1-1-2014

Directing Structure and Reactivity in Synthetic Uranium Complexes

Andrew James Lewis
University of Pennsylvania, andjlew@gmail.com

Directing Structure and Reactivity in Synthetic Uranium Complexes

Abstract
The coordination chemistry of uranium is not well understood. This fact is at the crux of all issues in modern synthetic uranium chemistry. Imposing simple design principles including steric pressure and coordinative saturation have proven most effective for the rational synthesis of uranium complexes. In this work, the effect of minor perturbations to the electronic structure on the gross molecular structure is investigated. Intramolecular non-covalent interactions are shown to influence the primary and secondary coordination sphere at uranium ions. Forces common in supramolecular assembly similarly control the orientation of ligands about the metal center. Insight is provided into the inverse trans influence, a thermodynamic phenomenon that preferentially stabilizes reactive uranium-ligand bonds in a preferred axial bonding orientation. Leveraging the inverse trans influence allowed for the first reported synthesis of uranium(VI)-alkyl and -acetylide complexes, and the establishment of an inverse trans influence ligand series. The role of covalency in stabilizing uranium-ligand bonds is explored.

Degree Type
Dissertation

Degree Name
Doctor of Philosophy (PhD)

Graduate Group
Chemistry

First Advisor
Eric J. Schelter

Keywords
Actinide, DFT, Electrochemistry, Non-Covalent Interactions, Synthesis, Uranium

Subject Categories
Chemistry | Inorganic Chemistry | Other Chemistry

DIRECTING STRUCTURE AND REACTIVITY IN SYNTHETIC URANIUM COMPLEXES

Andrew J. Lewis

A DISSERTATION

in

Chemistry

Presented to the Faculties of the University of Pennsylvania

in

Partial Fulfillment of the Requirements for the
Degree of Doctor of Philosophy

2014

Supervisor of Dissertation

_____

Prof. Eric J. Schelter
Assistant Professor of Chemistry

Graduate Group Chairperson

_____

Prof. Gary Molander
Hirschmann-Makineni Professor of Chemistry

Dissertation Committee:

Prof. Donald H. Berry, Professor of Chemistry
Prof. Patrick J. Walsh, Professor of Chemistry
Prof. Larry G. Sneddon, Blanchard Professor of Chemistry

Acknowledgements

First, I must acknowledge you, the reader, for taking the time to read these words. It means so much to me that you would be interested enough to skim through this dissertation. I sincerely hope that it does not disappoint.

Obviously none of this work could have been accomplished without the endless support of my advisor, Eric Schelter. I can say without a doubt that no one has spent more time working towards ensuring my success, and I will always be grateful to him for that. Eric has always taken my ideas seriously, and gave me boundless opportunity and scientific freedom. I have no doubt that he will continue to run an exceptionally successful research program in the future, and that any success that I have in the future can be attributed to the time I spent working with him.

I am grateful that I had the opportunity to work with the many fine members of the Schelter lab. We had an excellent group of graduate students that fostered a highly collaborative environment, providing never-ending intellectual and emotional support. I will really miss working with them. Of course I will not get a chance to miss working with Jerome Robinson, since we are bound to see each other every day in our new employment. For the rest of them, I will always look back at our time spent together fondly.

To my dissertation committee, Profs. Don Berry, Pat Walsh, and Larry Sneddon, I give thanks for the support throughout the years. Of course I cannot leave out the many contributions and creative insight by my honorary committee member, Prof. Chris Graves. If the reader notices any extraordinarily good ideas in this dissertation there was probably some contribution from one of these sources. I have always felt that they were on my side and were genuinely rooting for my academic success.

This work was greatly facilitated by the access to incredible experimental support. I am very grateful to the hard work of Dr. Pat Carroll, who taught me so much about X-ray crystallography and contributed long hours to produce the crystallographic data that makes up the bulk of this dissertation. There were many issues with these data that Pat bravely waded through, and the magnitude of his contribution cannot be overstated. Also, I must thank Dr. Jun Gu and Dr.

George Furst for their assistance in the NMR experiments. I got to know them better during my short stint filling the NMRs, and found that in addition to being very helpful, they were truly good people. Additionally, I am grateful to Dr. Eiko Nakamaru-Ogiso for assistance in collecting the EPR spectra, to Prof. Jay Kikkawa for his contribution to the magnetic data collection, and to Judith Currano for sharing her vast expertise on how to navigate the literature.

I want to thank my family for a lifetime of support. Though I may try to fight it, my father is still an inspiration to me, and there is no doubt that I inherited his spirit. My mother is an incredibly loving person, and always worked hard to care for me. I am glad to have these people in my life.

Finally, I acknowledge my wife, Dr. Jasmina Cheung-Lau. She is the person who puts meaning in my life. Her encouragement and support during my time in graduate school has been incomparable. Everything that I do now is part of a long-term plan to spend every moment of my life with her. There could be no stronger motivation.

ABSTRACT

DIRECTING STRUCTURE AND REACTIVITY IN SYNTHETIC URANIUM COMPLEXES

Andrew J. Lewis

Eric J. Schelter

The coordination chemistry of uranium is not well understood. This fact is at the crux of all issues in modern synthetic uranium chemistry. Imposing simple design principles including steric pressure and coordinative saturation have proven most effective for the rational synthesis of uranium complexes. In this work, the effect of minor perturbations to the electronic structure on the gross molecular structure is investigated. Intramolecular non-covalent interactions are shown to influence the primary and secondary coordination sphere at uranium ions. Forces common in supramolecular assembly similarly control the orientation of ligands about the metal center. Insight is provided into the inverse trans influence, a thermodynamic phenomenon that preferentially stabilizes reactive uranium-ligand bonds in a preferred axial bonding orientation. Leveraging the inverse trans influence allowed for the first reported synthesis of uranium(VI)–alkyl and –acetylide complexes, and the establishment of an inverse trans influence ligand series. The role of covalency in stabilizing uranium-ligand bonds is explored.

Table of Contents

List of Tables

Chapter 2

Chapter 3

Chapter 4

Chapter 5

Chapter 6

List of Figures

Chapter 1

Chapter 2

Chapter 3

Chapter 4

Chapter 5

Chapter 6

Chapter 1

Introduction

1.1 Uranium. Uranium is a unique element. Though it is true that in some instances it behaves like a transition metal, engaging in redox chemistry spanning multiple oxidation states, and in other times like a main group metal, displaying high Lewis acidity and coordination number, it is on the rare occasion when the uranium ion exhibits a previously unknown reaction pathway or coordination mode that makes this metal so exciting to the modern synthetic chemist. The study of the coordination chemistry and reactivity of uranium is not purely an academic pursuit by any means, as fundamental principles revealed by these investigations are directly relevant to development of nuclear fuels, nuclear waste management and remediation, extraction of uranium from complex mixtures, and the development of depleted uranium as a catalyst.

1.2 Challenges Faced by the Modern Synthetic Uranium Chemist. In 1978, Marks and coworkers wrote, "Currently two major goals in organoactinide chemistry are to design ways of manipulating coordinative unsaturation for optimum chemical reactivity and to develop meaningful chemical comparisons between organoactinide reaction patterns and those of transition metal organometallics."[1] Those words are still true today.

New developments in synthetic uranium chemistry have leveraged the many available oxidation states of the uranium ion. In coordination complexes, uranium is known to adopt oxidation states ranging from 2+ to 6+.[2-6] In general, oxidation and reduction reactions tend to proceed through 1-electron transfer processes when possible, similar to a first-row transition metal. Because of this fact, traditional organometallic reactions such as oxidative addition and reductive elimination involving 2-electron transfer with a uranium ion are essentially unknown. Clever methods for circumventing these restrictions have allowed for formal 2-electron processes. For example, formal reductive elimination of bibenzyl from Bn_4U^{IV} occurs upon treatment with an

α-diimine, to form the ene-diamide with retention of the uranium(IV) oxidation state.[7] Similarly, formal intermolecular oxidative addition reactions to uranium(III) or uranium(V) complexes have been demonstrated, though these reactions undoubtedly proceed through radical intermediates.[8, 9] In order to fully appreciate the redox chemistry of the uranium ion, some discussion of the coordination chemistry in the various oxidation states is warranted.

A single molecular example of uranium in the 2+ oxidation state was recently reported, in the complex [K(2.2.2-cryptand)][$(C_5H_4SiMe_3)_3U^{II}$], formed through reduction of the uranium(III) complex $C_5H_4SiMe_3)_3U^{III}$ with KC_8 in the presence of 2.2.2-cryptand.[2] The ability to generate uranium(II) under these conditions set a precedent for this oxidation state that will undoubtedly be explored in new reduction chemistry. In the molecular complex of uranium(II), the additional unpaired electron populates the $6d_{z2}$ orbital to yield a $5f^36d^1$ electron configuration, consistent with theoretical predictions.[10] The formal U(III/II) reduction potential was predicted to be similar to that of the Th(IV/III) reduction potential,[10] and thorium(III) complexes also have proven exceptionally rare.[11-15] New examples of uranium(II) complexes may well draw inspiration from the ligand environments that were shown to support throrium(III).

Trivalent uranium complexes are in some cases structurally analogous to related lanthanide(III) coordination complexes, though the uranium(III) ion is generally a potent reductant.[16-20] As a result, uranium(III) complexes undergo facile oxidation and are frequently unstable towards the disproportionation reaction 4 $U^{3+} \rightarrow 3\ U^{4+} + U^0$.[21] Complexes of uranium(III) that exhibit suitable stability have enabled a variety of small molecule activation reactions through one- or multi-electron reduction processes.[18, 22-28] The successful synthesis of many uranium(III) complexes can be traced to the development of $U^{III}[N(SiMe_3)_2]_3$ by Andersen,[29] a stable dark purple complex that acts as a suitable starting material for protonolysis reactions. Reported uranium(III) complexes typically exhibit intense, dark colors, and are not known to engage in metal-ligand multiple bonding.

In the absence of uranyl, the 4+ oxidation state is generally the most stable valence for uranium,[30] where the coordination chemistry resembles that of thorium(IV) or in some cases an

early transition metal such as zirconium(IV).[31-33] There is a growing interest in understanding the one-electron oxidation chemistry from uranium(IV) to uranium(V),[34-37] and developing electron-rich uranium(IV) complexes that perform 2-electron reduction reactions.[27, 38, 39] The high Lewis acidity of the uranium(IV) cation as well as the high ionicity of the uranium(IV)-ligand bond has given rise to a rich variety of organometallic pathways primarily involving favorable insertion, σ-bond metathesis, and protonolysis reactions.[26, 40] Although uranium(IV) complexes are typically not strong chromophores in the absence of ligand-based features, this oxidation state has been identified by characteristic emission features in the UV absorption spectrum, as well as diagnostic 5f-5f transitions in the near-IR spectrum.[41, 42] Furthermore, low symmetry uranium(IV) complexes are characterized by the presence of a singlet ground state, identifiable by low temperature magnetic susceptibility, and the absence of saturation of the magnetic moment at high applied field at low temperature.[43-45]

The pentavalent oxidation state of uranium is highly disfavored under aqueous conditions,[46] leading to the environmentally important disproportionation reaction $2\ U^{V}O_2^{+} + 4\ H^{+} \rightarrow U^{IV} + U^{VI}O_2^{2+} + 2\ H_2O$.[47] Furthermore, $U^{V}O_2^{+}$ is believed to act as an intermediate and terminal electron acceptor in the microbial reduction of uranyl,[48] a key process in bioremediation of nuclear waste. The coordination chemistry of pentavalent uranium complexes not containing uranyl has blossomed in recent times, with dramatic improvements in the quality of characterization of the $5f^1$ electron configuration.[49, 50] The variety of uranium(V) complexes that have been prepared was recently reviewed by Graves and Kiplinger.[5] Uranium(V) complexes can be identified by characteristic 5f-5f transitions in the NIR spectrum, as well as by EPR spectroscopy of the unpaired $5f^1$ electron; however, it has been noted that depending on the m_j value of the ground state, some uranium(V) complexes are EPR silent.[51]

The majority of hexavalent uranium complexes that have been investigated contain the $U^{VI}O_2^{2+}$ cation. Recent work from Hayton and coworkers has expanded the basic coordination chemistry of the uranium(VI) ion with simple ligand types including alkoxides,[52] amides,[53] ketimides,[54] and alkyls,[55] demonstrating the stability of the 6+ oxidation state in the absence of a

uranium-ligand multiple bond. In general, the U=O multiple bond lends incredible stability to the high valent state, shifting the U(VI/V) reduction potential over a 2 V range.[56] Uranium(VI) complexes typically appear diamagnetic by NMR spectroscopy, but are known to exhibit temperature independent paramagnetism.[57] Much of the recent work on uranium(VI) complexes has focused on the preparation of novel uranium-ligand multiple bonds,[58] with interest in understanding the role of covalency and the ability for the 5f and 6d orbitals to engage in bonding.

1.3 Covalency in Uranium-Ligand Bonding. There are many aspects that must be considered when discussing the nature of a uranium-ligand bond. It is important to realize that while the 5f valence orbitals of uranium are far more accessible for bonding than the 4f orbitals of the lanthanide elements, the metal-ligand bonds of both are of largely ionic character. The 5f orbitals are quite radially contracted and too high in energy to interact well with ligand-based atomic orbitals (Figure 1.3.1). As a result, ligand field effects are generally smaller or on the same order of magnitude as spin-orbit coupling.[49] Coordination geometries, about low-valent uranium complexes in particular, are more broadly influenced by steric and electrostatic interactions than driven by covalency. Increasingly, the role of covalency in directing the structure and bonding of uranium complexes has been examined.[50, 59-64]

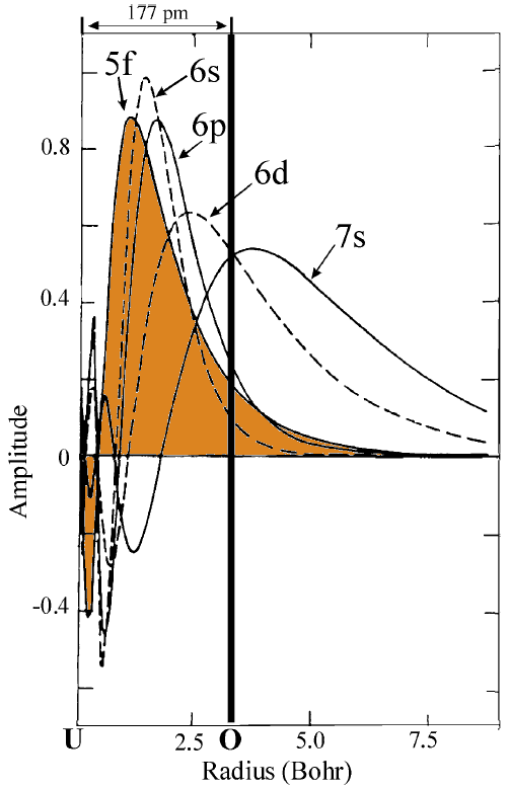

Figure 1.3.1 Radial amplitudes of the semi-core and valence orbitals of uranium, with the average U=O distance of 1.77 Å indicated with a black line. The uranium 5f orbital is shaded orange. Adapted with permission from Denning, R. G., *J. Phys. Chem. A* **2007,** *111*, 4125-4143.[65] Copyright 2007 American Chemical Society.

An archetypical example of metal-ligand covalency present in transition metal complexes is π-backbonding from electron-rich metals to a π-acidic ligand such as CO. In fact, CO is known to bind to uranium, first observed in the complex $(Cp')_3U(CO)$ (Cp' = C_5Me_4H), leading to speculation that a covalent π back-boding mechanism could be in effect.[66] However, more recent theoretical work has shown that electron donation into the CO π* orbital originates not from the uranium $5f^3$ electrons but from electrons localized in Cp'–U π-bonding orbitals. The role of covalency in uranium-ligand bonds is therefore not easy to identify. High valent uranium complexes exhibit more clearly defined and localized covalent bonding interactions, particularly in the presence of multiply-bonded ligands.[28, 58]

1.4 Strategies to Control the Structure and Reactivity at Uranium Ions.

1.4.1 Sterics. In the realm of directing structure and guiding reactivity in molecular uranium chemistry, ligands imposing a demanding steric profile have produced substantive results. Many of the most important recent accomplishments in reductive uranium chemistry have arisen from ligand sets that impose steric control (Figure 1.4.1.1). In landmark work from Meyer and coworkers, the reaction of CO_2 with a sterically encumbered uranium(III) complex, $U^{III}(OAr)_3tacn$, produced a $U^{IV}(\kappa^1\text{-OCO})$ complex,[22] the first example of a stable $CO_2^{-\cdot}$ radical anion complex and the first example of the linear κ^1-OCO coordination mode.[67] Relieving some of the steric bulk of the aryloxide ligand facilitated intermolecular two-electron reduction to form the $U^{IV}_2(\mu\text{-O})$ product with loss of CO.[68] Similarly, selective, reductive oligomerization of CO was demonstrated through steric control imparted by bulky ligands in the complex $(C_8H_6TMS_2)(C_5Me_5)U^{III}(THF)$,[25, 69] where CO dimerization could only be achieved with strict control of stoichiometry.[70] In contrast, selective dimerization of CO was observed at the more hindered $U^{III}[N(SiMe_3)_2]_3$, to form the ynediolate as the sole product.[71] The two-electron reduction of azide to form a monometallic uranium(V)-nitride was accomplished through use of a ligand set that imparted maximal steric hindrance, U(TREN^{TIPS}) (TREN^{TIPS} = $[N(CH_2CH_2NSi^iPr_3)_3]^{3-}$).[72] Whereas previous examples of azide reduction reactions had routinely produced dimeric or multinuclear structures,[23, 73, 74] the increased bulk of the substituted TREN ligand was sufficient to stabilize the U≡N multiple bond. In each of these examples, control over bonding and product formation can be directly attributed to steric pressure.

Steric encumbrance is undeniably effective in uranium chemistry. Much of the success in the development of uranium coordination chemistry arose from the "Cp^*_2U" framework ($Cp^* = C_5Me_5$),[1] and functionalized derivatives thereof, a ligand set that blocks all coordination save a sterically protected binding cleft.[75] Similarly, the three-fold symmetric "Cp_3U" and $U[N(SiMe_3)_2]_3$ frameworks have proven effective at guiding reactivity toward sterically protected open coordination sites.[4, 29]

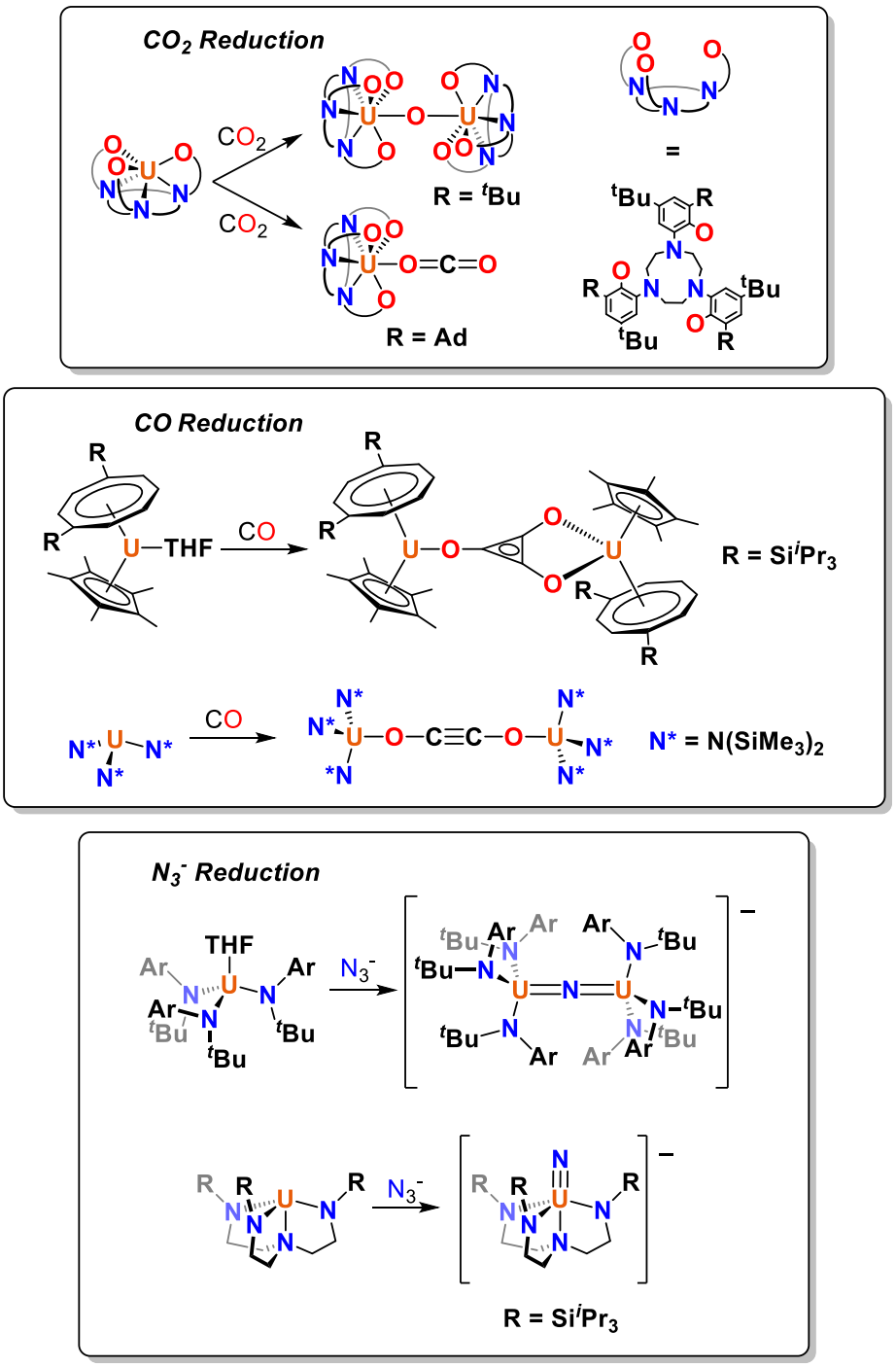

Figure 1.4.1.1 Controlling the outcome of small molecule reduction reactions with sterics. Steric hindrance at the uranium center is greater in the bottom reaction in each case.

1.4.2 Tethered Ligand Frameworks. As discussed in Section 1.3, the barrier to ligand reorganization in uranium complexes is low, particularly in low oxidation states. Furthermore,

simple mono-dentate ligands have a tendency to react in unexpected ways with uranium. In a classic example, treatment of $UI_3(THF)_4$ with an excess of $Li(OEt_2)$(dbabh) (dbabh = 2,3:5,6-dibenzo-7-azabicyclo[2.2.1]hepta-2,5-diene) surprisingly produced $[Li(THF)_n][U^{V}(dbabh)_6]$ through formal loss of "Li_3N".[76] Reactions such as these provide valuable insight into the type of reaction pathways accessible to uranium, but represent the lowest level of control over molecular architecture. In contrast, tethered, multi-dentate ligands such as derivatives of TREN ($[N(CH_2CH_2NR)_3]^{3-}$) impart inherent control over local coordination geometry. In an extreme example, reaction of a substituted TREN (R = $SiMe_2{}^tBu$) with UO_2^{2+} gave a mixed valent U(VI/V) dimeric complex in which one of the oxo ligands and one of the silyl groups is lost from the metal and TREN ligand respectively.[77] In spite of the dramatic reactivity, tetra-coordination of each of the TREN ligands with each metal center is retained in the product.

An enormous segment of synthetic uranium chemistry is dedicated towards the use of multi-dentate ligands. Three-fold symmetric ligands with mixed donors have been studied in great depth by the Meyer group,[16, 17, 22, 43, 68, 78-88] furnishing a variety of impressive results. Uranium complexes of ligands related to TREN have produced a wide variety of new chemistry from the groups of Scott and more recently Liddle.[27, 41, 72, 89-100] Pyrrole-based pacman ligands have enabled numerous transformations of uranyl in work from Arnold and coworkers.[101-110] Our efforts in preparing pyrrole-based multi-dentate complexes are presented in Chapter 5.

1.4.3 The Inverse *Trans* Influence. It has long been recognized that $U^{VI}O_2^{2+}$ complexes benefit from synergistic stabilization of the U=O multiple bonds through the inverse *trans* influence,[65, 111, 112] discussed in greater detail in Section 2.3. Recently, work from a number of groups,[39, 83, 87, 113] including ours,[37, 114, 115] have explored the possibility that the inverse *trans* influence could be used as a guiding force to stabilize other reactive uranium-ligand bonds, through coordination *trans* to a strong U=O multiple bond. Inverse *trans* influence stabilization has allowed for the synthesis of complexes containing $O=U^{VI}=S$ and $O=U^{VI}=Se$ multiple bonds,[39] the first molecular examples of heavy chalcogenide analogues of uranyl. Complexes of this type are of long standing interest, as at the extreme, US_2 isolated in an argon matrix was determined

to have a bent geometry, with an S–U–S angle of 118 ± 5°,[116] and US_2^{2+} was determined to be unstable toward S–S bond formation,[117] representing a breakdown of the inverse *trans* influence with the weaker sulfido ligand. Work from Meyer and coworkers has shown that in the rigid C_3 symmetric U[$(ArO)_3$tacn] framework, an oxo ligand moves into a sterically unfavorable geometry upon oxidation to orient *trans* to an aryloxide ligand, hinting at inverse *trans* influence stabilization.[83]

The work presented in Chapters 2 and 3 provide an investigation into the role of the inverse *trans i*nfluence in a structurally conserved framework. It is demonstrated that reactive metal ligand bonds can indeed be generally stabilized in both uranium(V) and uranium(VI) complexes, with the caveat that these advances do involve use of steric protection. It is our hope that the stabilization presented by the inverse *trans* influence may be used as a general design feature in the synthesis of previously unknown high valent uranium-ligand bonds.

1.4.4 Non-Covalent Interactions. The use of non-covalent interactions in structural design has been a universal tool in supramolecular chemistry, biochemistry, and bioinorganic modeling. Weak perturbations such as van der Waals' forces, hydrogen bonding, cation-π interactions, π-stacking, and dipolar interactions impose directionality and selectively stabilize a given structural arrangement.[118] Additionally, weak stabilizing forces have been applied toward the activation and stabilization of metal ligand bonds,[119, 120] a principle routinely applied in biological systems.[121] The ability to direct secondary structure and stabilize metal-ligand bonding addresses two of the major difficulties faced in synthetic uranium chemistry. Towards these goals, we have focused on designing systems that favor a particular geometry through interactions between functionalized aryl groups. The efforts in this vein are presented in Chapters 4 and 5. We have also examined the ability for non-covalent interactions to destabilize strong U=O multiple bonding in UO_2^{2+} cations, also presented in Chapter 5. New efforts in our group that make use of non-covalent interactions have primarily involved directing ligands through weak U←F-C contacts,[122] which has proven to be a fruitful method ripe for further discovery.

1.5 References.

(1) Manriquez, J. M.; Fagan, P. J.; Marks, T. J., *J. Am. Chem. Soc.* **1978,** *100*, 3939.
(2) MacDonald, M. R.; Fieser, M. E.; Bates, J. E.; Ziller, J. W.; Furche, F.; Evans, W. J., *J. Am. Chem. Soc.* **2013,** *135*, 13310.
(3) Korobkov, I.; Gambarotta, S., Trivalent Uranium: A Versatile Species for Molecular Activation. In *Prog. Inorg. Chem.*, John Wiley & Sons, Inc.: 2005; pp 321.
(4) Ephritikhine, M., *Organometallics* **2013,** *32*, 2464.
(5) Graves, C. R.; Kiplinger, J. L., *Chem. Commun.* **2009**, 3831.
(6) Baker, R. J., *Chem. - Eur. J.* **2012,** *18*, 16258.
(7) Kraft, S. J.; Fanwick, P. E.; Bart, S. C., *J. Am. Chem. Soc.* **2012,** *134*, 6160.
(8) Villiers, C.; Ephritikhine, M., *J. Organomet. Chem.* **1990,** *393*, 339.
(9) Spencer, L. P.; Yang, P.; Scott, B. L.; Batista, E. R.; Boncella, J. M., *Inorg. Chem.* **2009,** *48*, 11615.
(10) Bratsch, S. G.; Lagowski, J. J., *J. Phys. Chem.* **1986,** *90*, 307.
(11) Bruno, J. W.; Kalina, D. G.; Mintz, E. A.; Marks, T. J., *J. Am. Chem. Soc.* **1982,** *104*, 1860.
(12) Blake, P. C.; Lappert, M. F.; Atwood, J. L.; Zhang, H., *J. Chem. Soc., Chem. Commun.* **1986**, 1148.
(13) Parry, J. S.; Cloke; Coles, S. J.; Hursthouse, M. B., *J. Am. Chem. Soc.* **1999,** *121*, 6867.
(14) Blake, P. C.; Edelstein, N. M.; Hitchcock, P. B.; Kot, W. K.; Lappert, M. F.; Shalimoff, G. V.; Tian, S., *J. Organomet. Chem.* **2001,** *636*, 124.
(15) Walensky, J. R.; Martin, R. L.; Ziller, J. W.; Evans, W. J., *Inorg. Chem.* **2010,** *49*, 10007.
(16) Castro-Rodríguez, I.; Meyer, K., *Chem. Commun.* **2006**, 1353.
(17) Lam, O. P.; Anthon, C.; Meyer, K., *Dalton Trans.* **2009**, 9677.
(18) Arnold, P. L., *Chem. Commun.* **2011,** *47*, 9005.
(19) Mansell, S. M.; Kaltsoyannis, N.; Arnold, P. L., *J. Am. Chem. Soc.* **2011,** *133*, 9036.
(20) Mougel, V.; Camp, C.; Pecaut, J.; Coperet, C.; Maron, L.; Kefalidis, C. E.; Mazzanti, M., *Angew. Chem. Int. Ed.* **2012,** *51*, 12280.
(21) Odom, A. L.; Arnold, P. L.; Cummins, C. C., *J. Am. Chem. Soc.* **1998,** *120*.
(22) Castro-Rodriguez, I.; Nakai, H.; Zakharov, L. N.; Rheingold, A. L.; Meyer, K., *Science* **2004,** *305*, 1757.
(23) Evans, W. J.; Kozimor, S. A.; Ziller, J. W., *Science* **2005,** *309*, 1835.
(24) Hayton, T. W.; Boncella, J. M.; Scott, B. L.; Palmer, P. D.; Batista, E. R.; Hay, P. J., *Science* **2005,** *310*, 1941.
(25) Summerscales, O. T.; Cloke, F. G.; Hitchcock, P. B.; Green, J. C.; Hazari, N., *Science* **2006,** *311*, 829.
(26) Fox, A. R.; Bart, S. C.; Meyer, K.; Cummins, C. C., *Nature* **2008,** *455*, 341.
(27) King, D. M.; Tuna, F.; McInnes, E. J. L.; McMaster, J.; Lewis, W.; Blake, A. J.; Liddle, S. T., *Science* **2012,** *337*, 717.
(28) Hayton, T. W., *Chem. Commun.* **2013,** *49*, 2956.
(29) Andersen, R. A., *Inorg. Chem.* **1979,** *18*, 1507.
(30) Brennan, J. G.; Andersen, R. A.; Zalkin, A., *J. Am. Chem. Soc.* **1988,** *110*, 4554.
(31) Andersen, R. A., *Inorg. Chem.* **1979,** *18*, 1724.
(32) Turner, H. W.; Andersen, R. A.; Zalkin, A.; Templeton, D. H., *Inorg. Chem.* **1979,** *18*, 1221.

(33) Seaman, L. A.; Walensky, J. R.; Wu, G.; Hayton, T. W., *Inorg. Chem.* **2013,** *52*, 3556.
(34) Graves, C. R.; Scott, B. L.; Morris, D. E.; Kiplinger, J. L., *J. Am. Chem. Soc.* **2007,** *129*, 11914.
(35) Graves, C. R.; Yang, P.; Kozimor, S. A.; Vaughn, A. E.; Clark, D. L.; Conradson, S. D.; Schelter, E. J.; Scott, B. L.; Thompson, J. D.; Hay, P. J.; Morris, D. E.; Kiplinger, J. L., *J. Am. Chem. Soc.* **2008,** *130*, 5272.
(36) Graves, C. R.; Vaughn, A. E.; Schelter, E. J.; Scott, B. L.; Thompson, J. D.; Morris, D. E.; Kiplinger, J. L., *Inorg. Chem.* **2008,** *47*, 11879.
(37) Lewis, A. J.; Nakamaru-Ogiso, E.; Kikkawa, J. M.; Carroll, P. J.; Schelter, E. J., *Chem. Commun.* **2012,** *48*, 4977.
(38) Fortier, S.; Kaltsoyannis, N.; Wu, G.; Hayton, T. W., *J. Am. Chem. Soc.* **2011,** *133*, 14224.
(39) Brown, J. L.; Fortier, S.; Wu, G.; Kaltsoyannis, N.; Hayton, T. W., *J. Am. Chem. Soc.* **2013,** *135*, 5352.
(40) Weiss, C. J.; Marks, T. J., *Dalton Trans.* **2010,** *39*, 6576.
(41) Roussel, P.; Alcock, N. W.; Boaretto, R.; Kingsley, A. J.; Munslow, I. J.; Sanders, C. J.; Scott, P., *Inorg. Chem.* **1999,** *38*, 3651.
(42) Hashem, E.; Swinburne, A. N.; Schulzke, C.; Evans, R. C.; Platts, J. A.; Kerridge, A.; Natrajan, L. S.; Baker, R. J., *RSC Adv.* **2013,** *3*, 4350.
(43) Castro-Rodriguez, I.; Olsen, K.; Gantzel, P.; Meyer, K., *J. Am. Chem. Soc.* **2003,** *125*, 4565.
(44) Lewis, A. J.; Williams, U. J.; Kikkawa, J. M.; Carroll, P. J.; Schelter, E. J., *Inorg. Chem.* **2012,** *51*, 37.
(45) Lewis, A. J.; Williams, U. J.; Carroll, P. J.; Schelter, E. J., *Inorg. Chem.* **2013,** *52*, 7326.
(46) Selbin, J.; Ortego, J. D., *Chem. Rev.* **1969,** *69*, 657.
(47) Burdet, F.; Pécaut, J.; Mazzanti, M., *J. Am. Chem. Soc.* **2006,** *128*, 16512.
(48) Lovley, D. R.; Phillips, E. J.; Gorby, Y. A.; Landa, E. R., *Nature* **1991,** *350*, 413.
(49) Edelstein, N.; Brown, D.; Whittaker, B., *Inorg. Chem.* **1974,** *13*, 563.
(50) Lukens, W. W.; Edelstein, N. M.; Magnani, N.; Hayton, T. W.; Fortier, S.; Seaman, L. A., *J. Am. Chem. Soc.* **2013,** *135*, 10742.
(51) Rosen, R. K.; Andersen, R. A.; Edelstein, N. M., *J. Am. Chem. Soc.* **1990,** *112*, 4588.
(52) Fortier, S.; Wu, G.; Hayton, T. W., *Inorg. Chem.* **2008,** *47*, 4752.
(53) Seaman, L. A.; Fortier, S.; Wu, G.; Hayton, T. W., *Inorg. Chem.* **2011,** *50*, 636.
(54) Seaman, L. A.; Wu, G.; Edelstein, N.; Lukens, W. W.; Magnani, N.; Hayton, T. W., *J. Am. Chem. Soc.* **2012,** *134*, 4931.
(55) Fortier, S.; Walensky, J. R.; Wu, G.; Hayton, T. W., *J. Am. Chem. Soc.* **2011,** *133*, 11732.
(56) Fortier, S.; Hayton, T. W., *Coord. Chem. Rev.* **2010,** *254*, 197.
(57) Cuellar, E. A.; Marks, T. J., *Inorg. Chem.* **1981,** *20*, 2129.
(58) Hayton, T. W., *Dalton Trans.* **2010,** *39*, 1145.
(59) Jensen, M. P.; Bond, A. H., *IJ. Am. Chem. Soc.* **2002,** *124*, 9870.
(60) Arnold, P. L.; Turner, Z. R.; Kaltsoyannis, N.; Pelekanaki, P.; Bellabarba, R. M.; Tooze, R. P., *Chem. - Eur. J.* **2010,** *16*, 9623.
(61) Minasian, S. G.; Keith, J. M.; Batista, E. R.; Boland, K. S.; Clark, D. L.; Conradson, S. D.; Kozimor, S. A.; Martin, R. L.; Schwarz, D. E.; Shuh, D. K.; Wagner, G. L.; Wilkerson, M. P.; Wolfsberg, L. E.; Yang, P., *J. Am. Chem. Soc.* **2012**.

(62) Kaltsoyannis, N., *Inorg. Chem.* **2013,** *52*, 3407.
(63) Roy, L. E.; Bridges, N. J.; Martin, L. R., *Dalton Trans.* **2013,** *42*, 2636.
(64) Cantat, T.; Graves, C. R.; Scott, B. L.; Kiplinger, J. L., *Angew. Chem. Int. Ed.* **2009,** *48*, 3681.
(65) Denning, R. G., *J. Phys. Chem. A* **2007,** *111*, 4125.
(66) Parry, J.; Carmona, E.; Coles, S.; Hursthouse, M., *J. Am. Chem. Soc.* **1995,** *117*.
(67) Aresta, M., *Carbon dioxide as chemical feedstock*. John Wiley & Sons: 2010.
(68) Castro-Rodriguez, I.; Meyer, K., *J. Am. Chem. Soc.* **2005,** *127*, 11242.
(69) Summerscales, O. T.; Cloke, F. G. N.; Hitchcock, P. B.; Green, J. C.; Hazari, N., *J. Am. Chem. Soc.* **2006,** *128*, 9602.
(70) Frey, A. S.; Cloke, F. G. N.; Hitchcock, P. B.; Day, I. J.; Green, J. C.; Aitken, G., *J. Am. Chem. Soc.* **2008,** *130*, 13816.
(71) Arnold, P. L.; Turner, Z. R.; Bellabarba, R. M.; Tooze, R. P., *Chem. Sci.* **2011,** *2*, 77.
(72) King, D. M.; Tuna, F.; McInnes, E. J.; McMaster, J.; Lewis, W.; Blake, A. J.; Liddle, S. T., *Nat. Chem.* **2013,** *5*, 482.
(73) Fox, A. R.; Arnold, P. L.; Cummins, C. C., *J. Am. Chem. Soc.* **2010,** *132*, 3250.
(74) Fortier, S.; Wu, G.; Hayton, T. W., *J. Am. Chem. Soc.* **2010,** *132*, 6888.
(75) Ephritikhine, M., *Dalton Trans.* **2006**, 2501.
(76) Meyer, K.; Mindiola, D. J.; Baker, T. A.; Davis, W. M.; Cummins, C. C., *Angew. Chem. Int. Ed.* **2000,** *39*, 3063.
(77) Duval, P. B.; Burns, C. J.; Buschmann, W. E.; Clark, D. L.; Morris, D. E.; Scott, B. L., *Inorg. Chem.* **2001,** *40*, 5491.
(78) Castro-Rodriguez, I.; Nakai, H.; Gantzel, P.; Zakharov, L. N.; Rheingold, A. L.; Meyer, K., *J. Am. Chem. Soc.* **2003,** *125*, 15734.
(79) Nakai, H.; Hu, X.; Zakharov, L. N.; Rheingold, A. L.; Meyer, K., *Inorg. Chem.* **2004,** *43*, 855.
(80) Castro-Rodríguez, I.; Nakai, H.; Meyer, K., *Angew. Chem. Int. Ed.* **2006,** *45*, 2389.
(81) Bart, S. C.; Anthon, C.; Heinemann, F. W.; Bill, E.; Edelstein, N. M.; Meyer, K., *J. Am. Chem. Soc.* **2008,** *130*, 12536.
(82) Lam, O. P.; Feng, P. L.; Heinemann, F. W.; O'Connor, J. M.; Meyer, K., *J. Am. Chem. Soc.* **2008,** *130*, 2806.
(83) Kosog, B.; La Pierre, H. S.; Heinemann, F. W.; Liddle, S. T.; Meyer, K., *J. Am. Chem. Soc.* **2012,** *134*, 5284.
(84) Kosog, B.; Kefalidis, C. E.; Heinemann, F. W.; Maron, L.; Meyer, K., *J. Am. Chem. Soc.* **2012,** *134*, 12792.
(85) Lam, O. P.; Franke, S. M.; Heinemann, F. W.; Meyer, K., *J. Am. Chem. Soc.* **2012,** *134*, 16877.
(86) Lam, O. P.; Meyer, K., *Polyhedron* **2012,** *32*.
(87) Lam, O. P.; Franke, S. M.; Nakai, H.; Heinemann, F. W.; Hieringer, W.; Meyer, K., *Inorg. Chem.* **2012,** *51*, 6190.
(88) Franke, S. M.; Heinemann, F. W.; Meyer, K., *Chem. Sci.* **2013**.
(89) Scott, P.; Hitchcock, P. B., *J. Chem. Soc., Dalton Trans.* **1995**, 603.
(90) Roussel, P.; Hitchcock, P. B.; Tinker, N.; Scott, P., *Chem. Commun.* **1996**.
(91) Roussel, P.; Hitchcock, P. B.; Tinker, N. D.; Scott, P., *Inorg. Chem.* **1997,** *36*, 5716.
(92) Roussel, P.; Scott, P., *J. Am. Chem. Soc.* **1998,** *120*, 1070.

(93) Boaretto, R.; Roussel, P.; J. Kingsley, A.; J. Munslow, I.; J. Sanders, C.; W. Alcock, N.; Scott, P., *Chem. Commun.* **1999**, 1701.
(94) Roussel, P.; Boaretto, R.; Kingsley, A. J.; Alcock, N. W.; Scott, P., *J. Chem. Soc., Dalton Trans.* **2002**, 1423.
(95) Gardner, B. M.; McMaster, J.; Lewis, W.; Blake, A. J.; Liddle, S. T., *J. Am. Chem. Soc.* **2009,** *131*, 10388.
(96) Liddle, S. T.; McMaster, J.; Mills, D. P.; Blake, A. J.; Jones, C.; Woodul, W. D., *Angew. Chem. Int. Ed.* **2009,** *48*, 1077.
(97) Patel, D.; Moro, F.; McMaster, J.; Lewis, W.; Blake, A. J.; Liddle, S. T., *Angew. Chem. Int. Ed.* **2011,** *50*, 10388.
(98) Gardner, B. M.; Patel, D.; Lewis, W.; Blake, A. J.; Liddle, S. T., *Angew. Chem. Int. Ed.* **2011,** *50*, 10440.
(99) Gardner, B. M.; Lewis, W.; Blake, A. J.; Liddle, S. T., *Inorg. Chem.* **2011,** *50*, 9631.
(100) Gardner, B. M.; Stewart, J. C.; Davis, A. L.; McMaster, J.; Lewis, W.; Blake, A. J.; Liddle, S. T., *Proc. Natl. Acad. Sci.* **2012,** *109*, 9265.
(101) Arnold, P. L.; Patel, D.; Blake, A. J.; Wilson, C.; Love, J. B., *J. Am. Chem. Soc.* **2006,** *128*, 9610.
(102) Arnold, P. L.; Patel, D.; Wilson, C.; Love, J. B., *Nature* **2008,** *451*, 315.
(103) Arnold, P. L.; Pécharman, A.-F.; Hollis, E.; Yahia, A.; Maron, L.; Parsons, S.; Love, J. B., *Nat. Chem.* **2010,** *2*, 1056.
(104) Arnold, P. L.; Pécharman, A.-F.; Love, J. B., *Angew. Chem. Int. Ed.* **2011,** *50*, 9456.
(105) Arnold, P. L.; Hollis, E.; White, F. J.; Magnani, N.; Caciuffo, R.; Love, J. B., *Angew. Chem. Int. Ed.* **2011,** *50*, 887.
(106) Arnold, P. L.; Jones, G. M.; Odoh, S. O.; Schreckenbach, G.; Magnani, N.; Love, J. B., *Nat. Chem.* **2012,** *4*, 221.
(107) Jones, G. M.; Arnold, P. L.; Love, J. B., *Angew. Chem. Int. Ed.* **2012,** *51*, 12584.
(108) Arnold, P. L.; Jones, G. M.; Pan, Q.-J.; Schreckenbach, G.; Love, J. B., *Dalton Trans.* **2012,** *41*, 6595.
(109) Arnold, P. L.; Hollis, E.; Nichol, G. S.; Love, J. B.; Griveau, J.-C.; Caciuffo, R.; Magnani, N.; Maron, L.; Castro, L.; Yahia, A.; Odoh, S. O.; Schreckenbach, G., *J. Am. Chem. Soc.* **2013,** *135*, 3841.
(110) Jones, G. M.; Arnold, P. L.; Love, J. B., *Chem. - Eur. J.* **2013,** *19*, 10287.
(111) Tatsumi, K.; Hoffmann, R., *Inorg. Chem.* **1980,** *19*, 2656.
(112) O'Grady, E.; Kaltsoyannis, N., *J. Chem. Soc., Dalton Trans.* **2002**, 1233.
(113) La Pierre, H. S.; Meyer, K., *Inorg. Chem.* **2013,** *52*, 529.
(114) Lewis, A. J.; Carroll, P. J.; Schelter, E. J., *J. Am. Chem. Soc.* **2013,** *135*, 511.
(115) Lewis, A. J.; Carroll, P. J.; Schelter, E. J., *J. Am. Chem. Soc.* **2013,** *135*, 13185.
(116) Liang, B.; Andrews, L.; Ismail, N.; Marsden, C. J., *Inorg. Chem.* **2002,** *41*, 2811.
(117) Pereira, C. C. L.; Michelini, M. d. C.; Marçalo, J.; Gong, Y.; Gibson, J. K., *Inorg. Chem.* **2013,** *52*, 14162.
(118) Steed, J. W.; Turner, D. R.; Wallace, K., *Core concepts in supramolecular chemistry and nanochemistry*. John Wiley & Sons: 2007.
(119) Park, Y. J.; Ziller, J. W.; Borovik, A. S., *J. Am. Chem. Soc.* **2011,** *133*, 9258.
(120) Borovik, A., *Acc. Chem. Res.* **2005,** *38*, 54.
(121) Bertini, I., *Biological inorganic chemistry: structure and reactivity*. University Science Books: 2007.

(122) Yin, H.; Lewis, A. J.; Williams, U. J.; Carroll, P. J.; Schelter, E. J., *Chem. Sci.* **2013,** *4*, 798.

Chapter 2

The Synthesis of Pentavalent Uranium Tris-Amide Complexes

2.1 Introduction. The remarkable stability of the uranyl dication (UO_2^{2+}) is attributed to its linear *trans*-axial geometry,[1] which is a general feature of the high oxidation state chemistry of U, Np, Pu and Am.[2] The synthesis of new high valent uranium complexes with axial symmetry is desirable to draw comparisons with the complex electronic structures of the actinyl (AnO_2^{n+}) cations and for expanding the unique coordination chemistry and reactivity of uranium.[1, 3] High valent, axially-symmetric coordination complexes of uranium that have been reported include bis(imido)-,[4, 5] oxo/imido-,[6] oxo/nitrido-,[7] oxo/halo-[8] and imido/fluoro- complexes.[9]

2.2 Previous Studies of Pentavalent Uranium. Pentavalent uranium complexes are of particular interest because of the spectroscopic information that can be gained from the $5f^1$ electronic configuration, however there are few examples of pentavalent uranium complexes that allow for ligand substitution (Figure 2.2.1).[10] Mono(imido) complexes of type **A** have been explored extensively as precursors to a variety of U(V)–X derivatives,[11] and complexes **B**[12] and **C**[13] are promising candidates for new U(V) complexes. However, a general route to pentavalent uranium compounds in which axial ligands can be systematically varied is not currently available.

Portions of this chapter have been adapted from previous publications. Sections 2.1, 2.2, 2.4, 2.5, and 2.9.1-2.9.7 are adapted from "Pentavalent Uranium Trans-Dihalides and -Pseudohalides" Lewis, A. J.; Nakamaru-Ogiso, E.; Kikkawa, J. M.; Carroll, P. J.; Schelter, E. J. *Chem. Commun.* **2012**, *48*, 4977–4979 with permission from The Royal Society of Chemistry. Sections 2.6-2.8 and 2.9.12-2.9.15 are adapted with permission from "Tetrakis(bis(trimethylsilyl)amido)uranium(IV): Synthesis and Reactivity" **Lewis, A. J.**; Williams, U. J.; Carroll, P. J.; Schelter, E. J. *Inorg. Chem.* **2013**, *52*, 7326–7328.

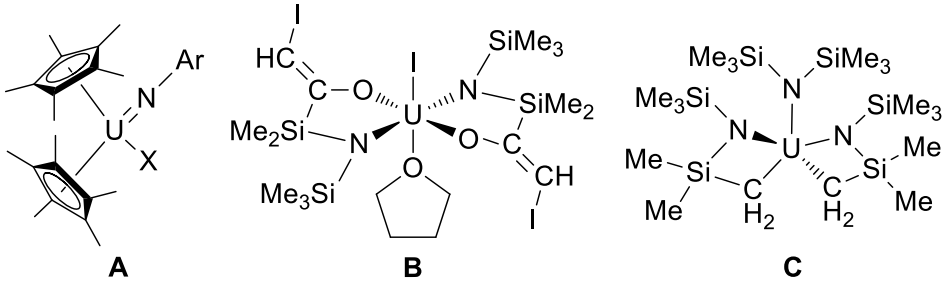

Figure 2.2.1 Representative pentavalent uranium complexes amenable to further ligand substitution.

2.3 The Inverse *Trans* Influence. Transition metal complexes, particularly those that are d^8 square planar, exhibit a thermodynamic phenomenon termed the *trans* influence, in which strong metal-ligand bonds destabilize metal-ligand bonds in the *trans* position. The origin of the *trans* influence can be understood on the basis of covalent as well as ionic bonding principles. Metal-ligand bonds that exhibit a high degree of covalency necessarily contain a high percentage of metal AO character within bonding orbitals. At a square planar coordination environment, metal-ligand σ-bonding is facilitated by the symmetric arrangement of ligand-based orbitals with the $d_x2\text{-}_y2$ orbital. An increase in metal AO character at a strong single metal ligand bond reduces the percentage of metal AO character in the *trans* metal ligand bond (Figure 2.3.1).[14, 15] The principle of "competition for ligand donation" represents the most wide-spread interpretation of the origin of the *trans* influence. Additional factors to consider are the fact that strong σ-bonding can result in partial population of the *trans* metal-ligand σ* orbital in some cases where the electronegativity of the two ligands differs, and π-back-bonding interactions present minor perturbation.[16] From an ionic perspective, a strong metal ligand bond imparts an effective buildup of positive charge at the metal center, which creates a dipole at the metal center oriented along the axis of the metal ligand bond. The subsequent buildup of negative charge at the *trans* position reduces the electrostatic attraction of the *trans* metal-ligand bond (Figure 2.3.2, left).[17]

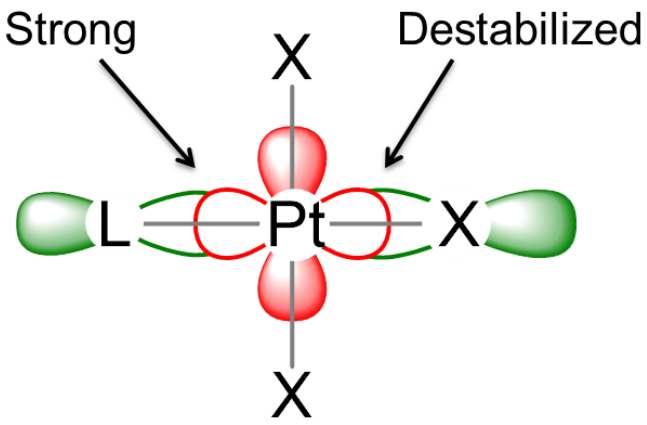

Figure 2.3.1 Schematic representation of the *trans* influence at d^8 square planar Pt^{2+} ion.

Axially symmetric complexes of high valent actinides exhibit a thermodynamic phenomenon that is opposite that of the *trans* influence. In the canonical example, the UO_2^{2+} (uranyl) moiety exhibits a linear O=U=O geometry in which the two strong U=O bonds synergistically stabilize one another in a preferential *trans* coordination, in contrast to the ubiquitous cis-dioxo geometry found in transition metal complexes.[18] In seminal work from Tasumi and Hoffmann, it was recognized that mixing of the filled, semi-core uranium $6p_z$ orbital with the $5f_z3$ orbital involved in σ-bonding along the primary axis, effectively lowered the energy of the σ-bonding orbital.[19] Later work by Denning suggested that the transfer of electron density from the $6p_z$ orbital effectively created a hole in the valence along the primary axis, leading to a buildup of positive charge in the position *trans* to the U=O bond.[20] The collective linear arrangement was therefore expected to impart a quadropole (Figure 2.3.2, right), in contrast to the effective dipole of the *trans* influence. The induced quadropole enhances trans-axial ligand to metal donation and weakens cis-equatorial bonding.[1] This satisfying explanation was demonstrated to not be wholly correct in later work by O'Grady and Kaltsoyannis, who used theoretical methods to show that suppression of uranium 5f-6p mixing in $[UOX_5]^-$ complexes (X = F^-, Cl^-, Br^-) through incorporation of the 6p orbitals in to the core pseudopotential led to only a partial reduction in the inverse *trans* influence.[21] The observed cis-destabilization could be partially rationalized based on the symmetric matching of the $5f_z3$ orbital with equatorial U-X π*

orbitals; conversely, stronger π-bonding ligands are expected to weaken axial σ-bonding,[22] though the ability for equatorial π-bonding to affect axial U=O bonding has been debated.[23, 24]

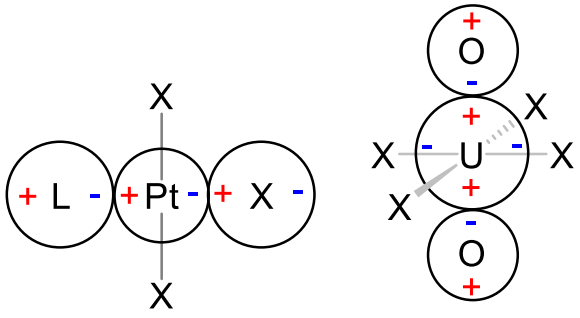

Figure 2.3.2 Comparison of charge polarization effects in the normal *trans* influence (left) and the inverse *trans* influence (right).

As a first step towards understanding the electronic origins of the inverse *trans* influence, we sought to prepare axially symmetric pentavalent uranium complexes in which the axial ligands could be systematically varied. Subtle changes in the preserved equatorial coordination sphere were expected to serve as a benchmark for comparing the inverse *trans* influence strength of various ligands.

2.4 Facile Synthesis of $U^{V}X_2[N(SiMe_3)_2]_3$ Complexes Through a Variety of Routes. Axial pentavalent uranium dihalide complexes were accessed through two oxidation routes (Scheme 2.4.1). Initial attempts to use CuF_2 to generate $U^{V}F_2[N(SiMe_3)_2]_3$ (**2.1-F**, Figure 2.4.1) directly from $U^{III}[N(SiMe_3)_2]_3$ were hindered by poor conversion. However, **2.1-F** was accessible through fluoride abstraction from [TEMPO][BF_4] (TEMPO = 2,2,6,6-tetramethylpiperidine-1-oxyl),[‡] or from [Ph_3C][PF_6]. The more potent oxidant AgF was also capable of producing **2.1-F**, though this heterogeneous reaction proceeded slowly. In contrast, treatment of $U^{III}[N(SiMe_3)_2]_3$ with excess CuX_2 (X = Cl^-, Br^-)[§] in toluene induced a rapid color change from dark purple to pale brown, and finally to dark red-brown (Scheme 2.4.1). This effective two-electron oxidation in one pot afforded black $U^{V}Cl_2[N(SiMe_3)_2]_3$ (**2.1-Cl**, Figure 2.4.2) or $U^{V}Br_2[N(SiMe_3)_2]_3$ (**2.1-Br**, Figure 2.4.3) respectively in good yields. WCl_6 was also found to be a suitable oxidant for the formation of **2.1-Cl**. The direct oxidation of uranium(III) to uranium(V) with copper or tungsten reagents was unknown prior to this work.[10]

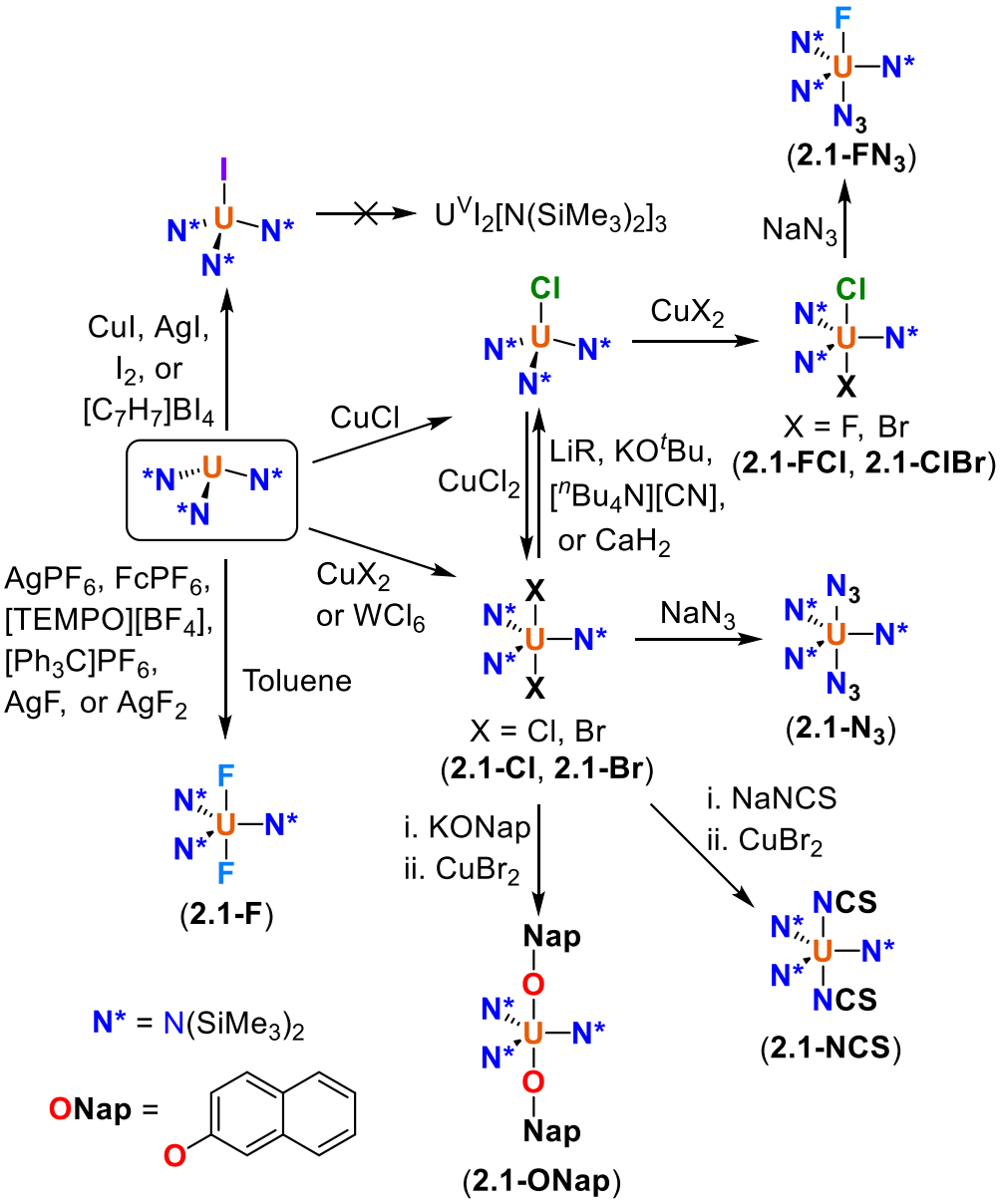

Scheme 2.4.1 Synthesis of uranium(IV) and uranium(V) tris-amide complexes.

On oxidation, two halide ions are installed axially into the tris-silylamide framework despite steric congestion. Steric crowding at the U(V) ion is evidenced in the ^{1}H NMR data; complexes **2.1-Cl** and **2.1-Br** exhibited restricted rotation of the trimethyl groups at room temperature. Restricted rotation in uranium tris-silylamide complexes has been observed previously.[9, 25] At room temperature, the spectrum of **2.1-F** recorded in benzene-d_6 displays a single, paramagnetically shifted and broadened peak (–1.53 ppm), whereas the spectra of **2.1-Cl**

displays three extremely broad features (0.84, –1.59, –4.01 ppm) and the spectrum of **2.1-Br** displays three well-resolved resonances in a 1:1:1 integration ratio (1.70, –1.01, –4.14 ppm). The restricted rotation in complexes **2.1-Cl** and **2.1-Br** is presumably due to the larger Cl^- and Br^- ions, respectively.

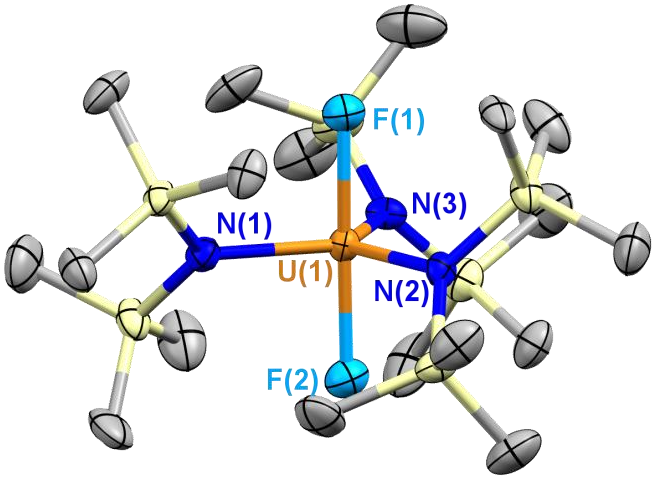

Figure 2.4.1 Thermal ellipsoid plot of **2.1-F** at 30% probability. Hydrogen atoms are omitted for clarity. Bond distances (Å) and angles (°): U(1)–F(1) 2.0562(19), U(1)–F(2) 2.0751(1), U(1)–N(1) 2.190(3), U(1)–N(2) 2.189(2), U(1)–N(3) 2.187(2), F(1)–U(1)–F(2) 178.35(8).

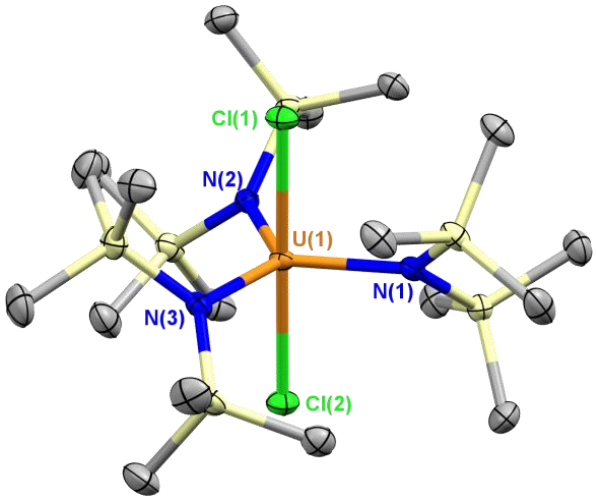

Figure 2.4.2 Thermal ellipsoid plot of **2.1-Cl** at 30% probability. Hydrogen atoms are omitted for clarity. Bond distances (Å) and angles (°): U(1)–Cl(1) 2.5704(5), U(1)–Cl(2) 2.5801(5), U(1)–N(1) 2.1687(16), U(1)–N(2) 2.1663(15), U(1)–N(3) 2.1614(16), Cl(1)–U(1)–Cl(2) 179.529(17).

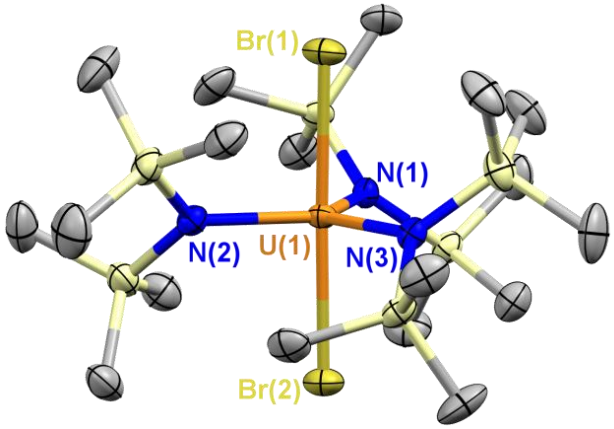

Figure 2.4.3 Thermal ellipsoid plot of **2.1-Br** at 30% probability. One of the two molecules from the asymmetric unit is depicted. Hydrogen atoms are omitted for clarity. Bond distances (Å) and angles (°): U(1)–Br(1) 2.7371(6), U(1)–Br(2) 2.7530(6), U(1)–N(1) 2.166(4), U(1)–N(2) 2.167(4), U(1)–N(3) 2.166(4), U(1')–Br(1') 2.7503(6), U(1')–Br(2') 2.7378(6), U(1')–N(1') 2.167(4), U(1')–N(2') 2.158(4), U(1')–N(3') 2.159(4), Br(1)–U(1)–Br(2) 178.382(19), Br(1')–U(1')–Br(2') 179.63(2).

The oxidation reactions could similarly be achieved in a stepwise fashion. As reported by Kiplinger,[26] addition of CuCl to $U^{III}[N(SiMe_3)_2]_3$ produced the known product $U^{IV}Cl[N(SiMe_3)_2]_3$ with no observable formation of **2.1-Cl** (Scheme 2.4.1). The synthesis of $U^{IV}Cl[N(SiMe_3)_2]_3$ from UCl_4 and $Na[N(SiMe_3)_2]$ is also well established.[27] Subsequent addition of $CuCl_2$ to an isolated sample of $U^{IV}Cl[N(SiMe_3)_2]_3$ re-suspended in THF resulted in complete conversion to **2.1-Cl** (Scheme 2.4.1). This stepwise one-electron oxidation represents a new pathway for accessing pentavalent uranium complexes, which we expected to be useful for installation of two different ligands in the axial positions of the tris-silylamide framework. To test this hypothesis we treated $U^{IV}Cl[N(SiMe_3)_2]_3$ with 5 equiv CuF_2 in THF, generating $U^{V}FCl[N(SiMe_3)_2]_3$ (**2.1-FCl**) (Scheme 2.4.1, Figure 2.4.4). This reaction required mild heating, likely due to the poor solubility of CuF_2. Complex **2.1-FCl** shows two broad, overlapping peaks in the ^{1}H NMR centered at –1.40 and –1.83 ppm in benzene-d_6, also indicating hindered rotation of the silylamide groups. Mixed halide complexes of uranium(V) have been reported in one instance,[28] but they were not structurally characterized. This route also allowed for the synthesis of $U^{V}BrCl[N(SiMe_3)_2]_3$ (**1-BrCl**, Figure 2.4.5), via treatment of $U^{IV}Cl[N(SiMe_3)_2]_3$ with $CuBr_2$.

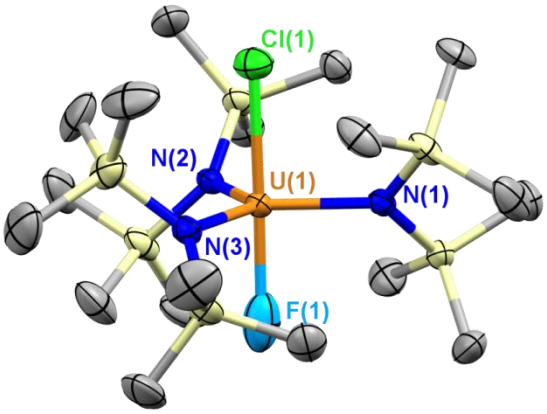

Figure 2.4.4 Thermal ellipsoid plot of **2.1-FCl** at 30% probability. Hydrogen atoms are omitted for clarity. Bond distances (Å) and angles (°): U(1)–Cl(1) 2.538(2), U(1)–Cl(1') 2.391(19), U(1)–F(1) 2.11(3), U(1)–F(1') 1.971(8), U(1)–N(1) 2.180(2), U(1)–N(2) 2.174(3), U(1)–N(3) 2.173(2), Cl(1)–U(1)–F(1) 178.8(6), Cl(1')–U(1)–F(1') 177.1(4).

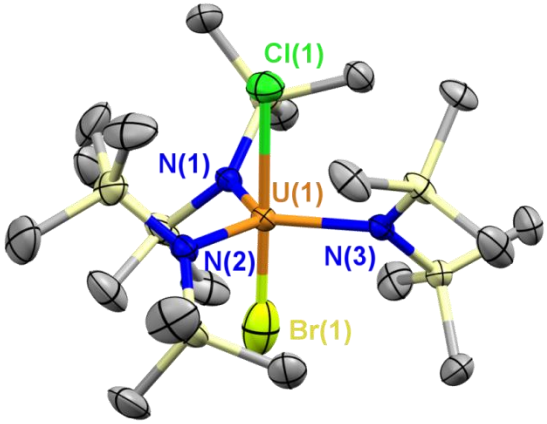

Figure 2.4.5 Thermal ellipsoid plot of **2.1-BrCl** at 30% probability. Hydrogen atoms are omitted for clarity. Bond distances (Å) and angles (°): U(1)–Cl(1) 2.56(4), U(1)–Cl(1') 2.56(4), U(1)–Br(1) 2.670(12), U(1)–Br(1') 2.628(18), U(1)–N(1) 2.152(6), U(1)–N(2) 2.174(5), U(1)–N(3) 2.163(5), Cl(1)–U(1)–Br(1) 179.4(12), Cl(1')–U(1)–Br(1') 179.4(12).

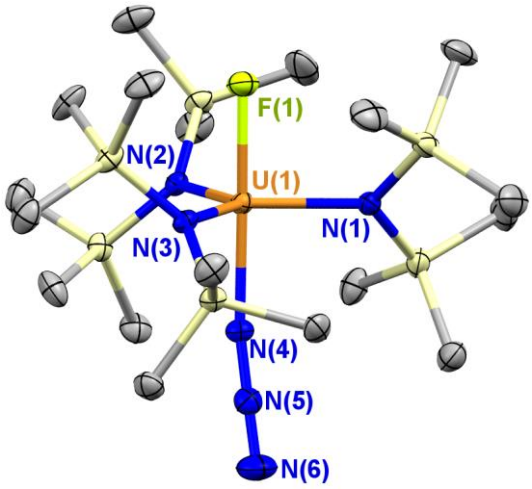

Figure 2.4.6 Thermal ellipsoid plot of **2.1-FN$_3$** at 30% probability. Hydrogen atoms are omitted for clarity. Bond distances (Å) and angles (°): U(1)–F(1) 2.065(2), U(1)–N(1) 2.194(3), U(1)–N(2) 2.183(3), U(1)–N(3) 2.186(3), U(1)–N(4) 2.210(3), F(1)–U(1)–N(4) 178.21(11).

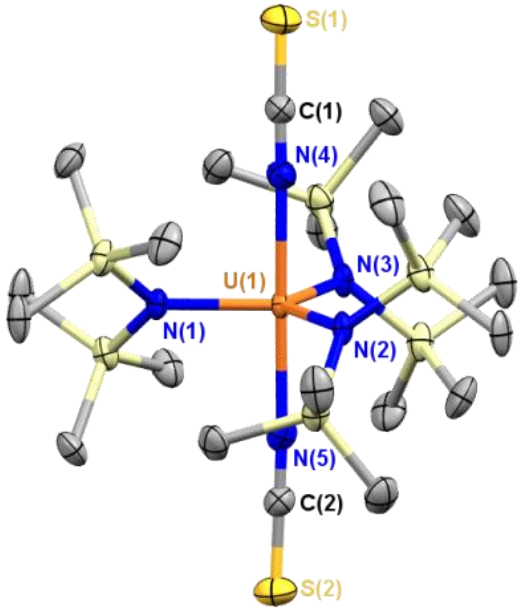

Figure 2.4.7 Thermal ellipsoid plot of **2.1-NCS** at 30% probability. Hydrogen atoms are omitted for clarity. Bond distances (Å) and angles (°): U(1)–N(1) 2.158(7), U(1)–N(2) 2.148(8), U(1)–N(3) 2.156(8), U(1)–N(4) 2.313(10), U(1)–N(5) 2.319(9), N(4)–C(1) 1.172(14), N(5)–C(2) 1.156(15), C(1)–S(1) 1.589(11), C(2)–S(2) 1.573(12), N(4)–U(1)–N(5) 179.3(3), U(1)–N(4)–C(1) 176.3(8), U(1)–N(5)–C(2) 175.5(11), N(4)–C(1)–S(1) 179.5(11), N(5)–C(2)–S(2) 178.4(11).

Compound **2.1-Cl** was found to be a viable starting material for substitution of the axial chlorides with pseudohalides. Addition of 2 equiv NaN_3 to a THF solution of **2.1-Cl** led to quantitative conversion to the reported diazide complex $U^{V}(N_3)_2[N(SiMe_3)_2]_3$ (**2.1-N$_3$**) (Scheme

2.4.1).[29] Analytically pure **2.1-N_3** was obtained from this reaction by suspending the crude product in hexanes followed by filtration, affording its isolation in 90% yield. Similarly, treatment of **2.1-FCl** with NaN_3 produced $U^{V}F(N_3)[N(SiMe_3)_2]_3$ (**2.1-FN_3**, Figure 2.4.6). In contrast, addition of an excess of anhydrous NaSCN to a THF solution of **2.1-Cl** generated a pale tan solution consistent with the formation of a U^{IV} product. However, subsequent *in situ* addition of $CuBr_2$ rapidly restored the characteristic dark red-brown color, producing the dithiocyanate complex $U^{V}(NCS)_2[N(SiMe_3)_2]_3$ (**2.1-NCS**) (Scheme 2.4.1, Figure 2.4.7). Notably, **2.1-NCS** is the first example of a U^{V}-thiocyanate complex, and exhibits the shortest U–NCS bonds for a uranium complex in any oxidation state.[30]

An aryloxide derivative of **2.1-X** was also synthesized and characterized. Addition of a slight excess of K(2-naphthoxide) (KONap) to a THF solution of **2.1-Cl** led to a color change from dark red to pale orange, with formation of a product that was identified by ^{1}H NMR as $[K(THF)_n][U^{IV}(ONap)_2[N(SiMe_3)_2]_3]$ (Figure 2.4.8). Despite the formal reduction of the uranium ion in this reaction, no obvious oxidation product could be identified. The uranium(IV) complex formed *in situ* was not isolated, but was treated with 4 equiv $CuBr_2$, resulting in rapid color change to dark red then to dark green. Extraction and recrystallization from hexanes afforded $U^{V}(ONap)_2[N(SiMe_3)_2]_3$ (**2.1-ONap**, Figure 2.4.9) as a black crystalline solid.

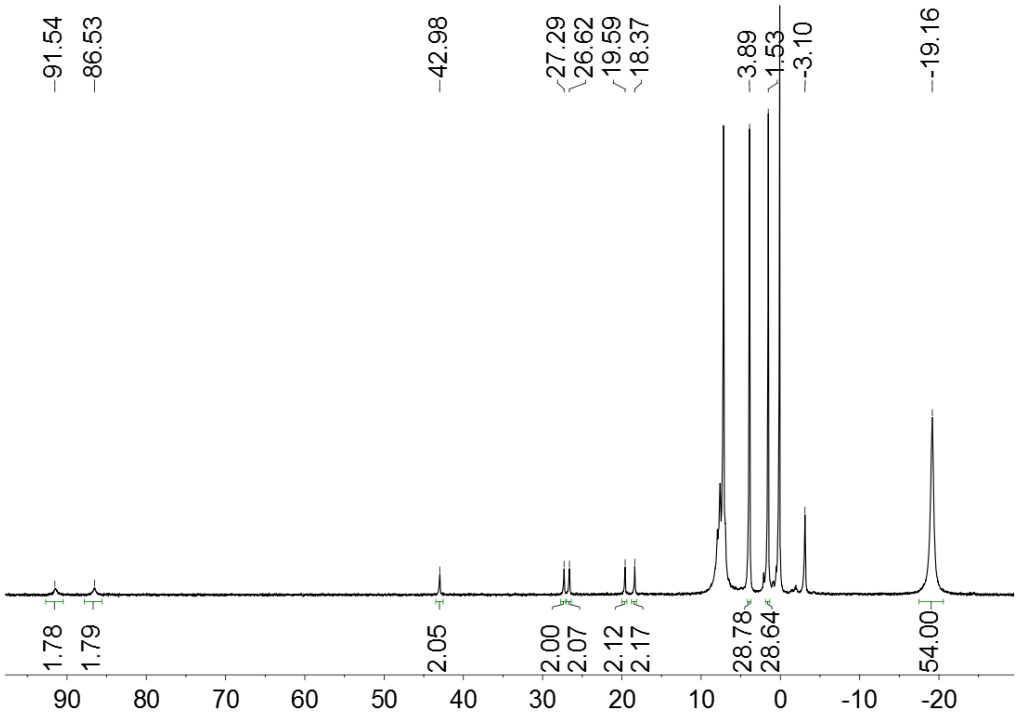

Figure 2.4.8 ^{1}H NMR of an aliquot taken from the reaction of **2.1-Cl** with 2 equiv KONap. The resonance indicated at –3.10 corresponds to $U[N(SiMe_3)_2]_4$.[31]

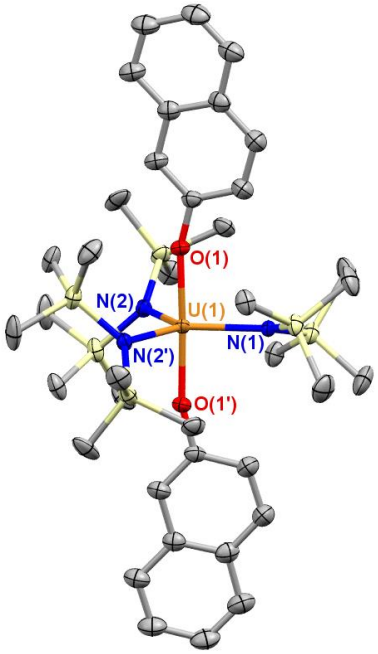

Figure 2.4.9 Thermal ellipsoid plot of **2.1-ONap** at 30% probability. Hydrogen atoms are omitted for clarity. Bond distances (Å) and angles (°): U(1)–O(1) 2.102(4), U(1)–N(1) 2.243(7), U(1)–N(2) 2.212(5), O(1)–U(1)–O(1') 177.7(2).

The ability for aryloxides to stabilize the uranium(V) center in **2.1-ONap** led us to consider the possibility of linking multiple uranium(V) ions through a *p*-hydroquinone type structure. Addition of 1 equiv *p*-benzoquinone to $U[N(SiMe_3)_2]_3$ immediately produced an insoluble black solid, presumably $[U[N(SiMe_3)_2]_3(\mu\text{-HQ})]_n$ (**2.1-HQ**, HQ = *p*-hydroquinonate). Similar results were obtained when *p*-fluoranil (tetrafluoro-*p*-benzoquinone) was used as an oxidant, to produce a black, utterly insoluble product. Attempts to obtain single crystals of the putative coordination chain polymer (Figure 2.4.10) were unsuccessful due to the very poor solubility of the product. However, the oxidation state assignment was supported by the variable temperature magnetic susceptibility data (Figure 2.4.11), which was analogous to that of **2.1-Cl** (vide infra).

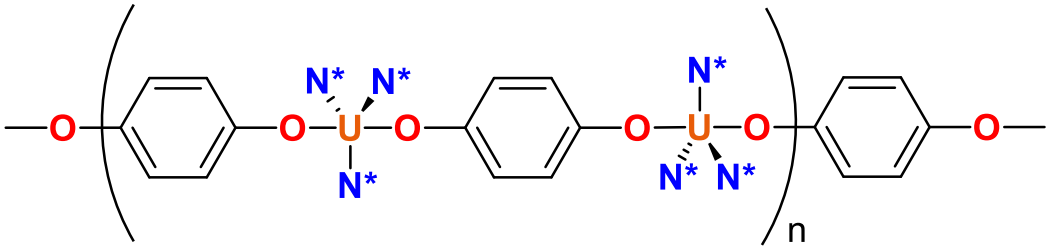

Figure 2.4.10 Proposed chain coordination polymer structure for **2.1-HQ**.

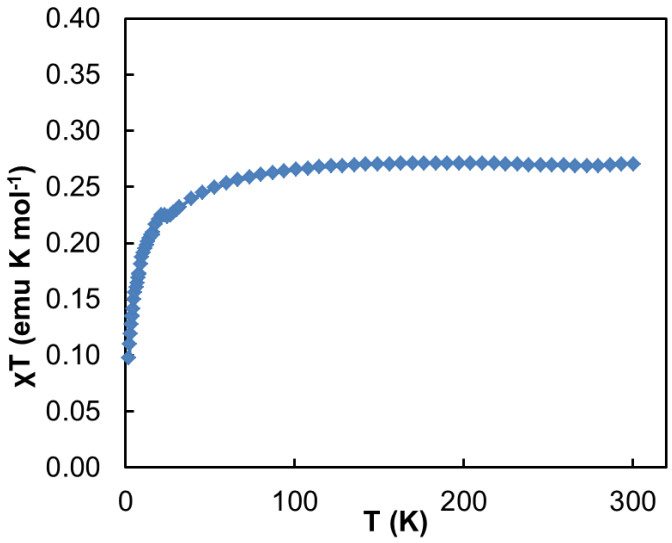

Figure 2.4.11 Temperature dependent magnetic susceptibility data for **2.1-HQ** at an applied field of 0.5 T.

Attempts to form other **2.1-X** derivatives were generally unsuccessful. Reaction of either **2.1-Cl** or **2.1-Br** with $[^{n}Bu_4N]CN$ led to reduction to the corresponding uranium(IV)-halide product.

This is in contrast to cyclometalated uranium(IV) derivatives of the tris(amido) framework, which were shown to readily undergo substitution with cyanide ligands, albeit from uranium-iodide precursors.[32] Similarly, reaction of **2.1-F** with Me_3SiCN led to no reaction, despite the utility of this reagent in forming other uranium-cyanide complexes through the favorable formation of Me_3SiF.[33] The inherent difficulty in installing the cyanide ligand in the **2.1-X** framework implies that it is thermodynamically unfavorable. Reaction of **2.1-Cl** with alkylsodium reagents such as $NaCH_2Ph$ and $NaCH_2SiMe_3$ at –21 °C, conditions known to be favorable for the formation of uranium-alkyl complexes, led to immediate reduction to uranium(IV), typically forming a mixture of the mono- and bis-metalacyclic products $U^{IV}(CH_2SiMe_2NSiMe_3)[N(SiMe_3)_2]_2$ and $[Na(THF)_x][U^{IV}(CH_2SiMe_2NSiMe_3)[N(SiMe_3)_2]_2]$,[34, 35] as judged by ^{1}H NMR. Attempts to react **2.1-Cl** or **2.1-Br** with 2 equiv NaCCPh in THF to form the corresponding uranium(V)-acetylide product led to no reaction.

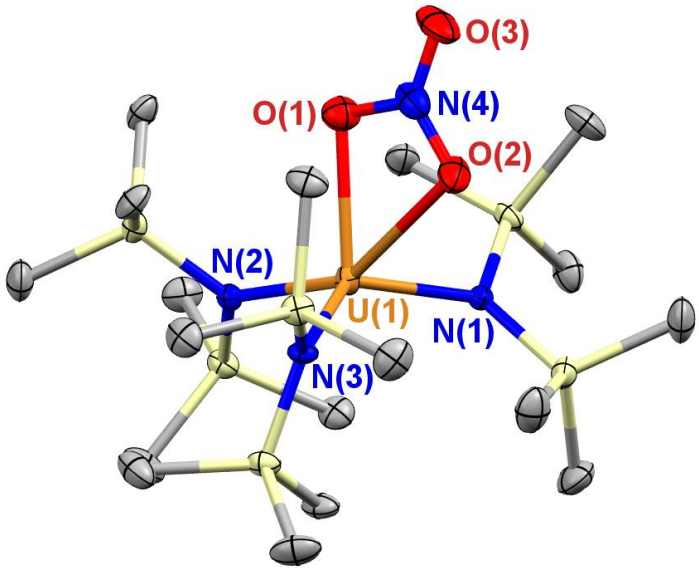

Figure 2.4.12 Thermal ellipsoid plot of $U^{IV}(\kappa^2\text{-}NO_3)[N(SiMe_3)_2]_3$ at 30% probability. Hydrogen atoms are omitted for clarity. Bond distances (Å) and angles (°): U(1)–O(1) 2.419(6), U(1)–O(2) 2.541(6), U(1)–N(1) 2.235(6), U(1)–N(2) 2.251(6), U(1)–N(3) 2.241(6), O(1)–U(1)–O(2) 51.8(2).

The successful synthesis of **2.1-Onap** suggested that more sterically encumbered ligand groups could be accessible in the **2.1-X** framework. We were particularly interested in whether uranium(IV) complex bearing a ligand in an κ^2 coordination mode could become κ^1 upon

installation of a second ligand in the *trans* position. Treatment of $U[N(SiMe_3)_2]_3$ with $AgNO_3$ led to a color change to light brown and formation of a single major product as judged by ^1H NMR spectroscopy. Crystallization of this product from hexanes at –21 °C revealed the structure to be $U^{IV}(\kappa^2\text{-}NO_3)[N(SiMe_3)_2]_3$ (Figure 2.4.12). This complex represents an unusual example of a low-coordinate, low-valent uranium-nitrate complex, as known uranium(IV)-nitrate complexes are either 10- or 12-coordinate.[36, 37] Additionally, one of the two oxygen atoms of the nitrate ligand binds 0.122 Å closer than the other, with U–O bond lengths of 2.419(6) and 2.541(6) Å. In a survey of the Cambridge Structure Database, $\kappa^2\text{-}NO_3$ complexes of uranium generally exhibit equivalent U–O bond lengths.[30] Attempts to oxidize $U^{IV}(\kappa^2\text{-}NO_3)[N(SiMe_3)_2]_3$ with a strong oxidant such as $AgPF_6$ proved fruitless, demonstrating the stabilization imparted by the chelation of the nitrate ligand.

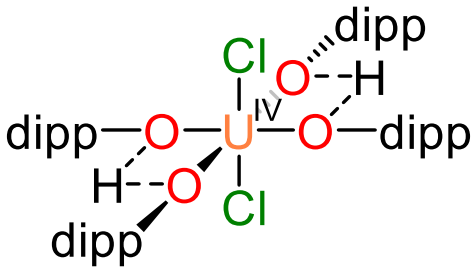

Figure 2.4.13 Connectivity of $U^{IV}(Hdipp)_2(dipp)_2Cl_2$ established by X-ray data. O-H hydrogen atoms were not located directly.

We additionally explored the reactivity of **2.1-Cl** toward protonolysis. For example, 2,6-di-*tert*-butylphenol was not reactive with **2.1-Cl** despite lengthy reaction times and heating. However, addition of 4 equiv 2,6-di-*iso*-propylphenol to an Et_2O solution of **2.1-Cl** formed $U^{IV}(Hdipp)_2(dipp)_2Cl_2$, dipp = O-2,6-^{i}Pr$_2$-C$_6H_3$, as the single observable product by ^1H NMR, isolated in 82% yield (Figure 2.4.13). We were unable to identify the corresponding oxidation product from this reaction; however, the isolation in 82% crystalline yield offers evidence against a disproportionation ($2\ U^{V} \rightarrow U^{IV} + U^{VI}$) mechanism. The room temperature ^1H NMR of $U^{IV}(Hdipp)_2(dipp)_2Cl_2$ shows the expected five resonances for a C_4 symmetric solution structure and an integration corresponding to two alcohol protons. The observed symmetry suggests that the O–H hydrogen atoms are not localized to individual aryloxide ligands at room temperature.

Variable temperature magnetic data collected on $U^{IV}(Hdipp)_2(dipp)_2Cl_2$ showed a χT product of 0.04 emu K mol^{-1} at 2 K (Figure 2.4.15). The field dependent moment collected for $U^{IV}(Hdipp)_2(dipp)_2Cl_2$ at 2 K does not saturate and achieves a value of 0.16 μ_B at 7 T (Figure 2.4.16). The small χT and *M(H)* values observed at the respective experimental limits of temperature and field are consistent with data reported for complexes with singlet ground states arising from a $5f^2$ configuration with a small amount of paramagnetic impurities.[38-40] The χT data for $U^{IV}(Hdipp)_2(dipp)_2Cl_2$ increase monotonically with temperature and achieve a room temperature χT product of 0.30 emu K mol^{-1}. The increase of χT with temperature for $U^{IV}(Hdipp)_2(dipp)_2Cl_2$ and the low room temperature χT value indicate the ground state is well isolated and that the complex shows a large temperature independent paramagnetism (TIP), from field-induced mixing of paramagnetic excited states (Figure S4).[41, 42]

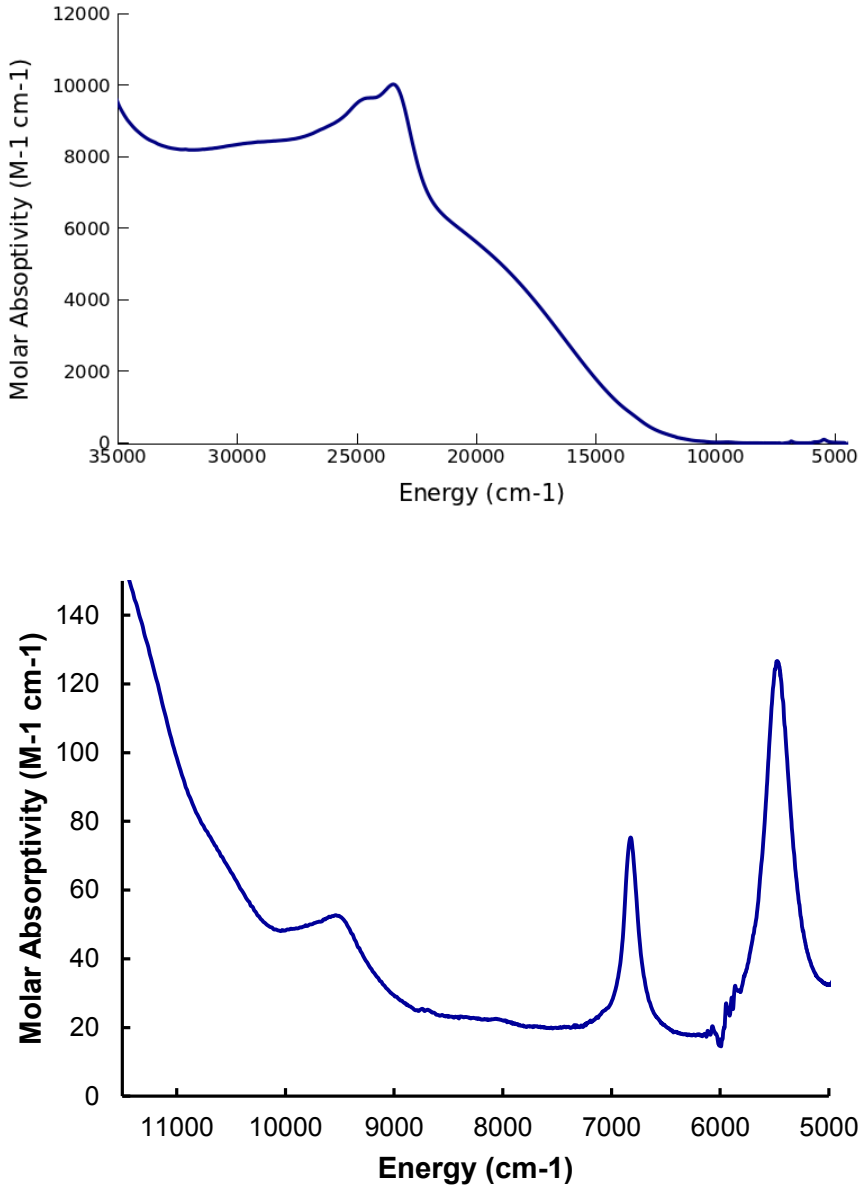

Figure 2.4.14 UV-Vis-NIR spectrum of $U^{IV}(Hdipp)_2(dipp)_2Cl_2$ showing the primary absorption features (top) and an expansion of the f-f absorption features (bottom).

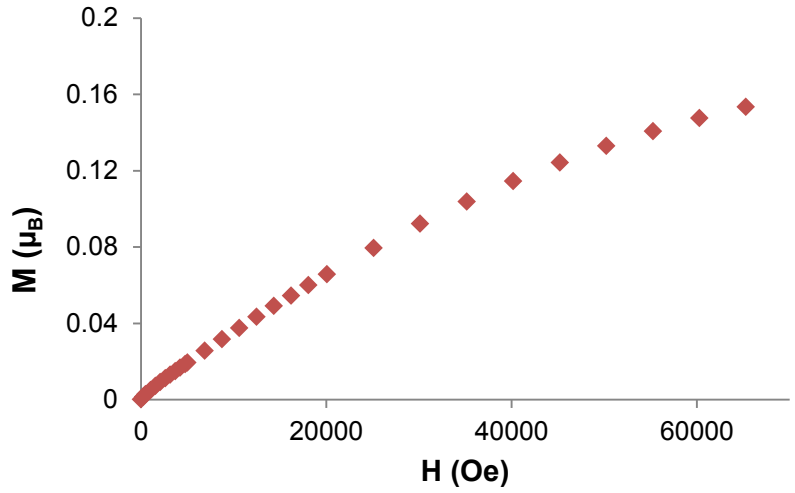

Figure 2.4.15 Field dependent magnetic data for $U^{IV}(Hdipp)_2(dipp)_2Cl_2$ collected at T = 2 K.

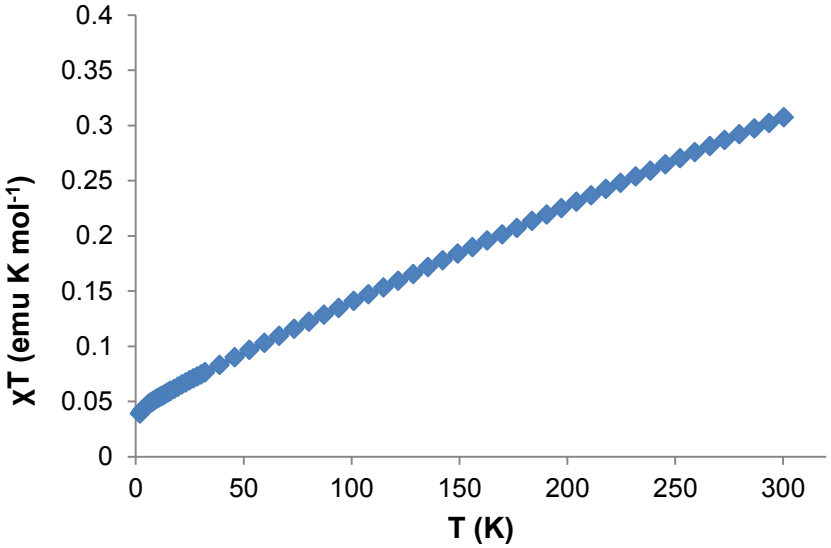

Figure 2.4.16. Temperature dependent magnetic data for $U^{IV}(Hdipp)_2(dipp)_2Cl_2$ collected at H = 2 T.

2.5 Characterization

2.5.1 X-Ray Structural Analysis. The X-ray structures of the **2-X** complexes all revealed trigonal bipyramidal uranium ions in a sterically congested framework. Mixed occupancy of the chloride and fluoride ligands in **2.1-FCl** precluded precise determination of the U–X, X = Cl^-, F^- bond distances because of overlap in the observed electron density. However, acceptable

refinement of **2.1-FCl** was obtained from refining the site occupancies of the chloride and fluoride anions. The average $U–N_{amide}$ bond lengths vary slightly depending on the axial ligand in the order $ONap^- > F^- > N_3^- \sim Cl^- \sim Br^- > NCS^-$ (Table 2.5.1.1).

Table 2.5.1.1 Average U–X and U–N(amide) bond distances (Å) in the **2.1-X** complexes.

	2.1-ONap	**2.1-F**	**2.1-Cl**	**2.1-Br**	**2.1-FCl**	**2.1-N_3**[a]	**2.1-NCS**
U–X	2.102(4)	2.066(2)	2.5753(5)	2.7446(6)	–[b]	2.226(3)	2.316(9)
U–N	2.222(7)	2.189(2)	2.166(2)	2.164(4)	2.176(2)	2.167(2)	2.154(8)

[a] Reported distances.[29] [b] Mixed occupancy of Cl^- and F^-.

The X-ray crystal structure of **2.1-Onap** displays an unusual structural distortion relative to the roughly D_3 symmetric arrangement in the other **2.1-X** complexes. The Si–N–Si plane of one of the $N(SiMe_3)_2^-$ ligands is forced into the equatorial plane of the complex to accommodate the naphthyl rings, resulting in a difference of only 17.9° rather than the more typical ~45°. Additionally, the two naphthoxide ligands are bound in the same orientation on both faces of the complex, with an 18.6° angle between the planes of the naphthyl rings. Despite the apparent steric crowding, the ^1H NMR exhibits a single peak for the $–SiMe_3$ groups at room temperature.

In addition to the uranium(V) complexes, the crystal structures of the uranium(IV) derivatives were collected as a point of reference (Figures 2.5.1.1–2.5.1.3). The syntheses of $U^{IV}F[N(SiMe_3)_2]_3$ and $U^{IV}Cl[N(SiMe_3)_2]_3$ were carried out through the reported procedures,[27, 43] and $U^{IV}I[N(SiMe_3)_2]_3$ was prepared as described in Section 2.6. Single crystals of each of these complexes were obtained from saturated solutions stored at –21 °C. Progressing from the smallest ligand, fluoride, to the much larger iodide, a significant structural distortion of the plane formed by the three nitrogen atoms of the $N(SiMe_3)_2^-$ ligands from the uranium ion was observed, due to steric repulsion of the halide ion. On this basis, it is possible that oxidation of $U^{IV}I[N(SiMe_3)_2]_3$ to form uranium(V)-dihalide products did not occur due to sterics rather than just due to the poor electron donation from the iodide ligand.

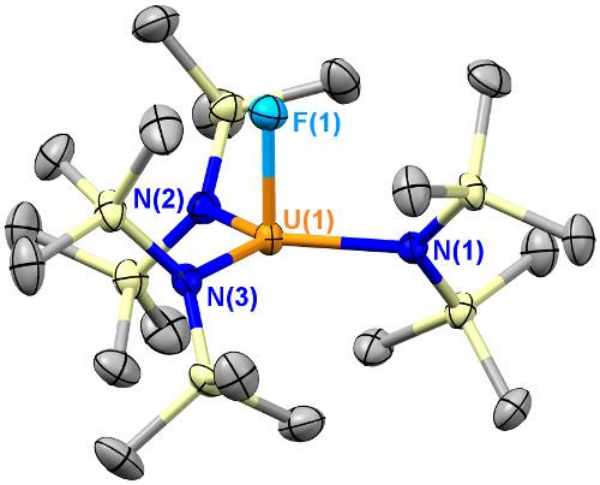

Figure 2.5.1.1 Thermal ellipsoid plot of $U^{IV}F[N(SiMe_3)_2]_3$ at 30% probability. Hydrogen atoms are omitted for clarity. Bond lengths (Å) and angles (°): U(1)–F(1) 2.0649(12), U(1)–N(1) 2.2498(16), U(1)–N(2), 2.2533(16), U(1)–N(3), 2.2530(15), N(1)–U(1)–F(1) 91.88(5), N(2)–U(1)–F(1) 93.70(6), N(3)–U(1)–F(1) 93.26(5).

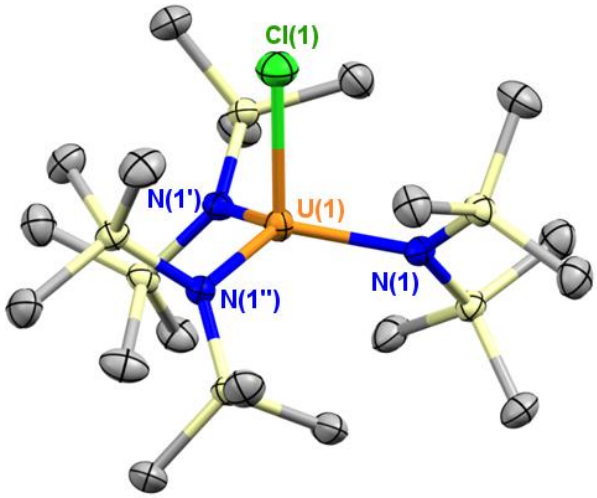

Figure 2.5.1.2 Thermal ellipsoid plot of $U^{IV}F[N(SiMe_3)_2]_3$ at 30% probability. Hydrogen atoms are omitted for clarity. Bond lengths (Å) and angles (°): U(1)-N(1) 2.233(2), U(1)-Cl(1) 2.592(1) N(1)-U(1)-Cl(1) 116.87(3).

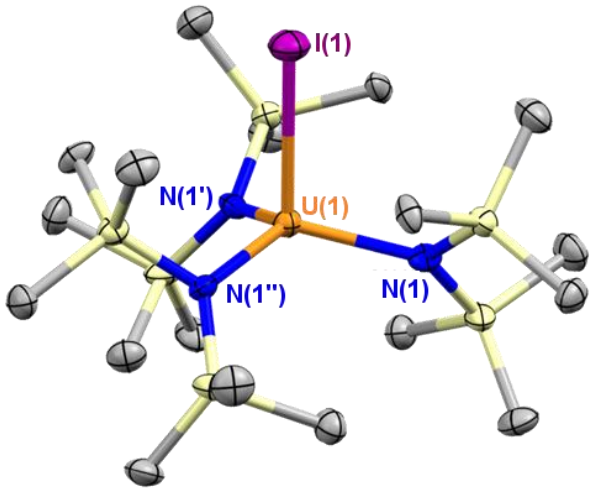

Figure 2.5.1.3 Thermal ellipsoid plot of $U^{IV}F[N(SiMe_3)_2]_3$ at 30% probability. Hydrogen atoms are omitted for clarity. Bond lengths (Å) and angles (°): U(1)-I(1) 2.9630(14), U(1)-N(1) 2.225(8), N(1)-U(1)-I(1) 115.91(13).

2.5.2 VT ^{1}H NMR Spectroscopy. We carried out VT ^{1}H NMR measurements on the halide derivatives of the **2.1-X** complexes to determine the barrier to rotation (Figure 2.5.2.1). Interestingly, the silylamide rotational barriers were found to scale directly with the ionic radii of their respective halides (Figure 2.5.2.2), by a factor of 6.96 kcal mol^{-1} $Å^{-1}$. An intercept of intercept of 0.04 kcal/mol was obtained, close to the ideal value of zero. We similarly determined the coalescence temperature and corresponding barrier to rotation in **2.1-N_3**. Using the empirical relation between established between the barrier to rotation and ionic radius in the dihalide congeners, we calculated an effective ionic radius for the azide ion of 1.58 Å, precisely the value obtained through analysis of the structure of KN_3,[44] further supporting the validity of this analysis. The complexes that display a single peak at room temperature have approximately the same shift (~–1.6ppm), so this empirical trend is useful for characterizing the ^{1}H-NMR spectra of related complexes.

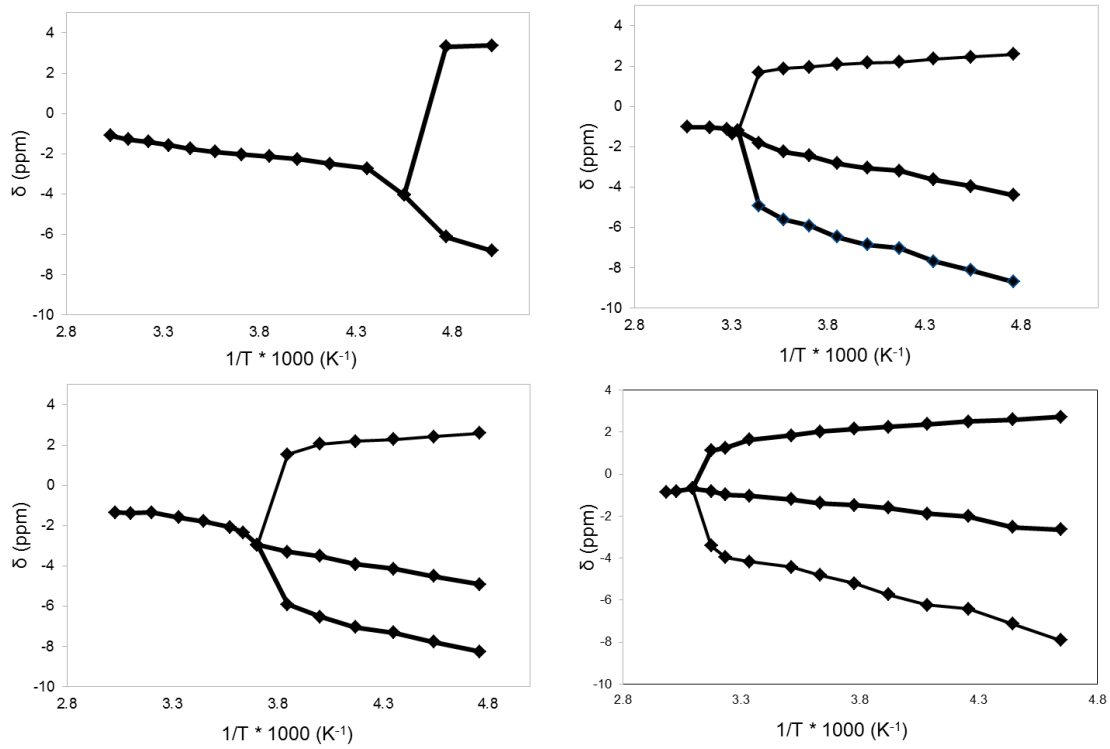

Figure 2.5.2.1 VT NMR data for **2.1-F** (top left), **2.1-Cl** (top right), **2.1-N_3** (bottom left) and **2.1-Br** (bottom right).

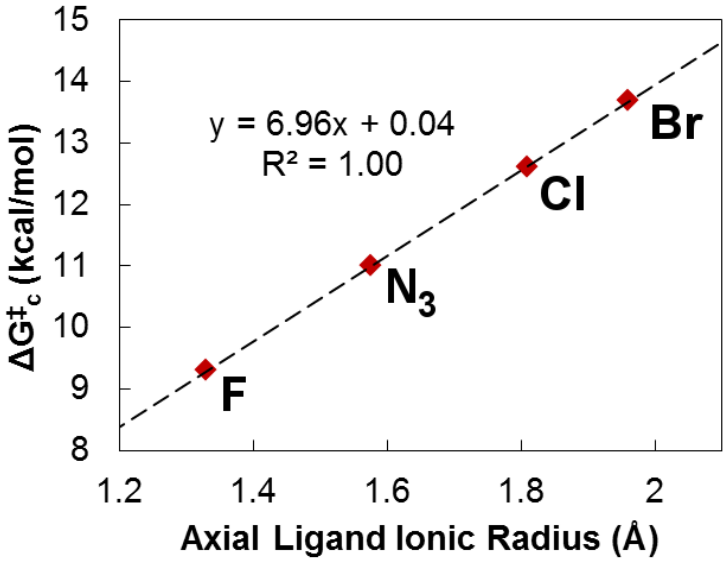

Figure 2.5.2.2 Correlation between axial ligand ionic radius and barrier to rotation of the –$SiMe_3$ groups in the **2.1-X** complexes.

2.5.3 Near-IR Spectroscopy. The **2.1-X** complexes showed absorption bands in the near-IR that are characteristic of interconfigurational 5f-5f transitions.[11, 45] Four bands are

expected for a pentavalent uranium complex in a D_3 geometry when spin-orbit coupling is much larger than the ligand field splitting energy (Figure 2.5.3.1).[45] As the spin-orbit coupling term is typically larger than the ligand field splitting, two sets of Stark levels comprising the $m_J = \pm 5/2$ (lower energy) and $m_J = \pm 7/2$ states are separated by ~7000 cm^{-1} ($\Delta E_{SOC} = 7/2\ \xi$; ξ ~2000 cm^{-1}). Given that the local symmetry at the uranium ion is maintained in the various complexes and that the spin orbit coupling parameter ξ is known to be essentially independent of the ligand set other uranium(V) complexes, the energy of the observed transitions can be used as a relative metric for the ligand field splitting parameters between the different complexes.

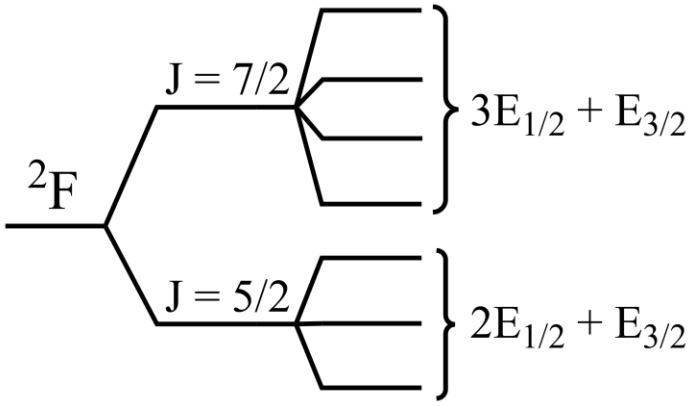

Figure 2.5.3.1 Splitting of the ^{2}F term due to spin-orbit coupling and crystal field splitting using a D_3' double group treatment (not to scale). Four absorption bands are expected in the NIR region of the spectrum based on transitions from the lowest Stark level of the J = 5/2 manifold to the four Stark levels of the J = 7/2 manifold.

The **2.1-X** complexes all displayed four primary absorption bands of varying intensity in the NIR spectra between 7000–14000 cm^{-1} (Figure 2.5.3.2). Some spectral broadening and shoulder peaks are noted in some of the peaks. The energy difference between the shoulder features and the primary absorptions in each case matches well with the expected axial uranium-ligand stretching frequency, confirmed through DFT calculations (vide infra). These features therefore are assigned as vibronic transitions along the primary axis. Vibronic transitions are common to octahedral uranium(V) complexes, where f-f transition intensity is much lower.[8, 46, 47] Since the axial metal-ligand vibrations are strongly associated with the highest energy f-f transition, these bands are assigned as transitions into the $5f_{z3}$ σ^* orbital. Notably, significant

vibronic intensity is observed in a lower energy band in **2.1-NCS**. This is attributed to greater mixing of the f-orbitals in **2.1-NCS**, indicating that the thiocyanate ligand does not impart a strong primary axis.

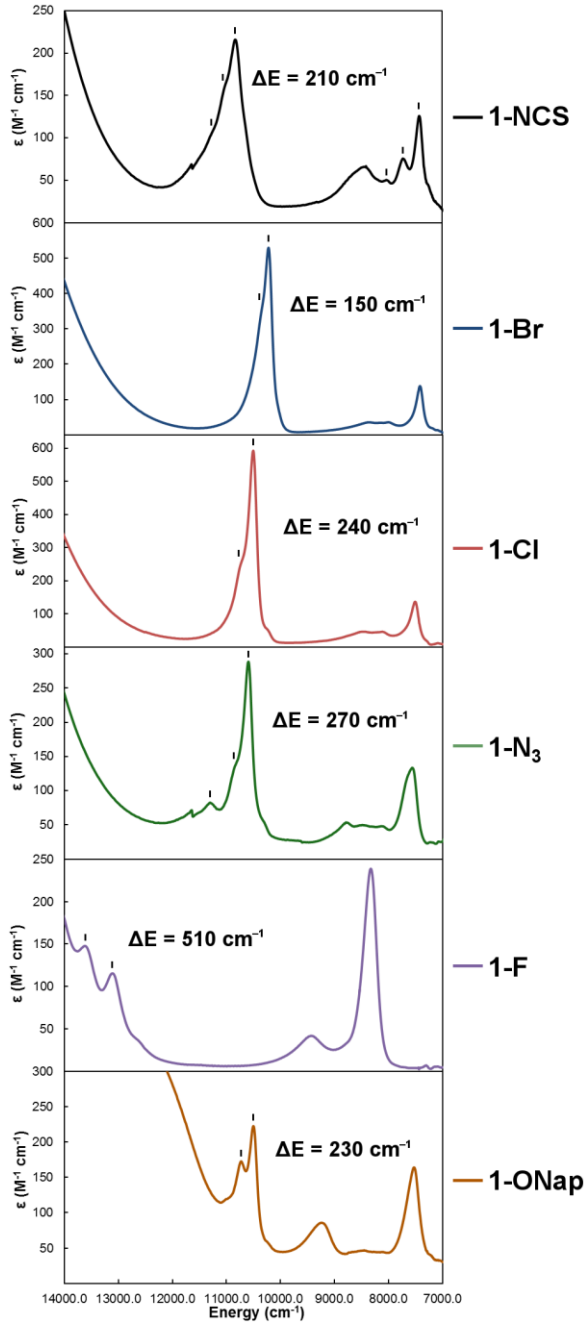

Figure 2.5.3.2 Near IR spectra of the **2.1-X** complexes in toluene.

2.5.4 EPR Spectroscopy. The EPR spectra of the **2.1-X** complexes were collected at 5 K with an X-band EPR spectrometer (Figures 2.5.4.1-2.5.4.6). All of the spectra exhibited a sharp signal centered at g ~ 2.2 and an extremely broad feature centered at g ~ 0.7. Similar spectra were reported by Hayton and coworkers for the compounds $U^{V}O[N(SiMe_3)_2]_3$ and $[Ph_3PCH_3][U^{V}O(CH_2SiMe_2NSiMe_3)[N(SiMe_3)_2]_2]$.[48, 49] In contrast, the EPR spectra of **2.1-N_3** and **2.1-NCS** exhibited extensive hyperfine coupling. In the case of **2.1-N_3**, assuming that the hyperfine coupling terms are equivalent between the chemically equivalent nitrogen atoms of the two azide ligands, and that each of the three nitrogen atoms exhibits a different coupling constant, a pentet of pentet of pentets would be expected, totaling 125 peaks. In spite of the apparent extensive coupling, calculation of the α-spin density from the DFT optimized structure of **2.1-N_3** did not show significant delocalization of the unpaired electron.

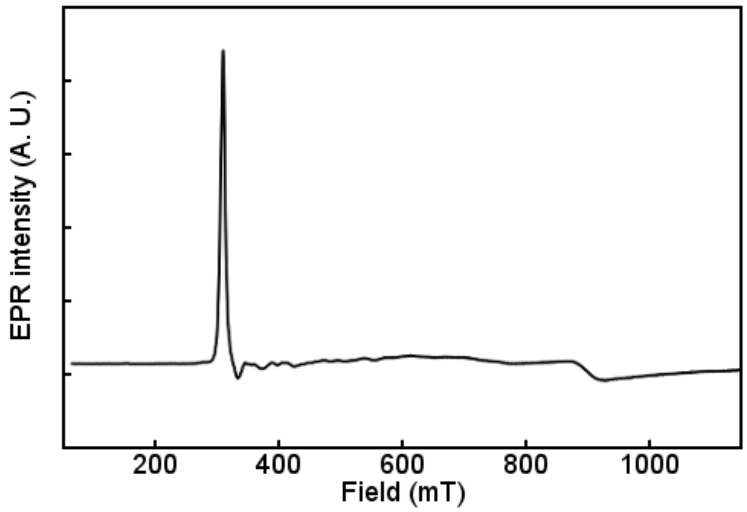

Figure 2.5.4.1 EPR spectrum of **2.1-Cl.**

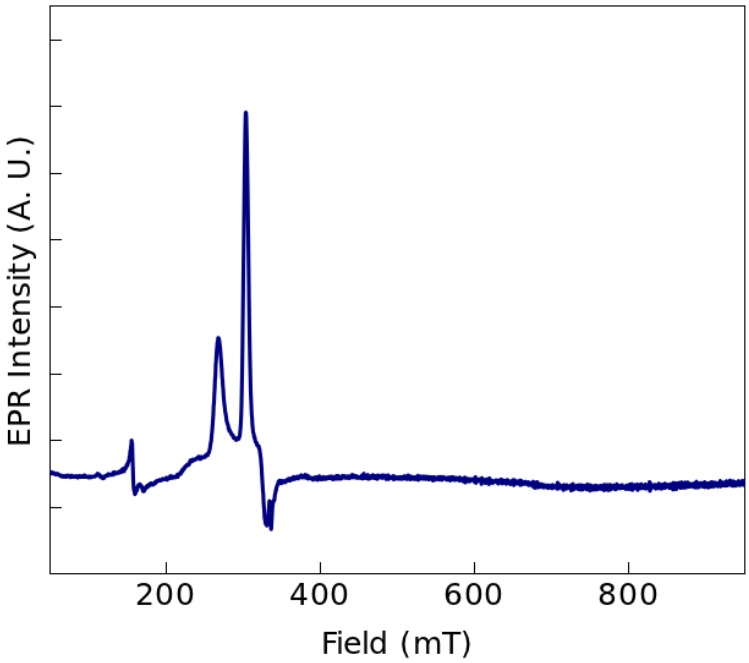

Figure 2.5.4.2 EPR spectrum of **2.1-F**.

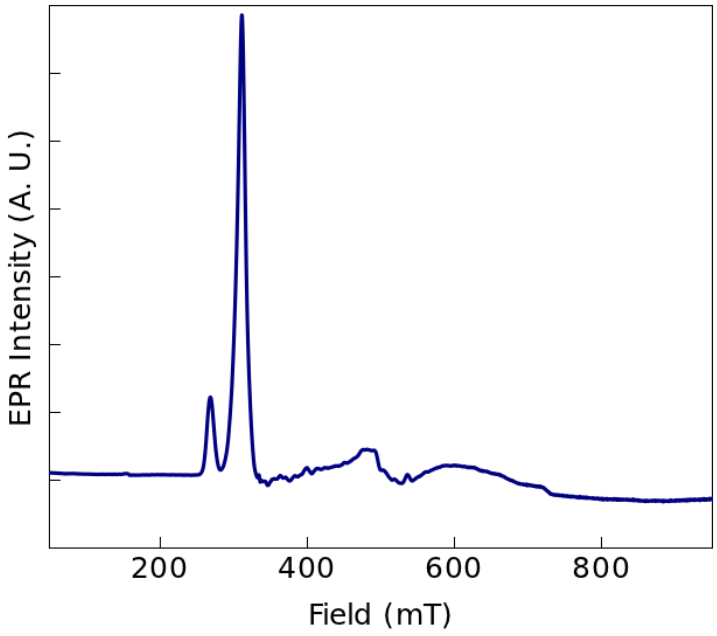

Figure 2.5.4.3 EPR spectrum of **2.1-Br**.

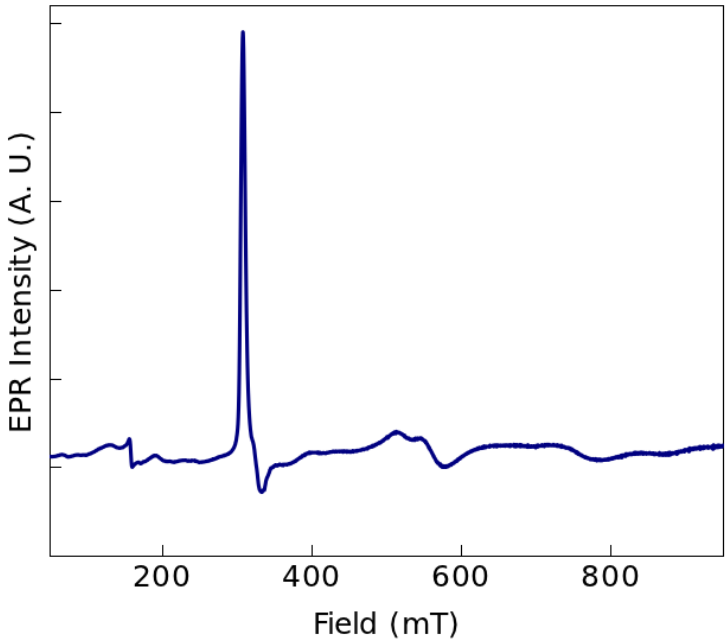

Figure 2.5.4.4 EPR spectrum of **2.1-FCl**.

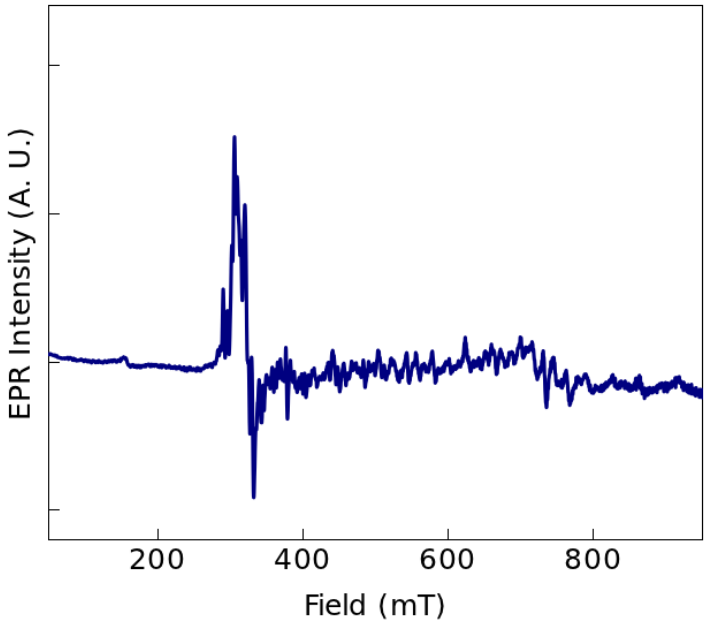

Figure 2.5.4.5 EPR spectrum of **2.1-N_3**.

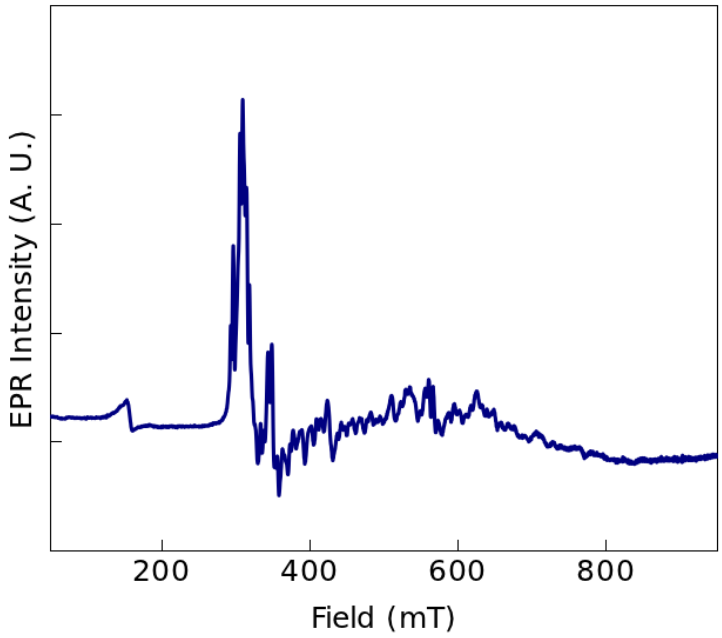

Figure 2.5.4.6 EPR spectrum of **2.1-NCS**.

2.5.5 Magnetism Data. The variable temperature magnetic response of **2.1-Cl**, **2.1-F**, and **2.1-NCS** each showed a small room temperature magnetic moment of ~1.5 μ_B, consistent with reported moments for uranium(V) complexes and a well-isolated orbital doublet ground state with TIP (Figures 2.5.5.1-2.5.5.3).[49-51] The variable field magnetic response measurement each reached a low value of ~0.4 μ_B. The nearly identical nature of the data suggested that the axial ligand had little effect on the magnetic behavior of the **2.1-X** complexes investigated.

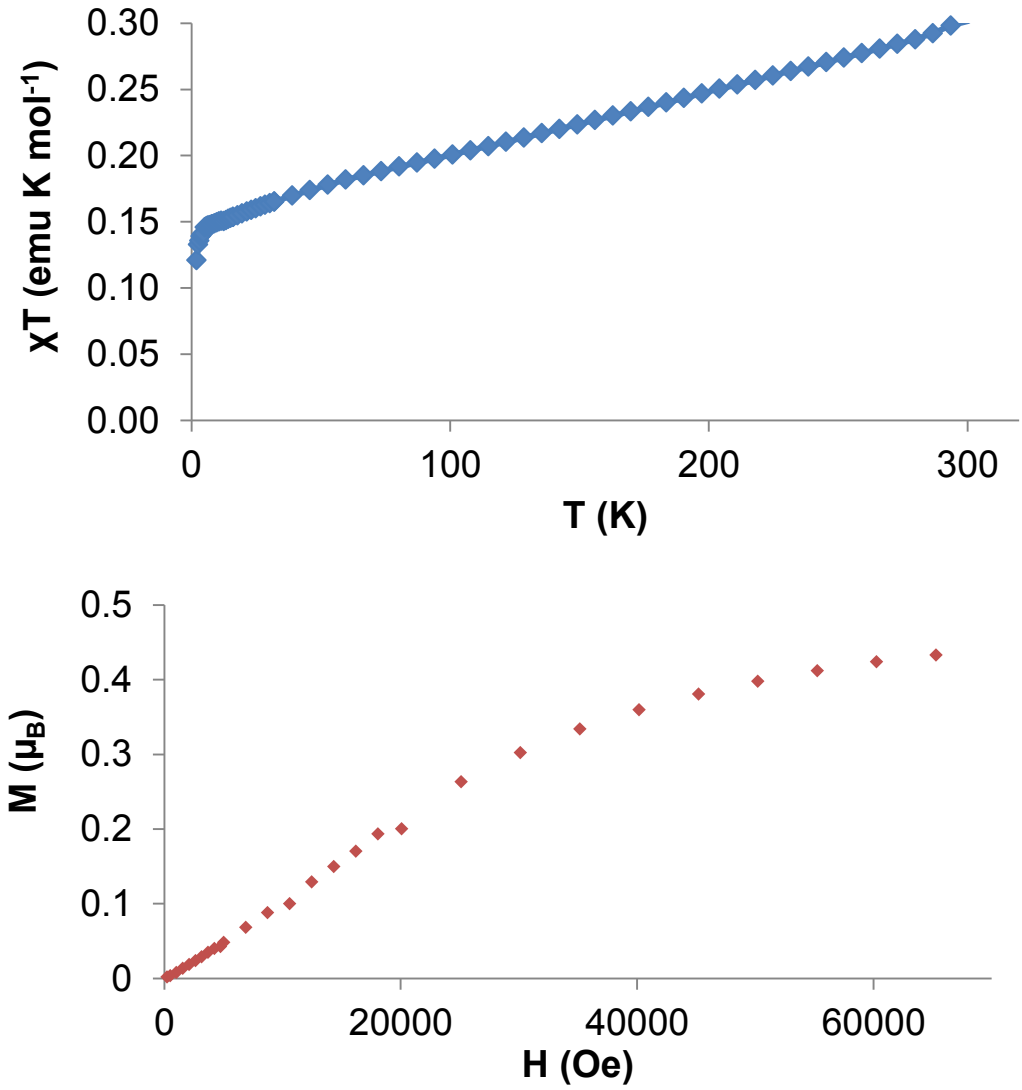

Figure 2.5.5.1 Temperature dependence at an applied field of 2 T (top) and field dependence at 2K (bottom) of the magnetic susceptibility of **2.1-Cl**.

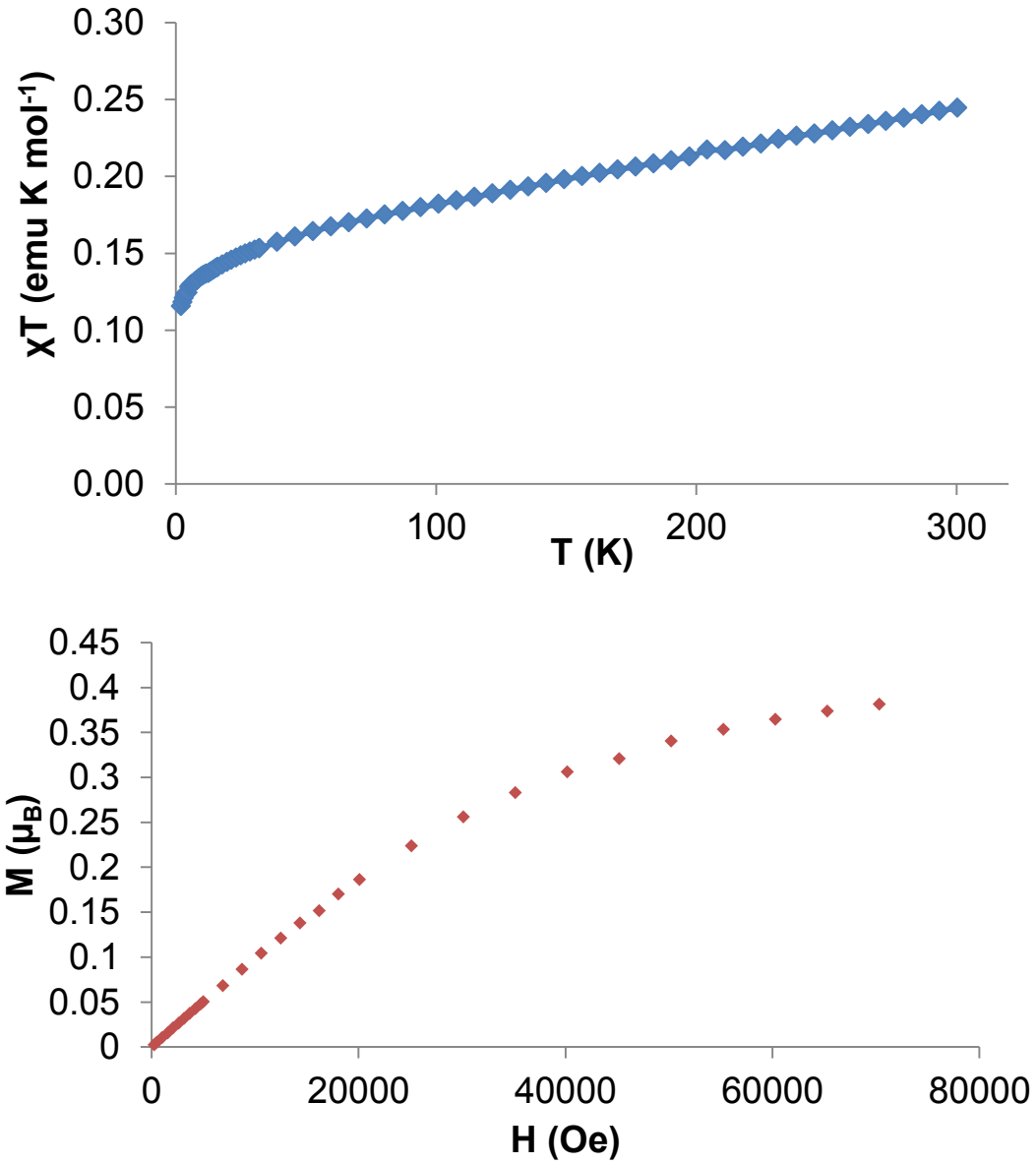

Figure 2.5.5.2 Temperature dependence at an applied field of 2 T (top) and field dependence at 2K (bottom) of the magnetic susceptibility of **2.1-F**.

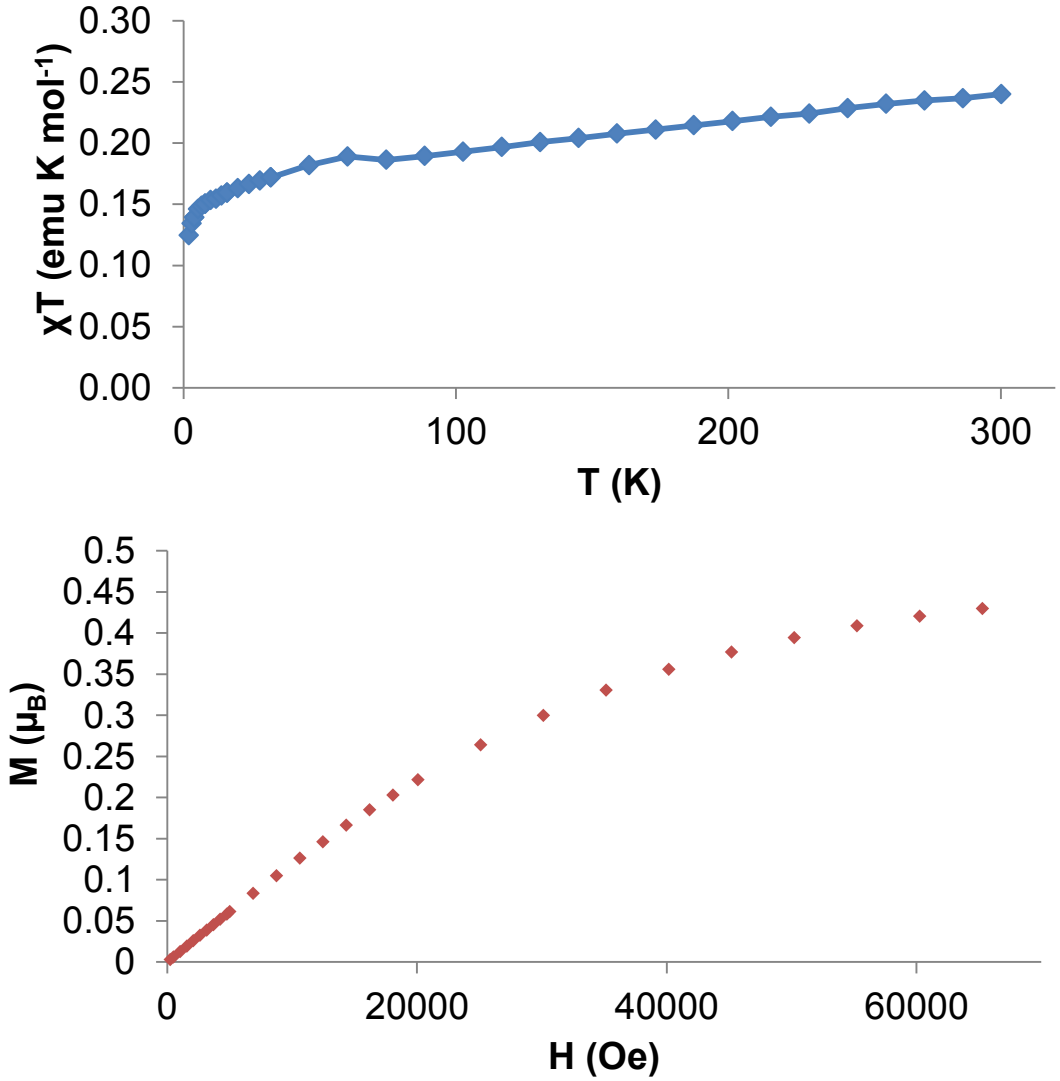

Figure 2.5.5.3 Temperature dependence at an applied field of 2 T (top) and field dependence at 2K (bottom) of the magnetic susceptibility of **2.1-NCS**.

2.5.6 Electrochemical Data. Electrochemical measurements were carried out on CH_2Cl_2 solutions of the **2.1-X** complexes in an effort to assess their stability (Table 2.5.7.1). Among the **2.1-X** complexes, reversible waves were observed in the cyclic voltammograms at $E_{1/2}$ ~ +0.9 V versus a ferrocene/ferrocenium internal standard. These waves are assigned to a U^{VI}/U^{V} redox process. The reduction feature of the U^{VI}/U^{V} wave became more reversible at faster scan rates, indicating that the U^{VI} product is unstable under the conditions of the experiment. The electrochemical accessibility of the U(VI/V) couple did not vary significantly between the dihalide

complexes, but the potential was ~100 mV greater in the pseudohalide complexes and ~150 mV lower in **2.1-ONap**. A second reversible feature was observed for each complex, assigned as a U^{V}/U^{IV} redox process, as the rest potential was measured between the two redox couples. The potential of this process was more sensitive to the identity of the axial ligand (Table 2.5.7.1). The potential was smallest for the difluoride complex **2.1-F** and largest for the dithiocyanate complex **2.1-NCS**. These data suggest that the donor strength of the axial ligand increases in the order $NCS^{-} < N_3^{-} < Br^{-} < Cl^{-} < F^{-} < Onap^{-}$.

2.5.7 Electronic Structure. Electronic structure calculations were performed on the optimized geometry of **2.1-Cl** using Gaussian '09 at the B3LYP hybrid DFT level of theory. Comparison of the calculated vibrational spectrum with that obtained experimentally showed excellent agreement (Figure 2.5.7.1).

Analysis of the molecular orbitals involved in bonding in **2.1-Cl** provided insight into the influence of the axial ligand on the electronic structure (Figure 2.5.7.2).[52] The singly occupied, highest energy filled orbital was determined to be ~41% uranium 5f-character, with ~10% chloride non-bonding p-character and ~43% amide non-bonding p-character. Significant uranium 5f-orbital character was identified in metal-ligand bonding. Partial mixing of the semi-core uranium $6p_z$ orbital (4.16 %) with the $5f_z3$ orbital (15.66 %) was noted in the σ-bonding HOMO-17. The LUMO through LUMO+5 were all of approximately 80–90% uranium 5f-character, with the remaining contribution involved in metal-ligand σ* and π* interactions. Minimal π-bonding was observed between the uranium(V) ion and the chloride ligands, with a calculated Mayer bond order[53] of 1.07 for each uranium–chloride bond. Extensive π-bonding was noted with the equatorial amide ligands, with a calculated Mayer bond order of 1.51 for each amide ligand. NBO analysis on **2.1-Cl** showed a charge of +1.38 on uranium, much lower than the formal oxidation state. A small ratio of NBO charge to oxidation state suggests significant covalent bonding.[54] The sum of these characterization studies indicates complex **2.1-Cl** shows particularly covalent bonding, and remarkable chemical stability.

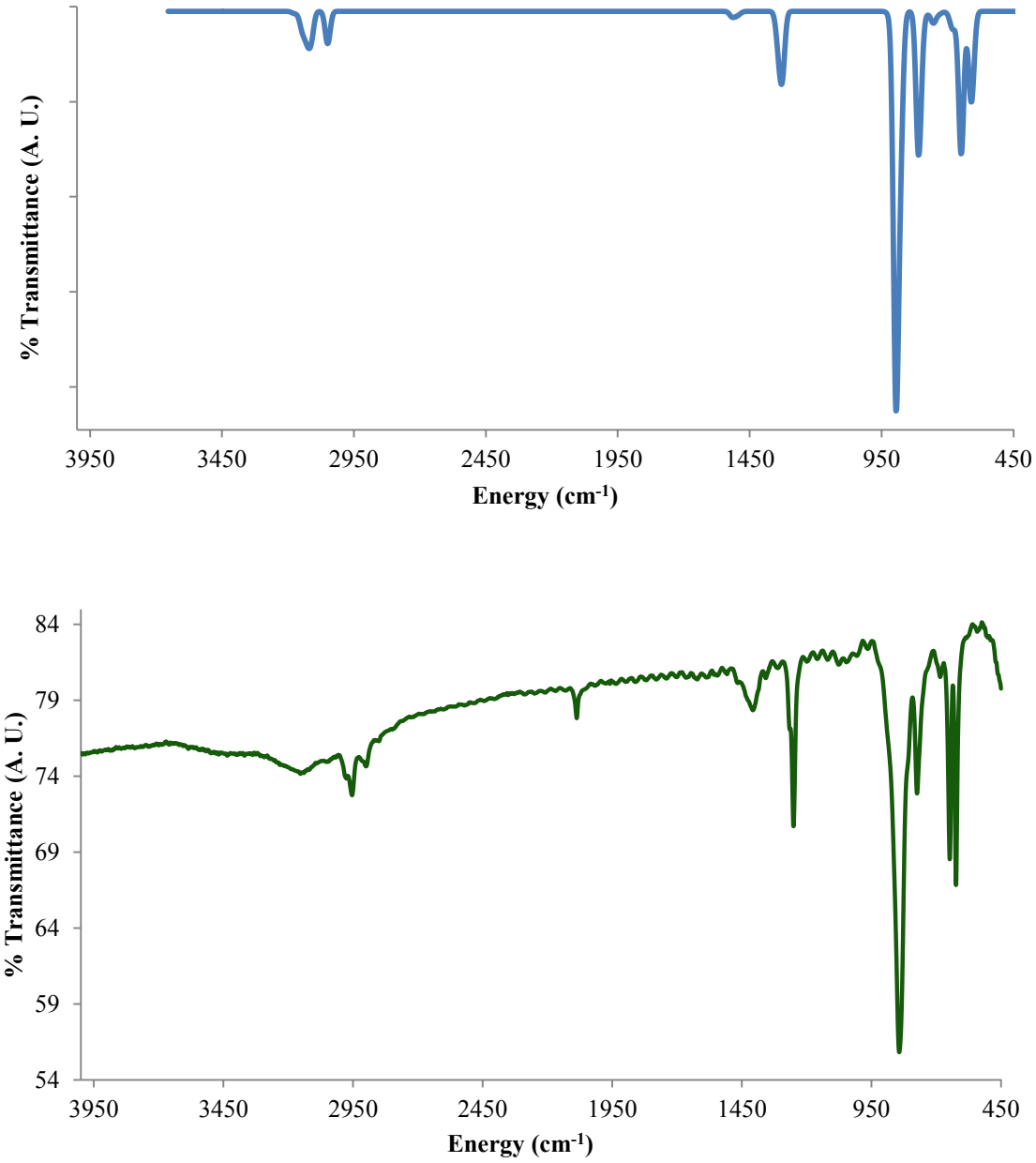

Figure 2.5.7.1 Calculated (top) and experimental (bottom) IR spectrum of **2.1-Cl**. Line broadening was applied to the calculated vibrational lines to better simulate the experimental spectrum.

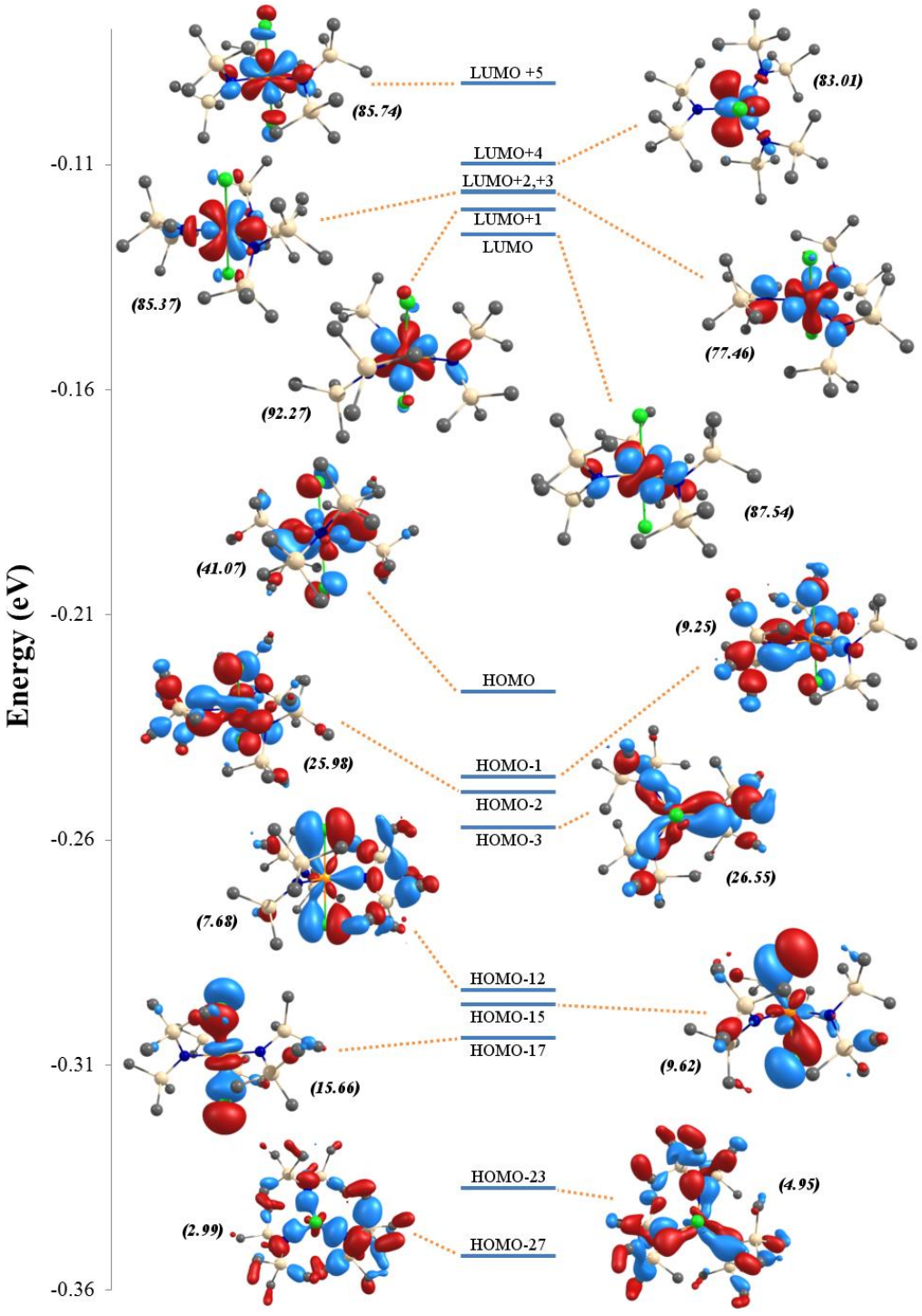

Figure 2.5.7.2 MO diagram of **2.1-Cl** depicting orbitals of significant uranium 5f character. Percent uranium 5f AO character for each MO is given in italics.

Table 2.5.7.1 Calculated and experimental bond metrics and electrochemical data for the **2.1-X** complexes.

	U–X Bond Length		U–N Bond Length		U-N	q_U	$E_{1/2}$	
	Exp.	Calc.	Exp.	Calc.	MBO	(NBO)	$U^{VI/V}$	$U^{V/IV}$
2.1-CN	–	2.488	–	2.168	1.589	1.31	–	–
2.1-NCS	2.316(9)	2.295	2.154(8)	2.191	1.554	1.56	1.01	–0.24
2.1-N_3	2.226(3)	2.229	2.167(3)	2.212	1.503	1.41	1.00	–0.41
2.1-Br	2.745(1)	2.773	2.164(4)	2.189	1.513	0.87	0.89	–0.37
2.1-Cl	2.575(1)	2.627	2.166(1)	2.192	1.459	1.00	0.91	–0.40
2.1-F	2.066(2)	2.067	2.189(2)	2.220	1.402	1.80	0.90	–0.63
2.1-ONap	2.102(4)	2.111	2.222(5)	2.262	1.379	1.74	0.76	–0.56

The observation of features of the inverse *trans* influence in the electronic structure of **2.1-Cl** led us to extend this analysis to the other **2.1-X** derivatives to determine the relative effect of the various axial ligands. DFT calculations on all of the **2.1-X** complexes gave good agreement with the experimental bond metrics (Table 2.5.7.1). The naphthyl groups in the **2.1-ONap** complex were truncated to phenyl groups for the sake of computational simplicity, yet the near co-planarity of the aryl rings and slight distortion of the U–O–C bonds from linearity was still reproduced. At the extremes the calculated equatorial U–N bond lengths followed the trend established by the X-ray crystal structures, where the U–N bond lengths of **2.1-ONap** differ experimentally ~ 0.068 Å and computationally by ~ 0.071 Å. Minor variations in the bond lengths among the intermediate complexes are too close to reliably differentiate.

A more significant trend was observed in the Mayer bond order of the equatorial U–N bonds, which vary following the order established from the potential of the $U^{V/IV}$ couple, indicating that as the U–N bond order increases the 5+ oxidation state becomes less stable relative to the 4+ state. This result is counterintuitive from a standard bonding perspective, as a larger MBO for an identical ligand in two complexes is expected to increase the electron density at the metal center, which should lead to a decrease in the reduction potential rather than the observed increase. The axial ligand therefore plays a significant role not only in stabilizing the high oxidation state, but in modulating the equatorial metal-ligand bonding, consistent with the cis-destabilization that arises from the inverse *trans* influence.

Extrapolating the observed trend to the hypothetical **2.1-CN** complex gave an indication of why we were not able to prepare this complex, as the equatorial bonding analysis showed that the U–N MBO was even higher than that of **2.1-NCS**, suggesting that the cyanide ligand is poor at stabilizing the 5+ oxidation state in this system.

Analysis of the molecular orbitals involved in bonding in the other **2.1-X** complexes yielded a similar valence structure. For example, in the MO diagram of **2.1-F** (Figure 2.5.7.3), destabilization of the F–U–F σ* interaction in the LUMO+5 was observed, signifying a stabilization of the axial σ-bonding relative to the other bonding MOs. Comparison of the LUMO through LUMO+5 of the **2.1-X** halide and pseudohalide complexes showed that progressing to the weaker axial donors led to a general stabilization of the σ* and π* orbitals, and finally substantial mixing of multiple f-orbitals in **2.1-NCS** (Figure 2.5.7.4). The poor ligand NCS^{-} did not impose a strong primary axis along the X–U–X vector, leading to mixing of the anti-bonding MOs. A notable exception to this trend was the complex **2.1-Cl**, where the LUMO+5 of primarily $5f_z3$ character was destabilized almost to the same extent as that of **2.1-F**; however, the relative energies of the π* MOs, the LUMO+3 and LUMO+4 in **2.1-F** and the LUMO+2 and LUMO+3 in **2.1-Cl**, showed that the fluoride ligand is a stronger π-donor. The ability for fluoride to act as a π-donor to high valent uranium has been investigated previously.[55]

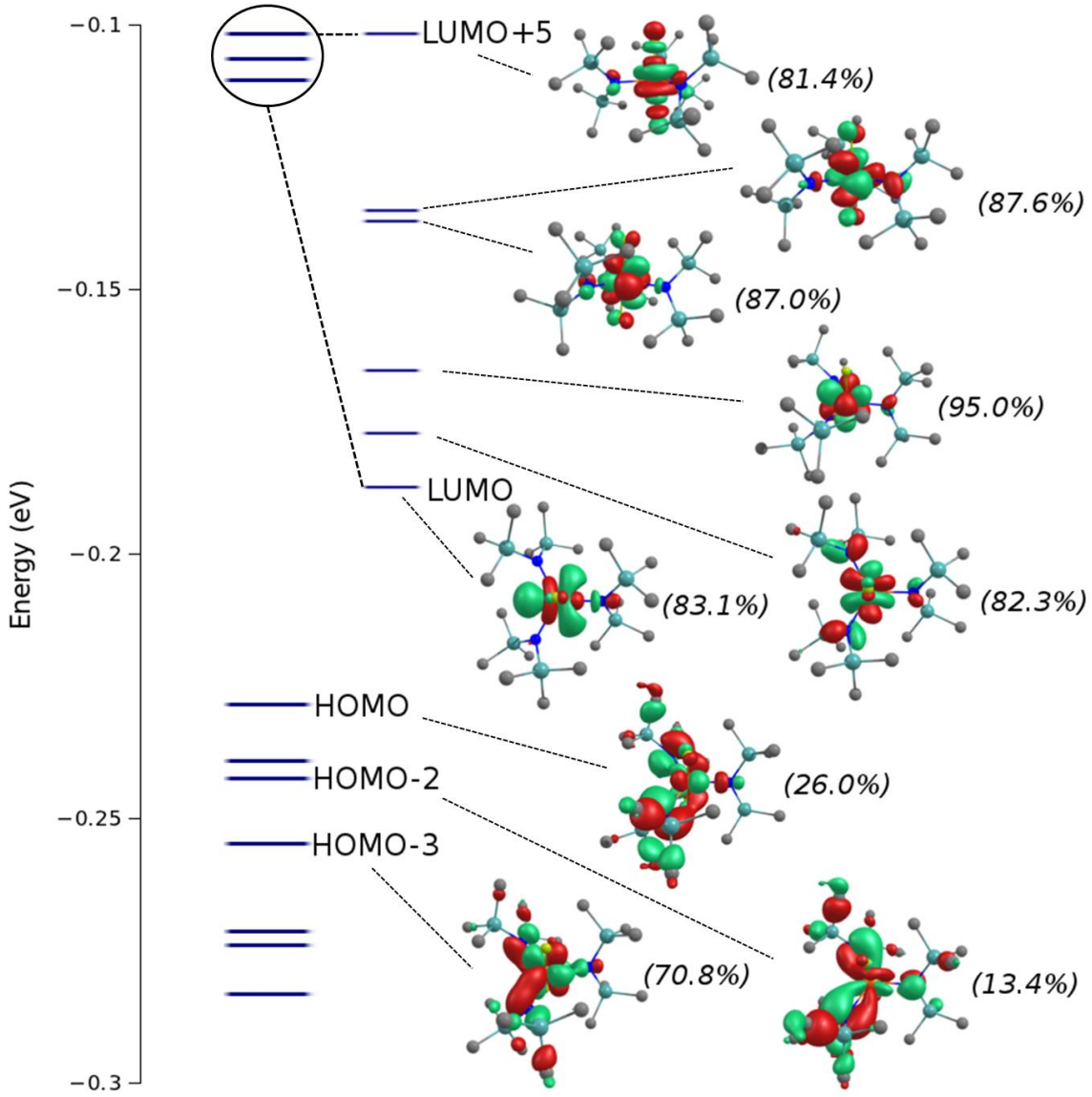

Figure 2.5.7.3 MO diagram of **2.1-F** depicting orbitals of significant uranium 5f character. Percent uranium 5f AO character for each MO is given in italics.

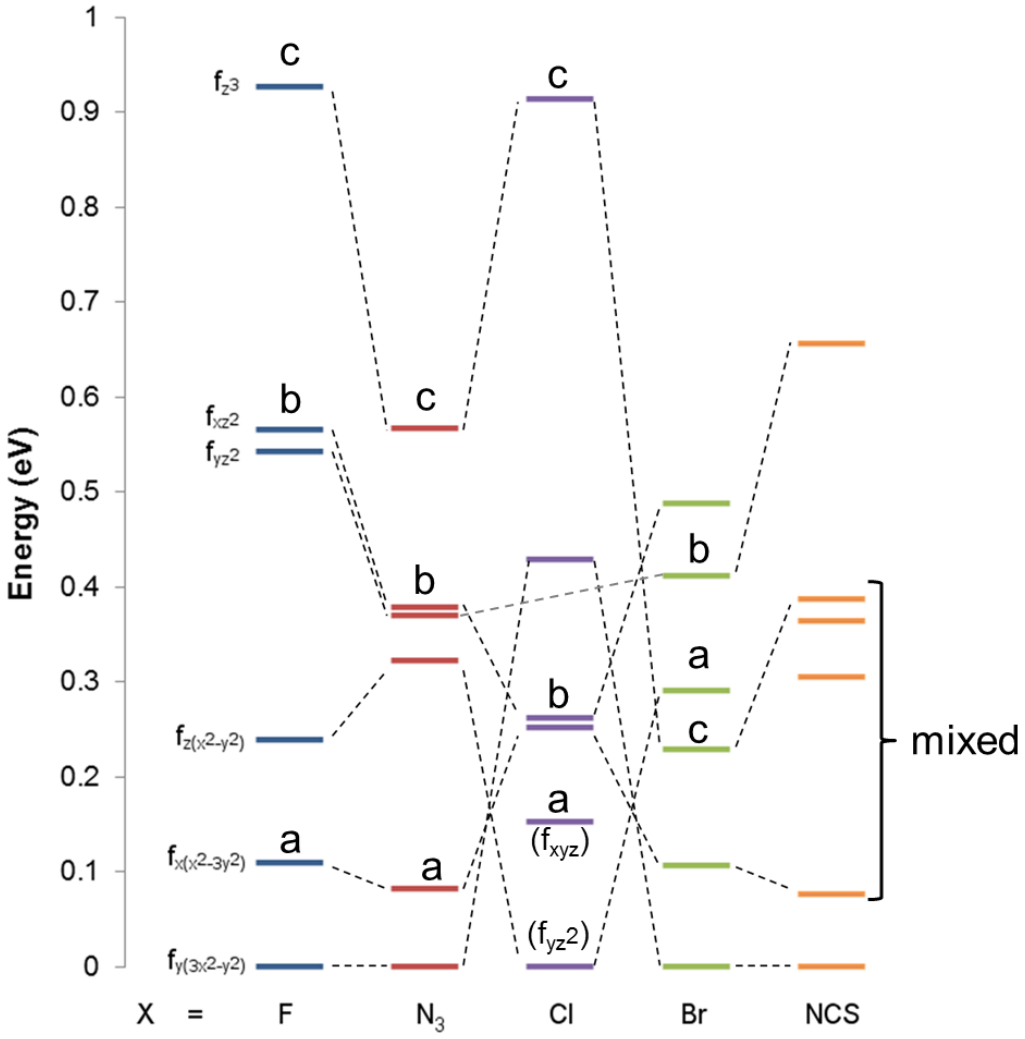

Figure 2.5.7.4 Correlation MO diagram of the **2.1-X** complexes illustrating the relative energy of molecular orbitals of primarily uranium 5f character, corresponding to the LUMO through LUMO+6. All energies are given relative to the non-bonding LUMO, which is of primarily $5f_{y(3x2-y2)}$ character in each complex except for **2.1-Cl**, in which the LUMO is predominately $5f_{yz}2$ in character. a = $U–N_{eq}$ π*, b = U–X π*, c = U–X σ*.

A better understanding of the effect of the axial ligand in the **2.1-X** complexes can be gleaned from the density of states (DOS) plots of the valence structure. The partial and total DOS plots for the **2.1-X** complexes quantify the relative amount each of the uranium center, equatorial amide ligands, and axial ligands contribute to the MO character at a particular energy level. A high degree of uranium AO character energetically matched to an LCAO originating from a set of ligands is a prerequisite feature for a bond. In the DOS plots of **2.1-OPh** (Figure 2.5.7.5), **2.1-F** (Figure 2.5.7.6), **2.1-Cl** (Figure 2.5.7.7), **2.1-Br** (Figure 2.5.7.8), and to a lesser extent **2.1-N_3**

(Figure 2.5.7.9) the appearance of uranium AO character is well matched to the AO character arising from the axial ligands. In contrast, in the **2.1-NCS** (Figure 2.5.7.10) and **2.1-CN** (Figure 2.5.7.11) DOS plots, it is apparent that uranium AO character is more strongly correlated to AO character arising from the equatorial amide ligands.

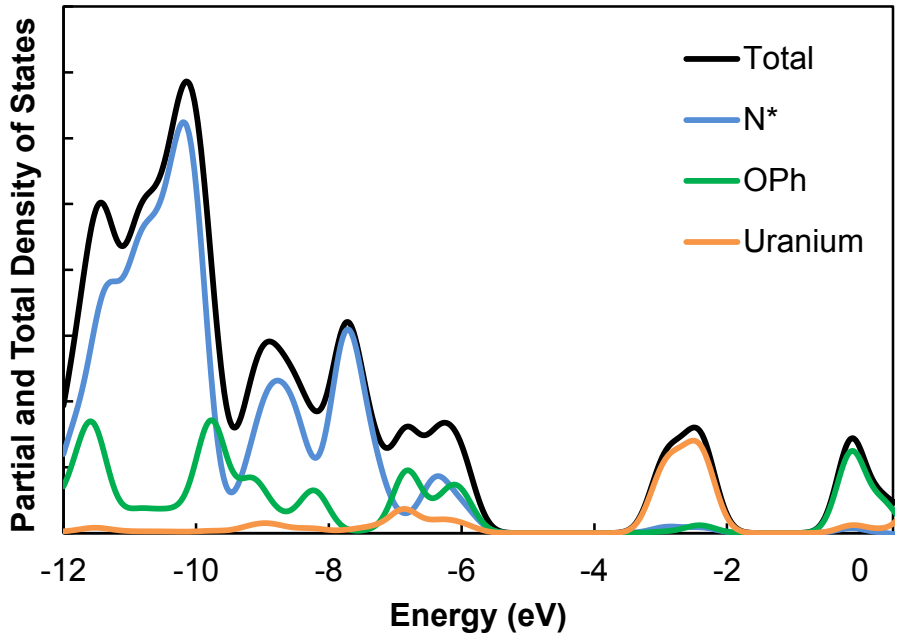

Figure 2.5.7.5 Density of states plot for **2.1-OPh**. HOMO = –5.94 eV, LUMO = –3.01 eV.

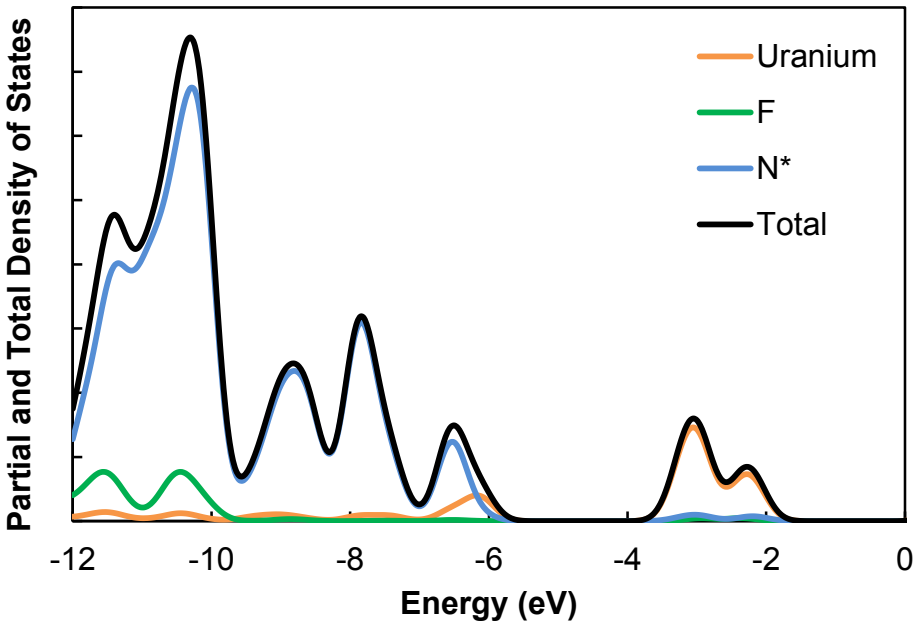

Figure 2.5.7.6 Density of states plot for **2.1-F**. HOMO = –6.14 eV, LUMO = –3.23 eV.

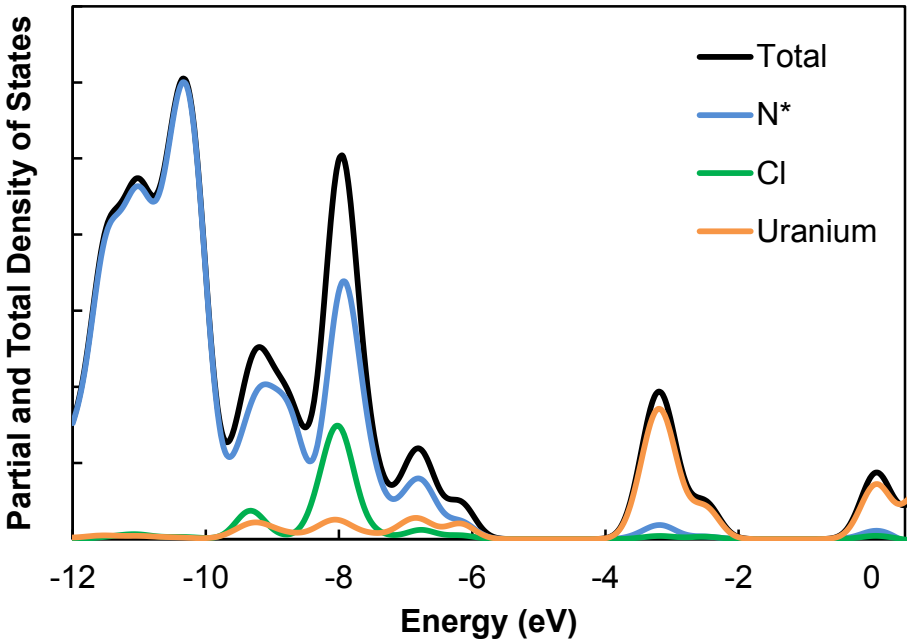

Figure 2.5.7.7 Density of states plot for **2.1-Cl**. HOMO = –6.18 eV, LUMO = -3.42 eV.

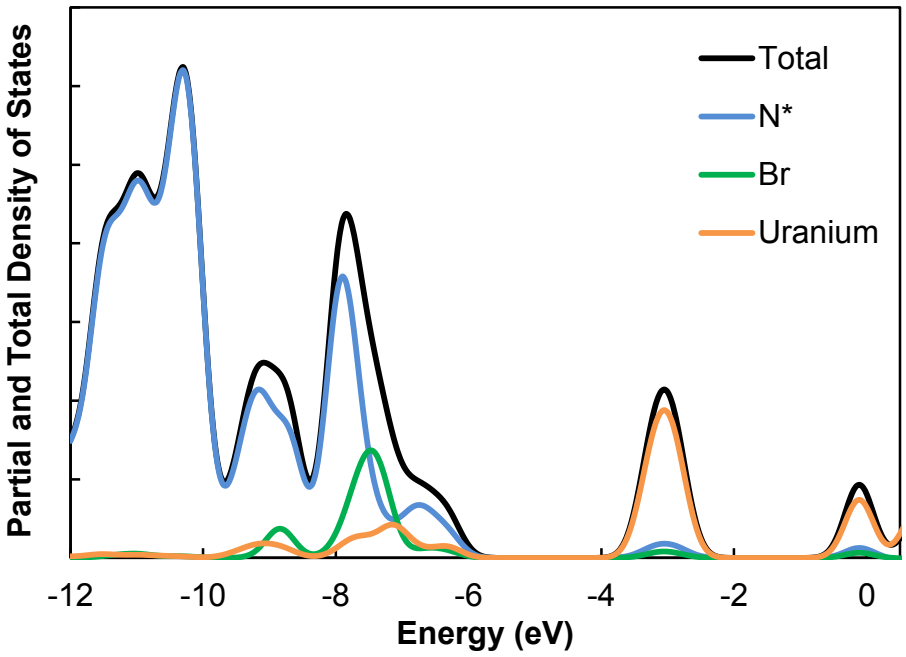

Figure 2.5.7.8 Density of states plot for **2.1-Br**. HOMO = –6.32 eV, LUMO = –3.31 eV.

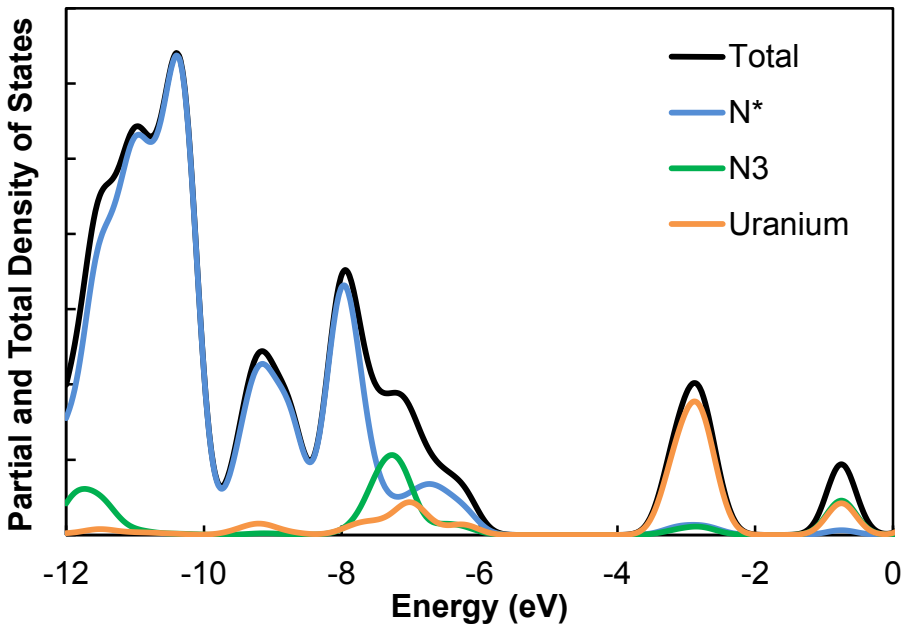

Figure 2.5.7.9 Density of states plot for **2.1-N_3**. HOMO = –6.22 eV, LUMO = –3.20 eV.

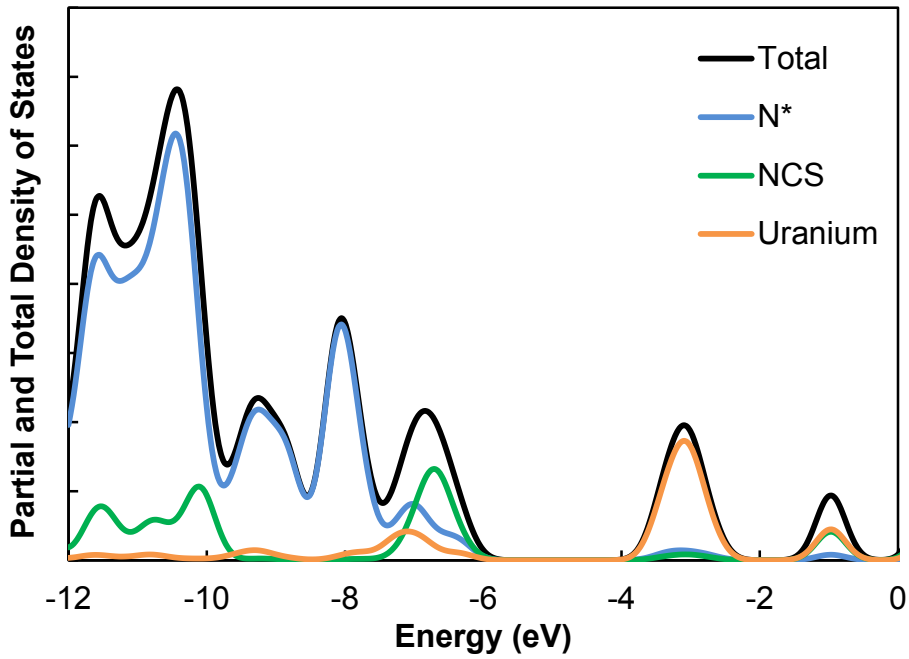

Figure 2.5.7.10 Density of states plot for **2.1-NCS**. HOMO = –6.34 eV, LUMO = –3.41 eV.

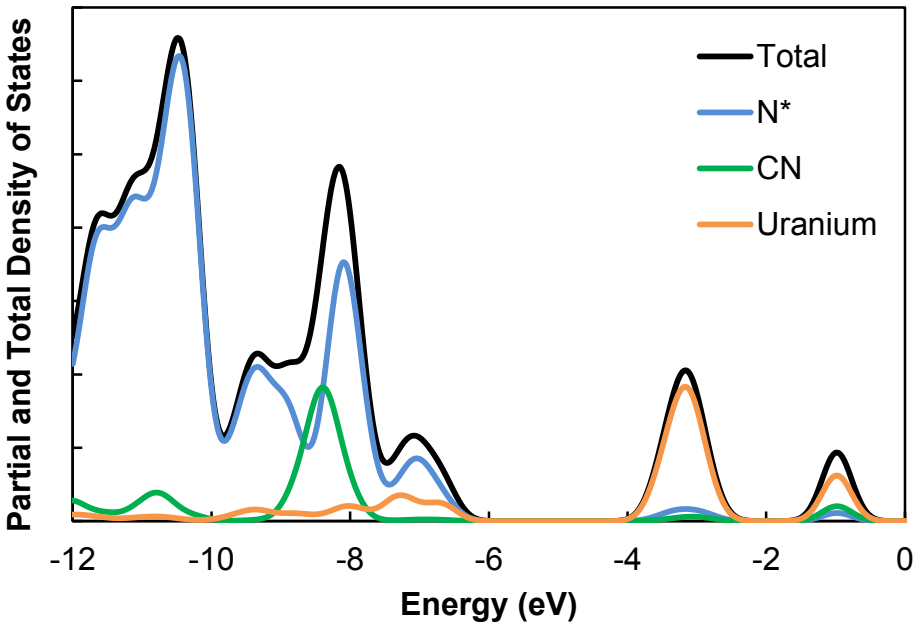

Figure 2.5.7.11 Density of states plot for **2.1-CN**. HOMO = –6.67 eV, LUMO = –3.50 eV.

Finally, the excess α-spin density in each of the **2.1-X** complexes was investigated to corroborate the results of the EPR experiments (Figures 2.5.7.12-2.5.7.16). All of the complexes

showed isolation of the α-spin to the uranium center, with minor excess β-spin density on the atoms directly bound to the uranium center due to spin contamination.[56] The absence of α-spin density on the azide ligands in **2.1-N_3** was surprising given the extensive coupling of the unpaired electron inferred from the EPR experiment.

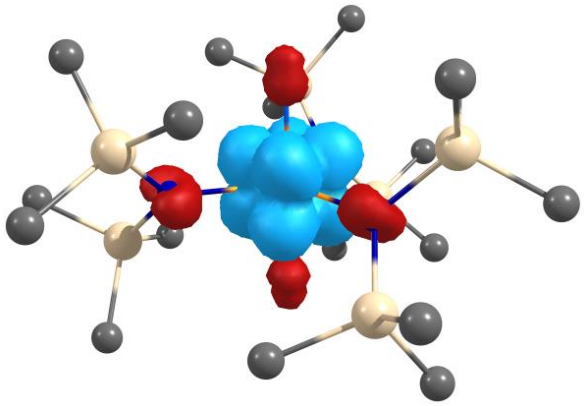

Figure 2.5.7.12 Spin density plot of **2.1-F**.

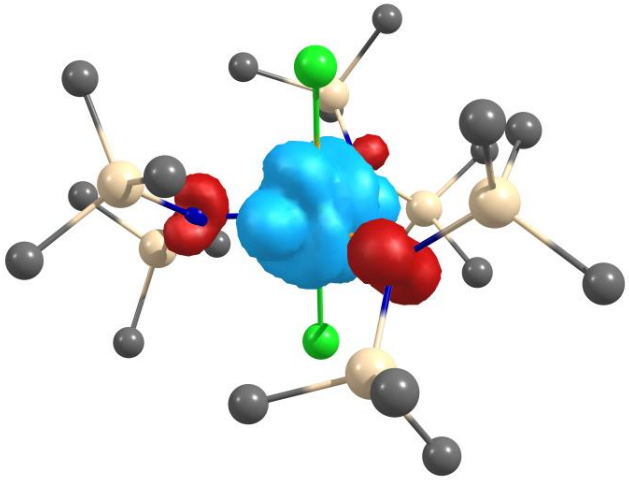

Figure 2.5.7.13 Spin density plot of **2.1-Cl**.

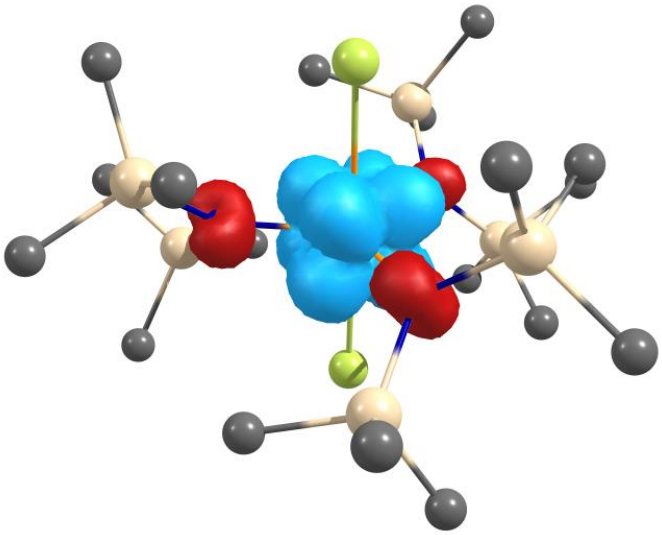

Figure 2.5.7.14 Spin density plot of **2.1-Br**.

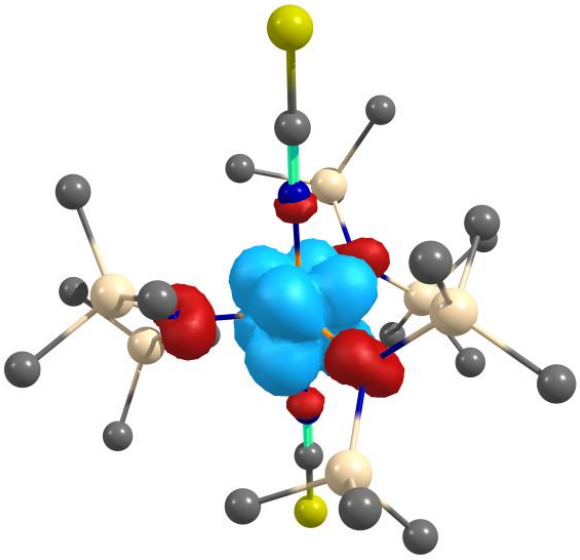

Figure 2.5.7.15 Spin density plot of **2.1-NCS**.

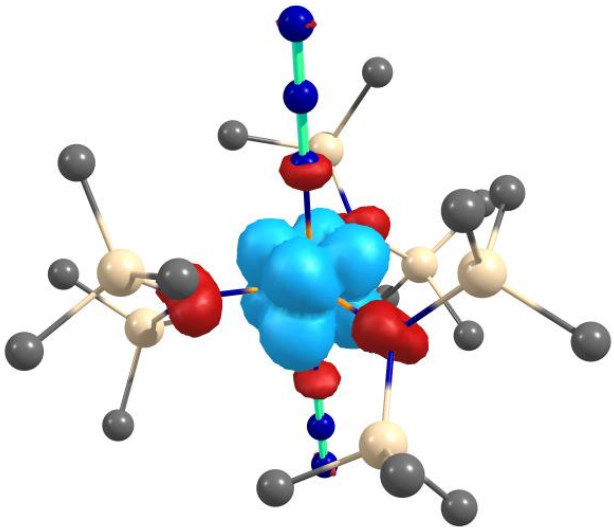

Figure 2.5.7.16 Spin density plot of **2.1-N_3**.

2.6 U[N(SiMe$_3$)$_2$]$_4$: A Common Side Product. In the course of investigating the one-electron oxidation chemistry of U[N(SiMe$_3$)$_2$]$_3$,[57] we noted a persistent side product by ^{1}H NMR at –3.2 ppm in d_6-benzene, particularly when these reactions were carried out in THF. Furthermore, attempts to generate a cationic uranium(IV) complex in THF repeatedly led to the rapid catalytic polymerization of the solvent, in which the ^{1}H NMR spectrum displayed *poly*-THF and the resonance at –3.2 ppm as the sole products. Extraction of this mixture with a 1:4 mixture of Et_2O:hexanes and crystallization at –21 °C allowed for an initial isolation of U[N(SiMe$_3$)$_2$]$_4$ (**2.2**) in low yield.

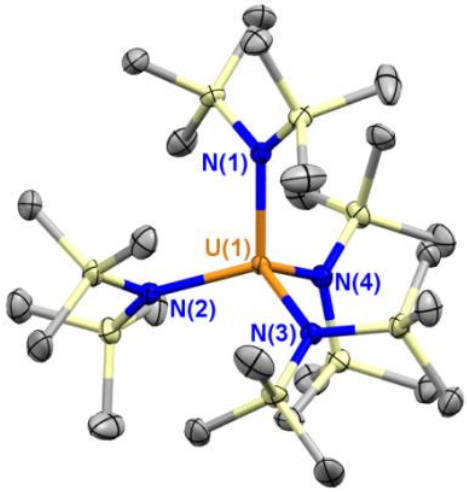

Figure 2.6.1 Thermal ellipsoid plot of **2.2** at 30% probability. Hydrogen atoms are omitted for clarity. Bond lengths (Å) and angles (deg): U(1)–N(1) 2.2941(17), U(1)–N(2) 2.2958(17), U(1)–N(3) 2.2977(17), U(1)–N(4) 2.3013(17), N(1)–U(1)–N(2) 111.12(6), N(1)–U(1)–N(3) 106.18(6), N(1)–U(1)–N(4) 111.72(6).

The crystal structure of **2.2** revealed a pseudo-tetrahedral coordination environment. Within each uranium-amide linkage, the two U–N–Si angles differ by ~12°. For comparison, the corresponding methyl group on the displaced trimethylsilyl group is ~ 4 Å from the uranium(IV) cation. Comparison of the average U–N bond lengths in **2.2** of 2.297(2) Å with the reported structure of $[K(THF)_6][U[N(SiMe_3)_2]_4]$ (**2.2-K**) of 2.432(7)[58] shows a difference of 0.135 Å. This difference is the same as the difference in ionic radii of six-coordinate uranium(III) and uranium(IV) ions.[59] Similar data are not available for a coordination number of four, but the difference is expected to be comparable. Also, the U–N bond lengths in **1** are only slightly longer than the average U–N bond lengths in $U[N(SiMe_2H)_2]_4$ of 2.281(5).[60] Therefore, the steric crowding enforced by the four amide ligands is not so substantial that it restricts U–N bonding.

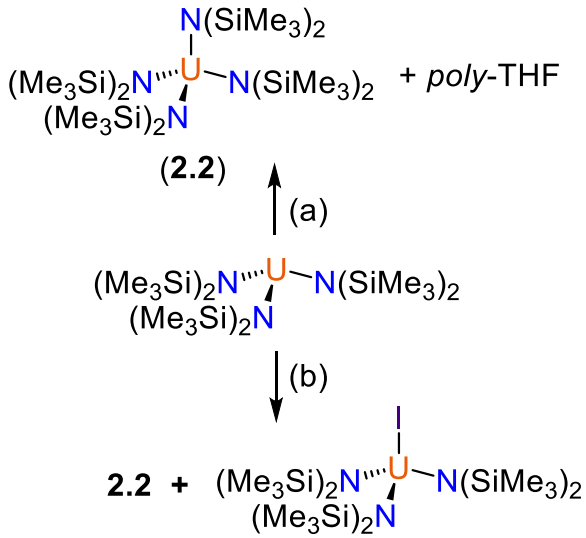

Scheme 2.6.1 Oxidation reactions of $U[N(SiMe_3)_2]_3$ to form **2.2** that proceeded in low yields; conditions: (a) THF, $AgBF_4$ or [TEMPO][BF_4] or $AgPF_6$ or $FcPF_6$ or [Ph_3C][PF_6]; (b) THF, CuI or AgI or I_2 or HgI_2.

$U[N(SiMe_3)_2]_3$ reacted with $AgBF_4$, [TEMPO][BF_4], $AgPF_6$, $FcPF_6$, or [Ph_3C][PF_6] in THF to produce **2.2** in low yields (Scheme 1). Oxidants containing the non-coordinating anions BF_4^- and PF_6^- produced **2.2** almost immediately and polymerized the solvent at varying rates, typically leading to solidification of the reaction mixture within 30 min to 1 h. PF_5,[61] and to a lesser extent BF_3,[62] are capable of initiating the ring opening polymerization of THF, however we observed THF polymerization even when we did not detect the expected fluorine abstraction product $UF[N(SiMe_3)_2]_3$.[43] The formation of **2.2** under these conditions is attributed to ligand redistribution.

Unlike the oxidants comprising the non-coordinating BF_4^- and PF_6^- anions, iodide-based oxidants, including CuI, AgI, I_2, and HgI_2, generated a mixture of **2.2** and $U^{IV}I[N(SiMe_3)_2]_3$,[49] which were in practice inseparable. This product distribution supports the proposed mechanism, as these iodide-based reagents can act either as inner sphere or outer sphere oxidants. An inner sphere oxidation pathway would form the uranium(IV)-iodide complex while the outer sphere oxidation leads to the formation of the cationic complex, which proceeds to form **2.2**.

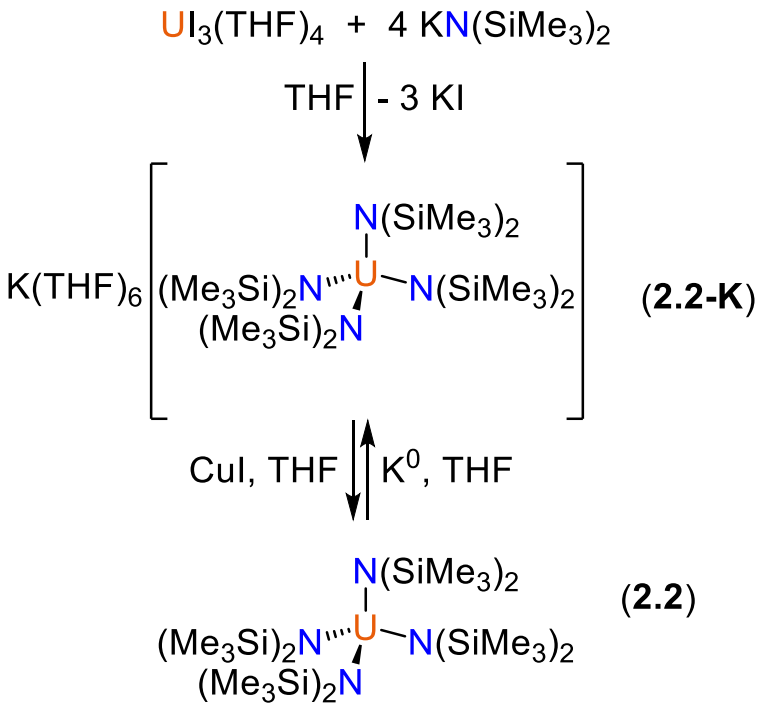

Scheme 2.6.2 Stepwise synthesis of **2.2** and **2.2-K**.

Since the synthesis of **2.2** through oxidative ligand-redistribution proceeded in inherently low yield, we pursued a more rational approach. We reasoned that direct oxidation of **2.2-K** would provide a convenient pathway for the synthesis of **2.2**. The synthesis of **2.2-K** has been previously reported through the reduction of $U[N(SiMe_3)_2]_3$ with KC_8 in THF under N_2; however, no yield was provided for **2.2-K**.[58] Addition of 4 equiv $KN(SiMe_3)_2$ to $UI_3(THF)_4$ in THF led to the formation of **2.2-K** as the sole uranium containing product, which was easily separated due to its high solubility in pentane, allowing for its isolation in 76% yield. Importantly, no evidence for a cyclometallated product was observed in this reaction.

Variable amide coordination with different alkali-metal salts of the $N(SiMe_3)_2^-$ ligand has been observed previously in the synthesis of uranyl complexes.[63] The ^{1}H NMR spectrum of **2.2-K** displayed variable peak positions among different samples, which prompted further investigation. The $-SiMe_3$ protons appeared between –6 and –10 ppm in C_6D_6, and a varying amount of $KN(SiMe_3)_2$ was observed from solutions of **2.2-K** . Interestingly, exposure of solid **2.2-K** to

dynamic vacuum for several hours resulted in complete conversion to $U[N(SiMe_3)_2]_3$ and $KN(SiMe_3)_2$ with loss of the associated THF resonances.

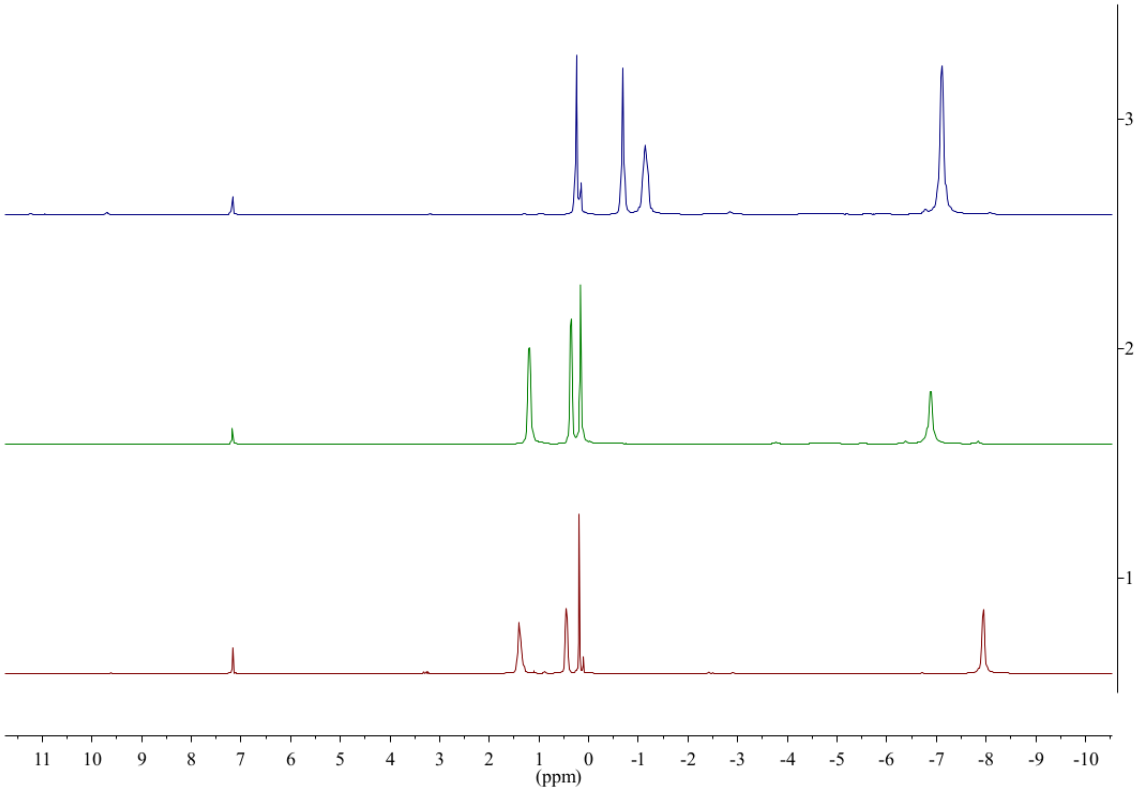

Figure 2.6.2 ^{1}H NMR spectra of **2.2-K** in C_6D_6, illustrating peak shifts as a function of THF solvation. $KN(SiMe_3)_2$ is observed at ~0.2 ppm in all cases due to partial loss in C_6D_6.

The direct oxidation of **2.2-K** with a mild oxidant such as CuI led to quantitative formation of **2.2**. Conversely, reaction of **2.2** with K^0 in THF produced **2.2-K**. The CuI oxidation of **2.2-K** formed *in situ* from $UI_3(THF)_4$ allowed for the direct one-pot synthesis of **2.2** in 94% yield. We also attempted to prepare **2.2** directly from a uranium(IV) precursor. The reaction of UCl_4 with 4 equiv $NaN(SiMe_3)_2$ is reported to form the metallacycle $U[N(SiMe_3)_2]_2(CH_2SiMe_2NSiMe_3)$.[34, 35, 64] In our hands no evidence for the formation of **2.2** was observed under these reaction conditions. We also attempted the reaction of $UI_4(OEt_2)_2$ with 4 equiv $NaN(SiMe_3)_2$, which also rapidly cyclometallated without formation of **2.2**, as judged by ^{1}H NMR spectroscopy. In contrast, the reaction of $UI_4(OEt_2)_2$ with 4 equiv $KN(SiMe_3)_2$ generated an approximately equimolar mixture of **2.2** and the cyclometallated product, as judge by ^{1}H NMR, that was not easily separated.

The steric bulk provided by the four trimethylsilylamide ligands prevents further reactivity at the metal center in **2.2**. Notably, cyclometallation through loss of $HN(SiMe_3)_2$ was not observed at room temperature, though complete conversion was observed after refluxing **2.2** in toluene for 2 h. We may therefore reasonably rule out **2.2** as an intermediate in the room temperature formation of $U[N(SiMe_3)_2]_2(CH_2SiMe_2NSiMe_3)$.[65] It was recently shown that $U[N(SiMe_3)_2]_3$ slowly disproportionates in arene solvent to form $[U[N(SiMe_3)_2]_2]_2(\mu\text{-}\eta^6\text{:}\eta^6\text{-arene})$ and $U[N(SiMe_3)_2]_2(CH_2SiMe_2NSiMe_3)$.[66] Based on our observations, it is likely that **2.2** initially forms in this reaction, then converts into **2.2** upon heating. In this context, DFT calculations were performed to assess the relative stability of **2.2** and $U[N(SiMe_3)_2]_2(CH_2SiMe_2NSiMe_3)$. Indeed, the conversion was found to be exothermic, with ΔG_{rxn} = -38.9 kcal/mol.

Despite the strong thermodynamic driving force for cyclometallation, experimentally the stability of **2.2** was greater than anticipated. For example, exposing a solution of **2.2-K** to air led to immediate formation of **2.2** as judged by ^{1}H NMR. A $CDCl_3$ solution of **2.2** left open to ambient atmosphere was quite stable, and exhibited approximately 50% decomposition to $HN(SiMe_3)_2$ over the course of 24 h, indicating that the complex decomposes only slowly in the presence of water but is stable to oxygen. Additionally, **2.2** was found to be stable on alumina. Although not strictly necessary given the high yield on recrystallization of **2.2** from pentane, it is remarkable that the use of flash chromatography through alumina is a viable means of purification of the complex.

2.7 Characterization of $U[N(SiMe_3)_2]_4$.

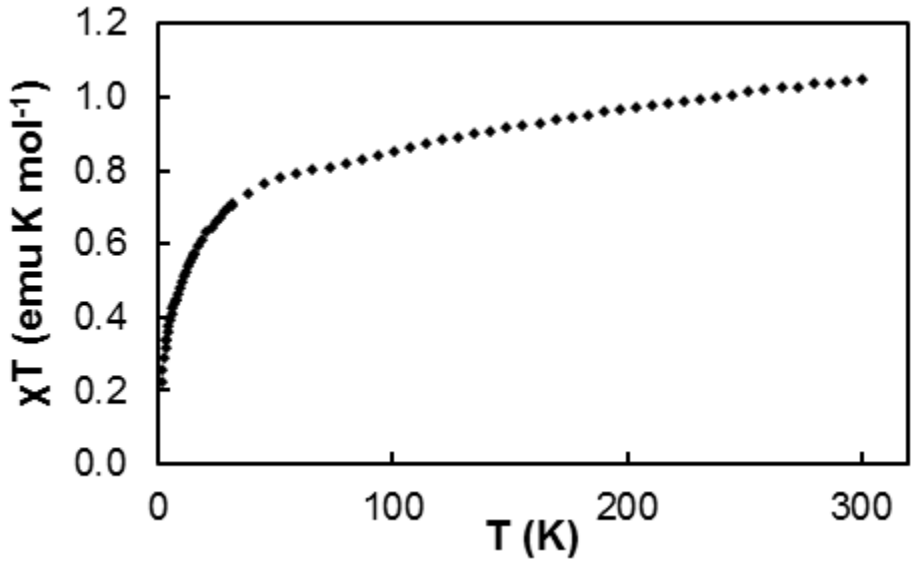

Figure 2.7.1 Temperature dependent magnetic susceptibility of **2.2** at an applied field of 2 T.

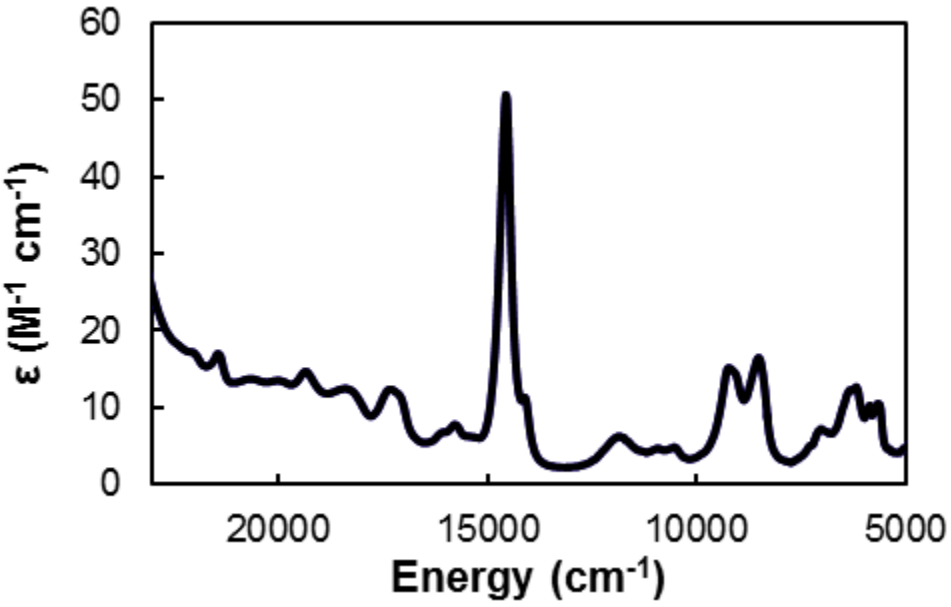

Figure 2.7.2 Near-IR spectrum of **2.2** as a 59.5 mM solution in toluene.

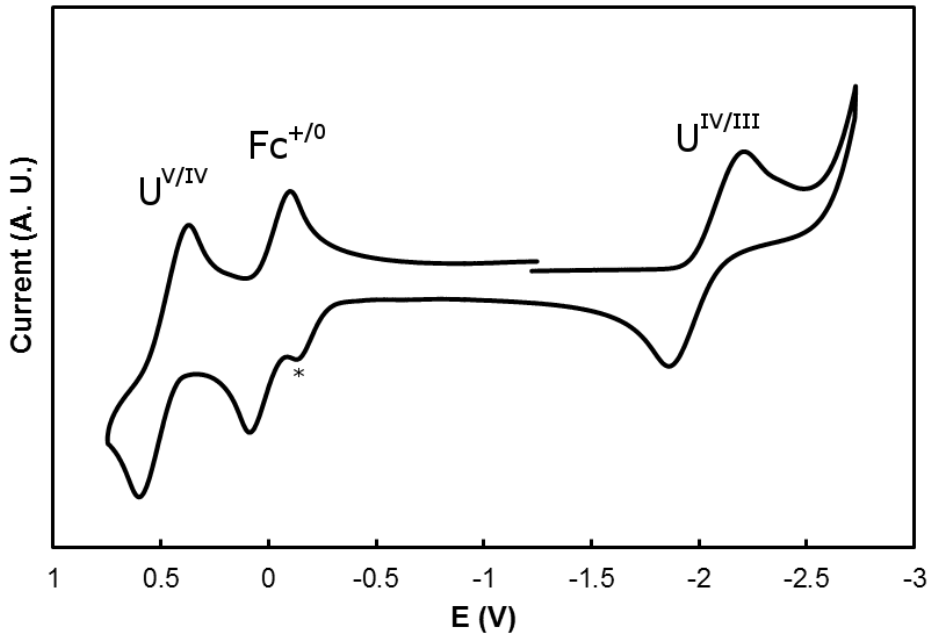

Figure 2.7.3 Cyclic voltammogram of **2.2** in acetonitrile referenced to an internal $Fc^{+/0}$, with 0.1 M [$^{n}Bu_4N$][PF_6] supporting electrolyte at a scan rate of 250 mV/s. The * denotes a minor impurity, which is attributed to Cu[$N(SiMe_3)_2$].

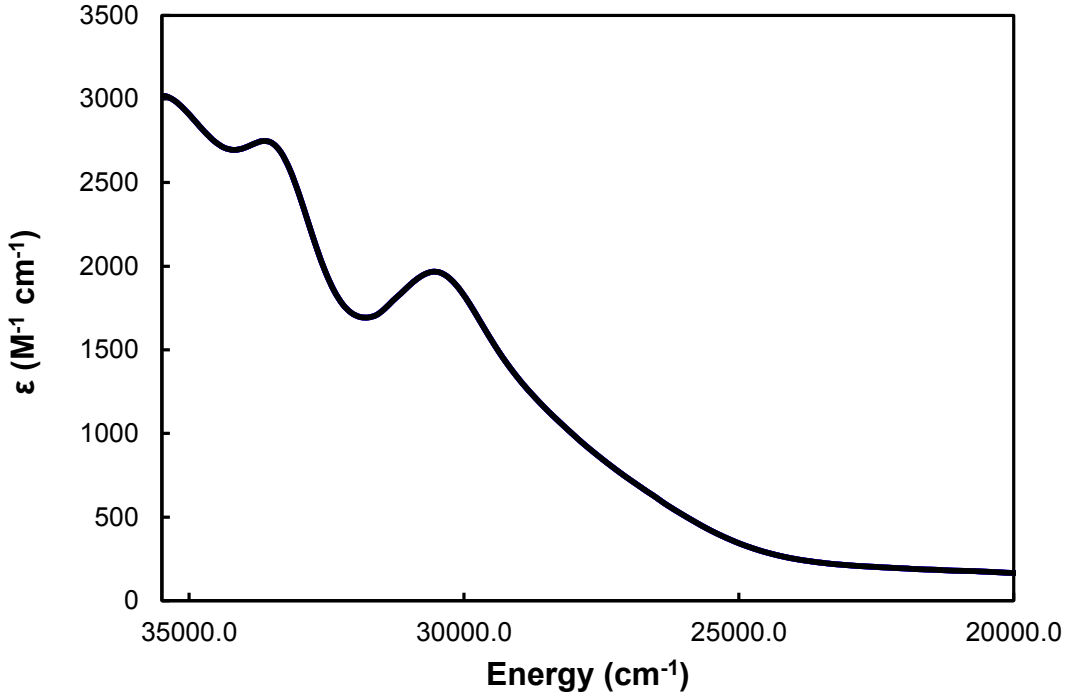

Figure 2.7.4 UV-vis spectrum of **2.2** as a 4.18 mM solution in toluene.

The high stability of **2.2** and its persistence as a product of the redox chemistry of $U[N(SiMe_3)_2]_3$ prompted us to perform complete characterization of the complex. Electrochemical measurements were carried out on **2.2** to assess its redox stability (Figure S1). In the cyclic voltammogram of **2.2** performed in CH_3CN, two sets of waves were observed, assigned to the $U^{V/IV}$ couple at +0.49 V and the $U^{IV/III}$ couple at –2.05 V versus Fc/Fc^+. The $U^{IV/III}$ reduction potential is shifted to a more negative potential than the reported $U^{IV/III}$ couple of $U[N(SiMe_3)_2]_3$ at –1.24 V,[67] consistent with the greater stabilization of the uranium(IV) oxidation state upon coordination of a fourth amide ligand. Despite the electrochemically accessible 5+ oxidation state, none of the oxidants that were used to produce **2.2** further oxidized the complex. Attempts to collect electrochemical data on **2.2-K** were hindered by the poor stability of the complex under the conditions of the experiment. Temperature dependent magnetic susceptibility measurements carried out on **2.2** yielded a room temperature moment μ_{eff} = 2.94 μ_B (Figure 2, top). The data showed a substantial decrease in the moment at low temperature and no saturation of the moment in the a field dependent measurement at 2 K, features characteristic of a uranium(IV) ion.[68, 69] The near-IR spectrum of **2.2** in toluene exhibited numerous transitions within a 5f state manifold (Figure 2, bottom).[70-72] Together the characterization data are consistent with signatures of a $5f^2$ uranium(IV) ion.

2.8 Appearance of $U[N(SiMe_3)_2]_4$ as a Side Product in Oxidation Reactions. As discussed in Section 2.6, numerous oxidation reactions with $U^{III}[N(SiMe_3)_2]_3$ produce **2.2** as a side product. Several representative reactions are presented in Figures 2.8.1–2.8.6.

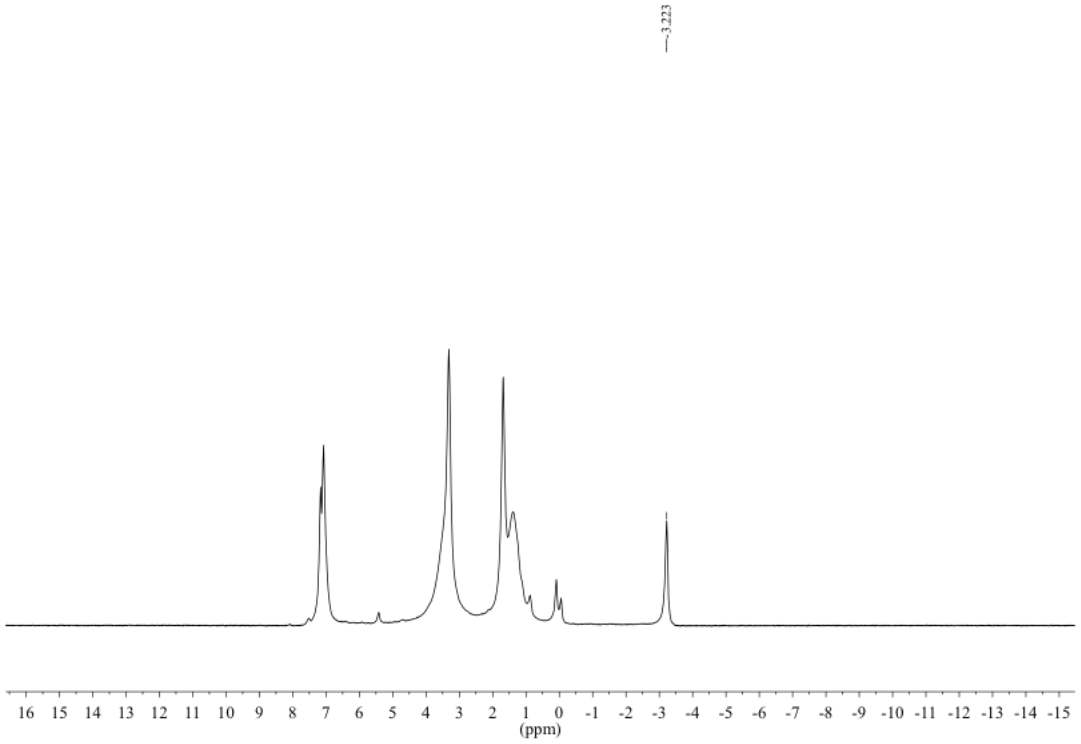

Figure 2.8.1 ^{1}H NMR spectrum of an aliquot from reaction of $U[N(SiMe_3)_2]_3$ with $[Ph_3C][PF_6]$ in THF.

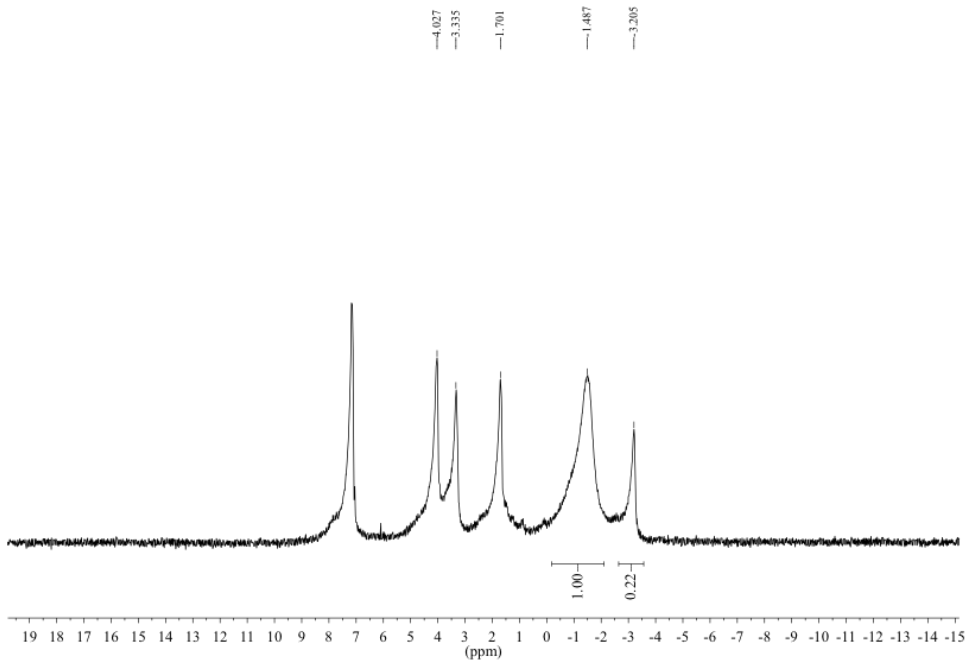

Figure 2.8.2 ^{1}H NMR spectrum of an aliquot from reaction of $U[N(SiMe_3)_2]_3$ with $FcPF_6$ in THF. The peak at -1.487 is $U^{V}F_2[N(SiMe_3)_2]_3$ and the peak at 4.027 is ferrocene.

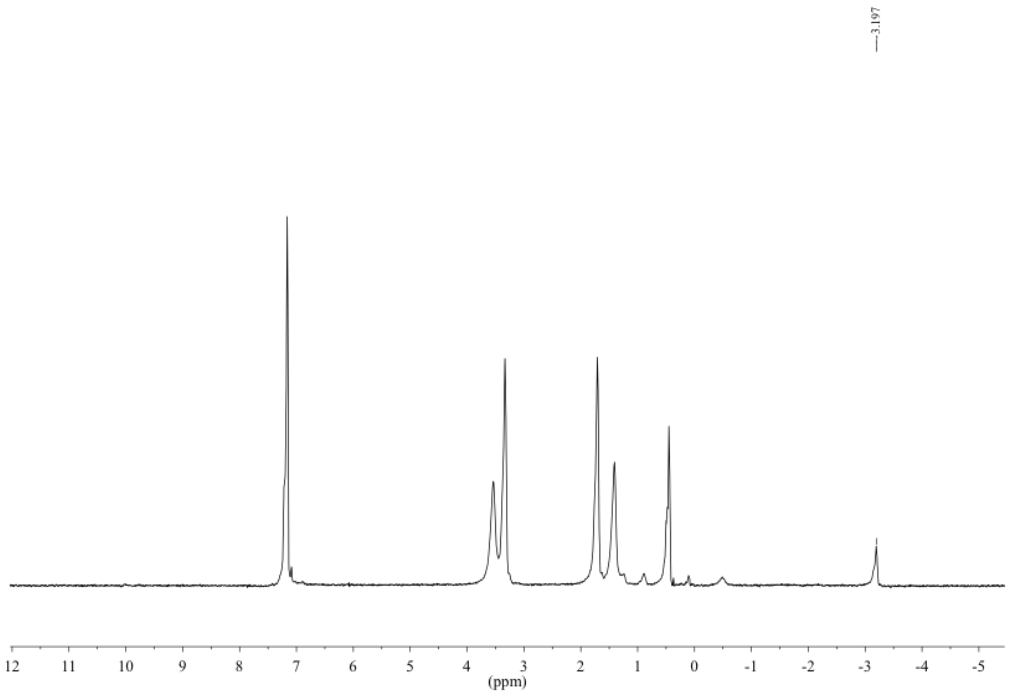

Figure 2.8.3 ^{1}H NMR spectrum of an aliquot from reaction of $U[N(SiMe_3)_2]_3$ with $AgPF_6$ in THF.

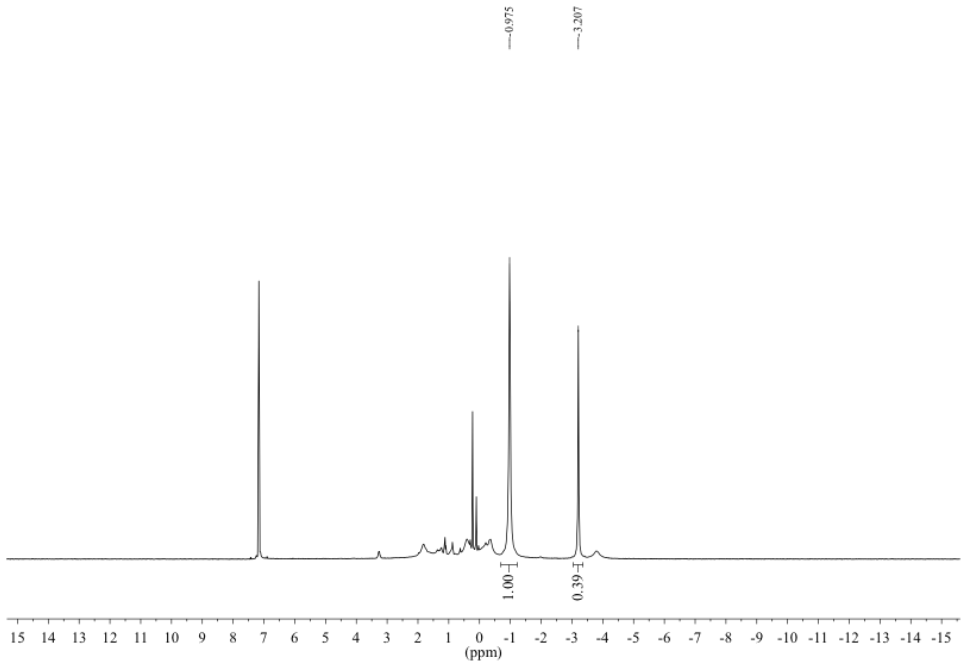

Figure 2.8.4 ^{1}H NMR spectrum of an aliquot from reaction of $U[N(SiMe_3)_2]_3$ with I_2 in THF. The peak at -0.975 is $U^{IV}I[N(SiMe_3)_2]_3$.

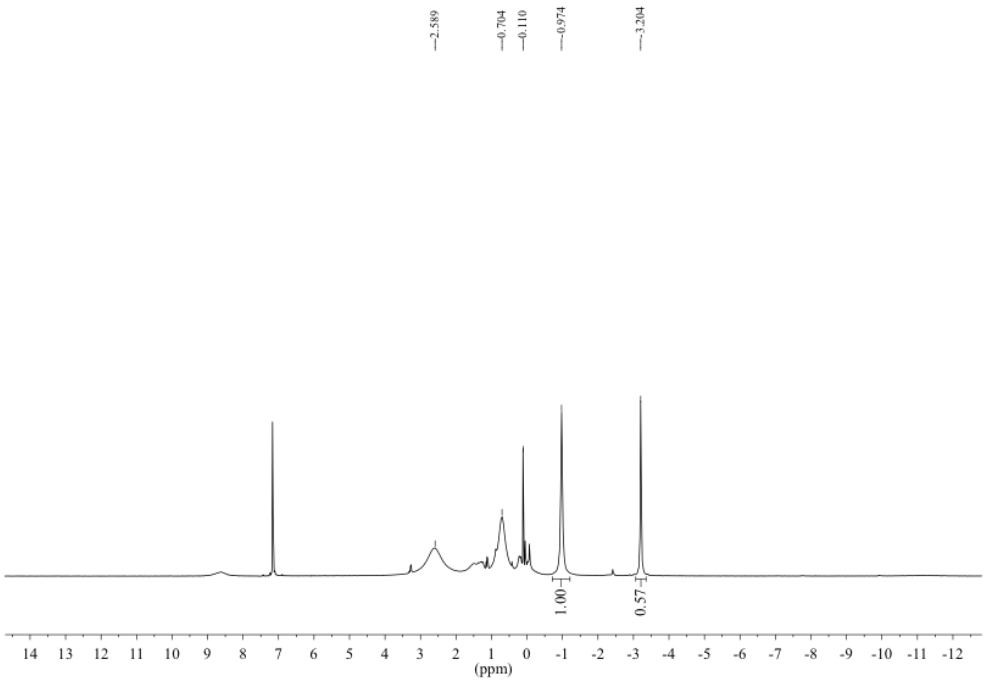

Figure 2.8.5 ^{1}H NMR spectrum of an aliquot from reaction of $U[N(SiMe_3)_2]_3$ with HgI_2 in THF. The peak at -0.975 is $U^{IV}I[N(SiMe_3)_2]_3$.

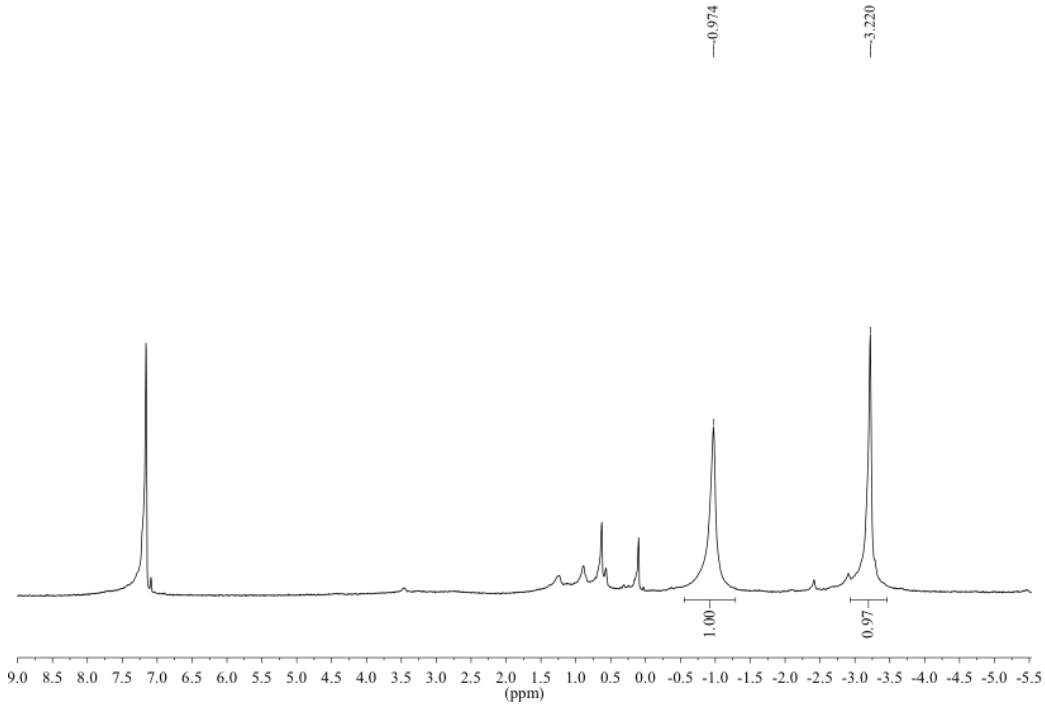

Figure 2.8.6 ^{1}H NMR spectrum of an aliquot from reaction of $U[N(SiMe_3)_2]_3$ with AgI in THF. The peak at -0.975 is $U^{IV}I[N(SiMe_3)_2]_3$.

2.9 Experimental

2.9.1 $U^{V}F_2[N(SiMe_3)_2]_3$ (2.1-F).

2.9.1.1 ***From $U^{III}[N(SiMe_3)_2]_3$ and $[Ph_3C][PF_6]$.*** A solution of $U[N(SiMe_3)_2]_3$ (250 mg, 0.35 mmol) in 10 mL of hexanes was added to a vial containing $[Ph_3C][PF_6]$ (270 mg, 0.70 mmol, 2.00 equiv). The resulting slurry turned from dark purple to dark red over about 20 minutes of stirring. After stirring for 5 h, the dark red solution was filtered through Celite packed on a coarse fritted filter and volatiles were removed under reduced pressure. The resulting residue was dissolved in $(Me_3Si)_2O$, filtered through Celite, and volatiles were removed under reduced pressure. Pentane (~10 mL) was added and this solution was stored at –21 °C overnight, which resulted in precipitation of residual Gomberg's dimer [4-(triphenylmethyl)-1-(diphenylmethylidene)-2,5-cyclohexadiene]. Filtration of this solution through Celite and removal of volatiles under reduced pressure produced **2.1-F** as a dark red solid. Yield: 187 mg, 0.25 mmol, 71%.

2.9.1.2 ***From $U^{III}[N(SiMe_3)_2]_3$ and AgF.*** A solution of $U[N(SiMe_3)_2]_3$ (100 mg, 0.14 mmol) in 5 mL of hexanes was added to a vial containing AgF (56 mg, 0.44 mmol, 3.14 equiv) in 3 mL of hexane. After stirring 32 h, the resulting dark red solution was filtered through Celite and volatiles were removed under reduced pressure. The resulting residue was dissolved in $(Me_3Si)_2O$, filtered, and concentrated under reduced pressure, yielding **2.1-F** as a dark red crystalline solid. Yield: 71 mg, 0.09 mmol, 68%.

2.9.1.3 ***From $U^{III}[N(SiMe_3)_2]_3$ and $[TEMPO][BF_4]$.*** A solution of $U[N(SiMe_3)_2]_3$ (140 mg, 0.19 mmol) in 5 mL of hexanes was added to a vial containing $[TEMPO][BF_4]$ (95 mg 0.39 mmol, 2.05 equiv). The resulting slurry rapidly turned dark red. After stirring 3 h, the mixture was filtered through Celite suspended in a glass pipette, and volatiles were removed under reduced pressure while heating to 50 ^{o}C to ensure removal of TEMPO. The resulting dark red residue was dissolved in $(Me_3Si)_2O$, filtered, and volatiles were removed under reduced pressure, yielding **2.1-F** as a dark red crystalline solid. Yield: 96 mg, 0.13 mmol, 65%. ^{1}H NMR (benzene-d_6): δ –1.53 (54H). IR (KBr): 2951 (w), 2899 (w), 1249 (s), 934 (w), 873 (s), 844 (s), 775 (m), 654 (s, $\nu_{U–N}$),

621 (s, ν_{U-N}), 511 (m, ν_{U-F} asymm. stretch) (cm^{-1}). Elemental analysis found (calculated) for $C_{18}H_{54}F_2N_3Si_6U$: C, 28.97 (28.55); H, 7.52 (7.19); N, 5.22 (5.55).

2.9.2 $U^{V}Cl_2[N(SiMe_3)_2]_3$ (2.1-Cl).

2.9.2.1 *From $U^{III}[N(SiMe_3)_2]_3$ and WCl_6.* To a stirring solution of $U[N(SiMe_3)_2]_3$ (30 mg, 0.04 mmol) in 4 mL of hexanes, WCl_6 (16 mg, 0.04 mmol, 1.00 equiv) was added, resulting in rapid color change to dark red-brown with a grey-black solid suspended. After stirring this slurry for 30 minutes, the solution was filtered through a Celite-packed coarse-porosity fritted filter and the volatiles were removed under reduced pressure. The black residue was dissolved in hexanes, filtered again through Celite and the volatiles were removed under reduced pressure. Recrystallization from minimal hexanes at –21 °C produced **2.1-Cl** as a black crystalline solid. Yield: 18 mg, 0.02 mmol, 54%. No $UCl[N(SiMe_3)_2]_3$ was observed in the ^1H NMR of an aliquot of this reaction despite the use of 1 equiv WCl_6.

2.9.2.2 *From $U^{III}[N(SiMe_3)_2]_3$ and $CuCl_2$.* A solution of $U[N(SiMe_3)_2]_3$ (100 mg, 0.14 mmol) in 5 mL of toluene was added to a vial containing $CuCl_2$ (75 mg, 0.56 mmol, 4.00 equiv), resulting in rapid color change to dark red-brown. After stirring this slurry for 3 h, 2 mL of THF was added and the solution was filtered through a Celite-packed coarse-porosity fritted filter and the volatiles were removed under reduced pressure. The black residue was dissolved in $(SiMe_3)_2O$, filtered again through Celite and volatiles were removed under reduced pressure. Recrystallization from minimal hexanes at –21 °C produced **2.1-Cl** as a black crystalline solid. Yield: 61 mg, 0.08 mmol, 55%.

2.9.2.3 *From $U^{IV}Cl[N(SiMe_3)_2]_3$ and $CuCl_2$.* A solution of $UCl[N(SiMe_3)_2]_3$ (**2**) (1.21 g, 1.59 mmol) in 15 mL of THF was added to a vial containing $CuCl_2$ (225 mg, 1.67 mmol, 1.10 equiv), resulting in a rapid color change to dark red-brown. After stirring this slurry for 5 h, the solution was filtered through Celite on a coarse porosity frit and the volatiles were removed under reduced pressure. The black residue was dissolved in $(SiMe_3)_2O$, again filtered through a Celite-packed coarse porosity fritted filter, and the volatiles were removed under reduced pressure. Recrystallization from minimal hexanes at –21 °C produced **2.1-Cl** as a black crystalline solid.

Yield 0.94 g, 1.19 mmol, 74%. ^{1}H NMR (benzene-d_6, RT): δ 0.84 (18H), –1.59 (18H), –4.01 (18H); (benzene-d_6, 32 °C): δ –1.11 (54H). IR (KBr, cm^{-1}): 2954 (w), 1403 (w), 1251 (s), 843 (s), 774 (m), 648 (s, $\nu_{U–N}$), 624 (s, $\nu_{U–N}$). Elemental analysis found (calculated) for $C_{18}H_{54}Cl_2N_3Si_6U$: C, 27.57 (27.36); H, 6.82 (6.89); N, 5.13 (5.32).

2.9.3 $U^{V}Br_2[N(SiMe_3)_2]_3$ (2.1-Br). A solution of $U[N(SiMe_3)_2]_3$ (250 mg, 0.35 mmol) in 10 mL of toluene was added to a vial containing $CuBr_2$ (311 mg, 1.39 mmol, 3.97 equiv). The resulting slurry was stirred for 17 h. The dark red solution was filtered through Celite on a coarse frit and volatiles were removed under reduced pressure. The black residue was dissolved in $(Me_3Si)_2O$, filtered through Celite, and concentrated under reduced pressure, yielding **2.1-Br** as a black crystalline solid. Yield: 251 mg, 0.29 mmol, 82%. ^{1}H NMR (benzene-d_6): δ 1.70 (18H), –1.01 (18H), –4.14 (18H). IR (KBr): 2956 (w), 1251 (s), 844 (s), 773 (m), 646 (s, ν_{U-N}), 623 (s, ν_{U-N}) (cm^{-1}). Elemental analysis found (calculated) for $C_{18}H_{54}Br_2N_3Si_6U$: C, 24.80 (24.60); H, 6.12 (6.19); N, 4.67 (4.78).

2.9.4 $U^{V}FCl[N(SiMe_3)_2]_3$ (2.1-FCl). To a vial containing CuF_2 (100 mg, 0.98 mmol, 4.90 equiv) stirring in 3 mL THF, $U^{IV}Cl[N(SiMe_3)_2]_3$ (150 mg, 0.20 mmol) dissolved in 5 mL THF was added. The mixture was heated at 50 ^{o}C for 3 h with stirring, resulting in a color change to dark red. Removal of volatiles under reduced pressure, dissolution in hexanes, filtration through Celite, and concentration, followed by storage at –21 ^{o}C produced **2.1-FCl** as a dark a black crystalline solid. Yield 74 mg, 0.10 mmol, 49%. ^{1}H NMR (benzene-d_6): δ –1.40 (27H), –1.83 (27H). IR (KBr): 2952 (w), 2900 (w), 1384 (m), 1250 (s), 906 (w), 847 (s), 775 (m), 650 (s, ν_{U-N}), 623 (s, ν_{U-N}), 495 (m, ν_{U-F} asymm. stretch) (cm^{-1}). Elemental analysis found (calculated) for $C_{18}H_{54}ClFN_3Si_6U$: C, 28.32 (27.95); H, 7.05 (7.04); N, 5.39 (5.43).

2.9.5 $U^{V}BrCl[N(SiMe_3)_2]_3$ (2.1-BrCl). To a vial containing $U^{IV}Cl[N(SiMe_3)_2]_3$ (400 mg, 0.53 mmol) in Et_2O, $CuBr_2$ (592 mg, 2.65 mmol, 5.0 equiv) was added. The mixture was stirred 2.5 h, over which time it became dark red. The mixture was filtered through Celite packed on a coarse fritted filter, and volatiles were removed under reduced pressure. The resulting black residue was extracted with pentane, filtered through Celite suspended in a glass pipet, and volatiles were

removed under reduced pressure to afford **2.1-BrCl** as a black solid. Yield: 220 mg, 0.26 mmol, 50%. ^{1}H NMR (benzene-d_6): δ 1.53 (18H), –1.38 (18H), –4.25 (18H).

2.9.6 $U^{V}(N_3)_2[N(SiMe_3)_2]_3$ (2.1-N_3). To a vial containing NaN_3 (10 mg, 0.154 mmol) stirring in 2 mL THF, **2.1-Cl** (60 mg, 0.08 mmol) dissolved in 5 mL THF was added. This mixture was stirred for 1.5 h, over which time no color change was observed. Filtration through Celite on a coarse porosity fritted filter, removal of the volatiles under reduced pressure, dissolution in pentane, filtration through Celite, and further removal of volatiles under reduced pressure yielded **2.1-N_3** as a dark red solid. Yield 55 mg, 0.07 mmol, 90%. Characterization data matched those previously reported.[9] Additional characterization: IR (KBr, cm^{-1}): 2954 (w), 2079 (s, ν_{N3}-asymm. stretch), 1359 (s, ν_{N3}-symm. stretch), 1251 (s), 844 (s), 773 (s), 650 (s, $\nu_{U–N(amide)}$), 622 (s, $\nu_{U–N(amide)}$) (cm^{-1}).

2.9.7 $U^{V}(NCS)_2[N(SiMe_3)_2]_3$ (2.1-NCS). To a vial containing **2.1-Cl** (150 mg, 0.19 mmol) dissolved in 3 mL THF, NaSCN (77 mg, 0.95 mmol, 5.00 equiv) was added as a solid. After stirring for ~30 min, the solution had become completely pale tan. To this mixture, $CuBr_2$ (250 mg, 1.12 mmol) was added as a solid, inducing a color change to dark red-brown and then dark green. After stirring for 3 h, the volatiles were removed under reduced pressure, and the residue was extracted with hexanes. Filtration through Celite packed on a coarse porosity fritted filter produced a dark red filtrate, which was concentrated and stored at –21 °C, producing **2.1-NCS** as opaque red plates collected in two crops. Yield 101 mg, 0.12 mmol, 64%. ^{1}H NMR (benzene-d_6): δ –1.47 (54H). IR (KBr, cm^{-1}): 2955 (w), 1994 (s, $\nu_{N=C}$ stretch), 1403 (w), 1253 (s), 841 (s), 775 (s), 683 (w), 647 (s, $\nu_{U–N(amide)}$), 626 (s, $\nu_{U–N(amide)}$) (cm^{-1}). The $\nu_{C=S}$ stretch was not located, likely due to overlap with silylamide vibrations. Elemental analysis found (calculated) for $C_{20}H_{54}N_5S_2Si_6U$: C, 28.94 (28.76); H, 6.42 (6.52); N, 8.64 (8.38).

2.9.8 $U(Onap)_2[N(SiMe_3)_2]_3$ (2.1-ONap). To a stirred, opaque solution of **1-Cl** (150 mg, 0.19 mmol) in THF, $K(THF)_{0.5}$(2-naphthoxide) (124 mg, 0.57 mmol, 3.0 equiv) was added, resulting in a color change to pale orange. After 30 minutes, $CuBr_2$ (212 mg, 0.95 mmol, 5.0 equiv) was added, resulting in a color change to red-black then to green-black. After 15 minutes,

volatiles were removed under reduced pressure, and the black residue was extracted with hexanes, filtered and volatiles were removed under reduced pressure. The black residue was dissolved in minimal Et_2O and stored at –21 °C to yield **2.1-Onap** as black crystals. Crystals suitable for X-ray diffraction were obtained from a concentrated hexanes solution stored at –21 °C. Yield: 111 mg, 0.11 mmol, 58%. ^{1}H NMR (benzene-d_6): 14.2 (2H), 12.7 (2H), 12.2 (2H), 10.0 (2H), 8.9 (2H), 8.7 (2H), 7.5 (2H), –1.9 (54H). ^{1}H NMR (benzene-d_6): 14.2 (2H), 12.7 (2H), 12.2 (2H), 10.0 (2H), 8.9 (2H), 8.7 (2H), 7.5 (2H), –1.9 (54H). IR (KBr): Elemental analysis found (calculated) for $C_{38}H_{68}N_3O_2Si_6U\cdot0.5Et_2O$: C, 46.15 (46.08); H, 6.72 (7.06); N, 3.54 (4.03).

2.9.9 $[U(HQ)[N(SiMe_3)_2]_3]_\infty$ (2.1-HQ). To a vial containing $U^{III}[N(SiMe_3)_2]_3$ (250 mg, 0.35 mmol) dissolved in Et_2O, *p*-benzoquinone (38 mg, 0.35 mmol, 1.0 equiv) was slowly added, resulting in a color change to pale brown then dark red brown over the course of the addition. Black solid immediately began to precipitate. After stirring 5 min, volatiles were removed under reduced pressure, then 10 mL Et_2O was added, then volatiles were removed under reduced pressure. This process was repeated with 10 mL THF twice. The resulting black microcrystalline solid was washed with 3 x 5 mL THF and dried under reduced pressure to yield **2.1-HQ**. Yield: 209 mg, 0.25 mmol (per monomer), 73%.

2.9.10 $U[N(SiMe_3)_2]_3(NO_3)$. To a vial containing $U^{III}[N(SiMe_3)_2]_3$ (150 mg, 0.21 mmol) in toluene, $AgNO_3$ (106 mg, 0.62 mmol, 3.0 equiv) was added, resulting in a color change to dark orange. After stirring 20 min, the mixture was filtered through Celite suspended in a glass pipet and concentrated under reduced pressure. Storage at –21 °C yielded orange crystals of $U[N(SiMe_3)_2]_3(NO_3)$, which were suitable for X-ray diffraction.

2.9.11 $U^{IV}H_2(dipp)_4Cl_2$. To a vial containing **2.1-Cl** (50 mg, 0.06 mmol) stirring in 2 mL Et_2O, 2,6-diisopropylphenol (45mg, 0.25 mmol, 4.17 equiv) was added as a neat liquid. After stirring for seven hours, no color change was observed, however no starting material could be identified in the ^{1}H NMR of an aliquot collected in benzene-d_6. The volatiles were removed under reduced pressure, and the crude product was dissolved in ~2 mL of hexanes. Brown needles of $U^{IV}H_2(dipp)_4Cl_2$ rapidly formed at –21 ^{o}C, collected in two crops. Yield 53 mg, 0.05 mmol 82%. ^{1}H

NMR (benzene-d_6): δ 9.01 (d, *J* = 7.2 Hz, 8H), 6.15 (t, *J* = 7.2 Hz, 4H), 4.17 (bs, 8H), 0.85 (bs, 48H), –7.9 (bs, 2H). Elemental analysis found (calculated) for $C_{46}H_{64}Cl_2O_4U$: C, 55.30 (55.81); H, 7.01 (6.52); N, 1.28 (N/A). Crystals used in combustion analysis were isolated by decanting the supernatant, which did not completely remove residual $HNTMS_2$. The presence of $HNTMS_2$ in crystalline samples was confirmed by ^{1}H NMR quantified against an internal mesitylene standard. Better agreement with the measure combustion analysis was obtained with the formula $C_{46}H_{64}Cl_2O_4U{\cdot}0.6C_6H_{19}NSi_2$: C, (54.80); H, (7.00); N (0.78).

2.9.12 $[K(THF)_6][U[N(SiMe_3)_2]_4]$ (2.2-K).

2.9.12.1 ***From $UI_3(THF)_4$.*** To a solution of $UI_3(THF)_4$ (250 mg, 0.275 mmol, 1.00 equiv) slurried in 5 mL THF, $KN(SiMe_3)_2$ (220 mg, 1.102 mmol, 4.00 equiv) in 3 mL THF was slowly added, resulting in a color change to dark purple and precipitation of a colorless solid. After stirring 40 minutes, this mixture was filtered through Celite packed on a coarse porosity fritted filter and the volatiles were removed under reduced pressure. The resulting purple residue was stirred in minimal pentane until the purple solid had dissolved, then filtered again through Celite. The purple filtrate was exposed to dynamic vacuum until all visible solvent was removed, which afforded **2.2-K** as a dark purple solid. Yield: 284 mg, 0.210 mmol, 76%.

2.9.12.2 ***From $U[N(SiMe_3)_2]_4$.*** A solution of **2.2** (25 mg, 0.028 mmol, 1.00 equiv) dissolved in 3 mL THF was added to a vial mirrored with K^0 (25 mg, 0.639 mmol, 22.84 equiv). This mixture was stirred for 1 h, then filtered to yield a dark purple solution. Removal of volatiles under reduced pressure yielded **2.2-K** as a dark purple solid. Yield: 20 mg, 0.015 mmol, 52%. ^{1}H NMR data were variable depending on extent of THF solvation, see Figure 2.6.2.

Continued application of dynamic vacuum to dry samples of **2.2-K** led to complete conversion to $U[N(SiMe_3)_2]_3$ and $KN(SiMe_3)_2$ as judged by ^{1}H NMR.

2.9.13 $U[N(SiMe_3)_2]_4$ (2.2).

2.9.13.1 ***From $UI_3(THF)_4$.*** To a solution of $UI_3(THF)_4$ (500 mg, 0.551 mmol, 1.00 equiv) slurried in 10 mL THF, $KN(SiMe_3)_2$ (440 mg, 2.206 mmol, 4.00 equiv) in 5 mL THF was slowly added, resulting in a color change to dark purple and precipitation of a colorless solid. After

stirring 15 minutes, CuI (210 mg, 1.102 mmol, 2.00 equiv) was added, resulting in a rapid color change to pale brown. After stirring for 30 minutes, the mixture filtered through Celite and the volatiles were removed under reduced pressure. The resulting tan solid was recrystallized from minimal pentane at –21 °C, affording **2.2** as a tan solid. Yield: 457 mg, 0.520 mmol, 94%.

2.9.13.2 ***From U[N(SiMe$_3$)$_2$]$_3$.*** Representative procedure: To a stirred THF solution of U[N(SiMe$_3$)$_2$]$_3$ (400 mg, 0.56 mmol, 1.00 equiv), [Ph$_3$C][PF$_6$] (432 mg, 1.11 equiv, 2.00 equiv) was added. The mixture was stirred until the solution appeared pale tan, which was then filtered through Celite and the volatiles were removed under reduced pressure. Allowing the reaction to proceed longer resulted in solidification of the reaction mixture, precluding further work-up. The resulting residue was extracted with a 4:1 hexanes:Et$_2$O mixture and recrystallized at –21 °C, producing pale yellow crystals of **2.2**. Yield: 43 mg, 0.049 mmol, 12 %. The calculated yield assumes a hypothetical 3:4 ratio of **2.2**:U[N(SiMe$_3$)$_2$]$_3$. Comparable results were obtained when AgBF$_4$, [TEMPO][BF$_4$], AgPF$_6$, or FcPF$_6$ were used as the oxidant.

^{1}H NMR (C$_6$D$_6$): δ –3.20 (72H). ^{1}H NMR (CDCl$_3$): δ –3.31 (72H). IR (KBr): 2953 (w), 1555 (w), 1400 (m), 1252 (s), 873 (s), 851 (s), 775 (m), 664 (m), 609 (m). Elemental analysis found (calculated) for C$_{24}$H$_{72}$N$_4$Si$_8$U: C, 33.12 (32.77); H, 8.20 (8.25); N, 6.04 (6.37).

2.9.14 U^{IV}[N(SiMe$_3$)$_2$]$_2$(CH$_2$SiMe$_2$NSiMe$_3$).

2.9.14.1 ***From UI$_4$(OEt$_2$)$_2$.*** To a slurry of UI$_4$(OEt$_2$)$_2$ (1.00 g, 1.12 mmol, 1.00 equiv) in 10 mL Et$_2$O, NaN(SiMe$_3$)$_2$ (821 mg, 4.48 mmol, 4.00 equiv) was added, resulting in a color change to pale tan and precipitation of a colorless solid. After stirring for 12 h, this mixture was filtered through Celite and the volatiles were removed under reduced pressure. The resulting brown residue was extracted with pentane and filtered through Celite, and recrystallized at –21 °C to produce U[N(SiMe$_3$)$_2$]$_2$(CH$_2$SiMe$_2$NSiMe$_3$) as a brown crystalline solid. Yield: 670 mg, 0.93 mmol, 83%.

2.9.14.2 ***From 2.2.*** A solution of **2.2** (50 mg, 0.057 mmol, 1.00 equiv) in 3 mL toluene was refluxed while stirring for 2 h. After cooling, volatiles were removed under reduced pressure. The resulting brown residue was extracted with pentane, filtered and recrystallized at –21 °C to

produce $U[N(SiMe_3)_2]_2(CH_2SiMe_2NSiMe_3)$ as a brown crystalline solid. Yield: 34 mg, 0.047 mmol, 83%.

Characterization of $U[N(SiMe_3)_2]_2(CH_2SiMe_2NSiMe_3)$ by ^1H NMR was consistent with previously reported data.[34]

2.9.15 $U^{IV}[N(SiMe_3)_2]_3I$. A solution of $U[N(SiMe_3)_2]_3$ (100 mg, 0.14 mmol) in 5 mL Et_2O was added to a stirring slurry of $[C_7H_7]BI_4$ (127 mg, 0.21 mmol) in 5 mL Et_2O. The solution rapidly turned pale yellow with a suspended orange solid. After stirring overnight, the residual orange solid was filtered off on a bed of Celite and the volatiles were removed from the filtrate under reduced pressure to yield a tan solid. Recrystallization from minimal hexane at -21°C produced $U^{IV}[N(SiMe_3)_2]_3I$ as tan needles (95 mg, 81%). ^1H NMR (benzene-d_6): δ -0.97 (54H). Elemental analysis found (calculated) for $C_{18}H_{54}IN_3Si_6U$: C, 25.85 (25.55); H, 6.56 (6.43); N, 4.71 (4.97).

2.10 X-Ray Data.

Table 2.10.1 Summary of structure determination.

	2.1-F	**2.1-Cl**	**2.1-Br**
Empirical formula	$C_{18}H_{54}Si_6N_3F_2U$	$C_{18}H_{54}Si_6N_3Cl_2U$	$C_{18}H_{54}Si_6N_3Br_2U$
Formula weight	757.21	790.11	879.03
Temperature	143(1) K	143(1) K	143(1) K
Wavelength	0.71073 Å	0.71073 Å	0.71073 Å
Crystal system	orthorhombic	orthorhombic	monoclinic
Space group	$P2_12_12_1$	$P2_12_12_1$	$P2_1/c$
a	11.7891(7) Å	11.9533(4) Å	12.5472(12) Å
b	12.4396(8) Å	12.5081(4) Å	15.7287(15) Å
c	22.9328(14) Å	22.8740(8) Å	36.278(3) Å
α	90	90	90
β	90	90	98.963(2)°
γ	90	90	90
Volume	3363.1(4) $Å^3$	3420.0(2) $Å^3$	7072.0(11) $Å^3$
Z	4	4	8
Density (calculated)	1.495 Mg/m^3	1.535 Mg/m^3	1.651 Mg/m^3
Absorption coefficient	5.062 mm^{-1}	5.125 mm^{-1}	7.066 mm^{-1}
F(000)	1508	1572	3432
Crystal size	0.50 x 0.38 x 0.25 mm^3	0.28 x 0.25 x 0.18 mm^3	0.30 x 0.15 x 0.15 mm^3
Theta range	1.78 to 27.63°	1.78 to 27.58°	1.64 to 27.50°
Index ranges	$-15 \le h \le 15$, $-16 \le k \le 16$, $-29 \le l \le 29$	$-15 \le h \le 15$, $-16 \le k \le 16$, $-29 \le l \le 29$	$-16 \le h \le 16$, $-20 \le k \le 20$, $-24 \le l \le 46$
Reflections	82945	65838	42607
Independent reflections	7771 [R(int) = 0.0520]	7776 [R(int) = 0.0218]	15933 [R(int) = 0.0344]

Completeness to theta = 27.52 °	99.40%	99.80%	97.90%
Max. and min. transmission	0.7456 and 0.4061	0.7456 and 0.6029	0.7456 and 0.4893
Data / restraints / parameters	7771 / 0 / 291	7776 / 0 / 290	15933 / 0 / 578
Goodness-of-fit on F^2	1.054	1.011	1.076
Final R indices [I>2sigma(I)]	R1 = 0.0176, wR2 = 0.0422	R1 = 0.0110, wR2 = 0.0280	R1 = 0.0341, wR2 = 0.0666
R indices (all data)	R1 = 0.0188, wR2 = 0.0427	R1 = 0.0116, wR2 = 0.0281	R1 = 0.0508, wR2 = 0.0742
Largest diff. peak and hole	1.643 and -0.561 e.Å^{-3}	0.467 and -0.340 e.Å^{-3}	1.000 and -1.672 e.Å^{-3}

	2.1-FCl	**2.1-FN_3**	**2.1-BrCl**
Empirical formula	$C_{18}H_{54}Si_6N_3FClU$	$C_{18}H_{54}Si_6N_6FU$	$C_{18}H_{54}Si_6N_3ClBrU$
Formula weight	773.66	780.24	834.57
Temperature	143(1) K	143(1) K	143(1) K
Wavelength	0.71073 Å	0.71073 Å	0.71069 Å
Crystal system	orthorhombic	monoclinic	orthorhombic
Space group	$P2_12_12_1$	$P2_1/n$	$P2_12_12_1$
a	11.8481(6) Å	18.0120(13) Å	11.9976(7) Å
b	12.5048(5) Å	11.7608(8) Å	12.5197(8) Å
c	22.9076(11) Å	18.2491(13) Å	22.9933(15) Å
α	90	90	90
β	90	115.970(2)°	90
γ	90	90	90
Volume	3393.9(3) Å^3	3475.5(4) Å^3	3453.7(4) Å^3
Z	4	4	4
Density (calculated)	1.514 Mg/m^3	1.491 Mg/m^3	1.605 Mg/m^3
Absorption coefficient	5.090 mm-1	4.899 mm^{-1}	6.154 mm^{-1}
F(000)	1540	1556	1644
Crystal size	0.20 x 0.15 x 0.05 mm^3	0.15 x 0.05 x 0.02 mm^3	0.40 x 0.25 x 0.22 mm^3
Theta range	1.78 to 27.54°	2.12 to 27.53°	1.77 to 27.57°
Index ranges	-15 ≤ h ≤ 15, -16 ≤ k ≤ 16, -29 ≤ l ≤ 29	-23 ≤ h ≤ 23, -15 ≤ k ≤ 15, -23 ≤ l ≤ 23	-15 ≤ h ≤ 14, -16 ≤ k ≤ 16, -29 ≤ l ≤ 29
Reflections	119534	84467	96397
Independent reflections	7818 [R(int) = 0.0539]	8003 [R(int) = 0.0669]	7881 [R(int) = 0.0424]
Completeness to theta = 27.52 °	100.00%	99.80%	99.10%
Max. and min. transmission	0.7456 and 0.5499	0.7456 and 0.5636	0.7456 and 0.5672
Data / restraints / parameters	7818 / 0 / 296	8003 / 0 / 307	7881 / 0 / 296
Goodness-of-fit on F^2	1.01	1.03	1.076
Final R indices [I>2sigma(I)]	R1 = 0.0194, wR2 = 0.0379	R1 = 0.0320, wR2 = 0.0542	R1 = 0.0328, wR2 = 0.0907

R indices (all data)	R1 = 0.0247, wR2 = 0.0394	R1 = 0.0589, wR2 = 0.0608	R1 = 0.0363, wR2 = 0.0939
Largest diff. peak and hole	0.622 and -0.663 e.Å^{-3}	0.817 and -0.643 e.Å^{-3}	1.897 and -1.876 e.Å^{-3}

	2.1-NCS	**2.1-Onap**	$U^{IV}(NO_3)[N(SiMe_3)_2]_3$
Empirical formula	$C_{20}H_{54}Si_6N_5S_2U$	$C_{38}H_{68}N_3Si_6O_2U$	$C_{18}H_{54}Si_6N_4O_3U$
Formula weight	835.37	1005.52	781.22
Temperature	143(1) K	143(1) K	143(1) K
Wavelength	0.71073 Å	0.71073 Å	0.71073 Å
Crystal system	monoclinic	monoclinic	monoclinic
Space group	$P2_1/n$	C2/c	$P2_1/n$
a	12.1020(3) Å	27.051(2) Å	10.4583(5) Å
b	15.1440(4) Å	11.9471(9) Å	30.7382(16) Å
c	20.9071(5) Å	18.0215(13) Å	11.7649(6) Å
α	90	90	90
β	90.1240(10)°	127.293(4)°	114.023(2)°
γ	90	90	90
Volume	3831.69(17) Å^3	4633.4(6) Å^3	3454.5(3) Å^3
Z	4	4	4
Density (calculated)	1.448 Mg/m^3	1.441 Mg/m^3	1.502 Mg/m^3
Absorption coefficient	4.550 mm^{-1}	3.692 mm^{-1}	4.930 mm^{-1}
F(000)	1668	2036	1560
Crystal size	0.20 x 0.15 x 0.05 mm^3	0.25 x 0.10 x 0.05 mm^3	0.25 x 0.10 x 0.10 mm^3
Theta range	1.66 to 27.53°	1.89 to 27.59°	2.01 to 27.55°
Index ranges	-15 ≤ h ≤ 15, -19 ≤ k ≤ 19, -27 ≤ l ≤ 26	-35 ≤ h ≤ 35, -15 ≤ k ≤ 15, -23 ≤ l ≤ 23	-13 ≤ h ≤ 12, 0 ≤ k ≤ 39, 0 ≤ l ≤ 15
Reflections	72576	47574	190603
Independent reflections	8785 [R(int) = 0.0365]	5358 [R(int) = 0.0965]	7952 [R(int) = 0.0570]
Completeness to theta = 27.52 °	99.60%	99.60%	99.80%
Max. and min. transmission	0.7456 and 0.5665	0.7456 and 0.4736	0.7456 and 0.4904
Data / restraints / parameters	8785 / 0 / 325	5358 / 234 / 332	7952 / 0 / 309
Goodness-of-fit on F^2	1.098	1.046	1.161
Final R indices [I>2sigma(I)]	R1 = 0.0646, wR2 = 0.1776	R1 = 0.0467, wR2 = 0.1182	R1 = 0.0488, wR2 = 0.1106
R indices (all data)	R1 = 0.0761, wR2 = 0.1889	R1 = 0.0668, wR2 = 0.1280	R1 = 0.0537, wR2 = 0.1129
Largest diff. peak and hole	5.541 and -2.138 e.Å^{-3}	2.639 and -0.717 e.Å^{-3}	6.769 and -2.105 e.Å^{-3}

	$U^{IV}F[N(SiMe_3)_2]_3$	$U^{IV}Cl[N(SiMe_3)_2]_3$	$U^{IV}I[N(SiMe_3)_2]_3$
Empirical formula	$C_{18}H_{54}Si_6N_3FU$	$C_{18}H_{54}Si_6N_3ClU$	$C_{18}H_{54}Si_6N_3IU$
Formula weight	738.21	754.66	846.11
Temperature	143(1) K	143(1) K	143(1) K

Wavelength	0.71073 Å	0.71073 Å	0.71073 Å
Crystal system	monoclinic	rhombohedral	rhombohedral
Space group	$P2_1/c$	R3c	R3m
a	8.7141(4) Å	18.4409(4) Å	18.2897(7) Å
b	18.2582(8) Å	18.4409(4) Å	18.2897(7) Å
c	21.1970(9) Å	16.9003(4) Å	8.6496(3) Å
α	90	90	90
β	97.711(2)°	90	90
γ	90	120	120
Volume	3342.0(3) $Å^3$	4977.25(19) $Å^3$	2505.76(16) $Å^3$
Z	4	6	3
Density (calculated)	1.467 Mg/m^3	1.511 Mg/m^3	1.682 Mg/m^3
Absorption coefficient	5.088 mm^{-1}	5.200 mm^{-1}	6.009 mm^{-1}
F(000)	1472	2256	1236
Crystal size	0.38 x 0.32 x 0.15 mm^3	0.25 x 0.25 x 0.12 mm^3	0.40 x 0.08 x 0.08 mm^3
Theta range	1.94 to 27.53°	2.21 to 27.50°	2.23 to 27.49°
Index ranges	$-11 \le h \le 11$, $-23 \le k \le 23$, $-27 \le l \le 27$	$-23 \le h \le 23$, $-19 \le k \le 23$, $-21 \le l \le 21$	$-23 \le h \le 11$, $0 \le k \le 23$, $0 \le l \le 11$
Reflections	116565	25931	23795
Independent reflections	7709 [R(int) = 0.0283]	2487 [R(int) = 0.0334]	742 [R(int) = 0.0148]
Completeness to theta = 27.52 °	99.90%	98.40%	100.00%
Max. and min. transmission	0.7456 and 0.4222	0.7456 and 0.4640	0.7456 and 0.5116
Data / restraints / parameters	7709 / 0 / 280	2487 / 1 / 95	742 / 7 / 93
Goodness-of-fit on F^2	1.123	1.035	1.152
Final R indices [I>2sigma(I)]	R1 = 0.0155, wR2 = 0.0348	R1 = 0.0150, wR2 = 0.0340	R1 = 0.0152, wR2 = 0.0436
R indices (all data)	R1 = 0.0187, wR2 = 0.0366	R1 = 0.0209, wR2 = 0.0355	R1 = 0.0153, wR2 = 0.0436
Largest diff. peak and hole	0.996 and -0.503 $e.Å^{-3}$	0.649 and -0.250 $e.Å^{-3}$	1.365 and -0.627 $e.Å^{-3}$

	2.2
Empirical formula	$C_{24}H_{72}Si_8N_4U$
Formula weight	879.61
Temperature	143(1) K
Wavelength	0.71073 Å
Crystal system	monoclinic
Space group	$P2_1/c$
a	15.9454(5) Å
b	11.5448(3) Å
c	23.1960(7) Å
α	90
β	90.003(2)°
γ	90
Volume	4270.1(2) $Å^3$

Z	4
Density (calculated)	1.368 Mg/m^3
Absorption coefficient	4.045 mm^{-1}
F(000)	1792
Crystal size	0.20 x 0.08 x 0.03 mm^3
Theta range	1.76 to 27.52°
Index ranges	-20 ≤ h ≤ 20, -14 ≤ k ≤ 14, -30 ≤ l ≤ 30
Reflections	80300
Independent reflections	9817 [R(int) = 0.0361]
Completeness to theta = 27.52 °	99.90%
Max. and min. transmission	0.7456 and 0.6247
Data / restraints / parameters	9817 / 0 / 359
Goodness-of-fit on F^2	1.011
Final R indices [I>2sigma(I)]	R1 = 0.0181, wR2 = 0.0378
R indices (all data)	R1 = 0.0279, wR2 = 0.0407
Largest diff. peak and hole	0.603 and -0.348 e.$Å^{-3}$

Table 2.10.2 Bond lengths of **2.1-F** (Å).

U1-F1	2.0562(19)	U1-F2	2.0751(18)	U1-N2	2.189(2)
U1-N3	2.187(2)	U1-N1	2.190(3)	U1-Si6	3.4104(9)
U1-Si4	3.4162(9)	U1-Si1	3.4171(10)	U1-Si5	3.4260(8)
U1-Si3	3.4312(9)	U1-Si2	3.4470(8)	Si1-N1	1.753(2)
Si1-C3	1.856(5)	Si1-C2	1.868(4)	Si1-C1	1.874(4)
Si2-N1	1.758(3)	Si2-C4	1.854(4)	Si2-C6	1.869(3)
Si2-C5	1.874(3)	Si3-N2	1.752(3)	Si3-C8	1.862(4)
Si3-C9	1.864(4)	Si3-C7	1.865(4)	Si4-N2	1.762(3)
Si4-C11	1.853(5)	Si4-C10	1.870(4)	Si4-C12	1.877(4)
Si5-N3	1.751(3)	Si5-C13	1.861(4)	Si5-C14	1.870(4)
Si5-C15	1.875(4)	Si6-N3	1.759(3)	Si6-C18	1.865(3)
Si6-C16	1.868(4)	Si6-C17	1.871(4)		

Table 2.10.3 Bond angles of **2.1-F** (°).

F1-U1-F2	178.35(8)	F1-U1-N2	92.15(8)
F1-U1-N3	89.06(8)	F2-U1-N3	89.29(8)
F1-U1-N1	90.28(8)	F2-U1-N1	90.66(8)
N3-U1-N1	118.67(9)	F1-U1-Si6	68.67(6)
N2-U1-Si6	102.98(7)	N3-U1-Si6	26.77(7)
F1-U1-Si4	72.47(5)	F2-U1-Si4	108.67(6)
N3-U1-Si4	135.85(7)	N1-U1-Si4	101.59(7)
F1-U1-Si1	110.97(6)	F2-U1-Si1	70.32(6)
N3-U1-Si1	132.23(7)	N1-U1-Si1	26.45(7)
Si4-U1-Si1	91.91(3)	F1-U1-Si5	109.18(6)
N2-U1-Si5	133.46(7)	N3-U1-Si5	26.14(7)
Si6-U1-Si5	52.92(2)	Si4-U1-Si5	157.43(2)
F1-U1-Si3	111.51(5)	F2-U1-Si3	68.71(5)
N3-U1-Si3	102.41(6)	N1-U1-Si3	133.91(7)
Si4-U1-Si3	52.80(2)	Si1-U1-Si3	108.82(2)
F1-U1-Si2	70.39(5)	F2-U1-Si2	110.10(5)
N3-U1-Si2	100.79(6)	N1-U1-Si2	25.86(6)
Si4-U1-Si2	109.47(2)	Si1-U1-Si2	52.31(2)

Si3-U1-Si2	156.74(2)	N1-Si1-C3	111.44(16)
C3-Si1-C2	107.4(2)	N1-Si1-C1	111.85(17)
C2-Si1-C1	104.8(2)	N1-Si1-U1	33.81(9)
C2-Si1-U1	79.58(13)	C1-Si1-U1	133.44(16)
N1-Si2-C6	110.64(14)	C4-Si2-C6	109.9(2)
C4-Si2-C5	107.77(16)	C6-Si2-C5	105.36(17)
C4-Si2-U1	112.11(14)	C6-Si2-U1	133.18(12)
N2-Si3-C8	111.68(18)	N2-Si3-C9	111.24(15)
N2-Si3-C7	111.80(19)	C8-Si3-C7	110.5(3)
N2-Si3-U1	33.28(8)	C8-Si3-U1	111.45(17)
C7-Si3-U1	134.14(17)	N2-Si4-C11	112.0(2)
C11-Si4-C10	106.7(2)	N2-Si4-C12	111.07(16)
C10-Si4-C12	106.7(2)	N2-Si4-U1	33.98(8)
C10-Si4-U1	77.77(11)	C12-Si4-U1	131.82(16)
N3-Si5-C14	112.56(15)	C13-Si5-C14	109.48(18)
C13-Si5-C15	107.2(2)	C14-Si5-C15	105.3(2)
C13-Si5-U1	112.44(12)	C14-Si5-U1	134.19(13)
N3-Si6-C18	111.00(13)	N3-Si6-C16	110.27(14)
N3-Si6-C17	111.44(17)	C18-Si6-C17	108.67(17)
N3-Si6-U1	34.06(8)	C18-Si6-U1	110.41(12)
C17-Si6-U1	136.00(13)	Si1-N1-Si2	119.01(15)
Si2-N1-U1	121.24(12)	Si3-N2-Si4	120.05(14)
Si4-N2-U1	119.28(13)	Si5-N3-Si6	120.36(15)
Si6-N3-U1	119.17(13)	N1-Si2-U1	32.90(8)
F2-U1-N2	88.56(8)	C5-Si2-U1	80.68(10)
N2-U1-N3	120.90(9)	C8-Si3-C9	106.3(2)
N2-U1-N1	120.41(10)	C9-Si3-C7	105.0(2)
F2-U1-Si6	109.71(6)	C9-Si3-U1	80.17(12)
N1-U1-Si6	132.61(7)	N2-Si4-C10	110.43(15)
N2-U1-Si4	26.74(7)	C11-Si4-C12	109.7(2)
Si6-U1-Si4	110.74(3)	C11-Si4-U1	114.70(16)
N2-U1-Si1	101.87(7)	N3-Si5-C13	111.27(16)
Si6-U1-Si1	155.15(2)	N3-Si5-C15	110.68(14)
F2-U1-Si5	69.29(6)	N3-Si5-U1	33.39(8)
N1-U1-Si5	100.92(7)	C15-Si5-U1	79.16(12)
Si1-U1-Si5	107.68(3)	C18-Si6-C16	108.63(19)
N2-U1-Si3	26.06(7)	C16-Si6-C17	106.7(2)
Si6-U1-Si3	93.47(2)	C16-Si6-U1	79.03(11)
Si5-U1-Si3	108.58(2)	Si1-N1-U1	119.74(14)
N2-U1-Si2	134.78(7)	Si3-N2-U1	120.66(13)
Si6-U1-Si2	108.14(2)	Si5-N3-U1	120.47(13)
Si5-U1-Si2	91.70(2)	C3-Si1-U1	113.18(14)
N1-Si1-C2	111.56(17)	N1-Si2-C4	111.76(16)
C3-Si1-C1	109.5(2)	N1-Si2-C5	111.22(13)

Table 2.10.4 Bond lengths of **2.1-Cl** (Å).

U1-N4	2.1614(16)	U1-N2	2.1663(15)	U1-N1	2.1687(16)
U1-Cl1	2.5704(5)	U1-Cl2	2.5801(5)	U1-Si4	3.3877(6)
U1-Si1	3.4009(6)	U1-Si6	3.4352(6)	U1-Si5	3.4429(5)
U1-Si2	3.4514(6)	N1-Si6	1.7736(16)	N1-Si5	1.7749(17)
N2-Si4	1.7710(16)	N2-Si3	1.7783(18)	N4-Si2	1.7689(17)
N4-Si1	1.7821(17)	Si1-C3	1.861(2)	Si1-C2	1.867(2)

Si1-C1	1.871(2)	Si2-C4	1.864(2)	Si2-C5	1.866(2)
Si2-C6	1.874(2)	Si3-C7	1.859(2)	Si3-C8	1.867(2)
Si3-C9	1.876(2)	Si4-C12	1.855(2)	Si4-C11	1.871(2)
Si4-C10	1.884(2)	Si5-C15	1.858(2)	Si5-C13	1.874(2)
Si5-C14	1.879(2)	Si6-C17	1.869(2)	Si6-C16	1.871(2)
Si6-C18	1.873(2)				

Table 2.10.5 Bond angles of **2.1-Cl** (°).

N4-U1-N2	125.52(6)	N4-U1-N1	118.71(6)
N4-U1-Cl1	90.42(4)	N2-U1-Cl1	88.51(4)
N4-U1-Cl2	89.60(4)	N2-U1-Cl2	91.86(4)
Cl1-U1-Cl2	179.529(17)	N4-U1-Si4	105.24(4)
N1-U1-Si4	132.61(4)	Cl1-U1-Si4	108.217(15)
N4-U1-Si1	27.32(4)	N2-U1-Si1	104.47(4)
Cl1-U1-Si1	71.112(15)	Cl2-U1-Si1	109.070(16)
N4-U1-Si6	99.88(4)	N2-U1-Si6	130.15(4)
Cl1-U1-Si6	69.979(16)	Cl2-U1-Si6	109.555(16)
Si1-U1-Si6	109.525(15)	N4-U1-Si5	133.62(4)
N1-U1-Si5	26.13(4)	Cl1-U1-Si5	108.320(15)
Si4-U1-Si5	108.099(16)	Si1-U1-Si5	157.735(15)
N4-U1-Si2	25.60(4)	N2-U1-Si2	140.53(4)
Cl1-U1-Si2	108.734(15)	Cl2-U1-Si2	71.144(15)
Si1-U1-Si2	52.916(14)	Si6-U1-Si2	89.322(14)
Si6-N1-Si5	117.78(9)	Si6-N1-U1	120.91(8)
Si4-N2-Si3	117.79(9)	Si4-N2-U1	118.38(9)
Si2-N4-Si1	118.60(9)	Si2-N4-U1	122.53(9)
N4-Si1-C3	110.76(10)	N4-Si1-C2	111.48(10)
N4-Si1-C1	110.79(9)	C3-Si1-C1	109.83(11)
N4-Si1-U1	33.82(5)	C3-Si1-U1	111.76(8)
C1-Si1-U1	79.54(7)	N4-Si2-C4	110.91(10)
C4-Si2-C5	109.59(11)	N4-Si2-C6	112.11(9)
C5-Si2-C6	104.66(11)	N4-Si2-U1	31.87(5)
C5-Si2-U1	132.19(8)	C6-Si2-U1	82.14(7)
N2-Si3-C8	110.02(8)	C7-Si3-C8	109.82(10)
C7-Si3-C9	108.45(10)	C8-Si3-C9	104.86(10)
N2-Si4-C11	111.85(10)	C12-Si4-C11	109.14(11)
C12-Si4-C10	108.97(11)	C11-Si4-C10	104.37(11)
C12-Si4-U1	113.29(8)	C11-Si4-U1	133.55(9)
N1-Si5-C15	110.66(9)	N1-Si5-C13	111.74(9)
N1-Si5-C14	111.91(9)	C15-Si5-C14	109.15(11)
N1-Si5-U1	32.56(5)	C15-Si5-U1	112.05(7)
C14-Si5-U1	133.78(8)	N1-Si6-C17	111.57(10)
C17-Si6-C16	108.77(10)	N1-Si6-C18	111.77(9)
C16-Si6-C18	109.63(10)	N1-Si6-U1	32.79(5)
C16-Si6-U1	110.92(7)	C18-Si6-U1	81.63(7)
N2-U1-N1	115.74(6)	N4-Si2-C5	111.14(10)
N1-U1-Cl1	89.20(4)	C4-Si2-C6	108.20(12)
N1-U1-Cl2	90.37(4)	C4-Si2-U1	112.85(8)
N2-U1-Si4	27.38(4)	N2-Si3-C7	110.70(9)
Cl2-U1-Si4	72.227(15)	N2-Si3-C9	112.81(8)
N1-U1-Si1	134.65(4)	N2-Si4-C12	110.91(9)
Si4-U1-Si1	92.686(15)	N2-Si4-C10	111.36(10)

N1-U1-Si6	26.29(4)	N2-Si4-U1	34.23(6)
Si4-U1-Si6	154.851(14)	C10-Si4-U1	79.08(8)
N2-U1-Si5	97.74(4)	C15-Si5-C13	108.66(11)
Cl2-U1-Si5	71.340(15)	C13-Si5-C14	104.49(11)
Si6-U1-Si5	52.425(15)	C13-Si5-U1	81.35(7)
N1-U1-Si2	100.17(4)	N1-Si6-C16	110.18(9)
Si4-U1-Si2	114.103(14)	C17-Si6-C18	104.75(11)
Si5-U1-Si2	109.223(13)	C17-Si6-U1	134.69(8)
Si5-N1-U1	121.31(8)	C3-Si1-C2	108.90(11)
Si3-N2-U1	123.81(8)	C2-Si1-C1	104.91(11)
Si1-N4-U1	118.86(9)	C2-Si1-U1	134.58(8)

Table 2.10.6 Bond lengths of **2.1-Br** (Å).

U1-N1	2.166(4)	U1-N3	2.166(4)	U1-N2	2.167(4)
U1-Br1	2.7371(6)	U1-Br2	2.7530(6)	U1-Si2	3.4141(14)
U1-Si3	3.4267(14)	U1-Si5	3.4471(15)	Si1-N1	1.780(4)
Si1-C3	1.864(6)	Si1-C2	1.864(5)	Si1-C1	1.874(6)
Si2-N1	1.782(4)	Si2-C4	1.868(5)	Si2-C5	1.871(6)
Si2-C6	1.874(5)	Si3-N2	1.784(4)	Si3-C8	1.858(6)
Si3-C7	1.863(5)	Si3-C9	1.875(6)	Si4-N2	1.775(4)
Si4-C11	1.861(6)	Si4-C12	1.871(7)	Si4-C10	1.877(6)
Si5-N3	1.787(4)	Si5-C14	1.866(6)	Si5-C13	1.873(6)
Si5-C15	1.883(6)	Si6-N3	1.780(4)	Si6-C17	1.870(7)
Si6-C16	1.874(7)	Si6-C18	1.880(6)	U1'-N2'	2.158(4)
U1'-N3'	2.159(4)	U1'-N1'	2.167(4)	U1'-Br2'	2.7378(6)
U1'-Br1'	2.7503(6)	U1'-Si6'	3.4256(15)	U1'-Si3'	3.4396(15)
U1'-Si4'	3.4487(15)	U1'-Si2'	3.4505(16)	U1'-Si1'	3.4506(16)
Si1'-N1'	1.782(5)	Si1'-C1'	1.862(6)	Si1'-C2'	1.865(7)
Si1'-C3'	1.869(6)	Si2'-N1'	1.788(5)	Si2'-C4'	1.850(7)
Si2'-C6'	1.876(7)	Si2'-C5'	1.879(7)	Si3'-N2'	1.776(4)
Si3'-C8'	1.861(7)	Si3'-C7'	1.870(7)	Si3'-C9'	1.883(6)
Si4'-N2'	1.792(4)	Si4'-C12'	1.872(6)	Si4'-C11'	1.874(6)
Si4'-C10'	1.882(6)	Si5'-N3'	1.786(4)	Si5'-C14'	1.873(6)
Si5'-C13'	1.880(6)	Si5'-C15'	1.881(6)	Si6'-N3'	1.781(4)
Si6'-C18'	1.852(6)	Si6'-C16'	1.872(6)	Si6'-C17'	1.876(6)

Table 2.10.7 Bond angles of **2.1-Br** (°).

N1-U1-N3	121.50(15)	N1-U1-N2	117.84(14)
N1-U1-Br1	90.29(10)	N3-U1-Br1	90.32(11)
N1-U1-Br2	89.63(10)	N3-U1-Br2	91.09(11)
Br1-U1-Br2	178.382(19)	N1-U1-Si2	27.04(10)
N2-U1-Si2	134.89(11)	Br1-U1-Si2	72.41(3)
N1-U1-Si3	135.52(10)	N3-U1-Si3	99.82(11)
Br1-U1-Si3	106.35(3)	Br2-U1-Si3	72.63(3)
N1-U1-Si5	102.47(11)	N3-U1-Si5	26.35(11)
Br1-U1-Si5	109.81(3)	Br2-U1-Si5	71.78(3)
Si3-U1-Si5	109.56(4)	N1-Si1-C3	111.0(3)
C3-Si1-C2	107.0(3)	N1-Si1-C1	111.3(2)
C2-Si1-C1	106.4(3)	N1-Si2-C4	112.0(2)
C4-Si2-C5	107.4(3)	N1-Si2-C6	110.9(2)

C5-Si2-C6	106.3(3)	N1-Si2-U1	33.55(12)
C5-Si2-U1	78.87(18)	C6-Si2-U1	131.46(19)
N2-Si3-C7	111.8(2)	C8-Si3-C7	108.5(3)
C8-Si3-C9	108.1(3)	C7-Si3-C9	105.1(3)
C8-Si3-U1	114.1(2)	C7-Si3-U1	132.96(19)
N2-Si4-C11	110.4(2)	N2-Si4-C12	110.7(3)
N2-Si4-C10	113.0(2)	C11-Si4-C10	107.2(3)
N3-Si5-C14	113.2(3)	N3-Si5-C13	111.1(2)
N3-Si5-C15	111.7(2)	C14-Si5-C15	102.7(3)
N3-Si5-U1	32.55(13)	C14-Si5-U1	136.1(2)
C15-Si5-U1	82.2(2)	N3-Si6-C17	111.8(3)
C17-Si6-C16	103.5(3)	N3-Si6-C18	109.7(3)
C16-Si6-C18	110.1(3)	Si1-N1-Si2	116.9(2)
Si2-N1-U1	119.4(2)	Si4-N2-Si3	116.7(2)
Si3-N2-U1	120.0(2)	Si6-N3-Si5	116.0(2)
Si5-N3-U1	121.1(2)	N2'-U1'-N3'	122.76(15)
N3'-U1'-N1'	118.32(16)	N2'-U1'-Br2'	89.87(10)
N1'-U1'-Br2'	89.41(11)	N2'-U1'-Br1'	90.36(10)
N1'-U1'-Br1'	90.72(11)	Br2'-U1'-Br1'	179.63(2)
N3'-U1'-Si6'	26.62(11)	N1'-U1'-Si6'	135.48(13)
Br1'-U1'-Si6'	73.02(3)	N2'-U1'-Si3'	26.09(11)
N1'-U1'-Si3'	134.33(13)	Br2'-U1'-Si3'	71.53(3)
Si6'-U1'-Si3'	90.14(4)	N2'-U1'-Si4'	26.32(11)
N1'-U1'-Si4'	99.43(12)	Br2'-U1'-Si4'	108.30(3)
Si6'-U1'-Si4'	113.45(4)	Si3'-U1'-Si4'	52.41(4)
N3'-U1'-Si2'	100.34(11)	N1'-U1'-Si2'	26.30(13)
Br1'-U1'-Si2'	71.17(3)	Si6'-U1'-Si2'	110.97(4)
Si4'-U1'-Si2'	108.50(4)	N2'-U1'-Si1'	99.77(11)
N1'-U1'-Si1'	26.12(13)	Br2'-U1'-Si1'	70.56(3)
Si6'-U1'-Si1'	157.29(4)	Si3'-U1'-Si1'	109.41(4)
Si2'-U1'-Si1'	52.41(5)	N1'-Si1'-C1'	112.0(3)
C1'-Si1'-C2'	103.7(3)	N1'-Si1'-C3'	111.3(3)
C2'-Si1'-C3'	108.4(3)	N1'-Si1'-U1'	32.36(14)
C2'-Si1'-U1'	82.4(2)	C3'-Si1'-U1'	113.2(2)
N1'-Si2'-C6'	111.2(3)	C4'-Si2'-C6'	107.8(3)
C4'-Si2'-C5'	109.2(3)	C6'-Si2'-C5'	104.5(3)
C4'-Si2'-U1'	112.5(2)	C6'-Si2'-U1'	133.9(2)
N2'-Si3'-C8'	111.8(3)	N2'-Si3'-C7'	109.9(3)
N2'-Si3'-C9'	112.0(2)	C8'-Si3'-C9'	107.9(3)
N2'-Si3'-U1'	32.28(13)	C8'-Si3'-U1'	114.1(2)
C9'-Si3'-U1'	81.55(18)	N2'-Si4'-C12'	110.8(3)
C12'-Si4'-C11'	108.9(3)	N2'-Si4'-C10'	112.1(2)
C11'-Si4'-C10'	108.5(3)	N2'-Si4'-U1'	32.28(13)
C11'-Si4'-U1'	112.8(2)	C10'-Si4'-U1'	81.92(19)
N3'-Si5'-C13'	110.4(2)	C14'-Si5'-C13'	108.2(3)
C14'-Si5'-C15'	103.1(3)	C13'-Si5'-C15'	110.1(3)
N3'-Si6'-C16'	111.0(2)	C18'-Si6'-C16'	109.6(3)
C18'-Si6'-C17'	108.4(3)	C16'-Si6'-C17'	104.8(3)
C18'-Si6'-U1'	114.0(2)	C16'-Si6'-U1'	79.84(18)
Si1'-N1'-Si2'	117.2(2)	Si1'-N1'-U1'	121.5(2)
Si3'-N2'-Si4'	117.0(2)	Si3'-N2'-U1'	121.6(2)
Si6'-N3'-Si5'	116.5(2)	Si6'-N3'-U1'	120.5(2)
N3-U1-N2	120.65(15)	Si3'-U1'-Si2'	157.08(4)
N2-U1-Br1	88.58(11)	N3'-U1'-Si1'	132.61(11)

N2-U1-Br2	90.02(11)	Br1'-U1'-Si1'	109.67(3)
N3-U1-Si2	100.48(11)	Si4'-U1'-Si1'	88.21(4)
Br2-U1-Si2	108.08(3)	N1'-Si1'-C2'	112.7(3)
N2-U1-Si3	26.80(11)	C1'-Si1'-C3'	108.4(3)
Si2-U1-Si3	159.67(4)	C1'-Si1'-U1'	133.4(3)
N2-U1-Si5	135.71(11)	N1'-Si2'-C4'	111.2(3)
Si2-U1-Si5	89.40(4)	N1'-Si2'-C5'	112.6(3)
N1-Si1-C2	112.4(2)	N1'-Si2'-U1'	32.48(15)
C3-Si1-C1	108.4(3)	C5'-Si2'-U1'	82.6(2)
N1-Si2-C5	111.1(2)	C8'-Si3'-C7'	109.8(3)
C4-Si2-C6	108.9(3)	C7'-Si3'-C9'	105.1(3)
C4-Si2-U1	115.45(19)	C7'-Si3'-U1'	130.9(3)
N2-Si3-C8	111.6(3)	N2'-Si4'-C11'	111.3(2)
N2-Si3-C9	111.4(2)	C12'-Si4'-C10'	105.1(3)
N2-Si3-U1	33.21(13)	C12'-Si4'-U1'	132.8(2)
C9-Si3-U1	79.92(18)	N3'-Si5'-C14'	112.1(3)
C11-Si4-C12	109.5(3)	N3'-Si5'-C15'	112.7(2)
C12-Si4-C10	105.9(3)	N3'-Si6'-C18'	110.8(3)
C14-Si5-C13	107.9(3)	N3'-Si6'-C17'	112.0(3)
C13-Si5-C15	109.8(3)	N3'-Si6'-U1'	32.90(13)
C13-Si5-U1	111.28(19)	C17'-Si6'-U1'	132.9(2)
N3-Si6-C16	112.5(2)	Si2'-N1'-U1'	121.2(2)
C17-Si6-C18	109.1(3)	Si4'-N2'-U1'	121.4(2)
Si1-N1-U1	123.6(2)	Si5'-N3'-U1'	123.0(2)
Si4-N2-U1	123.3(2)	N3'-U1'-Si4'	139.16(11)
Si6-N3-U1	122.9(2)	Br1'-U1'-Si4'	72.02(3)
N2'-U1'-N1'	118.86(16)	N2'-U1'-Si2'	133.77(11)
N3'-U1'-Br2'	88.23(11)	Br2'-U1'-Si2'	108.85(3)
N3'-U1'-Br1'	91.41(11)	N3'-U1'-Si3'	102.58(11)
N2'-U1'-Si6'	102.78(11)	Br1'-U1'-Si3'	108.60(3)
Br2'-U1'-Si6'	106.65(3)		

Table 2.10.8 Bond lengths of **2.1-FCl** (Å).

U1-F1'	1.971(8)	U1-F1	2.11(3)	U1-N3	2.173(2)
U1-N2	2.174(3)	U1-N1	2.180(2)	U1-Cl1'	2.391(19)
U1-Cl1	2.538(2)	U1-Si4	3.4134(10)	U1-Si1	3.4141(10)
U1-Si6	3.4248(9)	U1-Si5	3.4279(8)	U1-Si2	3.4291(10)
Si1-N1	1.769(3)	Si1-C3	1.853(5)	Si1-C2	1.871(4)
Si1-C1	1.875(4)	Si2-N1	1.754(3)	Si2-C4	1.861(4)
Si2-C5	1.870(4)	Si2-C6	1.875(4)	Si3-N2	1.768(3)
Si3-C7	1.865(4)	Si3-C8	1.870(4)	Si3-C9	1.878(3)
Si4-N2	1.768(2)	Si4-C12	1.856(4)	Si4-C10	1.867(4)
Si4-C11	1.871(4)	Si5-N3	1.773(3)	Si5-C15	1.858(3)
Si5-C13	1.868(4)	Si5-C14	1.871(4)	Si6-N3	1.762(3)
Si6-C18	1.865(4)	Si6-C16	1.869(3)	Si6-C17	1.874(4)

Table 2.10.9 Bond angles of **2.1-FCl** (°).

F1'-U1-F1	178.5(7)	F1'-U1-N3	87.9(2)
F1'-U1-N2	90.1(2)	F1-U1-N2	89.5(6)
F1'-U1-N1	92.2(2)	F1-U1-N1	89.2(7)

N2-U1-N1	121.26(10)	F1'-U1-Cl1'	177.1(4)
N3-U1-Cl1'	89.4(4)	N2-U1-Cl1'	91.9(4)
F1'-U1-Cl1	2.2(3)	F1-U1-Cl1	178.8(6)
N2-U1-Cl1	89.52(8)	N1-U1-Cl1	90.63(8)
F1'-U1-Si4	111.0(2)	F1-U1-Si4	69.1(6)
N2-U1-Si4	26.76(7)	N1-U1-Si4	102.36(7)
Cl1-U1-Si4	109.74(5)	F1'-U1-Si1	72.8(2)
N3-U1-Si1	135.57(7)	N2-U1-Si1	101.87(7)
Cl1'-U1-Si1	108.8(4)	Cl1-U1-Si1	70.81(5)
F1'-U1-Si6	68.3(2)	F1-U1-Si6	111.0(6)
N2-U1-Si6	132.12(7)	N1-U1-Si6	102.46(7)
Cl1-U1-Si6	70.19(5)	Si4-U1-Si6	155.18(3)
F1'-U1-Si5	107.9(2)	F1-U1-Si5	70.8(7)
N2-U1-Si5	99.94(7)	N1-U1-Si5	134.24(7)
Cl1-U1-Si5	110.12(5)	Si4-U1-Si5	107.62(3)
Si6-U1-Si5	52.82(3)	F1'-U1-Si2	110.9(2)
N3-U1-Si2	101.98(6)	N2-U1-Si2	135.50(7)
Cl1'-U1-Si2	68.9(4)	Cl1-U1-Si2	109.94(5)
Si1-U1-Si2	52.90(3)	Si6-U1-Si2	92.38(2)
N1-Si1-C3	111.46(19)	N1-Si1-C2	110.92(17)
N1-Si1-C1	110.97(15)	C3-Si1-C1	107.9(2)
N1-Si1-U1	33.86(8)	C3-Si1-U1	112.45(16)
C1-Si1-U1	79.26(11)	N1-Si2-C4	111.19(18)
C4-Si2-C5	110.3(2)	N1-Si2-C6	112.00(16)
C5-Si2-C6	104.8(2)	N1-Si2-U1	33.06(9)
C5-Si2-U1	132.91(16)	C6-Si2-U1	80.86(12)
N2-Si3-C8	110.60(14)	C7-Si3-C8	109.73(18)
C7-Si3-C9	108.17(17)	C8-Si3-C9	105.34(16)
C7-Si3-U1	111.83(14)	C8-Si3-U1	132.80(12)
N2-Si4-C12	111.28(16)	N2-Si4-C10	111.65(17)
N2-Si4-C11	111.68(17)	C12-Si4-C11	110.1(2)
N2-Si4-U1	33.63(9)	C12-Si4-U1	112.89(13)
C11-Si4-U1	133.10(16)	N3-Si5-C15	110.64(16)
C15-Si5-C13	107.6(2)	N3-Si5-C14	112.37(16)
C13-Si5-C14	105.35(19)	N3-Si5-U1	33.19(8)
C13-Si5-U1	79.70(11)	C14-Si5-U1	134.20(13)
N3-Si6-C16	110.87(14)	C18-Si6-C16	109.74(18)
C18-Si6-C17	105.5(2)	C16-Si6-C17	108.47(17)
C18-Si6-U1	80.31(12)	C16-Si6-U1	110.71(12)
Si2-N1-Si1	119.82(15)	Si2-N1-U1	120.91(14)
Si4-N2-Si3	118.01(15)	Si4-N2-U1	119.61(15)
Si6-N3-Si5	119.10(15)	Si6-N3-U1	120.64(13)
F1-U1-N3	91.1(6)	N1-U1-Si2	26.03(7)
N3-U1-N2	118.14(9)	Si4-U1-Si2	110.08(2)
N3-U1-N1	120.60(9)	Si5-U1-Si2	109.32(2)
F1-U1-Cl1'	2.5(10)	C3-Si1-C2	109.8(2)
N1-U1-Cl1'	88.6(4)	C2-Si1-C1	105.6(2)
N3-U1-Cl1	90.04(8)	C2-Si1-U1	133.44(17)
Cl1'-U1-Cl1	178.6(4)	N1-Si2-C5	111.28(18)
N3-U1-Si4	132.62(7)	C4-Si2-C6	107.1(2)
Cl1'-U1-Si4	71.6(4)	C4-Si2-U1	112.41(16)
F1-U1-Si1	108.7(7)	N2-Si3-C7	111.07(16)
N1-U1-Si1	26.88(7)	N2-Si3-C9	111.75(13)
Si4-U1-Si1	91.82(3)	N2-Si3-U1	32.06(8)

N3-U1-Si6	26.28(7)	C9-Si3-U1	81.98(10)
Cl1'-U1-Si6	108.9(4)	C12-Si4-C10	107.4(2)
Si1-U1-Si6	110.68(3)	C10-Si4-C11	104.5(2)
N3-U1-Si5	26.54(7)	C10-Si4-U1	79.88(13)
Cl1'-U1-Si5	69.7(4)	N3-Si5-C13	110.95(14)
Si1-U1-Si5	158.18(3)	C15-Si5-C14	109.75(18)
F1-U1-Si2	70.3(6)	C15-Si5-U1	111.76(12)
Si1-N1-U1	119.26(14)	N3-Si6-C18	110.45(15)
Si3-N2-U1	122.37(12)	N3-Si6-C17	111.63(18)
Si5-N3-U1	120.27(13)	N3-Si6-U1	33.08(8)
C17-Si6-U1	135.45(14)		

Table 2.10.10 Bond lengths of **2.1-FN_3** (Å).

U1-F1	2.065(2)	U1-N2	2.183(3)	U1-N3	2.186(3)
U1-N1	2.194(3)	U1-N4	2.210(3)	Si1-N1	1.761(3)
Si1-C3	1.849(5)	Si1-C1	1.869(5)	Si1-C2	1.868(5)
Si2-N1	1.760(3)	Si2-C6	1.858(5)	Si2-C4	1.866(5)
Si2-C5	1.870(5)	Si3-N2	1.770(4)	Si3-C7	1.862(5)
Si3-C9	1.867(5)	Si3-C8	1.867(5)	Si4-N2	1.768(4)
Si4-C12	1.867(6)	Si4-C10	1.870(5)	Si4-C11	1.870(5)
Si5-N3	1.759(3)	Si5-C15	1.866(5)	Si5-C14	1.862(5)
Si5-C13	1.875(5)	Si6-N3	1.763(3)	Si6-C16	1.863(5)
Si6-C18	1.868(5)	Si6-C17	1.866(5)	N4-N5	1.217(5)
N5-N6	1.150(5)				

Table 2.10.11 Bond angles of **2.1-FN_3** (°).

F1-U1-N2	90.45(11)	F1-U1-N3	89.80(11)
F1-U1-N1	89.73(11)	N2-U1-N1	117.32(13)
F1-U1-N4	178.21(11)	N2-U1-N4	90.41(13)
N1-U1-N4	91.26(12)	N1-Si1-C3	111.57(19)
C3-Si1-C1	108.6(2)	N1-Si1-C2	112.8(2)
C1-Si1-C2	105.7(2)	N1-Si2-C6	111.4(2)
C6-Si2-C4	110.6(2)	N1-Si2-C5	111.8(2)
C4-Si2-C5	107.1(3)	N2-Si3-C7	111.73(19)
C7-Si3-C9	108.4(2)	N2-Si3-C8	111.6(2)
C9-Si3-C8	108.8(2)	N2-Si4-C12	112.1(2)
C12-Si4-C10	106.6(3)	N2-Si4-C11	110.1(2)
C10-Si4-C11	109.7(3)	N3-Si5-C15	111.71(19)
C15-Si5-C14	109.0(2)	N3-Si5-C13	110.51(19)
C14-Si5-C13	108.8(2)	N3-Si6-C16	110.8(2)
C16-Si6-C18	106.2(2)	N3-Si6-C17	111.2(2)
C18-Si6-C17	105.9(2)	Si2-N1-Si1	120.38(18)
Si1-N1-U1	120.53(17)	Si3-N2-Si4	119.1(2)
Si4-N2-U1	120.14(19)	Si5-N3-Si6	119.16(19)
Si6-N3-U1	119.67(16)	N5-N4-U1	164.9(3)
N2-U1-N3	119.69(12)	N3-Si5-C14	111.90(19)
N3-U1-N1	122.99(12)	C15-Si5-C13	104.6(2)
N3-U1-N4	88.41(12)	N3-Si6-C18	111.36(19)
N1-Si1-C1	110.09(18)	C16-Si6-C17	111.1(2)
C3-Si1-C2	107.8(2)	Si2-N1-U1	119.06(17)

N1-Si2-C4	110.3(2)	Si3-N2-U1	120.72(18)
C6-Si2-C5	105.5(3)	Si5-N3-U1	121.16(17)
N2-Si3-C9	111.3(2)	N6-N5-N4	179.3(5)
C7-Si3-C8	104.7(3)	C12-Si4-C11	105.9(3)
N2-Si4-C10	112.2(2)		

Table 2.10.12 Bond lengths of **2.1-BrCl** (Å).

U1-N1	2.152(6)	U1-N3	2.163(5)	U1-N2	2.174(5)
U1-Cl1	2.56(4)	U1-Cl1'	2.56(4)	U1-Br1'	2.628(18)
U1-Br1	2.670(12)	U1-Si5	3.3970(18)	U1-Si3	3.4047(19)
U1-Si1	3.4404(18)	U1-Si2	3.4434(17)	U1-Si4	3.4468(18)
Si1-N1	1.779(5)	Si1-C1	1.872(8)	Si1-C3	1.876(7)
Si1-C2	1.880(9)	Si2-N1	1.791(6)	Si2-C4	1.860(8)
Si2-C6	1.871(7)	Si2-C5	1.876(8)	Si3-N2	1.767(6)
Si3-C7	1.851(8)	Si3-C8	1.866(9)	Si3-C9	1.874(9)
Si4-N2	1.765(6)	Si4-C12	1.873(8)	Si4-C10	1.880(8)
Si4-C11	1.887(8)	Si5-N3	1.775(5)	Si5-C14	1.867(8)
Si5-C13	1.879(8)	Si5-C15	1.890(9)	Si6-N3	1.786(5)
Si6-C16	1.858(7)	Si6-C17	1.868(7)	Si6-C18	1.885(7)

Table 2.10.13 Bond angles of **2.1-BrCl** (°).

N1-U1-N3	116.2(2)	N1-U1-N2	118.8(2)
N1-U1-Cl1	88.4(10)	N3-U1-Cl1	89.1(9)
N1-U1-Cl1'	90.2(11)	N3-U1-Cl1'	91.6(10)
Cl1-U1-Cl1'	178.7(14)	N1-U1-Br1'	89.1(5)
N2-U1-Br1'	90.1(4)	Cl1-U1-Br1'	0.7(15)
N1-U1-Br1	91.1(4)	N3-U1-Br1	91.5(3)
Cl1-U1-Br1	179.4(11)	Cl1'-U1-Br1	0.9(14)
N1-U1-Si5	133.09(15)	N3-U1-Si5	27.22(13)
Cl1-U1-Si5	108.8(10)	Cl1'-U1-Si5	72.3(10)
Br1-U1-Si5	71.9(3)	N1-U1-Si3	134.24(15)
N2-U1-Si3	26.95(15)	Cl1-U1-Si3	71.4(9)
Br1'-U1-Si3	70.9(4)	Br1-U1-Si3	108.7(3)
N1-U1-Si1	26.07(15)	N3-U1-Si1	130.61(14)
Cl1-U1-Si1	69.4(10)	Cl1'-U1-Si1	109.3(10)
Br1-U1-Si1	110.0(3)	Si5-U1-Si1	155.18(5)
N1-U1-Si2	26.37(15)	N3-U1-Si2	97.86(15)
Cl1-U1-Si2	107.7(10)	Cl1'-U1-Si2	71.1(11)
Br1-U1-Si2	72.0(3)	Si5-U1-Si2	108.28(5)
Si1-U1-Si2	52.43(5)	N1-U1-Si4	100.21(14)
N2-U1-Si4	25.81(15)	Cl1-U1-Si4	108.7(9)
Br1'-U1-Si4	108.6(4)	Br1-U1-Si4	70.9(3)
Si3-U1-Si4	52.75(5)	Si1-U1-Si4	89.40(4)
N1-Si1-C1	111.4(3)	N1-Si1-C3	110.2(3)
N1-Si1-C2	112.0(3)	C1-Si1-C2	104.7(4)
N1-Si1-U1	32.1(2)	C1-Si1-U1	81.9(2)
C2-Si1-U1	134.6(3)	N1-Si2-C4	110.4(3)
C4-Si2-C6	109.0(4)	N1-Si2-C5	111.6(3)
C6-Si2-C5	104.8(4)	N1-Si2-U1	32.25(17)
C6-Si2-U1	81.2(2)	C5-Si2-U1	133.1(3)

N2-Si3-C8	111.0(4)	C7-Si3-C8	109.1(4)
C7-Si3-C9	109.5(4)	C8-Si3-C9	104.2(4)
C7-Si3-U1	112.3(3)	C8-Si3-U1	134.0(3)
N2-Si4-C12	110.8(4)	N2-Si4-C10	113.0(3)
N2-Si4-C11	110.8(4)	C12-Si4-C11	111.3(4)
N2-Si4-U1	32.44(17)	C12-Si4-U1	112.6(3)
C11-Si4-U1	131.5(3)	N3-Si5-C14	112.7(3)
C14-Si5-C13	104.1(4)	N3-Si5-C15	110.2(3)
C13-Si5-C15	108.9(4)	N3-Si5-U1	33.88(17)
C13-Si5-U1	79.2(3)	C15-Si5-U1	112.5(3)
N3-Si6-C17	110.2(3)	C16-Si6-C17	109.7(4)
C16-Si6-C18	108.6(3)	C17-Si6-C18	104.0(3)
Si1-N1-U1	121.8(3)	Si2-N1-U1	121.4(3)
Si4-N2-U1	121.8(3)	Si3-N2-U1	119.2(3)
Si5-N3-U1	118.9(3)	Si6-N3-U1	123.8(2)
N3-U1-N2	124.9(2)	Cl1'-U1-Si4	71.4(10)
N2-U1-Cl1	90.4(9)	Si5-U1-Si4	113.73(5)
N2-U1-Cl1'	90.1(10)	Si2-U1-Si4	109.54(4)
N3-U1-Br1'	88.7(5)	C1-Si1-C3	109.7(4)
Cl1'-U1-Br1'	179.4(12)	C3-Si1-C2	108.7(4)
N2-U1-Br1	89.5(4)	C3-Si1-U1	110.9(2)
Br1'-U1-Br1	179.6(5)	N1-Si2-C6	111.4(3)
N2-U1-Si5	104.81(14)	C4-Si2-C5	109.5(4)
Br1'-U1-Si5	108.2(5)	C4-Si2-U1	112.1(3)
N3-U1-Si3	104.36(15)	N2-Si3-C7	111.6(4)
Cl1'-U1-Si3	109.5(11)	N2-Si3-C9	111.1(3)
Si5-U1-Si3	92.61(5)	N2-Si3-U1	33.90(17)
N2-U1-Si1	99.98(14)	C9-Si3-U1	79.9(3)
Br1'-U1-Si1	70.1(5)	C12-Si4-C10	108.1(4)
Si3-U1-Si1	109.32(5)	C10-Si4-C11	102.6(4)
N2-U1-Si2	134.10(15)	C10-Si4-U1	82.6(2)
Br1'-U1-Si2	108.3(5)	N3-Si5-C13	111.2(3)
Si3-U1-Si2	157.70(5)	C14-Si5-C15	109.5(4)
N3-U1-Si4	139.99(14)	C14-Si5-U1	134.1(3)
Si1-N1-Si2	116.8(3)	N3-Si6-C16	111.2(3)
Si4-N2-Si3	119.1(3)	N3-Si6-C18	113.0(3)
Si5-N3-Si6	117.3(3)		

Table 2.10.14 Bond lengths of **2.1-NCS** (Å).

U1-N2	2.148(8)	U1-N3	2.156(8)	U1-N1	2.158(7)
U1-N4	2.313(10)	U1-N5	2.319(9)	U1-Si6	3.398(3)
U1-Si5	3.417(3)	U1-Si4	3.420(3)	U1-Si3	3.425(3)
U1-Si2	3.425(3)	U1-Si1	3.432(3)	S1-C19	1.589(11)
S2-C20	1.573(12)	Si1-N1	1.739(8)	Si1-C2	1.858(12)
Si1-C3	1.881(14)	Si1-C1	1.909(13)	Si2-N1	1.829(9)
Si2-C6	1.848(13)	Si2-C4	1.865(12)	Si2-C5	1.884(12)
Si3-N2	1.769(8)	Si3-C9	1.880(12)	Si3-C7	1.889(13)
Si3-C8	1.905(13)	Si4-N2	1.785(8)	Si4-C11	1.854(11)
Si4-C12	1.881(12)	Si4-C10	1.887(12)	Si5-N3	1.749(9)
Si5-C14	1.869(13)	Si5-C13	1.885(12)	Si5-C15	1.903(12)
Si6-N3	1.784(9)	Si6-C17	1.847(13)	Si6-C18	1.885(13)
Si6-C16	1.897(13)	N4-C19	1.172(14)	N5-C20	1.156(15)

Table 2.10.15 Bond angles of **2.1-NCS** (°).

N2-U1-N3	119.2(3)	N2-U1-N1	120.6(3)
N2-U1-N4	90.5(3)	N3-U1-N4	90.2(3)
N2-U1-N5	90.1(3)	N3-U1-N5	89.7(3)
N4-U1-N5	179.3(3)	N2-U1-Si6	134.7(2)
N1-U1-Si6	100.6(2)	N4-U1-Si6	70.1(2)
N2-U1-Si5	100.5(2)	N3-U1-Si5	25.8(2)
N4-U1-Si5	109.1(2)	N5-U1-Si5	71.0(2)
N2-U1-Si4	26.7(2)	N3-U1-Si4	99.8(2)
N4-U1-Si4	71.3(2)	N5-U1-Si4	109.3(2)
Si5-U1-Si4	89.19(7)	N2-U1-Si3	26.1(2)
N1-U1-Si3	100.7(2)	N4-U1-Si3	108.5(2)
Si6-U1-Si3	158.66(8)	Si5-U1-Si3	110.59(8)
N2-U1-Si2	100.9(2)	N3-U1-Si2	135.2(2)
N4-U1-Si2	69.1(2)	N5-U1-Si2	110.6(2)
Si5-U1-Si2	158.54(7)	Si4-U1-Si2	109.50(7)
N2-U1-Si1	135.5(2)	N3-U1-Si1	101.4(2)
N4-U1-Si1	107.7(2)	N5-U1-Si1	71.7(2)
Si5-U1-Si1	110.48(8)	Si4-U1-Si1	158.79(7)
Si2-U1-Si1	53.14(8)	N1-Si1-C2	112.6(5)
C2-Si1-C3	110.8(6)	N1-Si1-C1	110.1(5)
C3-Si1-C1	108.1(8)	N1-Si1-U1	31.8(3)
C3-Si1-U1	111.5(5)	C1-Si1-U1	79.8(4)
N1-Si2-C4	109.4(6)	C6-Si2-C4	109.4(7)
C6-Si2-C5	109.6(6)	C4-Si2-C5	106.3(6)
C6-Si2-U1	112.8(4)	C4-Si2-U1	132.6(5)
N2-Si3-C9	111.4(5)	N2-Si3-C7	109.9(5)
N2-Si3-C8	110.1(5)	C9-Si3-C8	106.3(6)
N2-Si3-U1	32.3(3)	C9-Si3-U1	132.2(4)
C8-Si3-U1	79.4(4)	N2-Si4-C11	110.6(5)
C11-Si4-C12	108.9(6)	N2-Si4-C10	109.9(5)
C12-Si4-C10	105.9(6)	N2-Si4-U1	32.8(3)
C12-Si4-U1	80.6(4)	C10-Si4-U1	132.0(5)
N3-Si5-C13	111.6(5)	C14-Si5-C13	105.9(6)
C14-Si5-C15	111.0(6)	C13-Si5-C15	106.8(7)
C14-Si5-U1	131.8(4)	C13-Si5-U1	80.9(4)
N3-Si6-C17	111.0(5)	N3-Si6-C18	112.4(5)
N3-Si6-C16	109.9(6)	C17-Si6-C16	108.6(6)
N3-Si6-U1	33.7(3)	C17-Si6-U1	112.7(4)
C16-Si6-U1	133.2(5)	Si1-N1-Si2	118.5(4)
Si2-N1-U1	118.2(4)	Si3-N2-Si4	117.8(5)
Si4-N2-U1	120.5(4)	Si5-N3-Si6	119.4(5)
Si6-N3-U1	118.9(4)	C19-N4-U1	176.3(8)
N4-C19-S1	179.5(11)	N5-C20-S2	178.4(11)
N3-U1-N1	120.2(3)	C2-Si1-U1	132.8(4)
N1-U1-N4	90.1(3)	N1-Si2-C6	111.7(5)
N1-U1-N5	89.4(3)	N1-Si2-C5	110.3(5)
N3-U1-Si6	27.4(2)	N1-Si2-U1	33.7(2)
N5-U1-Si6	109.6(2)	C5-Si2-U1	79.0(4)
N1-U1-Si5	134.7(2)	C9-Si3-C7	110.9(6)
Si6-U1-Si5	53.18(9)	C7-Si3-C8	108.2(7)

N1-U1-Si4	136.1(2)	C7-Si3-U1	111.9(5)
Si6-U1-Si4	109.03(7)	N2-Si4-C12	111.2(5)
N3-U1-Si3	135.2(2)	C11-Si4-C10	110.3(6)
N5-U1-Si3	72.0(2)	C11-Si4-U1	112.1(4)
Si4-U1-Si3	52.82(7)	N3-Si5-C14	110.5(5)
N1-U1-Si2	28.1(2)	N3-Si5-C15	110.9(5)
Si6-U1-Si2	108.80(8)	N3-Si5-U1	32.5(3)
Si3-U1-Si2	89.62(7)	C15-Si5-U1	112.2(4)
N1-U1-Si1	25.1(2)	C17-Si6-C18	108.6(7)
Si6-U1-Si1	89.73(7)	C18-Si6-C16	106.1(7)
Si3-U1-Si1	110.39(8)	C18-Si6-U1	80.9(4)
N1-Si1-C3	109.3(5)	Si1-N1-U1	123.1(4)
C2-Si1-C1	105.9(6)	Si3-N2-U1	121.6(4)
C20-N5-U1	175.5(10)	Si5-N3-U1	121.7(4)

Table 2.10.16 Bond lengths of **2.1-ONap** (Å).

U1-O1	2.102(4)	U1-O1#1	2.102(4)	U1-N2#1	2.212(5)
U1-N2	2.212(5)	U1-N1	2.243(7)	U1-Si3'	3.426(6)
U1-Si3'#1	3.426(6)	U1-Si2'	3.436(5)	U1-Si2'#1	3.436(5)
O1-C1	1.370(8)	C1-C10	1.356(10)	C1-C2	1.411(11)
C2-C3	1.384(11)	C3-C4	1.384(12)	C4-C9	1.408(11)
C4-C5	1.437(11)	C5-C6	1.327(13)	C6-C7	1.415(15)
C7-C8	1.356(12)	C8-C9	1.385(11)	C9-C10	1.451(11)
N1-Si1#1	1.740(5)	N1-Si1	1.740(5)	N1-Si1'#1	1.784(6)
N1-Si1'	1.784(6)	Si1-C11	1.834(13)	Si1-C12	1.890(12)
Si1-C13	1.882(14)	Si1'-C13'	1.86(2)	Si1'-C12'	1.89(2)
Si1'-C11'	1.90(2)	N2-Si3'	1.736(8)	N2-Si2'	1.745(8)
N2-Si2	1.747(6)	N2-Si3	1.788(6)	Si2-C16	1.829(12)
Si2-C14	1.877(13)	Si2-C15	1.87(2)	C16-Si2'	1.759(13)
Si2'-C15'	1.87(3)	Si2'-C14'	1.90(2)	Si3-C19	1.844(10)
Si3-C17	1.883(12)	Si3-C18	1.882(14)	C19-Si3'	1.907(11)
Si3'-C18'	1.88(2)	Si3'-C17'	1.88(4)		

Symmetry transformations used to generate equivalent atoms:

#1 -x,y,-z+1/2

Table 2.10.17 Bond angles of **2.1-ONap** (°).

O1-U1-O1#1	177.7(2)	O1-U1-N2#1	88.83(19)
O1-U1-N2	89.87(19)	O1#1-U1-N2	88.83(19)
O1-U1-N1	91.13(12)	O1#1-U1-N1	91.13(12)
N2-U1-N1	124.89(13)	O1-U1-Si3'	108.84(16)
N2#1-U1-Si3'	126.45(17)	N2-U1-Si3'	26.04(17)
O1-U1-Si3'#1	70.52(16)	O1#1-U1-Si3'#1	108.84(16)
N2-U1-Si3'#1	126.45(17)	N1-U1-Si3'#1	105.43(11)
O1-U1-Si2'	68.53(16)	O1#1-U1-Si2'	109.73(16)
N2-U1-Si2'	26.07(18)	N1-U1-Si2'	136.26(10)
Si3'#1-U1-Si2'	103.40(15)	O1-U1-Si2'#1	109.73(16)
N2#1-U1-Si2'#1	26.07(18)	N2-U1-Si2'#1	94.11(17)
Si3'-U1-Si2'#1	103.40(15)	Si3'#1-U1-Si2'#1	51.97(15)
C1-O1-U1	164.8(4)	C10-C1-O1	121.8(7)

O1-C1-C2	119.0(6)	C3-C2-C1	121.2(8)
C3-C4-C9	119.8(8)	C3-C4-C5	122.8(8)
C6-C5-C4	120.9(9)	C5-C6-C7	119.9(9)
C7-C8-C9	118.9(9)	C8-C9-C4	121.2(8)
C4-C9-C10	118.5(7)	C1-C10-C9	120.7(8)
Si1#1-N1-Si1'#1	34.0(2)	Si1-N1-Si1'#1	104.2(4)
Si1-N1-Si1'	34.0(2)	Si1'#1-N1-Si1'	111.9(5)
Si1-N1-U1	121.5(2)	Si1'#1-N1-U1	124.0(2)
N1-Si1-C11	114.9(6)	N1-Si1-C12	109.9(4)
N1-Si1-C13	113.0(6)	C11-Si1-C13	103.1(8)
N1-Si1'-C13'	116.3(10)	N1-Si1'-C12'	108.1(7)
N1-Si1'-C11'	113.4(9)	C13'-Si1'-C11'	103.1(11)
Si3'-N2-Si2'	119.5(4)	Si3'-N2-Si2	77.8(3)
Si3'-N2-Si3	68.6(3)	Si2'-N2-Si3	87.4(3)
Si3'-N2-U1	120.0(3)	Si2'-N2-U1	120.1(4)
Si3-N2-U1	120.9(3)	N2-Si2-C16	113.5(5)
C16-Si2-C14	101.1(7)	N2-Si2-C15	112.2(6)
C14-Si2-C15	107.0(8)	Si2'-C16-Si2	62.6(4)
N2-Si2'-C15'	111.5(13)	C16-Si2'-C15'	94.2(13)
C16-Si2'-C14'	114.1(10)	C15'-Si2'-C14'	105.0(14)
C16-Si2'-U1	119.2(6)	C15'-Si2'-U1	139.1(12)
N2-Si3-C19	111.3(4)	N2-Si3-C17	114.8(4)
N2-Si3-C18	110.4(7)	C19-Si3-C18	106.4(7)
Si3-C19-Si3'	63.9(4)	N2-Si3'-C18'	110.7(7)
C18'-Si3'-C19	102.4(8)	N2-Si3'-C17'	113.8(11)
C19-Si3'-C17'	113.4(15)	N2-Si3'-U1	34.0(2)
C19-Si3'-U1	110.5(4)	C17'-Si3'-U1	134.1(13)
O1#1-U1-N2#1	89.87(19)	C12-Si1-C13	109.8(7)
N2#1-U1-N2	110.2(3)	C13'-Si1'-C12'	106.6(11)
N2#1-U1-N1	124.89(13)	C12'-Si1'-C11'	109.1(10)
O1#1-U1-Si3'	70.52(16)	Si2'-N2-Si2	64.6(3)
N1-U1-Si3'	105.43(11)	Si2-N2-Si3	116.5(3)
N2#1-U1-Si3'#1	26.04(18)	Si2-N2-U1	122.5(3)
Si3'-U1-Si3'#1	149.1(2)	N2-Si2-C14	110.4(4)
N2#1-U1-Si2'	94.11(17)	C16-Si2-C15	112.0(8)
Si3'-U1-Si2'	51.97(15)	N2-Si2'-C16	117.2(6)
O1#1-U1-Si2'#1	68.53(16)	N2-Si2'-C14'	112.6(8)
N1-U1-Si2'#1	136.26(10)	N2-Si2'-U1	33.9(2)
Si2'-U1-Si2'#1	87.5(2)	C14'-Si2'-U1	83.5(7)
C10-C1-C2	119.2(7)	C19-Si3-C17	108.9(6)
C4-C3-C2	120.5(8)	C17-Si3-C18	104.4(7)
C9-C4-C5	117.4(8)	N2-Si3'-C19	110.8(5)
C8-C7-C6	121.7(9)	C18'-Si3'-C17'	105.0(16)
C8-C9-C10	120.2(8)	C18'-Si3'-U1	78.0(7)
Si1#1-N1-Si1	117.1(4)	Si1'-N1-U1	124.0(2)
Si1#1-N1-Si1'	104.2(4)	C11-Si1-C12	105.8(7)
Si1#1-N1-U1	121.5(2)		

Symmetry transformations used to generate equivalent atoms:

#1 -x,y,-z+1/2

Table 2.10.18 Bond lengths of $U^{IV}(NO_3)[N(SiMe_3)_2]_3$ (Å).

U1-N1	2.235(6)	U1-N3	2.241(6)	U1-N2	2.251(6)

U1-O2	2.419(6)	U1-O1	2.541(6)	U1-N4	2.923(7)
U1-Si5	3.322(2)	U1-Si4	3.3612(19)	U1-Si2	3.420(2)
U1-Si1	3.456(2)	Si1-N1	1.731(6)	Si1-C3	1.867(10)
Si1-C1	1.870(9)	Si1-C2	1.877(10)	Si2-N1	1.748(6)
Si2-C5	1.854(9)	Si2-C4	1.865(9)	Si2-C6	1.876(9)
Si3-N2	1.757(6)	Si3-C7	1.861(9)	Si3-C8	1.876(9)
Si3-C9	1.878(8)	Si4-N2	1.754(6)	Si4-C11	1.866(9)
Si4-C12	1.868(8)	Si4-C10	1.875(8)	Si5-N3	1.732(6)
Si5-C14	1.866(9)	Si5-C15	1.866(10)	Si5-C13	1.884(8)
Si6-N3	1.767(6)	Si6-C18	1.862(9)	Si6-C16	1.873(9)
Si6-C17	1.877(9)	O1-N4	1.285(11)	O2-N4	1.291(10)
O3-N4	1.202(10)				

Table 2.10.19 Bond angles of $U^{IV}(NO_3)[N(SiMe_3)_2]_3$ (°).

N1-U1-N3	127.2(2)	N1-U1-N2	109.3(2)
N1-U1-O2	101.0(2)	N3-U1-O2	112.4(2)
N1-U1-O1	78.3(2)	N3-U1-O1	91.3(2)
O2-U1-O1	51.8(2)	N1-U1-N4	88.9(2)
N2-U1-N4	123.5(2)	O2-U1-N4	25.8(2)
N1-U1-Si5	117.22(15)	N3-U1-Si5	28.73(14)
O2-U1-Si5	137.77(16)	O1-U1-Si5	117.16(18)
N1-U1-Si4	131.79(16)	N3-U1-Si4	96.04(15)
O2-U1-Si4	76.44(16)	O1-U1-Si4	126.10(16)
Si5-U1-Si4	89.70(5)	N1-U1-Si2	26.85(15)
N2-U1-Si2	96.44(14)	O2-U1-Si2	79.67(16)
N4-U1-Si2	76.30(15)	Si5-U1-Si2	141.90(5)
N1-U1-Si1	25.52(16)	N3-U1-Si1	101.72(15)
O2-U1-Si1	115.86(16)	O1-U1-Si1	75.87(15)
Si5-U1-Si1	95.25(5)	Si4-U1-Si1	151.54(5)
N1-Si1-C3	112.2(4)	N1-Si1-C1	113.8(4)
N1-Si1-C2	108.9(4)	C3-Si1-C2	108.9(5)
N1-Si1-U1	33.8(2)	C3-Si1-U1	118.9(3)
C2-Si1-U1	75.8(3)	N1-Si2-C5	110.1(3)
C5-Si2-C4	108.5(5)	N1-Si2-C6	112.6(4)
C4-Si2-C6	107.3(4)	N1-Si2-U1	35.29(19)
C4-Si2-U1	137.1(3)	C6-Si2-U1	111.7(3)
N2-Si3-C8	112.4(4)	C7-Si3-C8	105.9(5)
C7-Si3-C9	105.5(4)	C8-Si3-C9	107.6(5)
N2-Si4-C12	109.4(3)	C11-Si4-C12	105.3(4)
C11-Si4-C10	108.9(4)	C12-Si4-C10	106.5(4)
C11-Si4-U1	106.7(3)	C12-Si4-U1	75.2(3)
N3-Si5-C14	115.1(4)	N3-Si5-C15	113.3(4)
N3-Si5-C13	107.5(3)	C14-Si5-C13	104.9(4)
N3-Si5-U1	38.45(19)	C14-Si5-U1	141.1(4)
C13-Si5-U1	72.6(2)	N3-Si6-C18	113.4(3)
C18-Si6-C16	107.1(5)	N3-Si6-C17	111.8(4)
C16-Si6-C17	109.0(4)	N4-O1-U1	93.8(5)
Si1-N1-Si2	120.1(3)	Si1-N1-U1	120.7(3)
Si4-N2-Si3	116.8(3)	Si4-N2-U1	113.5(3)
Si5-N3-Si6	118.0(3)	Si5-N3-U1	112.8(3)
O3-N4-O1	123.2(9)	O3-N4-O2	122.0(9)
O3-N4-U1	175.9(8)	O1-N4-U1	60.2(4)

N3-U1-N2	105.2(2)	C5-Si2-C6	106.2(5)
N2-U1-O2	97.8(2)	C5-Si2-U1	77.2(3)
N2-U1-O1	149.5(2)	N2-Si3-C7	112.8(3)
N3-U1-N4	103.8(2)	N2-Si3-C9	112.2(3)
O1-U1-N4	26.0(2)	N2-Si4-C11	111.6(3)
N2-U1-Si5	86.36(15)	N2-Si4-C10	114.5(4)
N4-U1-Si5	132.50(16)	N2-Si4-U1	37.89(19)
N2-U1-Si4	28.59(15)	C10-Si4-U1	142.3(3)
N4-U1-Si4	101.51(18)	C14-Si5-C15	108.2(5)
N3-U1-Si2	152.97(15)	C15-Si5-C13	107.3(4)
O1-U1-Si2	77.20(17)	C15-Si5-U1	109.5(3)
Si4-U1-Si2	110.55(5)	N3-Si6-C16	110.5(4)
N2-U1-Si1	123.68(15)	C18-Si6-C17	104.7(4)
N4-U1-Si1	95.68(16)	N4-O2-U1	99.5(5)
Si2-U1-Si1	51.98(5)	Si2-N1-U1	117.9(3)
C3-Si1-C1	107.4(5)	Si3-N2-U1	129.5(3)
C1-Si1-C2	105.2(5)	Si6-N3-U1	129.1(3)
C1-Si1-U1	130.8(4)	O1-N4-O2	114.8(7)
N1-Si2-C4	111.9(4)	O2-N4-U1	54.7(4)

Table 2.10.20 Bond lengths of $U^{IV}F[N(SiMe_3)_2]_3$ (Å).

U1-F1	2.0649(12)	U1-N1	2.2498(16)	U1-N3	2.2530(15)
U1-N2	2.2533(16)	U1-Si5	3.3851(5)	U1-Si1	3.3926(6)
U1-Si4	3.4346(6)	U1-Si3	3.4473(6)	Si1-N1	1.7224(17)
Si1-C3	1.867(2)	Si1-C2	1.867(2)	Si1-C1	1.877(2)
N1-Si2	1.7427(17)	Si2-C6	1.861(2)	Si2-C5	1.866(3)
Si2-C4	1.871(2)	N2-Si3	1.7302(17)	N2-Si4	1.7386(17)
Si3-C8	1.868(3)	Si3-C9	1.871(3)	Si3-C7	1.871(3)
N3-Si5	1.7307(16)	N3-Si6	1.7388(16)	Si4-C11	1.859(3)
Si4-C12	1.867(2)	Si4-C10	1.871(3)	Si5-C14	1.869(2)
Si5-C15	1.870(2)	Si5-C13	1.875(2)	Si6-C17	1.866(2)
Si6-C18	1.869(2)	Si6-C16	1.870(2)		

Table 2.10.21 Bond angles of $U^{IV}F[N(SiMe_3)_2]_3$ (°).

F1-U1-N1	91.88(5)	F1-U1-N3	93.26(5)
F1-U1-N2	93.70(6)	N1-U1-N2	117.50(6)
F1-U1-Si5	115.32(4)	N1-U1-Si5	131.25(4)
N2-U1-Si5	101.07(4)	F1-U1-Si1	113.41(4)
N3-U1-Si1	101.93(4)	N2-U1-Si1	128.02(4)
F1-U1-Si4	72.16(4)	N1-U1-Si4	131.57(4)
N2-U1-Si4	26.51(4)	Si5-U1-Si4	96.166(14)
F1-U1-Si3	114.01(4)	N1-U1-Si3	99.21(4)
N2-U1-Si3	25.96(4)	Si5-U1-Si3	104.453(14)
Si4-U1-Si3	52.463(15)	N1-Si1-C3	114.15(10)
C3-Si1-C2	108.80(11)	N1-Si1-C1	106.85(10)
C2-Si1-C1	107.48(12)	N1-Si1-U1	36.33(5)
C2-Si1-U1	126.43(8)	C1-Si1-U1	70.55(8)
Si1-N1-U1	116.69(8)	Si2-N1-U1	120.39(9)
N1-Si2-C5	108.26(9)	C6-Si2-C5	109.91(14)
C6-Si2-C4	106.58(13)	C5-Si2-C4	107.58(12)

Si3-N2-U1	119.28(9)	Si4-N2-U1	118.15(8)
N2-Si3-C9	113.81(11)	C8-Si3-C9	107.91(13)
C8-Si3-C7	107.94(13)	C9-Si3-C7	106.37(13)
C8-Si3-U1	127.08(10)	C9-Si3-U1	122.75(9)
Si5-N3-Si6	122.33(9)	Si5-N3-U1	115.75(8)
N2-Si4-C11	111.41(11)	N2-Si4-C12	109.14(10)
N2-Si4-C10	113.34(11)	C11-Si4-C10	107.56(14)
N2-Si4-U1	35.34(5)	C11-Si4-U1	106.38(10)
C10-Si4-U1	141.63(10)	N3-Si5-C14	113.63(10)
C14-Si5-C15	108.88(11)	N3-Si5-C13	106.88(9)
C15-Si5-C13	106.74(11)	N3-Si5-U1	36.83(5)
C15-Si5-U1	122.81(8)	C13-Si5-U1	70.13(7)
N3-Si6-C18	109.06(9)	C17-Si6-C18	108.68(12)
C17-Si6-C16	107.21(12)	C18-Si6-C16	107.87(11)
N1-U1-N3	121.06(6)	N2-Si3-C7	107.98(9)
N3-U1-N2	120.65(6)	N2-Si3-U1	34.76(6)
N3-U1-Si5	27.42(4)	C7-Si3-U1	73.31(7)
N1-U1-Si1	26.97(4)	Si6-N3-U1	121.87(8)
Si5-U1-Si1	105.222(15)	C11-Si4-C12	109.12(13)
N3-U1-Si4	105.61(4)	C12-Si4-C10	106.06(13)
Si1-U1-Si4	151.562(14)	C12-Si4-U1	78.77(8)
N3-U1-Si3	130.72(4)	N3-Si5-C15	113.67(10)
Si1-U1-Si3	103.185(14)	C14-Si5-C13	106.54(11)
N1-Si1-C2	113.18(10)	C14-Si5-U1	127.16(8)
C3-Si1-C1	105.90(13)	N3-Si6-C17	111.15(10)
C3-Si1-U1	123.50(8)	N3-Si6-C16	112.75(9)
Si1-N1-Si2	122.81(9)	Si3-N2-Si4	122.54(10)
N1-Si2-C6	110.66(10)	N2-Si3-C8	112.51(12)
N1-Si2-C4	113.78(11)		

Table 2.10.22 Bond lengths of $U^{IV}Cl[N(SiMe_3)_2]_3$ (Å).

U1-N1#1	2.233(2)	U1-N1#2	2.233(2)	U1-N1	2.233(2)
U1-Cl1	2.5920(13)	U1-Si2#1	3.4207(7)	U1-Si2#2	3.4207(7)
U1-Si2	3.4207(7)	Si1-N1	1.747(2)	Si1-C3	1.862(3)
Si1-C2	1.867(3)	Si1-C1	1.869(3)	Si2-N1	1.746(2)
Si2-C4	1.863(3)	Si2-C5	1.866(3)	Si2-C6	1.872(3)

Symmetry transformations used to generate equivalent atoms:

#1 -y+1,x-y,z #2 -x+y+1,-x+1,z

Table 2.10.23 Bond angles of $U^{IV}Cl[N(SiMe_3)_2]_3$ (°).

N1#1-U1-N1#2	116.87(3)	N1#1-U1-N1	116.87(3)
N1#1-U1-Cl1	100.31(5)	N1#2-U1-Cl1	100.31(5)
N1#1-U1-Si2#1	26.77(5)	N1#2-U1-Si2#1	137.23(5)
Cl1-U1-Si2#1	79.125(15)	N1#1-U1-Si2#2	105.07(5)
N1-U1-Si2#2	137.23(5)	Cl1-U1-Si2#2	79.125(15)
N1#1-U1-Si2	137.23(5)	N1#2-U1-Si2	105.07(5)
Cl1-U1-Si2	79.125(15)	Si2#1-U1-Si2	116.526(10)
N1-Si1-C3	114.85(11)	N1-Si1-C2	111.92(13)
N1-Si1-C1	109.37(12)	C3-Si1-C1	104.87(14)
N1-Si2-C4	111.74(13)	N1-Si2-C5	112.82(12)

N1-Si2-C6	109.42(14)	C4-Si2-C6	108.46(17)
N1-Si2-U1	35.19(7)	C4-Si2-U1	106.90(11)
C6-Si2-U1	78.93(13)	Si2-N1-Si1	119.89(12)
Si1-N1-U1	122.00(11)	N1-U1-Si2	26.77(5)
N1#2-U1-N1	116.87(3)	Si2#2-U1-Si2	116.526(10)
N1-U1-Cl1	100.31(5)	C3-Si1-C2	107.20(13)
N1-U1-Si2#1	105.07(5)	C2-Si1-C1	108.24(14)
N1#2-U1-Si2#2	26.77(5)	C4-Si2-C5	107.68(14)
Si2#1-U1-Si2#2	116.526(10)	C5-Si2-C6	106.51(16)
Si2-N1-U1	118.05(10)	C5-Si2-U1	140.90(9)

Symmetry transformations used to generate equivalent atoms:

#1 -y+1,x-y,z #2 -x+y+1,-x+1,z

Table 2.10.24 Bond lengths of $U^{IV}I[N(SiMe_3)_2]_3$ (Å).

U1-N1#1	2.225(8)	U1-N1#2	2.225(8)	U1-N1#3	2.225(8)
U1-N1	2.225(8)	U1-N1#4	2.225(8)	U1-N1#5	2.225(8)
U1-I1	2.9630(14)	Si1-N1	1.691(8)	Si1-C1	1.781(10)
Si1-C3#1	1.936(10)	Si1-C2#1	2.001(10)	Si2-N1	1.764(8)
Si2-C5	1.860(10)	Si2-C4	1.868(11)	Si2-C6	1.881(11)

Symmetry transformations used to generate equivalent atoms:

#1 x,x-y,z #2 -x+y,-x,z #3 -y,-x,z #4 -y,x-y,z #5 -x+y,y,z

Table 2.10.25 Bond angles of $U^{IV}I[N(SiMe_3)_2]_3$ (°).

N1#1-U1-N1#3	115.91(13)	N1#2-U1-N1	115.91(13)
N1#1-U1-N1#5	115.91(13)	N1#3-U1-N1#5	115.91(13)
N1#2-U1-I1	101.83(19)	N1#3-U1-I1	101.83(19)
N1#4-U1-I1	101.83(19)	N1#5-U1-I1	101.83(19)
N1-Si1-C3	111.8(4)	C1-Si1-C3	108.9(5)
C1-Si1-C2	105.0(5)	C3-Si1-C2	100.3(5)
N1-Si2-C4	111.5(5)	C5-Si2-C4	106.6(5)
C5-Si2-C6	107.6(5)	C4-Si2-C6	109.7(5)
Si1-N1-U1	126.9(4)	Si2-N1-U1	117.3(4)
N1#2-U1-N1#4	115.91(13)	N1-Si1-C2	105.6(4)
N1#1-U1-I1	101.83(19)	N1-Si2-C5	112.7(4)
N1-U1-I1	101.83(19)	N1-Si2-C6	108.7(4)
N1-Si1-C1	122.6(4)	Si1-N1-Si2	115.8(5)

Symmetry transformations used to generate equivalent atoms:

#1 x,x-y,z #2 -x+y,-x,z #3 -y,-x,z #4 -y,x-y,z #5 -x+y,y,z

Table 2.10.26 Bond lengths of **2.2** (Å).

U1-N4	2.2941(17)	U1-N2	2.2958(17)	U1-N3	2.2977(17)
U1-N1	2.3013(17)	U1-Si7	3.4444(6)	U1-Si4	3.4578(6)
U1-Si5	3.4616(6)	U1-Si1	3.4619(6)	Si1-N1	1.7493(19)
Si1-C2	1.872(3)	Si1-C3	1.878(3)	Si1-C1	1.878(2)
Si2-N1	1.7554(19)	Si2-C6	1.863(3)	Si2-C5	1.875(2)
Si2-C4	1.874(3)	Si3-N2	1.7559(18)	Si3-C9	1.861(2)
Si3-C8	1.872(3)	Si3-C7	1.874(3)	Si4-N2	1.7512(18)
Si4-C11	1.872(2)	Si4-C12	1.877(2)	Si4-C10	1.879(2)

Si5-N3	1.7471(18)	Si5-C13	1.874(2)	Si5-C15	1.877(2)
Si5-C14	1.879(3)	Si6-N3	1.7606(18)	Si6-C18	1.858(3)
Si6-C17	1.868(2)	Si6-C16	1.874(3)	Si7-N4	1.7532(19)
Si7-C20	1.875(2)	Si7-C21	1.875(3)	Si7-C19	1.876(2)
Si8-N4	1.7576(18)	Si8-C22	1.864(3)	Si8-C23	1.875(3)
Si8-C24	1.878(3)				

Table 2.10.27 Bond angles of **2.2** (°).

N4-U1-N2	106.04(6)	N4-U1-N3	110.36(6)
N4-U1-N1	111.72(6)	N2-U1-N1	111.12(6)
N4-U1-Si7	27.23(4)	N2-U1-Si7	87.64(4)
N1-U1-Si7	101.37(5)	N4-U1-Si4	87.94(4)
N3-U1-Si4	100.83(4)	N1-U1-Si4	137.57(4)
N4-U1-Si5	100.48(4)	N2-U1-Si5	137.70(4)
N1-U1-Si5	88.05(4)	Si7-U1-Si5	126.461(15)
N4-U1-Si1	137.93(5)	N2-U1-Si1	101.15(4)
N1-U1-Si1	26.81(5)	Si7-U1-Si1	126.969(16)
Si5-U1-Si1	78.945(15)	N1-Si1-C2	108.49(10)
C2-Si1-C3	107.10(13)	N1-Si1-C1	114.65(11)
C3-Si1-C1	104.19(12)	N1-Si1-U1	36.40(6)
C3-Si1-U1	131.87(9)	C1-Si1-U1	122.32(8)
N1-Si2-C5	115.01(11)	C6-Si2-C5	104.16(12)
C6-Si2-C4	110.15(16)	C5-Si2-C4	103.33(13)
N2-Si3-C8	112.59(11)	C9-Si3-C8	109.46(13)
C9-Si3-C7	102.95(12)	C8-Si3-C7	105.22(14)
N2-Si4-C12	113.99(11)	C11-Si4-C12	107.89(12)
C11-Si4-C10	106.04(12)	C12-Si4-C10	104.09(12)
C11-Si4-U1	71.93(7)	C12-Si4-U1	129.91(9)
N3-Si5-C13	115.61(10)	N3-Si5-C15	114.62(10)
N3-Si5-C14	107.66(10)	C13-Si5-C14	106.76(11)
N3-Si5-U1	36.24(6)	C13-Si5-U1	122.47(8)
C14-Si5-U1	71.80(7)	N3-Si6-C18	110.93(10)
C18-Si6-C17	103.85(13)	N3-Si6-C16	113.02(12)
C17-Si6-C16	103.66(13)	N4-Si7-C20	108.18(10)
C20-Si7-C21	107.39(12)	N4-Si7-C19	115.83(10)
C21-Si7-C19	104.83(12)	N4-Si7-U1	36.77(6)
C21-Si7-U1	130.72(9)	C19-Si7-U1	123.17(8)
N4-Si8-C23	114.57(11)	C22-Si8-C23	103.55(12)
C22-Si8-C24	109.60(13)	C23-Si8-C24	104.28(13)
Si1-N1-U1	116.78(9)	Si2-N1-U1	128.64(10)
Si4-N2-U1	116.74(8)	Si3-N2-U1	128.98(9)
Si5-N3-U1	117.05(9)	Si6-N3-U1	128.26(9)
Si7-N4-U1	116.00(9)	Si8-N4-U1	129.72(9)
N2-U1-N3	111.51(6)	N2-Si4-C10	116.16(11)
N3-U1-N1	106.18(6)	N2-Si4-U1	36.37(6)
N3-U1-Si7	137.06(4)	C10-Si4-U1	124.57(9)
N2-U1-Si4	26.89(4)	C13-Si5-C15	103.97(12)
Si7-U1-Si4	78.879(15)	C15-Si5-C14	107.74(12)
N3-U1-Si5	26.71(4)	C15-Si5-U1	132.05(9)
Si4-U1-Si5	126.315(15)	N3-Si6-C17	114.81(10)
N3-U1-Si1	88.02(4)	C18-Si6-C16	109.97(15)
Si4-U1-Si1	126.634(15)	N4-Si7-C21	114.02(11)

N1-Si1-C3	114.80(12)	C20-Si7-C19	106.03(12)
C2-Si1-C1	107.09(12)	C20-Si7-U1	71.68(8)
C2-Si1-U1	72.42(8)	N4-Si8-C22	111.27(10)
N1-Si2-C6	110.83(10)	N4-Si8-C24	112.93(11)
N1-Si2-C4	112.81(12)	Si1-N1-Si2	114.51(10)
N2-Si3-C9	111.33(10)	Si4-N2-Si3	114.24(10)
N2-Si3-C7	114.68(11)	Si5-N3-Si6	114.61(10)
N2-Si4-C11	108.14(9)	Si7-N4-Si8	114.23(10)

2.11 Coordinates of Optimized Geometries Obtained from DFT.

Table 2.11.1. Optimized coordinates of **2.1-F**.

U -0.00318906 -0.02271957 -0.02251214	F 0.00403995 -0.06092855 2.04694767
F -0.01440596 -0.04584015 -2.08727100	N 1.96161660 -1.06799366 -0.02357016
N -1.95858789 -1.08467680 -0.00139829	N -0.00231029 2.18719154 -0.00768001
Si 0.96786364 3.11631659 -1.19168949	Si 3.19654808 -0.71382575 1.21945738
Si -3.23845725 -0.69988779 -1.18679357	Si -0.94221007 3.11295376 1.20175983
Si -2.27551238 -2.37384187 1.19386834	Si 2.29838631 -2.37164909 -1.19692521
C 3.01804574 -1.84028212 2.73130505	H 3.81385644 -1.62543244 3.45634268
H 2.05904328 -1.66701742 3.23215781	H 3.07754687 -2.90325983 2.47566331
C 3.06804077 1.07603569 1.83083103	H 3.27544118 1.80631905 1.04118831
H 2.09899099 1.31599461 2.27481442	H 3.82762739 1.21788703 2.61154674
C 4.96590449 -0.86375059 0.54297572	H 5.66513339 -0.58161216 1.34120049
H 5.23971423 -1.87054225 0.21295643	H 5.13570271 -0.17820551 -0.29550807
C 3.01054309 -3.90424989 -0.32750982	H 3.19065609 -4.68824686 -1.07472815
H 3.95761743 -3.72250466 0.18970875	H 2.30245216 -4.30656446 0.40669384
C 0.71360863 -2.97232706 -2.05689147	H -0.14893891 -3.08732056 -1.39082424
H 0.41519672 -2.30868687 -2.87229633	H 0.92093327 -3.96256045 -2.48385261
C 3.48055050 -1.82387765 -2.57095037	H 3.55708925 -2.61459550 -3.32874718
H 3.10897699 -0.92161879 -3.07005180	H 4.49119551 -1.61340599 -2.20735565
C 1.90354509 4.54288781 -0.35483211	H 2.50612800 5.06338644 -1.11068640
H 1.25317268 5.28849389 0.11291959	H 2.59054589 4.17046808 0.41404133
C 2.30455731 2.05154765 -2.01562597	H 2.94455884 1.51667161 -1.30674530
H 1.88260878 1.31897397 -2.70857021	H 2.95102025 2.72537854 -2.59386048
C -0.10364413 3.80713550 -2.59204382	H -0.84073160 4.53712931 -2.24443917
H 0.53281098 4.30426741 -3.33580156	H -0.64417443 3.00280124 -3.10366212
C -2.40740765 2.11727210 1.87671900	H -3.14096583 1.85736749 1.10619906
H -2.10929793 1.20050873 2.39064575	H -2.92167375 2.75144341 2.61173225
C -1.72580221 4.67622112 0.45763558	H -2.32813724 5.16367378 1.23557730
H -1.00398703 5.41483874 0.09568828	H -2.39995757 4.43225865 -0.37166392
C 0.12032402 3.60864871 2.68917016	H -0.47019021 4.22526722 3.37944834
H 0.45466956 2.72402935 3.24260424	H 1.00769870 4.18343226 2.40535214
C -4.94726754 -0.60608266 -0.36118887	H -5.69507657 -0.33721291 -1.11876413
H -5.27298546 -1.54368130 0.09953020	H -4.97157167 0.17064846 0.41246330
C -3.27922344 -1.95802179 -2.60155533	H -4.00649301 -1.64611022 -3.36237159
H -2.29815003 -2.02210667 -3.08615947	H -3.55592683 -2.96382666 -2.27005924
C -2.97726479 1.00321315 -1.98091013	H -2.88700419 1.81718270 -1.25408889
H -2.10064211 1.03102569 -2.63287087	H -3.85934844 1.21772141 -2.59922661
C -3.28782998 -3.80812876 0.46352449	H -3.40525237 -4.57493184 1.24074381
H -4.29091505 -3.53200994 0.12491273	H -2.76614830 -4.27661157 -0.37919491
C -3.16374647 -1.71185573 2.72849044	H -3.39558612 -2.53512502 3.41652078
H -2.53208640 -0.99743937 3.26797055	H -4.10398087 -1.20823241 2.48049671

C -0.66020287 -3.19115282 1.76289125	H -0.16671371 -3.74576664 0.95662586
H 0.06094533 -2.49364357 2.19531968	H -0.91277882 -3.91974410 2.54533991

Table 2.11.2 Optimized coordinates of **2.1-Cl**.

U 0.00139108 -0.13807519 -0.00017212	Cl 0.05661945 -0.15637308 2.62578527
Cl -0.05337229 -0.14633161 -2.62627490	N 1.77352681 1.15720393 0.03665022
N 0.00556602 -2.32422145 -0.00444701	N -1.77805821 1.14766385 -0.03220697
Si -2.07002662 2.53412470 -1.15392132	Si 2.05770503 2.54127204 1.16332982
Si -1.11246045 -3.28054374 -1.06249509	Si -3.14357265 0.74911738 1.07840900
Si 1.12766014 -3.27949562 1.05025802	Si 3.14101235 0.77025266 -1.07565758
C 4.82183526 0.83824398 -0.19223341	H 5.09125744 1.82126256 0.20371371
H 5.59323445 0.55654888 -0.92177640	H 4.87153637 0.11673696 0.63135974
C -3.19863729 1.90135624 2.57630141	H -2.28763924 1.80005942 3.17518491
H -4.04675856 1.61858387 3.21434627	H -3.31871858 2.95512965 2.31011943
C 3.18890737 1.92821025 -2.56930501	H 2.27914162 1.82265178 -3.16931520
H 4.03963797 1.65419706 -3.20768830	H 3.30110437 2.98176332 -2.29878928
C -2.64666210 -2.28573374 -1.56758338	H -3.36311879 -2.19344527 -0.74595032
H -3.13966855 -2.86001650 -2.36410251	H -2.44559394 -1.29283258 -1.97531493
C 3.09102870 1.98715074 2.65078768	H 2.58244196 1.18980020 3.20194109
H 3.21840551 2.83578347 3.33581581	H 4.08816057 1.63210488 2.37507916
C -2.97921315 3.96656030 -0.29428119	H -3.97860738 3.71239814 0.07107963
H -3.09775242 4.77639672 -1.02638034	H -2.40757665 4.37123259 0.54858544
C -4.82432783 0.81043725 0.19437480	H -5.09861520 1.79305198 -0.19918289
H -5.59472758 0.52272939 0.92261935	H -4.86964021 0.09088779 -0.63118170
C -0.22144206 -3.86128557 -2.62413250	H 0.19701286 -3.01174940 -3.17269456
H -0.93607167 -4.36785021 -3.28571867	H 0.58814023 -4.56557825 -2.40977840
C -1.83032469 -4.78169062 -0.14787547	H -1.09450410 -5.53599557 0.14485448
H -2.54698629 -5.26995662 -0.82183745	H -2.38274063 -4.48077288 0.74943618
C 0.47426570 3.31036384 1.85918072	H -0.16228932 3.76762383 1.09750815
H 0.78943349 4.11124567 2.54238247	H -0.12714420 2.60454972 2.43427515
C 1.85120637 -4.77489779 0.13066657	H 1.11839156 -5.53158149 -0.16347601
H 2.57064574 -5.26195064 0.80254443	H 2.40140755 -4.46909060 -0.76635182
C 3.03789492 -1.00912240 -1.76376622	H 2.25167586 -1.65490422 -1.36347840
H 3.99338106 -1.51412673 -1.57343249	H 2.87835578 -0.97233078 -2.84599906
C 2.65819203 -2.28007066 1.55757867	H 3.37397814 -2.18324203 0.73589770
H 3.15358719 -2.85441765 2.35256995	H 2.45369096 -1.28889847 1.96783899
C -3.03069002 -1.03164455 1.76126724	H -2.24240051 -1.67266778 1.35746899
H -3.98429294 -1.54044386 1.57145808	H -2.86913589 -0.99720060 2.84326000
C 0.23968445 -3.86902312 2.61030044	H -0.18105328 -3.02303776 3.16257997
H 0.95643904 -4.37594473 3.26931200	H -0.56784702 -4.57503364 2.39379987
C -3.09901330 1.97941658 -2.64418456	H -2.58447347 1.18843893 -3.19896107
H -3.23253973 2.83031226 -3.32522068	H -4.09350961 1.61566577 -2.37033801
C -0.49110134 3.31586987 -1.84585571	H 0.14277831 3.77314635 -1.08197571
H -0.81105095 4.11822250 -2.52508712	H 0.11450080 2.61650073 -2.42442608
C 2.95720967 3.98283563 0.30881636	H 3.95896845 3.73737517 -0.05598681
H 3.06870833 4.79123197 1.04360698	H 2.38363776 4.38586661 -0.53350752

Table 2.11.3 Optimized coordinates of **2.1-Br**.

U -0.00327570 -0.02914364 0.00081940	Br -0.04096124 -0.06896462 -2.76971968
Br 0.06059948 -0.05599685 2.77424642	N -1.96932616 -1.00195144 0.02073567

N 0.06548240 2.15438787 -0.00367817	N 1.90149718 -1.10775885 -0.01045668
Si 2.17233761 -2.51286643 -1.11739513	Si -2.33359832 -2.40173805 1.10808616
Si -3.31838227 -0.48847110 -1.06883156	Si 1.17064630 3.09466319 -1.08988451
Si -0.97791073 3.16380652 1.08147114	C 3.37138459 -1.87720077 2.56803962
H 2.43885874 -1.86444199 3.14053816	H 4.17378880 -1.53852008 3.23727689
H 3.58972813 -2.91077909 2.28582276	Si 3.27948338 -0.69957936 1.08942437
C 4.94069473 -0.77146770 0.17028029	H 5.21096931 -1.76388177 -0.20204915
H 5.72563746 -0.46305225 0.87404605	H 4.96685635 -0.07428942 -0.67464338
C -0.01431161 3.73827712 2.60449646	H 0.39094064 2.88255276 3.15331084
H -0.69232437 4.27718649 3.27909722	H 0.81221273 4.41106319 2.35739976
C -3.38964008 -3.72564669 0.24666501	H -4.38909134 -3.39599777 -0.04938184
H -3.51654102 -4.55495441 0.95568177	H -2.88836162 -4.13023755 -0.63959025
C 3.06517536 -3.93713150 -0.23309840	H 4.07697945 -3.69915988 0.10685392
H 3.14770527 -4.76823306 -0.94656657	H 2.49417176 -4.30197716 0.62819776
C -0.76745309 -3.35944360 1.59839834	H 0.09015374 -2.74920219 1.88818094
H -0.45824706 -4.04722429 0.80525389	H -1.02913005 -3.96762671 2.47509038
C -4.97212986 -0.42791114 -0.13522435	H -5.31498321 -1.39371283 0.24685396
H -5.73823621 -0.06443183 -0.83342554	H -4.93720220 0.27435815 0.70534388
C 2.67972557 2.09803794 -1.65992818	H 3.40648801 1.96417644 -0.85354501
H 3.16849366 2.69591148 -2.44162355	H 2.45137126 1.12435051 -2.09591318
C -3.07948414 1.27007802 -1.76428708	H -2.21627016 1.82126457 -1.38572655
H -3.97397519 1.86664373 -1.54369713	H -2.96496104 1.22040306 -2.85206463
C 0.24939011 3.70596221 -2.62408875	H -0.19283200 2.86779199 -3.17129995
H 0.95783074 4.20756761 -3.29613186	H -0.54533736 4.41964421 -2.38707261
C -3.23825606 -1.84950986 2.67389776	H -2.62963253 -1.15490414 3.25991059
H -3.44491608 -2.72567357 3.30242251	H -4.19505251 -1.36612676 2.45392473
C -2.53454972 2.25838408 1.67640726	H -3.27148965 2.14246746 0.87656185
H -2.98792544 2.90102878 2.44387737	H -2.35525946 1.28539577 2.13663105
C -1.68347146 4.68185443 0.18101771	H -0.94045173 5.40771168 -0.16010002
H -2.34725135 5.20148710 0.88508168	H -2.29224967 4.38990050 -0.68199948
C 0.53647716 -3.28143469 -1.72808515	H -0.38346439 -2.84400145 -1.33250894
H 0.52598628 -4.34751340 -1.46838454	H 0.47537265 -3.19502883 -2.81776781
C 3.17445472 1.07513656 1.77710422	H 2.33311752 1.67349717 1.42156965
H 4.09564010 1.61528585 1.52435363	H 3.09162199 1.03831470 2.86849579
C 1.94805694 4.58276593 -0.19945429	H 1.23996726 5.34630040 0.13331740
H 2.63803658 5.06428372 -0.90550853	H 2.53980897 4.26830031 0.66742034
C 3.19106221 -2.03047365 -2.63601723	H 2.69507756 -1.24101073 -3.20900935
H 3.28741115 -2.90577571 -3.29240406	H 4.20028318 -1.69241864 -2.38388563
C -3.50181095 -1.65300220 -2.54934268	H -2.55866634 -1.73228088 -3.09922839
H -4.25143373 -1.23729542 -3.23590610	H -3.82672174 -2.66006674 -2.27397684

Table 2.11.4 Optimized coordinates of **2.1-N_3**.

U -0.00920489 -0.01125641 -0.01759102	N 0.18003270 -0.13343572 2.20248075
N -0.23844376 0.07453399 -2.23001948	N 0.31190560 -0.19090472 3.40284951
N -0.51443004 0.07380484 -3.40638027	N 0.43604116 -0.24527911 4.54475660
N -0.77333108 0.07332391 -4.52707494	N 0.86372990 2.01208229 0.00920913
N 1.38862212 -1.70876883 -0.22347189	N -2.20484155 -0.28472551 0.19409750
Si -3.35771322 0.67099932 -0.78668739	Si 0.40868450 3.20656863 1.27113663
Si 1.05057498 -3.01365795 -1.40619487	Si -2.88602248 -1.44594162 1.37498782
Si 2.84290390 -1.89305608 0.80972241	Si 2.05893421 2.54595265 -1.22041654
C 3.50552390 3.47779225 -0.41644207	H 3.21033414 4.37367906 0.13764019
H 4.20108936 3.79527840 -1.20448684	H 4.06248106 2.82956141 0.27012541

C -3.32077771 -0.61023169 3.01859375	H -2.44050782 -0.20799216 3.53066579
H -3.78573934 -1.34083524 3.69326153	H -4.03120876 0.21207646 2.88328944
C 1.25094030 3.64421479 -2.53487883	H 0.38117560 3.14659505 -2.97853027
H 1.96782874 3.83992619 -3.34307452	H 0.91999411 4.61098675 -2.14441116
C -0.76924184 -3.01895234 -1.98062653	H -1.11591772 -4.06008296 -2.01213326
H -0.86119650 -2.61281461 -2.99345068	H -1.47236536 -2.46998587 -1.34716953
C 1.63743891 3.20279374 2.71221291	H 1.60255867 2.26978837 3.28447798
H 1.39383395 4.01895326 3.40484216	H 2.66925999 3.34983516 2.37748746
C -4.76351931 1.36444002 0.28690642	H -5.37363759 0.59837495 0.77544983
H -5.43331687 1.95790125 -0.34943958	H -4.37707733 2.03093340 1.06686418
C -4.44875802 -2.31469551 0.72901636	H -5.30121481 -1.65019915 0.55858334
H -4.75789800 -3.05402677 1.47989242	H -4.25437154 -2.85928303 -0.20213353
C 2.12192124 -2.84619087 -2.95753804	H 2.00796812 -1.85583765 -3.41219291
H 1.81275559 -3.59096027 -3.70258440	H 3.18628335 -3.00064659 -2.75562145
C 1.32696510 -4.73351213 -0.64810962	H 2.34941877 -4.91927256 -0.30639778
H 1.09580458 -5.48769169 -1.41210520	H 0.65278293 -4.90851750 0.19863881
C -1.32993861 2.89059392 1.96353604	H -2.10499698 3.14210594 1.23149291
H -1.46686302 3.56192473 2.82228671	H -1.51109077 1.87255899 2.31551687
C 4.31844779 -2.61180542 -0.14890757	H 4.16837934 -3.62890816 -0.52270682
H 5.18473663 -2.63689962 0.52541979	H 4.58870751 -1.97713633 -1.00081824
C 2.86158016 1.10077613 -2.15556607	H 3.10412971 0.23521624 -1.53361369
H 3.80395449 1.47061396 -2.58159174	H 2.24133586 0.74779008 -2.98364309
C 3.49453240 -0.22919115 1.44835009	H 3.97210018 0.35091973 0.65153727
H 4.26860224 -0.44620887 2.19698970	H 2.74675661 0.40640741 1.92741652
C -1.68962063 -2.88139318 1.71654502	H -1.62991226 -3.56672572 0.86363668
H -2.09296837 -3.45407057 2.56266816	H -0.67307800 -2.58325332 1.98502539
C 2.49299295 -3.00298071 2.30371364	H 1.74561609 -2.56579872 2.97461979
H 3.41335611 -3.14138664 2.88589522	H 2.13599832 -3.99458918 2.00811674
C -4.10502123 -0.34458033 -2.19914730	H -3.32685040 -0.79274059 -2.82748958
H -4.70643934 0.31188339 -2.84172293	H -4.75592189 -1.14997483 -1.84654015
C -2.53203046 2.19102530 -1.58845485	H -1.61278309 2.53765787 -1.10761925
H -3.24547803 3.02492463 -1.55521574	H -2.29871385 2.00474332 -2.64199596
C 0.29234092 4.97759518 0.59063122	H 1.23440304 5.38838840 0.21614136
H -0.04449235 5.62895518 1.40811040	H -0.45147254 5.05273331 -0.21083843

Table 2.11.5 Optimized coordinates of **2.1-NCS**.

U 0.01570485 -0.02734121 0.00229595	C 0.03956730 -0.55213835 3.45714320
C 0.07426967 0.45384577 -3.45746427	S 0.05425916 -0.82818032 5.03068789
S 0.11665991 0.70375075 -5.03488923	N 0.02560261 -0.34550827 2.27609615
N 0.04104087 0.26893416 -2.27328732	N 2.15444016 -0.56003348 -0.06568690
N -0.57716333 2.05169158 0.27527288	N -1.63285214 -1.45137906 -0.20845712
Si -3.00774739 -1.21265864 -1.35034509	Si -1.61353886 -2.98631552 0.73298329
Si 2.78764118 -1.67271038 -1.33063378	Si 3.33826021 0.06202718 1.13920454
Si 0.17354846 3.37210234 -0.70178069	Si -1.79792895 2.56127508 1.50629820
C -3.29250099 0.60810905 -1.79233687	H -3.64718366 1.20353386 -0.94596991
H -4.08255579 0.62810752 -2.55549451	H -2.41888270 1.10490146 -2.21773616
C -4.65233013 -1.78175835 -0.58993109	H -4.70540905 -2.85364867 -0.37598796
H -5.45561683 -1.55217604 -1.30240984	H -4.87465864 -1.24199385 0.33769780
C -2.72034944 -2.14389004 -2.97188991	H -1.83441787 -1.77134940 -3.49703534
H -3.58177273 -1.99093889 -3.63494075	H -2.59994858 -3.22158742 -2.82784151
C -2.08158197 -4.47364490 -0.34985885	H -3.09630639 -4.43531561 -0.75720351
H -2.01301793 -5.37812961 0.26928904	H -1.38567302 -4.59709048 -1.18768239

C 0.13109843 -3.38261027 1.39870039	H 0.95465397 -2.77492241 1.01199576
H 0.36618454 -4.42594291 1.15192646	H 0.15225825 -3.28397783 2.48899456
C -2.77992407 -2.92869784 2.21957429	H -2.51068244 -2.12377632 2.91166403
H -2.70043899 -3.87388760 2.77286110	H -3.82855494 -2.79687433 1.93703338
C 3.58228726 -0.72748887 -2.76196506	H 2.87284904 -0.04925179 -3.24653755
H 3.93007524 -1.43825569 -3.52278977	H 4.44707364 -0.13783272 -2.44152943
C 1.41222722 -2.78338495 -2.02456952	H 1.10715609 -3.54881316 -1.30341631
H 1.83251809 -3.30788209 -2.89351604	H 0.51922567 -2.25968387 -2.37417178
C 4.05103352 -2.90145893 -0.62465300	H 4.96646827 -2.44070210 -0.24221740
H 4.34398731 -3.58780359 -1.43027301	H 3.61767293 -3.50858017 0.17836489
C 4.98231316 0.54596414 0.32047930	H 5.52155819 -0.28660416 -0.14089765
H 5.63765994 0.96999510 1.09277076	H 4.83828586 1.31889105 -0.44321715
C 3.67052914 -1.20486014 2.50374965	H 2.74723749 -1.50151723 3.01215612
H 4.33419732 -0.76479171 3.25934723	H 4.15454558 -2.11121085 2.12638481
C 2.73471803 1.66489656 1.95310054	H 2.72312246 2.50525987 1.25162349
H 3.45564007 1.91362581 2.74364023	H 1.75248381 1.59498964 2.42514367
C 1.80830602 2.82945602 -1.51560718	H 2.25296537 1.90917085 -1.12894173
H 2.54765468 3.62865178 -1.37566626	H 1.66894833 2.68974665 -2.59243416
C 0.61942329 4.86822843 0.37870435	H -0.23756621 5.35778936 0.85025718
H 1.10885018 5.61401037 -0.26179168	H 1.32955572 4.59810392 1.16854384
C -0.96579889 3.94819020 -2.09781730	H -1.18728659 3.13346262 -2.79549515
H -0.45463922 4.73407622 -2.67004919	H -1.91521150 4.36018167 -1.74386370
C -2.93757154 3.92700724 0.84346852	H -2.42665266 4.86124508 0.59353337
H -3.67779637 4.15836254 1.62082082	H -3.48873838 3.59626204 -0.04403407
C -0.95430364 3.17186437 3.08617009	H -0.37998529 2.37321895 3.56754292
H -1.71968772 3.49967951 3.80176020	H -0.27943475 4.01520365 2.91262256
C -2.97697694 1.16618573 2.01224035	H -3.66781042 0.87526474 1.21562194
H -3.58413869 1.55808918 2.83981013	H -2.47568704 0.26807645 2.37657156

Table 2.11.6 Optimized coordinates of **2.1-CN**.

U 0.00038021 -0.05358232 -0.01584104	C -0.03122047 -0.04143592 -2.50292131
N -0.04887624 -0.04635498 -3.67374353	C 0.05220096 -0.03575069 2.47300110
N 0.08149393 -0.03767923 3.64351584	N -1.95237695 -1.00593843 0.01146930
N 0.02312566 2.10554124 -0.00338085	N 1.93075715 -1.04730012 -0.00207073
Si 2.19389064 -2.42565860 -1.14301986	Si -2.26500184 -2.38597382 1.14418376
Si -3.31219645 -0.55136720 -1.09963284	Si 1.07418963 3.06513050 -1.13485024
Si -0.98428182 3.08841920 1.14692284	C 3.27459437 -1.80952036 2.62823094
Si 3.28770029 -0.65452251 1.13447124	C 4.97246304 -0.77298203 0.26640047
C 0.03412957 3.65396743 2.63522639	C -3.25411830 -3.77407920 0.30968174
C 3.00162258 -3.90127900 -0.26640233	C -0.64240352 -3.22484302 1.66146192
C -4.96824622 -0.53272693 -0.17229909	C 2.48041203 2.03865566 -1.88700289
C -3.11936196 1.18934928 -1.82035333	C 0.07600183 3.73891162 -2.59048758
C -3.16757176 -1.81605584 2.70059919	C -2.46953573 2.13539829 1.83856813
C -1.74629247 4.60199249 0.29090801	C 0.53036214 -3.07784237 -1.81581339
C 3.19324007 1.12827319 1.76595728	C 1.92437972 4.49863667 -0.22725420
C 3.24938884 -1.92612951 -2.62505506	C -3.39789976 -1.73694535 -2.56866861
H -4.21735717 -1.43130545 -3.23238158	H -3.57437690 -2.77749935 -2.28228115
H 2.38372651 -1.64408210 3.24228194	H 4.15184739 -1.59875565 3.25400721
H 3.31253265 -2.86693418 2.35067665	H 5.23725858 -1.77930939 -0.07209000
H 5.74113018 -0.45962065 0.98535434	H 5.03904476 -0.09912291 -0.59512157
H 0.35320103 2.79438421 3.23310525	H -0.59670809 4.28438512 3.27590995
H 0.91892063 4.23717207 2.36543608	H -4.25650413 -3.48403984 -0.01748562

H -3.37076443 -4.58506206 1.04080276	H -2.72223030 -4.18757343 -0.55431611
H 4.00912440 -3.70127661 0.10971377	H 3.08075591 -4.72286307 -0.99092367
H 2.39332047 -4.26008134 0.57160038	H 0.10099372 -2.57015963 2.12267438
H -0.17512236 -3.77265215 0.83721124	H -0.91503043 -3.96505225 2.42670823
H -5.26913592 -1.50257656 0.23455370	H -5.75017445 -0.21739857 -0.87550852
H -4.96054855 0.18863024 0.65265147	H 3.02422278 1.41126422 -1.17734333
H 3.20005686 2.75789180 -2.30178074	H 2.13433118 1.40643586 -2.70742356
H -3.10164274 1.98451669 -1.07057537	H -4.00406808 1.35827675 -2.45006000
H -2.24346725 1.29404917 -2.46388166	H -0.36984181 2.91963514 -3.16378147
H 0.75419313 4.27896194 -3.26452761	H -0.71951480 4.42885772 -2.29647858
H -2.53458873 -1.15271296 3.29818575	H -3.41158372 -2.68921748 3.31974555
H -4.10318669 -1.29373727 2.47904940	H -3.22039119 1.88335060 1.08520427
H -2.94863852 2.81492055 2.55737240	H -2.20363570 1.22997172 2.38710848
H -1.01878035 5.34039949 -0.05832018	H -2.39475604 5.10431383 1.02090674
H -2.37299800 4.31745141 -0.56148600	H -0.38854873 -2.66039679 -1.39114968
H 0.48813804 -4.16061650 -1.64095072	H 0.47406505 -2.89772494 -2.89348445
H 3.44733690 1.86099118 0.99397065	H 3.94537672 1.22036158 2.56148878
H 2.23199293 1.40009941 2.20684904	H 1.23741249 5.24618981 0.17957769
H 2.57631258 5.01252018 -0.94585860	H 2.55724214 4.14059258 0.59204196
H 2.76526379 -1.12569200 -3.19348687	H 3.35454058 -2.78967734 -3.29528757
H 4.25483280 -1.59668036 -2.34774674	H -2.47049948 -1.69006073 -3.14932407

Table 2.11.7 Optimized coordinates of **2.1-OPh**.

U -0.00432342 -0.04642133 0.01795883	Si 0.46052033 3.33927886 -1.05229560
Si 1.51723408 -1.59174557 2.87762713	Si -0.97204623 -2.91679866 1.83546595
Si -0.33542124 2.94853014 1.84672909	Si -1.54361585 -0.56135921 -3.17052156
Si 0.87622329 -2.25048404 -2.58614796	N 0.03064884 2.22236735 0.26437015
N 0.20804056 -1.58496499 1.65784116	N -0.24552548 -0.97809171 -2.00874560
O 2.09499445 -0.01676023 -0.18502836	O -2.09784082 -0.02240484 0.30195516
C 3.41143553 0.30135730 -0.27442927	C 3.86181171 1.56235730 0.14660832
C 5.21546861 1.88656601 0.06084280	C 6.13603092 0.96367916 -0.44080305
C 5.68721538 -0.29232494 -0.85489999	C 4.33569135 -0.62970533 -0.77442504
C 1.70664769 4.69575905 -0.57237202	C 1.27424473 2.38948896 -2.47948318
C -1.04117038 4.31332761 -1.69901581	C 2.28302384 0.11507371 3.16459113
C 0.89173980 -2.02876300 4.62419773	C 2.93669590 -2.76274487 2.42203764
C -1.83169724 -3.36463538 0.20104037	C -0.17047123 -4.57274736 2.32844784
C -2.30154654 -2.48864248 3.11821048	C -3.41241161 0.28714808 0.43466013
C -3.83053126 1.62603191 0.38074444	C -5.18193626 1.94361006 0.51212228
C -6.13291798 0.93736282 0.69626810	C -5.71660165 -0.39470891 0.74611863
C -4.36736841 -0.72608678 0.61670261	C -1.51273967 4.44036904 1.77531809
C -1.17588238 1.67177808 2.97659001	C 1.21443079 3.60443978 2.73045707
C -2.24536848 1.17416537 -2.90736626	C -0.92637213 -0.47213984 -4.97069910
C -3.00454315 -1.76600719 -3.08463777	C 1.70417362 -3.21238698 -1.17401529
C 0.00951737 -3.63712937 -3.56147124	C 2.22872421 -1.50202286 -3.68301866
H 3.14096358 2.26936836 0.54009165	H 5.54990177 2.86674587 0.39101724
H 3.98871017 -1.60369858 -1.09715483	H 1.29129490 5.42288806 0.13413152
H 1.96363125 5.24835998 -1.48641355	H 2.64105792 4.31053915 -0.15313033
H 2.31607762 2.15337938 -2.23666284	H 1.27903840 3.02689043 -3.37349626
H 0.78288099 1.45094556 -2.75271896	H -1.94359060 3.70712176 -1.80999540
H -0.80669286 4.74110552 -2.68293122	H -1.28116187 5.14874450 -1.03258499
H 2.66392509 0.60622497 2.26806297	H 3.13923514 -0.02448546 3.83862837
H 1.58768511 0.79225057 3.66974423	H 0.12553576 -1.31714303 4.95448182

H 1.74116062 -1.92929869 5.31339658	H 0.48878261 -3.03685412 4.75078470
H 2.59698109 -3.77063687 2.16576540	H 3.62599338 -2.84768931 3.27244095
H 3.51178745 -2.37381021 1.57421363	H -2.12149467 -2.51674456 -0.41945168
H -2.74147006 -3.93319593 0.43862090	H -1.19670029 -4.01861212 -0.40579833
H 0.53973514 -4.91030607 1.56454792	H -0.96831262 -5.32602047 2.38237120
H 0.34704088 -4.57786247 3.29104672	H -1.88627857 -2.40531873 4.12751901
H -3.07190478 -3.27068526 3.14263333	H -2.79651226 -1.54080187 2.88209307
H -3.08603575 2.39871966 0.22936912	H -5.49093390 2.98484378 0.46783039
H -4.04582342 -1.75948773 0.65697576	H -1.04964213 5.31546963 1.30630825
H -1.76768586 4.72336129 2.80552090	H -2.45221489 4.23736951 1.25194700
H -2.23659965 1.56651366 2.72641639	H -1.11266655 2.03540132 4.01081074
H -0.73972608 0.66678859 2.97031490	H 2.03161995 2.87882879 2.76427696
H 0.95932547 3.86181641 3.76722784	H 1.59465931 4.51366662 2.25407839
H -2.52986149 1.40284313 -1.87948879	H -3.15553291 1.25791042 -3.51646394
H -1.55109633 1.94305075 -3.25783068	H -0.14164262 0.28596570 -5.07961025
H -1.77160803 -0.15184148 -5.59478335	H -0.54883358 -1.40748128 -5.39159363
H -2.70687790 -2.81451295 -3.17634413	H -3.70278687 -1.54396284 -3.90247753
H -3.55709139 -1.65161182 -2.14524265	H 2.03425739 -2.60521217 -0.33150817
H 2.58350611 -3.72899690 -1.58318336	H 1.03370727 -3.98426019 -0.78211074
H -0.72987519 -4.15530484 -2.93998693	H 0.77507191 -4.37566846 -3.83629475
H -0.48744102 -3.32700188 -4.48430399	H 1.81838875 -1.07347257 -4.60276225
H 2.95438993 -2.27336011 -3.97333255	H 2.77598573 -0.70939830 -3.16243788
H -6.44611329 -1.18810873 0.88682894	H -7.18487558 1.18790663 0.79771736
H 6.39315910 -1.02101082 -1.24491997	H 7.18969141 1.21902996 -0.50601126

Table 2.11.8 Optimized coordinates of **2.3**.

U -0.00000200 0.00000200 -0.00000600	N 1.54162800 -0.98470000 1.41466300
N 0.98470900 1.54164000 -1.41466500	N -1.54164200 0.98469100 1.41466400
N -0.98470700 -1.54162500 -1.41467700	Si 2.23017700 -0.00016000 2.73515000
Si 2.09472600 -2.68569000 1.43803900	Si 2.68570300 2.09472800 -1.43802900
Si 0.00018400 2.23019900 -2.73515700	Si -2.23015000 0.00015600 2.73517600
Si -2.09477600 2.68567000 1.43802300	Si -0.00017100 -2.23018300 -2.73516200
Si -2.68569900 -2.09471800 -1.43804900	C 1.74003700 -0.52702500 4.49990500
H 0.73028700 -0.93901800 4.57717500	H 1.77687800 0.36206500 5.14378800
H 2.43281500 -1.26045900 4.92154900	C 1.64979700 1.80065700 2.58986400
H 1.63627400 2.20351200 1.57379200	H 2.34419500 2.42859000 3.16467300
H 0.65133200 1.93678300 3.01163800	C 4.13221600 0.03898200 2.75920100
H 4.57916500 -0.96033000 2.79948200	H 4.44973000 0.57113300 3.66611200
H 4.56466900 0.56253300 1.90198800	C 3.67766200 -2.96923600 0.42289100
H 3.53463400 -2.89611700 -0.65858200	H 4.05245500 -3.97963400 0.63398100
H 4.46746800 -2.26158500 0.69847800	C 2.52827400 -3.37251000 3.16069400
H 3.40647400 -2.91438900 3.62582300	H 2.75781800 -4.43740400 3.01856600
H 1.69664400 -3.31205400 3.86992400	C 0.74127500 -3.87034700 0.84219900
H 0.04793200 -4.08801900 1.66243000	H 1.19538400 -4.82174800 0.53557500
H 0.14861500 -3.49388100 0.00710000	C 3.37253300 2.52828900 -3.16067700
H 3.31207700 1.69666600 -3.86991500	H 4.43742700 2.75782800 -3.01854200
H 2.91441700 3.40649600 -3.62580000	C 2.96925300 3.67765100 -0.42286400
H 2.26160700 4.46746300 -0.69844300	H 3.97965400 4.05244200 -0.63394700
H 2.89613200 3.53461100 0.65860700	C 3.87035000 0.74126500 -0.84220100
H 3.49388000 0.14859800 -0.00710900	H 4.82175400 1.19536400 -0.53557100
H 4.08802000 0.04792900 -1.66243900	C 0.52705400 1.74005300 -4.49990900
H 1.26049700 2.43282300 -4.92154900	H -0.36203300 1.77690200 -5.14379700

H	0.93903700	0.73029900	-4.57717400	C	-1.80064000	1.64984100	-2.58987900
H	-1.93677800	0.65137600	-3.01165100	H	-2.42856100	2.34424500	-3.16469400
H	-2.20349900	1.63632700	-1.57380900	C	-0.03893600	4.13223900	-2.75920700
H	-0.56248700	4.56469800	-1.90199800	H	-0.57107600	4.44976000	-3.66612200
H	0.96038200	4.57917600	-2.79948100	C	-1.74000000	0.52706200	4.49991600
H	-0.73025900	0.93908100	4.57716600	H	-1.77681000	-0.36201900	5.14381400
H	-2.43279000	1.26048600	4.92155800	C	-1.64972700	-1.80064800	2.58991200
H	-1.63620800	-2.20352000	1.57384600	H	-2.34410100	-2.42858900	3.16474000
H	-0.65125300	-1.93674300	3.01167400	C	-4.13218800	-0.03903200	2.75925200
H	-4.57916100	0.96027000	2.79952300	H	-4.44967700	-0.57117600	3.66617600
H	-4.56463900	-0.56260700	1.90205400	C	-3.67773100	2.96916800	0.42288900
H	-3.53471400	2.89603700	-0.65858400	H	-4.05254300	3.97956100	0.63397000
H	-4.46751800	2.26150400	0.69849500	C	-2.52832000	3.37250600	3.16067300
H	-3.40650500	2.91437200	3.62581800	H	-2.75788900	4.43739300	3.01853200
H	-1.69668100	3.31207800	3.86989400	C	-0.74135900	3.87034900	0.84215100
H	-0.04801200	4.08804800	1.66237200	H	-1.19549300	4.82173600	0.53552000
H	-0.14870000	3.49388600	0.00705200	C	-0.52703000	-1.74003800	-4.49991800
H	-1.26046800	-2.43280900	-4.92156300	H	0.36206100	-1.77688400	-5.14379900
H	-0.93901400	-0.73028500	-4.57718600	C	1.80065100	-1.64982100	-2.58987100
H	1.93678900	-0.65135500	-3.01164100	H	2.42857700	-2.34422300	-3.16468100
H	2.20350200	-1.63630600	-1.57379800	C	0.03895200	-4.13222300	-2.75921100
H	0.56249800	-4.56468000	-1.90199800	H	0.57110000	-4.44974300	-3.66612200
H	-0.96036400	-4.57916200	-2.79949200	C	-3.87035400	-0.74126100	-0.84222300
H	-3.49388800	-0.14859400	-0.00712900	H	-4.82175700	-1.19536500	-0.53559700
H	-4.08802400	-0.04792500	-1.66246100	C	-3.37252100	-2.52828000	-3.16070000
H	-3.31206600	-1.69665600	-3.86993600	H	-4.43741600	-2.75782300	-3.01856900
H	-2.91440100	-3.40648500	-3.62582300	C	-2.96924700	-3.67764400	-0.42288600
H	-2.26159600	-4.46745300	-0.69846400	H	-3.97964500	-4.05243900	-0.63397300
H	-2.89613000	-3.53460400	0.65858500				

Table 2.11.9 Optimized coordinates of $U^{IV}(CH_2SiMe_2NSiMe_3)[N(SiMe_3)_2]_2$.

U	-0.05648800	-0.08069400	0.31349600	N	1.35411100	-1.75826400	-0.09685100
N	0.96858000	1.93249800	-0.07886600	N	-2.30699100	-0.19661100	-0.04630700
C	0.05774100	-1.37642200	2.34314300	Si	1.20314200	-2.59907700	1.47716800
Si	2.29288000	2.46058500	0.95559600	Si	0.44816900	2.93262800	-1.43253500
Si	2.42844500	-2.17001700	-1.42081900	Si	-3.25805500	0.85807800	0.98442300
Si	-3.02547700	-1.40409100	-1.10132200	C	2.16813300	4.28933800	1.45359400
C	-1.70895200	-1.98342500	-2.34296300	C	2.86598900	-2.79791200	2.36846600
C	2.26973600	1.46336200	2.57440600	C	-2.04975300	1.75650100	2.15977000
C	0.42976200	-4.32008600	1.28101700	C	3.99362600	2.17707100	0.16602400
C	4.25854100	-2.10307800	-0.92301300	C	-4.19983900	2.20094500	0.03148700
C	-4.50075500	-0.07300200	2.07229100	C	-0.61564700	4.40743400	-0.88724400
C	1.89150600	3.60521600	-2.46663400	C	2.18385000	-0.92856700	-2.83607800
C	-4.49484000	-0.74539700	-2.10529600	C	2.08691800	-3.90716000	-2.10599200
C	-3.61299600	-2.93410200	-0.14540600	C	-0.61725500	1.89069700	-2.61558700
H	0.49572600	-0.96113100	3.25855900	H	-0.91824300	-1.81758500	2.59080500
H	2.27318100	4.96986000	0.60070200	H	2.96768400	4.53455900	2.16473800
H	1.21184400	4.51257400	1.94147000	H	-1.42601800	-1.18959500	-3.04500000
H	-2.10781100	-2.81532000	-2.93792400	H	-0.79637100	-2.35518600	-1.85934100
H	3.52670400	-3.50448300	1.85245900	H	2.69585800	-3.18462700	3.38126700
H	3.40366700	-1.84728400	2.45999100	H	1.33941600	1.58461200	3.14273700
H	3.08564900	1.82558500	3.21385600	H	2.44185900	0.39003700	2.43164600

H	-1.29426800	2.37028900	1.64923400	-1.53843000	1.07115800	2.84892700
H	-2.63103400	2.45036300	2.78112000	-0.54501800	-4.26664900	0.78154000
H	0.27440300	-4.77974700	2.26540700	1.06360300	-4.99541200	0.69403000
H	4.13169100	1.12238200	-0.10022300	4.79523400	2.45034100	0.86455400
H	4.13356100	2.76768500	-0.74569800	4.53239500	-1.12832700	-0.50227300
H	4.89561400	-2.27473500	-1.80049600	4.51296100	-2.86523000	-0.17834800
H	-3.53162500	2.78819000	-0.60938500	-4.68443800	2.89516900	0.73045000
H	-4.98213200	1.77951000	-0.60932100	-5.29428100	-0.54465300	1.48028300
H	-4.98649100	0.61540800	2.77601900	-4.01188200	-0.85955100	2.65911400
H	-1.49035900	4.08388700	-0.31051000	-0.98401600	4.95636900	-1.76380400
H	-0.05631300	5.11482900	-0.26553200	2.52072100	4.30936400	-1.90999800
H	1.50379800	4.13950500	-3.34383800	2.53788200	2.79824800	-2.83155800
H	1.18341400	-1.00009200	-3.27995600	2.90719800	-1.12088900	-3.63884400
H	2.33743800	0.10430000	-2.49990000	-5.35373700	-0.49530700	-1.47124800
H	-4.83026400	-1.50793800	-2.82018500	-4.22966700	0.15179800	-2.67672400
H	2.30226400	-4.68811100	-1.36720800	2.71806600	-4.10282400	-2.98268900
H	1.04217200	-4.02539800	-2.41663400	-2.79524500	-3.38772100	0.42788300
H	-3.99758200	-3.69786800	-0.83385600	-4.41388800	-2.69491100	0.56326500
H	-0.03625800	1.10507000	-3.11357600	-1.00463200	2.54901200	-3.40457800
H	-1.48904700	1.42897400	-2.13593900			

2.12 References

(1) Denning, R. G., *J. Phys. Chem. A* **2007,** *111*, 4125.
(2) Spezia, R.; Siboulet, B.; Abadie, S.; Vuilleumier, R.; Vitorge, P., *J. Phys. Chem. B* **2011,** *115*, 3560.
(3) Kosog, B.; La Pierre, H. S.; Heinemann, F. W.; Liddle, S. T.; Meyer, K., *J. Am. Chem. Soc.* **2012,** *134*, 5284.
(4) Hayton, T. W.; Boncella, J. M.; Scott, B. L.; Palmer, P. D.; Batista, E. R.; Hay, P. J., *Science* **2005,** *310*, 1941.
(5) Spencer, L. P.; Yang, P.; Scott, B. L.; Batista, E. R.; Boncella, J. M., *J. Am. Chem. Soc.* **2008,** *130*, 2930.
(6) Hayton, T. W.; Boncella, J. M.; Scott, B. L.; Batista, E. R., *J. Am. Chem. Soc.* **2006,** *128*, 12622.
(7) Fortier, S.; Wu, G.; Hayton, T. W., *J. Am. Chem. Soc.* **2010,** *132*, 6888.
(8) Ryan, J. L., *J. Inorg. Nucl. Chem.* **1971,** *33*, 153.
(9) Burns, C. J.; Smith, W. H.; Huffman, J. C.; Sattelberger, A. P., *J. Am. Chem. Soc.* **1990,** *112*, 3237.
(10) Graves, C. R.; Kiplinger, J. L., *Chem. Commun.* **2009**, 3831.
(11) Graves, C. R.; Vaughn, A. E.; Schelter, E. J.; Scott, B. L.; Thompson, J. D.; Morris, D. E.; Kiplinger, J. L., *Inorg. Chem.* **2008,** *47*, 11879.
(12) Benaud, O.; Berthet, J.-C.; Thuery, P.; Ephritikhine, M., *Chem. Commun.* **2011,** *47*.
(13) Korobkov, I.; Gambarotta, S., *Inorg. Chem.* **2010,** *49*, 3409.
(14) Burdett, J. K.; Albright, T. A., *Inorg. Chem.* **1979,** *18*, 2112.
(15) Anderson, K. M.; Orpen, A. G., *Chem. Commun.* **2001**, 2682.
(16) Mitoraj, M. P.; Zhu, H.; Michalak, A.; Ziegler, T., *Int. J. Quantum Chem.* **2009,** *109*, 3379.
(17) Pinter, B.; Van Speybroeck, V.; Waroquier, M.; Geerlings, P.; De Proft, F., *Phys. Chem. Chem. Phys.* **2013,** *15*, 17354.

(18) Nugent, W.; Mayer, J., *Metal-Ligand Multiple Bonds*. Wiley: New York: 1988.
(19) Tatsumi, K.; Hoffmann, R., *Inorg. Chem.* **1980,** *19*, 2656.
(20) Denning, R., Electronic structure and bonding in actinyl ions. In *Complexes, Clusters and Crystal Chemistry*, Springer Berlin / Heidelberg: 1992; Vol. 79, pp 215.
(21) O'Grady, E.; Kaltsoyannis, N., *J. Chem. Soc., Dalton Trans.* **2002**, 1233.
(22) Clark, D. L.; Conradson, S. D.; Donohoe, R. J.; Keogh, D. W.; Morris, D. E.; Palmer, P. D.; Rogers, R. D.; Tait, C. D., *Inorg. Chem.* **1999,** *38*, 1456.
(23) Ingram, K. I. M.; Haller, L. J. L.; Kaltsoyannis, N., *Dalton Trans.* **2006**, 2403.
(24) Tsushima, S., *Dalton Trans.* **2011,** *40*, 6732.
(25) Berg, J. M.; Clark, D. L.; Huffman, J. C.; Morris, D. E.; Sattelberger, A. P.; Streib, W. E.; Van der Sluys, W. G.; Watkin, J. G., *J. Am. Chem. Soc.* **1992,** *114*, 10811.
(26) Thomson, R. K.; Graves, C. R.; Scott, B. L.; Kiplinger, J. L., *Inorg. Chem. Commun.* **2011,** *14*, 1742.
(27) Turner, H. W.; Andersen, R. A.; Zalkin, A.; Templeton, D. H., *Inorg. Chem.* **1979,** *18*, 1221.
(28) Holloway, J. H.; Staunton, G. M.; Berry, J. A.; Brown, D., *J. Less-Common Met.* **1986,** *120*, 71.
(29) Fortier, S.; Wu, G.; Hayton, T. W., *Dalton Trans.* **2010,** *39*, 352.
(30) Allen, F. H., *Acta. Crystallogr. B* **2002,** *58*, 380.
(31) Lewis, A. J.; Williams, U. J.; Carroll, P. J.; Schelter, E. J., *Inorg. Chem.* **2013,** *52*, 7326.
(32) Bénaud, O.; Berthet, J.-C.; Thuéry, P.; Ephritikhine, M., *Inorg. Chem.* **2011,** *50*, 12204.
(33) Thomson, R. K.; Graves, C. R.; Scott, B. L.; Kiplinger, J. L., *Dalton Trans.* **2010,** *39*, 6826.
(34) Dormond, A.; El Bouadili, A.; Aaliti, A.; Moise, C., *J. Organomet. Chem.* **1985,** *288*, C1.
(35) B n aud, O.; Berthet, J.-C.; Thu ry, P.; Ephritikhine, M., *Inorg. Chem.* **2010,** *49*, 8117.
(36) Rebizant, J.; Apostolidis, C.; Spirlet, M. R.; Andreetti, G. D.; Kanellakopulos, B., *Acta Crystallogr. Sect. C* **1988,** *44*, 2098.
(37) Crawford, M.-J.; Ellern, A.; Karaghiosoff, K.; Mayer, P., *Inorg. Chem.* **2009,** *48*, 10877.
(38) Stewart, J. L.; Andersen, R. A., *New J. Chem.* **1995,** *19*, 587.
(39) Schelter, E. J.; Morris, D. E.; Scott, B. L.; Thompson, J. D.; Kiplinger, J. L., *Inorg. Chem.* **2007,** *46*, 5528.
(40) Kozimor, S. A.; Bartlett, B. M.; Rinehart, J. D.; Long, J. R., *J. Am. Chem. Soc.* **2007,** *129*, 10672.
(41) Gonsalves, J. W.; Steenkamp, P. J.; Du, P. J. G. H., *Inorg. Chim. Acta* **1977,** *21*, 167.
(42) Siladke, N. A.; Meihaus, K. R.; Ziller, J. W.; Fang, M.; Furche, F.; Long, J. R.; Evans, W. J., *J. Am. Chem. Soc.* **2011**, Article ASAP.
(43) Stewart, J. L. *Tris[bis(trimethylsilyl)amido]uranium: compounds with tri-, tetra-, and pentavalent uranium*; Lawrence Berkeley Lab.: 1988; p 200 pp.
(44) Rao, K. R.; Trevino, S. F.; Prask, H.; Mical, R. D., *Phys. Rev. B* **1971,** *4*, 4551.
(45) Bart, S. C.; Anthon, C.; Heinemann, F. W.; Bill, E.; Edelstein, N. M.; Meyer, K., *J. Am. Chem. Soc.* **2008,** *130*, 12536.
(46) Edelstein, N.; Brown, D.; Whittaker, B., *Inorg. Chem.* **1974,** *13*, 563.

(47) Lukens, W. W.; Edelstein, N. M.; Magnani, N.; Hayton, T. W.; Fortier, S.; Seaman, L. A., *J. Am. Chem. Soc.* **2013,** *135*, 10742.
(48) Fortier, S.; Kaltsoyannis, N.; Wu, G.; Hayton, T. W., *J. Am. Chem. Soc.* **2011,** *133*, 14224.
(49) Fortier, S.; Brown, J. L.; Kaltsoyannis, N.; Wu, G.; Hayton, T. W., *Inorg. Chem.* **2012,** *51*, 1625.
(50) Selbin, J.; Ortego, J. D., *Chem. Rev.* **1969,** *69*, 657.
(51) Bourdeaux, E. A. M., L. N., *Theory and Applications of Molecular Paramagnetism*. Wiley: 1976.
(52) The initial analysis was performed with Gaussian '09 Rev. A.02, giving slightly different results.
(53) Bridgeman, A. J.; Cavigliasso, G.; Ireland, L. R.; Rothery, J., *J. Chem. Soc., Dalton Trans.* **2001**, 2095.
(54) Barros, N.; Maynau, D.; Maron, L.; Eisenstein, O.; Zi, G.; Andersen, R. A., *Organometallics* **2007,** *26*, 5059.
(55) Straka, M.; Patzschke, M.; Pyykkö, P., *Theor. Chem. Acc.* **2003,** *109*, 332.
(56) Baker, J.; Scheiner, A.; Andzelm, J., *Chem. Phys. Lett.* **1993,** *216*, 380.
(57) Lewis, A. J.; Nakamaru-Ogiso, E.; Kikkawa, J. M.; Carroll, P. J.; Schelter, E. J., *Chem. Commun.* **2012,** *48*, 4977.
(58) Evans, W. J.; Lee, D. S.; Rego, D. B.; Perotti, J. M.; Kozimor, S. A.; Moore, E. K.; Ziller, J. W., *J. Am. Chem. Soc.* **2004,** *126*, 14574.
(59) Shannon, R., *Acta Crystallogr. Sect. A* **1976,** *32*, 751.
(60) Mansell, S. M.; Perandones, B. F.; Arnold, P. L., *J. Organomet. Chem.* **2010,** *695*, 2814.
(61) Sims, I. D., *J. Chem. Soc.* **1964**, 864.
(62) Burrows, R. C.; Crowe, B. F., *J. Appl. Polym. Sci.* **1962,** *6*, 465.
(63) Burns, C. J.; Clark, D. L.; Donohoe, R. J.; Duval, P. B.; Scott, B. L.; Tait, C. D., *Inorg. Chem.* **2000,** *39*, 5464.
(64) Simpson, S. J.; Turner, H. W.; Andersen, R. A., *Inorg. Chem.* **1981,** *20*, 2991.
(65) Kaltsoyannis, N.; Scott, P., *The f Elements*. Oxford University Press: 1999.
(66) Arnold, P. L.; Mansell, S. M.; Maron, L.; McKay, D., *Nat. Chem.* **2012,** *4*, 668.
(67) Avens, L. R.; Barnhart, D. M.; Burns, C. J.; McKee, S. D.; Smith, W. H., *Inorg. Chem.* **1994,** *33*, 4245.
(68) Castro-Rodriguez, I.; Olsen, K.; Gantzel, P.; Meyer, K., *J. Am. Chem. Soc.* **2003,** *125*, 4565.
(69) Lewis, A. J.; Williams, U. J.; Kikkawa, J. M.; Carroll, P. J.; Schelter, E. J., *Inorg. Chem.* **2012,** *51*, 37.
(70) Roussel, P.; Alcock, N. W.; Boaretto, R.; Kingsley, A. J.; Munslow, I. J.; Sanders, C. J.; Scott, P., *Inorg. Chem.* **1999,** *38*, 3651.
(71) Yin, H.; Lewis, A. J.; Williams, U. J.; Carroll, P. J.; Schelter, E. J., *Chem. Sci.* **2013,** *4*, 798.
(72) Hashem, E.; Swinburne, A. N.; Schulzke, C.; Evans, R. C.; Platts, J. A.; Kerridge, A.; Natrajan, L. S.; Baker, R. J., *RSC Adv.* **2013,** *3*, 4350.

Chapter 3

The Synthesis of Hexavalent Uranium Tris-Amide Complexes: Insight into the Inverse Trans Influence

3.1 Introduction. The structure and bonding of complexes possessing axial symmetry is central to the chemistry of the actinides. Foremost among such complexes is the uranyl cation, UO_2^{2+}. This species accounts for the majority of the uranium in the environment, including 4.5 billion tons in the Earth's seawater alone.[1] The mobility of uranyl through groundwater is a major concern in the long term storage of nuclear waste, as insoluble uranium(IV) materials are slowly oxidized to the more soluble UO_2^{2+}, allowing for the migration of uranium into the environment.[2] Though numerous methods have now been developed to extract and chemically transform uranyl,[3-13] there are still unanswered fundamental questions about the electronic structure of this ion.

Uranyl is a ubiquitous moiety in the chemistry of uranium due to its extraordinary thermodynamic stability, which has been attributed to an inverse trans influence (ITI),[14-17] a phenomenon described in detail in section 2.3. Whereas a trans influence is the thermodynamic weakening of the metal-ligand bond trans to a strong metal-ligand bond, the ITI imparts a synergistic thermodynamic stabilization between strong metal-ligand bonds trans to one another. Much theoretical work has gone into investigating the origins of the ITI,[14-16, 18] and experimental inquiry into the ITI has largely focused on the uranyl cation and its imido analogs.[19-24] The prevailing theory of the ITI is that mixing of an axial 5f orbital with semi-core 6p character of equal

The majority of this chapter has been adapted from previous publications. Sections 3.1-3.6 and Tables 3.16.1-3.16.10 are adapted with permission from "Reductive Cleavage of Nitrite to form Terminal Uranium Mono-Oxo Complexes" Lewis, A. J.; Carroll, P. J.; Schelter, E. J. *J. Am. Chem. Soc.* **2013**, *135*, 511–518. Sections 3.7-3.10 and Tables 3.16.11-3.16.49 are adapted with permission from "Stable Uranium(VI) Methyl and Acetylide Complexes and the Elucidation of an Inverse Trans Influence Ligand Series" Lewis, A. J.; Carroll, P. J.; Schelter, E. J. *J. Am. Chem. Soc.* **2013**, *135*, 13185–13192.

parity enables the stabilization. However, a detailed picture of thermodynamic contributions of the ITI in the formation and stability of uranium complexes has remained elusive.

3.2 Uranyl Analogues. Though numerous complexes of uranyl have been synthesized, substitution of the equatorial ligand environment has only a small impact on the electronic structure, and does not yield significant insight into the ITI. Analysis of the electronic structure of uranyl shows that the axial ligands play a dominant role in the makeup of the molecular orbital diagram.[15, 17] One potential strategy is to systematically vary the trans-axial ligands at an axially symmetric uranium(VI) ion. In spite of the strong thermodynamic driving force for uranyl formation, other uranium(VI) complexes possessing multiply bonded ligands have become increasingly well known.[25, 26] A number of these uranyl analogues exhibit characteristics of the ITI, suggesting that this phenomenon extends beyond the U=O bonding in uranyl.

Simple uranium(VI) oxo halides of the formula $[Ph_4P][U^{VI}OX_5]$ (X = F, Cl, Br) have been known for over 40 years, synthesized through treatment of $U^{VI}O_2Cl_2$ with thionyl chloride and Ph_4PCl to form $[Ph_4P][U^{VI}OCl_5]$, and subsequent addition of HF or HBr to form the pentafluoride or pentabromide complexes respectively.[27] An ITI was observed in the related complex $CsU^{VI}OF_5$, where the IR spectrum showed separate vibrational bands for the *trans*-fluoride ligand at ~500 cm^{-1} and the *cis*-fluoride ligands at ~400 cm^{-1}.[28] The electronic structure of these complexes revealed features of the ITI, including shortening of the *trans*-halides relative to the *cis*-halides and $5f_z3\text{-}6p_z$ mixing.[16] Attempts to use these uranium(VI) oxo halides as starting materials for further chemistry have historically met with limited success. However, seminal work by Denning and coworkers showed that phosphorane imide ligands could be installed in one or both axial coordination sites, in products of the formulae: $[Ph_4P][U^{VI}O[NP(p\text{-}Tol)_3]Cl_4]$ and $[Ph_4P][U^{VI}[NP(p\text{-}Tol)_3]_2Cl_4]$.[20] While not formally a multiply bonded uranium imido complexes, these iminato ligands exhibited partial U=N multiple bond character.

Uranyl analogues with genuine multiply-bonded ligands have received significant attention recently. The largest family of complexes structurally analogous to uranyl comes from recent work in the synthesis of uranium(VI) *trans*-bis-imido complexes. Uranium complexes

containing two *cis*-coordinated imido ligands were originally reported by Burns and coworkers, in the synthesis of $(C_5Me_5)_2U^{VI}(NPh)_2$, with a 98.7(4) ° N–U–N bond angle.[29] The synthesis of *trans*-bis-imido complexes was elusive up until the last decade, which saw numerous examples of the successful preparation of these complexes.[22, 29-43] The electronic structure of the RN=U=NR moiety was observed to be directly analogous to that of uranyl, with greater covalency due to the better matching of electronegativity of uranium with nitrogen compared to oxygen.[22] Partial hydrolysis of uranium(VI) bis-imido complexes has also enabled the synthesis of uranium(VI) oxo-imido complexes.[33] The U=O bond is capable of stabilizing reactive uranium-ligand multiple bonds, which has facilitated the synthesis of other uranyl analogues. Recent work from Hayton and coworkers has demonstrated that a highly reductive uranium(VI) mono-oxo complex, $[(C_5Me_5)_2Co][U^{IV}O[N(SiMe_3)_2]_3$, undergoes two-electron oxidation with chalcogenide-transfer reagents to form $[(C_5Me_5)_2Co][U^{VI}OE[N(SiMe_3)_2]_3$ (E = S, Se, Te).[44]

The variety of uranyl analogues that have been reported suggested that the ITI extends to a variety of ligand types, and that the ITI stabilizes otherwise reactive bonds. However, unanswered questions remain in the electronic origin of the ITI stabilization, and how the ITI compares between different types of ligands. Systematic variation in the axial ligand of a uranium(VI) mono-oxo complex with a conserved equatorial ligand environment was pursued as a means to contribute to answering these questions.

3.3 Reductive Cleavage of Nitrite to Form $UOX[N(SiMe_3)_2]_3$ Complexes. The one-electron reduction of nitrite (NO_2^-) to form nitric oxide (NO) is a critical reaction in denitrification.[45] This reaction is catalyzed by iron- or copper-containing nitrite reductase (NiR) enzymes that are present in anaerobic bacteria. Synthetic work directed toward understanding this reactivity has focused primarily on Cu-complexes that reduce nitrite under biologically relevant conditions.[46-49] Fe–NO_2 complexes can be deoxygenated by PPh_3 to form biologically relevant dinitrosyl iron complexes (DNICs).[50, 51] Metalloporphyrin nitrite complexes, M = Mn,[52] Fe,[52] Cr,[53] or Mo,[54] undergo N–O bond cleavage upon UV photolysis to generate metal-oxo complexes, a reaction that occurs in reverse in the case of $[Fe^{IV}O(tmc)(OAc)]^+$ (tmc = 1,4,8,11-tetramethyl-1,4,8,11-

tetraazacyclotetradecane), where NO adds to form a transiently stable Fe^{III}-nitrite complex.[55] In contrast, the reactivity of lanthanide- and actinide-nitrite complexes has received little attention, amidst numerous recent examples of activation of other small molecules with these elements.[56, 57]

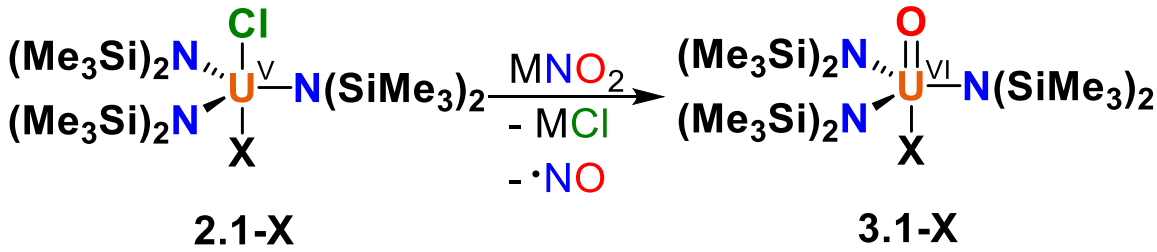

Scheme 3.3.1 Synthesis of terminal uranium(VI) mono-oxo complexes from reaction with nitrite.

We recently reported a methodology for the synthesis of several pentavalent uranium *trans*-dihalides of the formula $U^{V}X_2[N(SiMe_3)_2]_3$ ($X = F^-, Cl^-, Br^-$).[58] We hypothesized that reaction of small molecules with the uranium complexes containing favorable leaving groups in the axial positions could induce unusual reactivity. Indeed, upon treating $U^{V}[N(SiMe_3)_2]_3Cl_2$ with $NaNO_2$ in THF a significant color change of the reaction mixture from dark red to dark green was observed. Analysis of the product mixture revealed that no characteristic nitrite stretching bands could be identified by IR spectroscopy and no new paramagnetically shifted products could be observed in the ^1H NMR spectrum. X-ray structural analysis revealed the product of this reaction to be $U^{VI}OCl[N(SiMe_3)_2]_3$ (**3.1**) (Figure 3.3.1). The X-ray structure of **3.1-Cl** revealed a trigonal bipyramidal geometry in which mixed occupancy of the oxo- and chloro- ligand was observed at both sites. The product was isolated in 74% yield following recrystallization from $(Me_3Si)_2O$ (Scheme 3.3.1). This reaction represented the first example of a uranium(VI) terminal mono-oxo formed from a uranium(V)–halide complex.

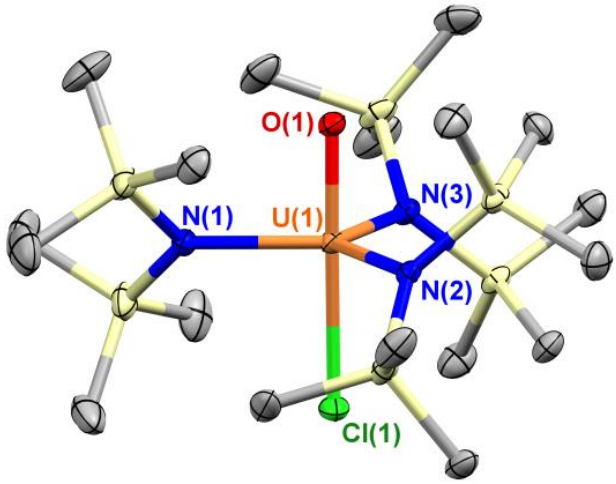

Figure 3.3.1 Thermal ellipsoid plot of **3.1-Cl** at 30% probability. Hydrogen atoms were omitted for clarity. Bond lengths (Å) and angles (deg): U(1)–O(1) 1.803(5), U(1)–O(1') 1.788(8), U(1)–Cl(1) 2.5369(17), U(1)–Cl(1') 2.546(3), U(1)–N(1) 2.196(2), U(1)–N(2) 2.193(2), U(1)–N(3) 2.191(2), O(1)–U(1)–Cl(1) 179.27(11), O(1')–U(1)–Cl(1') 178.6(2). The O(1) and Cl(1) atoms were disordered over the two axial positions.

Traditional methods to synthesize uranium mono-oxo complexes have focused on two-electron oxidation of uranium(III) or uranium(IV) precursors, with oxygen atom transfer reagents such as pyridine *N*-oxide, trimethylamine *N*-oxide, *N*-methylmorpholine-*N*-oxide, and 2,2,6,6-tetramethylpiperidine *N*-oxide.[59-65] Uranium mono-oxo complexes have also been prepared by double bond metathesis between uranium-imido complex and CO_2,[66] and through selective protonation of a single oxo ligand of uranyl.[67] The synthesis of **3.1-Cl** was also possible through the use of $AgNO_2$ without visible formation of Ag^0, proceeding over a shorter reaction time and in comparable yield. The increased reactivity of $AgNO_2$ towards $U^{V}Cl_2[N(SiMe_3)_2]_3$ is likely due to the higher lattice energy of AgCl than NaCl at 217 versus 184 kcal/mol respectively.[68]

The ^{1}H NMR spectrum of **3.1-Cl** exhibits two sharp resonances at 0.55 and 0.61 ppm in benzene-d_6 in a 1:1 ratio, due to the different chemical environments in each axial direction from the trigonal plane of the molecule. The appearance of two peaks at room temperature indicates hindered rotation about the U–N bonds caused by the collective arrangement of the bulky $–SiMe_3$ groups.[69] The U=O stretching peak was identified in the IR spectrum at 862 cm^{-1}, however this mode overlaps with strong vibrations from the amide ligands, supported by DFT calculations (*vide infra*).

Having isolated **3.1-Cl** directly through two routes from a uranium(V)-chloride precursor we next sought to expand the nitrite activation methodology to other uranium oxidation states. Complex **3.1-Cl** was similarly accessed by an alternative, stepwise pathway (Scheme 3.3.2). Addition of $AgNO_2$ to $U^{IV}Cl[N(SiMe_3)_2]_3$ in THF led to the formation of the known complex $U^{V}O[N(SiMe_3)_2]_3$,[65, 70] in an unprecedented direct oxidation of a uranium(IV) complex to a uranium(V)-oxo product. Subsequent oxidation of $U^{V}O[N(SiMe_3)_2]_3$ with $CuCl_2$ produced **3.1-Cl**. Additionally, **3.1-Cl** could be prepared in a two-electron oxidation from the addition of *N*-methylmorpholine-*N*-oxide to $U^{IV}Cl[N(SiMe_3)_2]_3$.

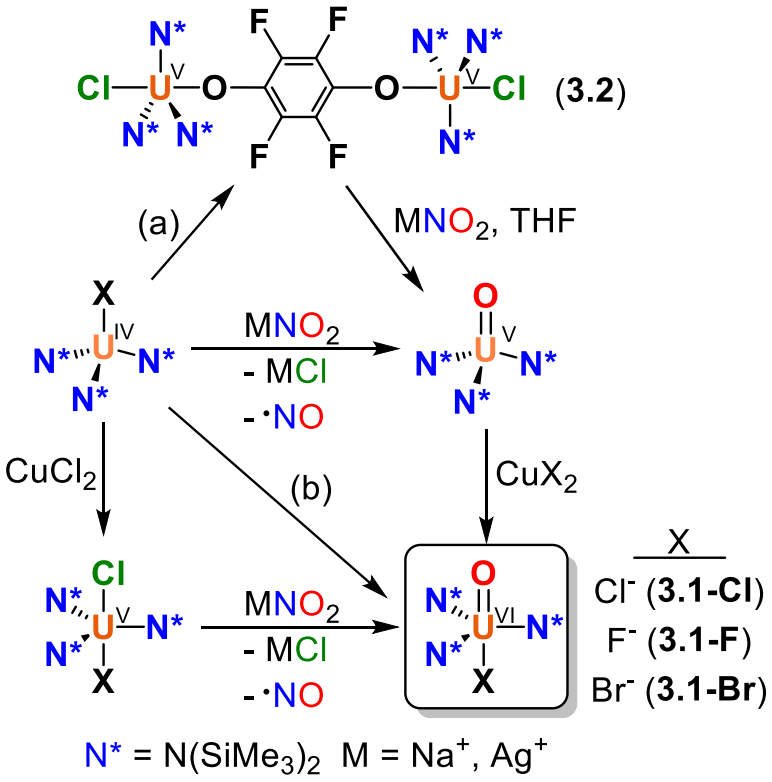

Scheme 3.3.2 Synthesis of uranium(VI) terminal mono-oxo complexes through various routes. (a) Fluoranil, Et_2O (b) *N*-methylmorpholine-*N*-oxide, Et_2O.

In the reaction of $U^{V}[N(SiMe_3)_2]_3Cl_2$ with NO_2^-, longer reaction times led to the formation of yellow $U^{VI}O_2[N(SiMe_3)_2]_2(THF)_2$ as a side product, which was identified by comparison of the ^1H NMR spectrum of the reported compound and confirmed by X-ray crystallography.[4, 71] Complete conversion to the uranyl product was observed after two days in the presence of excess NO_2^-.

The absence of available valence electrons on uranium in **3.1-Cl** implies that the second nitrite reduction occurs by means of oxidation of an $N(SiMe_3)_2^-$ ligand to the highly unstable bis(timethylsilyl)aminyl radical. The aminyl radical is known to elicit hydrogen atom abstraction from ethereal solvents to generate $HN(SiMe_3)_2$.[72] Indeed, the free amine $HN(SiMe_3)_2$ was detected by ^1H NMR as a product of the second oxidation reaction. Homolytic cleavage of a M–$N(SiMe_3)_2$ bond has been proposed in the one-electron reduction of a uranyl complex previously.[73] This second oxidation pathway was not observed when the reactions were performed in Et_2O, suggesting that uranyl formation is promoted in THF.

We expected that inhibiting the second nitrite substitution step would preclude uranyl formation. To test this hypothesis, we employed the uranium(V) complex $U^{V}ClF[N(SiMe_3)_2]_3$, which has one chloride ligand and one fluoride ligand in the axial positions. Our hypothesis was that addition of one equivalent of nitrite anion to $U^{V}ClF[N(SiMe_3)_2]_3$ would preferentially form a mono-oxo complex. Reaction of $U^{V}ClF[N(SiMe_3)_2]_3$ with $AgNO_2$ in Et_2O led to the formation of the expected product $U^{VI}OF[N(SiMe_3)_2]_3$ (**3.1-F**) (Figure 3.3.2). The corresponding reaction of $U^{V}ClF[N(SiMe_3)_2]_3$ with $NaNO_2$ also led to formation of **3.1-F** without the generation of uranyl, however, this reaction proceeded more slowly than the similar reaction to form **3.1-Cl**. An inverse trans effect of the U–Cl bond by the stronger U–F bond likely limits the rate of nitrite substitution and the utility of this pathway. Similar to **3.1-Cl**, treatment of $UF[N(SiMe_3)_2]_3$ with *N*-methylmorpholine-*N*-oxide also cleanly generated **3.1-F**.

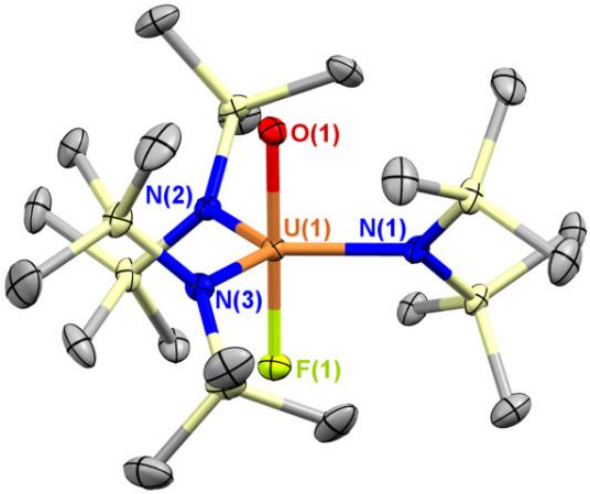

Figure 3.3.2 Thermal ellipsoid plot of **3.1-F** at 30% probability. Hydrogen atoms are omitted for clarity. Bond lengths (Å) and angles (deg): U(1)–O(1) 1.9198(16), U(1)–F(1) 1.9246(16), U(1)–N(1) 2.210(2), U(1)–N(2) 2.2060(19), U(1)–N(3) 2.2090(19), F(1)–U(1)–O(1) 179.07. U–F and U–O bond lengths are unreliable due to partial occupancy of these two atoms in the two axial positions.

The ^{1}H NMR spectrum of **3.1-F** was similar to that of **3.1-Cl**, with two sharp resonances in a 1:1 ratio. The ^{19}F NMR spectrum displayed a single peak at 586.8 ppm versus $CFCl_3$. ^{19}F NMR data for molecules containing U^{IV}–F bonds are rare and useful for the calibration of theoretical methods; compounds of the formula UF_nCl_{6-n} exhibit resonances between +750–790 ppm,[74] in which the shift is dependent on the nature of the trans U-F/Cl bonding.[75] In the IR spectrum of **3.1-F**, the U=O stretch was identified at 882 cm^{-1}, about 20 cm^{-1} higher in energy than that of **3.1-Cl**, consistent with a greater ITI stabilization by fluoride than chloride. A similar comparison of *trans*-fluoro versus *trans*-oxo ligand substitution on the energies of U–F stretching modes has been noted previously.[28]

Attempts to form the analogous uranium-oxo-bromide complex from reaction of $U^{V}Br_2[N(SiMe_3)_2]_3$ with nitrite were unsuccessful due to the rapid substitution of bromide with nitrite, leading to facile uranyl formation even at low temperature. However, addition of *N*-methylmorpholine-*N*-oxide to $U^{IV}Br[N(SiMe_3)_2]_3$ produced $U^{VI}OBr[N(SiMe_3)_2]_3$ (**3.1-Br**). The structure of **3.1-Br** was confirmed by X-ray diffraction of a single crystal obtained from recrystallization from pentane. The IR spectrum of **3.1-Br** showed a U=O stretching peak at 859 cm^{-1}, at slightly lower energy than that of **3.1-Cl**.

Having observed the ability for homolysis of a U–$N(SiMe_3)_2$ bond to induce nitrite reduction, we were interested in whether a deliberate ligand-based redox event could be exploited to reduce nitrite in a controlled fashion. Addition of *p*-fluoranil (FA, tetrafluoro-1,4-benzoquinone) to 2 equiv $U^{IV}Cl[N(SiMe_3)_2]_3$ led to an immediate color change from pale tan to dark brown. Recrystallization from pentane afforded $[U^{V}Cl[N(SiMe_3)_2]_3]_2(\mu_2\text{-FA})$ (**3.2**) as a black solid. Structural analysis, IR spectroscopy, near-IR absorption spectroscopy, and solution electrochemistry support the presence of two uranium(V) ions in the complex that are bridged by a tetrafluoro-*p*-phenylenediolate (Figure 3.3.3). The diolate ligand in **3.2** is the product of doubly-reduced FA.

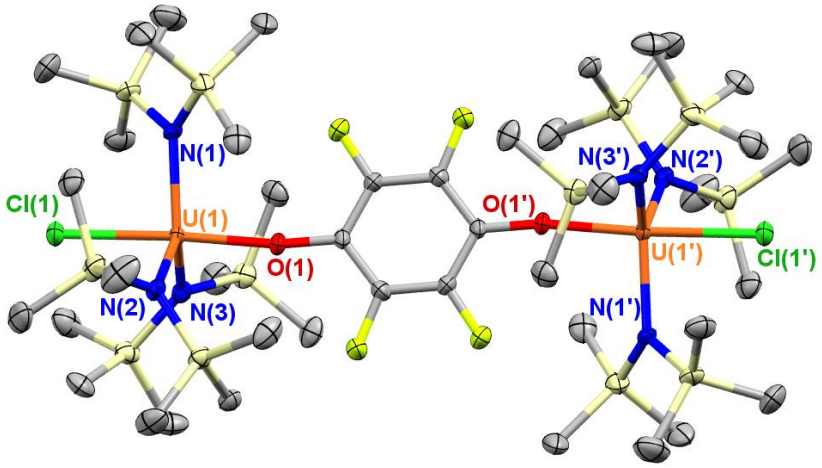

Figure 3.3.3 Thermal ellipsoid plot of **3.2** at 30% probability. Hydrogen atoms are omitted for clarity. Bond lengths (Å) and angles (deg): U(1)–Cl(1) 2.5852(19), U(1)–N(1) 2.166(7), U(1)–N(2) 2.189(6), U(1)–N(3) 2.189(6), U(1)–O(1) 2.145(5), O(1)–C(1) 1.353(8), Cl(1)–U(1)–O(1) 176.20(15), U(1)–O(1)–C(1) 169.3(5).

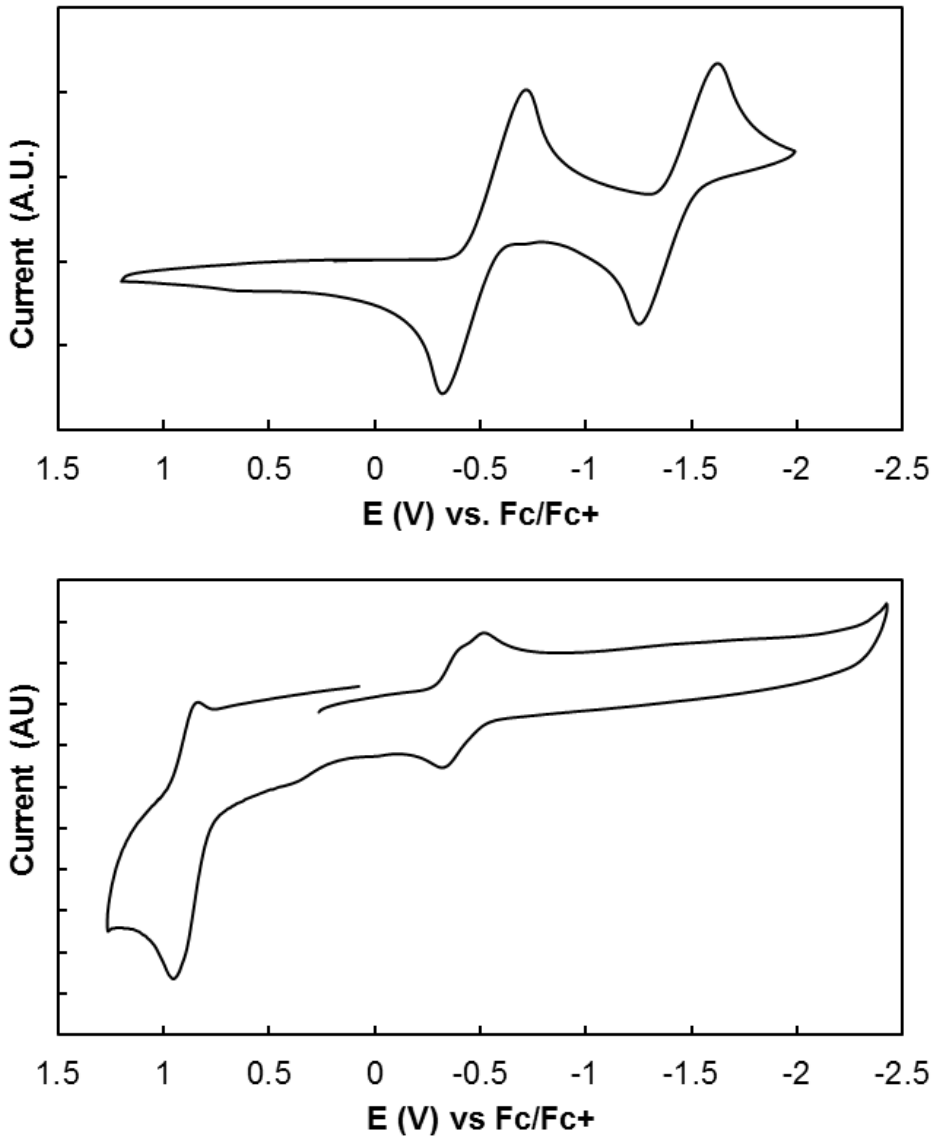

Figure 3.3.4 Cyclic votammogram of *p*-fluoranil (top) and **3.2** (bottom) in CH_2Cl_2 with 0.1 M [^{n}Bu$_4$N][PF_6] supporting electrolyte. Potentials are relative to an internal ferrocenium/ferrocene standard.

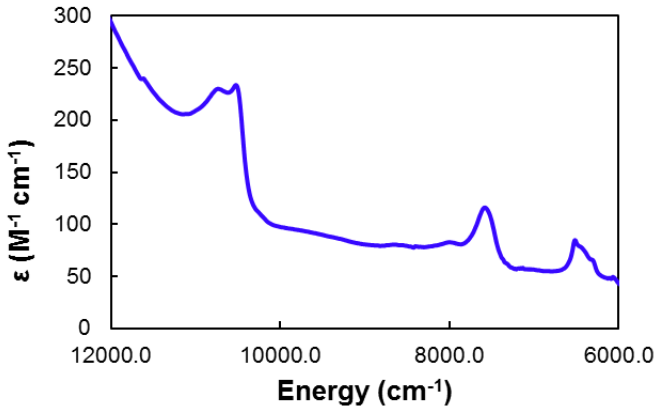

Figure 3.3.5 Near-IR spectrum of **3.2** in toluene.

The oxidation state of **3.2** is proposed to be U^{V}/U^{V}, based on the evidence provided by the characterization data. Electrochemical data displays both reduction and oxidation couples below and above the rest potential respectively, at potentials similar to those in $U^{V}Cl_2[N(SiMe_3)_2]_3$ (Figure 3.3.4). The near-IR spectrum, in which absorptions due to f-f transitions appear, exhibits few peaks, consistent with a U^{V} oxidation state assignment (Figure 3.3.5). The reduced nature of the fluoranil ligand is deduced from the IR spectrum, which shows no stretches consistent with carbonyl character, and multiple sharp bands consistent with a hydroquinone structure. Analysis of the bond lengths in **3.2** reveals a short U–O bond to both metal centers, consistent with the presence of negative charge on the oxygen rather than a neutral donor interaction. The internal bond lengths in the tetrafluorophenylene-1,4-diolate ligand are consistent with C–O single bonds and delocalized C–C bonds. Additionally, the complex is centered about a crystallographic 2-fold axis, necessitating an identical coordination environment at each metal center. These data strongly support a U^{V}/U^{V} assignment with a fully reduced hydroquinone-like ligand rather than possible U^{IV}/U^{IV} or U^{V}/U^{IV} with partial ligand reduction.

Multiple overlapping peaks between –3 and 0 ppm are present in the ^{1}H NMR spectrum of **3.2** due to the large steric demand of the axial ligands and the different chemical environment on each face of the complex. The resonances between –3 and 0 ppm coalesce into two broad peaks above 45 °C, centered at –0.74 and –1.16 ppm. A single paramagnetically shifted peak was observed in the ^{19}F NMR spectrum at room temperature. Addition of 2 equiv $NaNO_2$ to **3.2** in

THF led to formation of $U^{V}O[N(SiMe_3)_2]_3$ as the major product. Although this reaction formally proceeds through loss of NaCl and neutral fluoranil, a black insoluble solid is produced that contains a mixture of unidentified products that are readily separated. This reaction demonstrates the ability to install an oxo ligand at a uranium center without change in the metal oxidation state through use of a redox active supporting ligand. A similar strategy was employed by Bart *et al* to affect a 2-electron oxygen atom donation reaction in a U^{III}/U^{IV} transformation, in which one electron originates from a reduced bipyridyl ligand.[63]

3.4 Analysis of Nitrite Reduction Mechanism. The formation of **3.1** from nitrite reduction proceeds through formal loss of NO, however, gas evolution was not directly observed in the reaction of $U^{V}Cl_2[N(SiMe_3)_2]_3$ with $NaNO_2$, due to the slow reactivity. The sluggish reactivity is attributed to the poor solubility of $NaNO_2$ in common organic solvents. However, the formation of **3.1-Cl** proceeded more rapidly with $AgNO_2$ resulting in observable gas evolution. The presence of nitric oxide in the evolved gas was confirmed by exposing the gaseous products to a solution of $Mo(N^tBuAr)_3$, Ar = 3,5-dimethylphenyl, using a system of nested vials. Capture of the gaseous reaction products led to formation of the known compound $Mo(N^tBuAr)_3(NO)$ as judged by IR spectroscopy.[76]

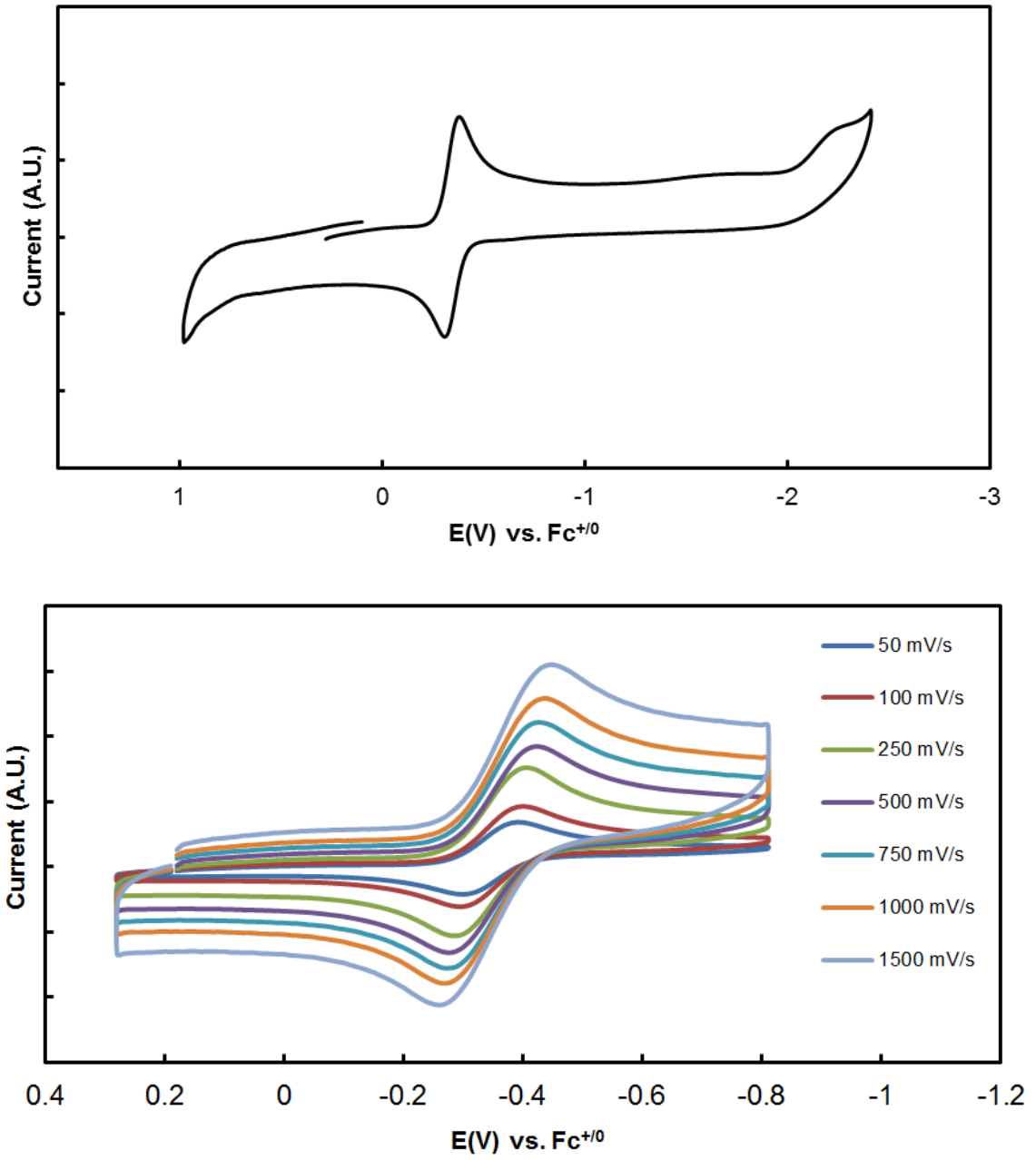

Figure 3.4.1 Cyclic votammogram of **3.1-Cl** in CH_2Cl_2 with 0.1 M [$^nBu_4N$][PF_6] supporting electrolyte (top). Scan rate dependence of isolated U(VI/V) couple (bottom). Potentials are relative to an internal ferrocenium/ferrocene standard.

Analysis of the electrochemical potentials involved in the oxidation processes that lead to **3.1-Cl** and to the higher oxidation uranyl product suggests that the nitrite reduction reaction is electrochemically unfavorable. Electrochemistry measurements performed on $U^{V}Cl_2[N(SiMe_3)_2]_3$ in CH_2Cl_2 revealed a U(VI/V) couple of +0.91 V versus Fc/Fc^+,[58] which is greater than the

reported aqueous standard reduction potential of the nitrite/nitric oxide couple of +0.52 V ($E°' = +0.37$ V) at pH = 7.[77] This difference is rationalized by electrochemical measurements on **3.1-Cl**, which show that the U(VI/V) couple is shifted to –0.35 V upon installation of the oxo-ligand, corresponding to a stabilization of 1.26 V (Figure 3.4.1). Similarly, the amide ligand oxidation in **3.1-Cl** is beyond the observable window of +1 V, yet the second oxidation to form the uranyl product is spontaneous. The electrochemical data imply that these reactions are mediated by the thermodynamic driving force of uranium-oxo bond formation rather than favorable electron transfer. To develop a detailed understanding of the thermochemistry involved in these reactions, we next studied species along the nitrite reduction reaction coordinate using DFT.

3.5 Theoretical Analysis of Reaction Coordinate. A computational investigation was carried out on the reaction pathway leading to complex **3.1-F**. DFT calculations were performed on $U^{V}ClF[N(SiMe_3)_2]_3$, several isomers of the intermediate $U^{V}(ONO)F[N(SiMe_3)_2]_3$, and $U^{VI}OF[N(SiMe_3)_2]_3$ (Figure 3.5.1). The synthesis of **3.1-F** implicates the initial associative formation of an unstable uranium-nitrite complex. In the proposed mechanism, homolytic cleavage of the N–O bond is accompanied by single electron transfer from the uranium(V) center, formally generating the uranium(VI)-oxo complex and nitric oxide. Given the potential for different possible nitrite coordination modes, we explored intermediates possessing κ^1-ONO, κ^2-O_2N, and κ^1-NO_2 linkages.

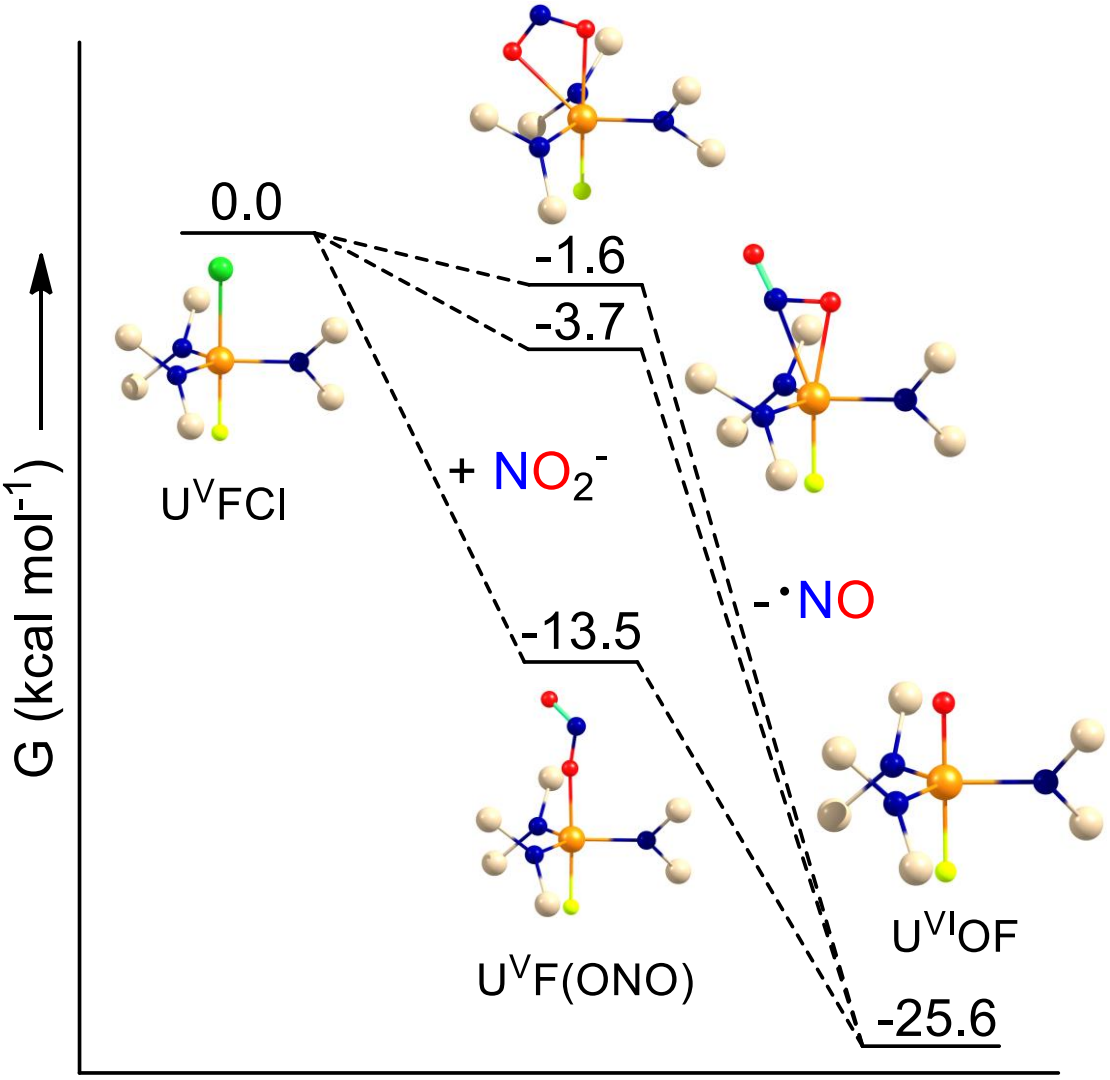

Figure 3.5.1 DFT calculated relative free energies for the proposed formation of **3.1-F** by reductive cleavage of nitrite. Methyl groups were removed for clarity.

A minimum was found for each of the isomers, except for the κ^1-NO_2 complex, which converged to an η^2-ONO structure. Of the three isomers the κ^1-ONO complex was found to be the lowest in energy. This complex exhibited a perturbation of the internal nitrite bond lengths with a proximal N–O bond of 1.383 Å and a distal N=O bond of 1.190 Å, indicative of alternating single and double bond character, as well as a short U–ONO bond length of 2.163 Å. The bonding arrangement in this intermediate is poised toward formation of a uranium-oxygen multiple bond and a nitrogen-oxygen multiple bond. In comparison, longer U–O bond lengths are noted in the

other calculated isomers, with approximately equal N–O bond lengths indicative of delocalization. Previous to this work, only one structurally characterized U–ONO complex wass known.[78] In that single example the nitrite ion bridges two uranyl ions. More recent work from Cantat and coworkers showed that $[Ph_4P]_2[UO_2(NO_2)_4]$ could be prepared from salt metathesis and oxidation of UCl_4.[79] In this example, the nitrite ligands exhibited both κ^1-ONO and κ^2-NO_2 coordination modes, in which the N–O bonds were 1.255(3) and 1.254(3) Å in the κ^2-NO_2 ligands and 1.305(3) and 1.211(3) in the proximal and distal N–O bonds of the κ^1-ONO ligands.[79]

The nitrite reduction mechanism proposed in the formation of **3.1-F** differs from that of nitrite reductases (NiR). In either the T2 copper center of the Cu-NiR enzymes or the heme-iron center of Fe-NiR,[80] nitrite is proposed to undergo one electron reduction to induce cleavage of the N–O bond. Similar reactivity has been demonstrated in synthetic iron complexes.[81, 82] However, in general, reductive cleavage of NO_2^- is coupled to proton transfer with formation of metal-nitrosyl complexes and H_2O.[83] Recent work from the Solomon group suggests that CuNiR forms a κ^2-O_2N complex, which is protonated to form Cu^I–(HNO_2) facilitating electron transfer to Cu^{II}–OH and nitric oxide.[84] The reactivity exhibited by uranium in the formation of **3.1-Cl** and **3.1-F** is fundamentally different from the reactivity of CuNiR, and is driven by formation of the U=O multiple bond. The U=O bond enthalpy is the primary driver for overcoming the barrier to electron transfer without the need for protonation. As axial, high valent uranium complexes are known to exert an ITI,[15-17] we next evaluated the electronic structures of our unique uranium(VI) compounds in detail.

3.6 Calculated Electronic Structures of 3.1-X Complexes. A computational investigation of the of the isoelectronic complexes $U^{VI}F_2[N(SiMe_3)_2]_3^+$ (***3.1-F₂***), $U^{VI}OF[N(SiMe_3)_2]_3$ (***3.1-OF***), and $U^{VI}O_2[N(SiMe_3)_2]_3^-$ (***3.1-O₂***)[85] was performed to better understand the effect of axial ligand substitution on the electronic structure at uranium. The complex ***3.1-F₂*** has not yet been isolated, but electrochemical data supports its stability on that timescale. The frequency calculation performed on ***3.1-OF*** gave a U=O stretching mode of 905 cm^{-1} and a U–F stretching

mode of 522 cm^{-1}, in reasonably good agreement with the experimentally observed values of 882 cm^{-1} and 504 cm^{-1}.

The optimized structures of the three complexes display a pronounced equatorial metal-ligand bond lengthening upon shifting from fluoro- to oxo-substitution, shown in Table 3.6.1. Similarly, the Mayer bond order (MBO) of the U–N bonds decreases with the increasing U–N bond lengths. These metrics are indicative of greater *cis*-destabilization by the oxo-ligands than the fluoride ligands. *Cis*-destabilization is recognized as a characteristic feature of an inverse *trans* influence (ITI),[16] though its precise origin is not completely understood.

Table 3.6.1 Comparison of computationally derived bonding metrics in ***3.1-F$_2$***, ***3.1-OF*** and ***3.1-O$_2$***.

	3.1-F$_2$	***3.1-OF***	***3.1-O$_2$***
U–N_{ave} calc'd (Å)	2.127	2.235	2.367
U–N_{ave} obs'd (Å)	-----	2.208(2)	2.310(5)
U–N_{ave} MBO	1.266	0.970	0.734
%U in U-N_{ave} NBOs	18.68	15.21	10.15
%U in U-F/O NBOs	8.37	17.65	19.45
U Natural Charge	1.924	1.702	1.725
N_{ave} Natural Charge	-1.352	-1.481	-1.597
U($6p_z$) depopulation	-0.140	-0.158	-0.181

NBO analysis showed a decreasing contribution of uranium AO character to the U–N bonding interactions upon substitution of fluoride with oxo ligands, along with an increase in contribution of uranium AO character to axial U–F/O bonding interactions. The natural charge on uranium decreaseed with oxo ligand substitution, while the natural charges on the amide nitrogen atoms became substantially more negative. These values suggested that the equatorial metal-ligand bonding was polarized away from the metal center by the stronger axial donor oxo ligands, suggestive of more ionic equatorial bonding. This means that the donation from the axial oxygen atom is much greater that the equatorial nitrogen atoms, rendering the equatorial bonding more ionic with increasing numbers of *trans*-oxo ligands. Therefore, the greater *cis*-destabilization exerted by the oxo ligands can largely be attributed to electrostatic effects, due to the smaller covalent component to the equatorial bonding compared to the axial bonding. This is reflected in the structure of the complex $[Na(THF)_2][UO_2(N(SiMe_3)_2)_3]$, in which a Na^+ ion is directly bound to

one uranyl-oxo ligand. The Na^+ cation attenuates the negative charge on the oxygen atom, and as a result the U–N bond lengths in this complex are shorter than those calculated for ***3.1-O₂***.

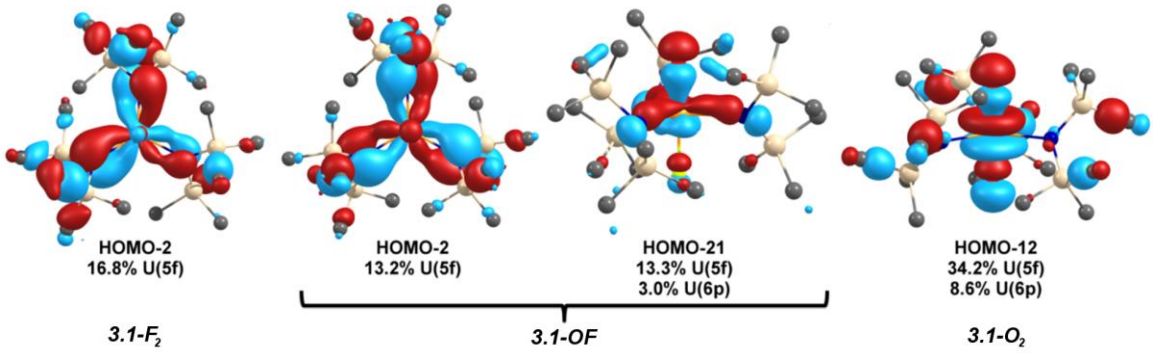

Figure 3.6.1. Comparison of occupied molecular orbitals of ***3.1-F₂*** (left), ***3.1-OF*** (center), and ***3.1-O₂*** (right) of greatest U(5f) orbital character.

The nature of the axial bonding in these complexes was further examined through orbital analysis. Analysis of the uranium AO character in the occupied orbitals showed greater U(5f) character contributing to equatorial bonding interactions for ***3.1-F₂***, and substantially more U(5f) character contributing to axial bonding interactions in ***3.1-O₂***, illustrated in Figure 3.6.1. The complex ***3.1-OF*** exhibited intermediate behavior, with U(5f) character contributing approximately equally to axial and equatorial bonding interactions. Fragment molecular orbital analysis showed depopulation of the filled uranium semi-core 6p AOs in all three complexes; however, while the $6p_x$ and $6p_y$ depopulation remained relatively constant, depopulation of the $6p_z$ orbital increased upon oxo substitution (Table 3.6.1). Notable U(6p) character was present in axial σ-bonding interactions (Figure 3.6.1), most pronounced in ***3.1-O₂***. Mixing of the uranium $6p_z$ and $5f_z3$ orbitals has been previously implicated in ITI stabilization of axial bonding.[17] The LUMO to LUMO+6 orbitals of each of the complexes are of primarily uranium(5f) character, as shown in Figure 3.6.2. Progressing from ***3.1-F₂*** to ***3.1-O₂***, there is a substantial increase in the axial U–O/U–F σ* and π* orbital energies, coupled to a decrease in the U–N σ* and π* orbital energies. This trend in orbital energies also suggests that greater axial covalent interactions diminish equatorial U(5f)-ligand covalent interactions.

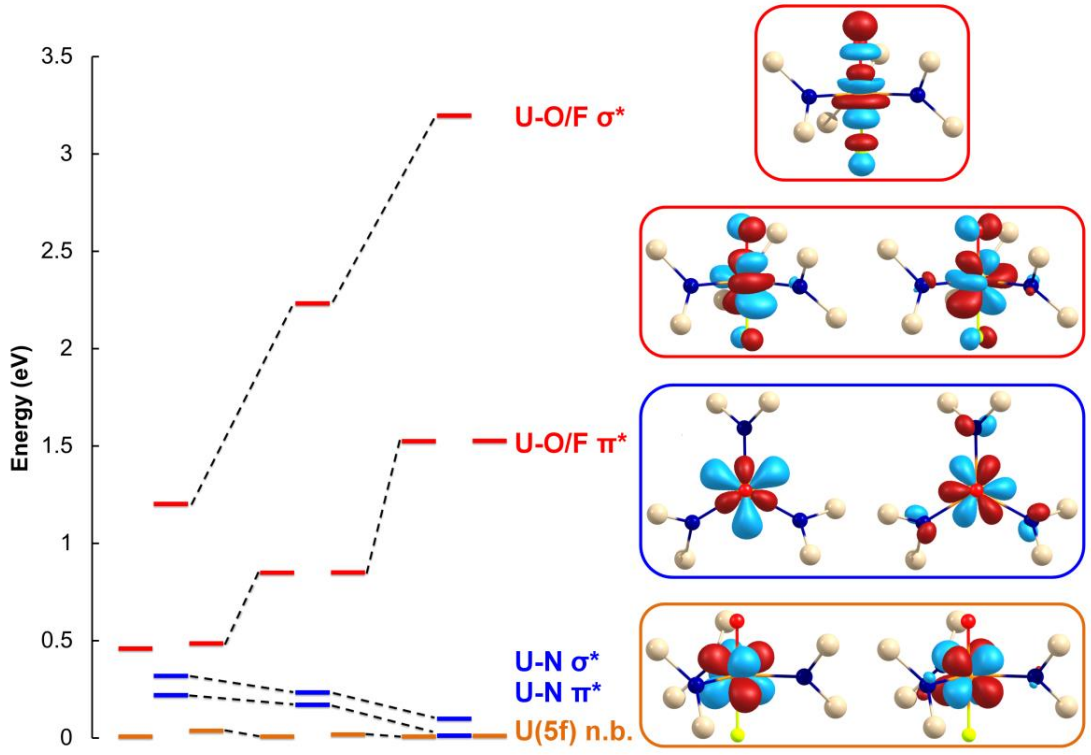

Figure 3.6.2 Correlation diagram between calculated LUMO to LUMO+6 orbitals for $U^{VI}F_2[N(SiMe_3)_2]_3^+$ (left), $U^{VI}OF[N(SiMe_3)_2]_3$ (middle), and $U^{VI}O_2[N(SiMe_3)_2]_3^-$ (right). Energies are plotted relative to the LUMO adjusted to 0 eV. Orbitals shown as degenerate pairs are not strictly degenerate, as each compound was optimized in C_1 rather than C_3 or D_3 symmetry. Orbitals shown are right are for ***3.1-OF***, with methyl groups removed for clarity.

3.7 High Valent Uranium Hydrocarbyl Complexes. High valent uranium carbon bonds have attracted attention historically following the work of Wilkinson.[86] Recently, significant effort has been made toward isolating high valent homoleptic uranium alkyl complexes,[87-89] following the successful syntheses of low valent derivatives.[90-93] Efforts from the Hayton group have demonstrated that homoleptic uranium(VI) alkyl complexes are thermally unstable,[87] which has prevented their crystallographic characterization and further exploration of their reactivity.

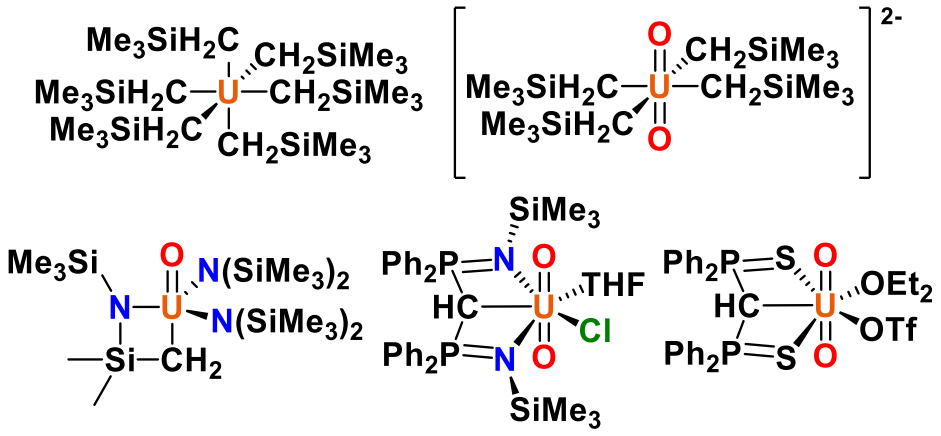

Figure 3.7.1 Known uranium(VI) hydrocarbyl-type complexes.[64, 87, 88, 94]

Several examples of complexes bearing uranium(VI)-carbon bonds supported by heteroatoms and/or chelating linkages have been reported (Figure 3.7.1).[64, 94-100] Recently, a uranyl(VI)-alkyl complex was structurally characterized: $[Li(DME)_{1.5}]_2[UO_2(CH_2SiMe_3)_4]$ and its stability attributed to "-ate" complex formation; even the uranyl(VI)-alkyl-ate complex was found to be unstable above –25 °C.[88, 101] A stable example of the parent unsupported uranium(VI) alkyl-linkage has proven elusive. In our work, we show that uranium(VI)-alkyl complexes can be stabilized by the inverse trans influence, by installing uranium-carbon bond trans to oxo ligands. We demonstrate that the ITI affords even greater stability to uranium(VI)-carbon bonds than that offered by –ate complex formation or the uranyl moiety.

3.8 Synthesis/Characterization of $U^{VI}OR[N(SiMe_3)_2]_3$ (R = CCPh, Me). Addition of *N*-methylmorpholine-*N*-oxide to an Et_2O solution of $U^{IV}Me[N(SiMe_3)_2]_3$ at –21 °C led to a rapid color change to dark red, cleanly producing the corresponding oxidation product $U^{VI}O(Me)[N(SiMe_3)_2]_3$ (**3.1-Me**) in 96% yield following recrystallization from pentane (Scheme 3.8.1). Solutions of **3.1-Me** kept at room temperature over several days exhibited no decomposition, a remarkable stability that stands in contrast to the two reported uranium(VI)-alkyl complexes.[87, 88] No example of a uranium(VI)-methyl complex has previously been reported. A single uranium(V)-methyl complex is known, which was not structurally characterized.[102]

The ^1H NMR spectrum of **3.1-Me** displayed two resonances for the –trimethylsilyl groups indicative of a sterically saturated C_3 symmetry, similar to related six coordinate tris(silylamido)

complexes.[58, 103, 104] A single resonance was observed for the methyl ligand at –2.57 ppm, comparable to the shift of the methylene protons in $U^{VI}O[N(SiMe_3)_2]_2[CH_2SiMe_2NSiMe_3]$ at –1.89 ppm.[105] Preparation of a $^{13}CH_3$ labeled derivative of **3.1-Me** allowed for straightforward determination of the ^{13}C NMR shift of the methyl group, which appeared at +301.0 ppm in benzene-d_6, consistent with other known uranium(VI)-carbon bonds.[88, 106] The large shift results from spin-orbit coupling effects at the uranium(VI) cation; the calculation of such chemical shifts is an area of on-going interest.[106]

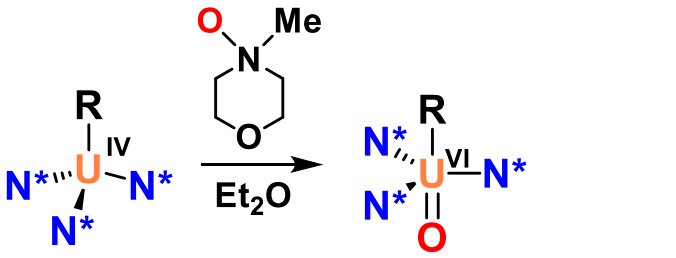

R = -Me (**3.1-Me**)
-CCPh (**3.1-CCPh**)

Scheme 3.8.1 Synthesis of **3.1-Me** and **3.1-CCPh**.

The single crystal structure of **3.1-Me** revealed the expected five coordinate uranium(VI) cation where the U–N bonds form a trigonal plane and range from 2.215(2)–2.225(2) Å (Figure 3.8.1). The oxo and methyl groups are located in a trans disposition with a U=O distance of 1.791(3) Å, which is in the range of reported uranium(VI) mono-oxo complexes.[103] The uranium(VI)–methyl distance is the shortest known U–terminal alkyl bond at 2.343(4) Å. Reported structurally characterized uranium(IV)-methyl complexes contain U–C bond lengths in the general range of ~2.4–2.5 Å.[60, 91, 107-120] Additionally, we performed structural analysis of the starting material: $U^{IV}Me[N(SiMe_3)_2]_3$ (Figure 3.8.2),[121] which exhibited a U–C bond length of 2.450(15). The U–C bond of $U^{VI}O[N(SiMe_3)_2]_2[CH_2SiMe_2NSiMe_3]$ is comparatively shorter at 2.319(2),[105] due to the strained nature of the four atom metalacycle. U–C bonds shorter than 2.3 Å are also present in complexes bearing phosphonium ylides, either neutral or deprotonated; the heteroatom stabilized U–C bonds are further shortened by chelation.[122-124]

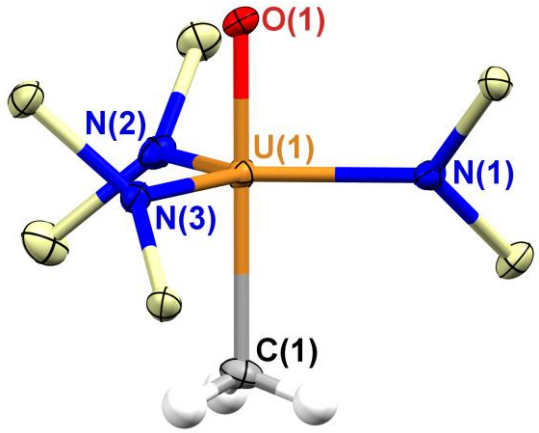

Figure 3.8.1 Thermal ellipsoid plot of **3.1-Me** at 30% probability. All methyl groups other than the methyl ligand are omitted for clarity. Bond lengths (Å) and angles (degrees): U(1)–O(1) 1.791(3), U(1)–C(1) 2.343(4), U(1)–N(1) 2.215(2), U(1)–N(2) 2.223(2), U(1)–N(3) 2.225(2), O(1)–U(1)–C(1) 178.95(18).

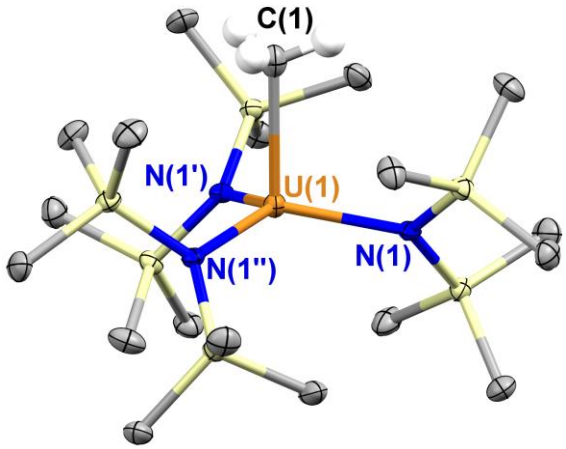

Figure 3.8.2 Thermal ellipsoid plot of $U^{IV}Me[N(SiMe_3)_2]_3$ at the 30% probability. Hydrogen atoms – except for those of the methyl group – are omitted for clarity. Bond lengths (Å) and angles (degrees): U(1)–N(1) 2.259(3), U(1)–C(1) 2.450(15), N(1)–U(1)–C(1) 99.48(8).

Analogous to the synthesis of **3.1-Me**, addition of *N*-methylmorpholine-*N*-oxide to an *in situ* generated solution of $U^{IV}(PhCC)[N(SiMe_3)_2]_3$ led to the formation of a dark brown product determined to be $U^{VI}O(PhCC)[N(SiMe_3)_2]_3$ (**3.1-CCPh**). We observed limited stability of the uranium(IV)-phenylacetylide precursor complex consistent with the literature report.[125] In contrast, samples of **3.1-CCPh** stored in C_6D_6 were stable for days with no noticeable decomposition by ^1H NMR spectroscopy. The stability of **3.1-CCPh** allowed for structural characterization of the complex (Figure 3.8.3) as well as elemental analysis. Complex **3.1-CCPh** represents the first

example of a uranium(VI)-acetylide complex. Additionally, there is only one example of a uranium(V)-acetylide complex that was not structurally characterized.[126]

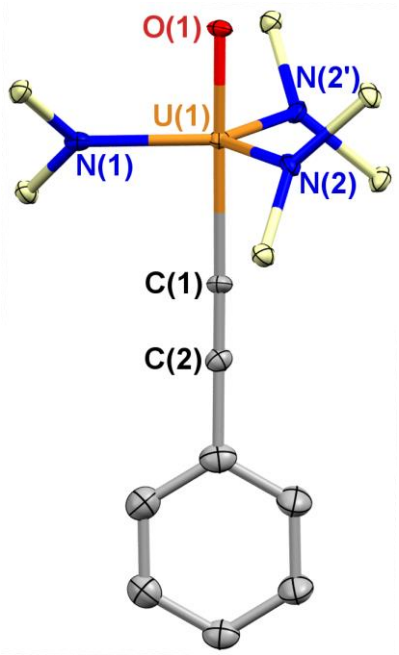

Figure 3.8.3 Thermal ellipsoid plot of **3.1-CCPh** at 30% probability. Methyl groups and hydrogen atoms are omitted for clarity. Bond lengths (Å) and angles (degrees): U(1)–O(1) 1.811(10), U(1)–C(1) 2.337(14), U(1)–N(1) 2.225(7), U(1)–N(2) 2.189(5), C(1)–C(2) 1.209(1), O(1)–U(1)–C(1) 177.2(7), U(1)–C(1)–C(2) 176.9(14).

The U–N bonds of **3.1-CCPh** are slightly longer than those observed in **3.1-Me**, ranging from 2.189(5) to 2.225(7). The U=O bond in **3.1-CCPh** is also slightly longer, at 1.811(10), than that in **3.1-Me**, indicating a more activated set of axial bonds. However, the U–C bond in **3.1-CCPh**, at 2.337(14), is slightly shorter than that of **3.1-Me**, likely a result of the smaller steric profile of the acetylide group. This U–C bond is shorter than other known uranium-phenylacetylide complexes, which are typically ~2.4 Å.[127]

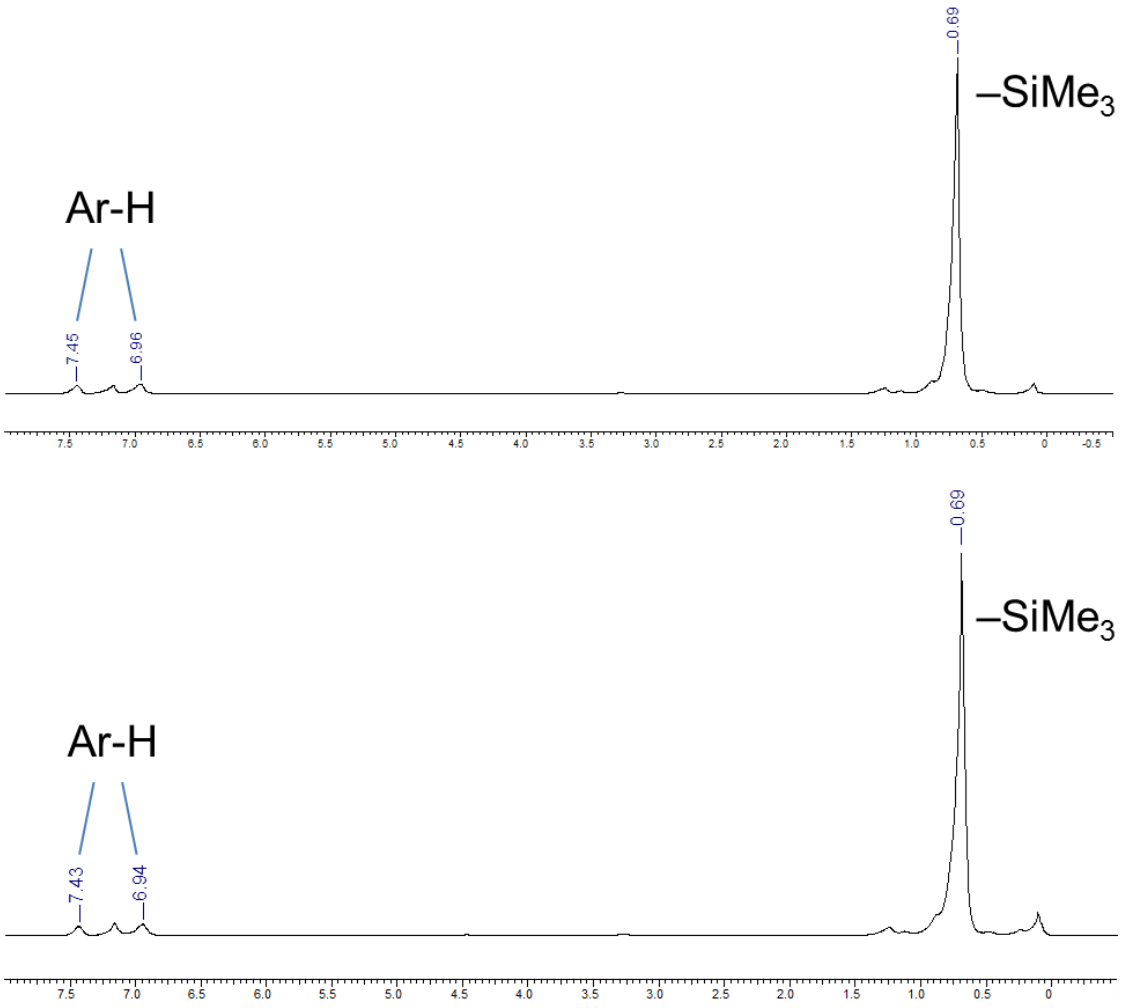

Figure 3.8.4 ^{1}H NMR spectrum of **1-CCPh** in C_6D_6 in a J Young tube at room temperature (top), and after storage for 14 days (bottom).

Given the room temperature stability of **3.1-CCPh** and **3.1-Me** we became interested in their resistance to thermolysis, especially given the potential for the complexes to cyclometalate to $U^{VI}O[N(SiMe_3)_2][CH_2SiMe_2NSiMe_3]$ with elimination of HCCPh or methane respectively. The complex **3.1-CCPh** was found to be rather unreactive, heating of C_6D_6 solutions of **3.1-CCPh** resulted in only minor decomposition as shown in Figure 3.8.4; the complex is evidently stable toward cyclometalation and elimination of HCCPh to at least 75 °C. Heating of **3.1-Me** at 75 °C in C_6D_6 induced decomposition to a mixture of as yet unidentified products. We expect the decomposition of **3.1-Me** is driven by the strong entropic component of methane elimination. It is evident that the trans disposition of the U–C bonds in **3.1-Me** and **3.1-CCPh** confers extraordinary

stability as compared to the two reported uranium(VI)-alkyl complexes. In this context DFT calculations were pursued to illuminate the electronic structure origins for the stability.

3.9 Calculated Electronic Structures. In order to study the remarkable electronic stabilization provided by the *trans*-oxo ligand in detail, computational studies were carried out. Hybrid DFT with the B3LYP functional using a 60 electron effective core potential was applied to uranium,[128] and the 6-31G* basis set for all other atoms. The phenylacetylide ligand in the model of **3.1-CCPh** was truncated to a methylacetylide group (**3.1-CCMe**).

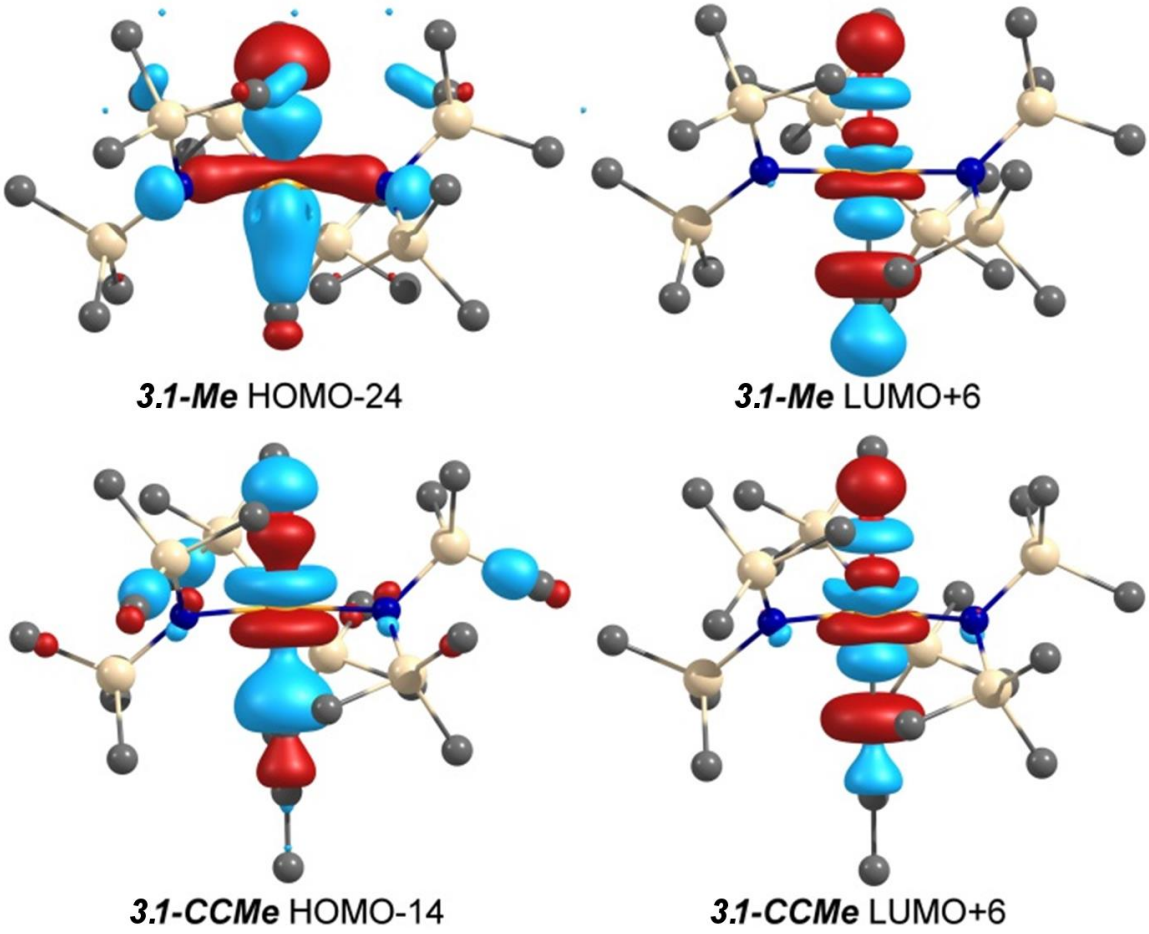

Figure 3.9.1 Molecular orbitals of **3.1-Me** (top) and **3.1-CCMe** (bottom) exhibiting σ-bonding (left) and σ*-anti-bonding (right) character.

Inspection of the axial uranium-ligand bonding in **3.1-Me** and **3.1-CCMe** revealed a general similarity to the electronic structure of the uranyl cation.[17] Critically, the calculations reveal that the molecular orbitals involved in U–O σ-bonding in **3.1-Me** and **3.1-CCMe** also

contained U–C bonding character (Figure 3.9.1). The mixing of U–O and U–C σ-bonding lowers the energy of the U–C orbital interaction, which is expected to strengthen the U–C bond and diminish the reducing strength of the coordinated alkyl group, such that it does not spontaneously reduce the uranium(VI) ion. Resistance to reduction is an essential feature, given that uranium(VI) can be a potent oxidant when not stabilized as uranyl.[8] In the case of **3.1-Me**, this interaction primarily involved a uranium f-d hybrid orbital in the HOMO–24 (Figure 3.9.1). The uranium $5f_{z3}$ orbital contributed significantly to U–C σ-bonding in the HOMO-3, with a smaller component of U–O σ-bonding. In contrast, in **3.1-CCMe**, the uranium $5f_{z3}$ AO showed approximately equal contribution to U–O and U–C σ-bonding in the HOMO–14 (Figure 3.9.1). Regardless, in both complexes the LUMO+6 corresponded to the uranium $5f_{z3}$ σ* interaction, with mixing of 42-52% uranium $5f_{z3}$ character and 10-15% uranium $6p_z$ character. Mixing of $6p_z$ character in axial σ-bonding is believed to be a significant contributor to ITI stabilization.[16] These σ and σ* orbitals are directly analogous to those present in the uranyl cation, where the $5f_{z3}/6p_z$ AOs contribute approximately equally to the σ* orbital.[17]

Natural Bond Orbital (NBO) analysis of **3.1-Me** and **3.1-CCMe** revealed substantial covalency of the U–C bonds. Calculated uranium natural charges of +1.66 and +1.53 for **3.1-Me** and **3.1-CCMe** respectively indicate greater charge donation than that previously calculated for the analogous uranyl complex of +1.73.[103] The natural charges on the methyl and acetylide ligands were –0.21 and –0.25 respectively. The uranium AO contributions to U–C bonding were, remarkably, 28.6% in **3.1-Me** and 25.3% in **3.1-CCMe**. These values are comparable to the 32.0% uranium AO contribution to U–C σ-bonding in $[(BIPM)U^{VI}OCl_2]$ (BIPM = bis(iminophosphorano)methanediide), which also exhibits a linear *trans*-CUO linkage.[64]

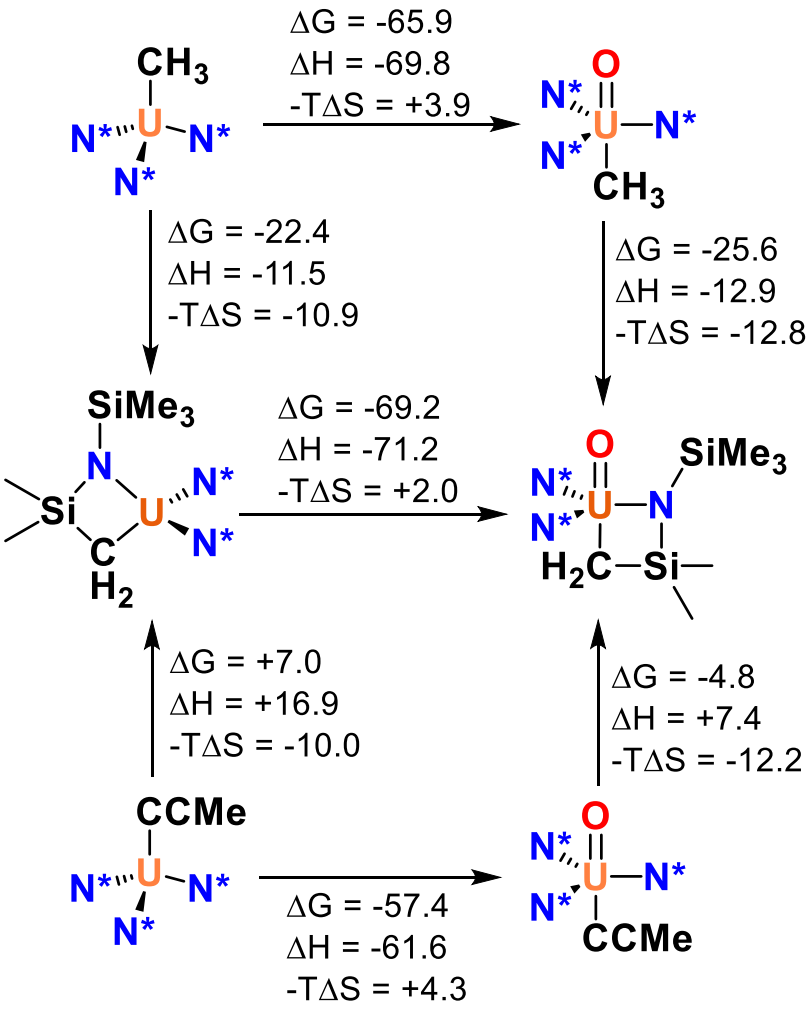

Figure 3.9.2 Computed thermodynamics of alkane/alkyne elimination reactions.

Given that complexes of the formula $U^{IV}R[N(SiMe_3)_2]_3$ are frequently reactive toward γ-deprotonation,[129] but were found to be rather stable in this context upon heating, the stability of **3.1-Me** and **3.1-CCMe** toward cyclometalation was also tested computationally. Comparison of the energies of the optimized structures with the known cyclometalated complex $U^{VI}O[N(SiMe_3)_2]_2[CH_2SiMe_2NSiMe_3]$ allowed for extraction of the thermodynamic parameters involved (Figure 3.9.2). The cyclometalation reactions of both complexes were calculated to be spontaneous, though the ΔH value was positive for **3.1-CCMe**, reflecting the relative pK_a of methane (~56)[130] versus that of phenylacetylene (28.7).[131] The cyclometalation reactions of **3.1-**

Me and **3.1-CCMe** were calculated to be more favorable than those of the corresponding uranium(IV) complexes.

In total, the electronic structures of **3.1-Me** and **3.1-CCMe** reveal stabilities engendered by the axial disposition of ligands. In particular, the *trans*-oxo group strengthens the U–C bonds and reduces the tendency for the coordinated hydrocarbyl groups to reduce the uranium(VI) cations. Noting this key interaction, we next considered its extent across a variety of ligand types.

3.10 Establishing an Inverse Trans Influence Ligand Series. With our unusual uranium(VI)-hydrocarbyl complexes in hand, computational analysis of related **3.1-X** complexes was performed with the goals of organizing common ligand types into an ITI series when trans to an oxo-group and determining the relative stabilization of the U–C bonds. Along with the compounds prepared here and in our previous work (X = Me^-, F^-, $CCPh^-$, Cl^-, and Br^-),[103] we also considered theoretical derivatives of interest (X = NMe_2^-, OMe^-, H^-, SPh^-, I^-, CN^-) (Figure 3.10.1). The five isolated **3.1-X** compounds and their six theoretical counterparts represent an important opportunity to examine the ITI in a structurally conserved framework. In the work of O'Grady and Kaltsoyannis, an increasing ITI was determined in complexes of the formula $[UOX_5]^-$, where X = Br^- < Cl^- < F^-,[16] providing us with a basis for comparison. In addition to the uranium(VI) complexes, DFT calculations were also performed on the isostructural uranium(V) complexes of the formula $[U^{V}OX[N(SiMe_3)_2]_3]^-$ (**3.3-X**) as well as uranium(IV) complexes of the formula $U^{IV}X[N(SiMe_3)_2]_3$ (**3.4-X**) (Figure 3.10.1). The optimized structure geometries were in good agreement with the available experimental structures (Tables 3.10.1).

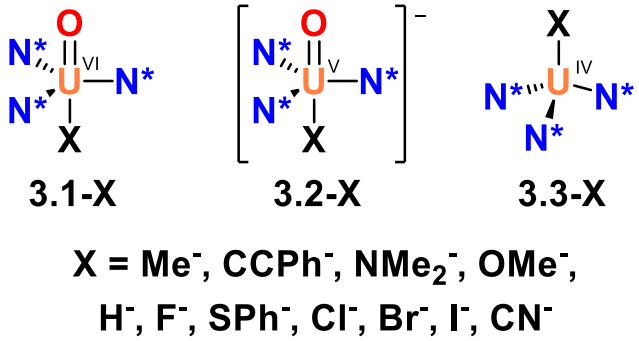

Figure 3.10.1 Computational models considered in this work.

Table 3.10.1 Comparison of optimized structures with reported structural parameters.

	U–N calc.	U–N exp.	U–X calc.	U–X exp.
3.1-Me	2.292	2.221(2)	2.351	2.343(4)
3.1-CCMe	2.236	2.201(8)	2.326	2.337(14)
3.1-F[103]	2.235	2.208(2)	2.029	–
3.1-Cl[103]	2.221	2.193(2)	2.584	2.5369(17)
3.1-Br[103]	2.218	2.200(3)	2.739	2.7311(19)
3.4-Me	2.279	2.259(3)	2.438	2.450(15)
3.4-H[132]	2.264	2.237(9)	2.034	–
3.4-I[65]	2.252	2.238(4)	3.044	2.9512(8)

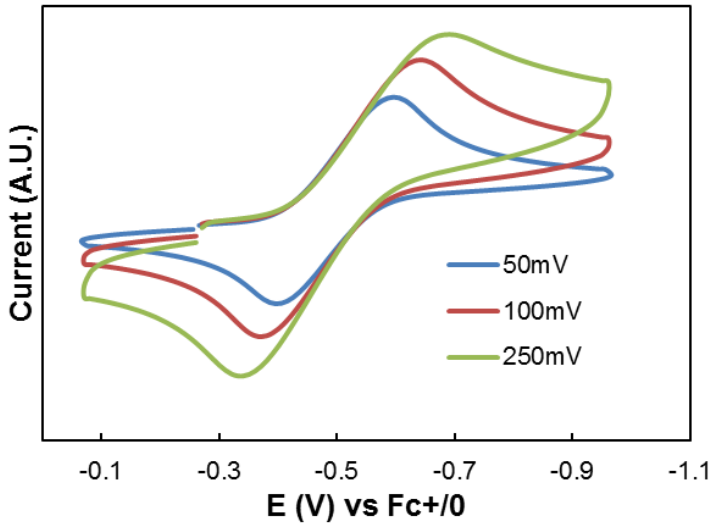

Figure 3.10.2 Cyclic voltammogram of **3.1-CCPh** in fluorobenzene at various scan rates.

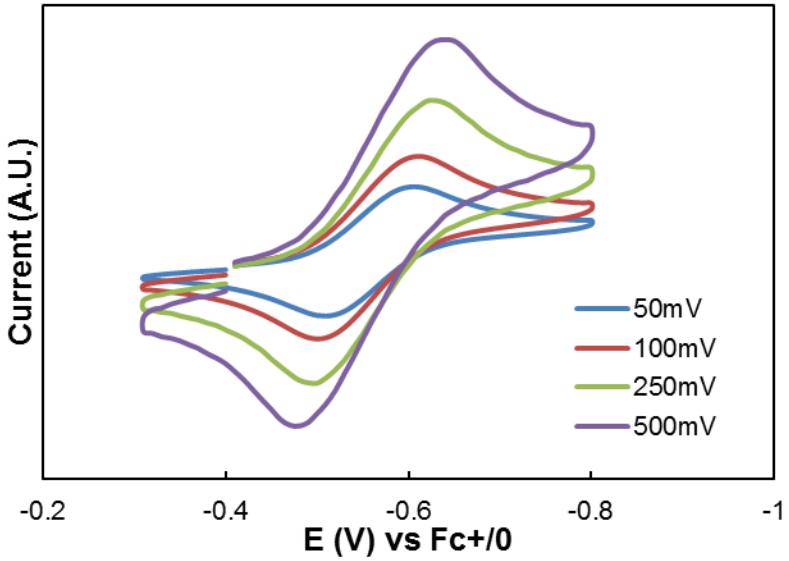

Figure 3.10.3 Cyclic voltammogram of **3.1-F** in fluorobenzene at various scan rates.

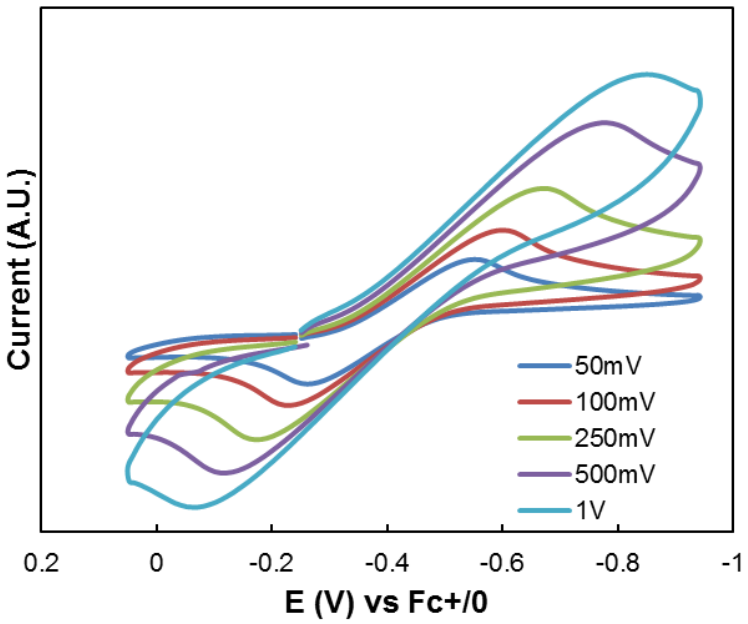

Figure 3.10.4 Cyclic voltammogram of **3.1-Cl** in fluorobenzene at various scan rates. Note that better reversibility, at a potential of –0.35 V, was observed previously in CH_2Cl_2 for the uranium(V/IV) couple.[103]

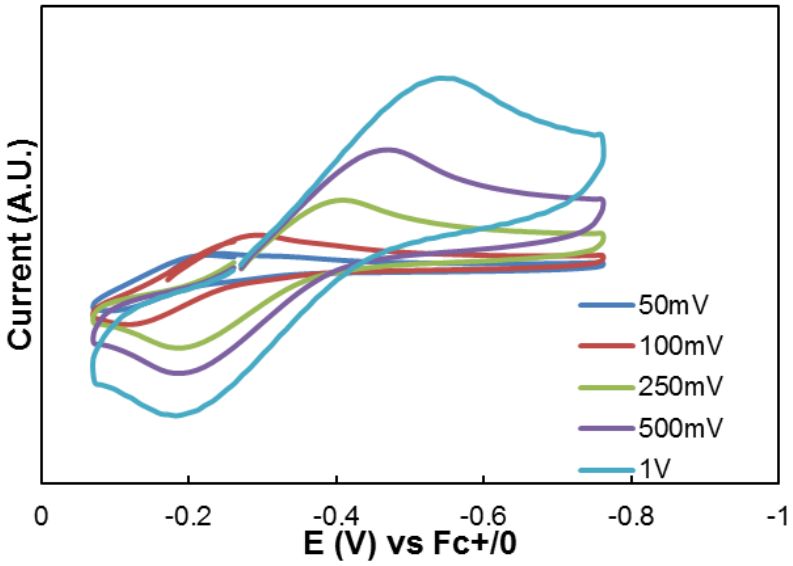

Figure 3.10.5 Cyclic voltammogram of **3.1-Br** in fluorobenzene at various scan rates. Note the large shift in potential and loss of reversibility at higher scan rates.

It has recently been established that within the **3.1-X** framework, strong axial donating ligands induce *cis*-destabilization through a decrease in the covalency of the equatorial

bonding.[103, 104] The presence of *cis*-destabilization may be ascertained from an increase in equatorial uranium-ligand bond length with a concomitant decrease in the equatorial metal-ligand bond order. The degree of equatorial uranium-ligand bond covalency is supported by NBO analysis. Build-up of negative natural charge on the donor nitrogen atoms (q_N) is indicative of a polarization toward greater ionicity. A decrease in uranium AO character of the equatorial metal-ligand bonds can be interpreted as a reduction in covalency.

Table 3.10.2 Equatorial bonding analysis for **3.1-X** complexes ordered by decreasing cis-destabilization.

	U–N Bond Length Calc.[a]	U–N Bond Length Expt.[a]	U–N MBO[b]	q_N[c]	%U AO[d]
3.1-NMe_2	2.292	–	0.892	–1.514	14.27
3.1-Me	2.255	2.221(2)	0.904	–1.503	14.41
3.1-OMe	2.261	–	0.913	–1.498	14.48
3.1-H	2.233	–	0.955	–1.491	14.84
3.1-F	2.235	2.208(2)	0.970	–1.481	15.21
3.1-CCMe	2.236	2.201(8)	0.971	–1.466	15.51
3.1-SPh	2.235	–	0.965	–1.457	15.98
3.1-Cl	2.221	2.193(2)	1.016	–1.444	15.63
3.1-Br	2.218	2.200(3)	0.990	–1.439	15.93
3.1-I	2.217	–	1.007	–1.438	15.98
3.1-CN	2.211	–	1.035	–1.438	16.48

[a] Average of three equatorial bonds, in Å. [b] Average equatorial Mayer bond order.[133] [c] Average natural charge on equatorial nitrogen atoms. [d] % contribution of uranium AO character to equatorial bonding.

The results of the DFT calculation on the **3.1-X** series demonstrated that all of the calculated metrics supported *cis*-destabilization resulting from the ITI exerted by the variable axial ligands. The computational analysis resulted in a positive correlation between the four variables: U–N bond lengths, U–N MBO, q_N, %U AO (Table 3.10.2). As the calculated equatorial U–N bond lengths increases, the calculated average equatorial U–N Mayer Bond Order decreases, the natural charge on the equatorial amide nitrogen atoms becomes more negative, and the percent uranium AO character involved in equatorial bonding decreases. Therefore, based solely on analysis of equatorial bonding, an approximate trend in ITI ligand strength was established.

While equatorial bonding analysis provides an indirect measurement of the donor strength of various ligands, the subtlety of the *cis*-destabilization changes across the series prompted us to consider direct analyses of the axial bonding. In the IR spectra of the **3.1-X**

complexes that were synthesized, as expected, the observed U=O stretching frequency was higher for the complexes that had a larger calculated *cis*-destabilization. However, frequency calculations performed on the **3.1-X** complexes revealed coupling of the primary U=O stretching mode with C–H and Si–C wagging and bending modes in the silylamide ligands due to their coincidental energies, which complicated simple analysis and correlation (Figure 3.10.6).

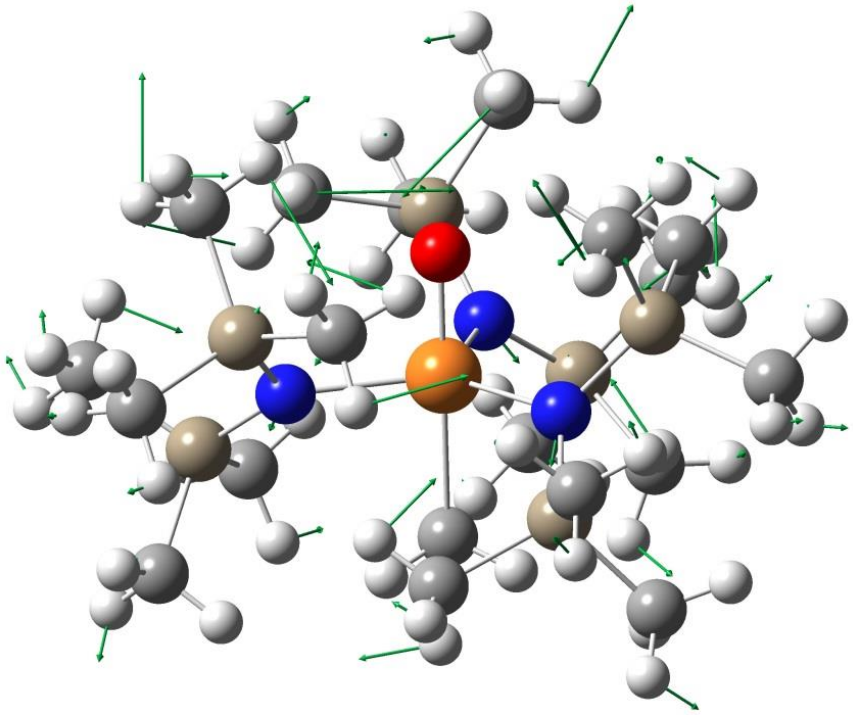

Figure 3.10.6 Silylamide ligand displacement vectors present in calculated vibrational mode of **3.1-Me** with greatest U=O stretching character. Displacement vectors have been enlarged for clarity. The U–O displacement vector is occluded by the bond.

A convenient, direct comparison of the donor strength of the various ligands in the **3.1-X** complexes can be extracted from the uranium(V/VI) reduction potentials. Given that the structure of the complexes is conserved, with the exception of the X ligand, a decrease in the reduction potential can be directly attributed to stronger axial donation to the uranium ion. The reduction potentials of the complexes were determined from the calculated ΔG obtained from comparison of the optimized free energies of the corresponding **3.1-X** and $[U^{V}OX[N(SiMe_3)_2]_3]^-$ (**3.3-X**) complexes, incorporating solvation effects using a PCM solvent continuum model following the recently reported procedure.[134] The calculation of reduction potentials of actinide complexes has

been demonstrated previously.[135-137] Indeed, measured electrochemical data for the complexes that have been prepared follow the predicted trend.

Table 3.10.3 Electronic stabilization of **3.1-X** complexes ordered by decreasing axial donor strength.

	$E_{1/2}$ $U^{V/VI}$		$\Delta G_{[O]}$ [c]	$\nu_{U=O}$ (Exp.)
	Calc.[a]	Exp.[b]		
3.1-H	–1.17	–	–68.0	–
3.1-Me	–1.01	–0.68[d]	–65.9	884
3.1-NMe_2	–0.94	–	*–56.3*[e]	–
3.1-OMe	–0.82	–	*–56.6*[e]	–
3.1-F	–0.66	–0.57	–59.5	882
3.1-CCMe	–0.71	–0.51	–57.4	878
3.1-SPh	–0.55	–	–54.7	–
3.1-Cl	–0.52	–0.43	–54.6	862
3.1-Br	–0.44	–0.21	–53.4	859
3.1-I	–0.42	–	–51.9	–
3.1-CN	–0.39	–	*–57.4*[e]	–

[a] In eV, referenced to the calculated $Fc^{+/0}$ couple. [b] In eV, referenced to $Fc^{+/0}$. [c] Calculated change in free energy for oxygen atom transfer analogous to Scheme 3.8.1, in kcal mol^{-1}. [d] Unstable under electrochemical conditions, decomposition was observed after initial scan. [e] Values in italics do not fit the trend, see text.

The calculated reduction potentials are observed to become more negative following the trend in *cis*-destabilization established from the equatorial bonding analysis (Tables 1 and 2). Despite the weakening of the equatorial bonding, the uranium ion becomes more electron rich, indicating stronger axial donation. Two notable exceptions to the trend determined in Table 3.10.3 were the **3.1-Me** and **3.1-H** complexes, which exhibited greater stabilization of the 6+ oxidation state than expected (*vide infra*).

To further support the trend in axial ligand strength, we also examined the thermodynamic driving force for U=O bond formation, $\Delta G_{[O]}$. Analysis of the oxygen atom transfer reaction from *N*-methylmorpholine-*N*-oxide to the **3.4-X** complexes to form the corresponding **3.1-X** complexes and *N*-methylmorpholine allowed for determination of the thermodynamic parameters. Following optimization of all the reactants and products, these calculations revealed a substantial enthalpic driving force in all cases (Table 3.10.3). Increased stabilization upon U=O bond formation correlated with an increase in *cis*-destabilization in the corresponding **3.1-X** complex (Table 3.10.2), and correlated with stabilization to reduction (Table 3.10.3). Deviation from this correlation was observed in the case of the π-donating alkoxide and amide ligands,

which overstabilized the 4+ oxidation state and the cyanide ligand, which understabilized the 4+ oxidation state, in the optimized uranium(IV) reactants (Figure 3.10.7). However, again the **3.1-Me** and **3.1-H** complexes were found to be more stable than suggested by *cis*-destabilization.

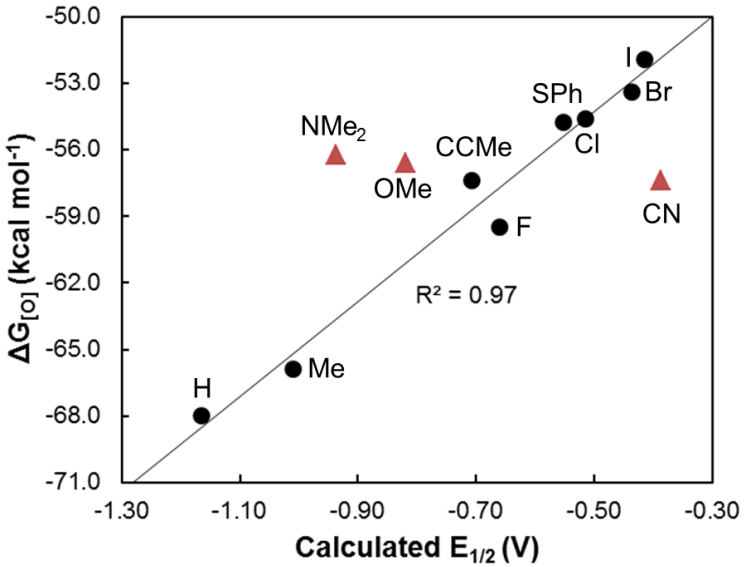

Figure 3.10.7 Correlation between calculated $E_{1/2}$ and $\Delta G_{[O]}$ values for the calculated **3.1-X** compounds. Red triangles = **3.1-NMe$_2$**, **3.1-OMe**, and **3.1-CN** (not included in linear fit), black circles = all other compounds.

Among the **3.1-X** complexes investigated, the ligands that were found to exert the largest *cis*-destabilization were those that engage in π-donation (X = NMe_2^-, OMe^-), followed by strong σ-donating ligands. Interestingly, the methyl and hydride derivatives exhibited larger ITI stabilizations than the NMe_2^- congener. Therefore, we propose that axial π-interactions are important in *cis*-destabilization, but have less impact on ITI stabilization than axial σ-interactions. This finding is consistent with the observation that mixing of the uranium $5f_{z3}$ and $6p_z$ atomic orbitals in the axial σ-bonding is a major contributor to ITI stabilization.[16, 17] The radial distribution of the uranium $5f_{xz2}$ and $5f_{yz2}$ orbitals involved in axial π-bonding allow for more significant interaction in equatorial bonding compared to the uranium $5f_{z3}$ orbital involved in axial σ-bonding, so perturbing the axial π-bonding has a larger effect on the equatorial bonding. In contrast, cyanide was predicted to exert the smallest ITI, which is surprising given that cyanide should be a reasonably strong σ-donating ligand.

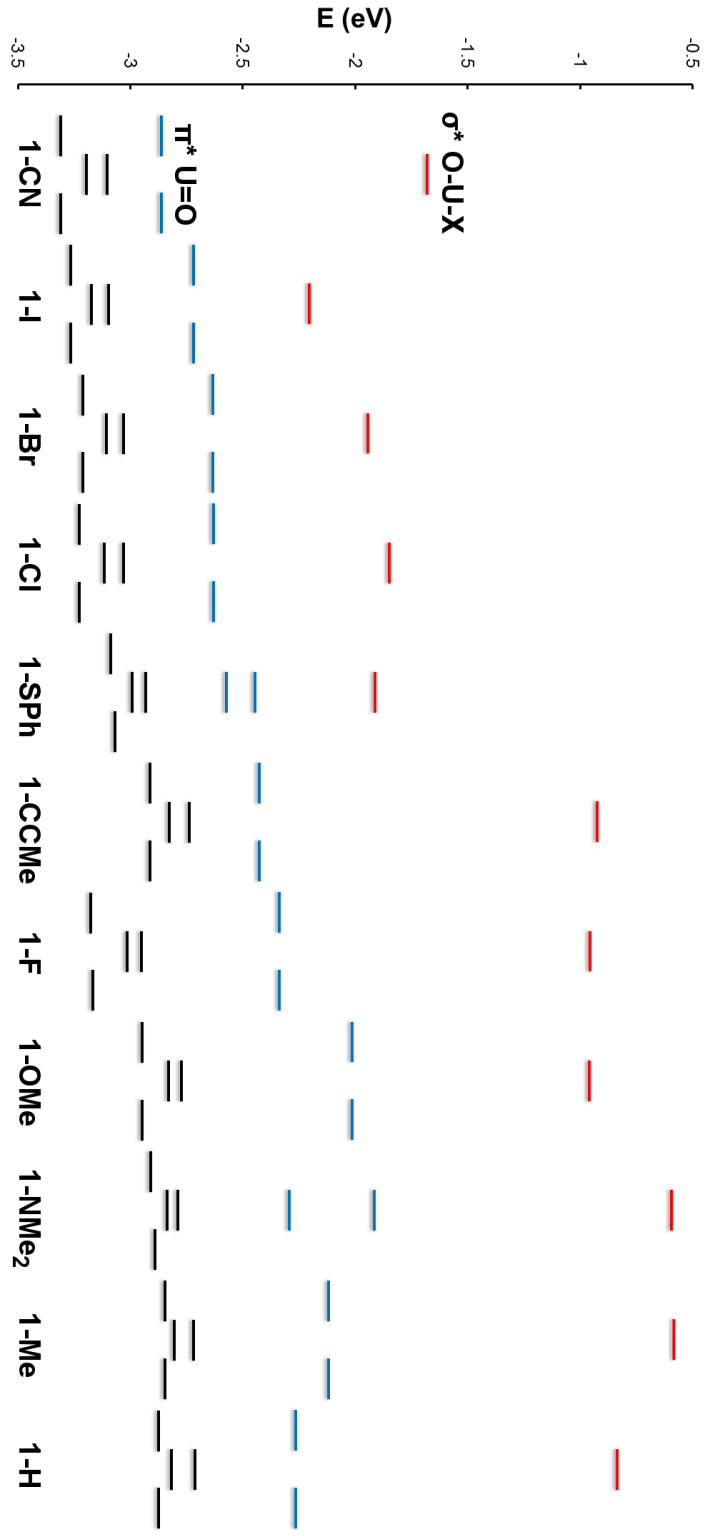

Figure 3.10.8 MO correlation diagram of the LUMO through LUMO+6 orbitals of the calculated **3.1-X** compounds, demonstrating the relative destabilization of the axial anti-bonding interactions.

Comparison of the molecular orbitals involved in the axial bonding in these complexes is difficult due to the various uranium f/d/p hybridizations that contribute as well as contributions from the silylamide ligands. However, the anti-bonding orbitals of primarily uranium 5f AO character are well isolated, allowing for the clearest interpretation of the bonding interactions (Figure 3.10.8). The destabilization of the uranium-ligand anti-bonding orbitals is expected to correlate with the stabilization of the bonding orbitals, though as noted recently by Lukens and Hayton,[138] the magnitude of stabilization of the filled orbitals will naturally be smaller than the destabilization of the unfilled orbitals. A selection of the relevant bonding and anti-bonding MOs are provided in Figures 3.10.9 and 3.10.10.

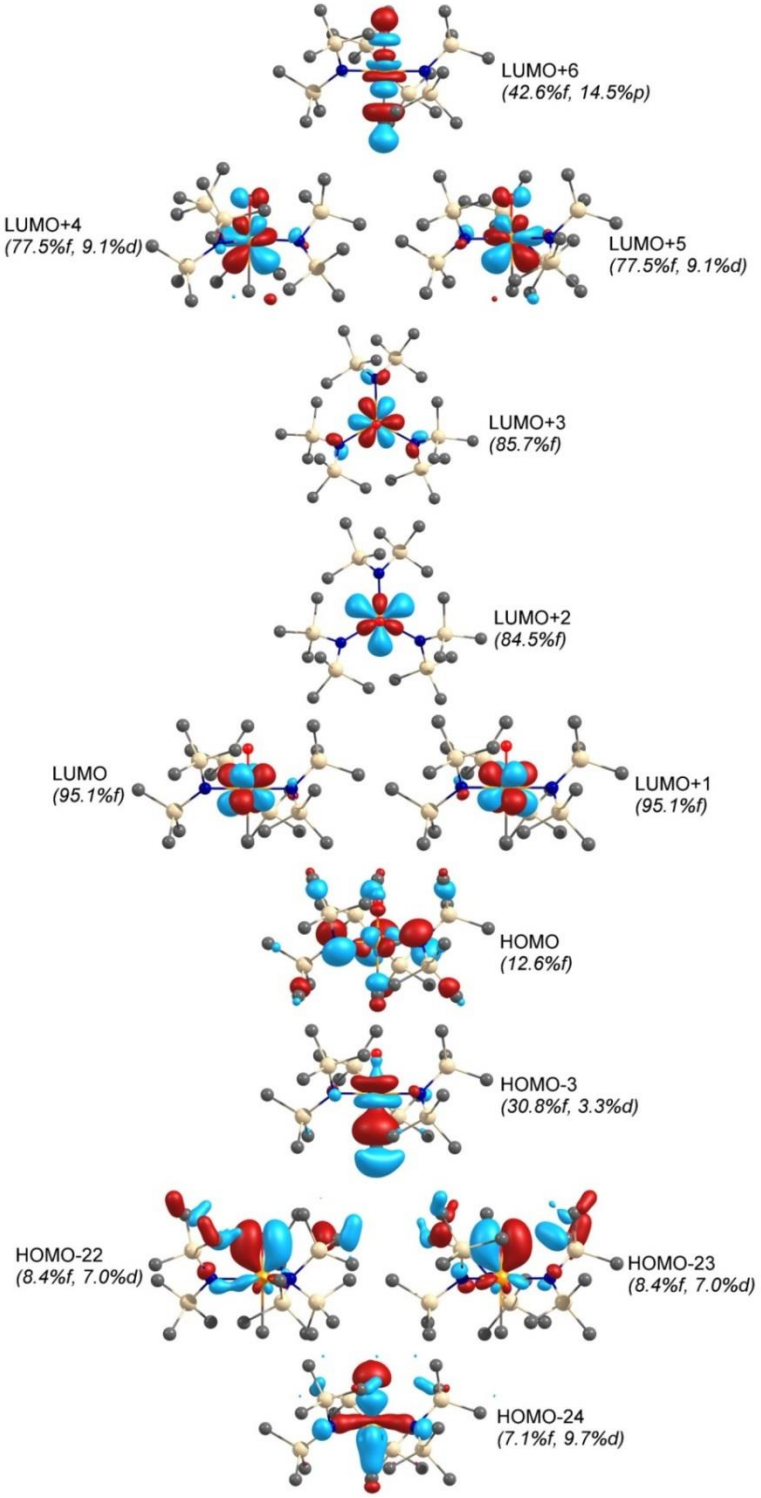

Figure 3.10.9 Selected molecular orbitals of **3.1-Me**, with %U AO character indicated.

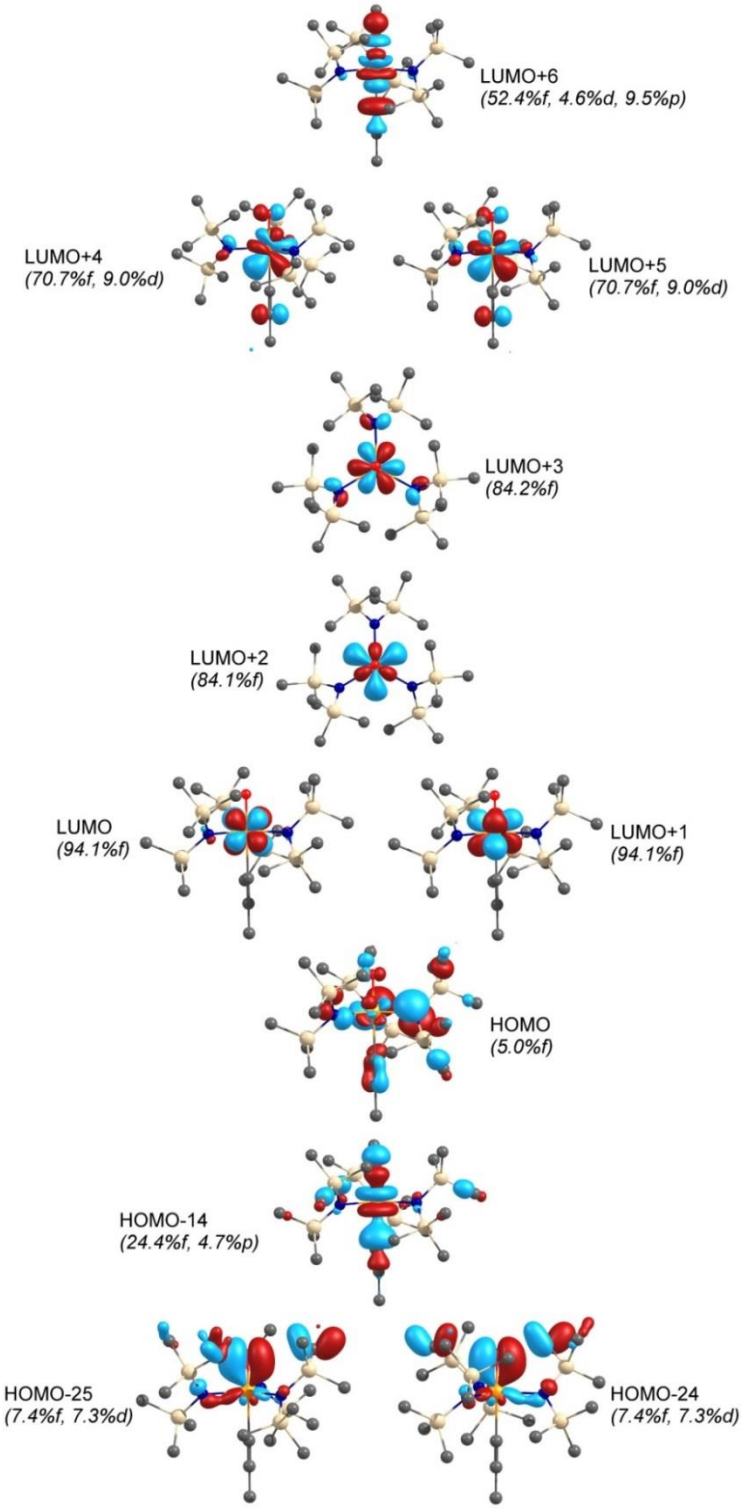

Figure 3.10.10 Selected molecular orbitals of **3.1-CCMe**, with %U AO character indicated.

As expected, stronger π-donating ligands impart the greatest destabilization of the axial π* interactions, and stronger σ-donating ligands similarly induce a large destabilization of the axial σ* interaction. The cyanide ligand destabilizes the axial σ* interaction, but shows the least destabilization of the axial π* interaction, thereby weakening the *trans*-U=O π-bonding. Computational analysis by Pyykkö et al suggested that the theoretical complex $U^{VI}(CN)_6$ would be much less stable than analogous UX_6 complexes (X = F^-, Cl^-), concluding that cyanide "is an anathema to uranium."[139] However, we contend that cyanide should lend more stability to uranium(VI) complexes when it does not coordinate along the primary axis. Indeed, uranyl(VI)-cyanide complexes of the formula $[UO_2(CN)_5]^{3-}$ are stable toward thermolysis in solution at 70 °C,[98] whereas the *cis*-alkyl complex $[UO_2(CHSiMe_3)_4]^{2-}$ complex is unstable above –25 °C.[88]

As a result of this experimental and theoretical data manifold we propose the following ligand stability series for the **3.1-X** complexes: $CN^- < I^- \approx Br^- < Cl^- \approx SPh^- < PhCC^- \approx F^- < MeO^- < NMe_2^- < Me^- < H^-$. The series developed from our analysis is similar to the series of uranium(V) compounds: $(C_5Me_5)_2U(=NAr)X$ (Ar = 2,6-diisopropylphenyl) that were organized: X = $OTf^- < I^- < Br^- < Cl^- < SPh^- < PhCC^- < F^- < [OPh^- \approx Me^- \approx Ph^-] << NPh_2^- < N=CPh_2^-$ according to their overall σ-/π-donor abilities.[102] In the case of the $(C_5Me_5)_2U(=NAr)X$ uranium(V) complexes, the imido and X ligands are in a *cis* geometry. A notable difference between the series is the ordering of the methyl group. In particular, the methyl group was determined to be more stabilizing in the **3.1-Me** compound than the alkoxide and amide groups **3.1-OMe** and **3.1-NMe_2**, whereas those groups create a more electron rich uranium(V) cation in the $(C_5Me_5)_2U(NAr)X$ series. The difference is ascribed to the difference in geometries between the **3.1-X** and $(C_5Me_5)_2U(NAr)X$ complexes; the σ-donation and associated larger ITI of **3.1-Me** induces a larger stability and reordering of the series.

3.11 Synthesis of $[U^VOX[N(SiMe_3)_2]_3]^-$ Complexes. Although the synthesis of the uranium(VI) cyanide **3.1-CN** was unsuccessful, we anticipated that starting from the 5+ oxidation state would avoid the reduction pathway. Indeed, the cyanide adduct was accessible through reaction of $[Et_4N]CN$ with $U^VO[N(SiMe_3)_2]_3$, generating $[Et_4N][UO(CN)[N(SiMe_3)_2]_3]$ (**3.3-CN**) as a

stable green product. The ^{1}H NMR spectrum of **3.3-CN** exhibited two resonances for the $–SiMe_3$ groups, at –1.14 and –1.92 ppm, in a 1:1 ratio, indicating hindered rotation around the U–N bonds. The oxidation state of **3.3-CN** was confirmed from the near-IR spectrum, which showed four primary absorption bands typical for related uranium(V) complexes (Figure 3.11.1).[65, 66, 105] As in the related *trans*-dihalide **2.1-X** complexes, splitting of the highest energy peak was observed, indicative of vibronic coupling along the primary axis. Surprisingly, the lowest energy transition was also split into two peaks of equal intensity. Electrochemical data collected on **3.3-CN** was showed a $U^{V/VI}$ couple at –0.26 V (Figure 3.11.2), in good agreement with the predicted potential of –0.39 V for **3.1-CN**. The experimental $U^{V/IV}$ couple exhibited substantial anodic and cathodic wave separation. The reduction potential was therefore obtained from the differential pulse voltammogram at –1.97 V, implicating a large kinetic barrier to oxidation of the formed uranium(IV) ion.

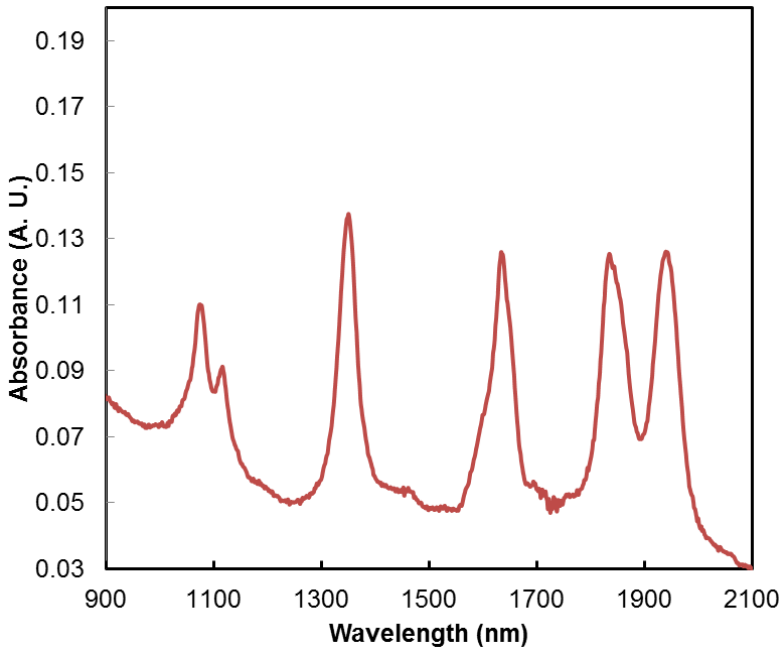

Figure 3.11.1 Near-IR spectrum of **3.3-CN** in CH_2Cl_2.

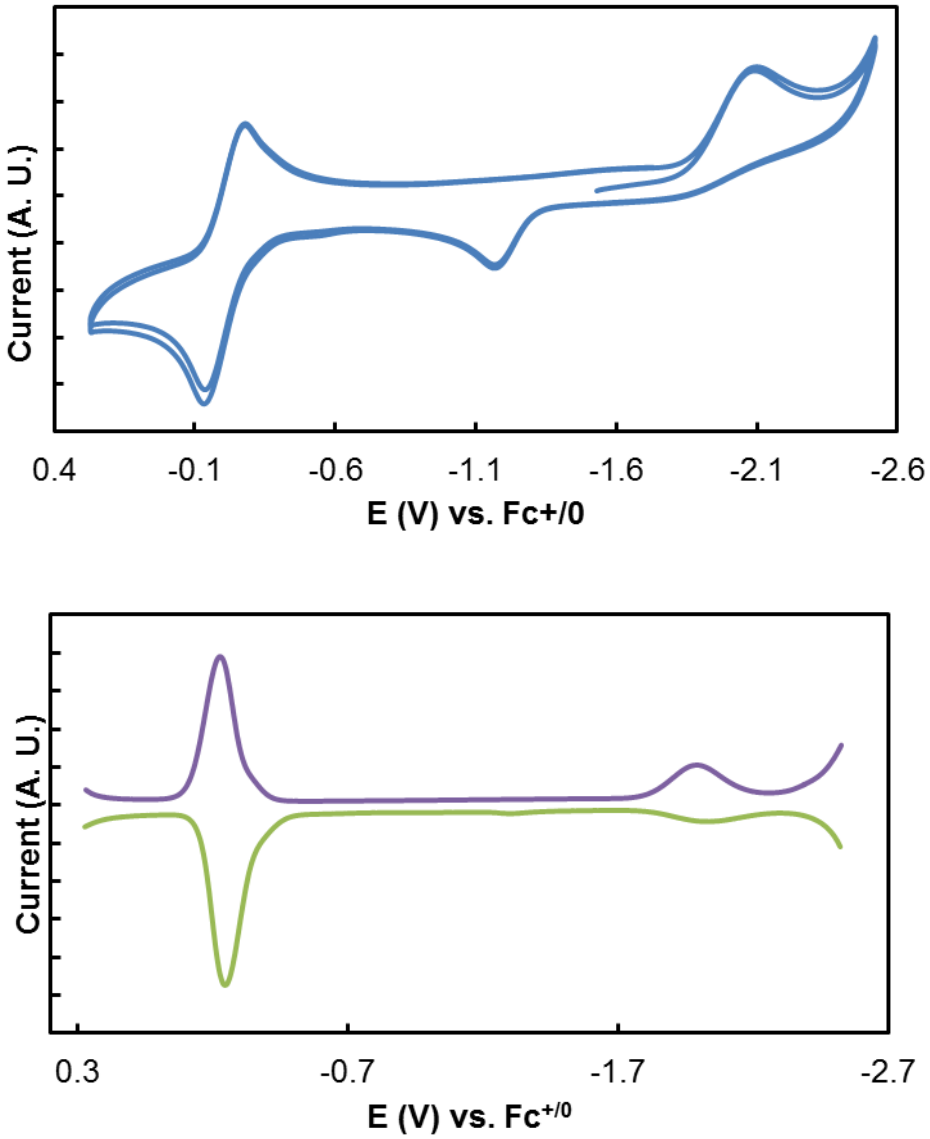

Figure 3.11.2 Cyclic voltammogram of **3.3-CN** in CH_2Cl_2 with 0.1 M [$^nBu_4N$][PF_6] at a scan rate of 250 mV/s (top) and differential pulse voltammogram of **3.3-CN**.

Attempts to form an acetylide adduct through addition of either NaCCPh or CuCCPh to $UO[N(SiMe_3)_2]_3$ led to no reaction, particularly surprising given the stability of the **3.1-CCPh**. However, treatment of **3.1-CCPh** with a reductant such as $NaCH_2Ph$ led to clean formation of orange $Na(THF)_6[UO(CCPh)[N(SiMe_3)_2]_3]$ (**3.3-CCPh**), where the oxidation product bibenzyl was conveniently separated with hexanes. This reduction also proceeded with NaSPh to primarily produce **3.3-CCPh** and PhSSPh, though significant formation of $UO[N(SiMe_3)_2]_3$ was also noted

by ^{1}H NMR in this reaction, limiting the usefulness of this pathway. Additionally, **3.3-CCPh** formed upon addition of NaO^{t}Bu to **3.1-CCPh**, but no oxidative side-product was detected by ^{1}H NMR.

The ^{1}H NMR spectrum of **3.3-CCPh** exhibited two resonances for the –$SiMe_3$ groups at –1.0 and –2.3 ppm, indicating hindered rotation about the U–N bonds, and the phenylacetylide ligand resonances were paramagnetically shifted to 12.3, 9.1, and 8.6 ppm.

Other **3.3-X** complexes were screened through simple adduct formation reactions. Addition of NaNCS, NaN_3, or NaBn in THF led to the formation of $Na[U^VO(NCS)[N(SiMe_3)_2]_3]$ (**3.3-NCS**), $Na[U^VO(N_3)[N(SiMe_3)_2]_3]$ (**3.3-N_3**), and $Na[U^VO(Bn)[N(SiMe_3)_2]_3]$ (**3.3-Bn**) respectively. The pseudo-halide complexes **3.3-NCS** and **3.3-N_3** exhibited intense green colors, whereas the **3.3-Bn** complex was orange. Complex formation was judged by the ^{1}H NMR spectra, which were directly analogous to **3.3-CN**, exhibiting two resonances for the –$SiMe_3$ groups in a 1:1 ratio in each complex. Crystallization of these complexes was possible from layering a concentrated THF solution with hexanes at –21 °C. However, rapid desolvation upon isolation of an individual crystal hindered X-ray structural analysis. Poor quality X-ray data was collected on a crystal of **3.3-N_3**, which established the proposed connectivity (Figure 3.11.3).

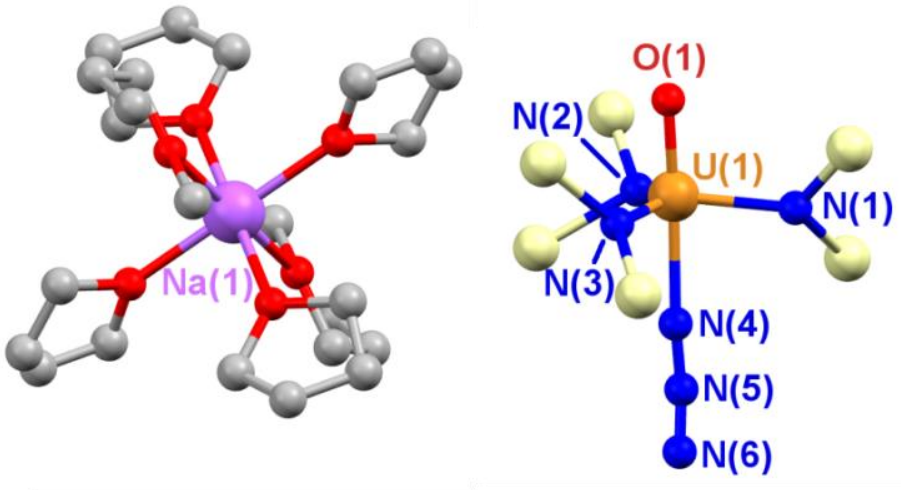

Figure 3.11.3 Structure of **3.3-N_3** established from X-ray data. Methyl groups are omitted for clarity, and hydrogen atoms were not included in the refinement.

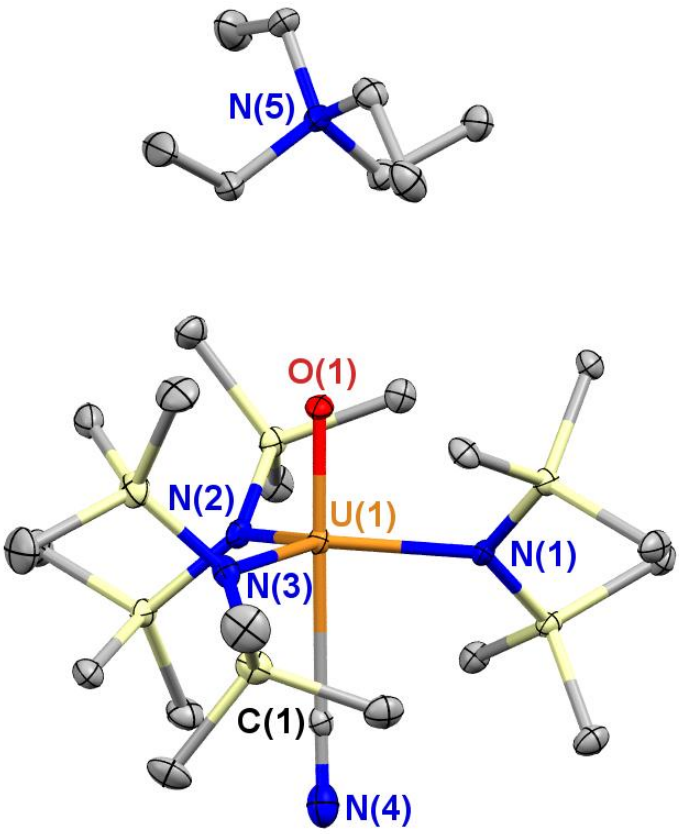

Figure 3.11.4 Thermal ellipsoid plot of **3.3-CN** at 30% probability. Hydrogen atoms are omitted for clarity.

Attempts to oxidize the **3.3-X** complexes to obtain new **3.1-X** complexes met with mixed success. Addition of $CuBr_2$ to a THF solution of **3.3-N_3** produced a dark green complex, which showed two resonances in the ^{1}H NMR at 0.58 and 0.41 ppm in a 1:1 ratio, analogous to the related **3.1-X** complexes. Crystallization from hexanes at –21 °C allowed for X-ray diffraction, which revealed the structure to be $U^{VI}O(N_3)[N(SiMe_3)_2]_3$ (**3.1-N_3**). Similarly, treatment of **3.3-NCS** with $CuBr_2$ in THF generated a dark green complex that produced a ^{1}H NMR spectrum almost identical to **3.1-N_3**, suggesting that $U^{VI}O(NCS)[N(SiMe_3)_2]_3$ (**3.1-NCS**) was formed. However, the stability of the putative **3.1-NCS** complex was very low, and decomposition was consistently observed within several days at –21 °C. The stability of **3.1-N_3** appeared slightly greater, but also decomposed within several days, preventing the complete characterization of these complexes.

The attempted oxidation of **3.3-CN** with $CuBr_2$ produced **3.1-Br**, presumably through transmetalation. Similarly, the reaction of **3.3-CN** with $AgPF_6$ generated **3.1-F** as the primary product. Addition of 0.5 equiv I_2 in THF to **3.3-CN** gave an unknown paramagnetic product with a single $–SiMe_3$ resonance in the ^1H NMR centered at –1.13 ppm. These observations led us to conclude that formation of **3.1-CN** was chemically challenging, in line with our previous observations that cyanide is a particularly poor ligand for uranium(VI).

Given the successful synthesis of the **3.3-X** complexes, the formation of uranium(V) complexes bearing a neutral adduct was tested. The coordination of a nitrile was pursued, due to the favorable steric profile of this ligand and the previous report of the stable uranium(III) complex $U^{III}(NC^tBu)_2[N(SiMe_3)_2]_3$.[140] Addition of Me_3SiCN to $U^{V}O[N(SiMe_3)_2]_3$ led to an immediate color change to pale orange. Crystallization from a hexanes solution stored at –21 °C revealed an unexpected structure – $U^{IV}(OSiMe_3)(NCSiMe_3)[N(SiMe_3)_2]_3$. This product is the result of silylation of the oxo ligand and reduction of the metal center, through formal loss of cyano radical, possibly to form cyanogen. Due to the presumable formation of hazardous side products this reaction was not to be repeated.

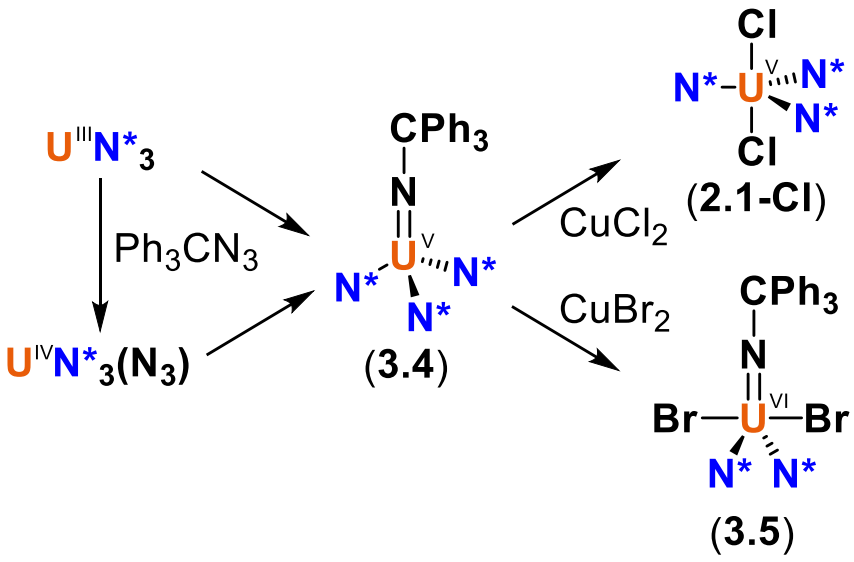

Scheme 3.12.1 Synthesis and reactivity of **3.4**.

3.12 Attempted Synthesis of Imido Analogues. Having established the synthesis of the **3.1-X** complexes, we sought to expand this reactivity to the potentially more chemically

interesting triphenylmethyl (trityl) imido ligand. Trityl functions as an effective protecting group in a variety of organic reactions, and the cleavage of Ph_3C–X bonds is a useful pathway for the oxidative installation of new uranium-ligand bonds,[67, 141, 142] including a recent example of the formation of a uranium-oxo multiple bond.[143] In fact, the low-temperature reaction of Ph_3CN_3 with $U^{III}[N(SiMe_3)_2]_3$ is known to form the product of one-electron oxidation, $U^{IV}(N_3)[N(SiMe_3)_2]_3$ through loss of trityl radical and formation of Gomberg's dimer.[140] Similarly, the reaction of $U^{III}(OAr)_3TACN$ with Me_3SiN_3 was reported to produce a mixture of both the uranium(V) mono-imido through two-electron oxidation as well as the uranium(IV) azide through loss of trimethylsilyl radical and subsequent formation of hexamethyldisilazane.[141] However, we found that formation of $U^{IV}(N_3)[N(SiMe_3)_2]_3$ through the low temperature addition of Ph_3CN_3 followed by addition of *N*-methylmorpholine-*N*-oxide, led to a color change to dark green and vigorous gas formation, to produce $U^{V}(=NCPh_3)[N(SiMe_3)_2]_3$ (**3.4**) in 93% yield (Scheme 3.12.1, Figure 3.12.1). More conveniently, the room temperature addition of Ph_3CN_3 to $U^{III}[N(SiMe_3)_2]_3$ in Et_2O directly generated **3.4** directly. When this reaction was performed in pyridine at room temperature only the uranium(IV) azide product was generated, and addition of *N*-methylmorpholine-*N*-oxide led to decomposition.

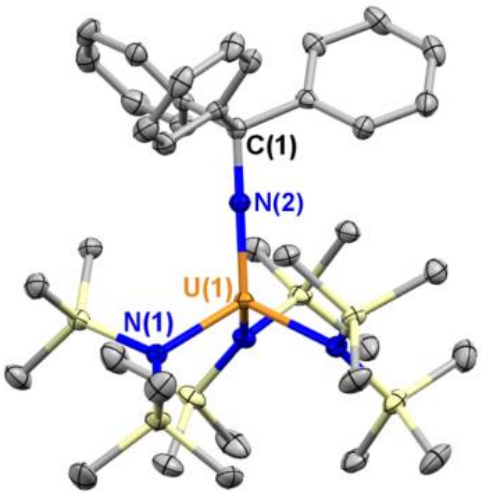

Figure 3.12.1 Thermal ellipsoid plot of **3.4** at 30% probability. Hydrogen atoms are omitted for clarity. Bond lengths (Å) and angles (°): U(1)–N(1) 2.264(3), U(1)–N(2) 1.959(5), N(2)–C(1) 1.478(7), N(1)–U(1)–N(2) 113.90(7), U(1)–N(2)–C(1) 180.0.

The X-ray crystal structure of **3.4** was obtained from a single crystal grown from a concentrated hexanes solution stored at –21 °C. The structure exhibited a C_3 symmetric geometry, in which the U–N–C bond angle was fixed at 180 °. This geometry is likely preferable to satisfy steric demands, but it is noted that the recently reported complex $[Li(12\text{-crown-}4)_2][U^{III}(NHCPh_3)[N(SiMe_3)_2]_3]$ exhibited a U–N–C bond angle of 151.2(3) °,[143] indicating that some flexibility is possible, albeit in the coordination sphere of the larger uranium(III) ion. The steric hindrance imposed by the trityl group appeared too great to install a *trans*-axial ligand, limiting the possibility of synthesizing imido derivatives of the **3.1-X** complexes. In spite of this, the cyclic voltammogram of **3.4** was collected to assess the accessibility of the 6+ and 4+ oxidation states, and to detect the possibility for electron transfer processes involving loss of the trityl group (Figure 3.12.2). Reversible $U^{VI/V}$ and $U^{V/IV}$ couples were observed at +0.38 V and –1.31 V respectively, in the range accessible by chemical means.

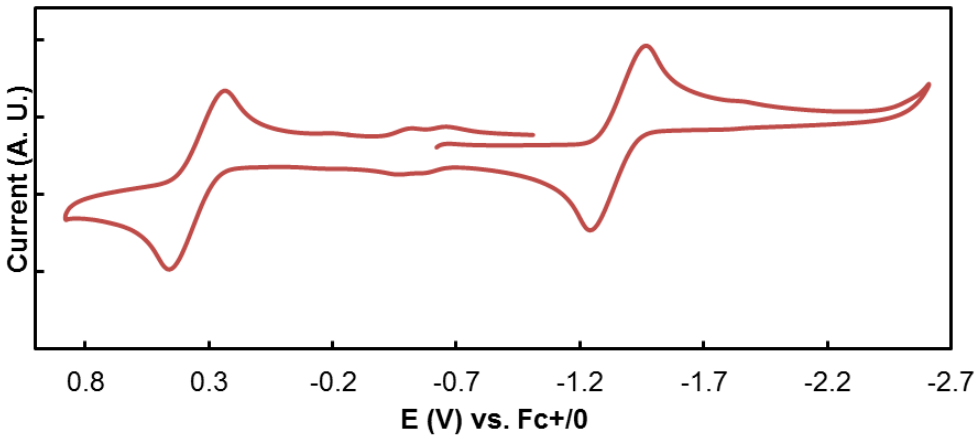

Figure 3.12.2 Cyclic voltammogram of **3.4** in CH_2Cl_2 at a scan rate of 250 mV/s, with 0.1 M $[^nBu_4N][PF_6]$ supporting electrolyte. A small, unidentified impurity centered at –0.54 V appeared in multiple experiments despite the use of a sample of high purity confirmed by ^1H NMR and elemental analysis.

The sterically hindered environment in **3.4** caused the oxidation reactions with Cu(II) salts to proceed with unexpected results (Scheme 3.12.1). Addition of $CuBr_2$ in THF produced a brown product that appeared to be diamagnetic by ^1H NMR, with a curious 2:1 ratio of $–N(SiMe_3)_2$ to $=NCPh_3$ ligands inferred from integration. X-ray structural analysis of a single crystal grown from

hexanes at –21 °C revealed the structure to be $U^{VI}Br_2(=NSiMe_3)[N(SiMe_3)_2]_3$ (**3.5**). Isolation of **3.5** was achieved in 83% yield, ruling out the possibility that **3.5** was a product of ligand redistribution. Additionally, no production of $[Cu[N(SiMe_3]_2]_4$ was observed,[144] ruling out transmetalation. Formation of **3.5** implies the formal loss of the aminyl radical, $\cdot N(SiMe_3)_2$.[72] We have previously observed loss of aminyl radical in the formation of $U^{VI}O_2(THF)_2[N(SiMe_3)_2]_2$ from the reaction of $U^{VI}OCl[N(SiMe_3)_2]_3$ with $NaNO_2$, which was attributed to the strong thermodynamic driving force of uranyl formation as well as the absence of valence electrons on the $5f^0$ metal center.[103] Similarly, $U–N(SiMe_3)_2$ and $Ln–N(SiMe_3)_2$ bond homolysis has led to single-electron reduction of uranyl in the work of Arnold et al,[145, 146] also to form strong metal-oxo bonds. We were therefore surprised at the ability to install weaker bromide ligands, especially considering the relatively poorer stability of the aminyl fragment relative to bromide radical. However, while this reaction proceeds cleanly in THF, no reaction was observed in toluene, a solvent less prone to hydrogen atom donation, implicating the need for hydrogen atom abstraction from solvent to form free $HN(SiMe_3)_2$. The synthesis of **3.5** is best described as a sterically induced reduction, a process common among $(C_5Me_5)_3Ln$ and $(C_5Me_5)_3U$ complexes.[147]

In contrast to $CuBr_2$, addition of $CuCl_2$ led to an immediate color change to dark red. The ^1H NMR spectrum of the product showed complete conversion to $U^{V}Cl_2[N(SiMe_3)_2]_3$, a compound previously reported by us.[58] This reaction most likely proceeds through transmetalation to form a "$Cu(NCPh_3)$" product; however, no other product could be identified from the intractable solid.

With no evidence for redox activity of the trityl functionality observed in the oxidation reactions, we also tested the reduction of **3.4**. Addition of KC_8 to a THF solution of **3.4** led to a slow color change to orange. This product was obtained in high purity immediately following filtration through Celite to separate the formed graphite, from which it was readily determined by ^1H NMR spectroscopy that the reduction product, $K(THF)_6[U^{IV}(=NCPh_3)[N(SiMe_3)_2]_3]$, was generated (Figure 3.12.3). Therefore, cleavage of the trityl group from the imido ligand will necessitate a different reaction pathway than the oxidation and reduction reactions reported here.

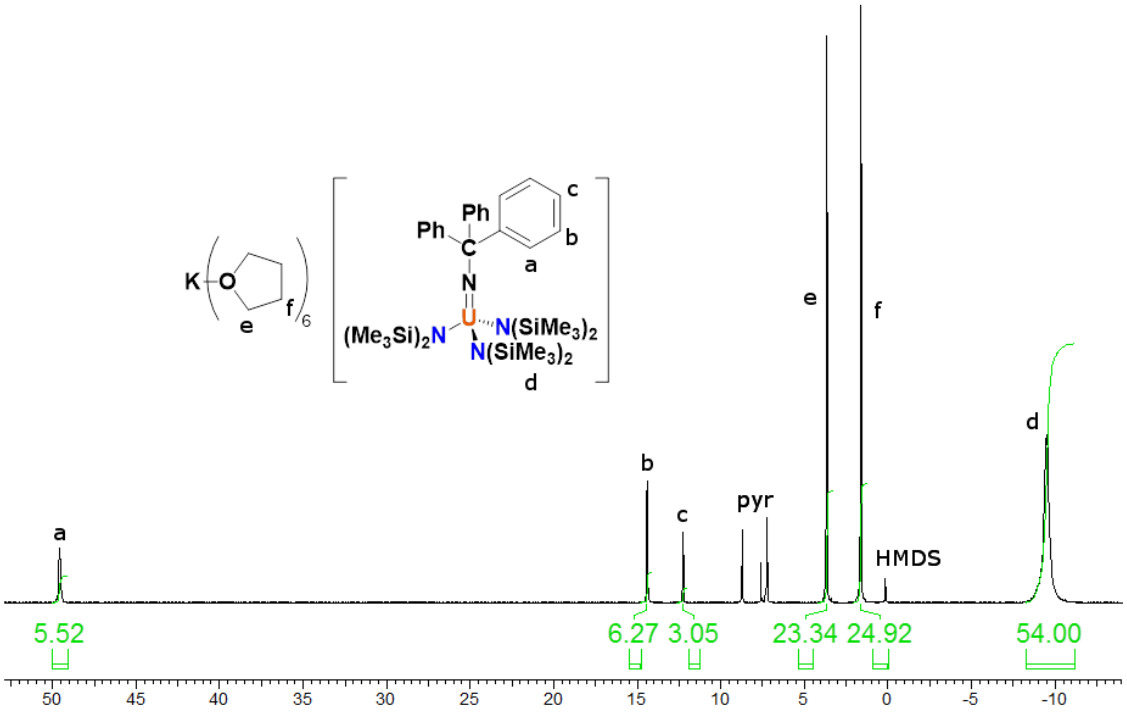

Figure 3.12.3 ^{1}H NMR of $K(THF)_6[U^{IV}(=NCPh_3)[N(SiMe_3)_2]_3]$ in pyridine-d_5.

3.13 Thermodynamics of Uranium Imido Reactions. The unusual reactivity exhibited by the mono-imido complex **3.4** led us to consider the thermodynamics of its formation and further oxidation (Figure 3.13.1). Since Ph_3CN_3 may act as either a one-electron or two-electron oxidant, the relative free energy changes of these processes were compared. The formation of the imido complex **3.4** was found to be exothermic in, with calculated ΔG_{rxn} = –30.5 kcal/mol. The formation of the intermediate uranium(IV) azide complex through C–N bond homolysis was exothermic by –35.3 kcal/mol. Reversibility of the C–N bond homolysis was found to be unfavorable, as the uranium(III) tritylazide adduct was predicted to be unstable relative to the uranium(IV) azide by 33.8 kcal/mol. The ability to isolate this product at low temperature suggests that the direct one-electron oxidation to form **3.4** possesses a large kinetic barrier. This observation suggests that *N*-methylmorpholine-*N*-oxide facilitates the one-electron transfer process, most likely through transient coordination to the uranium ion. As an alternative mechanism, the two-electron reduction of azide may be facilitated to generate the uranium(VI) nitrido complex which may recombine with the trityl radical to form **3.4**. Similar reactivity has been

observed in the reaction of the iron(IV) nitrido complex, $[PhB(MesIm)_3Fe^{IV}{\equiv}N]$,[148] with trityl radical to form the iron(III) imido complex, $[PhB(MesIm)_3Fe^{IV}{=}NCPh_3]$,[149] though the only reactivity of uranium(VI) nitrido complexes that has been reported thus far has been C-H activation.[150, 151] Calculation of the hypothetical uranium(VI) nitrido intermediate showed that it was in fact more energetically favorable than **3.4**.

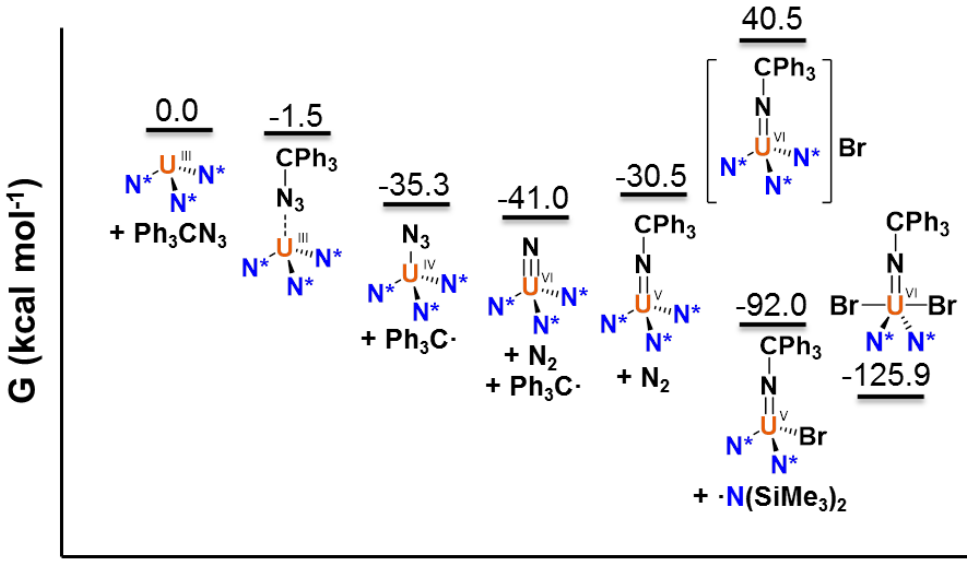

Figure 3.13.1 Calculated thermodynamics of the oxidation reactions involved in the synthesis of uranium mono-imido complexes.

3.14 Experimental.

3.14.1 $U^{VI}OCl[N(SiMe_3)_2]_3$ (3.1-Cl).

3.14.1.a *From $U^{V}Cl_2[N(SiMe_3)_2]_3$*. To a vial containing $U^{V}Cl_2[N(SiMe_3)_2]_3$ (75 mg, 0.09 mmol) stirring in 2 mL THF, $NaNO_2$ (52 mg, 0.95 mmol, 10.56 equiv) was added as a solid. After stirring 5 h, the volatiles were removed from the resulting green-black solution under reduced pressure. The black residue was dissolved in $(Me_3Si)_2O$, filtered through a Celite-packed coarse porosity fritted filter, and the volatiles were removed under reduced pressure, yielding pure **3.1-Cl** as a black crystalline solid. Yield 54 mg, 0.07 mmol, 74%. Alternatively, performing this reaction under the same conditions with $U^{V}Cl_2[N(SiMe_3)_2]_3$ (33 mg, 0.04 mmol) and $AgNO_2$ (6.4 mg, 0.04 mmol, 1.00 equiv) yielded **3.1-Cl** following recrystallization from $(Me_3Si)_2O$ in two crops. Yield 23 mg, 0.03 mmol, 72%.

3.14.1.b ***From $U^{V}O[N(SiMe_3)_2]_3$.*** To a vial containing $U^{V}O[N(SiMe_3)_2]_3$ (85 mg, 0.12 mmol) stirring in 5 mL THF, $CuCl_2$ (78 mg, 0.58 mmol, 5.02 equiv) was added, resulting in an immediate color change to dark green. After stirring 30 minutes, the solution was filtered and volatiles were removed under reduced pressure. The black residue was extracted with pentane and recrystallized at –25 °C, yielding **3.1-Cl** as a black crystalline solid. Yield 60 mg, 0.08 mmol, 67%.

3.14.1.c ***From $U^{IV}Cl[N(SiMe_3)_2]_3$.*** To a vial containing $U^{V}Cl[N(SiMe_3)_2]_3$ (117 mg, 0.16 mmol) stirring in 5 mL Et_2O, *N*-methylmorpholine-*N*-oxide (24 mg, 0.20 mmol, 1.32 equiv) was added, resulting in a rapid color change to dark green. After stirring 45 minutes, the solution was filtered through Celite suspended in a glass pipette to remove residual *N*-methylmorpholine-*N*-oxide, and the volatiles were removed from the filtrate for an hour to ensure removal of volatile *N*-methylmorpholine. The black residue was dissolved in $(Me_3Si)_2O$, filtered through a Celite suspended in a glass pipette, and the volatiles were removed under reduced pressure to yield **3.1-Cl** as a black crystalline solid. Yield 61 mg, 0.08 mmol, 51%.

^{1}H NMR (benzene-d_6): δ 0.61 (27H), 0.55 (27H). IR (KBr, cm^{-1}): 2954 (w), 1404 (w), 1249 (s), 862 (m, $\nu_{U=O}$), 844 (s), 773 (s), 681 (w), 650 (s, $\nu_{U–N(amide)}$), 621 (s, $\nu_{U–N(amide)}$) (cm^{-1}). Elemental analysis found (calculated) for $C_{18}H_{54}ClN_3OSi_6U$: C, 28.42 (28.05); H, 7.18 (7.06); N, 5.16 (5.45).

3.14.2 $U^{VI}OF[N(SiMe_3)_2]_3$ (3.1-F).

3.14.2.1 ***From $U^{V}ClF[N(SiMe_3)_2]_3$.*** To a vial containing $U^{V}ClF[N(SiMe_3)_2]_3$ (50 mg, 0.07 mmol) stirring in 5 mL Et_2O, $AgNO_2$ (50 mg, 0.32 mmol, 5.00 equiv) was added as a solid. Occasional bubble formation from the surface of the suspended $AgNO_2$ was noted. After stirring 1 h, the volatiles were removed under reduced pressure and another 5 mL Et_2O was added, along with another addition of $AgNO_2$ (50 mg, 0.32 mmol, 5.00 equiv). After an additional stirring 3 h, the resulting dark green solution was filtered through Celite suspended in a pipette and volatiles were removed from the filtrate under reduced pressure. The resulting black residue was dissolved

in $(SiMe_3)_2O$, filtered, and the volatiles were removed under reduced pressure, yielding pure **3.1-F** as a black solid. Yield 35 mg, 0.05 mmol, 71%.

3.14.2.2 ***From $U^{IV}F[N(SiMe_3)_2]_3$***. Preparation was analogous to the procedure for the synthesis of **3.1-Cl**, with $U^{IV}F[N(SiMe_3)_2]_3$ (52 mg, 0.07 mmol) and *N*-methylmorpholine-*N*-oxide (9 mg, 0.08 mmol, 1.09 equiv), yielding **3.1-F** as a black solid. Yield 37 mg, 0.05 mmol, 71%.

^{1}H NMR (benzene-d_6): δ 0.56 (27H), 0.48 (27H). ^{19}F NMR (benzene-d_6): δ 586.8 (1F). IR (KBr, cm^{-1}): 2953 (w), 1400 (w), 1248 (s), 882 (m, $\nu_{U=O}$), 841 (s), 773 (s), 682 (w), 653 (s $\nu_{U-N(amide)}$), 620 (s, $\nu_{U-N(amide)}$), 504 (m, ν_{U-F}) (cm^{-1}). Elemental analysis found (calculated) for $C_{18}H_{54}FN_3OSi_6U$: C, 29.03 (28.67); H, 6.91 (7.22); N, 5.49 (5.57).

3.14.3 $U^{VI}OBr[N(SiMe_3)_2]_3$ (3.1-Br). Preparation was analogous to the procedure for the synthesis of **3.1-Cl** (b), with $U^{V}O[N(SiMe_3)_2]_3$ (27 mg, 0.04 mmol) and $CuBr_2$ (20 mg, 0.09 mmol, 2.4 equiv). Recrystallization in minimal pentane at –21 °C yielded **3.1-Br** as a black crystalline solid. Yield 27 mg, 90%. ^{1}H NMR (benzene-d_6): δ 0.62 (54H). IR (KBr, cm^{-1}): 2953 (w), 1385 (m), 1250 (s), 931(w), 859 (m, $\nu_{U=O}$) 843 (s), 773 (s), 682 (w), 651 (s, $\nu_{U-N(amide)}$), 622 (s, $\nu_{U-N(amide)}$) (cm^{-1}). Elemental analysis found (calculated) for $C_{18}H_{54}BrN_3OSi_6U$: C, 26.89 (26.52); H, 6.42 (6.68); N, 5.05 (5.16).

3.14.4 $[U^{V}Cl[N(SiMe_3)_2]_3]_2(\mu_2\text{-FA})$ (3.2). To a vial containing $U^{IV}Cl[N(SiMe_3)_2]_3$ (50 mg, 0.066 mmol) stirring in 5 mL Et_2O, tetrafluoro-*p*-quinone (fluoranil, FA) (6 mg, 0.033 mmol, 1.00 equiv) dissolved in minimal Et_2O was added, causing an immediate color change from pale tan to dark brown. After stirring 15 minutes, the volatiles were removed under reduced pressure. The black residue was dissolved in pentane and filtered through Celite suspended in a glass pipette. Removal of volatiles under reduced pressure yielded **3.2** as a dark red-brown solid. Yield 46 mg, 0.027 mmol, 82%. ^{1}H NMR (47 °C, benzene-d_6): δ –0.74 (54H), –1.16 (54H). The room temperature ^{1}H NMR spectrum displayed multiple broad, overlapping peaks between 0 to –3 ppm. ^{19}F NMR (benzene-d_6): –138.8 (4F). IR (KBr, cm^{-1}): 3138 (m), 2958 (w), 2925(w), 1491(s), 1400 (s), 1299 (w), 1251(m), 1033 (m), 984 (m), 845 (s), 775 (w), 651 (m), 620 (m) (cm^{-1}).

Elemental analysis found (calculated) for $C_{42}H_{108}Cl_2F_4N_6O_2Si_{12}U_2 \cdot 0.5C_6H_{14}$: C, 31.43 (31.20); H, 6.09 (6.69); N, 4.76 (4.85).

3.14.5 $U^{V}O[N(SiMe_3)_2]_3$.

3.14.5.1 *From $U^{IV}Cl[N(SiMe_3)_2]_3$.* To a vial containing $U^{IV}Cl[N(SiMe_3)_2]_3$ (50 mg, 0.07 mmol) in 3 mL THF, $AgNO_2$ (10 mg, 0.07 mmol, 0.98 equiv) was added as a solid. Mild bubble formation was noted, along with a color change to red. After 6 h, the solution was filtered through Celite suspended in a glass pipette, and volatiles were removed under reduced pressure. The resulting red residue was extracted with pentane, filtered, and recrystallized at –21 °C to yield $U^{V}O[N(SiMe_3)_2]_3$ as a red solid. Yield: 24 mg, 0.03 mmol, 49%.

3.14.5.2 *From 2.* To a vial containing **3.2** (56 mg, 0.03 mmol) stirring in 5 mL THF, $NaNO_2$ (5 mg, 0.07 mmol, 2.19 equiv) suspended in minimal THF was slowly added. After stirring 12h, the resulting orange-red solution had a significant amount of black solid suspended in it. The solution was filtered through Celite suspended in a glass pipette and volatiles were removed under reduced pressure. Extraction with pentane, filtration, and recrystallization yielded $U^{V}O[N(SiMe_3)_2]_3$ as a red solid. Yield: 32 mg, 0.04 mmol, 65%.

Characterization data for $U^{V}O[N(SiMe_3)_2]_3$ was consistent with previously reported data.[65]

3.14.6 $U^{VI}O(Me)[N(SiMe_3)_2]_3$ (3.1-Me). To a Et_2O solution of $U^{IV}Me[N(SiMe_3)_2]_3$ (65 mg, 0.09 mmol, 1.0 equiv) cooled to –21 °C, *N*-methylmorpholine-*N*-oxide (11 mg, 0.09 mmol, 1.1 equiv) was added, causing and immediate color change to dark red. After stirring 30 minutes, the mixture was filtered through Celite suspended in a glass pipette. Volatiles were removed under reduced pressure, leaving a black residue. This residue was extracted with pentane and filtered. Storage at –21 °C gave black crystals of **3.1-Me**. Yield: 64 mg, 0.09 mmol, 96%. Single crystal suitable for X-ray analysis was grown in the same manner. Identical results were obtained when $U^{IV}(^{13}CH_3)[N(SiMe_3)_2]_3$ was used, to yield the ^{13}C-labeled analogue. ^1H NMR (benzene-d_6): 0.64 (27H), 0.62 (27H), –2.57 (3H). ^{13}C NMR (benzene-d_6): 301.0 (CH_3), 6.8 ($SiMe_3$). IR (KBr): 2954 (s), 2899 (w), 1401 (m), 1250 (s), 1181 (m), 931 (m), 884 (m), 841 (s), 774 (m), 659 (m), 613 (m).

Elemental analysis found (calculated) for $C_{19}H_{57}N_3OSi_6U$: C, 30.72 (30.42); H, 7.40 (7.66); N, 5.53 (5.60).

3.14.7 $U^{VI}O(CCPh)[N(SiMe_3)_2]_3$ (3.1-CCPh). To a Et_2O solution of $U^{III}[N(SiMe_3)_2]_3$ (250 mg, 0.35 mmol, 1.0 equiv), CuCCPh (114 mg, 0.69 mmol, 2.0 equiv) was added. This mixture was stirred for 3 h, over which time the suspended solid became slightly green and the solution turned brown. The mixture was then filtered through Celite to yield a light brown solution, then cooled to –21 °C. *N*-methylmorpholine-*N*-oxide (41 mg, 0.35 mmol, 1.0 equiv) was added, causing and immediate color change to dark brown. After stirring 30 minutes, the mixture was filtered through Celite suspended in a glass pipette. Volatiles were removed under reduced pressure, leaving a black residue. This residue was extracted with pentane and filtered. Storage at –21 °C gave black crystals of **3.1-CCPh**. Yield: 171 mg, 0.20 mmol, 59%. Single crystal suitable for X-ray analysis was grown in the same manner. ^{1}H NMR (benzene-d_6): 7.44 (2H), 6.95 (2H), 0.70 (54H). The *p*-H resonance could not be precisely located due to overlap with C_6D_5H at 7.16 ppm. ^{13}C NMR (benzene-d_6): 7.3 ($SiMe_3$). IR (KBr): 3166 (m), 2954 (m), 2056 (w, $\nu_{C\equiv C}$), 1542 (m), 1400 (s), 1257 (m), 1024 (w), 878 (m), 875 (s), 775 (m), 654 (m), 620 (m). Elemental analysis found (calculated) for $C_{26}H_{59}N_3OSi_6U$: C, 37.08 (37.34); H, 6.74 (7.11); N, 4.87 (5.02).

3.14.8 $[Et_4N][U^{V}O(CN)[N(SiMe_3)_2]_3]$ (3.3-CN). To a red-orange solution of $UO[N(SiMe_3)_2]_3$ (68 mg, 0.09 mmol) in 3 mL THF, $[Et_4N][CN]$ (14 mg, 0.09 mmol, 1 equiv) was added, resulting in an immediate color change to green-yellow. After stirring 20 minutes, the reaction mixture was filtered through Celite suspended in a glass pipet, and volatiles were removed under reduced pressure. The resulting green-yellow powder was rinsed with pentane to provide pure **3.3-CN**. Yield: mg, mmol, %. ^{1}H NMR (pyridine-d_5): 3.9 (8H), 1.7 (8H), –1.1 (27H), –1.9 (27H). IR (KBr): 3379 (m), 2923 (s), 2852 (m), 2058 (w, $\nu_{C\equiv N}$), 1540 (m), 1456 (m), 1384 (s), 1344 (m), 1181 (w), 1083 (w), 922 (s), 845 (s), 775 (m) 665 (m, ν_{U-N}), 612 (m, ν_{U-N}). Elemental analysis found (calculated) for $C_{35}H_{90}N_5OSi_6U$: C, 36.68 (36.38); H, 8.30 (8.37); N, 7.51 (7.86).

3.14.9 $[Et_4N][UO(CCPh)[N(SiMe_3)_2]_3]$ (3.3-CCPh). To a dark green-brown solution of $UO(CCPh)[N(SiMe_3)_2]_3$ (70 mg, 0.08 mmol) in THF, a THF solution of $NaCH_2Ph$ (10 mg, 0.09

mmol, 1.10 equiv) was added, resulting in an immediate color change to light brown-orange. After stirring for 10 min, $[Et_4N]Br$ (18 mg, 0.09 mmol, 1.10 equiv) was added, resulting in a slow color change to yellow-brown. After stirring 1.5 h, the cloudy mixture was filtered through Celite suspended in a glass pipet, and volatiles were removed under reduced pressure. The resulting brown residue was dissolved in Et_2O and filtered through Celite suspended in a glass pipet, then concentrated and stored at –21 °C to afford **3.3-CCPh** as a tan solid, which was rinsed with pentane and dried under reduced pressure. Yield: 54 mg, 0.06 mmol, 66%. ^{1}H NMR (benzene-d_6): 12.2 (2H), 9.1 (2H), 8.6 (1H), 4.4 (16H, THF), 1.8 (16H, THF), –1.0 (27H), –2.1 (27H). IR (KBr): 3383 (m), 2921 (s), 2852 (m), 1537 (s), 1455 (m), 1384 (vs), 1253 (m), 1181 (m), 1084 (m), 890 (s), 775 (m). 691 (w), 667 (m, $\nu_{U–N}$), 612 (m, $\nu_{U–N}$).

3.14.10 Na[UO(N$_3$)[N(SiMe$_3$)$_2$]$_3$] (3.3-N$_3$). To a red-orange solution of $UO[N(SiMe_3)_2]_3$ (20 mg, 0.03 mmol) in 3 mL THF, NaN_3 (18 mg, 0.28 mmol, 10.0 equiv) was added, resulting in a slow color change to green-yellow. After 1 h, volatiles were removed under reduced pressure, and the resulting yellow powder was rinsed with pentane to provide pure **3.3-N$_3$**. A bulk sample of **3.3-N$_3$** was not obtained in high purity due to continuous decomposition even at –21 °C. ^{1}H NMR (4:1 benzene-d_6:pyridine-d_5): 3.6 (12H), 1.5 (12H), –1.3 (27H), –1.9 (27H).

3.14.11 UO(N$_3$)[N(SiMe$_3$)$_2$]$_3$] (3.1-N$_3$). To a THF solution of $U^{V}O[N(SiMe_3)_2]_3$ (37 mg, 0.05 mmol), NaN_3 (33 mg, 0.51 mmol, 10.0 equiv) was added, resulting in a slow color change to green-yellow. After stirring 1 h, the mixture was filtered through Celite suspended in a glass pipet. To the green-yellow filtrate, $CuBr_2$ (22 mg, 0.10 mmol, 2.0 equiv) was added, resulting in an immediate color change to dark green. After stirring 15 minutes, the mixture was filtered through Celite suspended in a glass pipet, and volatiles were removed under vacuum. The resulting dark green residue was extracted with hexanes and recrystallized at –21 °C to afford green-black crystals of **3.1-N$_3$**. A bulk sample of **3.1-N$_3$** was not obtained in high purity due to continuous decomposition even at –21 °C. ^{1}H NMR (benzene-d_6): 0.6 (27H), 0.4 (27H).

3.14.12 Na[UO(NCS)[N(SiMe$_3$)$_2$]$_3$] (3.3-NCS). To a red-orange solution of $UO[N(SiMe_3)_2]_3$ (40 mg, 0.05 mmol) in 3 mL THF, NaNCS (9 mg, 0.11 mmol, 2.2 equiv) was

added, resulting in a color change to green-yellow. After 1 h, volatiles were removed under reduced pressure, and the resulting green-yellow powder was rinsed with pentane to provide pure **3.3-NCS**. A bulk sample of **3.3-NCS** was not obtained in high purity due to continuous decomposition even at –21 °C. ^{1}H NMR (4:1 benzene-d_6:pyridine-d_5): 3.6 (8H), 1.5 (8H), –1.1 (27H), –1.9 (27H).

3.15.13 UO(NCS)[N(SiMe$_3$)$_2$]$_3$ (3.1-NCS). To a solution of **3.3-NCS** prepared in situ as described in **3.14.12**, $CuBr_2$ (24 mg, 0.11 mmo, 2.2 equiv) was added, resulting in an immediate color change to dark green. After stirring 5 minutes, volatiles were removed under pressure, and the resulting black residue was extracted with hexanes. Filtration through Celite suspended in a glass pipet, followed by removal of volatiles under reduced pressure afforded crude **3.1-NCS**. Attempts to recrystallize this material led only to decomposition even at –21 °C. ^{1}H NMR (benzene-d_6): 0.6 (27H), 0.5 (27H).

3.14.14 Na[UO(Bn)[N(SiMe$_3$)$_2$]$_3$] (3.3-Bn). The procedure outlined in **3.14.12** was followed: $UO[N(SiMe_3)_2]_3$ (40 mg, 0.05 mmol), NaBn (6.2 mg, 0.05 mmol, 1.0 equiv). A bulk sample of **3.3-Bn** was not obtained in high purity due to continuous decomposition even at –21 °C. ^{1}H NMR (benzene-d_6): 6.21 (24H), 2.38 (24H), 0.32 (27H), –3.43 (27H).

3.14.15 U^{IV}(OSiMe$_3$)(NCSiMe$_3$)[N(SiMe$_3$)$_2$]$_3$. To an Et_2O solution of $U^{V}O[N(SiMe_3)_2]_3$ (40 mg, 0.05 mmol), $NCSiMe_3$ (10 mg, 0.10 mmol, 2.0 equiv) was added, resulting in a color change to dark brown. Removal of volatiles followed by recrystallization from hexanes produced crystals of $U^{IV}(OSiMe_3)(NCSiMe_3)[N(SiMe_3)_2]_3$ suitable for X-ray diffraction.

3.14.16 U^{VI}O[N(SiMe$_3$)$_2$]$_2$(κ$_2$-CH$_2$SiMe$_2$NSiMe$_3$). To a solution of $U^{IV}[N(SiMe_3)_2]_2(\kappa_2$-$CH_2SiMe_2NSiMe_3)$ (150 mg, 0.21 mmol) in Et_2O, *N*-methylmorpholine-*N*-oxide (37 mg, 0.32 mmol, 1.52 equiv) was added, resulting in an immediate color change to dark red. After stirring 5 minutes, volatiles were removed under reduced pressure. The resulting red-black residue was extracted with pentane and filtered through Celite suspended in a glass pipet, then volatiles were removed to afford pure $U^{VI}O[N(SiMe_3)_2]_2(\kappa_2$-$CH_2SiMe_2NSiMe_3)$. Yield: 121 mg, 0.16 mmol, 79%. Characterization data matched the previous report.[105]

3.14.17 $U^{V}(NCPh_3)[N(SiMe_3)_2]_3$ (3.4) To a solution of $U[N(SiMe_3)_2]_3$ (200 mg, 0.28 mmol) in 10 mL Et_2O cooled to –21 °C, Ph_3CN_3 (80 mg, 0.28 mmol, 1.00 equiv) was added, resulting in an immediate color change to pale brown. After stirring 15 minutes, *N*-methylmorpholine-*N*-oxide (66 mg, 0.56 mmol, 2.00 equiv) was added, resulting in the immediate evolution of gas and a color change to dark green. The mixture was stirred 20 minutes, and after filtration through Celite, volatiles were removed under reduced pressure. Recrystallization from minimal hexanes at –21 °C afforded **3.4** as a green-black crystalline solid. Yield: 272 mg, 0.28 mmol, 93%. ^{1}H NMR (benzene-d_6): 22.31 (6H), 10.20 (6H), 8.71 (3H), –3.94 (54H). Elemental analysis found (calculated) for $C_{37}H_{69}N_4Si_6U$: 45.58 (45.51); H 7.02 (7.12); N 5.75 (5.74).

3.14.18 $U^{VI}Br_2(NCPh_3)[N(SiMe_3)_2]_3$ (3.5) To a solution of **3.4** (40 mg, 0.04 mmol) in 5 mL of THF, $CuBr_2$ (46 mg, 0.21 mmol, 5.00 equiv) was added. After stirring for 10 minutes, volatiles were removed under reduced pressure. The resulting residue was extracted with pentane, filtered through Celite packed in a pipette, and stored at –21 °C to yield dark red-brown needles of **3.5**. Yield: 33 mg, 0.03 mmol, 83%. ^{1}H NMR (benzene-d_6): 7.72 (3H), 7.35 (6H), 7.02 (6H), 0.72 (36H). Elemental analysis found (calculated) for $C_{31}H_{51}Br_2N_3Si_4U$: C, 37.91 (38.15); H, 4.94 (5.27); N, 4.20 (4.31).

3.15 X-Ray Data.

Table 3.15.1 Summary of structure determination.

	3.1-Cl	**3.1-F**	**3.1-Br**
Empirical formula	$C_{18}H_{54}Si_6N_3OClU$	$C_{18}H_{54}Si_6N_3OFU$	$C_{18}H_{54}Si_6N_3OBrU$
Formula weight	770.66	754.21	815.12
Temperature	143(1) K	143(1) K	143(1) K
Wavelength	0.71073 Å	0.71073 Å	0.71073 Å
Crystal system	orthorhombic	orthorhombic	rhombohedral
Space group	$P2_12_12_1$	$P2_12_12_1$	R3c
a	11.8692(4) Å	11.8088(8) Å	18.5005(9) Å
b	12.5376(4) Å	12.4796(9) Å	18.5005(9) Å
c	22.9317(8) Å	22.9669(16) Å	16.9729(7) Å
α	90	90	90
β	90	90	90
γ	90	90	120
Volume	3412.5(2) $Å^3$	3384.6(4) $Å^3$	5031.0(4) $Å^3$
Z	4	4	6
Density (calculated)	1.500 Mg/m^3	1.480 Mg/m^3	1.614 Mg/m^3
Absorption coefficient	5.060 mm^{-1}	5.028 mm^{-1}	6.260 mm^{-1}

F(000)	1536	1504	2412
Crystal size	0.18 x 0.03 x 0.02 mm^3	0.55 x 0.42 x 0.20 mm^3	0.32 x 0.28 x 0.12 mm^3
Theta range	1.78 to 27.52°	1.94 to 27.53°	2.20 to 27.68°
Index ranges	-15 ≤ h ≤ 15, -16 ≤ k ≤ 16, -29 ≤ l ≤ 29	-15 ≤ h ≤ 15, -16 ≤ k ≤ 16, -29 ≤ l ≤ 29	-24 ≤ h ≤ 24, -24 ≤ k ≤ 24, -22 ≤ l ≤ 22
Reflections	69060	67229	62664
Independent reflections	7827 [R(int) = 0.0360]	7681 [R(int) = 0.0281]	2530 [R(int) = 0.0264]
Completeness to theta = 27.52 °	100.0 %	99.7 %	98.7 %
Max. and min. transmission	0.7456 and 0.5958	0.7456 and 0.4612	0.7456 and 0.4823
Data / restraints / parameters	7827 / 0 / 308	7681 / 0 / 290	2530 / 1 / 100
Goodness-of-fit on F^2	0.975	1.075	1.187
Final R indices [I>2sigma(I)]	R1 = 0.0170, wR2 = 0.0300	R1 = 0.0141, wR2 = 0.0328	R1 = 0.0245, wR2 = 0.0589
R indices (all data)	R1 = 0.0216, wR2 = 0.0307	R1 = 0.0150, wR2 = 0.0331	R1 = 0.0270, wR2 = 0.0606
Largest diff. peak and hole	0.591 and -0.275 e.$Å^{-3}$	1.005 and -0.476 e.$Å^{-3}$	0.630 and -2.500 e.$Å^{-3}$

	3.1-Me	**3.1-CCPh**	**3.4-Me**
Empirical formula	$C_{19}H_{57}N_3Si_6OU$	$C_{26}H_{59}Si_6N_3OU$	$C_{19}H_{57}N_3Si_6U$
Formula weight	750.25	836.33	734.25
Temperature	143(1) K	100(1) K	143(1) K
Wavelength	0.71073 Å	0.71073 Å	0.71073 Å
Crystal system	orthorhombic	monoclinic	rhombohedral
Space group	$P2_12_12_1$	P2/n	R3c
a	11.8834(13) Å	12.3823(8) Å	18.476(4) Å
b	12.5642(13) Å	12.1284(7) Å	18.476(4) Å
c	22.928(2) Å	13.0025(8) Å	16.940(4) Å
α	90	90	90
β	90	92.667(3)°	90
γ	90	90	120
Volume	3423.3(6) $Å^3$	1950.6(2) $Å^3$	5008.1(19) $Å^3$
Z	4	2	6
Density (calculated)	1.456 Mg/m^3	1.424 Mg/m^3	1.461 Mg/m^3
Absorption coefficient	4.967 mm^{-1}	4.367 mm^{-1}	5.088 mm^{-1}
F(000)	1504	840	2208
Crystal size	0.12 x 0.12 x 0.04 mm^3	0.28 x 0.25 x 0.15 mm^3	0.30 x 0.28 x 0.20 mm^3
Theta range	1.85 to 27.54°	2.78 to 27.57°	2.20 to 27.63°
Index ranges	-15 ≤ h ≤ 15, -15 ≤ k ≤ 16, -29 ≤ l ≤ 29	-16 ≤ h ≤ 16, -15 ≤ k ≤ 15, -16 ≤ l ≤ 16	-23 ≤ h ≤ 23, -23 ≤ k ≤ 23, -21 ≤ l ≤ 22
Reflections	67249	47798	35192
Independent reflections	7880 [R(int) = 0.0285]	4504 [R(int) = 0.0179]	2502 [R(int) = 0.0244]
Completeness to theta = 27.52 °	99.9 %	99.6 %	98.6 %

Max. and min. transmission	0.7456 and 0.5462	0.7456 and 0.6163	0.7456 and 0.6329
Data / restraints / parameters	7880 / 16 / 311	4504 / 0 / 192	2502 / 1 / 96
Goodness-of-fit on F^2	1.058	1.577	1.386
Final R indices [I>2sigma(I)]	R1 = 0.0156, wR2 = 0.0356	R1 = 0.0348, wR2 = 0.0973	R1 = 0.0210, wR2 = 0.0707
R indices (all data)	R1 = 0.0182, wR2 = 0.0366	R1 = 0.0350, wR2 = 0.0973	R1 = 0.0230, wR2 = 0.0868
Largest diff. peak and hole	0.793 and -0.496 e.Å^{-3}	2.759 and -4.128 e.Å^{-3}	2.113 and -1.297 e.Å^{-3}

	$UO_2(THF)_2$ $[N(SiMe_3)_2]_2$	**3.2**	**3.4**
Empirical formula	$C_{20}H_{52}Si_4N_2O_4U$	$C_{52}H_{132}Si_{12}N_6O_2F_4Cl_2U_2$	$C_{37}H_{69}N_4Si_6U$
Formula weight	735.03	1833.68	976.53
Temperature	143(1) K	143(1) K	143(1) K
Wavelength	0.71073 Å	0.71073 Å	0.71073 Å
Crystal system	triclinic	monoclinic	rhombohedral
Space group	$P\bar{1}$	$P2_1/c$	R-3
a	10.7070(12) Å	11.9455(10) Å	14.5991(10) Å
b	18.0278(18) Å	19.6016(16) Å	14.5991(10) Å
c	18.0287(18) Å	17.9892(15) Å	14.5991(10) Å
α	104.511(5)°	90	90
β	101.754(5)°	99.943(5)°	90
γ	101.706(5)°	90	120
Volume	3177.7(6) Å^3	4148.9(6) Å^3	8560.8(11) Å3
Z	4	2	6
Density (calculated)	1.536 Mg/m^3	1.468 Mg/m^3	1.137 Mg/m3
Absorption coefficient	5.283 mm^{-1}	4.182 mm^{-1}	2.993 mm-1
F(000)	1464	1848	2970
Crystal size	0.40 x 0.35 x 0.28 mm^3	0.18 x 0.10 x 0.04 mm^3	0.45 x 0.42 x 0.30 mm3
Theta range	1.96 to 27.63°	1.55 to 27.62°	2.38 to 27.55°
Index ranges	-13 ≤ h ≤ 13, -23 ≤ k ≤ 22, 0 ≤ l ≤ 23	-15 ≤ h ≤ 15, -23 ≤ k ≤ 24, -23 ≤ l ≤ 23	-18 ? h ? 18, -18 ? k ? 18, -60 ? l ? 59
Reflections	85341	122940	25970
Independent reflections	14639 [R(int) = 0.0604]	9535 [R(int) = 0.0613]	4369 [R(int) = 0.0328]
Completeness to theta = 27.52 °	99.1 %	98.7 %	99.00%
Max. and min. transmission	0.7456 and 0.4741	0.7456 and 0.5879	0.7456 and 0.5107
Data / restraints / parameters	14639 / 67 / 594	9535 / 4 / 380	4369 / 0 / 152
Goodness-of-fit on	1.087	1.191	0.635

F^2			
Final R indices [I>2sigma(I)]	R1 = 0.0397, wR2 = 0.1069	R1 = 0.0481, wR2 = 0.1096	R1 = 0.0278, wR2 = 0.0795
R indices (all data)	R1 = 0.0445, wR2 = 0.1118	R1 = 0.0679, wR2 = 0.1158	R1 = 0.0415, wR2 = 0.0923
Largest diff. peak and hole	2.512 and -3.874 e.Å^{-3}	1.825 and -1.490 e.Å^{-3}	1.560 and -0.512 e.Å-3

Table 3.15.2 Bond Distances in **3.1-Cl**, Å

U1-O1'	1.788(8)	U1-O1	1.803(5)	U1-N3	2.191(2)
U1-N2	2.193(2)	U1-N1	2.196(2)	U1-Cl1	2.5369(17)
U1-Cl1'	2.546(3)	U1-Si2	3.4273(8)	U1-Si6	3.4283(8)
U1-Si4	3.4331(7)	U1-Si3	3.4380(8)	U1-Si5	3.4408(8)
Si1-N1	1.764(2)	Si1-C2	1.865(3)	Si1-C3	1.869(3)
Si1-C1	1.874(3)	Si2-N1	1.767(2)	Si2-C6	1.859(3)
Si2-C4	1.874(3)	Si2-C5	1.874(3)	Si3-N2	1.758(2)
Si3-C8	1.856(3)	Si3-C7	1.869(3)	Si3-C9	1.874(3)
Si4-N2	1.770(2)	Si4-C10	1.860(3)	Si4-C12	1.866(3)
Si4-C11	1.872(3)	Si5-N3	1.756(2)	Si5-C13	1.856(3)
Si5-C14	1.866(3)	Si5-C15	1.868(3)	Si6-N3	1.774(2)
Si6-C18	1.856(4)	Si6-C17	1.865(3)	Si6-C16	1.866(3)

Table 3.15.3 Bond Angles in **3.1-Cl**, °

O1'-U1-O1	178.2(2)	O1'-U1-N3	91.32(18)
O1'-U1-N2	88.52(18)	O1-U1-N2	89.77(11)
O1'-U1-N1	89.98(19)	O1-U1-N1	90.39(12)
N2-U1-N1	118.65(7)	O1'-U1-Cl1	1.49(19)
N3-U1-Cl1	90.71(6)	N2-U1-Cl1	90.00(6)
O1'-U1-Cl1'	178.6(2)	O1-U1-Cl1'	1.67(14)
N2-U1-Cl1'	90.54(7)	N1-U1-Cl1'	91.33(7)
O1'-U1-Si2	110.68(19)	O1-U1-Si2	70.20(10)
N2-U1-Si2	132.91(6)	N1-U1-Si2	26.71(6)
Cl1'-U1-Si2	70.67(5)	O1'-U1-Si6	71.93(17)
N3-U1-Si6	26.82(6)	N2-U1-Si6	135.48(6)
Cl1-U1-Si6	70.92(3)	Cl1'-U1-Si6	108.16(6)
O1'-U1-Si4	108.76(18)	O1-U1-Si4	69.45(10)
N2-U1-Si4	26.60(5)	N1-U1-Si4	100.51(6)
Cl1'-U1-Si4	70.64(6)	Si2-U1-Si4	107.89(2)
O1'-U1-Si3	68.97(18)	O1-U1-Si3	109.55(10)
N2-U1-Si3	26.13(6)	N1-U1-Si3	132.55(6)
Cl1'-U1-Si3	109.83(6)	Si2-U1-Si3	155.45(2)
Si4-U1-Si3	52.73(2)	O1'-U1-Si5	110.34(18)
N3-U1-Si5	25.96(6)	N2-U1-Si5	102.17(5)
Cl1-U1-Si5	110.18(3)	Cl1'-U1-Si5	68.92(6)
Si6-U1-Si5	52.78(2)	Si4-U1-Si5	109.397(18)
N1-Si1-C2	110.97(12)	N1-Si1-C3	110.54(11)
N1-Si1-C1	112.12(11)	C2-Si1-C1	108.25(13)
N1-Si1-U1	32.51(6)	C2-Si1-U1	112.09(11)
C1-Si1-U1	81.85(8)	N1-Si2-C6	110.90(13)
C6-Si2-C4	108.43(16)	N1-Si2-C5	111.32(13)
C4-Si2-C5	103.87(16)	N1-Si2-U1	33.96(8)

C4-Si2-U1	80.55(10)	C5-Si2-U1	133.67(12)
N2-Si3-C7	110.69(12)	C8-Si3-C7	109.67(14)
C8-Si3-C9	105.53(15)	C7-Si3-C9	108.27(14)
C8-Si3-U1	80.56(9)	C7-Si3-U1	110.72(10)
N2-Si4-C10	110.43(13)	N2-Si4-C12	111.57(11)
N2-Si4-C11	112.09(12)	C10-Si4-C11	109.71(14)
N2-Si4-U1	33.71(7)	C10-Si4-U1	111.13(9)
C11-Si4-U1	134.78(10)	N3-Si5-C13	111.33(14)
C13-Si5-C14	107.37(16)	N3-Si5-C15	111.37(14)
C14-Si5-C15	104.62(17)	N3-Si5-U1	33.11(7)
C14-Si5-U1	81.06(10)	C15-Si5-U1	133.70(12)
N3-Si6-C17	111.13(13)	C18-Si6-C17	109.23(19)
C18-Si6-C16	108.45(17)	C17-Si6-C16	105.34(16)
C18-Si6-U1	112.06(12)	C17-Si6-U1	134.10(13)
Si1-N1-Si2	118.71(13)	Si1-N1-U1	121.92(10)
Si3-N2-Si4	119.77(12)	Si3-N2-U1	120.53(11)
Si5-N3-Si6	119.74(12)	Si5-N3-U1	120.94(11)
O1-U1-N3	90.00(12)	C2-Si1-C3	109.77(14)
N3-U1-N2	120.54(8)	C3-Si1-C1	105.00(13)
N3-U1-N1	120.82(8)	C3-Si1-U1	132.71(9)
O1-U1-Cl1	179.27(11)	N1-Si2-C4	112.24(13)
N1-U1-Cl1	89.12(6)	C6-Si2-C5	109.83(15)
N3-U1-Cl1'	88.33(8)	C6-Si2-U1	112.20(10)
Cl1-U1-Cl1'	179.04(6)	N2-Si3-C8	110.98(11)
N3-U1-Si2	102.20(6)	N2-Si3-C9	111.53(14)
Cl1-U1-Si2	109.49(3)	N2-Si3-U1	33.33(7)
O1-U1-Si6	109.71(10)	C9-Si3-U1	135.57(11)
N1-U1-Si6	101.39(6)	C10-Si4-C12	107.87(16)
Si2-U1-Si6	91.61(2)	C12-Si4-C11	104.97(15)
N3-U1-Si4	134.18(6)	C12-Si4-U1	80.09(9)
Cl1-U1-Si4	110.12(3)	N3-Si5-C14	111.90(13)
Si6-U1-Si4	158.09(2)	C13-Si5-C15	109.96(18)
N3-U1-Si3	102.35(6)	C13-Si5-U1	111.82(12)
Cl1-U1-Si3	70.43(3)	N3-Si6-C18	111.19(15)
Si6-U1-Si3	110.68(2)	N3-Si6-C16	111.28(12)
O1-U1-Si5	70.54(10)	N3-Si6-U1	33.87(7)
N1-U1-Si5	134.97(6)	C16-Si6-U1	79.76(9)
Si2-U1-Si5	109.73(2)	Si2-N1-U1	119.33(12)
Si3-U1-Si5	92.472(19)	Si4-N2-U1	119.69(10)
Si6-N3-U1	119.31(11)		

Table 3.15.4 Bond Distances in **3.1-F**, Å

U1-O1	1.9198(16)	U1-F1	1.9246(16)	U1-N2	2.2060(19)
U1-N3	2.2090(19)	U1-N1	2.210(2)	U1-Si5	3.4195(7)
U1-Si3	3.4275(8)	U1-Si6	3.4339(6)	U1-Si2	3.4379(8)
U1-Si4	3.4396(8)	Si1-N1	1.752(2)	Si1-C3	1.854(3)
Si1-C1	1.867(3)	Si1-C2	1.870(2)	Si2-N1	1.758(2)
Si2-C6	1.861(4)	Si2-C5	1.868(3)	Si2-C4	1.877(3)
Si3-N2	1.759(2)	Si3-C8	1.863(4)	Si3-C7	1.874(3)
Si3-C9	1.877(3)	Si4-N2	1.751(2)	Si4-C11	1.856(4)
Si4-C10	1.863(4)	Si4-C12	1.870(3)	Si5-N3	1.745(2)
Si5-C13	1.863(3)	Si5-C14	1.865(3)	Si5-C15	1.865(3)
Si6-N3	1.759(2)	Si6-C16	1.866(3)	Si6-C18	1.869(3)

Si6-C17	1.874(3)

Table 3.15.5 Bond Angles in **3.1-F**, °

O1-U1-F1	179.07(7)	O1-U1-N2	88.76(7)
O1-U1-N3	90.03(7)	F1-U1-N3	89.04(7)
O1-U1-N1	90.51(7)	F1-U1-N1	89.91(7)
N3-U1-N1	118.96(7)	O1-U1-Si5	110.25(5)
N2-U1-Si5	103.11(6)	N3-U1-Si5	26.45(5)
O1-U1-Si3	108.76(5)	F1-U1-Si3	71.97(5)
N3-U1-Si3	135.44(6)	N1-U1-Si3	101.38(6)
O1-U1-Si6	69.53(5)	F1-U1-Si6	109.56(5)
N3-U1-Si6	26.51(5)	N1-U1-Si6	101.21(5)
Si3-U1-Si6	157.36(2)	O1-U1-Si2	70.03(5)
N2-U1-Si2	101.87(6)	N3-U1-Si2	132.50(5)
Si5-U1-Si2	155.02(2)	Si3-U1-Si2	92.05(2)
O1-U1-Si4	68.80(5)	F1-U1-Si4	111.46(5)
N3-U1-Si4	102.83(5)	N1-U1-Si4	133.48(5)
Si3-U1-Si4	52.68(2)	Si6-U1-Si4	108.825(17)
N1-Si1-C3	111.41(13)	N1-Si1-C1	110.66(12)
N1-Si1-C2	111.62(10)	C3-Si1-C2	107.83(13)
N1-Si1-U1	33.28(6)	C3-Si1-U1	112.03(12)
C2-Si1-U1	80.65(8)	N1-Si2-C6	111.29(13)
C6-Si2-C5	107.36(18)	N1-Si2-C4	111.50(14)
C5-Si2-C4	104.81(17)	N1-Si2-U1	33.96(7)
C5-Si2-U1	79.85(11)	C4-Si2-U1	133.75(13)
N2-Si3-C7	110.96(12)	C8-Si3-C7	107.30(19)
C8-Si3-C9	110.07(19)	C7-Si3-C9	106.15(17)
C8-Si3-U1	114.24(14)	C7-Si3-U1	78.24(9)
N2-Si4-C11	111.52(15)	N2-Si4-C10	111.62(16)
N2-Si4-C12	111.51(12)	C11-Si4-C12	106.55(18)
N2-Si4-U1	33.62(7)	C11-Si4-U1	110.29(14)
C12-Si4-U1	80.57(10)	N3-Si5-C13	110.95(11)
C13-Si5-C14	106.01(17)	N3-Si5-C15	110.92(11)
C14-Si5-C15	108.80(14)	N3-Si5-U1	34.31(7)
C14-Si5-U1	135.99(11)	C15-Si5-U1	110.47(10)
N3-Si6-C18	111.32(11)	C16-Si6-C18	107.11(17)
C16-Si6-C17	109.53(15)	C18-Si6-C17	105.79(16)
C16-Si6-U1	111.55(9)	C18-Si6-U1	79.39(9)
Si1-N1-Si2	119.38(12)	Si1-N1-U1	120.93(10)
Si4-N2-Si3	120.47(12)	Si4-N2-U1	120.32(11)
Si5-N3-Si6	121.34(12)	Si5-N3-U1	119.24(10)
F1-U1-N2	91.75(7)	C6-Si2-C4	109.87(17)
N2-U1-N3	120.95(8)	C6-Si2-U1	112.34(11)
N2-U1-N1	120.08(8)	N2-Si3-C8	111.53(16)
F1-U1-Si5	68.88(5)	N2-Si3-C9	110.65(13)
N1-U1-Si5	132.55(5)	N2-Si3-U1	34.18(7)
N2-U1-Si3	26.62(6)	C9-Si3-U1	131.72(13)
Si5-U1-Si3	110.58(2)	C11-Si4-C10	110.3(2)
N2-U1-Si6	133.63(6)	C10-Si4-C12	104.98(19)
Si5-U1-Si6	52.953(19)	C10-Si4-U1	135.18(14)
F1-U1-Si2	110.61(5)	N3-Si5-C14	111.48(14)
N1-U1-Si2	26.38(5)	C13-Si5-C15	108.51(16)
Si6-U1-Si2	107.72(2)	C13-Si5-U1	79.46(9)

N2-U1-Si4	26.07(6)	N3-Si6-C16	111.10(13)
Si5-U1-Si4	93.967(18)	N3-Si6-C17	111.76(13)
Si2-U1-Si4	108.578(19)	N3-Si6-U1	34.08(7)
C3-Si1-C1	109.99(16)	C17-Si6-U1	134.76(11)
C1-Si1-C2	105.11(13)	Si2-N1-U1	119.66(11)
C1-Si1-U1	133.24(10)	Si3-N2-U1	119.20(11)
N1-Si2-C5	111.74(14)	Si6-N3-U1	119.41(10)

Table 3.15.6 Bond Distances in **3.1-Br**, Å

U1-O1	1.899(17)	U1-N1#1	2.200(3)	U1-N1#2	2.200(3)
U1-N1	2.200(3)	U1-Br1	2.731(2)	U1-Br1'	2.90(4)
U1-Si2#1	3.4383(15)	U1-Si2#2	3.4383(15)	U1-Si2	3.4383(15)
U1-Si1#1	3.4475(11)	U1-Si1#2	3.4475(11)	U1-Si1	3.4475(11)
N1-Si2	1.759(3)	N1-Si1	1.760(3)	Si1-C3	1.868(4)
Si1-C1	1.869(4)	Si1-C2	1.870(5)	Si2-C4	1.858(5)
Si2-C6	1.859(5)	Si2-C5	1.875(5)		

Symmetry transformations used to generate equivalent atoms:
#1 -x+y,-x,z #2 -y,x-y,z

Table 3.15.7 Bond Angles in **3.1-Br**, °

O1-U1-N1#1	84.89(8)	O1-U1-N1#2	84.89(8)
O1-U1-N1	84.89(8)	N1#1-U1-N1	119.22(2)
O1-U1-Br1	180	N1#1-U1-Br1	95.11(8)
N1-U1-Br1	95.11(8)	O1-U1-Br1'	0
N1#2-U1-Br1'	84.89(8)	N1-U1-Br1'	84.89(8)
O1-U1-Si2#1	65.36(2)	N1#1-U1-Si2#1	26.27(8)
N1-U1-Si2#1	98.44(8)	Br1-U1-Si2#1	114.64(2)
O1-U1-Si2#2	65.36(2)	N1#1-U1-Si2#2	98.44(8)
N1-U1-Si2#2	129.69(8)	Br1-U1-Si2#2	114.64(2)
Si2#1-U1-Si2#2	103.84(3)	O1-U1-Si2	65.36(2)
N1#2-U1-Si2	98.44(8)	N1-U1-Si2	26.27(8)
Br1'-U1-Si2	65.36(2)	Si2#1-U1-Si2	103.84(3)
O1-U1-Si1#1	104.30(2)	N1#1-U1-Si1#1	26.04(8)
N1-U1-Si1#1	137.19(8)	Br1-U1-Si1#1	75.70(2)
Si2#1-U1-Si1#1	52.30(3)	Si2#2-U1-Si1#1	90.82(3)
O1-U1-Si1#2	104.30(2)	N1#1-U1-Si1#2	137.19(8)
N1-U1-Si1#2	103.34(8)	Br1-U1-Si1#2	75.70(2)
Si2#1-U1-Si1#2	154.99(3)	Si2#2-U1-Si1#2	52.30(3)
Si1#1-U1-Si1#2	114.108(18)	O1-U1-Si1	104.30(2)
N1#2-U1-Si1	137.19(8)	N1-U1-Si1	26.04(8)
Br1'-U1-Si1	104.30(2)	Si2#1-U1-Si1	90.82(3)
Si2-U1-Si1	52.30(3)	Si1#1-U1-Si1	114.108(18)
Si2-N1-Si1	119.17(18)	Si2-N1-U1	120.14(16)
N1-Si1-C3	112.42(17)	N1-Si1-C1	111.53(19)
N1-Si1-C2	110.5(2)	C3-Si1-C2	105.8(3)
N1-Si1-U1	33.29(10)	C3-Si1-U1	137.09(14)
C2-Si1-U1	80.45(19)	N1-Si2-C4	113.46(18)
C4-Si2-C6	108.8(2)	N1-Si2-C5	111.4(2)
C6-Si2-C5	106.0(3)	N1-Si2-U1	33.60(10)
C6-Si2-U1	129.51(18)	C5-Si2-U1	78.5(2)
N1#1-U1-N1#2	119.22(2)	N1#2-U1-Si1#2	26.04(8)
N1#2-U1-N1	119.22(2)	Br1'-U1-Si1#2	104.30(2)
N1#2-U1-Br1	95.11(8)	Si2-U1-Si1#2	90.82(3)

N1#1-U1-Br1'	84.89(8)	N1#1-U1-Si1	103.34(8)
Br1-U1-Br1'	180	Br1-U1-Si1	75.70(2)
N1#2-U1-Si2#1	129.69(8)	Si2#2-U1-Si1	154.99(3)
Br1'-U1-Si2#1	65.36(2)	Si1#2-U1-Si1	114.108(18)
N1#2-U1-Si2#2	26.27(8)	Si1-N1-U1	120.67(16)
Br1'-U1-Si2#2	65.36(2)	C3-Si1-C1	107.1(2)
N1#1-U1-Si2	129.69(8)	C1-Si1-C2	109.2(3)
Br1-U1-Si2	114.64(2)	C1-Si1-U1	110.59(17)
Si2#2-U1-Si2	103.84(3)	N1-Si2-C6	111.3(2)
N1#2-U1-Si1#1	103.34(8)	C4-Si2-C5	105.4(3)
Br1'-U1-Si1#1	104.30(2)	C4-Si2-U1	118.48(16)
Si2-U1-Si1#1	154.99(3)		

Symmetry transformations used to generate equivalent atoms:
#1 -x+y,-x,z #2 -y,x-y,z

Table 3.15.8 Bond Distances in **3.1-Me**, Å

U1-O1	1.791(3)	U1-O1'	1.795(7)	U1-N2	2.215(2)
U1-N1	2.223(2)	U1-N3	2.225(2)	U1-C19	2.343(4)
U1-C19'	2.350(8)	U1-Si3	3.4319(8)	U1-Si2	3.4352(9)
U1-Si6	3.4417(9)	U1-Si5	3.4522(9)	U1-Si4	3.4628(8)
Si1-N1	1.751(2)	Si1-C2	1.869(3)	Si1-C3	1.870(3)
Si1-C1	1.879(3)	Si2-N1	1.753(2)	Si2-C5	1.865(4)
Si2-C4	1.868(4)	Si2-C6	1.875(3)	Si3-N2	1.754(2)
Si3-C8	1.865(3)	Si3-C9	1.869(3)	Si3-C7	1.877(3)
Si4-N2	1.748(2)	Si4-C12	1.868(4)	Si4-C11	1.872(4)
Si4-C10	1.878(3)	Si5-N3	1.754(3)	Si5-C15	1.855(4)
Si5-C14	1.868(4)	Si5-C13	1.875(4)	Si6-N3	1.740(2)
Si6-C16	1.861(4)	Si6-C18	1.864(4)	Si6-C17	1.870(4)

Table 3.15.9 Bond Angles in **3.1-Me**, °

O1-U1-O1'	177.1(4)	O1-U1-N2	89.99(12)
O1-U1-N1	90.68(12)	O1'-U1-N1	91.4(4)
O1-U1-N3	90.04(12)	O1'-U1-N3	90.7(4)
N1-U1-N3	119.87(8)	O1-U1-C19	178.95(18)
N2-U1-C19	90.05(16)	N1-U1-C19	88.38(16)
O1-U1-C19'	2.6(5)	O1'-U1-C19'	176.4(6)
N1-U1-C19'	92.2(4)	N3-U1-C19'	87.4(4)
O1-U1-Si3	69.34(10)	O1'-U1-Si3	108.2(4)
N1-U1-Si3	101.35(6)	N3-U1-Si3	134.28(6)
C19'-U1-Si3	71.1(4)	O1-U1-Si2	70.35(11)
N2-U1-Si2	132.81(6)	N1-U1-Si2	26.49(6)
C19-U1-Si2	108.89(16)	C19'-U1-Si2	71.2(4)
O1-U1-Si6	70.60(10)	O1'-U1-Si6	109.2(4)
N1-U1-Si6	134.33(6)	N3-U1-Si6	25.99(6)
C19'-U1-Si6	68.0(4)	Si3-U1-Si6	109.44(2)
O1-U1-Si5	108.81(10)	O1'-U1-Si5	72.8(4)
N1-U1-Si5	100.53(6)	N3-U1-Si5	26.13(6)
C19'-U1-Si5	106.4(4)	Si3-U1-Si5	158.06(2)
Si6-U1-Si5	52.10(2)	O1-U1-Si4	108.94(11)
N2-U1-Si4	25.54(6)	N1-U1-Si4	132.85(6)
C19-U1-Si4	71.42(16)	C19'-U1-Si4	109.3(4)
Si2-U1-Si4	155.13(2)	Si6-U1-Si4	92.82(2)
N1-Si1-C2	112.01(14)	N1-Si1-C3	111.45(12)

N1-Si1-C1	111.86(12)	C2-Si1-C1	107.94(15)
N1-Si2-C5	111.17(14)	N1-Si2-C4	111.73(15)
N1-Si2-C6	112.19(15)	C5-Si2-C6	107.91(18)
N1-Si2-U1	34.45(8)	C5-Si2-U1	111.81(12)
C6-Si2-U1	80.15(11)	N2-Si3-C8	111.34(14)
C8-Si3-C9	109.13(17)	N2-Si3-C7	111.30(12)
C9-Si3-C7	104.59(17)	N2-Si3-U1	34.29(7)
C9-Si3-U1	136.47(12)	C7-Si3-U1	79.74(10)
N2-Si4-C11	110.73(13)	C12-Si4-C11	105.95(18)
C12-Si4-C10	107.54(17)	C11-Si4-C10	108.94(17)
C12-Si4-U1	134.69(13)	C11-Si4-U1	79.73(11)
N3-Si5-C15	112.34(19)	N3-Si5-C14	111.48(17)
N3-Si5-C13	111.57(13)	C15-Si5-C13	108.2(2)
N3-Si5-U1	33.97(7)	C15-Si5-U1	114.89(16)
C13-Si5-U1	79.40(10)	N3-Si6-C16	111.17(17)
C16-Si6-C18	110.5(3)	N3-Si6-C17	111.97(14)
C18-Si6-C17	104.3(2)	N3-Si6-U1	34.07(8)
C18-Si6-U1	135.79(17)	C17-Si6-U1	80.62(11)
Si1-N1-U1	122.26(11)	Si2-N1-U1	119.06(12)
Si4-N2-U1	121.35(12)	Si3-N2-U1	119.22(11)
Si6-N3-U1	119.95(12)	Si5-N3-U1	119.91(12)
C5-Si2-C4	109.69(19)	C15-Si5-C14	107.9(2)
C4-Si2-C6	103.85(18)	C14-Si5-C13	105.1(2)
C4-Si2-U1	134.61(15)	C14-Si5-U1	133.14(17)
N2-Si3-C9	112.69(14)	N3-Si6-C18	112.10(18)
C8-Si3-C7	107.44(19)	C16-Si6-C17	106.4(2)
C8-Si3-U1	110.58(11)	C16-Si6-U1	109.85(17)
N2-Si4-C12	112.22(16)	Si1-N1-Si2	118.56(13)
N2-Si4-C10	111.23(13)	Si4-N2-Si3	119.35(13)
N2-Si4-U1	33.12(7)	Si6-N3-Si5	120.10(13)
C10-Si4-U1	112.85(12)		

Table 3.15.10 Bond Distances in **3.1-CCPh**, Å

U1-O1#1	1.811(10)	U1-O1	1.811(10)	U1-N1#1	2.189(5)
U1-N1	2.189(5)	U1-N2	2.225(7)	U1-C10	2.337(14)
U1-C10#1	2.337(14)	U1-Si1#1	3.3998(17)	U1-Si1	3.3998(17)
U1-Si3	3.4354(16)	U1-Si3#1	3.4354(16)	U1-Si2#1	3.4611(16)
Si1-N1	1.760(5)	Si1-C2	1.859(7)	Si1-C1	1.867(6)
Si1-C3	1.878(8)	Si2-N1	1.763(5)	Si2-C4	1.861(7)
Si2-C6	1.865(8)	Si2-C5	1.868(6)	Si3-N2	1.747(4)
Si3-C8	1.860(7)	Si3-C9	1.864(7)	Si3-C7	1.870(7)
N2-Si3#1	1.747(4)	C10-C11	1.209(18)	C11-C12	1.560(13)
C12-C14	1.379(11)	C12-C13	1.384(11)	C13-C13#2	1.397(15)
C14-C14#2	1.396(15)				

Symmetry transformations used to generate equivalent atoms:
#1 -x+1/2,y,-z+1/2 #2 -x+1/2,y,-z+3/2

Table 3.15.11 Bond Angles in **3.1-CCPh**, °

O1#1-U1-O1	177.0(8)	O1#1-U1-N1#1	87.2(4)
O1#1-U1-N1	91.2(4)	O1-U1-N1	87.2(4)
O1#1-U1-N2	91.5(4)	O1-U1-N2	91.5(4)
N1-U1-N2	122.21(12)	O1#1-U1-C10	3.7(8)
N1#1-U1-C10	90.8(5)	N1-U1-C10	90.2(5)

O1#1-U1-C10#1	177.2(7)	O1-U1-C10#1	3.7(8)
N1-U1-C10#1	90.8(5)	N2-U1-C10#1	89.0(5)
O1#1-U1-Si1#1	107.4(4)	O1-U1-Si1#1	71.9(4)
N1-U1-Si1#1	130.89(12)	N2-U1-Si1#1	102.77(3)
C10#1-U1-Si1#1	69.8(5)	O1#1-U1-Si1	71.9(4)
N1#1-U1-Si1	130.89(12)	N1-U1-Si1	27.08(12)
C10-U1-Si1	69.8(5)	C10#1-U1-Si1	110.6(4)
O1#1-U1-Si3	72.6(4)	O1-U1-Si3	110.3(4)
N1-U1-Si3	138.24(12)	N2-U1-Si3	26.32(3)
C10#1-U1-Si3	107.0(5)	Si1#1-U1-Si3	90.86(4)
O1#1-U1-Si3#1	110.3(4)	O1-U1-Si3#1	72.6(4)
N1-U1-Si3#1	102.10(12)	N2-U1-Si3#1	26.32(3)
C10#1-U1-Si3#1	71.1(5)	Si1#1-U1-Si3#1	112.41(4)
Si3-U1-Si3#1	52.64(6)	O1#1-U1-Si2#1	67.5(4)
N1#1-U1-Si2#1	25.63(12)	N1-U1-Si2#1	98.45(12)
C10-U1-Si2#1	71.2(5)	C10#1-U1-Si2#1	110.3(5)
Si1-U1-Si2#1	107.05(4)	Si3-U1-Si2#1	109.44(4)
N1-Si1-C2	112.2(3)	N1-Si1-C1	112.0(3)
N1-Si1-C3	111.3(3)	C2-Si1-C3	108.9(4)
N1-Si1-U1	34.49(15)	C2-Si1-U1	114.1(3)
C3-Si1-U1	133.3(2)	N1-Si2-C4	112.0(3)
C4-Si2-C6	105.1(4)	N1-Si2-C5	110.9(3)
C6-Si2-C5	109.0(3)	N1-Si2-U1	32.48(17)
C6-Si2-U1	135.8(2)	C5-Si2-U1	109.7(2)
N2-Si3-C9	110.6(2)	C8-Si3-C9	107.6(3)
C8-Si3-C7	105.5(4)	C9-Si3-C7	109.3(4)
C8-Si3-U1	79.5(2)	C9-Si3-U1	113.2(2)
Si1-N1-Si2	119.6(3)	Si1-N1-U1	118.4(2)
Si3-N2-Si3#1	121.4(4)	Si3-N2-U1	119.3(2)
C11-C10-U1	176.9(14)	C10-C11-C12	177.9(13)
C14-C12-C11	119.2(8)	C13-C12-C11	122.0(8)
C12-C14-C14#2	120.7(5)	O1-U1-Si2#1	110.2(4)
O1-U1-N1#1	91.2(4)	N2-U1-Si2#1	135.05(3)
N1#1-U1-N1	115.6(2)	Si1#1-U1-Si2#1	52.69(4)
N1#1-U1-N2	122.21(12)	Si3#1-U1-Si2#1	159.38(4)
O1-U1-C10	177.2(7)	C2-Si1-C1	107.7(3)
N2-U1-C10	89.0(5)	C1-Si1-C3	104.4(3)
N1#1-U1-C10#1	90.2(5)	C1-Si1-U1	79.5(2)
C10-U1-C10#1	178.0(10)	N1-Si2-C6	111.8(3)
N1#1-U1-Si1#1	27.08(12)	C4-Si2-C5	107.8(3)
C10-U1-Si1#1	110.6(4)	C4-Si2-U1	82.5(2)
O1-U1-Si1	107.4(4)	N2-Si3-C8	112.3(3)
N2-U1-Si1	102.77(3)	N2-Si3-C7	111.4(3)
Si1#1-U1-Si1	154.45(6)	N2-Si3-U1	34.4(2)
N1#1-U1-Si3	102.10(12)	C7-Si3-U1	133.3(3)
C10-U1-Si3	71.1(5)	Si2-N1-U1	121.9(3)
Si1-U1-Si3	112.41(4)	Si3#1-N2-U1	119.3(2)
N1#1-U1-Si3#1	138.24(12)	C14-C12-C13	118.8(7)
C10-U1-Si3#1	107.0(5)	C12-C13-C13#2	120.5(4)
Si1-U1-Si3#1	90.86(4)		

Symmetry transformations used to generate equivalent atoms:
#1 -x+1/2,y,-z+1/2 #2 -x+1/2,y,-z+3/2

Table 3.15.12 Bond Distances in **3.1-CCPh**, Å

U1-N1#1	2.259(3)	U1-N1	2.259(3)	U1-N1#2	2.259(3)
U1-C1	2.450(15)	U1-Si2#1	3.4361(12)	U1-Si2	3.4361(12)
U1-Si2#2	3.4361(12)	Si1-N1	1.734(3)	Si1-C3	1.860(5)
Si1-C4	1.869(4)	Si1-C2	1.884(4)	Si2-N1	1.738(3)
Si2-C5	1.868(4)	Si2-C6	1.875(4)	Si2-C7	1.881(6)

Symmetry transformations used to generate equivalent atoms:
#1 -x+y+1,-x+1,z #2 -y+1,x-y,z

Table 3.15.13 Bond Angles in **3.1-CCPh**, °

N1#1-U1-N1	117.34(4)	N1#1-U1-N1#2	117.34(4)
N1#1-U1-C1	99.48(8)	N1-U1-C1	99.48(8)
N1#1-U1-Si2#1	26.54(7)	N1-U1-Si2#1	137.62(7)
C1-U1-Si2#1	78.96(3)	N1#1-U1-Si2	104.51(7)
N1#2-U1-Si2	137.62(7)	C1-U1-Si2	78.96(3)
N1#1-U1-Si2#2	137.62(7)	N1-U1-Si2#2	104.51(7)
C1-U1-Si2#2	78.96(3)	Si2#1-U1-Si2#2	116.43(2)
N1-Si1-C3	112.4(2)	N1-Si1-C4	114.57(16)
N1-Si1-C2	109.65(19)	C3-Si1-C2	108.6(2)
N1-Si2-C5	112.19(17)	N1-Si2-C6	113.06(16)
N1-Si2-C7	110.0(3)	C5-Si2-C7	108.3(3)
N1-Si2-U1	35.49(9)	C5-Si2-U1	109.68(15)
C7-Si2-U1	78.2(3)	Si1-N1-Si2	120.37(17)
Si2-N1-U1	117.97(14)	Si2-U1-Si2#2	116.43(2)
N1-U1-N1#2	117.34(4)	C3-Si1-C4	107.2(2)
N1#2-U1-C1	99.48(8)	C4-Si1-C2	104.0(2)
N1#2-U1-Si2#1	104.51(7)	C5-Si2-C6	106.3(2)
N1-U1-Si2	26.54(7)	C6-Si2-C7	106.6(3)
Si2#1-U1-Si2	116.43(2)	C6-Si2-U1	139.92(13)
N1#2-U1-Si2#2	26.54(7)	Si1-N1-U1	121.65(15)

Symmetry transformations used to generate equivalent atoms:
#1 -x+y+1,-x+1,z #2 -y+1,x-y,z

Table 3.15.14 Bond Distances in $UO_2(THF)_2[N(SiMe_3)_2]_2$, Å

U1-O2	1.787(6)	U1-O1	1.794(6)	U1-N1	2.298(7)
U1-N2	2.325(7)	U1-O4	2.423(5)	U1-O3	2.445(6)
U1-Si4	3.450(2)	Si1-N1	1.726(7)	Si1-C3	1.869(10)
Si1-C2	1.879(11)	Si1-C1	1.904(10)	Si2-N1	1.754(7)
Si2-C4	1.869(9)	Si2-C5	1.870(11)	Si2-C6	1.879(10)
Si3-N2	1.739(7)	Si3-C8	1.844(10)	Si3-C7	1.877(11)
Si3-C9	1.886(10)	Si4-N2	1.736(8)	Si4-C11	1.878(11)
Si4-C12	1.879(10)	Si4-C10	1.882(10)	O3-C16	1.452(11)
O3-C13	1.457(11)	O4-C20	1.470(10)	O4-C17	1.473(10)
C13-C14	1.508(14)	C14-C15	1.519(16)	C15-C16	1.509(13)
C17-C18	1.511(13)	C18-C19	1.525(15)	C19-C20	1.510(12)
U1'-O1'	1.786(5)	U1'-O2'	1.798(6)	U1'-N2'	2.286(7)
U1'-N1'	2.295(6)	U1'-O4'	2.441(6)	U1'-O3'	2.451(6)
U1'-Si1'	3.421(2)	U1'-Si3'	3.458(3)	Si1'-N1'	1.727(7)
Si1'-C1'	1.866(12)	Si1'-C3'	1.870(11)	Si1'-C2'	1.879(10)
Si2'-N1'	1.748(7)	Si2'-C5'	1.868(11)	Si2'-C4'	1.870(12)
Si2'-C6'	1.896(11)	Si3'-N2'	1.766(7)	Si3'-C9'	1.863(11)
Si3'-C8'	1.876(10)	Si3'-C7'	1.887(10)	Si4'-N2'	1.729(7)

Si4'-C12'	1.863(11)	Si4'-C10'	1.868(11)	Si4'-C11'	1.889(11)
O3'-C13'	1.448(12)	O3'-C16'	1.471(13)	O4'-C20'	1.435(11)
O4'-C17'	1.460(10)	C13'-C14"	1.499(18)	C13'-C14'	1.527(14)
C14'-C15'	1.454(15)	C14"-C15'	1.510(18)	C15'-C16'	1.497(16)
C17'-C18'	1.499(15)	C18'-C19'	1.449(19)	C19'-C20'	1.483(16)

Table 3.15.15 Bond Angles in $UO_2(THF)_2[N(SiMe_3)_2]$, °

O2-U1-O1	179.1(3)	O2-U1-N1	91.6(3)
O2-U1-N2	92.0(3)	O1-U1-N2	89.0(3)
O2-U1-O4	87.4(2)	O1-U1-O4	92.6(2)
N2-U1-O4	88.6(2)	O2-U1-O3	85.5(2)
N1-U1-O3	92.5(2)	N2-U1-O3	90.4(2)
O2-U1-Si4	118.4(2)	O1-U1-Si4	62.5(2)
N2-U1-Si4	26.99(18)	O4-U1-Si4	85.20(15)
N1-Si1-C3	111.2(4)	N1-Si1-C2	114.7(4)
N1-Si1-C1	112.6(4)	C3-Si1-C1	109.1(5)
N1-Si2-C4	111.7(4)	N1-Si2-C5	114.4(5)
N1-Si2-C6	112.1(4)	C4-Si2-C6	108.9(5)
N2-Si3-C8	115.6(4)	N2-Si3-C7	113.4(4)
N2-Si3-C9	110.2(4)	C8-Si3-C9	104.2(5)
N2-Si4-C11	114.7(4)	N2-Si4-C12	111.1(4)
N2-Si4-C10	112.0(4)	C11-Si4-C10	103.5(5)
N2-Si4-U1	37.4(2)	C11-Si4-U1	151.1(4)
C10-Si4-U1	87.3(3)	C16-O3-C13	110.3(7)
C13-O3-U1	121.2(5)	C20-O4-C17	110.5(6)
C17-O4-U1	128.2(5)	Si1-N1-Si2	117.5(4)
Si2-N1-U1	118.6(3)	Si4-N2-Si3	118.3(4)
Si3-N2-U1	126.0(4)	O3-C13-C14	104.6(8)
C16-C15-C14	102.7(9)	O3-C16-C15	105.0(8)
C17-C18-C19	103.3(8)	C20-C19-C18	103.2(8)
O1'-U1'-O2'	179.3(3)	O1'-U1'-N2'	93.8(3)
O1'-U1'-N1'	92.4(3)	O2'-U1'-N1'	87.7(3)
O1'-U1'-O4'	87.8(3)	O2'-U1'-O4'	91.5(2)
N1'-U1'-O4'	88.5(2)	O1'-U1'-O3'	88.4(3)
N2'-U1'-O3'	88.2(2)	N1'-U1'-O3'	92.2(2)
O1'-U1'-Si1'	117.8(2)	O2'-U1'-Si1'	62.38(19)
N1'-U1'-Si1'	27.03(17)	O4'-U1'-Si1'	97.98(15)
O1'-U1'-Si3'	119.7(2)	O2'-U1'-Si3'	60.08(19)
N1'-U1'-Si3'	146.83(18)	O4'-U1'-Si3'	84.89(16)
Si1'-U1'-Si3'	122.44(6)	N1'-Si1'-C1'	113.8(5)
C1'-Si1'-C3'	102.1(6)	N1'-Si1'-C2'	111.2(4)
C3'-Si1'-C2'	107.9(5)	N1'-Si1'-U1'	37.1(2)
C3'-Si1'-U1'	85.5(3)	C2'-Si1'-U1'	99.1(3)
N1'-Si2'-C4'	111.7(5)	C5'-Si2'-C4'	102.1(6)
C5'-Si2'-C6'	105.5(6)	C4'-Si2'-C6'	109.5(7)
N2'-Si3'-C8'	112.0(4)	C9'-Si3'-C8'	104.2(6)
C9'-Si3'-C7'	102.3(5)	C8'-Si3'-C7'	109.2(4)
C9'-Si3'-U1'	150.8(4)	C8'-Si3'-U1'	98.5(3)
N2'-Si4'-C12'	113.2(5)	N2'-Si4'-C10'	111.3(4)
N2'-Si4'-C11'	114.7(4)	C12'-Si4'-C11'	102.1(6)
C13'-O3'-C16'	109.7(8)	C13'-O3'-U1'	127.2(6)
C20'-O4'-C17'	109.4(7)	C20'-O4'-U1'	126.5(5)
Si1'-N1'-Si2'	119.5(4)	Si1'-N1'-U1'	115.8(4)
Si4'-N2'-Si3'	119.8(4)	Si4'-N2'-U1'	123.6(3)

O3'-C13'-C14"	106.4(13)	O3'-C13'-C14'	103.1(10)
C15'-C14'-C13'	105.7(11)	C13'-C14"-C15'	104.3(14)
C14'-C15'-C14"	33.3(15)	C16'-C15'-C14"	108.0(12)
O4'-C17'-C18'	104.8(8)	C19'-C18'-C17'	106.8(9)
O4'-C20'-C19'	106.0(8)	O2'-U1'-O3'	92.3(3)
O1-U1-N1	87.5(3)	O4'-U1'-O3'	176.2(2)
N1-U1-N2	175.6(2)	N2'-U1'-Si1'	147.15(16)
N1-U1-O4	88.9(2)	O3'-U1'-Si1'	84.24(16)
O1-U1-O3	94.5(2)	N2'-U1'-Si3'	27.17(16)
O4-U1-O3	172.8(2)	O3'-U1'-Si3'	96.50(16)
N1-U1-Si4	149.03(17)	N1'-Si1'-C3'	113.2(4)
O3-U1-Si4	97.08(15)	C1'-Si1'-C2'	108.1(6)
C3-Si1-C2	105.5(5)	C1'-Si1'-U1'	147.5(4)
C2-Si1-C1	103.3(5)	N1'-Si2'-C5'	114.4(4)
C4-Si2-C5	107.2(6)	N1'-Si2'-C6'	112.9(5)
C5-Si2-C6	102.0(6)	N2'-Si3'-C9'	116.3(5)
C8-Si3-C7	104.1(6)	N2'-Si3'-C7'	112.1(4)
C7-Si3-C9	108.7(6)	N2'-Si3'-U1'	36.2(2)
C11-Si4-C12	105.0(5)	C7'-Si3'-U1'	87.0(3)
C12-Si4-C10	110.1(5)	C12'-Si4'-C10'	108.6(6)
C12-Si4-U1	96.0(3)	C10'-Si4'-C11'	106.3(7)
C16-O3-U1	128.5(5)	C16'-O3'-U1'	123.1(6)
C20-O4-U1	121.2(5)	C17'-O4'-U1'	123.9(5)
Si1-N1-U1	123.8(4)	Si2'-N1'-U1'	124.6(3)
Si4-N2-U1	115.6(4)	Si3'-N2'-U1'	116.6(3)
C13-C14-C15	102.9(8)	C14"-C13'-C14'	32.7(14)
O4-C17-C18	104.5(7)	C14'-C15'-C16'	102.8(11)
O4-C20-C19	104.0(7)	O3'-C16'-C15'	105.5(10)
O2'-U1'-N2'	86.1(2)	C18'-C19'-C20'	104.7(11)
N2'-U1'-N1'	173.8(2)	N2'-U1'-O4'	91.5(2)

Table 3.15.16 Bond Distances in **3.2**

U1-O1	2.145(5)	U1-N1	2.166(7)	U1-N2	2.189(6)
U1-N3	2.189(6)	U1-Cl1	2.5852(19)	U1-Si1	3.378(2)
U1-Si3	3.442(2)	U1-Si6	3.451(2)	U1-Si5	3.465(2)
N1-Si2	1.771(7)	N1-Si1	1.773(7)	N2-Si3	1.763(7)
N2-Si4	1.772(6)	N3-Si5	1.729(8)	N3-Si6	1.806(7)
C1-Si1	1.855(9)	C2-Si1	1.855(9)	C3-Si1	1.868(11)
C4-Si2	1.888(11)	C5-Si2	1.873(10)	C6-Si2	1.875(10)
C7-Si3	1.872(10)	C8-Si3	1.872(9)	C9-Si3	1.871(11)
C10-Si4	1.855(12)	C11-Si4	1.883(11)	C12-Si4	1.868(10)
C13-Si5	1.857(9)	C14-Si5	1.883(10)	C15-Si5	1.870(11)
C16-Si6	1.853(11)	C17-Si6	1.865(11)	C18-Si6	1.838(11)
C19-O1	1.353(8)	C19-C21	1.376(10)	C19-C20	1.391(10)
C20-F1	1.346(8)	C20-C21#1	1.377(10)	C21-F2	1.340(8)
C21-C20#1	1.377(10)	C22-C23	1.498(16)	C23-C24	1.464(15)
C24-C25	1.437(16)	C25-C26	1.458(15)		

Symmetry transformations used to generate equivalent atoms:
#1 -x+1,-y+1,-z+1

Table 3.15.17 Bond Angles in **3.2**

O1-U1-N1	91.2(2)	O1-U1-N2	92.8(2)
O1-U1-N3	96.7(2)	N1-U1-N3	122.8(3)

O1-U1-Cl1	176.20(15)	N1-U1-Cl1	85.66(17)
N3-U1-Cl1	86.83(17)	O1-U1-Si1	71.41(15)
N2-U1-Si1	133.37(17)	N3-U1-Si1	104.96(19)
O1-U1-Si3	73.41(15)	N1-U1-Si3	97.76(18)
N3-U1-Si3	138.8(2)	Cl1-U1-Si3	104.82(7)
O1-U1-Si6	114.31(15)	N1-U1-Si6	100.09(18)
N3-U1-Si6	27.2(2)	Cl1-U1-Si6	68.48(7)
Si3-U1-Si6	160.30(6)	O1-U1-Si5	82.53(15)
N2-U1-Si5	101.55(18)	N3-U1-Si5	24.5(2)
Si1-U1-Si5	118.55(6)	Si3-U1-Si5	115.09(7)
Si2-N1-Si1	117.1(4)	Si2-N1-U1	125.1(3)
Si3-N2-Si4	116.3(4)	Si3-N2-U1	120.7(3)
Si5-N3-Si6	116.5(3)	Si5-N3-U1	123.9(4)
O1-C19-C21	122.9(7)	O1-C19-C20	122.4(7)
F1-C20-C21#1	117.0(7)	F1-C20-C19	120.9(7)
F2-C21-C19	118.5(7)	F2-C21-C20#1	118.2(7)
C19-O1-U1	169.3(5)	N1-Si1-C2	111.0(4)
C2-Si1-C1	108.0(5)	N1-Si1-C3	111.6(4)
C1-Si1-C3	106.0(5)	N1-Si1-U1	34.6(2)
C1-Si1-U1	78.2(3)	C3-Si1-U1	134.8(4)
N1-Si2-C6	111.4(4)	C5-Si2-C6	105.8(5)
C5-Si2-C4	106.2(5)	C6-Si2-C4	108.3(5)
N2-Si3-C8	111.3(4)	C9-Si3-C8	111.5(4)
C9-Si3-C7	110.1(6)	C8-Si3-C7	102.2(5)
C9-Si3-U1	106.5(4)	C8-Si3-U1	82.2(3)
N2-Si4-C10	111.5(5)	N2-Si4-C12	112.3(4)
N2-Si4-C11	112.3(4)	C10-Si4-C11	109.5(6)
N3-Si5-C13	112.7(4)	N3-Si5-C15	106.5(4)
N3-Si5-C14	115.8(5)	C13-Si5-C14	102.3(5)
N3-Si5-U1	31.6(2)	C13-Si5-U1	124.8(4)
C14-Si5-U1	128.7(4)	N3-Si6-C18	111.3(5)
C18-Si6-C16	104.7(6)	N3-Si6-C17	111.7(5)
C16-Si6-C17	108.5(6)	N3-Si6-U1	33.6(2)
C16-Si6-U1	82.2(3)	C17-Si6-U1	112.3(4)
C25-C24-C23	115.8(17)	C24-C25-C26	115.0(17)
N1-U1-N2	115.4(2)	N1-Si1-C1	110.5(4)
N2-U1-N3	120.6(3)	C2-Si1-C3	109.5(5)
N2-U1-Cl1	86.60(17)	C2-Si1-U1	111.6(3)
N1-U1-Si1	27.70(18)	N1-Si2-C5	113.5(4)
Cl1-U1-Si1	106.36(7)	N1-Si2-C4	111.3(4)
N2-U1-Si3	26.13(16)	N2-Si3-C9	108.1(4)
Si1-U1-Si3	109.10(6)	N2-Si3-C7	113.6(4)
N2-U1-Si6	134.90(17)	N2-Si3-U1	33.1(2)
Si1-U1-Si6	90.60(7)	C7-Si3-U1	138.1(4)
N1-U1-Si5	142.83(18)	C10-Si4-C12	103.1(5)
Cl1-U1-Si5	101.27(7)	C12-Si4-C11	107.7(5)
Si6-U1-Si5	51.51(7)	C13-Si5-C15	109.8(5)
Si1-N1-U1	117.7(3)	C15-Si5-C14	109.8(5)
Si4-N2-U1	122.9(3)	C15-Si5-U1	74.9(3)
Si6-N3-U1	119.2(4)	N3-Si6-C16	113.1(4)
C21-C19-C20	114.7(6)	C18-Si6-C17	107.1(6)
C21#1-C20-C19	122.1(7)	C18-Si6-U1	135.3(4)
C19-C21-C20#1	123.3(7)	C24-C23-C22	107.6(16)

Symmetry transformations used to generate equivalent atoms:
#1 -x+1,-y+1,-z+1

Table 3.15.18 Bond Distances in **3.4**

U1-N1	1.959(5)	U1-N2#1	2.264(3)	U1-N2	2.264(3)
U1-N2#2	2.264(3)	U1-Si1#1	3.3706(10)	U1-Si1#2	3.3706(10)
U1-Si1	3.3706(10)	Si1-N2	1.748(3)	Si1-C10	1.870(4)
Si1-C9	1.871(4)	Si1-C8	1.881(4)	Si2-N2	1.752(3)
Si2-C13	1.858(4)	Si2-C11	1.860(5)	Si2-C12	1.874(5)
N1-C1	1.478(7)	C1-C2#1	1.548(4)	C1-C2	1.548(4)
C1-C2#2	1.548(4)	C2-C3	1.387(5)	C2-C7	1.388(5)
C3-C4	1.384(5)	C4-C5	1.377(6)	C5-C6	1.371(6)
C6-C7	1.388(5)				

Table 3.15.19 Bond Angles in **3.4**

N1-U1-N2#1	113.90(7)	N1-U1-N2	113.90(7)
N1-U1-N2#2	113.90(7)	N2#1-U1-N2#2	104.70(8)
N1-U1-Si1#1	93.420(17)	N2#1-U1-Si1#1	28.34(8)
N2#2-U1-Si1#1	132.68(8)	N1-U1-Si1#2	93.420(17)
N2-U1-Si1#2	132.68(8)	N2#2-U1-Si1#2	28.34(7)
N1-U1-Si1	93.420(17)	N2#1-U1-Si1	132.68(8)
N2#2-U1-Si1	97.45(8)	Si1#1-U1-Si1	119.647(4)
N2-Si1-C10	116.23(19)	N2-Si1-C9	111.30(18)
N2-Si1-C8	109.20(16)	C10-Si1-C8	104.2(2)
N2-Si1-U1	37.95(10)	C10-Si1-U1	128.78(18)
C8-Si1-U1	71.29(12)	N2-Si2-C13	111.65(17)
C13-Si2-C11	109.5(2)	N2-Si2-C12	113.58(19)
C11-Si2-C12	106.0(3)	C1-N1-U1	180
Si1-N2-U1	113.71(14)	Si2-N2-U1	129.28(16)
N1-C1-C2	108.8(2)	C2#1-C1-C2	110.1(2)
C2#1-C1-C2#2	110.1(2)	C2-C1-C2#2	110.1(2)
C3-C2-C1	122.4(3)	C7-C2-C1	119.3(3)
C5-C4-C3	120.6(4)	C4-C5-C6	119.9(4)
C6-C7-C2	121.2(4)	N2-Si2-C11	111.77(19)
N2#1-U1-N2	104.70(8)	C13-Si2-C12	103.9(2)
N2-U1-N2#2	104.70(8)	Si1-N2-Si2	116.77(17)
N2-U1-Si1#1	97.45(8)	N1-C1-C2#1	108.8(2)
N2#1-U1-Si1#2	97.45(8)	N1-C1-C2#2	108.8(2)
Si1#1-U1-Si1#2	119.647(4)	C3-C2-C7	118.3(3)
N2-U1-Si1	28.34(7)	C2-C3-C4	120.3(4)
Si1#2-U1-Si1	119.647(4)	C5-C6-C7	119.7(4)
C10-Si1-C9	107.1(2)	C9-Si1-U1	123.04(14)
C9-Si1-C8	108.41(19)		

Symmetry transformations used to generate equivalent atoms:
#1 -y+1,x-y,z #2 -x+y+1,-x+1,z

3.16 Coordinates of Optimized Geometries.

Table 3.16.1 DFT optimized coordinates of UClF[$N(SiMe_3)_2$]$_3$.

U	0.000540	-0.021812	-0.006828	H	2.399725	5.208456	0.972536
F	-0.003348	-0.040537	-2.065140	H	1.008111	5.437385	-0.087584
Cl	-0.004645	-0.043194	2.612751	C	2.592721	2.219620	1.643788

Si	-3.301083	-0.670811	1.087197	H	2.400861	1.241295	2.088426
Si	-2.254827	-2.351366	-1.246643	H	3.072148	2.838123	2.414956
Si	1.043527	3.153346	1.072552	H	3.318136	2.097310	0.832408
Si	-0.976503	3.086514	-1.226102	C	-2.311139	2.010109	-2.035920
Si	3.197535	-0.683121	-1.249752	H	-2.911815	1.424732	-1.334832
Si	2.290569	-2.458343	1.075573	H	-1.885043	1.320443	-2.768999
N	-1.961971	-1.040051	-0.055674	H	-2.994224	2.686395	-2.567294
N	0.027855	2.173111	-0.045758	C	-1.900541	4.510617	-0.375655
N	1.932409	-1.098491	-0.044689	H	-2.552664	4.141314	0.424103
C	-3.250582	1.129821	1.681763	H	-2.537208	5.012099	-1.116278
H	-2.299933	1.434840	2.124252	H	-1.241909	5.270691	0.055504
H	-4.018876	1.236378	2.459880	C	0.058533	3.767193	-2.659024
H	-3.504749	1.832958	0.881093	H	0.747625	4.561933	-2.360292
C	-5.008945	-0.821829	0.263709	H	-0.612260	4.178334	-3.424948
H	-5.111829	-0.143105	-0.590780	H	0.645670	2.970144	-3.128651
H	-5.763967	-0.527685	1.005057	C	2.897861	1.004393	-2.063353
H	-5.264461	-1.830540	-0.074888	H	2.082173	0.965469	-2.789688
C	-3.267957	-1.814289	2.593410	H	3.816090	1.272746	-2.602854
H	-3.360075	-2.868742	2.313584	H	2.685673	1.815674	-1.361356
H	-4.106004	-1.572796	3.260276	C	4.905587	-0.559295	-0.429197
H	-2.341901	-1.692502	3.163911	H	4.910237	0.201061	0.360476
C	-3.376580	-1.809278	-2.672545	H	5.642222	-0.254783	-1.184212
H	-4.407490	-1.613707	-2.364099	H	5.258471	-1.496856	0.010835
H	-3.400805	-2.601922	-3.432049	C	3.251274	-1.928699	-2.675785
H	-2.990585	-0.903569	-3.153594	H	3.586408	-2.925097	-2.374498
C	-3.000245	-3.879997	-0.401394	H	3.938683	-1.565966	-3.451241
H	-2.331001	-4.268228	0.375277	H	2.260885	-2.029984	-3.134059
H	-3.127171	-4.670783	-1.152431	C	3.223064	-1.873248	2.613017
H	-3.978338	-3.706078	0.057112	H	4.179279	-1.405035	2.355826
C	-0.646838	-2.957697	-2.058748	H	3.436524	-2.728248	3.267600
H	-0.353992	-2.318882	-2.895665	H	2.633917	-1.151879	3.187240
H	-0.837660	-3.965454	-2.451050	C	3.318964	-3.827360	0.248348
H	0.212902	-3.035381	-1.386139	H	2.789289	-4.275480	-0.599810
C	0.058273	3.694256	2.593496	H	3.472780	-4.621183	0.991624
H	-0.810756	4.304811	2.326988	H	4.307180	-3.512541	-0.098990
H	0.696401	4.293693	3.255833	C	0.708333	-3.368179	1.600605
H	-0.294360	2.828788	3.163019	H	-0.070476	-2.734983	2.031622
C	1.754690	4.707200	0.238357	H	0.992955	-4.094925	2.373955
H	2.381261	4.455912	-0.624879	H	0.277463	-3.937915	0.769511

Table 3.16.2 DFT optimized coordinates of NO_2^-.

N	0.000000	0.470402	0.000000
O	1.076435	-0.205801	0.000000
O	-1.076435	-0.205801	0.000000

Table 3.16.3 DFT optimized coordinates of $U(\kappa^1\text{-ONO})F[N(SiMe_3)_2]_3$.

U	-0.002757	0.014943	-0.103008	C	-1.640099	-4.730376	0.280682
F	0.010177	0.004587	-2.167159	H	-2.276726	-4.501752	-0.581727
O	-0.012102	0.096178	2.058525	H	-2.272496	-5.225011	1.029955
N	-0.284781	-0.084466	3.402565	H	-0.888290	-5.457810	-0.039980
O	0.211690	0.743511	4.097502	C	-2.476582	-2.212823	1.648969
Si	3.241750	0.777477	1.019800	H	-2.280887	-1.231044	2.084579
Si	2.221929	2.373944	-1.382198	H	-2.947410	-2.823167	2.431631
Si	-0.933534	-3.149954	1.065767	H	-3.212775	-2.093747	0.846892

Si	1.069788	-3.106390	-1.244017	C	2.393665	-2.019113	-2.055110
Si	-3.212651	0.571893	-1.370417	H	3.008266	-1.457139	-1.345966
Si	-2.370967	2.367920	0.965219	H	1.961997	-1.308635	-2.764565
N	1.935070	1.093941	-0.162819	H	3.065264	-2.684532	-2.614076
N	0.046114	-2.189679	-0.089602	C	2.016612	-4.500431	-0.367736
N	-1.975770	1.028997	-0.156152	H	2.668416	-4.104939	0.419983
C	3.135592	-0.985605	1.716900	H	2.657188	-5.008784	-1.100261
H	2.176634	-1.237214	2.175883	H	1.372046	-5.260851	0.083831
H	3.902635	-1.077018	2.497917	C	0.053716	-3.832351	-2.668243
H	3.357352	-1.743244	0.957591	H	-0.639715	-4.616028	-2.349837
C	4.962715	0.851943	0.215150	H	0.731417	-4.269598	-3.413244
H	5.060611	0.125561	-0.599982	H	-0.528372	-3.051196	-3.169761
H	5.709434	0.590742	0.976716	C	-2.872338	-1.130755	-2.134561
H	5.232876	1.836610	-0.178960	H	-2.028710	-1.107028	-2.828713
C	3.199208	1.986904	2.472907	H	-3.766692	-1.420156	-2.702440
H	3.272976	3.030712	2.151298	H	-2.683844	-1.921352	-1.402263
H	4.044072	1.785867	3.144820	C	-4.934374	0.440270	-0.579067
H	2.278420	1.875001	3.054159	H	-4.943858	-0.298595	0.230834
C	3.320107	1.784632	-2.807686	H	-5.650960	0.104136	-1.339898
H	4.340227	1.545338	-2.491944	H	-5.310243	1.384284	-0.172557
H	3.383267	2.572240	-3.569969	C	-3.267761	1.791794	-2.817914
H	2.898848	0.893815	-3.286506	H	-3.595882	2.794184	-2.527523
C	2.998783	3.916566	-0.590732	H	-3.961650	1.422959	-3.584646
H	2.349021	4.333208	0.187959	H	-2.279687	1.882891	-3.282978
H	3.117315	4.685138	-1.365750	C	-3.352706	1.763218	2.468219
H	3.984588	3.747091	-0.146997	H	-4.308791	1.314890	2.178045
C	0.608952	2.992752	-2.172221	H	-3.569824	2.608514	3.134114
H	0.191630	2.276476	-2.883679	H	-2.801866	1.018964	3.052912
H	0.850628	3.911832	-2.722861	C	-3.373819	3.744603	0.123244
H	-0.175869	3.250722	-1.453239	H	-2.824031	4.190195	-0.713666
C	0.071005	-3.638039	2.594749	H	-3.547411	4.539732	0.860437
H	0.980875	-4.190708	2.339612	H	-4.352484	3.426788	-0.248741
H	-0.536831	-4.279316	3.246465	C	-0.806357	3.247992	1.582177
H	0.360946	-2.759141	3.180059	H	-0.092864	2.605112	2.103279

Table 3.16.4 DFT optimized coordinates of $U(\eta^2\text{-ONO})F[N(SiMe_3)_2]_3$.

U	0.002717	-0.052029	-0.043885	C	1.637559	-3.489207	1.238354
F	-0.017763	-0.019966	-2.104484	H	0.852759	-3.249376	1.956751
Si	0.484747	3.175806	1.231016	H	2.239727	-4.296374	1.678113
Si	-1.397207	2.957066	-1.167647	H	1.178088	-3.900502	0.332948
Si	2.845038	-2.072616	0.856193	C	2.608077	1.677127	-1.992909
Si	3.250999	0.037872	-1.290783	H	2.322264	2.417455	-1.241673
Si	-1.931956	-2.557592	-1.364330	H	1.763428	1.534587	-2.670436
Si	-3.278619	-1.083164	0.957079	H	3.433232	2.108063	-2.576545
N	-0.304594	2.129466	-0.004002	C	4.909045	0.498210	-0.480931
N	2.126852	-0.726712	-0.110723	H	4.765911	1.275173	0.279332
N	-1.853987	-1.256234	-0.126460	H	5.571290	0.915747	-1.250857
C	2.100022	2.427333	1.886602	H	5.440169	-0.331389	-0.007191
H	1.991260	1.447210	2.355991	C	3.525823	-1.058311	-2.812035
H	2.478201	3.112222	2.658006	H	4.086025	-1.973857	-2.607114
H	2.871894	2.356577	1.114021	H	4.079491	-0.491478	-3.571983
C	1.025174	4.852271	0.514833	H	2.562705	-1.342539	-3.252014
H	1.736529	4.734195	-0.310430	C	-0.216298	-2.930976	-2.101616
H	1.540113	5.406055	1.311181	H	-0.056324	-2.361216	-3.020901

H	0.202596	5.481873	0.162805	H	-0.183526	-3.999844	-2.349752
C	-0.651319	3.495873	2.709244	H	0.641975	-2.736865	-1.450549
H	-1.611286	3.930494	2.414416	C	-2.530164	-4.187561	-0.597227
H	-0.164878	4.197614	3.399493	H	-1.866012	-4.514417	0.211667
H	-0.850520	2.570363	3.257945	H	-2.515445	-4.966144	-1.371302
C	-0.450271	3.879103	-2.525287	H	-3.548254	-4.143474	-0.198355
H	0.154562	4.708987	-2.148534	C	-3.038061	-2.111374	-2.832895
H	-1.173366	4.292401	-3.240926	H	-4.095894	-2.020038	-2.571024
H	0.212559	3.205331	-3.078064	H	-2.950337	-2.894256	-3.598075
C	-2.543407	4.193515	-0.290557	H	-2.719336	-1.167704	-3.288779
H	-3.176229	3.703542	0.457964	C	-3.228861	-2.315881	2.393255
H	-3.209245	4.639988	-1.040828	H	-3.242978	-3.355329	2.050717
H	-2.016436	5.014049	0.205932	H	-4.112118	-2.163926	3.027488
C	-2.545308	1.752777	-2.074975	H	-2.344289	-2.185946	3.024125
H	-2.007481	1.168264	-2.825466	C	-4.913278	-1.338760	0.022423
H	-3.304032	2.353157	-2.594460	H	-5.034313	-0.623678	-0.799343
H	-3.072653	1.053604	-1.420097	H	-5.736864	-1.167380	0.728164
C	3.571537	-1.408364	2.473595	H	-5.041910	-2.346031	-0.385911
H	4.335194	-0.645570	2.286260	C	-3.410070	0.658912	1.686736
H	4.045633	-2.225042	3.033116	H	-2.563546	0.939685	2.317615
H	2.809605	-0.968142	3.124636	H	-4.311710	0.683961	2.313538
C	4.228409	-3.000742	-0.067398	H	-3.532885	1.424674	0.914140
H	3.829193	-3.561932	-0.919988	N	0.087601	-0.984385	2.321919
H	4.639726	-3.737149	0.636153	O	0.123544	-1.530926	3.398810
H	5.063158	-2.392901	-0.423555	O	-0.246077	0.274899	2.273387

Table 3.16.5 DFT optimized coordinates of $U(\kappa^2\text{-}O_2N)F[N(SiMe_3)_2]_3$.

U	0.003073	0.202408	-0.031078	C	-2.193006	-2.025514	2.045844
F	0.044088	0.299229	-2.091508	H	-1.891706	-1.134671	2.601895
Si	3.471735	0.542826	0.922085	H	-2.672047	-2.706995	2.762457
Si	2.295394	2.370579	-1.221924	H	-2.946642	-1.733380	1.310347
Si	-0.739452	-2.967474	1.284436	C	2.378311	-1.950399	-2.075031
Si	1.107782	-2.984199	-1.126911	H	3.123617	-1.468734	-1.438380
Si	-3.196562	0.079693	-1.43161	H	1.907217	-1.176381	-2.686207
Si	-3.003117	1.945928	0.960273	H	2.909574	-2.631826	-2.753317
N	2.058794	0.979267	-0.100428	C	2.082823	-4.369642	-0.260955
N	0.131855	-2.009548	0.033151	H	2.770853	-3.992569	0.501976
N	-2.168545	0.716992	-0.084500	H	2.684303	-4.883845	-1.022289
C	3.330438	-1.193848	1.648439	H	1.446175	-5.124862	0.210332
H	2.401972	-1.356202	2.199374	C	0.071184	-3.822610	-2.477407
H	4.161601	-1.326416	2.353993	H	-0.776057	-4.400406	-2.098609
H	3.421396	-1.971811	0.886561	H	0.725467	-4.516471	-3.022481
C	5.082500	0.540043	-0.087460	H	-0.312929	-3.096519	-3.200120
H	5.042440	-0.177039	-0.915549	C	-2.428554	-1.360153	-2.385560
H	5.902741	0.230478	0.573604	H	-1.554420	-1.078231	-2.973236
H	5.352028	1.515178	-0.504336	H	-3.202369	-1.717270	-3.078730
C	3.689125	1.721846	2.391085	H	-2.154469	-2.200672	-1.742515
H	3.869362	2.759134	2.095988	C	-4.848400	-0.656495	-0.818702
H	4.557165	1.386769	2.974697	H	-5.064576	-1.553114	-1.412706
H	2.823131	1.710590	3.060848	H	-5.694350	0.025994	-0.937492
C	3.102163	1.837754	-2.845876	H	-4.817085	-0.965186	0.231737
H	4.099473	1.409660	-2.704160	C	-3.494946	1.451084	-2.707371
H	3.201173	2.704672	-3.512236	H	-3.915266	2.366826	-2.280222
H	2.484240	1.092899	-3.357893	H	-4.183040	1.100645	-3.487624

C	3.311957	3.764389	-0.429581	H	-2.549380	1.715357	-3.196750
H	2.794792	4.178249	0.443703	C	-2.994917	1.508227	2.805229
H	3.409347	4.571454	-1.167766	H	-3.569425	0.592369	2.984638
H	4.321884	3.480296	-0.121852	H	-3.505430	2.321067	3.339110
C	0.640459	3.200438	-1.647432	H	-2.014114	1.386632	3.267300
H	0.050947	2.654144	-2.386831	C	-4.868410	2.153360	0.620503
H	0.888262	4.178269	-2.082658	H	-5.130401	2.385004	-0.415444
H	0.009667	3.411759	-0.777099	H	-5.179397	3.012283	1.230386
C	0.387322	-3.440359	2.731663	H	-5.465584	1.296214	0.942800
H	1.281336	-3.994631	2.432300	C	-2.320170	3.692966	0.674554
H	-0.175431	-4.069373	3.434240	H	-1.299212	3.830449	1.036590
H	0.706558	-2.545111	3.276021	H	-2.959376	4.406355	1.211154
C	-1.523518	-4.548708	0.578349	H	-2.354740	3.961034	-0.388241
H	-2.264708	-4.325227	-0.197855	N	0.334898	1.342045	2.700533
H	-2.054082	-5.052508	1.397123	O	0.346858	0.098616	2.385592
H	-0.809601	-5.266547	0.164333	O	0.086081	2.080022	1.715642

Table 3.16.6 DFT optimized coordinates of Cl^-.

Cl	0.000000	0.000000	0.000000

Table 3.16.7 DFT optimized coordinates of **3.1-F**.

U	-0.001743	-0.000911	-0.007821	H	-0.005444	5.704040	-1.376790
O	-0.002781	-0.000953	-1.807748	H	1.328373	5.415267	-0.258035
F	0.001556	-0.003414	2.021006	C	-1.463008	2.981826	-1.754600
Si	2.659685	-1.917396	-1.218888	H	-1.651158	1.984978	-2.160659
Si	1.170887	-3.078978	1.199195	H	-1.700221	3.708202	-2.543690
Si	0.333939	3.260151	-1.218459	H	-2.166803	3.156776	-0.932607
Si	2.084608	2.551768	1.199446	C	2.841895	1.051581	2.085338
Si	-3.253199	0.530874	1.198825	H	3.087455	0.215904	1.421421
Si	-2.993330	-1.345126	-1.216780	H	2.194314	0.667846	2.878530
N	1.380546	-1.757086	0.018441	H	3.781332	1.381059	2.548844
N	0.832661	2.072933	0.020619	C	3.546344	3.412719	0.343221
N	-2.214639	-0.316548	0.020529	H	4.028884	2.742867	-0.378287
C	3.308795	-0.222270	-1.765648	H	4.298062	3.678827	1.097910
H	2.538263	0.430361	-2.182909	H	3.275800	4.331044	-0.186551
H	4.062081	-0.382722	-2.548981	C	1.384833	3.678493	2.552411
H	3.803995	0.310943	-0.946135	H	1.070681	4.655846	2.173605
C	4.204511	-2.810819	-0.560599	H	2.145421	3.849475	3.325382
H	4.651585	-2.268627	0.280795	H	0.519083	3.212190	3.036774
H	4.952331	-2.836296	-1.364330	C	-2.327760	1.934583	2.083647
H	4.034851	-3.843734	-0.242108	H	-1.669636	1.562286	2.873264
C	2.031035	-2.831548	-2.752228	H	-3.080139	2.583218	2.551497
H	1.644314	-3.828117	-2.513459	H	-1.727592	2.565620	1.419325
H	2.843448	-2.953434	-3.480247	C	-4.728863	1.367050	0.341486
H	1.229348	-2.266001	-3.239913	H	-4.388436	2.113365	-0.386133
C	2.489789	-3.028013	2.558165	H	-5.331275	1.892296	1.094310
H	3.496049	-3.244513	2.186504	H	-5.393569	0.673365	-0.182232
H	2.253991	-3.769397	3.332802	C	-3.878385	-0.634539	2.555468
H	2.513765	-2.042889	3.038259	H	-4.566590	-1.397663	2.179864
C	1.196541	-4.777007	0.346055	H	-4.407742	-0.058372	3.325645
H	0.378960	-4.865219	-0.379271	H	-3.040847	-1.147645	3.042353
H	1.051193	-5.560417	1.101413	C	-3.452481	-0.349509	-2.759895
H	2.130546	-4.999554	-0.178993	H	-4.108774	0.496484	-2.529239
C	-0.510179	-2.988053	2.080221	H	-3.973970	-0.990250	-3.482708

H	-0.519669	-2.239461	2.877312	H	-2.554893	0.043073	-3.250333
H	-0.697460	-3.968318	2.538283	C	-4.552357	-2.218346	-0.566637
H	-1.355139	-2.777467	1.415685	H	-4.321487	-2.877886	0.277936
C	1.432989	3.162952	-2.756313	H	-4.949922	-2.849946	-1.372244
H	2.491795	3.314923	-2.520725	H	-5.356613	-1.544916	-0.255933
H	1.137729	3.931835	-3.481861	C	-1.854480	-2.765635	-1.744167
H	1.332295	2.187781	-3.245150	H	-0.897772	-2.431681	-2.154127
C	0.346253	5.047650	-0.569617	H	-2.365561	-3.339987	-2.528744
H	-0.343262	5.173791	0.273141	H	-1.652428	-3.456875	-0.917676

Table 3.16.8 DFT optimized coordinates of $UO_2[N(SiMe_3)_2]_3^-$.

U	-0.003100	-0.003346	-0.006381	H	-2.315798	2.809327	1.122322
O	0.003031	-0.008010	-1.794626	H	-1.887507	3.640122	2.624826
O	-0.014062	0.002230	1.784495	C	1.325877	3.467397	2.718987
N	-2.315315	-0.513760	-0.014038	H	2.319561	3.827623	2.428403
N	0.713570	2.253947	-0.010784	H	1.453794	2.481731	3.180723
N	1.596916	-1.746306	-0.001974	H	0.930457	4.149683	3.484037
Si	-2.986186	-1.533156	1.235589	C	2.788579	1.415402	-2.084436
Si	-3.355300	0.163694	-1.242109	H	3.222736	0.699942	-1.375804
Si	0.149522	3.350673	1.226427	H	3.615946	1.850875	-2.662269
Si	1.836330	2.818802	-1.223626	H	2.150654	0.849427	-2.768448
Si	1.540762	-2.981299	-1.235278	C	3.222656	3.916185	-0.489386
Si	2.820311	-1.812611	1.242546	H	3.815169	3.350028	0.240773
C	-1.724144	-2.771289	1.935968	H	2.856785	4.817880	0.013802
H	-0.893422	-2.276345	2.445969	H	3.905555	4.238400	-1.287746
H	-1.301358	-3.415205	1.154976	C	1.002258	3.816939	-2.616336
H	-2.228197	-3.423954	2.662770	H	0.201322	3.227497	-3.078450
C	-3.667586	-0.553797	2.719611	H	1.726025	4.074867	-3.401856
H	-2.870519	0.041877	3.178880	H	0.557945	4.749914	-2.251213
H	-4.070511	-1.227290	3.488725	C	-0.162248	-3.131879	-2.070371
H	-4.467393	0.135207	2.423920	H	-0.983640	-3.189771	-1.346100
C	-4.403788	-2.661099	0.615800	H	-0.185326	-4.053733	-2.668449
H	-5.267111	-2.117775	0.216677	H	-0.369089	-2.286790	-2.732581
H	-4.763060	-3.283016	1.447498	C	2.795839	-2.696976	-2.639817
H	-4.048284	-3.339529	-0.170040	H	3.831955	-2.741419	-2.284757
C	-4.997063	0.837705	-0.524391	H	2.641411	-1.708587	-3.088306
H	-4.798542	1.643942	0.193439	H	2.679841	-3.449082	-3.432410
H	-5.601435	0.082357	-0.010178	C	1.852385	-4.738347	-0.541029
H	-5.612924	1.259416	-1.330719	H	1.079481	-5.007651	0.190220
C	-3.798506	-1.079186	-2.616441	H	2.824309	-4.856768	-0.049910
H	-2.883795	-1.488235	-3.062006	H	1.803721	-5.473502	-1.356355
H	-4.375524	-0.595508	-3.416738	C	4.525025	-2.399241	0.596362
H	-4.388874	-1.922294	-2.239971	H	4.518043	-3.405051	0.162365
C	-2.600729	1.671871	-2.122292	H	5.247326	-2.404200	1.424506
H	-1.800963	1.384763	-2.810216	H	4.909524	-1.712772	-0.168625
H	-2.181241	2.404982	-1.423079	C	3.203478	-0.111535	2.000913
H	-3.388682	2.177875	-2.697889	H	2.366088	0.278352	2.585490
C	-0.123873	5.138133	0.595535	H	3.452623	0.636404	1.238312
H	0.778881	5.619463	0.203869	H	4.072495	-0.202676	2.667610
H	-0.495727	5.760501	1.421485	C	2.354123	-2.957636	2.691475
H	-0.881458	5.160707	-0.197884	H	1.423268	-2.618347	3.160747
C	-1.557379	2.870825	1.912504	H	3.137343	-2.960721	3.462186
H	-1.541469	1.910227	2.433801	H	2.201317	-3.992566	2.363753

Table 3.16.9 DFT optimized coordinates of $UF_2[N(SiMe_3)_2]_3^+$.

U	0.000581	0.002234	-0.016623	H	-1.919480	-1.305675	-2.721518
F	-0.002132	0.018294	2.040142	H	-2.984047	-2.703372	-2.545596
F	0.011653	-0.002407	-2.067927	C	0.121305	-3.738980	-2.597720
N	-1.849761	1.045664	-0.012199	H	0.876122	-4.452289	-2.257107
N	1.836383	1.071858	-0.008245	H	-0.510137	-4.252416	-3.334287
N	0.012456	-2.122016	-0.005482	H	0.632997	-2.922158	-3.117227
Si	-0.978452	-3.093420	-1.211220	C	2.454243	-2.049974	1.837111
Si	-3.158318	0.673158	1.225601	H	3.181673	-1.825049	1.050745
Si	3.180205	0.697057	-1.204714	H	2.173115	-1.120582	2.336275
Si	0.992391	-3.077467	1.221895	H	2.974159	-2.667430	2.582079
Si	2.168029	2.401990	1.216712	C	1.749565	-4.614472	0.423328
Si	-2.204497	2.390881	-1.213378	H	2.364754	-5.107173	1.187758
C	-2.999356	1.825979	2.707567	H	1.025418	-5.352470	0.068341
H	-3.845784	1.648495	3.383309	H	2.413545	-4.359713	-0.409866
H	-2.082835	1.625143	3.272455	C	-0.082860	-3.539497	2.698565
H	-3.010013	2.885384	2.436090	H	0.491704	-4.200339	3.360145
C	-3.007547	-1.111005	1.831547	H	-0.359955	-2.654876	3.281681
H	-3.198455	-1.848734	1.046031	H	-0.998966	-4.067542	2.419525
H	-2.057261	-1.345910	2.314539	C	4.838924	0.617097	-0.301452
H	-3.791139	-1.244725	2.589740	H	5.610925	0.380052	-1.045165
C	-4.875800	0.796217	0.446308	H	5.136490	1.548606	0.187062
H	-5.600277	0.503702	1.217712	H	4.857945	-0.179526	0.450258
H	-5.158145	1.794767	0.102399	C	3.202121	1.979876	-2.584518
H	-4.997046	0.099249	-0.390197	H	3.936872	1.669602	-3.338462
C	-2.955314	3.870564	-0.309124	H	2.229007	2.045537	-3.082615
H	-3.144567	4.655151	-1.053319	H	3.480177	2.981158	-2.245565
H	-3.905579	3.660670	0.188449	C	2.917847	-0.997629	-2.004102
H	-2.268339	4.287244	0.435452	H	2.712876	-1.811255	-1.301547
C	-0.606843	2.999769	-2.025807	H	2.126801	-0.984921	-2.757259
H	0.215659	3.201929	-1.332697	H	3.856909	-1.249058	-2.514757
H	-0.246014	2.316173	-2.797909	C	3.160178	3.810505	0.439497
H	-0.848641	3.953041	-2.514242	H	3.274258	4.583472	1.211043
C	-3.341548	1.775734	-2.583774	H	4.164239	3.540552	0.102626
H	-3.437518	2.569858	-3.335462	H	2.629387	4.270687	-0.400967
H	-2.926782	0.896679	-3.088000	C	3.059590	1.689310	2.715424
H	-4.347979	1.526898	-2.237151	H	3.352793	2.512401	3.379449
C	-1.869176	-4.504267	-0.322549	H	2.405211	1.023691	3.288030
H	-2.478830	-5.033270	-1.066607	H	3.965840	1.136301	2.453039
H	-1.205714	-5.242645	0.135307	C	0.544851	3.187530	1.783710
H	-2.550227	-4.135044	0.451759	H	0.055253	3.763889	0.992114
C	-2.322150	-2.018716	-1.998579	H	-0.176330	2.487298	2.209526
H	-2.950397	-1.475394	-1.286168	H	0.804461	3.897845	2.580443

Table 3.16.10 DFT optimized coordinates of ·NO.

N	0.000000	0.000000	-0.617709
O	0.000000	0.000000	0.540495

Table 3.16.11 Optimized Coordinates of **3.1-Me**.

U	0.00000000	0.00000000	0.05854000	O	0.00000000	0.00000000	-1.73572713
C	0.00000000	0.00000000	2.40931919	H	0.22340802	1.00858508	2.76591321
H	0.76175606	-0.69776905	2.76591321	H	-0.98516408	-0.31081502	2.76591321
N	-0.23740002	2.24211417	0.05699400	N	-1.82302814	-1.32665210	0.05699400
N	2.06042816	-0.91546307	0.05699400	Si	-3.08100323	-1.07824008	-1.18900709

Si	-1.39449610	3.09447124	1.10230608	Si	0.60671905	3.20734724	-1.18900709
Si	-1.98264315	-2.75490421	1.10230608	Si	2.47428519	-2.12910716	-1.18900709
Si	3.37713926	-0.33956703	1.10230608	C	2.94903823	1.30471410	1.97115215
C	0.97800008	-3.19316825	-1.66039413	C	-2.60443520	1.90158515	1.97115215
C	2.27636517	2.44355719	-1.66039413	C	-0.52994204	4.06547331	2.48559119
C	-0.34460403	-3.20629924	1.97115215	C	-2.70339221	-2.04694116	-2.77155921
C	-0.42100703	3.36467626	-2.77155921	C	-3.25583225	-2.49167919	2.48559119
C	-3.25436525	0.74961106	-1.66039413	C	-4.81779637	-1.55787312	-0.57683005
C	-2.50215219	4.29268433	0.12729901	C	1.05974108	4.95127038	-0.57683005
C	-2.46649719	-4.31326933	0.12729901	C	3.75805529	-3.39339726	-0.57683005
C	3.12439824	-1.31773610	-2.77155921	C	4.96864938	0.02058600	0.12729901
C	3.78577329	-1.57379312	2.48559119	H	3.88167230	1.87093014	2.09231216
H	2.53835319	1.13935609	2.97220123	H	2.25352617	1.95328815	1.42813511
H	0.63968805	-3.81938329	-0.82770706	H	1.28829510	-3.86966929	-2.46842919
H	0.12545201	-2.61737820	-2.02827915	H	-2.81836021	0.97496708	1.42813511
H	-3.56110827	2.42616118	2.09231216	H	-2.25588717	1.62860012	2.97220123
H	2.98783823	2.46367719	-0.82770706	H	2.70708421	3.05053023	-2.46842919
H	2.20399017	1.41733411	-2.02827915	H	0.12836701	3.42114826	3.08105223
H	-1.28100810	4.48660935	3.16691024	H	0.07473201	4.89423637	2.10440016
H	0.56483404	-2.92825523	1.42813511	H	-0.32056302	-4.29709133	2.09231216
H	-0.28246502	-2.76795621	2.97220123	H	-1.76510014	-1.70162913	-3.21945125
H	-3.50190026	-1.89156814	-3.50874027	H	-2.61825720	-3.12419124	-2.59392320
H	-0.59110405	2.37943618	-3.21945125	H	0.11280401	3.97851930	-3.50874027
H	-1.39650010	3.82957329	-2.59392320	H	-3.02698423	-1.59940512	3.08105223
H	-3.24501325	-3.35269026	3.16691024	H	-4.27589833	-2.38239818	2.10440016
H	-3.62752628	1.35570511	-0.82770706	H	-3.99537931	0.81913906	-2.46842919
H	-2.32944218	1.20004409	-2.02827915	H	-4.93408438	-2.61353220	-0.31332802
H	-5.53560742	-1.34252110	-1.37950311	H	-5.11584039	-0.96038707	0.29290902
H	-1.95309415	5.07720039	-0.40185903	H	-3.18958524	4.78837136	0.82564206
H	-3.11168824	3.75809429	-0.61022305	H	0.20365602	5.57980843	-0.31332802
H	1.60514612	5.46523743	-1.37950311	H	1.72620113	4.91064138	0.29290902
H	-3.42043826	-4.23002932	-0.40185903	H	-2.55205919	-5.15644739	0.82564206
H	-1.69876113	-4.57384835	-0.61022305	H	4.73042736	-2.96627522	-0.31332802
H	3.93046130	-4.12271631	-1.37950311	H	3.38964026	-3.95025430	0.29290902
H	2.35620418	-0.67780705	-3.21945125	H	3.38909626	-2.08695116	-3.50874027
H	4.01475731	-0.70538205	-2.59392320	H	5.37353143	-0.84717107	-0.40185903
H	5.74164343	0.36807603	0.82564206	H	4.81044937	0.81575406	-0.61022305
H	2.89861722	-1.82174314	3.08105223	H	4.52602134	-1.13391909	3.16691024
H	4.20116732	-2.51183719	2.10440016				

Table 3.16.12 Optimized Coordinates of **3.1-CCMe**.

U	0.00000000	0.00000000	0.17455650	O	0.00000000	0.00000000	1.96906101
N	-0.32374514	2.21199303	0.13774607	N	2.07751473	-0.82562500	0.13774607
N	-1.75376958	-1.38636803	0.13774607	Si	3.28468815	-0.25248125	1.32754916
Si	0.53275495	3.29342031	-0.99691316	Si	-1.42368890	2.97086401	1.32754916
Si	2.58580819	-2.10808948	-0.99691316	Si	-1.86099925	-2.71838276	1.32754916
Si	-3.11856313	-1.18533084	-0.99691316	C	-3.32141974	0.61527338	-1.56465894
C	-0.19286408	-3.10728566	2.14590520	C	2.19355225	2.56879719	-1.56465894
C	-2.59455628	1.72066803	2.14590520	C	-0.52096904	3.66877831	-2.52742283
C	1.12786750	-3.18407056	-1.56465894	C	3.52135743	-1.48469833	2.74688664
C	-0.47489225	3.79193415	2.74688664	C	3.43773974	-1.38321673	-2.52742283
C	2.78742036	1.38661763	2.14590520	C	4.95833556	0.09211571	0.49239949
C	1.02362003	4.95651365	-0.21426316	C	-2.55894232	4.24798670	0.49239949
C	3.78065672	-3.36473778	-0.21426316	C	-2.39939323	-4.34010241	0.49239949

C	-3.04646518	-2.30723583	2.74688664	C	-4.80427675	-1.59177587	-0.21426316
C	-2.91677070	-2.28556158	-2.52742283	H	-3.68249079	1.25940953	-0.75554675
H	-4.08785713	0.62584282	-2.35204840	H	-2.41785733	1.06284330	-1.98362565
H	0.64806532	-3.18200990	1.44967616	H	-0.28816757	-4.08127490	2.64474542
H	0.06821210	-2.36415870	2.90410653	H	2.12937796	1.56250422	-1.98362565
H	2.93192604	2.55942581	-0.75554675	H	2.58592435	3.22726671	-2.35204840
H	-3.07973407	1.02976392	1.44967616	H	-3.39040395	2.29019788	2.64474542
H	-2.08152755	1.12300594	2.90410653	H	-0.77231415	2.74925927	-3.06528980
H	0.02981322	4.32494599	-3.21397364	H	-1.45757799	4.17245306	-2.26536155
H	0.28847937	-2.62534752	-1.98362565	H	0.75056475	-3.81883534	-0.75554675
H	1.50193279	-3.85310953	-2.35204840	H	2.55952476	-1.71095820	3.22102757
H	4.17394276	-1.04551952	3.51289647	H	3.97053224	-2.43000222	2.42892183
H	0.20197089	3.07209257	3.22102757	H	-1.18152492	4.13750022	3.51289647
H	0.11917753	4.65358290	2.42892183	H	2.76708545	-0.70578596	-3.06528980
H	3.73060649	-2.18829200	-3.21397364	H	4.34223934	-0.82392696	-2.26536155
H	2.43166875	2.15224598	1.44967616	H	3.67857152	1.79107701	2.64474542
H	2.01331545	1.24115277	2.90410653	H	5.42306258	-0.78952630	0.03986798
H	5.65862494	0.48147610	1.24307014	H	4.85880557	0.85425221	-0.28979943
H	0.18022545	5.57180484	0.11334526	H	1.57438676	5.53433872	-0.96862674
H	1.69358767	4.81925300	0.64214228	H	-2.02778146	5.09127310	0.03986798
H	-3.24628300	4.65977489	1.24307014	H	-3.16920690	3.78072295	-0.28979943
H	4.73521181	-2.94198224	0.11334526	H	4.00568455	-4.13062829	-0.96862674
H	3.32680169	-3.87631644	0.64214228	H	-3.39528112	-4.30174681	0.03986798
H	-2.41234193	-5.14125100	1.24307014	H	-1.68959867	-4.63497516	-0.28979943
H	-2.76149565	-1.36113436	3.22102757	H	-2.99241784	-3.09198070	3.51289647
H	-4.08970978	-2.22358068	2.42892183	H	-4.91543727	-2.62982260	0.11334526
H	-5.58007132	-1.40371043	-0.96862674	H	-5.02038936	-0.94293656	0.64214228
H	-1.99477130	-2.04347331	-3.06528980	H	-3.76041971	-2.13665398	-3.21397364
H	-2.88466134	-3.34852610	-2.26536155	C	0.00000000	0.00000000	-2.15138344
C	0.00000000	0.00000000	-3.38011494	C	0.00000000	0.00000000	-4.83922304
H	-0.15876738	1.01124857	-5.23418489	H	0.95515064	-0.36812770	-5.23418489
H	-0.79638326	-0.64312087	-5.23418489				

Table 3.16.13 Optimized Coordinates of **3.1-NMe_2**.

U	-0.05204763	-0.01466540	-0.09116999	O	-0.08395752	-0.13720720	1.69017735
N	1.23996798	1.87110647	0.12806488	N	-2.31912018	0.20594159	0.04844638
N	1.04384176	-2.03216189	-0.06208028	N	-0.15325966	0.11939480	-2.23727394
C	-1.07129960	1.03755811	-2.91551756	H	-0.51762152	1.80627611	-3.47095956
H	-1.69156168	0.48297628	-3.63350999	H	-1.73445533	1.52722743	-2.20694240
C	0.58074251	-0.65751663	-3.23327886	H	1.24772901	-1.37405755	-2.76960494
H	-0.12308304	-1.21400183	-3.87000051	H	1.17549879	0.00334955	-3.88132742
Si	1.10458723	3.30819721	-0.91223715	Si	2.62776989	-2.37125197	-0.78656099
Si	0.45369959	-3.26753437	1.08818950	Si	2.48937902	1.97281162	1.40479123
Si	-3.46997351	-0.73028017	-0.93378064	Si	-3.00020182	1.05910682	1.46883907
C	2.01359159	3.03441377	-2.55724642	H	3.09508984	2.97242799	-2.38559538
H	1.83634753	3.86882033	-3.24810289	H	1.71101671	2.10912216	-3.05676368
C	-0.71765779	3.80506548	-1.21872731	H	-1.45547345	3.05320341	-0.93136143
H	-0.89431401	4.06713227	-2.26884333	H	-0.93381452	4.69832587	-0.62060859
C	1.80491945	4.93623093	-0.21000745	H	1.23117585	5.28504846	0.65537141
H	1.67928725	5.68997636	-1.00015527	H	2.86234067	4.92883105	0.06513813
C	2.05118628	3.20884601	2.77839434	H	2.01295690	4.25013044	2.44851047
H	2.80762694	3.13988572	3.57152258	H	1.08278423	2.96379201	3.23013163
C	2.80774015	0.34406134	2.31852393	H	2.02690243	0.12444822	3.05057308

H	3.75962322	0.45274370	2.85627957	H	2.89846528 -0.52641227 1.66456593
C	4.18832110	2.41993341	0.66540378	H	4.56574515 1.59476715 0.05042504
H	4.90613627	2.57269905	1.48232298	H	4.20054145 3.32104897 0.04658264
C	2.54674450	-3.64321155	-2.20269135	H	2.36381522 -4.65222148 -1.82019181
H	3.51189227	-3.66124790	-2.72645761	H	1.77071796 -3.43334828 -2.94660022
C	3.41835976	-0.77064866	-1.47028916	H	2.79310498 0.12679190 -1.41480817
H	3.71289836	-0.89682087	-2.51924891	H	4.32973472 -0.55221778 -0.90152443
C	3.91425377	-3.06586807	0.43070443	H	4.12029721 -2.38001385 1.25967872
H	4.85548133	-3.20595749	-0.11848833	H	3.64220224 -4.03554431 0.85908500
C	1.22051952	-3.10619539	2.81313936	H	2.30967482 -3.21228140 2.80788309
H	0.81381156	-3.88785312	3.46826928	H	0.97863517 -2.13585338 3.25795759
C	-1.42724461	-3.19617760	1.30998280	H	-1.81363899 -2.20922985 1.57451494
H	-1.68788963	-3.87437469	2.13393116	H	-1.95820981 -3.55039731 0.42034263
C	0.75807868	-5.04235136	0.46825013	H	0.32317661 -5.20330602 -0.52519563
H	0.25744256	-5.73334185	1.15958869	H	1.81191615 -5.33546872 0.42614729
C	-4.54306305	0.33636972	-2.08730941	H	-5.23522627 0.97710099 -1.53246464
H	-5.14730419	-0.32620832	-2.72180147	H	-3.95521136 0.97830955 -2.75119891
C	-2.59544078	-2.00944595	-2.04485755	H	-1.70935281 -2.47068882 -1.59630636
H	-2.29786703	-1.59008113	-3.01075535	H	-3.30759631 -2.81935663 -2.25142011
C	-4.68666036	-1.74280006	0.12244985	H	-4.17210187 -2.47595038 0.75197918
H	-5.35242197	-2.29774679	-0.55223869	H	-5.32078013 -1.13079024 0.77128989
C	-3.19219954	-0.07413620	2.97634739	H	-3.84371613 -0.93268335 2.78548866
H	-3.62771445	0.49426841	3.80868380	H	-2.21844015 -0.45226388 3.30513576
C	-1.94359590	2.53469694	2.01829702	H	-0.89227841 2.28926879 2.18245084
H	-2.35146434	2.89292457	2.97345084	H	-1.99456806 3.36887250 1.31126999
C	-4.69597320	1.84196740	1.09672485	H	-4.63832910 2.55067644 0.26206880
H	-5.00743611	2.41065366	1.98315681	H	-5.49374574 1.12608987 0.87566899

Table 3.16.14 Optimized Coordinates of **3.1-OMe**.

U	0.00000000	0.00000000	0.01545777	O	0.00000000 0.00000000 1.81459252
N	-2.26048627	-0.01392086	0.03424783	N	1.14229895 -1.95067810 0.03424783
N	1.11818732	1.96459896	0.03424783	O	0.00000000 0.00000000 -1.99190767
C	0.00000000	0.00000000	-3.40549401	H	0.36350703 -0.96512533 -3.77282057
H	-1.01757657	0.16775634	-3.77282057	H	0.65406954 0.79736899 -3.77282057
Si	-3.19996024	-1.04605812	-1.05936760	Si	0.69406721 3.29427592 -1.05936760
Si	2.35615234	2.26563939	1.28127238	Si	-3.14017744 0.90766809 1.28127238
Si	2.50589303	-2.24821780	-1.05936760	Si	0.78402510 -3.17330747 1.28127238
C	-4.03000216	-0.04965267	-2.44623235	H	-4.82906890 0.60133940 -2.07764538
H	-4.46968385	-0.72844971	-3.18889565	H	-3.30188900 0.58626809 -2.96445466
C	-2.12298621	-2.36428092	-1.91808681	H	-1.28705187 -2.73383210 -1.31549137
H	-1.71395363	-2.01087554	-2.86897409	H	-2.76383777 -3.22697336 -2.14347513
C	-4.53133678	-2.03866708	-0.13379227	H	-4.07557289 -2.71839835 0.59582312
H	-5.08836179	-2.65368630	-0.85302924	H	-5.25907740 -1.41990188 0.39970148
C	-3.42945008	-0.11451017	2.84977532	H	-3.97220472 -1.04495483 2.65191098
H	-4.01337769	0.46560115	3.57613770	H	-2.47551077 -0.37400746 3.32194118
C	-2.20891425	2.48067060	1.78550058	H	-1.19802276 2.29355889 2.15510429
H	-2.77143778	2.96065865	2.59794048	H	-2.14721723 3.20438461 0.96493682
C	-4.81715279	1.55580611	0.65579809	H	-4.69100623 2.21961585 -0.20787551
H	-5.27707850	2.15003898	1.45660210	H	-5.53367650 0.77683882 0.37817652
C	1.97200061	3.51491058	-2.44623235	H	2.93530965 3.88142664 -2.07764538
H	1.60398597	4.23508461	-3.18889565	H	2.15866756 2.56638571 -2.96445466
C	-0.98603423	3.02070045	-1.91808681	H	-1.72404211 2.48153567 -1.31549137
H	-0.88449249	2.48976516	-2.86897409	H	-1.41272203 4.00704040 -2.14347513
C	0.50013091	4.94358630	-0.13379227	H	-0.31641558 4.88874883 0.59582312

H	0.24602115	5.73349373	-0.85302924	H	1.39986760	5.26444557	0.39970148
C	1.61555632	3.02724597	2.84977532	H	1.08114493	3.96250761	2.65191098
H	2.40991127	3.24288645	3.57613770	H	0.91385543	2.33085894	3.32194118
C	3.25278089	0.67264056	1.78550058	H	2.58529165	-0.10926130	2.15510429
H	3.94972449	0.91980619	2.59794048	H	3.84868709	0.25735236	0.96493682
C	3.75594401	3.39387363	0.65579809	H	4.26774683	2.95272263	-0.20787551
H	4.50052763	3.49506455	1.45660210	H	3.43960041	4.40388504	0.37817652
C	2.05800155	-3.46525791	-2.44623235	H	1.89375925	-4.48276605	-2.07764538
H	2.86569788	-3.50663490	-3.18889565	H	1.14322144	-3.15265380	-2.96445466
C	3.10902044	-0.65641953	-1.91808681	H	3.01109399	0.25229644	-1.31549137
H	2.59844612	-0.47888961	-2.86897409	H	4.17655980	-0.78006704	-2.14347513
C	4.03120587	-2.90491922	-0.13379227	H	4.39198847	-2.17035048	0.59582312
H	4.84234064	-3.07980742	-0.85302924	H	3.85920980	-3.84454368	0.39970148
C	1.81389376	-2.91273580	2.84977532	H	2.89105979	-2.91755279	2.65191098
H	1.60346642	-3.70848761	3.57613770	H	1.56165534	-1.95685149	3.32194118
C	-1.04386664	-3.15331116	1.78550058	H	-1.38726888	-2.18429759	2.15510429
H	-1.17828672	-3.88046485	2.59794048	H	-1.70146986	-3.46173698	0.96493682
C	1.06120878	-4.94967975	0.65579809	H	0.42325940	-5.17233849	-0.20787551
H	0.77655088	-5.64510356	1.45660210	H	2.09407611	-5.18072386	0.37817652

Table 3.16.15 Optimized Coordinates of **3.1-H**.

U	0.00000000	0.00000000	-0.09146439	H	0.00000000	0.00000000	1.82802721
O	0.00000000	0.00000000	-1.89001594	N	0.68362860	2.11980573	0.07447264
N	1.49399131	-1.65194260	0.07447264	N	-2.17761991	-0.46786313	0.07447264
Si	1.84343030	2.76065666	-1.12297650	Si	0.00000000	3.24131435	1.27659125
Si	1.46908365	-2.97678580	-1.12297650	Si	2.80706057	-1.62065718	1.27659125
Si	-2.80706057	-1.62065718	1.27659125	Si	-3.31251395	0.21612914	-1.12297650
C	3.04236097	1.40571763	-1.69056832	H	3.66941609	1.03969652	-0.86959296
H	3.71484776	1.83567502	-2.44521450	H	2.54459478	0.54787508	-2.15131889
C	0.94788985	3.43177454	-2.64970290	H	0.39983995	2.63067947	-3.15786577
H	1.67016910	3.84739586	-3.36416948	H	0.23339788	4.22317993	-2.39816939
C	2.96180009	4.13003695	-0.42481832	H	2.42519992	5.02365965	-0.09086200
H	3.65297193	4.44390941	-1.21834804	H	3.57073551	3.77111017	0.41301753
C	-1.50065852	2.49778597	2.17144329	H	-2.27600280	2.11039284	1.50317319
H	-1.95702384	3.29752864	2.77072665	H	-1.21832241	1.69296631	2.85811441
C	-0.62579117	4.83956561	0.46048625	H	0.16129743	5.41423220	-0.03887273
H	-1.06908574	5.49051469	1.22549276	H	-1.40337495	4.62835701	-0.28296017
C	1.24366913	3.68608707	2.63607268	H	1.62683423	2.78420574	3.12706002
H	0.74802147	4.29700337	3.40202839	H	2.10136761	4.25438508	2.26397819
C	2.49805901	-2.53678396	-2.64970290	H	2.07831528	-1.66161129	-3.15786577
H	2.49685800	-3.37010680	-3.36416948	H	3.54068216	-2.31371846	-2.39816939
C	-0.30379331	-3.33762070	-1.69056832	H	-0.93430444	-3.69765581	-0.86959296
H	-0.26768268	-4.13499004	-2.44521450	H	-0.79782365	-2.47762126	-2.15131889
C	2.09581687	-4.63001260	-0.42481832	H	3.13801692	-4.61211457	-0.09086200
H	2.02205247	-5.38552121	-1.21834804	H	1.48050945	-4.97790275	0.41301753
C	2.57041048	-2.92009260	2.63607268	H	1.59777579	-2.80098264	3.12706002
H	3.34730335	-2.79630728	3.40202839	H	2.63372175	-3.94703028	2.26397819
C	4.50408234	-1.87783176	0.46048625	H	4.60821390	-2.84680376	-0.03887273
H	5.28946805	-1.81940193	1.22549276	H	4.70996222	-1.09882015	-0.28296017
C	2.91347536	0.05071541	2.17144329	H	2.96565521	0.91587983	1.50317319
H	3.83425549	0.04606804	2.77072665	H	2.07531303	0.20861500	2.85811441
C	-3.81407961	-0.76599448	2.63607268	H	-3.22461002	0.01677690	3.12706002
H	-4.09532482	-1.50069609	3.40202839	H	-4.73508936	-0.30735480	2.26397819

C	-1.41281685	-2.54850139	2.17144329	H	-0.68965241	-3.02627266	1.50317319
H	-1.87723165	-3.34359667	2.77072665	H	-0.85699063	-1.90158131	2.85811441
C	-3.87829117	-2.96173385	0.46048625	H	-4.76951132	-2.56742842	-0.03887273
H	-4.22038231	-3.67111274	1.22549276	H	-3.30658728	-3.52953686	-0.28296017
C	-2.73856766	1.93190308	-1.69056832	H	-2.73511165	2.65795929	-0.86959296
H	-3.44716508	2.29931503	-2.44521450	H	-1.74677113	1.92974618	-2.15131889
C	-5.05761696	0.49997564	-0.42481832	H	-5.56321682	-0.41154509	-0.09086200
H	-5.67502440	0.94161179	-1.21834804	H	-5.05124497	1.20679258	0.41301753
C	-3.44594886	-0.89499058	-2.64970290	H	-2.47815523	-0.96906818	-3.15786577
H	-4.16702710	-0.47728906	-3.36416948	H	-3.77408004	-1.90946147	-2.39816939

Table 3.16.16 Optimized Coordinates of **3.1-SPh**.

U	0.34033723	0.02440976	0.24792882	O	1.43022223	0.08136917	1.68156645
N	-1.32318558	0.61486020	1.61164814	N	0.94037856	-2.11633459	-0.03549722
N	1.65482379	1.56473188	-0.69663290	S	-1.03897846	0.04799660	-2.04974772
C	-2.79221447	-0.03429824	-2.39655641	C	-3.34332932	-1.22862838	-2.89083932
C	-3.60121948	1.11075021	-2.32558452	C	-4.67927512	-1.27584866	-3.29056911
H	-2.72039392	-2.11296192	-2.97377616	C	-4.93622875	1.05550993	-2.72979234
H	-3.18387668	2.04169205	-1.95986842	C	-5.48208770	-0.13599759	-3.21064062
H	-5.08990038	-2.20760275	-3.67072226	H	-5.54884124	1.95124318	-2.66888747
H	-6.52104320	-0.17465898	-3.52575223	Si	-2.83929394	-0.32300037	1.74692034
Si	1.03346500	3.01535655	-1.54550142	Si	3.43308031	1.50138146	-0.44994381
Si	-1.00299702	1.82694551	2.89898947	Si	1.37080257	-2.81509322	-1.62808863
Si	1.17900579	-3.18269805	1.38635587	C	-4.36448795	0.65947373	1.21076035
H	-4.57090243	1.50471942	1.87404360	H	-5.24083943	-0.00228690	1.23427556
H	-4.27041214	1.03846224	0.18960952	C	-2.74545354	-1.88933426	0.66958359
H	-1.73642935	-2.23760597	0.42186140	H	-3.27971194	-1.74643254	-0.27349000
H	-3.23566525	-2.71002576	1.20946889	C	-3.17716224	-0.90268243	3.52671194
H	-2.36554783	-1.51373375	3.93378780	H	-4.08443472	-1.52198965	3.51661485
H	-3.35923929	-0.07841283	4.22432652	C	-0.27939880	1.02782342	4.45566066
H	-0.94646390	0.28605194	4.90570543	H	-0.08662310	1.80262953	5.20929610
H	0.67341520	0.53810854	4.22913838	C	0.21481755	3.16175114	2.33002163
H	1.15615107	2.76733505	1.94014194	H	0.45848006	3.78080874	3.20410540
H	-0.22428497	3.82157834	1.57502573	C	-2.56732702	2.79375159	3.37886598
H	-3.00736102	3.30684259	2.51593524	H	-2.28012216	3.56553264	4.10537418
H	-3.34839766	2.18482170	3.84405043	C	1.19056239	2.83311180	-3.42305380
H	2.23170631	2.75897243	-3.75205207	H	0.74552283	3.70582948	-3.91922458
H	0.65721670	1.94266167	-3.77259948	C	-0.79482413	3.39055229	-1.14498100
H	-1.24810956	2.76142430	-0.37339674	H	-1.39530236	3.27576324	-2.05287387
H	-0.88520483	4.43239751	-0.81200974	C	1.93590670	4.60219597	-1.00692305
H	1.76978153	4.80727569	0.05705757	H	1.50279146	5.43979332	-1.57071014
H	3.01412615	4.61280007	-1.18710798	C	3.96110221	2.48951730	1.07763932
H	3.68469459	3.54692923	1.02395342	H	5.05148481	2.43517728	1.19340301
H	3.51057380	2.06487906	1.98170487	C	4.08228054	-0.26171705	-0.22131735
H	3.60195602	-0.80419651	0.59375590	H	5.15315853	-0.18929385	0.01327407
H	3.99207611	-0.85646279	-1.13582314	C	4.39045362	2.11900062	-1.97425379
H	4.17085191	1.49921402	-2.85180782	H	5.46313173	2.01236559	-1.76398342
H	4.21546124	3.16255011	-2.24962947	C	-0.04142899	-3.87888659	-2.30823325
H	-0.20669276	-4.78438295	-1.71630572	H	0.18277825	-4.18712350	-3.33764487
H	-0.97683451	-3.31039928	-2.32479478	C	1.79599343	-1.49198912	-2.93386125
H	1.96262332	-0.48479534	-2.54112405	H	1.00028237	-1.41279610	-3.68032101
H	2.71797556	-1.79499621	-3.44721108	C	2.93428156	-3.89724821	-1.54250127
H	3.81440621	-3.30691361	-1.26312739	H	3.11807533	-4.29812091	-2.54863580

H	2.87285182	-4.74989509	-0.86047906	C	2.97587748	-3.20235039	1.98593169
H	3.69317726	-3.46263443	1.20200658	H	3.08097481	-3.93802113	2.79419165
H	3.25749254	-2.22458550	2.39210339	C	0.11745020	-2.66991101	2.86934543
H	0.23196915	-1.62405725	3.16150738	H	0.43220659	-3.28481653	3.72362505
H	-0.94441793	-2.87347920	2.70070764	C	0.61041764	-4.96666092	1.04538784
H	-0.44745300	-4.99479017	0.75799705	H	0.70825273	-5.53837628	1.97796121
H	1.18048181	-5.49720751	0.27765010				

Table 3.16.17 Optimized Coordinates of **3.1-Cl**.

U	0.00000000	0.00000000	0.03966401	Cl	0.00000000	0.00000000	-2.54456039
O	0.00000000	0.00000000	1.83856308	N	-2.10605222	0.70548175	0.03836516
N	0.44206099	-2.17663560	0.03836516	N	1.66399123	1.47115385	0.03836516
Si	-3.26501031	0.05476954	1.24645083	Si	-2.71664915	1.96651421	-1.08472704
Si	1.58507334	-2.85496664	1.24645083	Si	-0.34472669	-3.33594429	-1.08472704
Si	3.06137584	1.36943007	-1.08472704	Si	1.67993697	2.80019710	1.24645083
C	-2.66000629	-1.54936376	2.05972499	H	-2.23072111	-2.27961321	1.36765028
H	-3.52820715	-2.02485354	2.53585728	H	-1.91604876	-1.34992729	2.83551608
C	-3.56182023	1.26785674	2.67013568	H	-2.61168722	1.55342937	3.13525003
H	-4.17492598	0.78212610	3.44067501	H	-4.07591221	2.18299539	2.36364260
C	-4.91649973	-0.39069539	0.41850556	H	-5.42944684	0.45832800	-0.04314055
H	-5.59248386	-0.81003499	1.17523182	H	-4.77561115	-1.15469374	-0.35530275
C	-1.34501288	3.15629517	-1.63925170	H	-0.99336148	3.78397154	-0.81310872
H	-1.78428464	3.82829521	-2.38935805	H	-0.47942062	2.67843584	-2.10246309
C	-3.98673337	3.12242310	-0.26736188	H	-4.89734174	2.62840414	0.08330192
H	-4.28784573	3.86802315	-1.01537874	H	-3.55197597	3.66847694	0.57746943
C	-3.52213874	1.19265398	-2.61256976	H	-2.80395774	0.59636229	-3.18378450
H	-3.90311045	1.98217878	-3.27330542	H	-4.36492879	0.54581747	-2.34656151
C	0.68291396	-3.71855517	2.67013568	H	-0.03946569	-3.03850217	3.13525003
H	1.41012192	-4.00665500	3.44067501	H	0.14742664	-4.62134121	2.36364260
C	2.67179152	-1.52895115	2.05972499	H	3.08956350	-0.79205455	1.36765028
H	3.51767818	-2.04309025	2.53585728	H	2.12709571	-0.98438326	2.83551608
C	2.79660200	-4.06246597	0.41850556	H	2.31779973	-4.93120288	-0.04314055
H	3.49775280	-4.43821558	1.17523182	H	3.38779969	-3.55845371	-0.35530275
C	0.72820073	-3.64658862	-2.61256976	H	0.88551398	-2.72647978	-3.18378450
H	0.23493805	-4.37128219	-3.27330542	H	1.70977260	-4.05304795	-2.34656151
C	-0.71073104	-5.01382392	-0.26736188	H	0.17240611	-5.55542442	0.08330192
H	-1.20588345	-5.64739489	-1.01537874	H	-1.40100623	-4.91033989	0.57746943
C	-2.06092535	-2.74296291	-1.63925170	H	-2.78033474	-2.75226204	-0.81310872
H	-2.42325859	-3.45938343	-2.38935805	H	-2.07988317	-1.75440836	-2.10246309
C	2.79393801	2.45393464	-2.61256976	H	1.91844376	2.13011750	-3.18378450
H	3.66817240	2.38910341	-3.27330542	H	2.65515619	3.50723048	-2.34656151
C	3.40593824	-0.41333226	-1.63925170	H	3.77369622	-1.03170950	-0.81310872
H	4.20754322	-0.36891178	-2.38935805	H	2.55930379	-0.92402748	-2.10246309
C	4.69746441	1.89140082	-0.26736188	H	4.72493563	2.92702029	0.08330192
H	5.49372918	1.77937175	-1.01537874	H	4.95298220	1.24186295	0.57746943
C	-0.01178523	3.07831490	2.05972499	H	-0.85884239	3.07166775	1.36765028
H	0.01052897	4.06794379	2.53585728	H	-0.21104695	2.33431055	2.83551608
C	2.11989773	4.45316136	0.41850556	H	3.11164710	4.47287489	-0.04314055
H	2.09473104	5.24825057	1.17523182	H	1.38781146	4.71314745	-0.35530275
C	2.87890627	2.45069843	2.67013568	H	2.65115291	1.48507279	3.13525003
H	2.76480406	3.22452890	3.44067501	H	3.92848557	2.43834582	2.36364260

Table 3.16.18 Optimized Coordinates of **3.1-Br**.

U	0.00000000	0.00000000	-0.12131579	Br	0.00000000	0.00000000	2.61757053
O	0.00000000	0.00000000	-1.92454300	N	-0.85602225	2.04559677	-0.14544601
N	2.19954989	-0.28146137	-0.14544601	N	-1.34352764	-1.76413540	-0.14544601
Si	-0.25232406	3.36368214	0.91268742	Si	-2.78687216	-1.90036012	0.91268742
Si	-1.10282053	-3.05686608	-1.36861179	Si	-2.09591341	2.48350363	-1.36861179
Si	3.03919621	-1.46332202	0.91268742	Si	3.19873394	0.57336244	-1.36861179
C	-1.44144914	3.69036660	2.34836700	H	-2.41385580	4.06960778	2.01907536
H	-1.00485835	4.43608097	3.02583764	H	-1.60893930	2.77459406	2.92552405
C	1.45878939	2.98364173	1.66061248	H	2.03553786	2.20936012	1.14621591
H	1.36785016	2.67254480	2.70497426	H	2.05649327	3.90421464	1.63008347
C	0.00000000	4.97494361	-0.06426695	H	0.76545017	4.85577523	-0.83995985
H	0.35913259	5.74475419	0.63204182	H	-0.90220225	5.36554350	-0.54319612
C	-1.30803692	3.20825703	-2.92969483	H	-0.69862824	4.09524708	-2.73096312
H	-2.09379051	3.49457885	-3.64090287	H	-0.67300365	2.46292429	-3.42124629
C	-3.13406183	0.99304308	-1.90990606	H	-2.54364308	0.16196363	-2.30122911
H	-3.79512220	1.33489084	-2.71815560	H	-3.77568210	0.61631082	-1.10678912
C	-3.37898225	3.70295793	-0.67546868	H	-3.89438024	3.28241564	0.19601644
H	-4.13863413	3.87414724	-1.44979093	H	-2.97929012	4.68027580	-0.39018783
C	-2.47522666	-3.09351488	2.34836700	H	-2.31745583	-4.12526433	2.01907536
H	-3.33932964	-3.08827334	3.02583764	H	-1.59839929	-2.78067933	2.92552405
C	-3.31330423	-0.22847219	1.66061248	H	-2.93113092	0.65814744	1.14621591
H	-2.99841677	-0.15167941	2.70497426	H	-4.40939570	-0.17113190	1.63008347
C	-4.30842755	-2.48747181	-0.06426695	H	-4.58794979	-1.76498833	-0.83995985
H	-5.15466936	-2.56135915	0.63204182	H	-4.19559583	-3.46410181	-0.54319612
C	-2.12441363	-2.73692172	-2.92969483	H	-3.19727388	-2.65265334	-2.73096312
H	-1.97949881	-3.56056520	-3.64090287	H	-1.79645317	-1.81430040	-3.42124629
C	0.70703038	-3.21069870	-1.90990606	H	1.13155692	-2.28384134	-2.30122911
H	0.74151172	-3.95411766	-2.71815560	H	1.35410022	-3.57799203	-1.10678912
C	-1.51736451	-4.77776343	-0.67546868	H	-0.89546522	-5.01384004	0.19601644
H	-1.28579286	-5.52123592	-1.44979093	H	-2.56359268	-4.92027883	-0.39018783
C	3.91667580	-0.59685173	2.34836700	H	4.73131162	0.05565655	2.01907536
H	4.34418799	-1.34780763	3.02583764	H	3.20733859	0.00608527	2.92552405
C	1.85451484	-2.75516954	1.66061248	H	0.89559305	-2.86750756	1.14621591
H	1.63056661	-2.52086539	2.70497426	H	2.35290242	-3.73308274	1.63008347
C	4.30842755	-2.48747181	-0.06426695	H	3.82249962	-3.09078691	-0.83995985
H	4.79553677	-3.18339504	0.63204182	H	5.09779808	-1.90144167	-0.54319612
C	3.43245056	-0.47133531	-2.92969483	H	3.89590212	-1.44259373	-2.73096312
H	4.07328932	0.06598634	-3.64090287	H	2.46945683	-0.64862388	-3.42124629
C	2.42703145	2.21765563	-1.90990606	H	1.41208616	2.12187771	-2.30122911
H	3.05361048	2.61922682	-2.71815560	H	2.42158188	2.96168120	-1.10678912
C	4.89634676	1.07480551	-0.67546868	H	4.78984545	1.73142440	0.19601644
H	5.42442701	1.64708867	-1.44979093	H	5.54288281	0.24000303	-0.39018783

Table 3.16.19 Optimized Coordinates of **3.1-I**.

U	0.00000000	0.00000000	0.21689375	O	0.00000000	0.00000000	2.02008835
I	0.00000000	0.00000000	-2.80228932	N	2.04359932	-0.85859126	0.27254234
N	-0.27823782	2.19910456	0.27254234	N	-1.76536150	-1.34051330	0.27254234
Si	3.41220282	-0.24996769	-0.72309859	Si	-1.92257978	-2.83007047	-0.72309859
Si	-3.03906105	-1.07438760	1.51596282	Si	2.44997748	-2.09471027	1.51596282
Si	-1.48962303	3.08003817	-0.72309859	Si	0.58908357	3.16909788	1.51596282
C	3.82260063	-1.44407585	-2.13266161	H	4.21782897	-2.39997793	-1.77492103
H	4.58212038	-0.99341877	-2.78515248	H	2.93765620	-1.64779521	-2.74476051
C	3.06693660	1.46170111	-1.48574518	H	2.29688856	2.05349206	-0.98169861

H	2.77121722	1.37708421	-2.53470720	H	3.99809806	2.04227097	-1.43988057
C	4.97779555	0.01047835	0.32542365	H	4.82449918	0.77869001	1.09179700
H	5.77328733	0.36916263	-0.34173000	H	5.35274572	-0.88838372	0.82255886
C	3.10677195	-1.29642390	3.10193601	H	3.98575676	-0.66601634	2.93764622
H	3.38631645	-2.08080359	3.81736092	H	2.32962300	-0.68288672	3.57068763
C	0.95921742	-3.15567446	2.01163110	H	0.08033218	-2.58271153	2.31352566
H	1.26905145	-3.75797171	2.87673781	H	0.66678663	-3.85374597	1.22097638
C	3.70519156	-3.36829223	0.87114558	H	3.32353541	-3.88488008	-0.01733806
H	3.84606739	-4.12771781	1.65186814	H	4.69199067	-2.96482668	0.62755791
C	-3.16190669	-2.58843132	-2.13266161	H	-4.18735634	-2.45275807	-1.77492103
H	-3.15138608	-3.47152327	-2.78515248	H	-2.89586062	-1.72018729	-2.74476051
C	-0.26759800	-3.38689556	-1.48574518	H	0.62993201	-3.01590987	-0.98169861
H	-0.19301870	-3.08848661	-2.53470720	H	-0.23039049	-4.48358997	-1.43988057
C	-2.47982326	-4.31613658	0.32542365	H	-1.73788426	-4.56748386	1.09179700
H	-2.56693944	-5.18439481	-0.34173000	H	-3.44573573	-4.19142191	0.82255886
C	-2.67612201	-2.04233148	3.10193601	H	-2.56966545	-3.11875844	2.93764622
H	-3.49518700	-1.89223428	3.81736092	H	-1.75620875	-1.67606933	3.57068763
C	-3.21250295	0.74713058	2.01163110	H	-2.27685988	1.22178606	2.31352566
H	-3.88902470	0.77995506	2.87673781	H	-3.67083522	1.34941883	1.22097638
C	-4.76962242	-1.52464390	0.87114558	H	-5.02617254	-0.93582605	-0.01733806
H	-5.49774219	-1.26693317	1.65186814	H	-4.91361056	-2.58096978	0.62755791
C	-0.66069394	4.03250718	-2.13266161	H	-0.03047263	4.85273600	-1.77492103
H	-1.43073431	4.46494204	-2.78515248	H	-0.04179559	3.36798251	-2.74476051
C	-2.79933859	1.92519445	-1.48574518	H	-2.92682057	0.96241781	-0.98169861
H	-2.57819852	1.71140240	-2.53470720	H	-3.76770757	2.44131900	-1.43988057
C	-2.49797229	4.30565823	0.32542365	H	-3.08661492	3.78879385	1.09179700
H	-3.20634788	4.81523217	-0.34173000	H	-1.90700999	5.07980563	0.82255886
C	-0.43064994	3.33875538	3.10193601	H	-1.41609131	3.78477478	2.93764622
H	0.10887054	3.97303787	3.81736092	H	-0.57341425	2.35895606	3.57068763
C	2.25328554	2.40854388	2.01163110	H	2.19652771	1.36092547	2.31352566
H	2.61997324	2.97801665	2.87673781	H	3.00404859	2.50432715	1.22097638
C	1.06443086	4.89293613	0.87114558	H	1.70263714	4.82070613	-0.01733806
H	1.65167479	5.39465095	1.65186814	H	0.22161989	5.54579646	0.62755791

Table 3.16.20 Optimized Coordinates of **3.1-CN**.

U	0.00000000	0.00000000	0.11789985	C	0.00000000	0.00000000	-2.32590748
N	0.00000000	0.00000000	-3.49616637	O	0.00000000	0.00000000	1.91914446
N	-0.31595270	2.18569592	0.02790862	N	2.05084454	-0.81922490	0.02790862
N	-1.73489184	-1.36647103	0.02790862	Si	3.28789915	-0.25239784	1.20208965
Si	0.55785521	3.25580334	-1.12505420	Si	-1.42536664	2.97360311	1.20208965
Si	2.54068080	-2.11101845	-1.12505420	Si	-1.86253252	-2.72120528	1.20208965
Si	-3.09853601	-1.14478489	-1.12505420	C	-3.26268868	0.66014736	-1.68592140
C	-0.19898707	-3.12224163	2.02334358	C	2.20304873	2.49549761	-1.68592140
C	-2.60444704	1.73344867	2.02334358	C	-0.49237910	3.62175361	-2.65434568
C	1.05963995	-3.15564496	-1.68592140	C	3.51934778	-1.48895693	2.61637762
C	-0.47019936	3.79232305	2.61637762	C	3.38272018	-1.38446399	-2.65434568
C	2.80343410	1.38879296	2.02334358	C	4.94985048	0.07163621	0.34223144
C	1.06901879	4.90670244	-0.33412673	C	-2.53696402	4.25087816	0.34223144
C	3.71481957	-3.37914865	-0.33412673	C	-2.41288646	-4.32251436	0.34223144
C	-3.04914842	-2.30336612	2.61637762	C	-4.78383836	-1.52755379	-0.33412673
C	-2.89034108	-2.23728962	-2.65434568	H	-3.61830324	1.31147946	-0.88061140
H	-4.02570730	0.67645750	-2.47628635	H	-2.35776349	1.09709556	-2.11300927
H	0.64733305	-3.19091532	1.33324612	H	-0.30006277	-4.10259770	2.50826907
H	0.05670722	-2.39040412	2.79436771	H	2.12899438	1.49333530	-2.11300927

H	2.94492614	2.47780279	-0.88061140	H	2.59868303	3.14813604	-2.47628635
H	-3.08708025	1.03485080	1.33324612	H	-3.40292244	2.31116083	2.50826907
H	-2.09850430	1.14609217	2.79436771	H	-0.66035090	2.71526704	-3.24406080
H	0.03239650	4.34264153	-3.29488064	H	-1.46644921	4.05176967	-2.39907584
H	0.22876912	-2.59043086	-2.11300927	H	0.67337709	-3.78928225	-0.88061140
H	1.42702427	-3.82459354	-2.47628635	H	2.55824916	-1.70721409	3.09553523
H	4.17888032	-1.05407705	3.37879638	H	3.96044141	-2.43696411	2.29603584
H	0.19936619	3.06911581	3.09553523	H	-1.17658266	4.14605505	3.37879638
H	0.13025212	4.64832493	2.29603584	H	2.68166568	-0.78575287	-3.24406080
H	3.74463963	-2.19937696	-3.29488064	H	4.24216007	-0.75590256	-2.39907584
H	2.43974721	2.15606452	1.33324612	H	3.70298521	1.79143687	2.50826907
H	2.04179708	1.24431195	2.79436771	H	5.39786835	-0.81593823	-0.11516335
H	5.66344262	0.45219626	1.08480400	H	4.85069388	0.83469869	-0.43858813
H	0.23266182	5.53685199	-0.01698078	H	1.63664567	5.47336749	-1.08420836
H	1.72819539	4.75934154	0.52882326	H	-1.99231093	5.08266021	-0.11516335
H	-3.22333476	4.67858705	1.08480400	H	-3.14821721	3.78347479	-0.43858813
H	4.67872356	-2.96991704	-0.01698078	H	3.92175245	-4.15406047	-1.08420836
H	3.25761299	-3.87633188	0.52882326	H	-3.40555739	-4.26672198	-0.11516335
H	-2.44010786	-5.13078332	1.08480400	H	-1.70247668	-4.61817347	-0.43858813
H	-2.75761535	-1.36190172	3.09553523	H	-3.00229767	-3.09197799	3.37879638
H	-4.09069353	-2.21136081	2.29603584	H	-4.91138538	-2.56693494	-0.01698078
H	-5.55839813	-1.31930701	-1.08420836	H	-4.98580837	-0.88300966	0.52882326
H	-2.02131479	-1.92951417	-3.24406080	H	-3.77703613	-2.14326457	-3.29488064
H	-2.77571086	-3.29586711	-2.39907580				

Table 3.16.21 Optimized Coordinates of **3.3-Me**.

U	-0.00551990	-0.00757208	0.04992342	O	-0.02179594	-0.01829660	-1.77012362
C	-0.01715002	-0.01141165	2.48797376	H	0.64140268	0.77854796	2.86602284
H	0.33885346	-0.97845049	2.86157471	H	-1.03185854	0.16221373	2.86378242
N	0.91886542	2.17703869	0.08406327	N	-2.37148429	-0.31510410	0.07113737
N	1.45896222	-1.87216761	0.07317659	Si	-3.28740972	0.48153232	-1.18878986
Si	0.29760799	3.44580990	1.10423245	Si	2.07806258	2.58057723	-1.16525123
Si	-3.16647435	-1.47031643	1.10253320	Si	1.22287735	-3.07773635	-1.17437035
Si	2.86666826	-1.96041329	1.09608738	C	3.24320183	-0.32947142	2.01567972
C	-0.61508941	-3.36456501	-1.57202999	C	-1.32297200	2.97989562	2.00070499
C	3.21228525	1.12176881	-1.60908063	C	1.50618493	3.96028427	2.48866904
C	-1.95607509	-2.63166763	2.01775033	C	-3.37069794	-0.52199828	-2.80290296
C	1.25840610	3.15064761	-2.78411416	C	-4.22346743	-0.66779899	2.47425424
C	-2.58251426	2.18920462	-1.64139714	C	-5.09153669	0.88453737	-0.68483332
C	-0.15028359	5.04032230	0.14662362	C	3.31594863	3.95050739	-0.65349616
C	-4.31580788	-2.66843391	0.15147284	C	1.83425598	-4.82800606	-0.69225344
C	2.07912158	-2.62807829	-2.81220689	C	4.47690242	-2.33439039	0.13389712
C	2.72556940	-3.28348167	2.46333357	H	4.32482450	-0.27461575	2.20098726
H	2.73962335	-0.28475590	2.98666982	H	2.96150148	0.57224767	1.46098856
H	-1.14041483	-3.84678963	-0.73887682	H	-0.69219666	-4.03424998	-2.44030774
H	-1.14644781	-2.44174596	-1.82105949	H	-1.97247406	2.30499282	1.43196105
H	-1.89421207	3.89957443	2.18849448	H	-1.13092258	2.50792654	2.96919856
H	3.88074805	0.86155317	-0.77996376	H	3.84281508	1.40584563	-2.46358711
H	2.65556110	0.22446672	-1.89223544	H	1.78668350	3.09370007	3.10036582
H	1.04261555	4.70160380	3.15446141	H	2.43020107	4.39728880	2.09339390
H	-1.04414336	-2.86111238	1.45501442	H	-2.46724097	-3.58512470	2.20943419
H	-1.64878938	-2.22175813	2.98486438	H	-2.35636590	-0.68729085	-3.18255185
H	-3.94023938	0.01333507	-3.57511342	H	-3.84111734	-1.50154719	-2.65668302
H	0.63070815	2.34480201	-3.18058931	H	2.01099359	3.40122226	-3.54444877

H 0.62324227 4.03173145 -2.63592483	H -3.62444839 0.03869104 3.06253609
H -4.61201822 -1.42969432 3.16447039	H -5.07995770 -0.11636112 2.07011663
H -2.65522630 2.89349794 -0.80414018	H -3.16824946 2.60637173 -2.47282948
H -1.53792395 2.14612554 -1.96184562	H -5.69650725 0.00483048 -0.43916494
H -5.59071737 1.40420564 -1.51456609	H -5.11598188 1.55579365 0.18283250
H 0.69332640 5.47883088 -0.39719166	H -0.52259681 5.80173537 0.84627701
H -0.94628354 4.84461357 -0.58245303	H 2.85004546 4.91758367 -0.43452077
H 4.03081810 4.10964079 -1.47276955	H 3.89308340 3.65251424 0.23078697
H -5.11047046 -2.16442543 -0.40954736	H -4.79774268 -3.36229557 0.85446854
H -3.73881870 -3.26912497 -0.56243819	H 2.91225796 -4.89400325 -0.50814606
H 1.60014025 -5.52362647 -1.51022946	H 1.32072019 -5.19509479 0.20512902
H 1.67553409 -1.68100885 -3.18675836	H 1.90621495 -3.39899471 -3.57580556
H 3.16280755 -2.51114337 -2.69212262	H 4.45035079 -3.28154208 -0.41595641
H 5.32616457 -2.38166203 0.82981851	H 4.68733269 -1.53904170 -0.59142904
H 1.83762968 -3.10865737 3.08397784	H 3.60322218 -3.25603778 3.12420930
H 2.64730322 -4.29654800 2.05363919	

Table 3.16.22 Optimized Coordinates of **3.3-CCMe**.

U -0.00899700 -0.00183800 -0.21470302	O -0.02174400 -0.01477500 -2.03301715
N -2.35315218 -0.27136502 -0.14933901	N 1.41699011 -1.85835114 -0.13899001
N 0.94986307 2.13282816 -0.13320001	Si 1.18582709 -3.13456024 -1.31949710
Si -3.14758424 -1.32144010 1.00307408	Si -3.31880725 0.57469304 -1.33985210
Si 2.71862921 -2.01362216 1.02406208	Si 2.18788317 2.54210719 -1.30610110
Si 0.41454703 3.36176826 0.99486908	C -1.38255110 3.11791424 1.56836312
C 3.00173623 1.03157808 -2.12514216	C -2.03425016 -2.75386621 1.57685312
C -2.40031518 2.01367115 -2.18041517	C -3.75219029 -0.40200403 2.55619819
C 3.37295926 -0.33887603 1.64302413	C 2.44439219 -3.07043524 -2.74789421
C -3.90339530 -0.54188004 -2.76843321	C 2.22535817 -3.02746523 2.55815420
C -0.52135004 -3.10671924 -2.15850417	C 1.28599810 -4.87942137 -0.54005004
C -4.67719736 -2.23295717 0.29655702	C -4.86960137 1.39413711 -0.57419805
C 4.29122133 -2.84357222 0.31354402	C 3.64794328 3.49619627 -0.52061904
C 1.52461712 3.58708927 -2.75494421	C 0.38201403 5.12684739 0.25308802
C 1.50002811 3.45544427 2.55538719	H -2.09684816 3.26692125 0.75006106
H -1.60567412 3.87065929 2.33824018	H -1.56365012 2.13322816 2.00623515
H 3.34751326 0.27835402 -1.40958311	H 3.87822830 1.37606210 -2.69231820
H 2.31515817 0.53602204 -2.81694921	H -1.07464708 -2.41785519 1.97844315
H -1.83732014 -3.46079826 0.76217206	H -2.55144019 -3.30808425 2.37321118
H -1.85635714 2.65452320 -1.47789911	H -3.13491224 2.64429920 -2.70093120
H -1.67567413 1.64619813 -2.91170822	H -2.90294222 0.06364800 3.06723224
H -4.24239833 -1.08849608 3.26044725	H -4.46884434 0.38873903 2.30412218
H 2.59297220 0.28711402 2.08306216	H 3.85839829 0.23167602 0.84292506
H 4.13000632 -0.52562704 2.41836519	H 2.41930118 -2.08306916 -3.22385725
H 2.19728317 -3.81881229 -3.51359427	H 3.47225126 -3.25584125 -2.41748718
H -3.04020123 -1.03608408 -3.23007625	H -4.40596134 0.05129400 -3.54503327
H -4.59879635 -1.32197910 -2.44030019	H 1.39271711 -2.53947619 3.07608923
H 3.06448724 -3.11127924 3.26278225	H 1.90802115 -4.04253231 2.29241517
H -1.35279210 -2.99529923 -1.45399711	H -0.66416905 -4.05922331 -2.68844320
H -0.59736404 -2.29080217 -2.88207822	H 2.24325717 -5.09616839 -0.05342300
H 1.13112108 -5.64142943 -1.31642610	H 0.49702404 -5.00950338 0.21146902
H -5.48254142 -1.56672912 -0.03107600	H -5.09109939 -2.88915122 1.07499708
H -4.40461534 -2.86767822 -0.55545304	H -5.55025843 0.68559805 -0.08953601
H -5.44021639 1.91806914 -1.35355611	H -4.57959035 2.13849216 0.17828701
H 4.14061532 -3.87167030 -0.03284200	H 5.06101738 -2.87133322 1.09742008
H 4.69928436 -2.26676617 -0.52556004	H 3.35521726 4.44411834 -0.05591300

H	4.40139333	3.72368129	-1.28739310	H	4.13576132	2.88809522	0.25166302
H	0.67187505	3.07664724	-3.21808124	H	2.29752117	3.71593829	-3.52524827
H	1.19016809	4.58330635	-2.44583519	H	1.35903411	5.49294044	-0.08036101
H	0.01279700	5.82602243	1.01640408	H	-0.30330002	5.18293939	-0.60148104
H	1.48172711	2.49401719	3.07986224	H	1.13581209	4.22910532	3.24555125
H	2.54380220	3.68682628	2.31241718	C	-0.02587600	-0.00593800	2.23575417
C	-0.03461800	-0.00709900	3.46547426	C	-0.05612400	-0.00205300	4.92773438
H	-1.07179808	-0.16019101	5.31514540	H	0.58090104	-0.79541206	5.34168840
H	0.30480502	0.95343508	5.33191942				

Table 3.16.23 Optimized Coordinates of **3.3-NMe$_2$**.

U	-0.09139668	-0.01116831	0.06309346	O	-0.18691930	0.10221765	-1.74344357
N	1.60697806	-1.73469481	-0.12970179	N	-2.46992501	-0.46552573	-0.05297545
N	0.88658258	2.17807751	0.08219013	N	-0.27612012	-0.13030913	2.28324138
C	-1.04960292	-1.17832431	2.93389712	H	-0.41615481	-1.86759599	3.51717435
H	-1.78863802	-0.74462590	3.62921294	H	-1.60735090	-1.76175054	2.19884049
C	0.24433670	0.79823916	3.27289877	H	0.69579848	1.66432570	2.79231395
H	-0.56481537	1.16968422	3.92645283	H	1.00015756	0.33021900	3.92886268
Si	1.71647493	-3.05560033	1.00903766	Si	2.42635915	2.58888883	0.79465455
Si	0.18271065	3.32315700	-1.04630056	Si	2.72702925	-1.71567379	-1.48056138
Si	-3.68863020	0.32906528	0.90372611	Si	-2.98944038	-1.37956111	-1.45420949
C	2.35169884	-2.49010074	2.71292980	H	3.40949320	-2.20673677	2.63814144
H	2.27243377	-3.29035956	3.46135420	H	1.80656595	-1.61625402	3.07822641
C	0.05786202	-3.98471761	1.20254759	H	-0.82635559	-3.34545657	1.24365160
H	0.06162981	-4.60805285	2.10744041	H	-0.07074833	-4.65268969	0.34152141
C	2.86957441	-4.52546848	0.57498223	H	2.55011002	-5.05759969	-0.32762223
H	2.80268251	-5.23890190	1.40901867	H	3.92569476	-4.26540535	0.45709453
C	2.48207243	-3.16955214	-2.69700158	H	2.74971653	-4.14526369	-2.27826818
H	3.09739922	-3.01481595	-3.59416688	H	1.43493095	-3.22161717	-3.02039758
C	2.65366764	-0.17793996	-2.58916535	H	1.76034582	-0.17270146	-3.21775241
H	3.54218452	-0.18541389	-3.23717646	H	2.65488842	0.76112315	-2.02855807
C	4.56104762	-1.73017616	-0.92301301	H	4.80163984	-0.79520616	-0.40150406
H	5.21404323	-1.78823976	-1.80520548	H	4.83416964	-2.55466826	-0.25740652
C	2.33526414	3.93435655	2.15284494	H	2.04880027	4.91210183	1.75143619
H	3.31972831	4.04624648	2.62887786	H	1.61603152	3.68091132	2.94101656
C	3.28240871	1.10013341	1.62114946	H	3.07655293	0.14830211	1.12126615
H	2.99622420	0.98430847	2.67170873	H	4.36926779	1.25874688	1.59546235
C	3.70520141	3.25514195	-0.46214235	H	3.95124713	2.50689726	-1.22505475
H	4.63660723	3.51138445	0.06185548	H	3.36382345	4.15638315	-0.98384243
C	0.87085202	3.19968660	-2.81449865	H	1.94801581	3.39632783	-2.85797371
H	0.37102658	3.92374206	-3.47288216	H	0.69604169	2.19545035	-3.21250682
C	-1.70325579	3.13217613	-1.18771246	H	-2.02102189	2.10633871	-1.39762719
H	-2.06002508	3.75813868	-2.01770929	H	-2.21483732	3.47025944	-0.27921214
C	0.39874255	5.15272765	-0.52135861	H	-0.01734451	5.33850683	0.47646722
H	-0.14764215	5.79064672	-1.23001096	H	1.44121567	5.49154087	-0.51683114
C	-4.69852368	-0.83392136	2.03837380	H	-5.32021884	-1.53276072	1.46852363
H	-5.36547937	-0.24427469	2.68321211	H	-4.04759917	-1.42737029	2.69110027
C	-3.00171745	1.66875198	2.07597847	H	-2.18572481	2.25618266	1.64288382
H	-2.63693823	1.24761651	3.01737529	H	-3.81427744	2.36702129	2.32164639
C	-4.98654854	1.26908906	-0.14432507	H	-4.51068602	2.06484439	-0.72969579
H	-5.72693701	1.74156226	0.51660549	H	-5.53439121	0.62857085	-0.84460534
C	-3.23207301	-0.31941707	-3.01651939	H	-4.01091459	0.44028194	-2.88072127
H	-3.51838857	-0.94221797	-3.87534282	H	-2.29589657	0.19245496	-3.26172079
C	-1.78749248	-2.78318529	-1.90708049	H	-0.76288796	-2.43553549	-2.06478900

H -2.12582950 -3.25387890 -2.84111850	H -1.76814663 -3.56191195 -1.13559773
C -4.64078006 -2.31818467 -1.18764767	H -4.57129028 -3.02120320 -0.34806645
H -4.86548056 -2.90567566 -2.08889586	H -5.50066113 -1.66477825 -1.00249304

Table 3.16.24 Optimized Coordinates of **3.3-OMe**.

U -0.00168187 0.00189893 -0.02505389	O -0.01730888 0.00563691 -1.86043103
N 2.20296844 -0.92819342 -0.02984389	N -1.91128424 -1.44014053 -0.00921089
N -0.30966582 2.37369073 -0.00554989	O 0.02328813 -0.00093804 2.04388626
C 0.08129815 -0.00995297 3.43849637	H -0.58482095 -0.78236184 3.84911740
H 1.10438548 -0.21866772 3.78180040	H -0.22831107 0.96282473 3.84628641
Si 2.64495306 -2.21127597 1.05211819	Si 0.64066399 3.39631998 1.02717619
Si -1.34064877 3.08265052 -1.22247599	Si 3.30550691 -0.42784202 -1.28433199
Si -3.25788766 -1.18761417 1.05981319	Si -2.01443776 -2.64990675 -1.25947598
C 3.85625147 -1.65774144 2.41990829	H 4.81813013 -1.32640423 2.01371927
H 4.05409149 -2.47346226 3.12972335	H 3.43322340 -0.81831489 2.98618734
C 1.16734989 -2.97959785 1.98544526	H 0.25619091 -3.04761498 1.38127721
H 0.91505219 -2.42264912 2.89298033	H 1.43806517 -4.00023160 2.28873128
C 3.44828797 -3.71134910 0.17246112	H 2.74057746 -4.15456500 -0.53957393
H 3.70903895 -4.48614383 0.90674918	H 4.35995473 -3.46334296 -0.38300992
C 3.12532215 -1.44652732 -2.88207511	H 3.30536149 -2.51474618 -2.71410110
H 3.82625178 -1.10360143 -3.65551417	H 2.10748394 -1.33507257 -3.27354514
C 3.08057064 1.39669984 -1.77474703	H 2.04869328 1.63002859 -2.05277405
H 3.71958741 1.62705865 -2.63834809	H 3.37178483 2.07179325 -0.96086796
C 5.15224217 -0.52017775 -0.77841695	H 5.35486936 0.12929655 0.08227212
H 5.77178875 -0.16174996 -1.61252302	H 5.50037543 -1.52780440 -0.52298093
C -0.35801506 4.18646381 2.45131530	H -1.13408096 4.87026791 2.08964127
H 0.29802429 4.75195767 3.12777835	H -0.85787014 3.40777114 3.04120634
C 2.08246323 2.48111169 1.87946025	H 2.54804620 1.72462321 1.23900420
H 1.76933983 1.97773827 2.79837232	H 2.85884839 3.20936971 2.15046428
C 1.50038129 4.82669215 0.08858012	H 2.20506484 4.42811899 -0.65197194
H 2.07380157 5.45250590 0.78627217	H 0.80163943 5.48056632 -0.44435192
C -0.41639318 3.46959069 -2.84153111	H 0.41742803 4.16415577 -2.68201110
H -1.08780377 3.91181489 -3.59031117	H -0.00436401 2.54527512 -3.26200614
C -2.81499252 1.97425461 -1.68496102	H -2.50928525 0.96496792 -1.97609204
H -3.35146711 2.41768499 -2.53524508	H -3.52610347 1.88640173 -0.85456596
C -2.18434284 4.71078360 -0.66469794	H -2.82421768 4.54067780 0.21027113
H -2.83052835 5.07913183 -1.47413000	H -1.48410378 5.51420050 -0.41134692
C -3.38182404 -2.50354642 2.43870929	H -3.56814182 -3.50833773 2.04178127
H -4.19047540 -2.26489041 3.14369735	H -2.44336892 -2.54423027 3.00668334
C -3.21660272 0.48824301 1.97369926	H -2.85195070 1.31034252 1.34752021
H -2.58777063 0.45967678 2.86812633	H -4.23562011 0.74392677 2.29551728
C -4.94568681 -1.16988125 0.15790012	H -4.98096283 -0.34265623 -0.56169693
H -5.75993206 -1.01708925 0.88001918	H -5.16073668 -2.09246759 -0.39325492
C -2.80154863 -1.99164267 -2.86219611	H -3.81929216 -1.61924490 -2.69463110
H -2.84911667 -2.77093179 -3.63549017	H -2.20065161 -1.16195787 -3.25217114
C -0.31499675 -3.35930471 -1.74210702	H 0.40306835 -2.58552376 -2.02968205
H -0.43205493 -4.03495191 -2.60107609	H 0.12656100 -3.94153121 -0.92388696
C -3.00809291 -4.21211809 -0.76173295	H -2.55705726 -4.70610858 0.10840812
H -2.98717002 -4.92896912 -1.59435001	H -4.06082622 -4.02098538 -0.52313993

Table 3.16.25 Optimized Coordinates of **3.3-H**.

U 0.00000000 0.00000000 0.11878069	H 0.00000000 0.00000000 -1.88656633
O 0.00000000 0.00000000 1.95106667	N -2.23612676 -0.70282659 -0.09351365
N 1.72672907 -1.58512928 -0.09351365	N 0.50939770 2.28795588 -0.09351365

Si	-2.85125042	-1.83322956	1.09079366	Si	-3.32061760	-0.01107443	-1.27288815
Si	3.01324858	-1.55264052	1.09079366	Si	1.66989954	-2.87020198	-1.27288815
Si	1.65071806	2.88127641	-1.27288815	Si	-0.16199816	3.38587008	1.09079366
C	-1.51550799	-3.04653110	1.68970653	H	-1.13537676	-3.67119484	0.87239851
H	-1.94648375	-3.71794344	2.44593121	H	-0.66390039	-2.53379394	2.14709709
C	-3.53541624	-0.96265804	2.63863638	H	-2.74027408	-0.37952774	3.11715906
H	-3.91164492	-1.68820066	3.37295945	H	-4.35423998	-0.27546521	2.39421256
C	-4.24388611	-2.97378225	0.44011118	H	-5.13661453	-2.43447815	0.10409906
H	-4.55577602	-3.65381020	1.24499725	H	-3.89646708	-3.59311020	-0.39606766
C	-2.59223678	1.49662860	-2.17424486	H	-2.22014154	2.26705957	-1.49058367
H	-3.37645669	1.95124296	-2.79642870	H	-1.75973913	1.21359770	-2.82671145
C	-4.94565047	0.63150639	-0.49493569	H	-5.52461678	-0.15133908	0.00870782
H	-5.59109689	1.07272762	-1.26707819	H	-4.73603619	1.41241250	0.24687208
C	-3.80244150	-1.23194247	-2.65595084	H	-2.90263497	-1.61563922	-3.15209372
H	-4.41913117	-0.73373139	-3.41696393	H	-4.36654851	-2.09296236	-2.28112130
C	2.60139443	-2.58043126	2.63863638	H	1.69881770	-2.18338310	3.11715906
H	3.41784712	-2.54348354	3.37295945	H	2.41567986	-3.63314983	2.39421256
C	3.39612732	0.21079714	1.68970653	H	3.74703638	0.85233231	0.87239851
H	4.19307535	0.17326734	2.44593121	H	2.52628012	0.69194236	2.14709709
C	4.69731403	-2.18842206	0.44011118	H	4.67662718	-3.23119960	0.10409906
H	5.44218049	-2.11851266	1.24499725	H	5.05995825	-1.57788437	-0.39606766
C	2.96811423	-2.67703970	-2.65595084	H	2.85050210	-1.70593600	-3.15209372
H	2.84499561	-3.46021416	-3.41696393	H	3.99583283	-2.73506076	-2.28112130
C	1.92592466	-4.59881214	-0.49493569	H	2.89337187	-4.70878893	0.00870782
H	1.86653908	-5.37839579	-1.26707819	H	1.14483299	-4.80773391	0.24687208
C	-0.00000000	-2.99325721	-2.17424486	H	-0.85326041	-3.05622876	-1.49058367
H	-0.00159763	-3.89971874	-2.79642870	H	-0.17113687	-2.13077764	-2.82671145
C	0.83432728	3.90898218	-2.65595084	H	0.05213287	3.32157523	-3.15209372
H	1.57413556	4.19394556	-3.41696393	H	0.37071568	4.82802312	-2.28112130
C	2.59223678	1.49662860	-2.17424486	H	3.07340195	0.78916919	-1.49058367
H	3.37805432	1.94847579	-2.79642870	H	1.93087600	0.91717994	-2.82671145
C	3.01972581	3.96730576	-0.49493569	H	2.63124490	4.86012801	0.00870782
H	3.72455783	4.30566814	-1.26707819	H	3.59120320	3.39532141	0.24687208
C	-1.88061933	2.83573397	1.68970653	H	-2.61165962	2.81886253	0.87239851
H	-2.24659159	3.54467610	2.44593121	H	-1.86237972	1.84185158	2.14709709
C	-0.45342792	5.16220431	0.44011118	H	0.45998735	5.66567776	0.10409906
H	-0.88640445	5.77232285	1.24499725	H	-1.16349117	5.17099457	-0.39606766
C	0.93402181	3.54308929	2.63863638	H	1.04145638	2.56291083	3.11715906
H	0.49379780	4.23168421	3.37295945	H	1.93856012	3.90861504	2.39421256

Table 3.16.26 Optimized Coordinates of **3.3-F**.

U	-0.00134051	0.00174641	-0.04339771	O	0.01250956	0.00103320	-1.87577536
F	-0.02016514	0.00609256	2.02976367	N	-2.35512816	0.06354822	0.02122280
N	1.12627766	-2.06951979	0.04234956	N	1.22096367	2.01656546	0.03516613
Si	-3.25303001	-0.80674297	-1.20062036	Si	-3.20319809	1.05288493	1.18394587
Si	2.32946087	-2.40240082	-1.18269282	Si	0.69336107	-3.30500055	1.19693605
Si	2.50089962	2.25001939	1.19821996	Si	0.93059048	3.22037135	-1.19914057
C	-2.36242895	-2.38023211	-1.78684499	H	-1.38016325	-2.16754887	-2.21744535
H	-2.96987538	-2.87066150	-2.56074150	H	-2.22527919	-3.10027629	-0.97107937
C	-4.94619824	-1.45846287	-0.58988165	H	-4.81783234	-2.15674277	0.24651971
H	-5.43723940	-2.00878837	-1.40445923	H	-5.63639901	-0.67323137	-0.26243208
C	-3.58793760	0.24353153	-2.75178777	H	-4.15084822	1.15392553	-2.51459077
H	-4.15913021	-0.32118691	-3.50152622	H	-2.63936420	0.54726627	-3.20947951
C	-4.02217388	0.02944794	2.56811261	H	-4.82655119	-0.61474470	2.19556166

H	-4.44727121	0.68353084	3.34193701	H	-3.27597851 -0.61553567 3.04795059
C	-4.56120070	2.13988679	0.38843368	H	-4.11986615 2.83373149 -0.33826793
H	-5.06053777	2.74196093	1.16016609	H	-5.33542379 1.56656581 -0.13360277
C	-2.07616183	2.30091456	2.07466691	H	-1.41665999 1.81410904 2.79848012
H	-2.70563273	3.02182832	2.61480880	H	-1.43942073 2.86799420 1.38628408
C	1.58388540	-3.14988460	-2.76577586	H	1.03580968 -4.07729058 -2.56040841
H	2.36495563	-3.37594333	-3.50480215	H	0.88346780 -2.44053379 -3.22064862
C	3.71397417	-3.59717136	-0.61360551	H	4.26892007 -3.18594397 0.23875693
H	4.42975976	-3.72863609	-1.43698148	H	3.35821989 -4.59328294 -0.32837073
C	3.28990276	-0.84571733	-1.70131677	H	2.63651621 -0.05344537 -2.07703619
H	3.99624597	-1.10492370	-2.50280526	H	3.87412875 -0.43583649 -0.86834359
C	-0.92762127	-2.93815180	2.12361519	H	-1.74959683 -2.65906067 1.45460652
H	-0.80909131	-2.12784668	2.84825838	H	-1.23478236 -3.84273501 2.66687449
C	0.39017855	-5.00911015	0.38319231	H	-0.43511035 -4.94768318 -0.33733218
H	0.10827763	-5.74748210	1.14669438	H	1.26219515 -5.40387033 -0.15012732
C	2.00941139	-3.54175496	2.55566487	H	2.95703995 -3.92336000 2.15981101
H	1.65990331	-4.24471085	3.32451960	H	2.21785019 -2.58399229 3.04818522
C	2.96910806	0.65795974	2.13048721	H	2.21619775 0.39039056 2.87721784
H	3.92469196	0.81960615	2.64855094	H	3.09201590 -0.20766042 1.46980766
C	4.13678158	2.82700475	0.39265268	H	4.49250055 2.08196518 -0.33003853
H	4.91568516	2.94361581	1.15887850	H	4.05151114 3.78267428 -0.13694670
C	2.05675680	3.51084983	2.55779920	H	1.92273038 4.52550411 2.16682232
H	2.84226341	3.54835653	3.32528843	H	1.12122641 3.21879979 3.05055261
C	1.97766281	2.93699013	-2.76235342	H	3.05173152 2.93746110 -2.54134399
H	1.78785191	3.71315903	-3.51647373	H	1.72752854 1.96662924 -3.20597750
C	1.26691615	5.01596413	-0.62567116	H	0.61740705 5.29107617 0.21449113
H	1.04209587	5.70428923	-1.45234280	H	2.30228814 5.20110452 -0.31898565
C	-0.88776853	3.27262862	-1.75305986	H	-1.24205451 2.30818976 -2.12800974
H	-0.99896025	4.00761797	-2.56295417	H	-1.55120445 3.58122214 -0.93593854

Table 3.16.27 Optimized Coordinates of **3.3-SPh**.

U	-0.36012625	-0.02517884	0.27545667	O	-1.41536007 -0.06991226 1.75742516
N	1.45461451	-0.55633476	1.66075174	N	-1.01500356 2.18467410 -0.07814749
N	-1.69900566	-1.67454144	-0.67941303	S	1.02592472 -0.04836520 -2.18583446
C	2.77016740	0.01372549	-2.53807350	C	3.32533749 1.17503525 -3.11071456
C	3.60779320	-1.10487209	-2.37393982	C	4.66425777 1.21441754 -3.50042817
H	2.69069332	2.04417813	-3.25483836	C	4.94642692 -1.06112172 -2.76692042
H	3.20059672	-2.01071830	-1.93873426	C	5.48525319 0.09683644 -3.33202882
H	5.06597031	2.12532432	-3.93963338	H	5.57112177 -1.94108605 -2.62815225
H	6.52852465	0.12770919	-3.63686619	Si	2.92556812 0.39686167 1.70952269
Si	-1.04155374	-3.09994225	-1.46983121	Si	-3.43415465 -1.63310687 -0.38011803
Si	1.15973405	-1.69571283	2.96924327	Si	-1.48228723 2.80108744 -1.65750122
Si	-1.24588887	3.23656523	1.31258143	C	4.49117438 -0.55434000 1.19814384
H	4.71543222	-1.38176167	1.87992461	H	5.35631767 0.12338026 1.19952374
H	4.39734374	-0.96157237	0.18665660	C	2.81911085 1.91632326 0.56681594
H	1.82300448	2.36933361	0.51057316	H	3.12747632 1.67886245 -0.45476295
H	3.50221777	2.68801625	0.94831790	C	3.30950330 1.09755600 3.44761644
H	2.49899396	1.73501756	3.81799103	H	4.21936833 1.71194019 3.39627085
H	3.48610807	0.31710653	4.19672173	C	0.42619514 -0.88037930 4.52266278
H	1.08601780	-0.11485391	4.94595562	H	0.23859685 -1.63094918 5.30290484
H	-0.52802994	-0.40544852	4.27101166	C	-0.03347085 -3.09185407 2.47755232
H	-0.98919705	-2.72826019	2.08974037	H	-0.24901545 -3.69307460 3.37208013
H	0.40747522	-3.76034556	1.72990641	C	2.73388952 -2.63352483 3.51723515
H	3.17658151	-3.18791148	2.68063829	H	2.46402513 -3.36553001 4.29108606

H	3.51249999	-1.98668425	3.93614533	C	-1.21800910	-3.03170566	-3.36073242
H	-2.26518473	-2.97759710	-3.67876328	H	-0.77082134	-3.92087566	-3.82671696
H	-0.69765478	-2.14912617	-3.74930920	C	0.80870758	-3.41156613	-1.09590785
H	1.24172020	-2.75963010	-0.33086050	H	1.39782683	-3.27301772	-2.00784447
H	0.94435626	-4.44758502	-0.75674906	C	-1.86335866	-4.72657575	-0.88283123
H	-1.67992877	-4.88641550	0.18690444	H	-1.40370923	-5.56652550	-1.42283227
H	-2.94400069	-4.78400357	-1.04751794	C	-3.92875758	-2.57864462	1.19496212
H	-3.63957173	-3.63474780	1.16228685	H	-5.01495719	-2.53166123	1.35322191
H	-3.44203084	-2.12124055	2.06397931	C	-4.13376430	0.12022075	-0.18259947
H	-3.63978030	0.68530406	0.61016549	H	-5.19922189	0.03762699	0.07568467
H	-4.06621633	0.69955576	-1.10981819	C	-4.46129188	-2.33408623	-1.83458645
H	-4.28254808	-1.75376423	-2.74842057	H	-5.52923565	-2.24173321	-1.59253652
H	-4.26806553	-3.38604516	-2.06791757	C	-0.12939310	3.89084972	-2.43333374
H	0.05044974	4.80511425	-1.85657063	H	-0.40211319	4.18530947	-3.45603082
H	0.81149521	3.33146306	-2.48267576	C	-1.90674363	1.44061003	-2.93010803
H	-2.03514681	0.44136808	-2.50222112	H	-1.12268242	1.35712505	-3.68834124
H	-2.84810670	1.70333775	-3.43229779	C	-3.08079381	3.85425736	-1.60513984
H	-3.93473115	3.24599484	-1.28248803	H	-3.29985418	4.21244371	-2.62098678
H	-3.03265729	4.73124204	-0.95183080	C	-3.02625663	3.21798223	1.98310872
H	-3.76875353	3.47882871	1.22146771	H	-3.13195125	3.92739737	2.81543958
H	-3.26951060	2.21872337	2.36161972	C	-0.13155103	2.80653138	2.78990948
H	-0.20301448	1.75895582	3.09147703	H	-0.44546253	3.42210305	3.64494601
H	0.92006188	3.03887419	2.59080654	C	-0.77711934	5.05919665	0.96162720
H	0.27206897	5.13513660	0.64960905	H	-0.88535034	5.63927530	1.88868298
H	-1.38606677	5.54936200	0.19528042				

Table 3.16.28 Optimized Coordinates of **3.3-Cl**.

U	0.00000000	0.00000000	0.09700672	Cl	0.00000000	0.00000000	-2.58190207
O	0.00000000	0.00000000	1.92328400	N	-0.50900378	2.27582687	0.04595786
N	-1.71642199	-1.57872364	0.04595786	N	2.22542577	-0.69710323	0.04595786
Si	-1.65866212	2.90467257	1.21602364	Si	0.22597953	3.40147388	-1.08515394
Si	-1.68618918	-2.88877982	1.21602364	Si	-3.05875255	-1.50503293	-1.08515394
Si	2.83277302	-1.89644095	-1.08515394	Si	3.34485130	-0.01589275	1.21602364
C	-2.71359785	1.56669645	2.06062266	H	-3.13365647	0.83636773	1.36171165
H	-3.55391132	2.05844709	2.57108827	H	-2.13464505	1.01119289	2.80347272
C	-0.81970061	3.84351969	2.64553436	H	-0.04478712	3.21336924	3.09795134
H	-1.55167475	4.08799330	3.42759393	H	-0.34696286	4.77813323	2.32563007
C	-2.94091201	4.07618693	0.41685367	H	-2.49723319	4.95095080	-0.07072170
H	-3.63832219	4.44337311	1.18237210	H	-3.53113416	3.54187401	-0.33813016
C	1.96503612	2.87142548	-1.64577662	H	2.69325646	2.95643261	-0.83051279
H	2.29204411	3.54763540	-2.44842081	H	2.01001723	1.85200446	-2.03667547
C	0.54193037	5.14295841	-0.35456099	H	-0.36291884	5.67077215	-0.03504385
H	1.02623032	5.76054622	-1.12390348	H	1.22246359	5.09822163	0.50440278
C	-0.83407640	3.66049461	-2.64258287	H	-0.96696106	2.71284851	-3.17493159
H	-0.35634430	4.37265148	-3.32952403	H	-1.82816406	4.05037019	-2.39363264
C	-2.91873538	-2.63164140	2.64553436	H	-2.76046584	-1.64547141	3.09795134
H	-2.76446867	-3.38778640	3.42759393	H	-3.96450333	-2.68954526	2.32563007
C	-0.00000000	-3.13339290	2.06062266	H	0.84251253	-3.13200997	1.36171165
H	-0.00571181	-4.10700103	2.57108827	H	0.19160380	-2.35425329	2.80347272
C	-2.05962543	-4.58499797	0.41685367	H	-3.03903258	-4.63814278	-0.07072170
H	-2.02891289	-5.37256600	1.18237210	H	-1.30178579	-4.82898890	-0.33813016
C	-2.75304312	-2.55257865	-2.64258287	H	-1.86591520	-2.19383710	-3.17493159
H	-3.60865512	-2.49492896	-3.32952403	H	-2.59364145	-3.60842162	-2.39363264
C	-4.72489782	-2.10215374	-0.35456099	H	-4.72957334	-3.14968302	-0.03504385

H	-5.50189449	-1.99153157	-1.12390348	H	-5.02642124	-1.49042629	0.50440278
C	-3.46924548	0.26605846	-1.64577662	H	-3.90697397	0.85421221	-0.83051279
H	-4.21836443	0.21115073	-2.44842081	H	-2.60889152	0.81472375	-2.03667547
C	3.58711952	-1.10791595	-2.64258287	H	2.83287626	-0.51901142	-3.17493159
H	3.96499942	-1.87772253	-3.32952403	H	4.42180551	-0.44194858	-2.39363264
C	1.50420935	-3.13748395	-1.64577662	H	1.21371751	-3.81064481	-0.83051279
H	1.92632032	-3.75878613	-2.44842081	H	0.59887430	-2.66672821	-2.03667547
C	4.18296745	-3.04080467	-0.35456099	H	5.09249218	-2.52108915	-0.03504385
H	4.47566419	-3.76901463	-1.12390348	H	3.80395765	-3.60779534	0.50440278
C	2.71359785	1.56669645	2.06062266	H	2.29114394	2.29564224	1.36171165
H	3.55962314	2.04855395	2.57108827	H	1.94304125	1.34306040	2.80347272
C	5.00053744	0.50881104	0.41685367	H	5.53626577	-0.31280803	-0.07072170
H	5.66723507	0.92919289	1.18237210	H	4.83291996	1.28711489	-0.33813016
C	3.73843600	-1.21187829	2.64553436	H	2.80525296	-1.56789784	3.09795134
H	4.31614342	-0.70020690	3.42759393	H	4.31146619	-2.08858797	2.32563007

Table 3.16.29 Optimized Coordinates of **3.3-Br**.

U	-0.01568253	-0.00328266	0.14671582	Br	-0.03497051	0.03644017	-2.70105144
O	-0.03904613	-0.03630825	1.96782476	N	-2.35338533	0.03802651	0.14490793
N	1.15104765	-2.01327358	0.12404840	N	1.20876783	1.96963519	0.15023564
Si	-3.32519781	-0.94843677	-0.93568811	Si	0.83196238	3.33709588	-0.89068243
Si	2.45864046	2.18173076	1.36905974	Si	-3.16964499	0.96301632	1.39530478
Si	2.52650610	-2.32841964	-0.92496230	Si	0.73371420	-3.21889696	1.33632430
C	-4.07648644	0.05719892	-2.36297615	H	-4.76188923	0.83502687	-2.00807074
H	-4.63052698	-0.59206221	-3.05484252	H	-3.27364209	0.54447427	-2.92796773
C	-2.36861263	-2.39369609	-1.73355637	H	-1.54938495	-2.77871675	-1.11700026
H	-1.93400948	-2.10601759	-2.69384626	H	-3.06769424	-3.22481114	-1.90259287
C	-4.76012050	-1.82948048	-0.02507143	H	-4.36617748	-2.52021553	0.73098305
H	-5.33601848	-2.42538458	-0.74680610	H	-5.46148704	-1.15543210	0.47727494
C	-3.56922861	-0.06271705	2.94760377	H	-4.20729574	-0.92597198	2.72934654
H	-4.08013243	0.55303022	3.70072060	H	-2.63959668	-0.43473038	3.39326766
C	-2.16420960	2.45597207	2.00909264	H	-1.19248980	2.16539555	2.41544876
H	-2.73277923	2.94424115	2.81334596	H	-1.99853911	3.20420700	1.22610489
C	-4.80007370	1.76179040	0.79052381	H	-4.60922388	2.44462497	-0.04691352
H	-5.23375972	2.35682731	1.60617580	H	-5.56268235	1.04661061	0.46504167
C	2.03267132	3.48504312	-2.35706783	H	3.06702009	3.65146703	-2.03541897
H	1.74639028	4.31714097	-3.01522671	H	2.00540479	2.56314704	-2.94873351
C	-0.92439643	3.29176812	-1.63065382	H	-1.66854995	2.82751406	-0.97518370
H	-0.95059991	2.74878164	-2.57844326	H	-1.24955336	4.32552657	-1.81408860
C	0.86211253	5.00712292	0.04501808	H	0.09282985	5.03039447	0.82718429
H	0.63278778	5.81532411	-0.66349798	H	1.82038753	5.24754269	0.51671800
C	1.82250638	3.05141177	2.93697658	H	1.40879444	4.04469531	2.73309338
H	2.63081056	3.16659310	3.67212119	H	1.03323438	2.44682927	3.39852485
C	3.22713754	0.55014428	1.96669184	H	2.48103264	-0.15392115	2.34149018
H	3.91671956	0.77994360	2.79161395	H	3.80919877	0.04795923	1.18653708
C	3.97308868	3.15916509	0.72637243	H	4.43341215	2.64049533	-0.12391356
H	4.72770157	3.21571627	1.52313227	H	3.75364106	4.18383185	0.40876745
C	2.09941382	-3.48891584	-2.36969474	H	1.79491984	-4.48689079	-2.03526102
H	2.96320704	-3.60735773	-3.03848217	H	1.27767309	-3.06164999	-2.95579223
C	3.28264170	-0.76577770	-1.70901488	H	3.26962149	0.10843638	-1.05034908
H	2.76379396	-0.48184297	-2.62752298	H	4.33276314	-0.97792160	-1.95515898
C	3.99949239	-3.09872335	0.02354891	H	4.38102509	-2.39736236	0.77604859
H	4.81860961	-3.30451044	-0.67945437	H	3.76370195	-4.03623826	0.53700197
C	1.75085604	-3.04495139	2.93427649	H	2.83013461	-3.07772793	2.74915720

H	1.50414945	-3.84733554	3.64308505	H	1.52139415	-2.08802901	3.41623766
C	-1.09200776	-3.16703263	1.86599285	H	-1.40042981	-2.18827774	2.24123587
H	-1.22971953	-3.89434600	2.67901053	H	-1.77150867	-3.45352360	1.05536928
C	0.93853826	-5.01631209	0.71313341	H	0.30283095	-5.19969240	-0.16201710
H	0.61193685	-5.70554412	1.50420656	H	1.96301893	-5.29123027	0.44218502

Table 3.16.30 Optimized Coordinates of **3.3-I**.

U	0.00000000	0.00000000	0.24701352	O	0.00000000	0.00000000	2.07648789
I	0.00000000	0.00000000	-2.91113017	N	0.90652234	2.13647093	0.27139954
N	-2.30349927	-0.28316409	0.27139954	N	1.39697694	-1.85330684	0.27139954
Si	0.29198530	3.47425392	-0.69677066	Si	2.86279950	-1.98999365	-0.69677066
Si	1.11450128	-3.08406912	1.50064793	Si	2.11363157	2.50722098	1.50064793
Si	-3.15478480	-1.48426027	-0.69677066	Si	-3.22813284	0.57684814	1.50064793
C	1.46757267	3.93678790	-2.11751583	H	2.43752813	4.30100966	-1.76135989
H	1.02392637	4.72141663	-2.74602025	H	1.64517975	3.06057042	-2.75136352
C	-1.40910920	3.14243253	-1.49332207	H	-2.02620679	2.41794503	-0.95269054
H	-1.30558014	2.76972946	-2.51566932	H	-1.96758278	4.08863416	-1.52608505
C	-0.00000000	5.05839395	0.33611293	H	-0.77071538	4.89107916	1.09832702
H	-0.36199371	5.85548284	-0.32828743	H	0.89253176	5.43671874	0.84501108
C	1.33728475	3.15308439	3.11272082	H	0.73174065	4.05315023	2.96224379
H	2.11706315	3.38968320	3.84960187	H	0.69171873	2.37946466	3.54357031
C	3.18580859	1.02124959	2.00751286	H	2.60110015	0.14815667	2.30721952
H	3.79467172	1.32562470	2.87084795	H	3.87507945	0.71660842	1.21283380
C	3.41169417	3.78780838	0.92331435	H	3.95269082	3.42323006	0.04138687
H	4.15020511	3.93062536	1.72445971	H	3.00067259	4.77211392	0.67654088
C	2.67557199	-3.23934916	-2.11751583	H	2.50601957	-4.26146612	-1.76135989
H	3.57690356	-3.24745456	-2.74602025	H	1.82794186	-2.95505267	-2.75136352
C	3.42598100	-0.35089190	-1.49332207	H	3.10710521	0.54577404	-0.95269054
H	3.05144615	-0.25419916	-2.51566932	H	4.52465244	-0.34034041	-1.52608505
C	4.38069766	-2.52919698	0.33611293	H	4.62115649	-1.77808048	1.09832702
H	5.25199374	-2.61424567	-0.32828743	H	4.26207067	-3.49131455	0.84501108
C	2.06200881	-2.73466476	3.11272082	H	3.14426074	-2.66028112	2.96224379
H	1.87702018	-3.52827207	3.84960187	H	1.71481748	-1.78877832	3.54357031
C	-0.70847621	-3.26961597	2.00751286	H	-1.17224264	-2.32669715	2.30721952
H	-0.74931120	-3.94909445	2.87084795	H	-1.31693863	-3.71422146	1.21283380
C	1.57449120	-4.84851800	0.92331435	H	0.98825878	-5.13474568	0.04138687
H	1.32891886	-5.55949575	1.72445971	H	2.63243560	-4.98471565	0.67654088
C	-4.14314466	-0.69743873	-2.11751583	H	-4.94354770	-0.03954355	-1.76135989
H	-4.60082993	-1.47396207	-2.74602025	H	-3.47312161	-0.10551776	-2.75136352
C	-2.01687180	-2.79154063	-1.49332207	H	-1.08089842	-2.96371907	-0.95269054
H	-1.74586600	-2.51553030	-2.51566932	H	-2.55706966	-3.74829375	-1.52608505
C	-4.38069766	-2.52919698	0.33611293	H	-3.85044112	-3.11299868	1.09832702
H	-4.89000003	-3.24123716	-0.32828743	H	-5.15460243	-1.94540420	0.84501108
C	-3.39929355	-0.41841963	3.11272082	H	-3.87600140	-1.39286912	2.96224379
H	-3.99408334	0.13858887	3.84960187	H	-2.40653621	-0.59068634	3.54357031
C	-2.47733238	2.24836637	2.00751286	H	-1.42885751	2.17854048	2.30721952
H	-3.04536052	2.62346976	2.87084795	H	-2.55814083	2.99761304	1.21283380
C	-4.98618536	1.06070963	0.92331435	H	-4.94094960	1.71151563	0.04138687
H	-5.47912399	1.62887038	1.72445971	H	-5.63310817	0.21260173	0.67654088

Table 3.16.31 Optimized Coordinates of **3.3-CN**.

U	-0.00665570	0.00164672	0.15038475	C	-0.00969607	0.00992794	-2.40445173
N	-0.00597249	0.00876454	-3.57614720	O	-0.02222354	0.01450063	1.96995948
N	0.89556190	-2.12587178	0.02065045	N	-2.31741019	0.31093884	0.02862470

N	1.43906544	1.80813592	0.03365058	Si	-3.32915200	-0.51466246	1.20185718
Si	0.31731003	-3.33406313	-1.12210887	Si	2.13310842	-2.59227130	1.18121426
Si	-3.07062362	1.38708607	-1.13965328	Si	1.22467936	3.11024020	1.19644818
Si	2.75041156	1.93183014	-1.13465786	C	3.36268855	0.23722641	-1.73903609
C	-0.48409466	3.10870781	2.03308104	C	-1.46775062	-3.01623328	-1.69393962
C	2.99387557	-1.11388430	2.01014951	C	1.40171636	-3.45466363	-2.67651257
C	-1.90538017	2.78799388	-1.68687444	C	-3.90489090	0.61766112	2.61975214
C	1.43585147	-3.62538927	2.62071766	C	-3.67626207	0.48534275	-2.69759200
C	-2.45124473	-1.97040190	2.05717637	C	-4.88163927	-1.29303461	0.40497050
C	0.21695315	-5.09230529	-0.37476416	C	3.55119636	-3.58400925	0.37242291
C	-4.57738734	2.33853273	-0.44108347	C	1.35097042	4.83702250	0.38741660
C	2.47999685	3.04390042	2.62588214	C	4.33159858	2.73050975	-0.41260900
C	2.27270808	2.94240347	-2.67022046	H	3.84032766	-0.33772500	-0.93766133
H	4.11965602	0.40768560	-2.51763435	H	2.57660600	-0.37962732	-2.18078788
H	-1.31701000	2.96684957	1.33607345	H	-0.62936606	4.08145709	2.52397336
H	-0.55637856	2.32345183	2.79023610	H	-1.62515815	-2.02560320	-2.12683402
H	-2.19067021	-3.15617073	-0.88189916	H	-1.70645226	-3.75191152	-2.47506560
H	3.37174535	-0.37137594	1.29999395	H	3.85406624	-1.49319726	2.57990055
H	2.32335688	-0.59751262	2.70287081	H	1.36296537	-2.51674479	-3.24044708
H	1.04454227	-4.25790924	-3.33563167	H	2.44970434	-3.66316100	-2.43193328
H	-0.93434483	2.44506849	-2.05305955	H	-1.73248120	3.50520487	-0.87578779
H	-2.38513116	3.33449845	-2.51108666	H	-3.03676400	1.08984371	3.09482772
H	-4.43245496	0.03538154	3.38782833	H	-4.57670957	1.41449762	2.28368255
H	0.60085143	-3.09055995	3.08846455	H	2.20469101	-3.78470660	3.38924571
H	1.06938383	-4.60776050	2.30470851	H	-2.83045205	0.06049679	-3.24790136
H	-4.19951457	1.17957532	-3.36947392	H	-4.36816879	-0.32910029	-2.45236614
H	-1.89608334	-2.61636872	1.36847382	H	-3.20938659	-2.59314739	2.55254976
H	-1.74485661	-1.61703206	2.81300501	H	-5.53791124	-0.56532258	-0.08476940
H	-5.47570053	-1.80831653	1.17237033	H	-4.59701725	-2.03869594	-0.34790121
H	1.18003545	-5.49280412	-0.04084125	H	-0.17752928	-5.77811157	-1.13725515
H	-0.47005849	-5.12070451	0.47968119	H	3.22486231	-4.52231100	-0.08937815
H	4.30737301	-3.83482920	1.12909434	H	4.04599245	-2.98884900	-0.40510688
H	-5.41021405	1.69459156	-0.13809244	H	-4.95450073	3.01725366	-1.21861801
H	-4.29946115	2.95307119	0.42382132	H	2.31396196	5.03181823	-0.09688820
H	1.20294725	5.61338578	1.15063875	H	0.56818708	4.96539633	-0.37038384
H	2.44571374	2.06042896	3.10926670	H	2.23541013	3.79945346	3.38514629
H	3.50989133	3.22007497	2.29756044	H	4.20030948	3.76696431	-0.08319048
H	5.11086819	2.73004435	-1.18731022	H	4.71599373	2.15625555	0.43915980
H	1.48207762	2.43137378	-3.22951255	H	3.13550853	3.06027263	-3.34029444
H	1.91261773	3.94381058	-2.40829057				

Table 3.16.32 Optimized Coordinates of **3.4-Me**.

U	-0.03021168	-0.04642021	0.30098606	C	-0.10422979	-0.08722871	2.73719463
H	-1.12010379	-0.00570400	3.14777001	H	0.32820568	-1.00690982	3.15537152
H	0.47153040	0.74907687	3.16165576	N	1.49908578	1.59501511	-0.09424094
N	-2.19204181	0.57833504	-0.05339318	N	0.69398872	-2.17417009	-0.07988231
Si	1.32081890	2.79262847	-1.38450209	Si	2.87983708	1.74861067	1.01065575
Si	-3.13075872	-0.20180184	-1.33071645	Si	-2.98605565	1.73873052	1.02491043
Si	1.81190374	-2.58722336	-1.38603968	Si	0.13022316	-3.46332883	0.99871899
C	-0.30419612	2.49568884	-2.32054467	H	-0.35044616	1.50457466	-2.79226332
H	-0.37057414	3.22969841	-3.13461107	H	-1.19461116	2.60761688	-1.69667482
C	1.27955129	4.57360872	-0.72577158	H	0.51231472	4.71071401	0.04460295
H	1.05934849	5.27109879	-1.54440926	H	2.23980124	4.87702196	-0.29206631
C	2.66430915	2.72457900	-2.72718554	H	3.64542530	3.05952661	-2.37904491

H	2.36749734	3.38358116	-3.55412485	H	2.78232344	1.71579745	-3.13712418
C	2.52869478	2.95515466	2.43208653	H	2.33047089	3.96587393	2.05749723
H	3.39318777	3.01493979	3.10608774	H	1.66336986	2.65232106	3.03173988
C	4.47594193	2.34880828	0.17174020	H	4.76989800	1.71080032	-0.66930184
H	5.28832224	2.31584763	0.90975814	H	4.41399182	3.37981393	-0.19331709
C	3.33436159	0.05564927	1.74543381	H	2.53359222	-0.43894981	2.30370521
H	4.16531099	0.20038777	2.44891747	H	3.68295790	-0.63627913	0.96999097
C	-2.03365209	-1.45824088	-2.24554704	H	-1.20402105	-0.98333334	-2.78691657
H	-2.65268852	-1.95534468	-3.00432128	H	-1.61220886	-2.24208451	-1.60930859
C	-4.63225586	-1.14251157	-0.64979987	H	-4.34897842	-1.85850820	0.13023664
H	-5.12798070	-1.70129871	-1.45414016	H	-5.37817713	-0.46372514	-0.21914593
C	-3.76437386	0.95993987	-2.69273227	H	-4.53853892	1.64913469	-2.34421834
H	-4.20306513	0.35379890	-3.49678961	H	-2.95792892	1.55631745	-3.13273553
C	-3.92175882	0.89254290	2.44304761	H	-4.75120270	0.28268247	2.06671358
H	-4.34771746	1.64623937	3.11825606	H	-3.27929895	0.23823147	3.04183369
C	-4.25145441	2.85636845	0.15143127	H	-3.82502314	3.37556135	-0.71431985
H	-4.58812960	3.62276344	0.86211565	H	-5.14306660	2.31574196	-0.18562657
C	-1.69943693	2.93122372	1.75113351	H	-0.85047176	2.44466967	2.24047988
H	-2.18610117	3.55888937	2.50933771	H	-1.30466638	3.60077882	0.97844508
C	2.35555939	-1.01470338	-2.29988220	H	1.51773100	-0.48304488	-2.77091653
H	3.03245606	-1.30866362	-3.11313780	H	2.88758804	-0.29954850	-1.66689481
C	3.38518325	-3.43813492	-0.74739419	H	3.88857173	-2.83855191	0.02011495
H	4.09457132	-3.58846955	-1.57155895	H	3.17979665	-4.42363218	-0.31262093
C	1.06313287	-3.69420417	-2.73716376	H	0.87960128	-4.72023231	-2.40623956
H	1.76103433	-3.74228823	-3.58372794	H	0.11672774	-3.29085134	-3.11443338
C	1.30177482	-3.74165478	2.46538831	H	2.29117300	-4.06056958	2.11698233
H	0.91198403	-4.53144556	3.12072793	H	1.44469066	-2.84493029	3.07737726
C	-0.06206872	-5.15797582	0.15994498	H	-0.74819674	-5.12674732	-0.69353172
H	-0.48272575	-5.85802644	0.89410520	H	0.88669343	-5.58347864	-0.18480934
C	-1.61499955	-3.05303879	1.63508086	H	-1.74163443	-2.04557641	2.04484240
H	-1.87104818	-3.75160087	2.44271112	H	-2.35843423	-3.18995137	0.84039789

Table 3.16.33 Optimized Coordinates of **3.4-CCMe**.

U	-0.02314237	-0.04700238	0.25214867	C	-0.09616370	-0.09463725	2.63965539
C	-0.09260389	-0.08281789	3.87070802	C	-0.09233387	-0.07039568	5.33167716
H	0.06952884	-1.07672746	5.73823769	H	0.70088936	0.57795128	5.72483580
H	-1.04787184	0.29746671	5.72633470	N	1.51404514	1.57581508	-0.12796254
N	-2.16881148	0.59410598	-0.10475242	N	0.65020022	-2.18221574	-0.11758427
Si	1.36251299	2.77762170	-1.41679884	Si	2.86748822	1.72772578	1.01783612
Si	-3.12555437	-0.16014303	-1.38407408	Si	-2.95554444	1.72325705	1.02044744
Si	1.76380847	-2.61703555	-1.41904598	Si	0.08324451	-3.44792506	0.99563185
C	-0.25133932	2.49108917	-2.37651782	H	-0.30272558	1.49798623	-2.84392182
H	-0.29761414	3.22048599	-3.19607881	H	-1.14931564	2.61798337	-1.76614076
C	1.31943568	4.55568461	-0.75182531	H	0.52684508	4.69623039	-0.00833680
H	1.13665623	5.26100703	-1.57296411	H	2.26678444	4.84382344	-0.28132964
C	2.72931005	2.69739194	-2.73436074	H	3.70786282	3.01563701	-2.36387677
H	2.46035258	3.36390339	-3.56478539	H	2.83992954	1.68819850	-3.14570262
C	2.41389950	2.82564288	2.49317785	H	2.10321019	3.82714690	2.17434266
H	3.27233836	2.94150515	3.16780771	H	1.59181609	2.38384706	3.06658966
C	4.45113232	2.44643513	0.24926879	H	4.81786423	1.84785658	-0.59204447
H	5.23376045	2.44316220	1.01965405	H	4.34260970	3.48117466	-0.09419568
C	3.37122568	0.01841424	1.67214162	H	2.57315526	-0.50518392	2.20852129
H	4.19696572	0.15183287	2.38429568	H	3.73533187	-0.63346390	0.86971675
C	-2.04555127	-1.42109422	-2.31342627	H	-1.19950381	-0.95454973	-2.83683812

H	-2.66430076	-1.89200919	-3.08890678	H	-1.64931060	-2.22378790	-1.68449404
C	-4.63167044	-1.09102550	-0.70104597	H	-4.34328274	-1.83372082	0.05154322
H	-5.15399138	-1.61807856	-1.50994999	H	-5.35575759	-0.41306751	-0.23376096
C	-3.74643185	1.02760902	-2.72886092	H	-4.48467213	1.74559601	-2.36095615
H	-4.22619082	0.44208125	-3.52467208	H	-2.92687025	1.59344482	-3.18489189
C	-3.74368155	0.81896004	2.48705409	H	-4.51684554	0.11260069	2.16326190
H	-4.21481480	1.53582341	3.17250751	H	-2.98723758	0.26050335	3.04842383
C	-4.31950149	2.77442559	0.21429567	H	-3.94926684	3.36128740	-0.63405906
H	-4.69580150	3.48280534	0.96419522	H	-5.17650128	2.18529073	-0.13061329
C	-1.68699957	2.96838659	1.68033538	H	-0.83347302	2.49826736	2.17851371
H	-2.17741866	3.61040617	2.42448321	H	-1.30792961	3.61964860	0.88467399
C	2.29690262	-1.05233951	-2.35495486	H	1.45489528	-0.51853374	-2.81665414
H	2.95880671	-1.35392816	-3.17763402	H	2.84398700	-0.33638198	-1.73565032
C	3.34354375	-3.44713837	-0.77136297	H	3.86215105	-2.81426039	-0.04184872
H	4.03788456	-3.63944482	-1.59964507	H	3.14081400	-4.40905540	-0.28601385
C	1.01221395	-3.74642767	-2.74905219	H	0.83361317	-4.76710663	-2.39947648
H	1.70567307	-3.80695429	-3.59846514	H	0.06274410	-3.35164070	-3.12771937
C	1.20762258	-3.60407929	2.51139105	H	2.23819220	-3.84590205	2.22532952
H	0.85147470	-4.40115279	3.17725812	H	1.22394047	-2.66912836	3.08075821
C	-0.02804124	-5.17415175	0.20718140	H	-0.70961967	-5.19796141	-0.65016446
H	-0.42367955	-5.86804038	0.96080246	H	0.94023147	-5.56965082	-0.11848651
C	-1.68640598	-3.05623301	1.56353803	H	-1.80355177	-2.06413503	2.01297957
H	-1.97779966	-3.78388932	2.33304748	H	-2.40168651	-3.15240228	0.73783737

Table 3.16.34 Optimized Coordinates of **3.4-NMe_2**.

U	-0.73740447	0.18580524	0.58709370	N	0.45224149	-0.21710921	2.42102500
C	1.19570806	-1.45766608	2.63477081	H	1.10559805	-2.12619564	1.77438137
H	2.26757770	-1.25977330	2.80369915	H	0.82655329	-2.00238288	3.52053816
C	0.61746944	0.64082090	3.58955187	H	1.68103192	0.86014298	3.78099991
H	0.10054005	1.59568698	3.46838652	H	0.21912705	0.16229368	4.50027088
N	0.60079321	1.71892785	-0.51205964	N	-2.80340665	1.10005984	1.05905438
N	-1.00804149	-1.99948220	-0.06000932	Si	0.00703384	3.02344221	-1.55726817
Si	2.35922083	1.70362019	-0.24947929	Si	-4.27306900	0.66005458	0.17570325
Si	-2.92885848	2.19335182	2.44396332	Si	-0.32182788	-2.55634986	-1.59028177
Si	-1.83301432	-3.16722266	0.98440991	C	-1.88450750	3.10700208	-1.60821213
H	-2.34032815	2.22044507	-2.06281005	H	-2.15897316	3.96180483	-2.24099514
H	-2.34281913	3.25308677	-0.62810675	C	0.57083965	4.73815555	-0.95837677
H	0.19967214	4.94285771	0.05311140	H	0.16640024	5.51380309	-1.62180897
H	1.65881383	4.85944519	-0.94067972	C	0.49690718	2.82299600	-3.38470960
H	1.56210266	2.96963221	-3.58032713	H	-0.05225643	3.56252343	-3.98270024
H	0.22243358	1.83038822	-3.76180258	C	2.84116923	2.67212143	1.30882065
H	2.52802531	3.72021382	1.23410881	H	3.93003956	2.66100680	1.44892155
H	2.38613908	2.25467379	2.21212672	C	3.40499552	2.43418616	-1.66440532
H	3.29246075	1.86777038	-2.59551920	H	4.45821359	2.35568708	-1.36254073
H	3.21077961	3.48831363	-1.88429511	C	3.03426517	-0.06589908	-0.12559048
H	2.56462913	-0.68341425	0.64305172	H	4.10519213	-0.01819598	0.11312753
H	2.94248357	-0.58419716	-1.08742283	C	-3.83798818	-0.33758538	-1.38497590
H	-3.40562977	0.30180907	-2.16487190	H	-4.76906490	-0.74890569	-1.79738440
H	-3.15870631	-1.17652649	-1.21380762	C	-5.45591581	-0.37653127	1.24282532
H	-5.00469564	-1.31303036	1.58710801	H	-6.35828082	-0.63250191	0.67215188
H	-5.78206442	0.17561713	2.13310902	C	-5.30564148	2.11111785	-0.49505692
H	-5.89610667	2.61784351	0.27268334	H	-6.01118324	1.70904534	-1.23485066
H	-4.69389860	2.86248682	-1.00522251	C	-2.90864668	1.23070404	4.08104636
H	-3.84356040	0.66649268	4.19114921	H	-2.83169874	1.91046808	4.93962050

H	-2.08925059	0.50917741	4.14736752	C	-4.48922277	3.27250231	2.53166905
H	-4.58694286	3.95005501	1.67751018	H	-4.41123509	3.89205264	3.43547030
H	-5.41613618	2.69504015	2.61617012	C	-1.50150975	3.45897490	2.38592015
H	-0.53449604	3.07607758	2.03987756	H	-1.34060851	3.91044199	3.37365112
H	-1.77571322	4.26775076	1.69698191	C	-0.09082099	-1.06209823	-2.74153945
H	-1.05796898	-0.65113998	-3.05884658	H	0.43496824	-1.38707218	-3.64903432
H	0.49607984	-0.24164397	-2.31225343	C	1.36504360	-3.39854479	-1.36854745
H	2.09351875	-2.74268808	-0.87970350	H	1.77982740	-3.68348074	-2.34443475
H	1.28580150	-4.31035241	-0.76618256	C	-1.41935148	-3.77629726	-2.54654584
H	-1.52423336	-4.74285393	-2.04078779	H	-0.96119696	-3.97121408	-3.52523498
H	-2.42490504	-3.37975356	-2.72670968	C	-0.76959369	-4.70271044	1.33897719
H	-0.59401947	-5.30780688	0.44159581	H	-1.28146533	-5.34533586	2.06727046
H	0.20810252	-4.44161052	1.75968145	C	-3.48160432	-3.80018047	0.28218687
H	-4.18375426	-2.98644888	0.07330321	H	-3.95503302	-4.45885707	1.02264361
H	-3.36129246	-4.37794995	-0.63897923	C	-2.26302213	-2.38803931	2.66246851
H	-1.38454738	-2.16408614	3.27392886	H	-2.87726144	-3.10882194	3.21907013
H	-2.85416661	-1.46954904	2.57744899				

Table 3.16.35 Optimized Coordinates of **3.4-OMe**.

U	-1.14287093	0.52425625	0.56621112	O	-0.06634776	0.06614699	2.26929066
C	0.65980866	-0.21713103	3.43831289	H	0.40477013	0.49749776	4.23125505
H	0.42864455	-1.22967194	3.79342538	H	1.73800612	-0.15287413	3.24336698
N	0.17766778	2.25078193	-0.17604978	N	-3.15880098	0.94123581	1.59079253
N	-0.92491329	-1.45503725	-0.56519579	Si	-0.57443158	3.67494705	-0.88438565
Si	1.91182406	2.23743880	0.15760690	Si	-4.67503096	0.47156421	0.82864909
Si	-3.16369543	1.62022160	3.22070423	Si	-0.66913749	-1.51677926	-2.30788941
Si	-0.84129528	-2.95119692	0.37467495	C	-2.45877892	3.41082874	-0.94401438
H	-2.76056139	2.63311846	-1.65896360	H	-2.92662558	4.34220258	-1.28965525
H	-2.90606802	3.17107370	0.02688576	C	-0.26116348	5.24194747	0.14132138
H	-0.58566327	5.11383436	1.18076160	H	-0.80969546	6.09497598	-0.27864250
H	0.80055397	5.51552445	0.16018274	C	-0.06566295	4.04258862	-2.67590962
H	0.98019593	4.34996271	-2.76933237	H	-0.68545133	4.86012066	-3.06778924
H	-0.21810728	3.17295723	-3.32465912	C	2.30381172	2.95757585	1.86999524
H	2.00016141	4.00889197	1.93819097	H	3.38066341	2.90982383	2.07858824
H	1.78495373	2.41419084	2.66738385	C	2.94774273	3.22173548	-1.09631261
H	2.81280742	2.85987898	-2.12204365	H	4.01021930	3.10593055	-0.84427363
H	2.72961855	4.29575135	-1.08758975	C	2.58196625	0.46188356	0.07825365
H	2.06857277	-0.23406387	0.75013308	H	3.64376417	0.46085594	0.35839347
H	2.51244138	0.05661127	-0.93843179	C	-4.30288700	-0.37657068	-0.83195181
H	-3.80546503	0.29026080	-1.55021793	H	-5.25374310	-0.67129845	-1.29528732
H	-3.69226300	-1.27930409	-0.73426321	C	-5.67223215	-0.75970854	1.87598306
H	-5.08321150	-1.64940167	2.12712090	H	-6.56366128	-1.09311003	1.32879057
H	-6.01646840	-0.31657212	2.81800300	C	-5.82028975	1.92615152	0.40325826
H	-6.22773549	2.42391639	1.28848138	H	-6.66998998	1.55929027	-0.18787078
H	-5.30422075	2.68347221	-0.19790688	C	-3.01640394	0.26796730	4.54333016
H	-3.87027733	-0.41857894	4.50077777	H	-2.98906133	0.70198473	5.55133801
H	-2.10840770	-0.33011537	4.41097828	C	-4.71805214	2.62960030	3.64489083
H	-4.86253958	3.47619363	2.96409461	H	-4.60260832	3.03962421	4.65714181
H	-5.63809910	2.03436180	3.64168028	C	-1.71857678	2.83846345	3.41846863
H	-0.74151146	2.41273263	3.16544439	H	-1.66290104	3.17662424	4.46167966
H	-1.86712127	3.72944936	2.79582311	C	-0.61188652	0.24977628	-3.00485983
H	-1.54766537	0.80468045	-2.85108521	H	-0.46456942	0.19055819	-4.09146970
H	0.20467067	0.84961764	-2.59223069	C	0.97541545	-2.34685541	-2.77000015
H	1.82477207	-1.84887400	-2.28756130	H	1.13521237	-2.30307944	-3.85513198

H	1.00582149	-3.40345072	-2.47886995	C	-2.05636467	-2.38540904	-3.27201776
H	-2.12401933	-3.45710637	-3.06290315	H	-1.87408823	-2.27123885	-4.34897452
H	-3.03443061	-1.94087713	-3.05519313	C	0.92563240	-3.31015889	0.96522553
H	1.61332463	-3.45083304	0.12302983	H	0.95649977	-4.22212990	1.57570042
H	1.31476872	-2.48675181	1.57436046	C	-1.43946463	-4.49352448	-0.56105513
H	-2.48390803	-4.40467174	-0.88087646	H	-1.37491756	-5.35777888	0.11317745
H	-0.83578025	-4.72673448	-1.44479775	C	-1.96458428	-2.83350526	1.90170426
H	-1.72589093	-1.99394150	2.56268885	H	-1.86395002	-3.75176187	2.49559079
H	-3.01913714	-2.74379858	1.61545735				

Table 3.16.36 Optimized Coordinates of **3.4-H**.

U	-0.02776729	-0.04979817	0.09480163	H	-0.21721040	-0.15353342	2.11704288
N	1.49480204	1.61123929	-0.18636361	N	-2.17968630	0.59716926	-0.12463181
N	0.69010787	-2.18030639	-0.17327426	Si	1.36818828	2.80658756	-1.47915647
Si	2.79144702	1.73779174	1.01561902	Si	-3.16023418	-0.12148486	-1.40091656
Si	-2.91021137	1.64820670	1.10382875	Si	1.80854423	-2.62954790	-1.46102732
Si	0.13387410	-3.39106635	1.00196024	C	-0.22287304	2.49010436	-2.46884757
H	-0.25070393	1.49389422	-2.93266167	H	-0.27154479	3.21368643	-3.29326120
H	-1.13134172	2.60702812	-1.87054819	C	1.29073617	4.58936503	-0.83227135
H	0.49064134	4.72583648	-0.09567210	H	1.10327295	5.28374125	-1.66160516
H	2.23105037	4.89596639	-0.35881864	C	2.77732208	2.72733052	-2.74923053
H	3.74675471	3.01436406	-2.33107102	H	2.55875216	3.41713827	-3.57531192
H	2.88339282	1.72429282	-3.17705141	C	2.40999334	3.01489714	2.36400036
H	2.25539318	4.01947199	1.95526695	H	3.24114902	3.07131260	3.07921690
H	1.50816288	2.74441403	2.92488820	C	4.47944833	2.18627114	0.26886552
H	4.76804746	1.51407927	-0.54736437	H	5.24541197	2.10441739	1.05120635
H	4.51683949	3.21299456	-0.11260286	C	3.01959990	0.06349982	1.88186892
H	2.12460191	-0.27561951	2.41716774	H	3.81270606	0.17267843	2.63378035
H	3.33005491	-0.73348387	1.19640432	C	-2.06785317	-1.33400792	-2.38601990
H	-1.27760516	-0.82888584	-2.95884871	H	-2.70130675	-1.84411245	-3.12388112
H	-1.59880241	-2.11636177	-1.77864844	C	-4.63593243	-1.10115367	-0.72192474
H	-4.32124152	-1.87103476	-0.00832868	H	-5.17278987	-1.59991810	-1.53919495
H	-5.35531773	-0.45141038	-0.20936945	C	-3.82861941	1.10815247	-2.68207475
H	-4.55492749	1.80910799	-2.25913449	H	-4.33552846	0.55319977	-3.48285574
H	-3.02677939	1.69459868	-3.14368418	C	-3.66445781	0.64986291	2.52649257
H	-4.43697729	-0.04616290	2.18021450	H	-4.12514035	1.31669407	3.26709518
H	-2.89034119	0.06574199	3.03729034	C	-4.26684418	2.77645604	0.39855930
H	-3.89822913	3.39791137	-0.42585609	H	-4.61551058	3.45221559	1.19052429
H	-5.14209964	2.22409709	0.03769226	C	-1.59106034	2.79835050	1.83316411
H	-0.76920056	2.25145190	2.30818512	H	-2.05321255	3.41983844	2.61166878
H	-1.16601441	3.47437366	1.08264691	C	2.28764445	-1.07281764	-2.44117968
H	1.42947891	-0.59571419	-2.93523384	H	2.97908041	-1.36573442	-3.24236685
H	2.79072211	-0.31318659	-1.83516495	C	3.41498262	-3.38983841	-0.79535856
H	3.93911402	-2.70060655	-0.12244340	H	4.09616799	-3.62756312	-1.62269979
H	3.23762013	-4.31886874	-0.24088569	C	1.06988692	-3.81862804	-2.74331493
H	0.91440525	-4.82869358	-2.35335150	H	1.75120942	-3.89814852	-3.60080935
H	0.10740090	-3.45430100	-3.12118370	C	1.22833846	-3.42253220	2.54671187
H	2.27880804	-3.61001052	2.29444730	H	0.90500645	-4.21335724	3.23614080
H	1.17918567	-2.46916343	3.08405773	C	0.08115195	-5.15931583	0.30857321
H	-0.58997132	-5.24646456	-0.55307892	H	-0.30183459	-5.82623304	1.09228829
H	1.06405431	-5.54184457	0.01126780	C	-1.65004233	-2.99686409	1.51912401
H	-1.78855242	-1.97341336	1.88673315	H	-1.94077470	-3.66648881	2.33953085
H	-2.35324571	-3.16626837	0.69462496				

Table 3.16.37 Optimized Coordinates of **3.4-F**.

U	0.01110200	-0.01672500	-0.13700501	F	0.05760800	-0.11814801	-2.20815417
N	-1.78952214	-1.39100011	0.08883501	N	-0.37612303	2.21559317	0.06718100
N	2.14523916	-0.77674506	0.07903601	Si	-1.77908614	-2.57132620	1.39524611
Si	-3.05246223	-1.43872211	-1.15461009	Si	-1.40548911	2.82242422	1.36179911
Si	0.23478002	3.31506625	-1.18523109	Si	3.18500624	-0.14278201	1.35063010
Si	2.77906221	-1.91521415	-1.12537709	C	-0.16137301	-2.35849118	2.38174218
C	-1.82687214	-4.36130033	0.76744306	C	-3.17719424	-2.35978118	2.66020220
C	-4.73619436	-2.02026116	-0.49302004	C	-3.33283826	0.30046702	-1.85288614
C	-2.56910320	-2.58011420	-2.58797420	C	-1.97853315	1.34914110	2.42070319
C	-2.96436323	3.69179328	0.71794005	C	-0.53182404	3.99729730	2.57042719
C	0.45716603	5.10512439	-0.58835004	C	-0.91307607	3.35249325	-2.69194121
C	1.94926515	2.75051021	-1.76888714	C	2.20314717	1.14643309	2.34933518
C	4.72635336	0.72606905	0.66629005	C	3.74799029	-1.44137811	2.61587820
C	4.24282632	-2.95403223	-0.50022704	C	3.33452125	-1.02042308	-2.69835821
C	1.43235311	-3.17227124	-1.58384912	H	0.74810906	-2.43577519	1.77444114
H	-0.10971201	-3.16150024	3.12888624	H	-0.11944801	-1.41662011	2.94628723
H	-2.76024021	-4.58436435	0.23712002	H	-1.75353014	-5.06425239	1.60738012
H	-1.00020808	-4.57335235	0.07978301	H	-3.18954624	-1.35034411	3.08624324
H	-3.03109123	-3.06534123	3.48900127	H	-4.16625332	-2.55433819	2.23439117
H	-4.72152436	-3.04940723	-0.11694701	H	-5.46758343	-1.98553115	-1.31114210
H	-5.11104439	-1.37417211	0.30928202	H	-3.70211328	0.99238208	-1.08677308
H	-4.09068931	0.25507202	-2.64617620	H	-2.43167318	0.73368306	-2.29848418
H	-1.66991612	-2.21253917	-3.09571624	H	-3.37378726	-2.63011220	-3.33301326
H	-2.36787818	-3.60210927	-2.24654917	H	-2.55903719	0.60931605	1.86055414
H	-2.62412420	1.72808913	3.22391225	H	-1.14957909	0.82862206	2.92058622
H	-2.72659421	4.58992935	0.13596401	H	-3.60252328	4.00371930	1.55485512
H	-3.55703727	3.03125223	0.07455901	H	0.38299103	3.55107827	2.97707323
H	-1.19925509	4.20947732	3.41627126	H	-0.26291402	4.95574838	2.11668616
H	-0.47799404	5.57739744	-0.26735702	H	0.85042507	5.70138844	-1.42220211
H	1.17502409	5.18256040	0.23598602	H	-0.94699607	2.37239318	-3.18085824
H	-0.55726004	4.08017931	-3.43285626	H	-1.93874615	3.62718127	-2.41956118
H	2.69260520	2.81808722	-0.96560907	H	2.28490517	3.40956026	-2.58073420
H	1.96510415	1.72912913	-2.16377216	H	1.81584114	1.97086115	1.74126613
H	2.87167122	1.58689212	3.10088124	H	1.36488210	0.70848205	2.90952422
H	5.38383843	0.03415200	0.12691401	H	5.31499141	1.16756409	1.48084811
H	4.45853934	1.53161112	-0.02702600	H	2.90179222	-2.01318615	3.01487623
H	4.23460032	-0.93961207	3.46278027	H	4.46662034	-2.15409616	2.19981617
H	5.12191739	-2.35814618	-0.23074502	H	4.55002735	-3.63707028	-1.30321210
H	3.97350530	-3.56872927	0.36598803	H	2.49047319	-0.50140704	-3.16512124
H	3.73777129	-1.73124313	-3.43111226	H	4.11460232	-0.27875102	-2.48970919
H	1.15065309	-3.78664229	-0.71996805	H	1.81928914	-3.85124429	-2.35522318
H	0.52227304	-2.71870521	-1.99104915				

Table 3.16.38 Optimized Coordinates of **3.4-SPh**.

U	-0.77948677	0.33470532	0.66567336	S	0.36188671	0.52804796	3.12309626
C	1.19328793	-0.79377912	4.00044722	C	0.49478086	-1.57217393	4.93731519
C	2.57169121	-1.00476543	3.83569950	C	1.15784943	-2.55630877	5.67157232
C	3.22804013	-1.99224815	4.57248106	C	2.52501660	-2.77541216	5.48994958
H	-0.56490639	-1.39856515	5.09392166	H	3.12764022	-0.38657813	3.13881113
H	0.60177420	-3.15040191	6.39259092	H	4.29523872	-2.14360061	4.43083770
H	3.03850208	-3.54200195	6.06366186	N	0.49461757	1.79063900	-0.49323487

N	-2.82830179	1.19164768	1.07752945	N	-0.75187338	-1.80407522	-0.08507430
Si	-0.04724047	3.10628469	-1.55800923	Si	2.25106206	1.63490066	-0.21903027
Si	-4.33010858	0.61629304	0.32261612	Si	-2.98031334	2.42229391	2.36586491
Si	-0.36251324	-2.30413949	-1.74332212	Si	-1.05172697	-3.06959015	1.12651169
C	-1.93736700	3.19048882	-1.62867488	H	-2.37287721	2.27752286	-2.05378970
H	-2.21772128	4.01587373	-2.29651625	H	-2.41171733	3.36397362	-0.66068932
C	0.59166358	4.79419209	-0.96916012	H	0.32202573	4.99217410	0.07423201
H	0.15843728	5.59325874	-1.58469446	H	1.68172632	4.87756232	-1.05040148
C	0.46576527	2.90869456	-3.37786076	H	1.53878443	3.02258846	-3.55217241
H	-0.04462943	3.68496068	-3.96383672	H	0.16212637	1.93861205	-3.78613050
C	2.87065080	2.73474189	1.19075141	H	2.70442773	3.79540959	0.96989684
H	3.95036225	2.59378779	1.33338535	H	2.37211393	2.50286148	2.13685874
C	3.32027570	2.04917795	-1.73448051	H	3.05575615	1.45551727	-2.61609793
H	4.36288438	1.81491294	-1.48073718	H	3.28755660	3.10725552	-2.01482558
C	2.67260006	-0.18667118	0.14022340	H	2.06685016	-0.68718874	0.90423029
H	3.70962106	-0.23327988	0.49904706	H	2.61998070	-0.78435715	-0.77663252
C	-3.95056859	-0.73231629	-0.95608805	H	-3.30679425	-0.37407522	-1.77021551
H	-4.89961099	-1.03520614	-1.41821744	H	-3.48578858	-1.62635785	-0.53400189
C	-5.52789725	-0.12454306	1.59670094	H	-5.06221058	-0.91718584	2.19291032
H	-6.39591913	-0.55863773	1.08357918	H	-5.90761040	0.63078142	2.29452555
C	-5.30370025	1.92263906	-0.65492800	H	-5.79909239	2.66403367	-0.02276021
H	-6.08648078	1.40575928	-1.22625354	H	-4.67494996	2.46006750	-1.37194085
C	-3.22702878	1.62994119	4.06788245	H	-4.12561290	1.00248005	4.09145762
H	-3.34431904	2.40712728	4.83432334	H	-2.36947924	1.01056468	4.34837329
C	-4.42672185	3.63115897	2.12180081	H	-4.38352218	4.16167498	1.16443887
H	-4.36392381	4.38579053	2.91740267	H	-5.41142894	3.15875710	2.20492631
C	-1.44397546	3.53944210	2.39311259	H	-0.47746121	3.02704127	2.43072049
H	-1.49419480	4.16308309	3.29578883	H	-1.43806055	4.21315130	1.52856502
C	-0.02703080	-0.78762367	-2.83208667	H	-0.90815080	-0.13885479	-2.92147876
H	0.20724210	-1.13946726	-3.84561058	H	0.80685472	-0.16752936	-2.49458611
C	1.16830753	-3.42569662	-1.80815351	H	2.02634115	-2.99240119	-1.28282539
H	1.46321587	-3.59391704	-2.85217083	H	0.97331911	-4.40946598	-1.36489674
C	-1.75447383	-3.23093127	-2.64513878	H	-1.96044463	-4.22090992	-2.22954593
H	-1.44937756	-3.37238744	-3.69077828	H	-2.69374843	-2.66829721	-2.65106323
C	0.55492372	-3.76644024	1.84214533	H	1.13100409	-4.29320262	1.07241988
H	0.33742352	-4.48539277	2.64235832	H	1.19795349	-2.99008521	2.26768264
C	-2.04747584	-4.55804926	0.49270366	H	-2.98917768	-4.26966093	0.01286123
H	-2.29672228	-5.18958391	1.35604268	H	-1.48586818	-5.18294901	-0.21032204
C	-2.13116422	-2.33068680	2.50641041	H	-1.81195293	-1.35870390	2.90241832
H	-2.12652357	-3.02102598	3.35967126	H	-3.16885273	-2.23202068	2.16838804

Table 3.16.39 Optimized Coordinates of **3.4-Cl**.

U	-0.01401602	-0.02705338	0.30821248	Cl	-0.04823821	-0.03997634	2.91129853
N	1.52175486	1.56735237	-0.10706822	N	-2.15499461	0.58476896	-0.08058364
N	0.64261248	-2.15367937	-0.08670117	Si	1.35245331	2.77859133	-1.39180281
Si	2.90831938	1.72430789	1.00950635	Si	-3.10097501	-0.17308951	-1.37216768
Si	-2.97084694	1.71707472	1.03051430	Si	1.76134414	-2.59404657	-1.38856139
Si	0.07439540	-3.43258255	1.01888898	C	-0.27726941	2.50384285	-2.32613332
H	-0.33498685	1.51958664	-2.81071597	H	-0.33597777	3.24808087	-3.13149302
H	-1.16559738	2.62000133	-1.70023118	C	1.32566219	4.54944526	-0.71064416
H	0.54822873	4.68402965	0.04957868	H	1.12693520	5.26082545	-1.52273247
H	2.28234963	4.83341756	-0.25740229	C	2.69390809	2.69977734	-2.73428842
H	3.67815028	3.02450246	-2.38589372	H	2.40248819	3.36390669	-3.55899394
H	2.80113052	1.69110963	-3.14736286	C	2.48412436	2.83150400	2.48414326

H	2.20103947	3.83997144	2.16127844	H	3.34928632	2.92734885	3.15302844
H	1.65539127	2.41829841	3.06842600	C	4.46854682	2.44384378	0.19641471
H	4.81438705	1.84455888	-0.65316659	H	5.26981786	2.43923252	0.94738536
H	4.35358309	3.47885616	-0.14346447	C	3.44433302	0.01623227	1.63970309
H	2.66916252	-0.53751906	2.17794341	H	4.27560597	0.15798889	2.34344893
H	3.81414308	-0.61359705	0.82243999	C	-2.00687894	-1.41950111	-2.30169041
H	-1.15085233	-0.94751169	-2.80352181	H	-2.61374610	-1.87609463	-3.09487434
H	-1.62397412	-2.23152569	-1.67745548	C	-4.59994547	-1.11855719	-0.69591159
H	-4.30715646	-1.86583573	0.05020555	H	-5.11774760	-1.64224207	-1.50987586
H	-5.32934138	-0.45011367	-0.22355410	C	-3.72583238	1.01463984	-2.71455429
H	-4.48942957	1.70897611	-2.35410611	H	-4.17589895	0.42324136	-3.52325174
H	-2.91401701	1.60531473	-3.15201627	C	-3.73209862	0.81484305	2.51045208
H	-4.49530235	0.09440997	2.19355385	H	-4.21486111	1.53284692	3.18624286
H	-2.97329141	0.27418173	3.08545105	C	-4.36466131	2.71640090	0.21186223
H	-4.01363104	3.30794028	-0.64115246	H	-4.76028108	3.41889259	0.95731940
H	-5.20451360	2.09961771	-0.12610978	C	-1.73523314	3.01725809	1.64798327
H	-0.84549097	2.60404894	2.13322008	H	-2.23639836	3.64824757	2.39420585
H	-1.40890708	3.67328438	0.83265943	C	2.30396039	-1.03485064	-2.32665076
H	1.46593683	-0.49991016	-2.79386875	H	2.96672580	-1.34455336	-3.14563966
H	2.85249211	-0.31849678	-1.70960863	C	3.33181127	-3.43215396	-0.73130193
H	3.84642723	-2.80699637	0.00725944	H	4.03183462	-3.62031258	-1.55570017
H	3.12214821	-4.39728461	-0.25567961	C	1.01123737	-3.72169557	-2.72031062
H	0.82859267	-4.74199474	-2.37242242	H	1.71178471	-3.78350454	-3.56380862
H	0.06615842	-3.32534714	-3.10746659	C	1.20256916	-3.60281469	2.52849808
H	2.22605745	-3.86362681	2.23380415	H	0.83623698	-4.39662616	3.19244215
H	1.24339744	-2.67533921	3.10818283	C	-0.03806394	-5.15187225	0.21755369
H	-0.71635214	-5.17046128	-0.64236552	H	-0.43951334	-5.84683471	0.96707214
H	0.93014186	-5.54994447	-0.10456429	C	-1.70037322	-3.05055300	1.57867658
H	-1.84875189	-2.05320213	2.00584030	H	-1.97966929	-3.76610280	2.36355146
H	-2.40973399	-3.18086167	0.75257794				

Table 3.16.40 Optimized Coordinates of **3.4-Br**.

U	-0.01610266	-0.02564827	0.33262895	Br	-0.04524743	-0.03243591	3.09539519
N	1.51805254	1.56533759	-0.08927903	N	-2.15421259	0.58432868	-0.06728356
N	0.64061327	-2.15000709	-0.07099709	Si	1.34107596	2.78353412	-1.36862235
Si	2.92652159	1.71649406	1.00406027	Si	-3.09552994	-0.18404008	-1.35818132
Si	-2.98344238	1.73426533	1.01846765	Si	1.76335513	-2.58253793	-1.37414445
Si	0.07008758	-3.44646786	1.01546126	C	-0.29771302	2.52208658	-2.29011766
H	-0.36233861	1.54139725	-2.78085657	H	-0.35876906	3.27230416	-3.08976021
H	-1.18097403	2.63687866	-1.65733130	C	1.33202419	4.55117501	-0.67890866
H	0.56665712	4.68595585	0.09333753	H	1.12458606	5.26662757	-1.48520201
H	2.29657144	4.82907547	-0.23884065	C	2.66451875	2.70616934	-2.72936651
H	3.65458567	3.02741901	-2.39507701	H	2.36133076	3.37493228	-3.54608047
H	2.76320517	1.69952903	-3.14934415	C	2.54055693	2.84238260	2.47474240
H	2.26441778	3.85121321	2.14722588	H	3.41815978	2.93346523	3.12793806
H	1.71694277	2.44345902	3.07555093	C	4.47867373	2.41306082	0.15565239
H	4.79931543	1.80567628	-0.69810107	H	5.29467968	2.40008462	0.89050839
H	4.37128139	3.44820032	-0.18591743	C	3.46394358	0.00920172	1.63536448
H	2.69503478	-0.53707974	2.18959640	H	4.30693564	0.15293818	2.32471661
H	3.81894066	-0.62625548	0.81606491	C	-1.99963767	-1.43690415	-2.27594714
H	-1.13854619	-0.96913738	-2.77294237	H	-2.60378412	-1.89140736	-3.07240149
H	-1.62376923	-2.24933345	-1.64853777	C	-4.59797379	-1.12242095	-0.68010132
H	-4.31006615	-1.85913411	0.07824943	H	-5.10914395	-1.65743673	-1.49087764
H	-5.33146158	-0.44829714	-0.22243990	C	-3.71441148	0.99026726	-2.71555300

H	-4.49765276	1.67136519	-2.37302702	H	-4.13746763	0.38763292	-3.53052314
H	-2.90548696	1.59437307	-3.13969511	C	-3.76955119	0.85046587	2.49593711
H	-4.53736814	0.13672999	2.17527818	H	-4.25062386	1.57766235	3.16301614
H	-3.02097742	0.30522931	3.07932946	C	-4.36524373	2.72302864	0.16748602
H	-4.00525613	3.29944104	-0.69197260	H	-4.76528868	3.43909196	0.89756823
H	-5.20408281	2.10309370	-0.16701912	C	-1.75885471	3.04610859	1.63394769
H	-0.87659777	2.64318493	2.14092907	H	-2.27463267	3.68768251	2.36103900
H	-1.42181241	3.68969322	0.81319220	C	2.31180609	-1.01940672	-2.30182611
H	1.47636865	-0.48330935	-2.77224570	H	2.97903002	-1.32720275	-3.11794224
H	2.85654109	-0.30458594	-1.67997528	C	3.32963046	-3.42978965	-0.71859110
H	3.83913343	-2.81672837	0.03338562	H	4.03498191	-3.60448903	-1.54141078
H	3.11721417	-4.40260412	-0.26026720	C	1.01761059	-3.69815806	-2.71885826
H	0.83761669	-4.72291045	-2.38326201	H	1.72064673	-3.74792096	-3.56109752
H	0.07236156	-3.30057599	-3.10408971	C	1.19655278	-3.64147868	2.52324597
H	2.22082668	-3.89510655	2.22521363	H	0.83024254	-4.44783180	3.17191489
H	1.23381396	-2.72396666	3.11852412	C	-0.03918202	-5.15449504	0.18934883
H	-0.71443586	-5.16296405	-0.67303486	H	-0.44391409	-5.85797611	0.92913604
H	0.92990039	-5.54965707	-0.13336424	C	-1.70776075	-3.07807033	1.57414713
H	-1.85624717	-2.09170479	2.02559544	H	-1.99076727	-3.81299387	2.33958916
H	-2.41275653	-3.18794854	0.74149550				

Table 3.16.41 Optimized Coordinates of **3.4-I**.

U	-0.01799439	-0.02432094	0.48151307	I	-0.03057506	-0.00492384	3.52541242
N	1.48536460	1.55661382	-0.05100187	N	-2.14163953	0.54346538	-0.02598270
N	0.67020006	-2.10621046	-0.03989342	Si	1.28185780	2.78725678	-1.32246262
Si	2.94766689	1.70162800	0.97716014	Si	-3.06855316	-0.25006788	-1.32003119
Si	-3.00024770	1.73788586	0.99221677	Si	1.80860292	-2.53189558	-1.33960716
Si	0.06307471	-3.43334351	0.99138297	C	-0.37121982	2.54804759	-2.21868999
H	-0.43698498	1.57786813	-2.72830842	H	-0.44625300	3.31751886	-2.99859113
H	-1.24422634	2.64205046	-1.56966627	C	1.30340220	4.54777640	-0.61398171
H	0.56972381	4.67831166	0.18895098	H	1.06463832	5.26863251	-1.40672836
H	2.28514344	4.82282434	-0.21185710	C	2.57171450	2.72449319	-2.71653939
H	3.56925532	3.04927357	-2.41009966	H	2.23893043	3.40009482	-3.51599352
H	2.66375888	1.72369947	-3.15098952	C	2.65920242	2.87107675	2.43612889
H	2.43126376	3.88741105	2.09516809	H	3.55904319	2.92532686	3.06272609
H	1.83280732	2.53337584	3.06910621	C	4.48001761	2.34597962	0.05686860
H	4.74296606	1.73226549	-0.81134292	H	5.32517744	2.30312272	0.75683451
H	4.39053987	3.38549760	-0.27542823	C	3.48109631	-0.00716048	1.61063281
H	2.71387127	-0.57730418	2.14308448	H	4.30435145	0.14205584	2.32226269
H	3.86478894	-0.62612331	0.79193385	C	-1.97484100	-1.51515100	-2.21720568
H	-1.10647674	-1.04998713	-2.70255089	H	-2.57392288	-1.96771392	-3.01854872
H	-1.60709641	-2.32481289	-1.58289200	C	-4.58562601	-1.16578110	-0.64267234
H	-4.31983156	-1.88079202	0.14371606	H	-5.07798194	-1.72321504	-1.45008448
H	-5.32887559	-0.47676404	-0.22460243	C	-3.67800483	0.89916291	-2.70427325
H	-4.50152624	1.54899647	-2.39835849	H	-4.04468735	0.27359847	-3.52922706
H	-2.87992351	1.53305684	-3.10372620	C	-3.87814449	0.91328206	2.45160297
H	-4.64495429	0.20748891	2.11181118	H	-4.37685400	1.67123574	3.06975938
H	-3.17719492	0.36939584	3.09254195	C	-4.31796092	2.73935811	0.06000835
H	-3.91706662	3.25854414	-0.81738109	H	-4.70133729	3.50520265	0.74747607
H	-5.17570901	2.13921788	-0.26195162	C	-1.77582985	3.04470540	1.62251259
H	-0.87428999	2.65463981	2.10604759	H	-2.28765946	3.65897455	2.37551737
H	-1.46804339	3.71310578	0.81035471	C	2.39562305	-0.97571768	-2.24836595
H	1.57042381	-0.44320429	-2.73888328	H	3.08471389	-1.28689203	-3.04475993
H	2.92031994	-0.25920410	-1.61262702	C	3.34134156	-3.42766268	-0.66891951

H	3.83394704	-2.85854833	0.12719317	H	4.07042471	-3.57457347	-1.47630789
H	3.10040291	-4.41818090	-0.26570023	C	1.06997408	-3.61810778	-2.71334598
H	0.86565937	-4.64519005	-2.40029243	H	1.79419642	-3.66525247	-3.53770474
H	0.14192451	-3.19970857	-3.11698188	C	1.20178573	-3.75717751	2.46657089
H	2.20230661	-4.05920494	2.13584985	H	0.79832516	-4.56786538	3.08713020
H	1.30864797	-2.87240309	3.10172393	C	-0.14642391	-5.09384660	0.09298915
H	-0.81181654	-5.02725213	-0.77454522	H	-0.60236270	-5.79755386	0.80227437
H	0.79939869	-5.53675229	-0.23640156	C	-1.69230073	-3.01011358	1.58921687
H	-1.83986903	-2.00165811	1.99185349	H	-1.95149644	-3.69607315	2.40661064
H	-2.42058182	-3.16716463	0.78511343				

Table 3.16.42 Optimized Coordinates of **3.4-CN**.

U	-0.96581928	0.20402922	0.40225219	C	0.04830448	-0.08970117	2.64294238
N	0.57352743	-0.22310938	3.68057578	N	0.50753158	1.59896047	-0.55898043
N	-2.84837698	1.20212595	1.11737350	N	-0.90295571	-1.92786772	-0.31731172
Si	0.05674618	2.96773732	-1.59223134	Si	2.23006453	1.37943850	-0.13681014
Si	-4.39531253	0.77455354	0.36966048	Si	-2.82743535	2.28007502	2.54061310
Si	-0.54293376	-2.40354833	-1.98608317	Si	-1.17519045	-3.19610678	0.90803418
C	-1.83443006	3.06533825	-1.72264929	H	-2.27886090	2.16715027	-2.17364096
H	-2.09140181	3.90156879	-2.38622460	H	-2.32836913	3.23892608	-0.76291762
C	0.67567248	4.62445133	-0.90699632	H	0.32754212	4.80372732	0.11634137
H	0.31139686	5.44912287	-1.53330790	H	1.77017042	4.68327267	-0.89711755
C	0.66225293	2.82713954	-3.38599823	H	1.74806505	2.91041298	-3.48626809
H	0.21584843	3.64135077	-3.97243872	H	0.35623556	1.88283931	-3.84906588
C	2.70676550	2.37908003	1.39710485	H	2.47769183	3.44447875	1.28210462
H	3.78408693	2.28886494	1.58829450	H	2.18361916	2.01407288	2.28762575
C	3.41986048	1.86132196	-1.53604416	H	3.22875591	1.30616951	-2.46116558
H	4.44049214	1.61865510	-1.21215431	H	3.40316067	2.93064234	-1.77324858
C	2.58183183	-0.45401440	0.20740294	H	1.99348143	-0.89268698	1.01990658
H	3.63298180	-0.53867610	0.51478030	H	2.45202936	-1.07192350	-0.68811465
C	-4.06608099	-0.48337906	-1.02189310	H	-3.44554958	-0.07766505	-1.83349615
H	-5.03171604	-0.73751808	-1.47887252	H	-3.61307740	-1.42210816	-0.68858317
C	-5.59495597	-0.02607556	1.60000403	H	-5.14843784	-0.89012863	2.10412252
H	-6.49897222	-0.36922807	1.08049951	H	-5.91360513	0.67916434	2.37645311
C	-5.30568953	2.21007758	-0.47140364	H	-5.68514074	2.94935126	0.23948520
H	-6.16849732	1.80737918	-1.01877963	H	-4.67247041	2.73419726	-1.19492435
C	-3.04889683	1.30481981	4.14609687	H	-3.97135845	0.71249968	4.13882841
H	-3.10069879	1.98884494	5.00319190	H	-2.20816224	0.62447162	4.31672989
C	-4.18090202	3.61286453	2.48954710	H	-4.12848703	4.23346953	1.58786894
H	-4.03809485	4.27559859	3.35315900	H	-5.19556919	3.20557050	2.56193803
C	-1.18808204	3.22974243	2.60253075	H	-0.29928214	2.59370942	2.65885561
H	-1.18394762	3.85072158	3.50833281	H	-1.07968927	3.90269392	1.74419508
C	-0.14383737	-0.86263828	-3.02036773	H	-0.98468658	-0.15766521	-3.07555223
H	0.05630054	-1.18405283	-4.05115496	H	0.73207994	-0.31018747	-2.66998251
C	0.94760156	-3.57149094	-2.09220536	H	1.83926507	-3.13895587	-1.62430510
H	1.18920375	-3.77872831	-3.14276561	H	0.75632110	-4.53536337	-1.60633250
C	-2.00281308	-3.22453509	-2.87935282	H	-2.24844149	-4.21530977	-2.48737925
H	-1.74918698	-3.34471623	-3.94098036	H	-2.90863298	-2.60969077	-2.82633709
C	0.43613584	-3.71161827	1.75178271	H	1.18041691	-4.05589386	1.02406063
H	0.25187250	-4.53540484	2.45357092	H	0.87396180	-2.88512776	2.32124947
C	-1.99077503	-4.76779249	0.22141079	H	-2.95923702	-4.56894228	-0.25069914
H	-2.17014817	-5.44981800	1.06304235	H	-1.36526852	-5.30459652	-0.49997135
C	-2.39575515	-2.54552483	2.21169737	H	-2.12803913	-1.59156433	2.67963238
H	-2.44025634	-3.27546980	3.03099631	H	-3.40723123	-2.45625538	1.79806929

Table 3.16.43 Optimized Coordinates of $U^{VI}O[N(SiMe_3)_2]_2(CH_2SiMe_2\mathit{N}SiMe_3)$.

U	-0.00587371	0.02783615	-0.07322929	O	0.05716615	-0.04287491	-1.86689281
N	-0.12048214	2.25421572	-0.02259794	N	-1.91448920	-1.20506912	-0.04625922
N	2.05327292	-0.86032260	0.12498843	Si	-0.50624869	3.54151037	-1.17046635
Si	0.22751143	2.48172680	1.69864425	Si	-3.38942594	-0.82693432	0.85911045
Si	3.33785543	-0.46094460	-1.04199975	Si	-2.00579659	-2.55172068	-1.21462985
Si	2.35719415	-2.11053928	1.34311980	C	-2.30633145	4.09616638	-0.93346492
C	-0.98861969	3.60596248	2.61399686	C	0.61959855	5.04456971	-0.88917709
C	-3.39251401	0.95406674	1.52234456	C	1.98119459	3.10631321	2.04025905
C	-0.31660628	2.98990677	-2.96679987	C	0.08592882	0.64396789	2.17087897
C	-4.95078847	-0.90484736	-0.22287028	C	-3.60388770	-1.96642526	2.36108742
C	3.14428004	1.31336594	-1.67647088	C	3.47018039	-1.50509658	2.75759157
C	-2.70392870	-1.97596301	-2.87672521	C	0.73224947	-2.68635709	2.16325782
C	5.07254970	-0.52431659	-0.26493086	C	-3.03012364	-4.01918109	-0.56528138
C	-0.29638040	-3.31797801	-1.52553722	C	3.30570521	-1.62190461	-2.53783937
C	3.14941091	-3.66635586	0.59588264	H	-2.54627174	4.92148385	-1.61635499
H	-2.50550767	4.44209823	0.08719406	H	-0.88701165	4.64472648	2.27623065
H	0.38869392	5.83056119	-1.61972238	H	0.49509771	5.48295963	0.10862202
H	-0.77177936	3.58839344	3.68950328	H	-2.03017839	3.30559693	2.47218565
H	-3.00577742	3.27904788	-1.14999636	H	-4.43382872	1.22674427	1.73890672
H	1.67749260	4.78274658	-1.01023277	H	2.14469931	4.10552534	1.62034515
H	-0.67401921	3.78859949	-3.63001265	H	-2.83393945	1.07374376	2.45514604
H	2.16177160	3.16582119	3.12143631	H	-3.01349009	1.68580169	0.80070066
H	-5.82639354	-0.66918314	0.39626074	H	-4.47105368	-1.65455973	2.95771091
H	-0.89316318	2.08531293	-3.18413184	H	0.72689609	2.78467368	-3.22820136
H	-0.83318815	0.37151603	2.69989597	H	2.73454832	2.43568656	1.61171467
H	-4.90553305	-0.15621608	-1.02342549	H	-2.72147887	-1.92547828	3.01186728
H	0.95400105	0.22945798	2.68752598	H	3.19883701	2.05459566	-0.87053193
H	-5.13216793	-1.87752107	-0.68883663	H	-3.75473428	-3.01289649	2.07625661
H	2.20286633	1.45958187	-2.21258546	H	3.09799659	-0.57615649	3.20649357
H	3.96157523	1.52926102	-2.37763787	H	-2.08388379	-1.17007633	-3.28501665
H	5.16634534	0.17901517	0.57082832	H	-3.73010595	-1.60350031	-2.79014769
H	3.50215066	-2.26282058	3.55169365	H	0.48285962	-2.08779370	3.04534972
H	-0.14928576	-2.69410678	1.51202459	H	4.49916916	-1.32406181	2.43136730
H	-4.08696031	-3.79975249	-0.38513514	H	5.80473622	-0.22497009	-1.02650417
H	-2.70702899	-2.79953828	-3.60235337	H	-2.60625517	-4.41338715	0.36620764
H	5.36764111	-1.51542479	0.09521819	H	0.87806438	-3.72081083	2.50185796
H	0.46364454	-2.61001521	-1.86603860	H	2.35549898	-1.53536553	-3.07691449
H	-2.98757374	-4.82657459	-1.30841478	H	4.11061250	-1.36461597	-3.23858411
H	0.08582629	-3.83677349	-0.63901313	H	3.43672985	-2.67114287	-2.25175760
H	-0.40958482	-4.07197486	-2.31652314	H	4.12848232	-3.47759907	0.14300989
H	3.29330417	-4.41618715	1.38490313	H	2.50883413	-4.11287995	-0.17317633

Table 3.16.44 Optimized Coordinates of N-methylmorpholine-*N*-oxide.

C	0.63755220	-1.16085042	1.17264583	C	-0.42095012	-0.05994085	1.22208947
C	-0.42095012	-0.05994085	-1.22208947	C	0.63755220	-1.16085042	-1.17264583
H	-1.42833121	-0.47938043	1.22804780	H	-0.31119641	0.59629869	2.08878015
H	1.65495679	-0.74030566	1.24225965	H	0.50070450	-1.83887689	2.02079211
H	-1.42833121	-0.47938043	-1.22804780	H	-0.31119641	0.59629869	-2.08878015
H	0.50070450	-1.83887689	-2.02079211	H	1.65495679	-0.74030566	-1.24225965
N	-0.42095012	0.83924324	0.00000000	O	0.51076447	-1.95071725	-0.00000000
O	-1.53712800	1.60659484	0.00000000	C	0.77375499	1.74883887	0.00000000
H	0.67729586	2.37328494	-0.88787329	H	0.67729586	2.37328494	0.88787329

H 1.72895023 1.21264982 0.00000000

Table 3.16.45 Optimized Coordinates of N-methylmorpholine.

C	0.97801562	-1.17634334	0.32965014	C	-0.23853198 -1.20026645 -0.60390952
C	-0.23848965	1.20028031	-0.60390244	C	0.97805882 1.17631970 0.32965369
H	0.12393620	-1.26097503	-1.63948441	H	-0.85486068 -2.08745623 -0.41320396
H	0.66206269	-1.23127595	1.38574512	H	1.64335867 -2.02318628 0.13074850
H	0.12397821	1.26097902	-1.63947786	H	-0.85479041 2.08748672 -0.41319192
H	1.64343127	2.02314282	0.13076205	H	0.66210474 1.23125245 1.38574856
N	-1.07503193	0.00001856	-0.48950718	O	1.75237652 -0.00002251 0.11658942
C	-1.96888304	0.00001486	0.66274601	H	-1.47718359 -0.00010270 1.65250885
H	-2.61333917	0.88543855	0.61419042	H	-2.61350519 -0.88528368 0.61406231

Table 3.16.46 Optimized Coordinates of Cp_2Fe.

Fe	0.00000000	0.00000000	0.00000000	C	0.81934337 1.91218925 0.00000000
H	1.88162568	2.12051526	0.00000000	C	0.00000000 1.73055374 1.15458986
H	0.33188314	1.77743459	2.18405063	C	-1.32515147 1.43732320 0.71354590
H	-2.17405167	1.22083759	1.34963978	C	-0.81934337 -1.91218925 -0.00000000
H	-1.88162568	-2.12051526	-0.00000000	C	0.00000000 -1.73055374 -1.15458986
C	-0.00000000	1.73055374	-1.15458986	C	0.00000000 -1.73055374 1.15458986
H	0.33188314	1.77743459	-2.18405063	H	-0.33188314 -1.77743459 2.18405063
H	-0.33188314	-1.77743459	-2.18405063	C	-1.32515147 1.43732320 -0.71354590
C	1.32515147	-1.43732320	0.71354590	C	1.32515147 -1.43732320 -0.71354590
H	-2.17405167	1.22083759	-1.34963978	H	2.17405167 -1.22083759 1.34963978
H	2.17405167	-1.22083759	-1.34963978		

Table 3.16.47 Optimized Coordinates of $[Cp_2Fe]^+$.

Fe	0.00000000	0.00000000	0.00000000	C	0.82082616 1.92715050 0.00000000
H	1.88381136	2.13167444	0.00000000	C	-0.00000000 1.74636077 1.15656522
H	0.33262503	1.79040419	2.18578902	C	-1.32783119 1.45434271 0.71477391
H	-2.17651655	1.23688902	1.35066441	C	-0.82082616 -1.92715050 -0.00000000
H	-1.88381136	-2.13167444	-0.00000000	C	-0.00000000 -1.74636077 -1.15656522
C	-0.00000000	1.74636077	-1.15656522	C	0.00000000 -1.74636077 1.15656522
H	0.33262503	1.79040419	-2.18578902	H	-0.33262503 -1.79040419 2.18578902
H	-0.33262503	-1.79040419	-2.18578902	C	-1.32783119 1.45434271 -0.71477391
C	1.32783119	-1.45434271	0.71477391	C	1.32783119 -1.45434271 -0.71477391
H	-2.17651655	1.23688902	-1.35066441	H	2.17651655 -1.23688902 1.35066441
H	2.17651655	-1.23688902	-1.35066441		

Table 3.16.48 Optimized Coordinates of HCCMe.

C	0.00000000	0.00000000	0.21901242	C	-0.00000000 -0.00000000 1.42629757
H	-0.00000000	-0.00000000	2.49220165	C	0.00000000 0.00000000 -1.24156018
H	-0.00000000	1.02249656	-1.63823350	H	0.88550800 -0.51124828 -1.63823350
H	-0.88550800	-0.51124828	-1.63823350		

Table 3.16.49 Optimized Coordinates of CH_4.

C	0.00000000	0.00000000	0.00000000	H	0.63139706 0.63139706 0.63139706
H	-0.63139706	-0.63139706	0.63139706	H	-0.63139706 0.63139706 -0.63139706
H	0.63139706	-0.63139706	-0.63139706		

Table 3.16.50 Optimized Coordinates of $U^{III}[N(SiMe_3)_2]_3$.

U	0.00369015	-0.00612090	-0.37105958	N	1.87892097 -1.32473735 0.10510482
N	-2.09015646	-0.93551103	0.10413631	N	0.24281635 2.26400836 0.09227991
Si	1.97763494	-2.51254795	1.38412528	Si	3.11331729 -1.09554429 -1.09700866

Si	-3.18938232	-0.40186278	1.35672168	Si	-2.49989399	-2.16331405	-1.06042559
Si	1.26979303	2.98633476	1.31354782	Si	-0.65799191	3.19874896	-1.06812541
C	0.56523228	-2.20320487	2.61638516	H	0.66955824	-1.23620949	3.12405901
H	0.56762289	-2.97753851	3.39443221	H	-0.42117643	-2.23505311	2.13610919
C	1.78461929	-4.29556815	0.75434752	H	0.84383114	-4.42845342	0.20589871
H	1.77928959	-5.00344716	1.59356163	H	2.59918610	-4.58874921	0.08214666
C	3.60909335	-2.42997812	2.35497744	H	4.47375453	-2.69645160	1.73465190
H	3.58706680	-3.13121874	3.19926816	H	3.78918123	-1.42727848	2.76071682
C	3.66544504	-2.68487710	-1.97745704	H	4.19547418	-3.36120171	-1.29640363
H	4.35138835	-2.44915819	-2.80148718	H	2.81661267	-3.23915611	-2.39575395
C	4.67564891	-0.21458626	-0.48028372	H	4.44012055	0.74874832	-0.01320401
H	5.37135143	-0.02427772	-1.30794806	H	5.20778590	-0.81703623	0.26510606
C	2.37206852	0.02998843	-2.47186019	H	1.47150031	-0.38472301	-2.95421419
H	3.11271465	0.10917629	-3.27805812	H	2.16623605	1.06196047	-2.15324151
C	-2.24857336	0.66009165	2.62056031	H	-1.50929336	0.07247838	3.17843471
H	-2.95180722	1.07554975	3.35415240	H	-1.73161449	1.50707493	2.15244771
C	-4.60470817	0.66948014	0.67501029	H	-4.22264912	1.52297218	0.10140506
H	-5.21813835	1.07106439	1.49223569	H	-5.26971352	0.10354509	0.01282538
C	-3.97813343	-1.84273488	2.31268201	H	-4.64259684	-2.44714644	1.68286912
H	-4.58095889	-1.46272483	3.14777917	H	-3.21765912	-2.51290594	2.73134269
C	-4.17858806	-1.90179042	-1.91012055	H	-5.01142993	-2.01699206	-1.20607010
H	-4.32566022	-2.63785044	-2.71117618	H	-4.26031872	-0.90248439	-2.35459408
C	-2.46919992	-3.93625157	-0.38713923	H	-1.50624188	-4.17518097	0.07931671
H	-2.64062782	-4.66409489	-1.19098617	H	-3.24616073	-4.09219107	0.36999327
C	-1.18742147	-2.10617488	-2.46509527	H	-1.11641295	-1.13271467	-2.97600649
H	-1.49093961	-2.81618770	-3.24533221	H	-0.18268975	-2.42229702	-2.14978774
C	1.71923873	1.67956126	2.61551077	H	0.83881011	1.34844011	3.18018389
H	2.43144307	2.09621783	3.33956817	H	2.19129971	0.79578709	2.16830236
C	2.89789453	3.64526540	0.58747094	H	3.44687863	2.85887041	0.05523721
H	3.55355503	4.02537427	1.38172162	H	2.73100559	4.46381735	-0.12221539
C	0.43070285	4.42770209	2.22450726	H	0.25101705	5.28699488	1.56672411
H	1.06451571	4.77854042	3.04934800	H	-0.53432766	4.13012914	2.65186637
C	0.37946284	4.47067374	-2.02300935	H	0.73749811	5.27403267	-1.36820012
H	-0.21797189	4.93940724	-2.81574029	H	1.25861988	4.01259628	-2.49198740
C	-2.16802953	4.09929772	-0.35889982	H	-2.83362000	3.41121829	0.17494754
H	-2.75102006	4.57744576	-1.15686077	H	-1.87330825	4.88282891	0.34817677
C	-1.33854569	1.97619020	-2.38911088	H	-0.55481001	1.41585148	-2.92613094
H	-1.85490518	2.55577498	-3.16558673	H	-2.08774455	1.26971768	-2.00155409

Table 3.16.51 Optimized Coordinates of $U^{III}(N_3CPh_3)[N(SiMe_3)_2]_3$.

U	-1.54304307	0.02073467	0.07044620	N	-2.11883447	-0.35701334	-2.09844319
N	-1.68259613	2.14901005	0.86451253	N	-2.06434564	-1.67213122	1.49728833
N	0.68488625	-0.14558275	-0.01512895	N	1.90258540	-0.14250199	-0.13817098
N	2.87686527	-0.06240431	0.65558258	C	4.23267261	-0.07509061	0.00497003
C	5.25746954	-0.11958550	1.16207147	C	4.87083583	-0.05750793	2.50584162
C	6.62548913	-0.22515605	0.86580170	C	5.82719144	-0.10442553	3.52540282
H	3.81998514	0.02780153	2.75343192	C	7.57852751	-0.26574518	1.88108162
H	6.94911716	-0.27946508	-0.16915732	C	7.18284735	-0.20777710	3.22015700
H	5.50349535	-0.05739340	4.56215568	H	8.63178376	-0.34724254	1.62524110
H	7.92460568	-0.24388556	4.01367119	C	4.42529929	-1.36421600	-0.82769424
C	5.20657834	-1.40137670	-1.99057838	C	3.88650123	-2.57079522	-0.35336353
C	5.42203000	-2.60261314	-2.67196164	H	5.64682778	-0.48854090	-2.37754831
C	4.09740600	-3.76866570	-1.03438123	H	3.30585456	-2.57268540	0.56334132
C	4.86468028	-3.79043423	-2.20131667	H	6.02760092	-2.60262733	-3.57466607

H	3.66495524	-4.68754648	-0.64714396	H	5.02941060	-4.72358172	-2.73333025
C	4.35786753	1.22930504	-0.81552586	C	4.96142124	2.37279559	-0.27461662
C	3.76140266	1.33397226	-2.08328585	C	4.98398078	3.57702778	-0.98230813
H	5.41656773	2.32726326	0.70820790	C	3.78678435	2.53499086	-2.79316689
H	3.27929454	0.46893364	-2.52561953	C	4.40106421	3.66382565	-2.24639703
H	5.46201849	4.44732641	-0.54008866	H	3.32612691	2.58455955	-3.77636412
H	4.42482831	4.59868338	-2.80017485	Si	-3.37003507	0.58067681	-2.92066475
Si	-1.14027032	-1.50858054	-3.02873097	Si	-2.87850535	2.64396539	2.06526002
Si	-0.43701672	3.30169934	0.34153228	Si	-3.49232338	-2.70060835	1.33201336
Si	-0.88443567	-2.03499426	2.77558645	C	-4.13771755	1.81321670	-1.69539375
H	-4.63032333	1.31852573	-0.84709159	H	-4.92029242	2.37869195	-2.21846470
H	-3.42311648	2.53702226	-1.29309057	C	-2.67679092	1.57938580	-4.37849567
H	-1.83618033	2.21218775	-4.07199916	H	-3.45391468	2.23165531	-4.79760591
H	-2.32423414	0.93160122	-5.18999917	C	-4.83179266	-0.44211802	-3.57182316
H	-4.56100669	-1.10435973	-4.39934330	H	-5.60675641	0.24333017	-3.94046375
H	-5.28390461	-1.05634639	-2.78532668	C	0.37852910	-0.67510998	-3.79785847
H	0.09684060	0.11902869	-4.49906165	H	0.98286043	-1.40793218	-4.34822701
H	1.01665244	-0.22986492	-3.02673089	C	-2.08338534	-2.36529129	-4.43765325
H	-2.96768397	-2.90457363	-4.08004454	H	-1.41529980	-3.10196177	-4.90321418
H	-2.40443069	-1.67704583	-5.22753758	C	-0.54447708	-2.91027517	-1.89624512
H	0.03597181	-2.57161963	-1.03153139	H	0.11336210	-3.57342560	-2.47356036
H	-1.38139571	-3.51519989	-1.52883782	C	-3.96994914	1.15590289	2.51761983
H	-4.53204177	0.76405302	1.65856057	H	-4.71782839	1.48130120	3.25287646
H	-3.41410540	0.32406825	2.95954480	C	-2.07276064	3.26907181	3.66634612
H	-1.38426931	2.52904449	4.09038798	H	-2.83966774	3.48473332	4.42161579
H	-1.50391859	4.19267871	3.50675207	C	-4.08884626	3.97900305	1.46706734
H	-3.61003773	4.94579126	1.28704770	H	-4.85964913	4.13174457	2.23438253
H	-4.59873562	3.68038629	0.54430670	C	1.11326071	3.20038309	1.42344551
H	0.87598067	3.43306597	2.46881300	H	1.86600540	3.92367439	1.08409940
H	1.58078319	2.21019976	1.40165470	C	-0.99963201	5.11754732	0.36468189
H	-1.86789239	5.29518796	-0.27980805	H	-0.17617376	5.73594292	-0.01676881
H	-1.24224991	5.48674330	1.36737466	C	0.00417607	2.95698554	-1.47437319
H	0.20304248	1.90616995	-1.71269584	H	0.91678151	3.50661364	-1.73761584
H	-0.79815152	3.30498475	-2.13653500	C	-4.48907035	-2.17279107	-0.19504445
H	-4.84341492	-1.13470551	-0.13376830	H	-5.38640552	-2.80250743	-0.25966207
H	-3.93836220	-2.28199038	-1.13312614	C	-3.04263235	-4.53245521	1.11086717
H	-2.36660230	-4.68726105	0.26205311	H	-3.94877680	-5.12477640	0.92871157
H	-2.55516114	-4.95019512	1.99967299	C	-4.71712529	-2.58237385	2.77861858
H	-4.31997506	-2.97993662	3.71670612	H	-5.61604813	-3.16262798	2.53072219
H	-5.03320086	-1.54920191	2.96028071	C	0.45277430	-3.22648902	2.15593598
H	0.02034642	-4.18083609	1.83283483	H	1.18329339	-3.44090200	2.94672663
H	0.99652582	-2.80412602	1.30394162	C	-1.63527301	-2.80979901	4.34011368
H	-2.38238588	-2.16105912	4.81074444	H	-0.82558542	-2.95849072	5.06680435
H	-2.09745660	-3.78779796	4.16756083	C	-0.05698727	-0.43456562	3.37481970
H	0.47012491	0.12473314	2.59406842	H	0.69181081	-0.69027519	4.13650051
H	-0.78406772	0.23828018	3.84477388				

Table 3.16.52 Optimized Coordinates of $U^{IV}(N_3)[N(SiMe_3)_2]_3$.

U	0.00519421	-0.01255555	0.11081105	N	-0.31521624	2.20906547	-0.19328690
N	-1.80375952	-1.34305019	-0.24482186	N	2.10120044	-0.81646425	-0.24901207
Si	-1.37670260	2.84686867	-1.45591902	Si	0.38953261	3.33793360	0.98716144
Si	-1.80192424	-2.50917090	-1.57107483	Si	-3.13707912	-1.35667638	0.92874454
Si	3.13249214	-0.18717735	-1.53866113	Si	2.76092230	-2.01378019	0.88391968

C	-2.12198168	1.40649517	-2.44541334	H	-1.36258266	0.78973025	-2.94605952
H	-2.74928808	1.82671083	-3.24272867	H	-2.75100792	0.74270334	-1.84594004
C	-2.81936170	3.85069698	-0.74108620	H	-3.39989003	3.26467243	-0.01940849
H	-3.50094412	4.16442535	-1.54231133	H	-2.47948650	4.75878243	-0.22966968
C	-0.49474331	3.92131182	-2.74932923	H	-0.12361083	4.86804643	-2.34676609
H	-1.20143348	4.16151242	-3.55490518	H	0.35293567	3.39453001	-3.20174439
C	-0.74414610	3.56411461	2.48876030	H	-1.72930853	3.94542224	2.19587009
H	-0.30851085	4.27877854	3.19886772	H	-0.90020804	2.62010306	3.02235084
C	0.74109307	5.06853793	0.28569942	H	1.43735328	5.04278256	-0.56007126
H	1.20970953	5.66843694	1.07712815	H	-0.15850598	5.60530943	-0.03450930
C	2.07626755	2.70124768	1.58254836	H	2.05700282	1.68811592	1.99765487
H	2.44235372	3.36375071	2.37832136	H	2.81773150	2.72287426	0.77512450
C	-0.16421218	-2.35327311	-2.52703640	H	-0.03450297	-1.37369803	-3.00846247
H	-0.17273450	-3.09252609	-3.33892062	H	0.72406678	-2.55124732	-1.91883202
C	-1.92677005	-4.30002192	-0.95652475	H	-1.12988975	-4.54070249	-0.24337794
H	-1.84506664	-4.99951099	-1.79855391	H	-2.88347389	-4.49966547	-0.45967255
C	-3.16289962	-2.24087254	-2.86558520	H	-4.16734750	-2.42884481	-2.47578244
H	-3.00143634	-2.93193102	-3.70370713	H	-3.14586755	-1.22311382	-3.27032073
C	-2.78469743	-2.54598577	2.36182044	H	-2.63494577	-3.57046906	2.00116092
H	-3.62462016	-2.56290549	3.06830519	H	-1.88823268	-2.25932861	2.92217875
C	-4.80985046	-1.86680901	0.18567561	H	-5.11849338	-1.21119887	-0.63638487
H	-5.57409871	-1.79025593	0.97039753	H	-4.82697902	-2.89924126	-0.18070374
C	-3.40897340	0.39111611	1.61694458	H	-2.50462623	0.85933386	2.01966205
H	-4.13736023	0.34646037	2.43740526	H	-3.82172214	1.05791096	0.85032424
C	2.20322593	1.18228113	-2.47374758	H	1.30812276	0.81421826	-2.99460166
H	2.86761388	1.57994410	-3.25246908	H	1.90191903	2.02137118	-1.83997900
C	4.73748294	0.57191556	-0.86944516	H	4.53465429	1.34986054	-0.12450361
H	5.31233230	1.03071881	-1.68428178	H	5.38451303	-0.17549923	-0.39552014
C	3.58911403	-1.46490029	-2.86676236	H	4.26299673	-2.24636697	-2.50362083
H	4.09477175	-0.95428814	-3.69712938	H	2.69892459	-1.95550568	-3.27681350
C	3.55275064	-1.18791678	2.39479717	H	4.37946168	-0.53067675	2.09986089
H	3.95904303	-1.94336685	3.07969141	H	2.83489029	-0.58244636	2.95813047
C	4.08138056	-3.15146853	0.12665804	H	3.69920047	-3.72123611	-0.72772819
H	4.38912350	-3.87584902	0.89235475	H	4.98400529	-2.62145575	-0.19663621
C	1.38329361	-3.18994496	1.45771710	H	0.50178895	-2.69339264	1.87728481
H	1.77969064	-3.84564365	2.24423065	H	1.04882411	-3.83439512	0.63557635
N	0.02402270	-0.08446528	2.33118844	N	0.03510191	-0.19571436	3.53791543
N	0.04608896	-0.29619164	4.68131473				

Table 3.16.53 Optimized Coordinates of $U^{VI}(N)[N(SiMe_3)_2]_3$.

U	-0.00001094	-0.00003312	-0.49335636	N	1.37398781	-1.69270100	0.13116636
N	-2.15327545	-0.34197059	0.13107580	N	0.78002435	2.03542162	0.13152213
N	-0.00101699	0.00044578	-2.23805826	Si	1.97901846	2.71173133	-1.00825628
Si	0.16021793	3.08112496	1.42308963	Si	2.59073027	-1.67736117	1.42173830
Si	-2.74677703	-1.39768489	1.42736925	Si	1.35772013	-3.07170352	-1.00595253
Si	-3.34045432	0.35523775	-1.00890339	C	1.44775638	3.55030171	2.73798790
H	1.92402563	2.66774163	3.17804309	H	0.93662682	4.08688235	3.54858160
H	2.23820936	4.20500853	2.36076879	C	-1.21582018	2.19301944	2.37681759
H	-2.07030650	1.92406504	1.75082839	H	-1.57618031	2.85966739	3.17149325
H	-0.86199535	1.27794101	2.86933063	C	2.51480048	-0.03937482	2.37232513
H	2.71570040	0.83279978	1.74505022	H	3.27039882	-0.06389746	3.16874582
H	1.54527814	0.11791604	2.86257834	C	4.35086302	-1.85674972	0.73200505
H	4.51585493	-2.83036168	0.25626309	H	5.08234938	-1.76393090	1.54535915
H	4.57896197	-1.08437820	-0.01110949	C	3.12929188	1.33401900	-1.62573741

H	3.76781323	0.95239449	-0.82093782	H	3.78893865	1.75585988	-2.39618068
H	2.61182186	0.48674168	-2.08851890	C	-3.79581975	-0.51447106	2.74113384
H	-3.26817364	0.33785089	3.18201050	H	-4.00769919	-1.22518164	3.55131005
H	-4.75665935	-0.15510145	2.36274179	C	-3.77833690	-2.83856691	0.74466761
H	-4.70119455	-2.49905475	0.26040592	H	-4.06827693	-3.51171632	1.56194657
H	-3.21900163	-3.42852140	0.00987060	C	2.35218231	-3.02384158	2.73965506
H	1.35182380	-2.98967511	3.18409230	H	3.07684603	-2.85224224	3.54691858
H	2.51733271	-4.03687735	2.36271076	C	-1.28854366	-2.14235111	2.38223374
H	-0.63468843	-2.75823865	1.75965848	H	-1.68526772	-2.77741904	3.18533126
H	-0.66643961	-1.37679285	2.86411431	C	1.13194147	3.51279538	-2.50039580
H	0.56360689	2.76904855	-3.06977426	H	1.87734173	3.95508945	-3.17410596
H	0.44175200	4.30933496	-2.19946549	C	-0.56878722	4.69323633	0.73391058
H	0.18896043	5.32215160	0.25247086	H	-1.01088688	5.28187343	1.54827025
H	-1.35548913	4.50246437	-0.00465660	C	3.13632237	4.00727398	-0.23892954
H	2.62075463	4.91221570	0.09979916	H	3.85697089	4.31430716	-1.00848183
H	3.70974857	3.60753680	0.60466488	C	-3.60999560	-0.78114568	-2.49924013
H	-2.68169879	-0.90194225	-3.06838928	H	-4.36623128	-0.35908401	-3.17384097
H	-3.95357549	-1.77672846	-2.19572794	C	-5.04116274	0.70586503	-0.23789905
H	-5.56263165	-0.19421731	0.10467079	H	-5.67106785	1.17130548	-1.00763032
H	-4.98312082	1.40518368	0.60345746	C	-2.72673551	2.04098622	-1.62872222
H	-2.71090362	2.78430493	-0.82347781	H	-3.42638984	2.40189374	-2.39481212
H	-1.73699536	2.01648594	-2.09755362	C	-0.41202251	-3.37932967	-1.61914693
H	-1.05920666	-3.74088763	-0.81202825	H	-0.37882966	-4.16158891	-2.38959447
H	-0.88868007	-2.50805264	-2.08115992	C	2.47313765	-2.74286001	-2.50011440
H	2.10919067	-1.88331256	-3.07367173	H	2.48770909	-3.61290653	-3.16936502
H	3.50696385	-2.53695543	-2.19981323	C	1.90059452	-4.72066253	-0.23410885
H	2.94301797	-4.72779361	0.10166438	H	1.80289529	-5.49992833	-1.00164343
H	1.26929215	-5.01428770	0.61178792				

Table 3.16.54 Optimized Coordinates of **3.4**.

U	0.59551699	0.00150002	0.00005003	N	-1.34721916	-0.00836197	-0.00190097
N	1.36347704	-1.24083108	1.76203417	N	1.34920206	2.15529018	0.19220105
N	1.36761504	-0.90590606	-1.95404512	C	-0.68694910	0.91258209	-3.24393021
Si	0.70259198	-2.87224120	2.05453719	Si	2.56851313	-0.67922505	2.95661826
C	-2.82649427	-0.00818396	-0.00247597	C	-3.35247431	0.25392206	1.43791014
C	-4.42911039	1.11181913	1.70017516	H	-4.89900342	1.65697218	0.88974010
C	-4.91738042	1.27834215	3.00063626	H	-5.75085450	1.95432421	3.17420327
C	-4.34429338	0.58494910	4.06479634	H	-4.72347441	0.71416811	5.07505142
C	-3.27678231	-0.28114598	3.81511333	H	-2.82054528	-0.83450702	4.63240439
C	-2.79101127	-0.44113899	2.51883423	H	-1.95881621	-1.11030905	2.33986421
C	-0.67735713	-3.28020622	0.82269109	H	-1.64487520	-2.85505018	1.09639112
H	-0.79621414	-4.37192731	0.80469709	H	-0.47913711	-2.97743120	-0.21115698
C	-0.03601008	-3.05016121	3.79723132	H	0.72738698	-3.02986822	4.58302938
H	-0.55625013	-4.01394028	3.87311233	H	-0.76432713	-2.26309114	4.02168734
C	1.96007306	-4.28516732	1.84997417	H	2.46053710	-4.26435232	0.87679910
H	1.40988402	-5.23374638	1.91176618	H	2.73258813	-4.30611232	2.62191923
C	1.73443908	0.14898902	4.44736337	H	1.14391603	1.02925609	4.17884535
H	2.49821314	0.47000404	5.16792643	H	1.06680402	-0.54893103	4.96521041
C	3.66681121	-2.04685116	3.69287132	H	3.12415217	-2.78225021	4.29524936
H	4.38968427	-1.55531812	4.35777937	H	4.24026325	-2.58467920	2.93057825
C	3.81196124	0.52064104	2.18162020	H	4.46093528	-0.00402801	1.47128814
H	4.45312729	0.93100007	2.97291526	H	3.34454821	1.35776510	1.66021016
C	-3.35189531	1.10819413	-0.94996304	C	-4.43570039	0.90956212	-1.81601010
H	-4.91108343	-0.06259595	-1.87692011	C	-4.92423542	1.95277220	-2.60992017

H	-5.76361550	1.76763119	-3.27543822	C	-4.34437037	3.21829230	-2.54906416
H	-4.72392339	4.02888336	-3.16547421	C	-3.26923028	3.43188730	-1.68280110
H	-2.80724224	4.41411038	-1.61860909	C	-2.78313625	2.38899222	-0.89664804
H	-1.94453819	2.56629823	-0.23495499	C	-3.35412632	-1.38624606	-0.49436601
C	-4.44412141	-2.02973211	0.10715004	H	-4.92178544	-1.59101907	0.97559811
C	-4.93610245	-3.23792019	-0.39811100	H	-5.78016451	-3.71614523	0.09240304
C	-4.35277841	-3.82442924	-1.51947109	H	-4.73462545	-4.76307731	-1.91217512
C	-3.27128333	-3.18823820	-2.13396113	H	-2.80678429	-3.62883724	-3.01283720
C	-2.78223728	-1.98641511	-1.62539709	H	-1.93963321	-1.50674408	-2.10738513
Si	0.67805302	3.21998127	1.45684714	Si	2.55407716	2.91680923	-0.88635504
C	-0.69955010	2.34605620	2.41882222	H	-1.66597117	2.36595521	1.91154618
H	-0.82428010	2.87157125	3.37514629	H	-0.49440009	1.29977912	2.66989523
C	-0.06662403	4.81464139	0.73764309	H	0.69339303	5.49047341	0.32988806
H	-0.59353007	5.35878845	1.53234215	H	-0.79037609	4.61104738	-0.05919297
C	1.92373611	3.75124130	2.79252224	H	2.39694514	2.89550623	3.28453928
H	1.36983607	4.30279534	3.56423530	H	2.71711118	4.40778634	2.42871222
C	1.72221810	3.78177730	-2.35696115	H	1.14428905	3.10103225	-2.98788620
H	2.48595516	4.25187433	-2.99045820	H	1.04325105	4.57270637	-2.01882312
C	3.63608725	4.24918733	-0.06583997	H	3.08412221	5.12892739	0.27952505
H	4.35132630	4.59421934	-0.82460103	H	4.21862929	3.85897129	0.77551709
C	3.81437925	1.65604112	-1.52645308	H	4.45745229	1.30800109	-0.71020902
H	4.45997830	2.14239216	-2.26963914	H	3.35937020	0.78252206	-1.99671312
Si	0.69644799	-0.35257901	-3.51183323	Si	2.58184013	-2.21252916	-2.06701012
H	-1.65220418	0.46057307	-3.00793220	H	-0.81130211	1.47336714	-4.18006429
H	-0.48623908	1.65708315	-2.46592315	C	-0.04033807	-1.78068912	-4.52769831
H	0.72391799	-2.46972017	-4.90412834	H	-0.56829311	-1.37216108	-5.39921241
H	-0.76188513	-2.36959915	-3.95074427	C	1.94084610	0.53921505	-4.64084632
H	2.41252914	1.39457811	-4.14673728	H	1.38607006	0.92971809	-5.50473739
H	2.73523715	-0.10304400	-5.02760335	C	1.76193005	-3.92455629	-2.07543113
H	1.18905801	-4.13456930	-1.16816706	H	2.53098010	-4.70280036	-2.16800813
H	1.08045400	-4.03283529	-2.92676119	C	3.66722521	-2.16917017	-3.62898925
H	3.11930817	-2.32084617	-4.56418832	H	4.38803526	-2.99317023	-3.54024024
H	4.24344926	-1.24194310	-3.71688325	C	3.84032822	-2.12155116	-0.65448802
H	4.47603228	-1.23552510	-0.76296303	H	4.49356827	-3.00286324	-0.70074202
H	3.38396319	-2.09322016	0.33643906				

Table 3.16.55 Optimized Coordinates of $[U^{VI}(NCPh_3)[N(SiMe_3)_2]_3]Br$.

U	0.14856001	-0.00506700	-0.00591800	Br	6.27660950	0.03335500	0.03761500
N	-1.79076014	-0.00188900	-0.00245200	N	0.92648907	-0.87934607	-1.88774114
N	0.90395107	-1.21309009	1.68822213	N	0.90563207	2.06907816	0.18463501
C	-1.10970709	2.18892017	2.43309319	Si	0.27155902	-0.25199602	-3.44291526
Si	2.16620817	-2.20665517	-2.05608016	C	-3.27775825	0.00493300	0.00167000
C	-3.80349429	-1.35626810	-0.53439804	C	-4.86538637	-2.03569516	0.07727801
H	-5.31646342	-1.64169112	0.98018407	C	-5.36479144	-3.22436024	-0.46538604
H	-6.18720146	-3.73181729	0.03175500	C	-4.81702837	-3.75364129	-1.63213012
H	-5.20461140	-4.67727936	-2.05296916	C	-3.76580929	-3.07870323	-2.25764917
H	-3.33173226	-3.47259426	-3.17306124	C	-3.27020425	-1.89551114	-1.71364613
H	-2.45665919	-1.38338011	-2.21158617	C	-1.08786708	1.02345008	-3.08816123
H	-2.07714816	0.58766805	-2.93945722	H	-1.15310209	1.67626113	-3.96885130
H	-0.90065607	1.69550413	-2.24224317	C	-0.49487604	-1.64367112	-4.48022534
H	0.26671902	-2.27477118	-4.95065838	H	-1.09264708	-1.19741909	-5.28565440
H	-1.15268209	-2.29601018	-3.89701030	C	1.49617912	0.66189105	-4.56314635
H	1.87895715	1.57750612	-4.10495131	H	0.94106307	0.95483607	-5.46520044
H	2.35103118	0.06480700	-4.88336037	C	1.28022810	-3.87764630	-2.23037217

H	0.66198805	-4.14067032	-1.36805311	H	2.03836416	-4.66386136	-2.34273018
H	0.64185905	-3.91105430	-3.11956224	C	3.26088725	-2.04571216	-3.59441728
H	2.73450921	-2.13930416	-4.54962135	H	3.98111130	-2.87302922	-3.53926927
H	3.84516130	-1.12037309	-3.59833527	C	3.35766526	-2.23133117	-0.60537305
H	4.11498031	-1.43559111	-0.65982805	H	3.91192730	-3.17946924	-0.64189905
H	2.87933422	-2.17372317	0.37275203	C	-3.78636029	0.22248802	1.45460211
C	-4.83491037	1.10198408	1.75408713	H	-5.29107941	1.69379413	0.96951707
C	-5.31320242	1.22831609	3.06265523	H	-6.12537245	1.92069015	3.26762525
C	-4.75783337	0.47440604	4.09452031	H	-5.12934239	0.57365405	5.11066939
C	-3.71971628	-0.41481703	3.80545229	H	-3.28017225	-1.01677108	4.59666235
C	-3.24458425	-0.53683404	2.50139819	H	-2.44024719	-1.23069509	2.29199918
C	-3.79410329	1.15456509	-0.90851907	C	-4.87609837	0.98029207	-1.78169013
H	-5.34743839	0.00937600	-1.87774715	C	-5.36978840	2.05024815	-2.53542319
H	-6.20854847	1.88583114	-3.20657125	C	-4.79603536	3.31547225	-2.42719819
H	-5.17944740	4.14615531	-3.01317623	C	-3.72375829	3.50375627	-1.55174212
H	-3.26856925	4.48546734	-1.44891911	C	-3.23385525	2.43541219	-0.80322106
H	-2.40349618	2.59821420	-0.12784901	Si	0.25586902	-2.87907022	1.90466514
Si	2.12703816	-0.69446905	2.93846522	C	-1.09498108	-3.20199525	0.61257904
H	-2.08643516	-2.87271022	0.92831407	H	-1.14732409	-4.28845533	0.46266804
H	-0.91753207	-2.77760621	-0.38275203	C	-0.52137204	-3.09982524	3.62154928
H	0.23619502	-3.17510124	4.40884434	H	-1.09740309	-4.03430831	3.63290728
H	-1.20104009	-2.28492917	3.89021730	C	1.49536111	-4.29430733	1.68044613
H	1.92487815	-4.32361633	0.67585205	H	0.93862007	-5.23024440	1.82743714
H	2.31898018	-4.28634533	2.39627018	C	1.21286009	-0.01595700	4.45873134
H	0.59055805	0.85641207	4.24269233	H	1.95520315	0.28726302	5.20869240
H	0.57235504	-0.77443506	4.92138238	C	3.21729325	-2.10515316	3.58067427
H	2.68581420	-2.88305322	4.13829132	H	3.93214030	-1.64100112	4.27327833
H	3.80733829	-2.57380320	2.78711721	C	3.32442425	0.57861205	2.25233017
H	4.09283931	0.13354001	1.60320712	H	3.86393330	1.02232208	3.10051524
H	2.85438922	1.39633911	1.70575813	Si	0.26287802	3.11071124	1.50582211
Si	2.14134916	2.87695722	-0.88866507	H	-2.09328016	2.28209417	1.96955715
H	-1.18019109	2.63581920	3.43375026	H	-0.93263607	1.12025909	2.60103120
C	-0.48528404	4.71233936	0.81544306	H	0.28158202	5.41589842	0.47445304
H	-1.05413608	5.20978940	1.61177612	H	-1.16934009	4.53441334	-0.02073100
C	1.49569411	3.60623027	2.85579922	H	1.83937014	2.74705721	3.43824026
H	0.95980407	4.27489133	3.54376927	H	2.37680718	4.14082331	2.49752019
C	1.24884009	3.84316729	-2.25896018	H	0.64214605	3.21577724	-2.91724622
H	2.00431615	4.33901833	-2.88265822	H	0.59773405	4.62380735	-1.85149914
C	3.22672825	4.14602432	0.00638600	H	2.69102621	5.00848138	0.41514703
H	3.92827730	4.52717635	-0.74777906	H	3.83309929	3.69523028	0.79810206
C	3.33969526	1.62972912	-1.61763612	H	4.10281431	1.30486210	-0.89490307
H	3.88590930	2.11886016	-2.43588919	H	2.86582522	0.73915006	-2.03106916

Table 3.16.56 Optimized Coordinates of $U^{V}(NCPh_3)[N(SiMe_3)_2]_2Br$.

U	0.62396008	-0.12229822	-0.21536826	Br	0.65571209	-0.44769336	-2.95228642
N	-1.29725472	-0.17613085	0.03323287	N	2.37019096	-1.43834941	0.29650912
N	1.32334373	1.99962387	0.04325783	C	0.60821172	0.81888648	2.66001749
C	-2.74589683	-0.25715552	0.27011748	C	-3.32562100	-1.49525089	-0.46812219
C	-4.33399895	-2.29916453	0.08015964	H	-4.69625499	-2.10870291	1.08490251
C	-4.88649344	-3.35554315	-0.65076365	H	-5.66459056	-3.96662467	-0.20021211
C	-4.44435420	-3.62411750	-1.94498353	H	-4.87164535	-4.44663597	-2.51243514
C	-3.45012092	-2.81907698	-2.50651523	H	-3.10032561	-3.00738258	-3.51826335
C	-2.90186434	-1.76391539	-1.77831112	H	-2.13496739	-1.14443965	-2.23133885
C	-2.90875266	-0.33867099	1.81123434	C	-3.28936890	0.77226884	2.57537606

H	-3.55965727	1.69856660	2.08148806	C	-3.32834110	0.70699407	3.97177520
H	-3.63065249	1.58414481	4.53819164	C	-2.98693788	-0.47089045	4.63443885
H	-3.02219782	-0.52277341	5.71932670	C	-2.60309084	-1.58680038	3.88594483
H	-2.33948280	-2.51568388	4.38539920	C	-2.56162730	-1.51746304	2.49392890
H	-2.27400454	-2.39679800	1.92724225	C	-3.49121457	0.97699029	-0.30380915
C	-4.89434611	1.02418551	-0.25389345	H	-5.44632215	0.19496476	0.17745925
C	-5.59339770	2.11803573	-0.75939494	H	-6.67916258	2.13007524	-0.70869234
C	-4.90496921	3.18847046	-1.33724005	H	-5.44955510	4.03826390	-1.74005431
C	-3.51377367	3.14987025	-1.39588946	H	-2.96137774	3.96823650	-1.84940819
C	-2.81443092	2.05410488	-0.87844682	H	-1.73285226	2.03791912	-0.92611261
Si	1.93220419	-3.15469105	0.13454357	Si	4.04645584	-1.05430697	0.76393362
C	0.04261597	-3.26473935	-0.03249511	H	-0.50124605	-2.92559646	0.85578807
H	-0.19424438	-4.33075844	-0.15015921	H	-0.39740953	-2.77853163	-0.91235400
C	2.36385631	-4.15310395	1.68936470	H	3.44040389	-4.21184424	1.88133409
H	1.99404086	-5.18122437	1.58336520	H	1.88970902	-3.72075820	2.57892776
C	2.65353951	-3.98322616	-1.40438317	H	2.42228064	-3.39420632	-2.29946314
H	2.20554302	-4.97716189	-1.53395620	H	3.73834454	-4.11396220	-1.35578384
C	4.20676065	-0.95981330	2.65347936	H	3.63442910	-0.12826775	3.08017702
H	5.25739941	-0.80694684	2.93267776	H	3.86651454	-1.88102942	3.14026140
C	5.30636693	-2.33939361	0.15505737	H	5.15650156	-3.34759835	0.55479273
H	6.30507268	-2.01083183	0.47212935	H	5.31785410	-2.40660869	-0.93845669
C	4.62586245	0.58101576	0.02175907	H	4.69945537	0.50488702	-1.06881002
H	5.62596925	0.82031688	0.40633424	H	3.96134611	1.41666487	0.25329067
Si	1.09913454	2.42915419	1.73957450	Si	1.72548257	3.23018866	-1.18286098
H	-0.31633167	0.32817039	2.32074872	H	0.37997847	1.11834988	3.69122262
H	1.41325959	0.07747104	2.73198277	C	-0.29850147	3.67852555	2.00535212
H	-0.06347090	4.65489811	1.56591229	H	-0.47732940	3.83590644	3.07676900
H	-1.23422538	3.32831377	1.55532129	C	2.65438001	3.04597430	2.62939357
H	3.50931302	2.37869421	2.47373358	H	2.46202598	3.09180009	3.70942438
H	2.94980349	4.04863361	2.30603887	C	0.15971291	3.80338011	-2.08009354
H	-0.31819564	2.97911245	-2.62181725	H	0.40714842	4.58081546	-2.81440983
H	-0.57356527	4.22489873	-1.38287019	C	2.53149261	4.77533267	-0.42188736
H	1.90075479	5.28734225	0.31344643	H	2.72773564	5.49060396	-1.23141944
H	3.49341872	4.55177332	0.05292089	C	2.94403780	2.60088411	-2.48591294
H	3.95081450	2.47090888	-2.07667635	H	3.00765551	3.34683373	-3.28938815
H	2.62979595	1.65611015	-2.93983493				

Table 3.16.57 Optimized Coordinates of **3.5**.

U	-0.58449154	-0.12896508	0.02113704	Br	-0.26814744	-0.39979244	-2.72461873
Br	-0.73574791	-0.29438545	2.78040405	Si	-0.49527158	3.26547635	0.92850127
Si	-2.20877910	2.62320441	-1.50727997	Si	-2.09815596	-3.02852495	-0.55731030
Si	-3.94406074	-1.02281149	0.88959295	N	1.30457779	-0.27102405	0.10276381
N	-1.14590691	1.98803184	-0.18335288	N	-2.36663268	-1.35213117	0.06221149
C	2.79052347	-0.31302992	0.08555550	C	3.28759930	0.00365422	1.52004915
C	4.25027159	0.98468365	1.78991830	C	4.68038045	1.22710655	3.09773447
C	4.15634042	0.49503933	4.16134465	C	3.19372867	-0.48418477	3.90624888
C	2.76527126	-0.72385000	2.60172620	C	3.35377909	0.69696582	-0.94652675
C	4.68689399	0.56561838	-1.37098190	C	5.24842673	1.47279246	-2.26818148
C	4.48452425	2.52751354	-2.77353290	C	3.15874239	2.66238774	-2.36676675
C	2.60120923	1.75711507	-1.45870194	C	3.21505604	-1.74122362	-0.37146450
C	2.87772006	-2.15443697	-1.67182697	C	3.26316409	-3.40487852	-2.14984082
C	4.00780181	-4.26950900	-1.34262960	C	4.36179682	-3.86437097	-0.05779266
C	3.97062600	-2.61028452	0.42454871	C	1.09473270	2.76904331	1.81397706
C	0.01528462	4.84310059	-0.00469301	C	-1.76740346	3.69577809	2.26227058

C	-1.15810851	3.29910296	-2.92915782	C	-3.37433169	4.00187339	-0.90524407
C	-3.39902122	1.33560940	-2.23253876	C	-2.70801293	-3.22257796	-2.33137018
C	-2.91575477	-4.38302904	0.48452632	C	-0.24080895	-3.36937435	-0.39940603
C	-4.12499331	-2.00653475	2.49813551	C	-5.35722589	-1.48708419	-0.28745700
C	-4.16086476	0.78282212	1.39610077	H	1.03072404	1.84810939	2.39480030
H	1.94491339	2.68970268	1.13174549	H	1.31928499	3.58279557	2.51807589
H	0.40560244	5.54576603	0.74366967	H	0.83215322	4.63877213	-0.70660964
H	-0.78013424	5.35694421	-0.54956704	H	-1.38857339	4.52926485	2.86802916
H	-1.91359883	2.84163037	2.93238617	H	-2.74313793	3.98758227	1.86377747
H	-0.48731646	2.52721951	-3.31888768	H	-1.81658850	3.61445560	-3.74901985
H	-0.55661508	4.16448084	-2.63690960	H	-4.05956386	3.64790025	-0.12753597
H	-2.87553545	4.89749360	-0.52666621	H	-3.98852067	4.30833235	-1.76283789
H	-2.93770810	0.38054672	-2.48724412	H	-3.78863467	1.76676106	-3.16506911
H	-4.25735068	1.15041021	-1.58073363	H	-2.49497480	-4.23710000	-2.69269293
H	-2.22122824	-2.51129004	-3.00388310	H	-3.79110879	-3.06935318	-2.39576963
H	-2.58974476	-5.34557606	0.06739634	H	-2.60310200	-4.35492647	1.53285019
H	-4.00946572	-4.36990271	0.44994812	H	-0.05075091	-4.35479159	-0.84569842
H	0.06829182	-3.43237245	0.65161214	H	0.44268198	-2.69315002	-0.92317603
H	-3.20675586	-1.95972313	3.09191154	H	-4.92411749	-1.54428855	3.09222189
H	-4.39108435	-3.05540402	2.34757154	H	-5.28470517	-0.96061701	-1.24519106
H	-5.39533465	-2.56155626	-0.49810064	H	-6.31539862	-1.21313328	0.17312496
H	-4.15519272	1.49402906	0.56969710	H	-3.40450688	1.09036965	2.12250845
H	-5.14014891	0.85756406	1.88854531	H	4.27269543	-2.31530153	1.42180699
H	2.30636073	-1.49053566	-2.31173857	H	2.98638453	-3.70001190	-3.15867634
H	4.31400360	-5.24310685	-1.71622947	H	4.95102441	-4.51867870	0.57955004
H	2.01233719	-1.48202377	2.42248580	H	2.76706567	-1.05972246	4.72319033
H	4.48964918	0.68581634	5.17799170	H	5.42670909	1.99640097	3.27828747
H	4.67044227	1.57264562	0.98302306	H	5.28997566	-0.25584079	-0.99680170
H	6.28249734	1.34802427	-2.57868903	H	4.91724858	3.22955015	-3.48114917
H	2.54457482	3.46804291	-2.76048100	H	1.56522675	1.87682413	-1.16849306

Table 3.16.58 Optimized Coordinates of Ph_3CN_3.

N	-0.15574753	-0.02713115	1.93532659	N	-1.08064584	-0.71445533	2.37216470
N	-1.89976799	-1.31326309	2.89714335	C	0.00030829	0.03444089	0.43204171
C	-1.32065155	0.58286930	-0.14636601	C	-2.42996346	-0.26344549	-0.31404224
H	-2.33461337	-1.32724468	-0.12266027	C	-3.65944390	0.24211888	-0.73824121
H	-4.50090013	-0.43385381	-0.86429754	C	-3.80748514	1.60496645	-0.99874744
H	-4.76389053	1.99861862	-1.33213129	C	-2.71652908	2.45715040	-0.82459110
H	-2.81858367	3.52159038	-1.01864805	C	-1.48721715	1.95190271	-0.39884397
H	-0.65218774	2.62962207	-0.26118596	C	0.38790290	-1.36318228	-0.10326223
C	1.17440723	-2.21304778	0.68837555	H	1.45817046	-1.89871735	1.68753588
C	1.59938774	-3.45042174	0.20638194	H	2.20335926	-4.09357231	0.84091097
C	1.25439884	-3.86063875	-1.08277245	H	1.58352186	-4.82569490	-1.45830799
C	0.48341427	-3.01895928	-1.88393272	H	0.20739365	-3.32355602	-2.89004682
C	0.05368193	-1.78134869	-1.39925935	H	-0.55368537	-1.14559451	-2.03501564
C	1.18660455	0.99007561	0.18549112	C	1.80953090	1.68659308	1.22666365
H	1.45467134	1.55639380	2.24187783	C	2.88263980	2.54456105	0.96739930
H	3.35368725	3.07320370	1.79204407	C	3.34576481	2.72318803	-0.33474029
H	4.18032300	3.38973367	-0.53500535	C	2.72647258	2.03445833	-1.38098178
H	3.07628805	2.16170419	-2.40204394	C	1.66056553	1.17534439	-1.12219549
H	1.19684103	0.64156356	-1.9457303				

Table 3.16.59 Optimized Coordinates of $Ph_3C\cdot$.

C	-1.91334562	5.09437581	7.54834134	C	-1.55180744	6.08371000	8.56605439

C	-1.97582506	7.43133051	8.46755900	H	-2.56287556	7.73798455	7.60777387
C	-1.63056938	8.37056906	9.43433779	H	-1.96062859	9.40023824	9.32226016
C	-0.85601188	8.00001995	10.53782920	H	-0.58944883	8.73415945	11.29321051
C	-0.42823751	6.67439516	10.65849130	H	0.16502684	6.37002749	11.51705037
C	-0.76561486	5.73337143	9.69059150	H	-0.44173669	4.70415950	9.80754168
C	-0.98278083	4.01499715	7.21076589	C	0.41933648	4.21231124	7.23957441
H	0.80912293	5.19187148	7.49742459	C	1.30098396	3.18549687	6.91625457
H	2.37149203	3.37361802	6.93469825	C	0.81827363	1.92288769	6.55881566
H	1.50825905	1.12150281	6.30918581	C	-0.56209145	1.70312069	6.52604768
H	-0.95097284	0.72328685	6.26069074	C	-1.44747544	2.72888998	6.84221791
H	-2.51569226	2.53749747	6.82989750	C	-3.20814940	5.18378439	6.86860613
C	-3.35652942	4.80616743	5.51196071	H	-2.48611063	4.46326353	4.96174759
C	-4.58665472	4.89393932	4.86744534	H	-4.66439803	4.60921429	3.82120891
C	-5.71481959	5.35422250	5.55315573	H	-6.67524391	5.41916106	5.04917179
C	-5.59369669	5.72974668	6.89447458	H	-6.46506296	6.07869605	7.44280318
C	-4.36390305	5.65031929	7.54076384	H	-4.28911728	5.92897731	8.58706770

Table 3.16.60 Optimized Coordinates of N_2.

N	0.00000000	0.00000000	0.55265300	N	0.00000000	0.00000000	-0.55265300

Table 3.16.61 Optimized Coordinates of $\cdot N(SiMe_3)_2$.

N	0.00000400	0.00049500	0.48505900	Si	1.67694000	0.00408700	0.03989800
Si	-1.67693600	-0.00401300	0.03992500	C	2.01417300	-0.33272200	-1.79563700
C	2.55642000	-1.30950300	1.08224400	C	2.31918300	1.73302000	0.48926100
C	-2.31938400	-1.73178500	0.49341700	C	-2.01415500	0.32835200	-1.79642400
C	-2.55624800	1.31219800	1.07910600	H	1.52610900	0.41251900	-2.43518600
H	3.08953400	-0.30599900	-2.01463400	H	1.64290600	-1.32035700	-2.09587500
H	2.42397200	-1.11156500	2.15140000	H	2.16582000	-2.31296700	0.87647700
H	3.63210000	-1.32160200	0.86525400	H	3.39560800	1.79792400	0.28532300
H	1.82075900	2.51392100	-0.09604800	H	2.15770600	1.94887000	1.55056200
H	-3.39581800	-1.79704800	0.28964300	H	-1.82105900	-2.51412900	-0.09004700
H	-2.15791100	-1.94513600	1.55522300	H	-3.08951900	0.30115600	-2.01534600
H	-1.64280900	1.31521500	-2.09909300	H	-1.52614300	-0.41850800	-2.43412300
H	-2.42374100	1.11688000	2.14873700	H	-2.16559400	2.31512600	0.87084400
H	-3.63194000	1.32383400	0.86215300				

3.17 References

(1) Zhou, L.; Bosscher, M.; Zhang, C.; Özçubukçu, S.; Zhang, L.; Zhang, W.; Li, C. J.; Liu, J.; Jensen, M. P.; Lai, L.; He, C., *Nat. Chem.* **2014,** *advance online publication*.

(2) Nash, K. L.; Jensen, M. P.; Schmidt, M. A., *J. Alloys Compd.* **1998,** *271–273*, 257.

(3) Franczyk, T. S.; Czerwinski, K. R.; Raymond, K. N., *J. Am. Chem. Soc.* **1992,** *114*, 8138.

(4) Arnold, P. L.; Patel, D.; Blake, A. J.; Wilson, C.; Love, J. B., *J. Am. Chem. Soc.* **2006,** *128*, 9610.

(5) Arnold, P. L.; Patel, D.; Wilson, C.; Love, J. B., *Nature* **2008,** *451*, 315.

(6) Schnaars, D. D.; Wu, G.; Hayton, T. W., *J. Am. Chem. Soc.* **2009,** *131*, 17532.

(7) Arnold, P. L.; Pécharman, A.-F.; Hollis, E.; Yahia, A.; Maron, L.; Parsons, S.; Love, J. B., *Nat. Chem.* **2010,** *2*, 1056.

(8) Fortier, S.; Hayton, T. W., *Coord. Chem. Rev.* **2010,** *254*, 197.

(9) Beer, S.; Berryman, O. B.; Ajami, D.; Rebek Jr, J., *Chem. Sci.* **2010,** *1*, 43.

(10) Sather, A. C.; Berryman, O. B.; Rebek, J., *J. Am. Chem. Soc.* **2010,** *132*, 13572.
(11) Schnaars, D. D.; Wu, G.; Hayton, T. W., *Inorg. Chem.* **2011,** *50*, 4695.
(12) Brown, J. L.; Mokhtarzadeh, C. C.; Lever, J. M.; Wu, G.; Hayton, T. W., *Inorg. Chem.* **2011,** *50*, 5105.
(13) Sather, A. C.; Berryman, O. B.; Moore, C. E.; Rebek, J., *Chem. Commun.* **2013**.
(14) Tatsumi, K.; Hoffmann, R., *Inorg. Chem.* **1980,** *19*, 2656.
(15) Denning, R., Electronic structure and bonding in actinyl ions. In *Complexes, Clusters and Crystal Chemistry*, Springer Berlin / Heidelberg: 1992; Vol. 79, pp 215.
(16) O'Grady, E.; Kaltsoyannis, N., *J. Chem. Soc., Dalton Trans.* **2002**, 1233.
(17) Denning, R. G., *J. Phys. Chem. A* **2007,** *111*, 4125.
(18) Shamov, G. A.; Schreckenbach, G.; Vo, T. N., *Chem. - Eur. J.* **2007,** *13*, 4932.
(19) Brown, D. R.; Denning, R. G.; Jones, R. H., *J. Chem. Soc., Chem. Commun.* **1994,** *0*, 2601.
(20) Brown, D. R.; Denning, R. G., *Inorg. Chem.* **1996,** *35*, 6158.
(21) Williams, V. C.; Müller, M.; Leech, M. A.; Denning, R. G.; Green, M. L. H., *Inorg. Chem.* **2000,** *39*, 2538.
(22) Hayton, T. W.; Boncella, J. M.; Scott, B. L.; Palmer, P. D.; Batista, E. R.; Hay, P. J., *Science* **2005,** *310*, 1941.
(23) Kovács, A.; Konings, R. J. M., *ChemPhysChem* **2006,** *7*, 455.
(24) Spencer, L. P.; Yang, P.; Minasian, S. G.; Jilek, R. E.; Batista, E. R.; Boland, K. S.; Boncella, J. M.; Conradson, S. D.; Clark, D. L.; Hayton, T. W.; Kozimor, S. A.; Martin, R. L.; MacInnes, M. M.; Olson, A. C.; Scott, B. L.; Shuh, D. K.; Wilkerson, M. P., *J. Am. Chem. Soc.* **2013,** *135*, 2279.
(25) Hayton, T. W., *Dalton Trans.* **2010,** *39*, 1145.
(26) Hayton, T. W., *Chem. Commun.* **2013,** *49*, 2956.
(27) Bagnall, K. W.; du Preez, J. G. H.; Gellatly, B. J.; Holloway, J. H., *J. Chem. Soc., Dalton Trans.* **1975**, 1963.
(28) Joubert, P.; Bougon, R.; Gaudreau, B., *Can. J. Chem.* **1978,** *56*, 1874.
(29) David, S. J. A.; Carol, J. B.; David, C. S., *J. Am. Chem. Soc.* **1992,** *114*.
(30) Warner, B. P.; Scott, B. L.; Burns, C. J., *Angew. Chem. Int. Ed.* **1998,** *37*, 959.
(31) Kiplinger, J. L.; Morris, D. E.; Scott, B. L.; Burns, C. J., *Chem. Commun.* **2002**, 30.
(32) Hayton, T. W.; Boncella, J. M.; Scott, B. L.; Batista, E. R.; Hay, P. J., *J. Am. Chem. Soc.* **2006,** *128*, 10549.
(33) Hayton, T. W.; Boncella, J. M.; Scott, B. L.; Batista, E. R., *J. Am. Chem. Soc.* **2006,** *128*, 12622.
(34) Spencer, L. P.; Yang, P.; Scott, B. L.; Batista, E. R.; Boncella, J. M., *J. Am. Chem. Soc.* **2008,** *130*, 2930.
(35) Spencer, L. P.; Gdula, R. L.; Hayton, T. W.; Scott, B. L.; Boncella, J. M., *Chem. Commun.* **2008**, 4986.
(36) Spencer, L. P.; Schelter, E. J.; Yang, P.; Gdula, R. L.; Scott, B. L.; Thompson, J. D.; Kiplinger, J. L.; Batista, E. R.; Boncella, J. M., *Angew. Chem. Int. Ed.* **2009,** *48*, 3795.
(37) Evans, W. J.; Traina, C. A.; Ziller, J. W., *J. Am. Chem. Soc.* **2009,** *131*, 17473.
(38) Spencer, L. P.; Yang, P.; Scott, B. L.; Batista, E. R.; Boncella, J. M., *Inorg. Chem.* **2009,** *48*, 2693.
(39) Spencer, L. P.; Yang, P.; Scott, B. L.; Batista, E. R.; Boncella, J. M., *C. R. Chim.* **2010,** *13*, 758.
(40) Swartz, D. L.; Spencer, L. P.; Scott, B. L.; Odom, A. L.; Boncella, J. M., *Dalton Trans.* **2010,** *39*, 6841.

(41) Seaman, L. A.; Fortier, S.; Wu, G.; Hayton, T. W., *Inorg. Chem.* **2011,** *50*, 636.
(42) Jilek, R. E.; Spencer, L. P.; Lewis, R. A.; Scott, B. L.; Hayton, T. W.; Boncella, J. M., *J. Am. Chem. Soc.* **2012,** *134*, 9876.
(43) Cladis, D. P.; Kiernicki, J. J.; Fanwick, P. E.; Bart, S. C., *Chem. Commun.* **2013,** *49*, 4169.
(44) Brown, J. L.; Fortier, S.; Lewis, R. A.; Wu, G.; Hayton, T. W., *J. Am. Chem. Soc.* **2012,** *134*, 15468.
(45) Merkle, A. C.; Lehnert, N., *Dalton Trans.* **2012,** *41*, 3355.
(46) Kujime, M.; Izumi, C.; Tomura, M.; Hada, M.; Fujii, H., *J. Am. Chem. Soc.* **2008,** *130*, 6088.
(47) Woollard-Shore, J. G.; Holland, J. P.; Jones, M. W.; Dilworth, J. R., *Dalton Trans.* **2010,** *39*, 1576.
(48) Chuang, W. J.; Lin, I. J.; Chen, H. Y.; Chang, Y. L.; Hsu, S. C., *Inorg. Chem.* **2010,** *49*, 5377.
(49) Kumar, M.; Dixon, N. A.; Merkle, A. C.; Zeller, M.; Lehnert, N.; Papish, E. T., *Inorg. Chem.* **2012,** *51*, 7004.
(50) Tsai, F.-T.; Kuo, T.-S.; Liaw, W.-F., *J. Am. Chem. Soc.* **2009,** *131*, 3426.
(51) Tsai, F.-T.; Chen, P.-L.; Liaw, W.-F., *J. Am. Chem. Soc.* **2010,** *132*, 5290.
(52) Suslick, K. S.; Watson, R. A., *Inorg. Chem.* **1991,** *30*, 912.
(53) Yamaji, M.; Hama, Y.; Miyazaki, Y.; Hoshino, M., *Inorg. Chem.* **1992,** *31*, 932.
(54) Hoshino, M.; Iimura, Y.; Konishi, S., *J. Phys. Chem. A* **1992,** *96*, 179.
(55) Owen, T. M.; Rohde, J.-U., *Inorg. Chem.* **2011,** *50*, 5283.
(56) Fox, A. R.; Bart, S. C.; Meyer, K.; Cummins, C. C., *Nature* **2008,** *455*, 341.
(57) Arnold, P. L., *Chem. Commun.* **2011,** *47*, 9005.
(58) Lewis, A. J.; Nakamaru-Ogiso, E.; Kikkawa, J. M.; Carroll, P. J.; Schelter, E. J., *Chem. Commun.* **2012,** *48*, 4977.
(59) Arney, D. S. J.; Burns, C. J., *J. Am. Chem. Soc.* **1995,** *117*, 9448.
(60) Zi, G.; Jia, L.; Werkema, E. L.; Walter, M. D.; Gottfriedsen, J. P.; Andersen, R. A., *Organometallics* **2005,** *24*, 4251.
(61) Cantat, T.; Graves, C. R.; Scott, B. L.; Kiplinger, J. L., *Angew. Chem. Int. Ed.* **2009,** *48*, 3681.
(62) Fortier, S.; Wu, G.; Hayton, T. W., *J. Am. Chem. Soc.* **2010,** *132*, 6888.
(63) Kraft, S. J.; Walensky, J.; Fanwick, P. E.; Hall, M. B.; Bart, S. C., *Inorg. Chem.* **2010,** *49*, 7620.
(64) Mills, D. P.; Cooper, O. J.; Tuna, F.; McInnes, E. J. L.; Davies, E. S.; McMaster, J.; Moro, F.; Lewis, W.; Blake, A. J.; Liddle, S. T., *J. Am. Chem. Soc.* **2012,** *134*, 10047.
(65) Fortier, S.; Brown, J. L.; Kaltsoyannis, N.; Wu, G.; Hayton, T. W., *Inorg. Chem.* **2012,** *51*, 1625.
(66) Bart, S. C.; Anthon, C.; Heinemann, F. W.; Bill, E.; Edelstein, N. M.; Meyer, K., *J. Am. Chem. Soc.* **2008,** *130*, 12536.
(67) Arnold, P. L.; Pécharman, A.-F.; Love, J. B., *Angew. Chem. Int. Ed.* **2011,** *50*, 9456.
(68) Lide, D. R., *CRC Handbook of Chemistry and Physics*. 86th ed.; CRC Press: Boca Raton, FL, 2005-2006.
(69) Burns, C. J.; Smith, W. H.; Huffman, J. C.; Sattelberger, A. P., *J. Am. Chem. Soc.* **1990,** *112*, 3237.
(70) Andersen, R. A., *Inorg. Chem.* **1979,** *18*, 1507.
(71) Barnhart, D. M.; Burns, C. J.; Sauer, N. N.; Watkin, J. G., *Inorg. Chem.* **1995,** *34*, 4079.

(72) Roberts, B. P.; Winter, J. N., *J. Chem. Soc., Chem. Commun.* **1978**, 545.
(73) Arnold, P. L.; Hollis, E.; White, F. J.; Magnani, N.; Caciuffo, R.; Love, J. B., *Angew. Chem. Int. Ed.* **2011,** *50*, 887.
(74) Downs, A. J.; Gardner, C. J., *J. Chem. Soc., Dalton Trans.* **1984**, 2127.
(75) Straka, M.; Kaupp, M., *Chem. Phys.* **2005,** *311*, 45.
(76) Laplaza, C. E.; Odom, A. L.; Davis, W. M.; Cummins, C. C.; Protasiewicz, J. D., *J. Am. Chem. Soc.* **1995,** *117*, 4999.
(77) Averill, B. A., *Chem. Rev.* **1996,** *96*, 2951.
(78) Sun, D.; Zhang, N.; Xu, Q.-J.; Huang, R.-B.; Zheng, L.-S., *Inorg. Chem. Commun.* **2010,** *13*, 859.
(79) Dulong, F.; Pouessel, J.; Thuery, P.; Berthet, J.-C.; Ephritikhine, M.; Cantat, T., *Chem. Commun.* **2013,** *49*, 2412.
(80) Williams, P. A.; Fulop, V.; Garman, E. F.; Saunders, N. F. W.; Ferguson, S. J.; Hajdu, J., *Nature* **1997,** *389*, 406.
(81) Harris, T. D.; Betley, T. A., *J. Am. Chem. Soc.* **2011,** *133*, 13852.
(82) Villar-Acevedo, G.; Nam, E.; Fitch, S.; Benedict, J.; Freudenthal, J.; Kaminsky, W.; Kovacs, J. A., *J. Am. Chem. Soc.* **2011,** *133*, 1419.
(83) Leferink, N. G. H.; Han, C.; Antonyuk, S. V.; Heyes, D. J.; Rigby, S. E. J.; Hough, M. A.; Eady, R. R.; Scrutton, N. S.; Hasnain, S. S., *Biochemistry* **2011,** *50*, 4121.
(84) Ghosh, S.; Dey, A.; Sun, Y.; Scholes, C. P.; Solomon, E. I., *J. Am. Chem. Soc.* **2008,** *131*, 277.
(85) Compound numbers in italics denote computational model compounds.
(86) Sigurdson, E. R.; Wilkinson, G., *J. Chem. Soc., Dalton Trans.* **1977**.
(87) Fortier, S.; Walensky, J. R.; Wu, G.; Hayton, T. W., *J. Am. Chem. Soc.* **2011,** *133*, 11732.
(88) Seaman, L. A.; Hrobarik, P.; Schettini, M. F.; Fortier, S.; Kaupp, M.; Hayton, T. W., *Angew. Chem. Int. Ed.* **2013,** *52*, 3259.
(89) Seaman, L. A.; Walensky, J. R.; Wu, G.; Hayton, T. W., *Inorg. Chem.* **2013,** *52*, 3556.
(90) Van der Sluys, W. G.; Burns, C. J.; Sattelberger, A. P., *Organometallics* **1989,** *8*.
(91) Fortier, S.; Melot, B. C.; Wu, G.; Hayton, T. W., *J. Am. Chem. Soc.* **2009,** *131*, 15512.
(92) Kraft, S. J.; Fanwick, P. E.; Bart, S. C., *J. Am. Chem. Soc.* **2012,** *134*, 6160.
(93) Kraft, S. J.; Fanwick, P. E.; Bart, S. C., *Organometallics* **2013,** *32*, 3279.
(94) Tourneux, J.-C.; Berthet, J.-C.; Cantat, T.; Thuéry, P.; Mézailles, N.; Ephritikhine, M., *J. Am. Chem. Soc.* **2011,** *133*, 6162.
(95) Sarsfield, M. J.; Steele, H.; Helliwell, M.; Teat, S. J., *Dalton Trans.* **2003**.
(96) Mungur, S. A.; Liddle, S. T.; Wilson, C.; Sarsfield, M. J.; Arnold, P. L., *Chem. Commun.* **2004,** *0*, 2738.
(97) Maynadie, J.; Berthet, J.-C.; Thuery, P.; Ephritikhine, M., *Chem. Commun.* **2007,** *0*, 486.
(98) Berthet, J.-C.; Thuery, P.; Ephritikhine, M., *Chem. Commun.* **2007,** *0*, 604.
(99) Schettini, M. F.; Wu, G.; Hayton, T. W., *Chem. Commun.* **2012,** *48*, 1484.
(100) Cooper, O. J.; Mills, D. P.; McMaster, J.; Tuna, F.; McInnes, E. J.; Lewis, W.; Blake, A. J.; Liddle, S. T., *Chem. - Eur. J.* **2013,** *19*, 7071.
(101) Berthet, J.-C.; Siffredi, G.; Thuery, P.; Ephritikhine, M., *Dalton Trans.* **2009,** *0*, 3478.
(102) Graves, C. R.; Vaughn, A. E.; Schelter, E. J.; Scott, B. L.; Thompson, J. D.; Morris, D. E.; Kiplinger, J. L., *Inorg. Chem.* **2008,** *47*, 11879.

(103) Lewis, A. J.; Carroll, P. J.; Schelter, E. J., *J. Am. Chem. Soc.* **2013,** *135*, 511.
(104) Brown, J. L.; Fortier, S.; Wu, G.; Kaltsoyannis, N.; Hayton, T. W., *J. Am. Chem. Soc.* **2013,** *135*, 5352.
(105) Fortier, S.; Kaltsoyannis, N.; Wu, G.; Hayton, T. W., *J. Am. Chem. Soc.* **2011,** *133*, 14224.
(106) Hrobárik, P.; Hrobáriková, V.; Greif, A. H.; Kaupp, M., *Angew. Chem. Int. Ed.* **2012,** *51*, 10884.
(107) Lukens, W. W.; Beshouri, S. M.; Blosch, L. L.; Stuart, A. L.; Andersen, R. A., *Organometallics* **1999,** *18*, 1235.
(108) Kiplinger, J. L.; John, K. D.; Morris, D. E.; Scott, B. L.; Burns, C. J., *Organometallics* **2002,** *21*, 4306.
(109) Barnea, E.; Andrea, T.; Kapon, M.; Berthet, J.-C.; Ephritikhine, M.; Eisen, M. S., *J. Am. Chem. Soc.* **2004,** *126*, 10860.
(110) Evans, W. J.; Kozimor, S. A.; Hillman, W. R.; Ziller, J. W., *Organometallics* **2005,** *24*, 4676.
(111) Evans, W. J.; Kozimor, S. A.; Ziller, J. W., *Organometallics* **2005,** *24*, 3407.
(112) Pool, J. A.; Scott, B. L.; Kiplinger, J. L., *J. Alloys Compd.* **2006,** *418*, 178.
(113) Evans, W. J.; Miller, K. A.; Ziller, J. W.; DiPasquale, A. G.; Heroux, K. J.; Rheingold, A. L., *Organometallics* **2007,** *26*, 4287.
(114) Schelter, E. J.; Veauthier, J. M.; Graves, C. R.; John, K. D.; Scott, B. L.; Thompson, J. D.; Pool-Davis-Tournear, J. A.; Morris, D. E.; Kiplinger, J. L., *Chem. - Eur. J.* **2008,** *14*, 7782.
(115) Evans, W. J.; Walensky, J. R.; Furche, F.; Ziller, J. W.; DiPasquale, A. G.; Rheingold, A. L., *Inorg. Chem.* **2008,** *47*, 10169.
(116) Evans, W. J.; Walensky, J. R.; Ziller, J. W.; Rheingold, A. L., *Organometallics* **2009,** *28*.
(117) Thomson, R. K.; Graves, C. R.; Scott, B. L.; Kiplinger, J. L., *Eur. J. Inorg. Chem.* **2009,** *2009*.
(118) Evans, W. J.; Siladke, N. A.; Ziller, J. W., *Chem. - Eur. J.* **2010,** *16*, 796.
(119) Evans, W. J.; Walensky, J. R.; Ziller, J. W., *Inorg. Chem.* **2010,** *49*, 1743.
(120) Newell, B. S.; Schwaab, T. C.; Shores, M. P., *Inorg. Chem.* **2011,** *50*, 12108.
(121) Turner, H. W.; Andersen, R. A.; Zalkin, A.; Templeton, D. H., *Inorg. Chem.* **1979,** *18*, 1221.
(122) Cramer, R. E.; Maynard, R. B.; Paw, J. C.; Gilje, J. W., *J. Am. Chem. Soc.* **1981,** *103*.
(123) Fortier, S.; Walensky, J. R.; Wu, G.; Hayton, T. W., *J. Am. Chem. Soc.* **2011,** *133*, 6894.
(124) Cooper, O. J.; Mills, D. P.; McMaster, J.; Moro, F.; Davies, E. S.; Lewis, W.; Blake, A. J.; Liddle, S. T., *Angew. Chem. Int. Ed.* **2011,** *50*, 2383.
(125) Dormond, A.; El Bouadili, A. A.; Moise, C., *J. Chem. Soc., Chem. Commun.* **1985,** *0*, 914.
(126) Graves, C. R.; Scott, B. L.; Morris, D. E.; Kiplinger, J. L., *Organometallics* **2008,** *27*, 3335.
(127) Newell, B. S.; Rapp , A. K.; Shores, M. P., *Inorg. Chem.* **2010,** *49*, 1595.
(128) K ch le, W.; Dolg, M.; Stoll, H.; Preuss, H., *J. Chem. Phys.* **1994,** *100*, 7535.
(129) Simpson, S. J.; Turner, H. W.; Andersen, R. A., *Inorg. Chem.* **1981,** *20*, 2991.
(130) Bordwell, F. G., *Acc. Chem. Res.* **1988,** *21*, 456.
(131) Bordwell, F. G.; Drucker, G. E.; Andersen, N. H.; Denniston, A. D., *J. Am. Chem. Soc.* **1986,** *108*, 7310.

(132) Andersen, R. A.; Zalkin, A.; Templeton, D. H., *Inorg. Chem.* **1981,** *20*.
(133) Bridgeman, A. J.; Cavigliasso, G.; Ireland, L. R.; Rothery, J., *J. Chem. Soc., Dalton Trans.* **2001**, 2095.
(134) Konezny, S. J.; Doherty, M. D.; Luca, O. R.; Crabtree, R. H.; Soloveichik, G. L.; Batista, V. S., *J. Phys. Chem. C* **2012,** *116*.
(135) Graves, C. R.; Yang, P.; Kozimor, S. A.; Vaughn, A. E.; Clark, D. L.; Conradson, S. D.; Schelter, E. J.; Scott, B. L.; Thompson, J. D.; Hay, P. J.; Morris, D. E.; Kiplinger, J. L., *J. Am. Chem. Soc.* **2008,** *130*, 5272.
(136) Elkechai, A.; Mani, Y.; Boucekkine, A.; Ephritikhine, M., *Inorg. Chem.* **2012,** *51*, 6943.
(137) Steele, H. M.; Guillaumont, D.; Moisy, P., *J. Phys. Chem. A* **2013**.
(138) Lukens, W. W.; Edelstein, N. M.; Magnani, N.; Hayton, T. W.; Fortier, S.; Seaman, L. A., *J. Am. Chem. Soc.* **2013,** *135*, 10742.
(139) Straka, M.; Patzschke, M.; Pyykkö, P., *Theor. Chem. Acc.* **2003,** *109*, 332.
(140) Stewart, J. L. *Tris[bis(trimethylsilyl)amido]uranium: compounds with tri-, tetra-, and pentavalent uranium*; Lawrence Berkeley Lab.: 1988; p 200 pp.
(141) Castro-Rodriguez, I.; Olsen, K.; Gantzel, P.; Meyer, K., *J. Am. Chem. Soc.* **2003,** *125*, 4565.
(142) Arnold, P. L.; Turner, Z. R.; Kaltsoyannis, N.; Pelekanaki, P.; Bellabarba, R. M.; Tooze, R. P., *Chem. - Eur. J.* **2010,** *16*, 9623.
(143) Smiles, D. E.; Wu, G.; Hayton, T. W., *J. Am. Chem. Soc.* **2013,** *136*, 96.
(144) James, A. M.; Laxman, R. K.; Fronczek, F. R.; Maverick, A. W., *Inorg. Chem.* **1998,** *37*, 3785.
(145) Arnold, P. L.; Hollis, E.; Nichol, G. S.; Love, J. B.; Griveau, J.-C.; Caciuffo, R.; Magnani, N.; Maron, L.; Castro, L.; Yahia, A.; Odoh, S. O.; Schreckenbach, G., *J. Am. Chem. Soc.* **2013,** *135*, 3841.
(146) Jones, G. M.; Arnold, P. L.; Love, J. B., *Chem. - Eur. J.* **2013,** *19*, 10287.
(147) Evans, W. J.; Davis, B. L., *Chem. Rev.* **2002,** *102*, 2119.
(148) PhB(MesIm) = phenyltris(1-mesitylimidazol-2-ylidene)borate
(149) Scepaniak, J. J.; Young, J. A.; Bontchev, R. P.; Smith, J. M., *Angew. Chem. Int. Ed.* **2009,** *48*, 3158.
(150) Thomson, R. K.; Cantat, T.; Scott, B. L.; Morris, D. E.; Batista, E. R.; Kiplinger, J. L., *Nat. Chem.* **2010,** *2*, 723.
(151) King, D. M.; Tuna, F.; McInnes, E. J.; McMaster, J.; Lewis, W.; Blake, A. J.; Liddle, S. T., *Nat. Chem.* **2013,** *5*, 482.

Chapter 4

Controlling the Primary and Secondary Coordination Sphere with Electron Deficient Diarylamide Ligands Incorporating Non-Covalent Interactions

4.1 Electron-Deficient Non-Symmetric Diarylamide Ligands. The coordination geometries at mid- to low valent uranium ions are typically non-directional and unpredictable.[1] Applying electron-rich ligand systems with large steric demands to confer stability and direct reactivity has been a fruitful approach in uranium chemistry.[2] Multidentate ligands derived from TREN, TREN = tris(2-aminoethyl)amine, have been extensively explored in this context, as they are electron-rich and direct coordination to a confined pocket.[3-6] These multidentate amide ligands typically prevent oligomerization that has been observed for monodentate uranium-amide complexes without sufficient steric protection.[7, 8] Conversely, stable monomeric uranium complexes can be obtained in relatively open ligand frameworks incorporating energetically weaker contributions such as *β*-agostic interactions to the coordination sphere of uranium ions.[9-12] The combination of sterically demanding ligands and weak agostic interactions has been shown to enforce geometries that direct reactivity.[13] We reasoned that fluorinated diarylamide ligands would engage in non-covalent interactions, to direct the secondary coordination sphere around a uranium ion. The coordination chemistry of low valent uranium as well as uranyl with the NAr^{F}Ph$^-$ ligand was investigated, due to the ability for this ligand type to engage in cooperative π-stacking interactions as well as dative C-F→M interactions.

Portions of this chapter have been adapted from a previous publication. Sections 4.1, 4.2, and 4.5.1-4.5.7 are adapted from "Fluorinated Diarylamide Complexes of Uranium(III, IV) Incorporating Ancillary Fluorine-to-Uranium Dative Interactions" Yin, H.; Lewis, A. J.; Williams, U. J.; Carroll, P. J.; Schelter, E. J. *Chem. Sci.* **2013**, *4*, 798–805 with permission from The Royal Society of Chemistry.

4.2 Low Valent Uranium Complexes of the NAr^{F}Ph$^-$ Ligand.

4.2.1 Synthesis and Characterization. The amine HNAr^{F}Ph was prepared in 83% yield on a 10 g scale by a single step Buchwald-Hartwig cross-coupling reaction of 3,5-bis(trifluoromethyl)bromobenzene and aniline.[14] In addition to full spectroscopic characterization, the structure of HNAr^{F}Ph was determined by X-ray diffraction (Figure 4.2.1.1). Deprotonation with KH in THF provided KNAr^{F}Ph as the 0.5 THF solvate in 85% yield, which was recrystallized from a THF solution layered with hexanes at –21 °C to reveal solvation with 3 THF molecules prior to application of vacuum (Figure 4.2.1.2). Alternately, the solvent-free deprotonated ligand was obtained through reaction of HNAr^{F}Ph with KH in Et_2O in 87% yield.

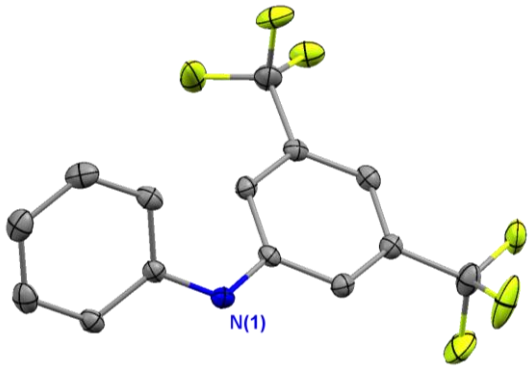

Figure 4.2.1.1 Thermal ellipsoid plot of HNAr^{F}Ph at 30% probability. Hydrogen atoms are omitted for clarity.

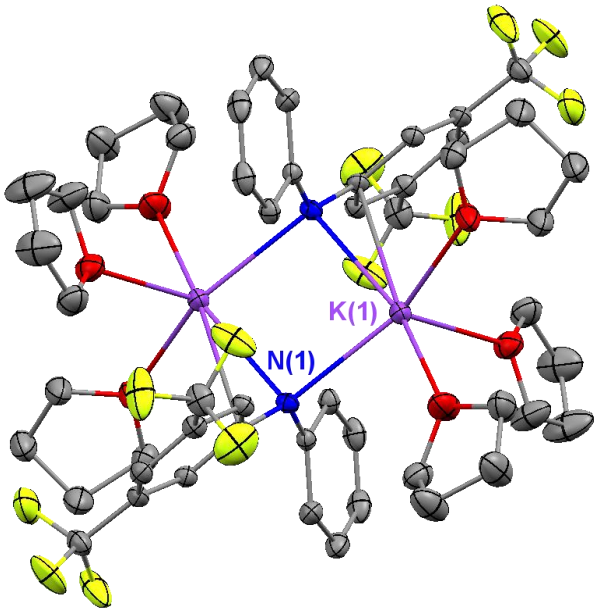

Figure 4.2.1.2 Thermal ellipsoid plot of $[KNAr^FPh(THF)_3]_2$ at 30% probability. Hydrogen atoms are omitted for clarity.

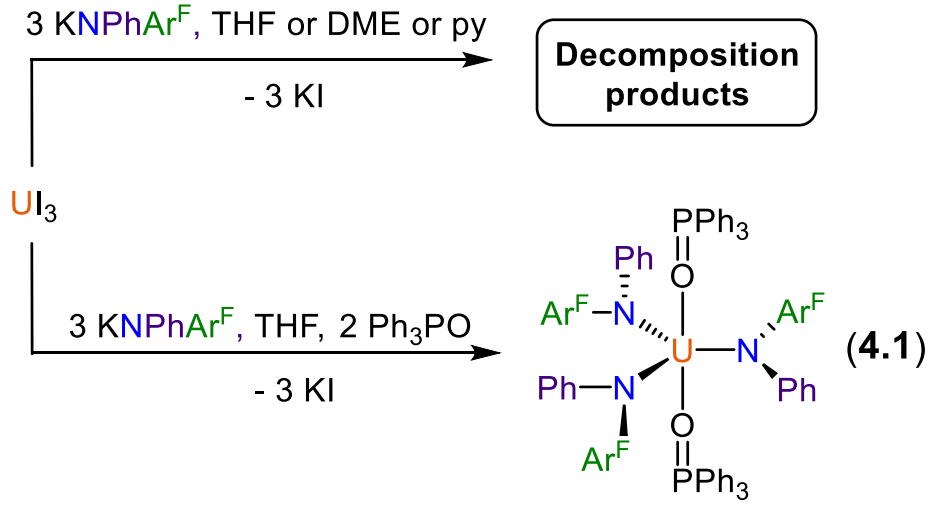

Scheme 4.2.1.1 Synthesis of **4.1** and attempted synthesis of alternate solvates.

As a first step towards exploring the coordination chemistry of the NAr^FPh^- ligand, we set out to synthesize low valent uranium derivatives. However, attempts to synthesize U(III)-$NPhAr^F$ solvate complexes met with little success. Addition of 3 equiv $KNPhAr^F$ to a THF, pyridine, or DME solution of UI_3 cooled to –21 °C led to the initial formation of a dark purple solution with apparent precipitation of KI in each case (Scheme 4.2.1.1). Monitoring these reactions by *in situ*

^{1}H and ^{19}F NMR showed apparent initial complex formation. However, removal of solvent or addition of non-coordinating solvent such as hexanes or pentane routinely led to further reactions, typically generating red or brown solutions indicative of oxidation products. In one instance we were able to isolate a few crystals of one of a decomposition product, characterized by X-ray crystallography as [K(py)][U(F)(NPhAr$^F_2$)$_4$(py)] (Figure 4.2.1.3). This unlikely product is indicative of the instability of the initially formed U(III) complex. Interestingly, the K^+ ion exhibited close contact with both the coordinated fluoride ligand as well as the CF_3 groups of the Ar^F rings, indicating that these peripheral non-covalent interactions may guide the overall structure.

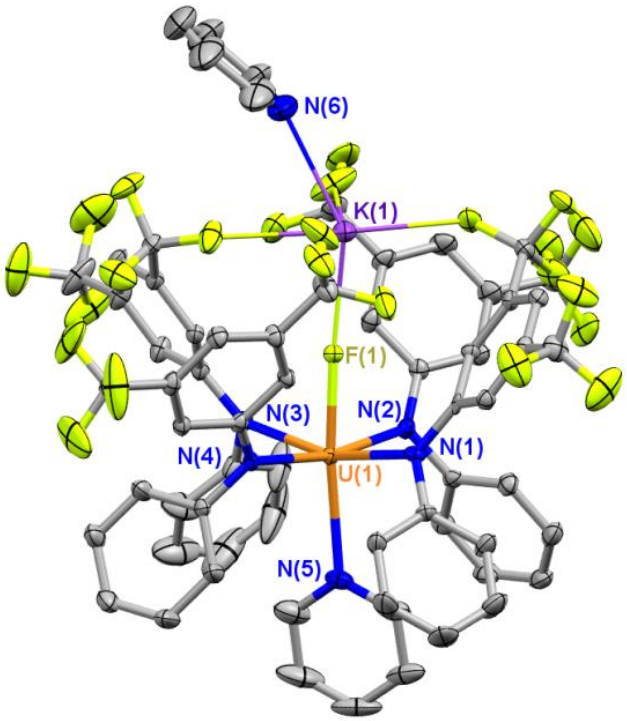

Figure 4.2.1.3 Thermal ellipsoid plot of [K(py)][U^{IV}(F)(NPhAr^F)$_4$(py)] at 30% probability. Hydrogen atoms are omitted for clarity. Bond lengths (Å) and angles (°):U(1)−F(25) 2.143(3), U(1)−N(1) 2.402(4), U(1)−N(2) 2.385(4), U(1)−N(3) 2.351(4), U(1)−N(4) 2.382(4), U(1)−N(5) 2.630(4).

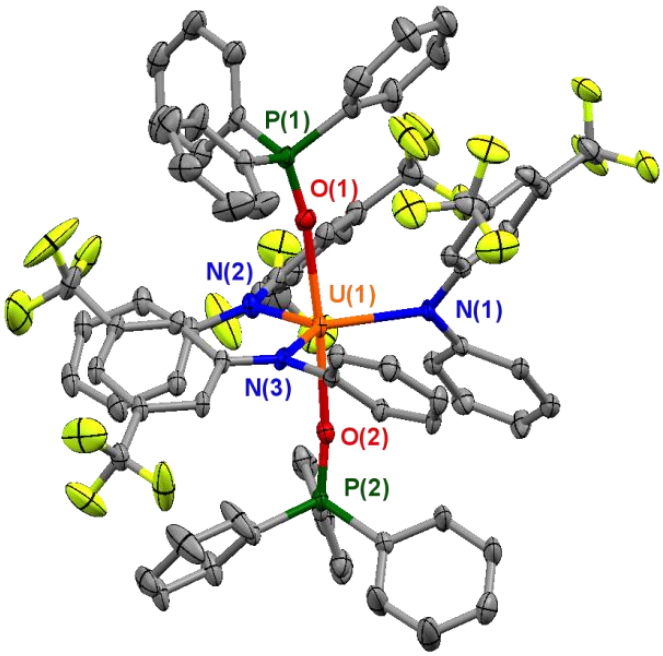

Figure 4.2.1.4 Thermal ellipsoid plot of $U^{III}(NPhAr^F)_3(OPPh_3)_2$ (**4.1**) at 30% probability. Hydrogen atoms omitted for clarity. Selected bond length (Å) and angles (deg): U(1)–N(1) 2.390(5), U(1)–N(2) 2.426(5), U(1)–N(3) 2.390(5), U(1)–O(1) 2.388(5), U(1)–O(2) 2.387(4); U(1)–O(1)–P(1) 169.7(3), U(1)–O(2)–P(2) 172.3(3), O(1)–U(1)–O(2) 175.99(14), N(1)–U(1)–N(2) 118.53(17), N(2)–U(1)–N(3) 122.26(17), N(1)–U(1)–N(3) 119.20(17).

In contrast, addition of 2 equiv triphenylphosphine oxide to UI_3, followed by subsequent addition of 3 equiv $KNPhAr^F$ led to the formation of green-black solution and precipitation of KI (Scheme 4.2.1.1). Recrystallization from a toluene solution layered with pentane afforded dark green $U(NPhAr^F)_3(OPPh_3)_2$ (**4.1**) in 76% yield. The ^{1}H NMR spectrum of **4.1** showed the expected eight peaks for a C_3 symmetric complex, with resonances between +18 and -7 ppm. The ^{19}F NMR spectrum similarly showed a single peak at room temperature. The ^{31}P NMR showed a single broad peak centered at 266.2 ppm, extremely shifted due to the close proximity of the phosphorous atoms to the metal center. The X-ray crystal structure of **4.1** revealed an approximately trigonal bi-pyramidal geometry, in which the phenyl groups of the Ph_3PO ligands cooperatively direct the aryl groups of the $NPhAr^{F-}$ ligands into the equatorial plane (Figure 4.2.1.4). We therefore rationalized the stability of **4.1** based on the steric protection provided by the collective arrangement of the ligands as well as inert nature of the strong donor Ph_3PO

ligands. Inter-ligand π-stacking interactions were not observed between the –Ar^F and –Ph rings in the structure of **4.1**.

Inspired by the ability for Ph_3PO to stabilize a reactive U(III) center, similar ligand types were investigated. Use of 2 equiv Ph_3PCH_2 rather than Ph_3PO led to formation of a dark green product that exhibited resonances in the ^1H and ^{19}F NMR spectra that resembled **4.1**. This product displayed poor stability and was not successfully characterized. Use of Ph_3PS also led to initial formation of a stable U(III) adduct as judged by comparison of the NMR spectra with **4.1**, however this product decomposed to an unidentified pale orange product overnight at –21 °C. Finally, use of 2 equiv Ph_3AsS produced a dark red product, which was recrystallized from fluorobenzene at –21 °C. Poor resolution X-ray data collected on a crystal obtained from this reaction suggested that the product was multinuclear, with 2 NAr^{F}Ph$^-$ ligands per uranium center and numerous bridging sulfur atoms. Several examples of complexes containing bridging uranium-sulfur bonds are now known,[15-21] and a uranium-sulfur cluster has been reported in one instance.[18] Unsuccessful refinement of this structure prevented assessment of oxidation state of the metal ions or the nature of the bonding.

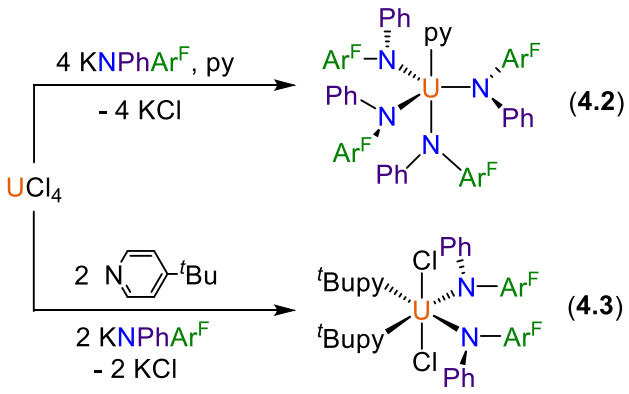

(**4.2**)

(**4.3**)

Scheme 4.2.1.2 Synthesis of U(IV)-(NArFPh) complexes in the presence of different donor co-ligands, py = pyridine and ^{t}Bupy = *p-tert*-butylpyridine.

We next sought to investigate the role of other co-ligands in biasing the synthesis of U(IV) complexes. Reaction of UCl_4 with 4 equiv KNPhAr^F in THF generally yielded a mixture of products as judged by ^{19}F NMR. The same reaction performed in pyridine generated the dark red pyridine adduct U(NPhAr^F)$_4$(py) (**4.2**) as the major product, isolated in 60% yield following

extraction from boiling hexanes. Eight broad peaks were observed in the ^{1}H NMR spectrum of **4.2** between 42 and –7 ppm, and a single resonance in the ^{19}F NMR at -64.3 ppm. X-ray crystallography shows the geometry of **4.2** is best described as a pyridine adduct of the trigonal pyramidal UN_4 core (Figure 4.2.1.5). Again, essentially no π-stacking was observed between the aryl rings of the NAr^{F}Ph$^-$ ligands.

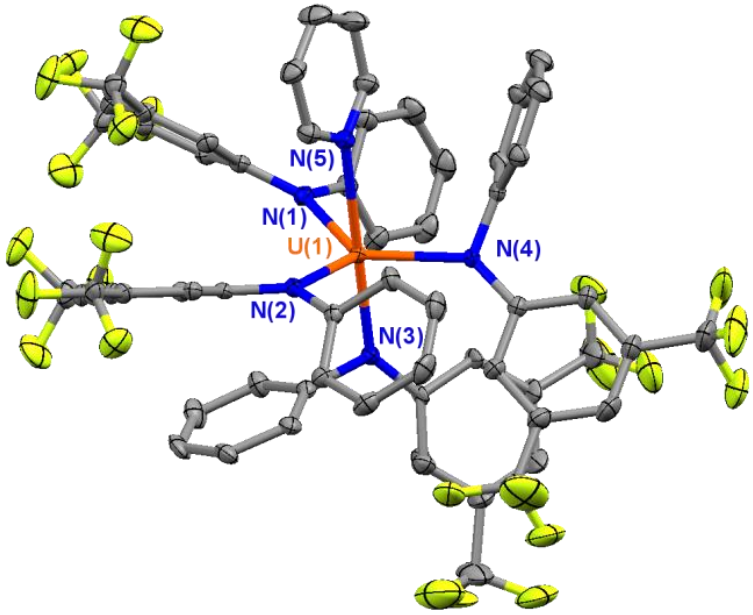

Figure 4.2.1.5 Thermal ellipsoid of U^{IV}(NPhAr^F)$_4$(py) (**4.2**) at 30% probability. Hydrogen atoms are omitted for clarity. Selected bond length (Å) and angles (deg): U(1)–N(1) 2.298(3), U(1)–N(2) 2.290(3), U(1)–N(3) 2.283(3), U(1)–N(4) 2.279(3), U(1)–N(5) 2.637; N(1)–U(1)–N(2) 116.68(12), N(1)–U(1)–N(4) 126.16, N(2)–U(1)–N(4) 114.81(12), N(3)–U(1)–N(5) 178.08(12).

We observed that the outcome of the substitution reaction could be significantly biased by slight difference in the co-ligands. Addition of 2-4 equivalents of KNPhAr^F to a solution of UCl_4 in the presence of *p*-^{t}Bu-pyridine (^{t}Bupy) routinely produced yellow U(NPhAr^F)$_2$(^{t}Bupy)$_2$Cl$_2$ (**4.3**) as the major product despite the presence of additional equivalents of ligand. Use of the appropriate stoichiometry and recrystallization from Et_2O/pentane at –21 °C led to the isolation of **4.3** in 88% yield. Although the ^{1}H NMR spectrum of **4.3** is not fully assignable due to severe broadening, only one resonance is observed in the ^{19}F NMR spectrum. Multiple crystalline polymorphs of **4.3** could be obtained depending on the solvent used. Crystallization from hexanes at –21 °C produced pale yellow plates, from Et_2O/pentane at –21 °C produced dark yellow needles, and from

toluene/hexanes at –21 °C produced dark red blocks. The X-ray crystal structures of two polymorphs of **4.3** are shown in Figure 4.2.1.6. Diffraction data was collected on both the yellow plate (**4.3a**) and dark red block polymorph (**4.3b**), which revealed an almost identical structure, with the exception of a single disordered toluene molecule nestled between the ^{t}Bupy ligands in **4.3b**. This small perturbation causes a distortion of the other aryl groups along the equatorial plane of the complex, allowing the Ar^F groups to come into closer contact with one another (centroid to centroid distance of 3.73 *versus* 3.61 Å respectively).

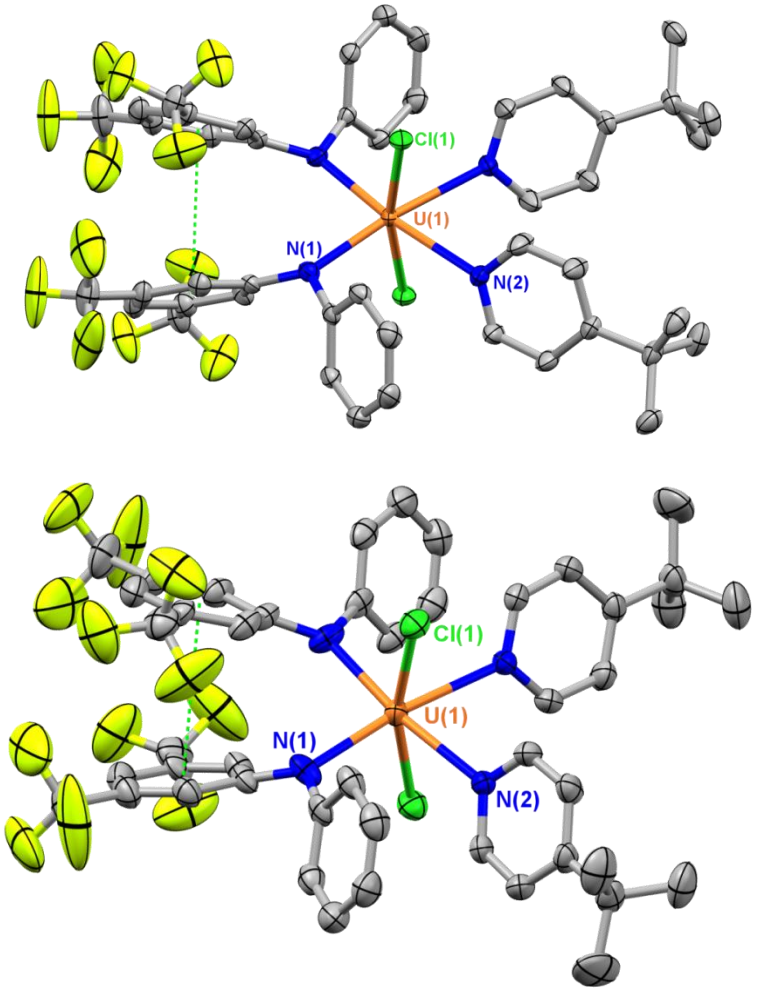

Figure 4.2.1.4 Thermal ellipsoid of **4.3a** (top) and **4.3b** (bottom) at 30% probability. Hydrogen atoms are omitted for clarity. The short π-π stacking distance is illustrated as a green dotted line. Selected bond length (Å) and angles (deg): **4.3a** U(1)–N(1) 2.248(3), U(1)–N(2) 2.587(3), U(1)–Cl(1) 2.6475(8), N(1)–U(1)–N(2) 101.81(10), N(1)–U(1)–N(1') 83.73(14), N(2)–U(1)–N(2') 72.85(13), Cl(1)–U(1)–Cl(1') 167.27(4); **4.3b** U(1)–N(1) 2.289(4), U(1)–N(2) 2.560(3), U(1)–Cl(1) 2.6349(12), N(1)–U(1)–N(2) 97.91, N(1)–U(1)–N(1′) 87.9(2), N(2)–U(1)–N(2′) 76.65(15), Cl(1)–U(1)–Cl(1′) 164.51(5).

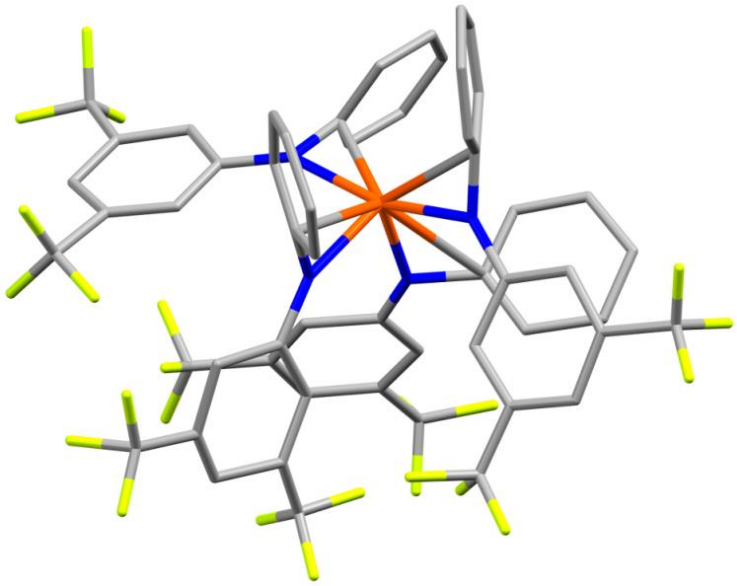

Figure 4.2.1.5 Structure of **4.4** determined from low quality X-ray diffraction data. Only connectivity of this complex could be established.

In an attempt to determine whether a U(IV) complex of NAr^{F}Ph would be stable in the absence of neutral co-ligands, we prepared an unsolvated derivative. Addition of KNPhAr^F to a solution of $UI_4(Et_2O)_2$ in Et_2O produced a red solution with precipitation of KI. Storage of a concentrated hexanes solution at –21 °C precipitated a dark red amorphous solid assigned as U(NPhAr^F)$_4$ (**4.4**). The ^{1}H NMR spectrum of **4.4** in C_6D_6 shows 5 peaks in a 2:1:2:1:2 ratio and only a single sharp resonance is observed in the ^{19}F NMR spectrum, clearly indicating symmetric ligand environments of the monomeric complex in solution. A low resolution structure of **4.4** obtained from crystals grown from a concentrated pentane solution stored at –21 °C confirmed the proposed connectivity and monomeric structure (Figure 4.2.1.5).

4.2.2 ^{1}H NMR Spectra.

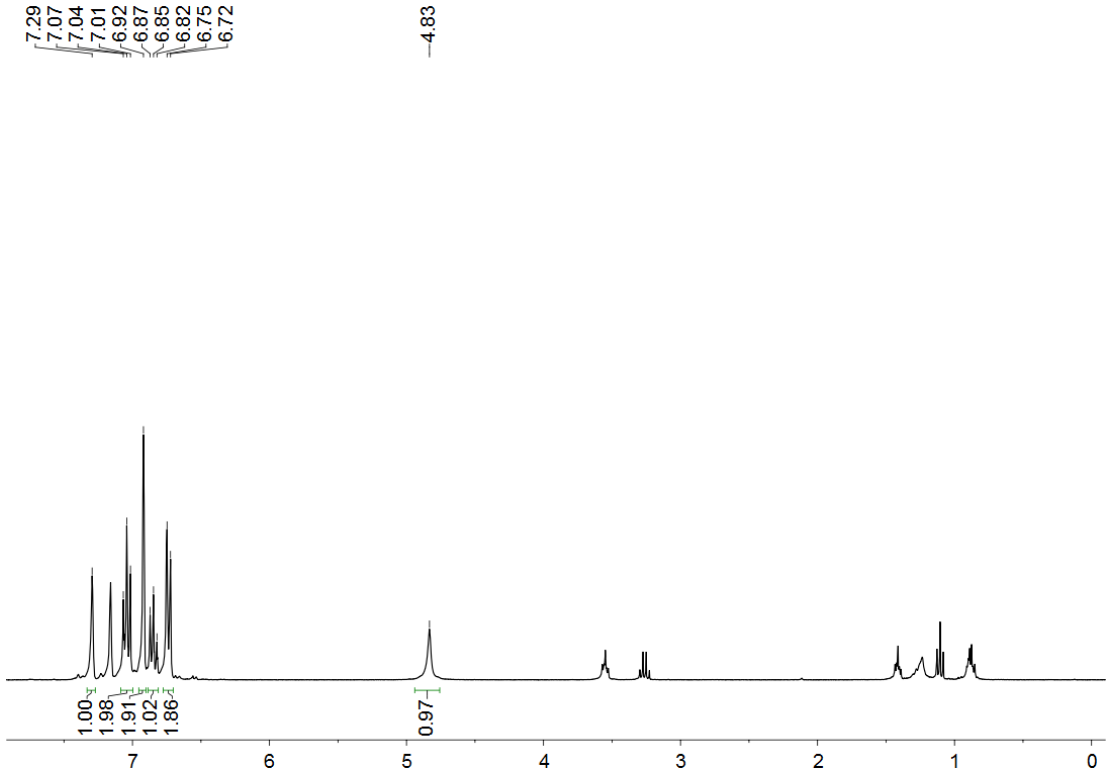

Figure 4.2.2.1 ^{1}H NMR of **HNPhAr^F** in benzene-d_6.

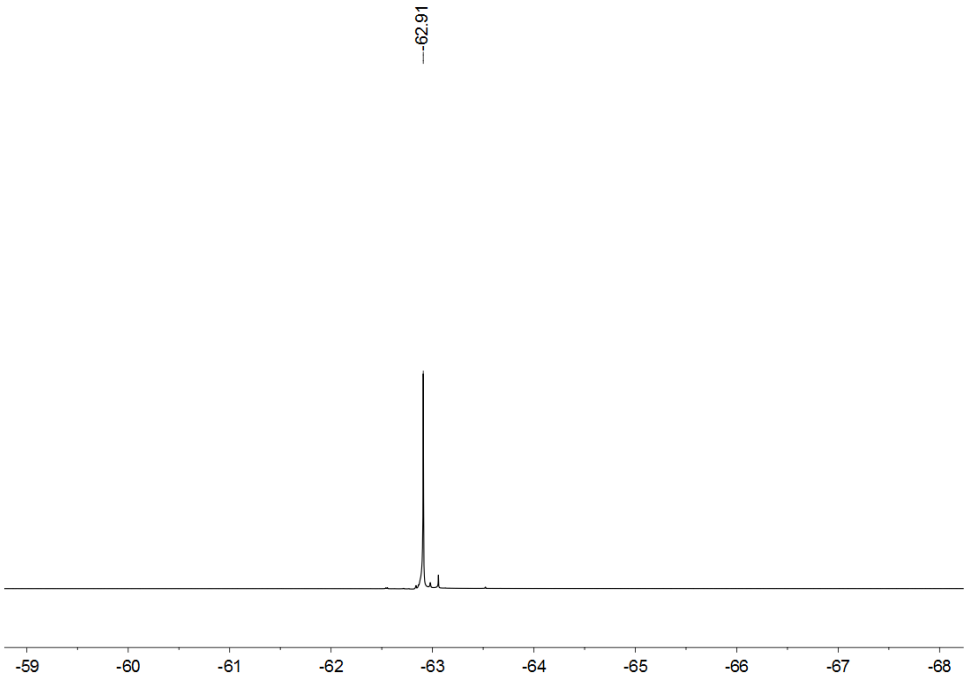

Figure 4.2.2.2 ^{19}F NMR of **HNPhAr^F** in benzene-d_6.

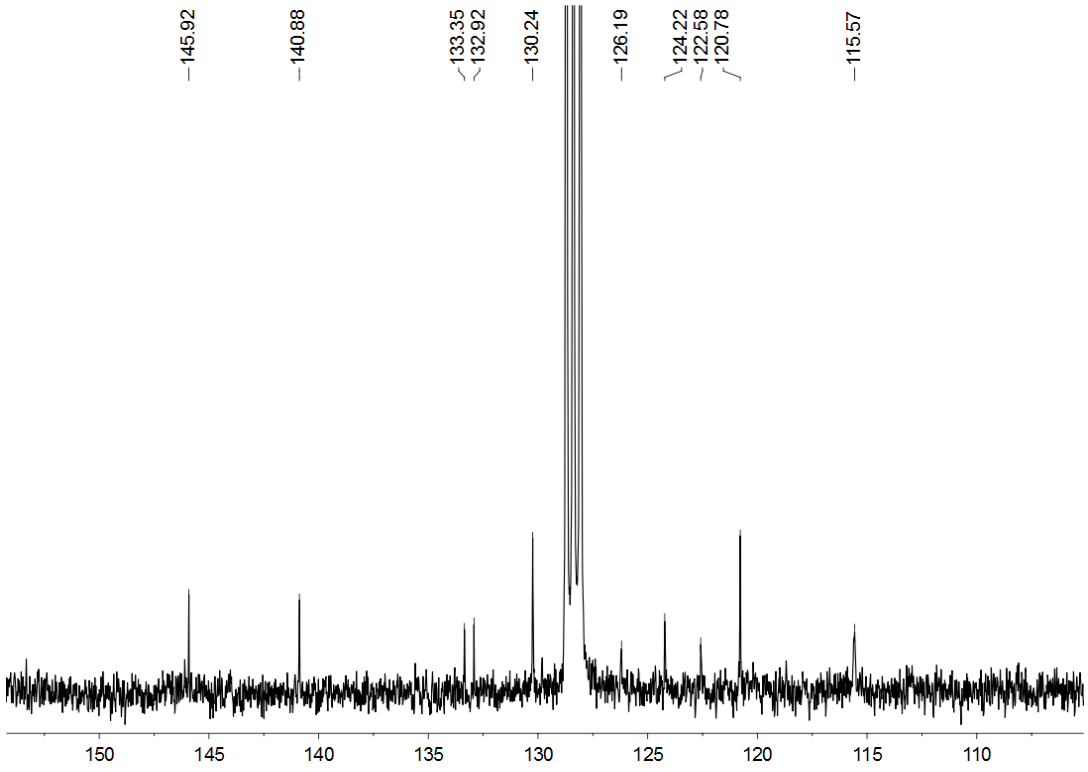

Figure 4.2.2.3 ^{13}C NMR of **HNPhAr^{F}** in benzene-d_6.

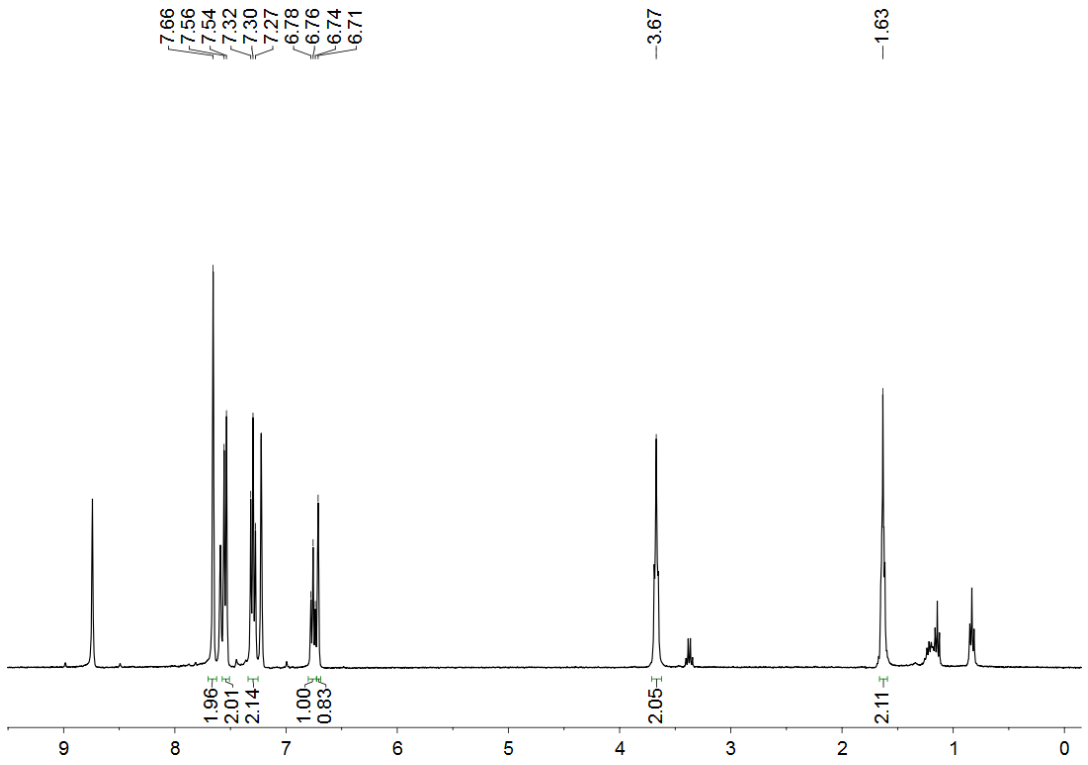

Figure 4.2.2.4 ^{1}H NMR of **KNPhAr^{F}(THF)$_{0.5}$** in pyridine-d_5.

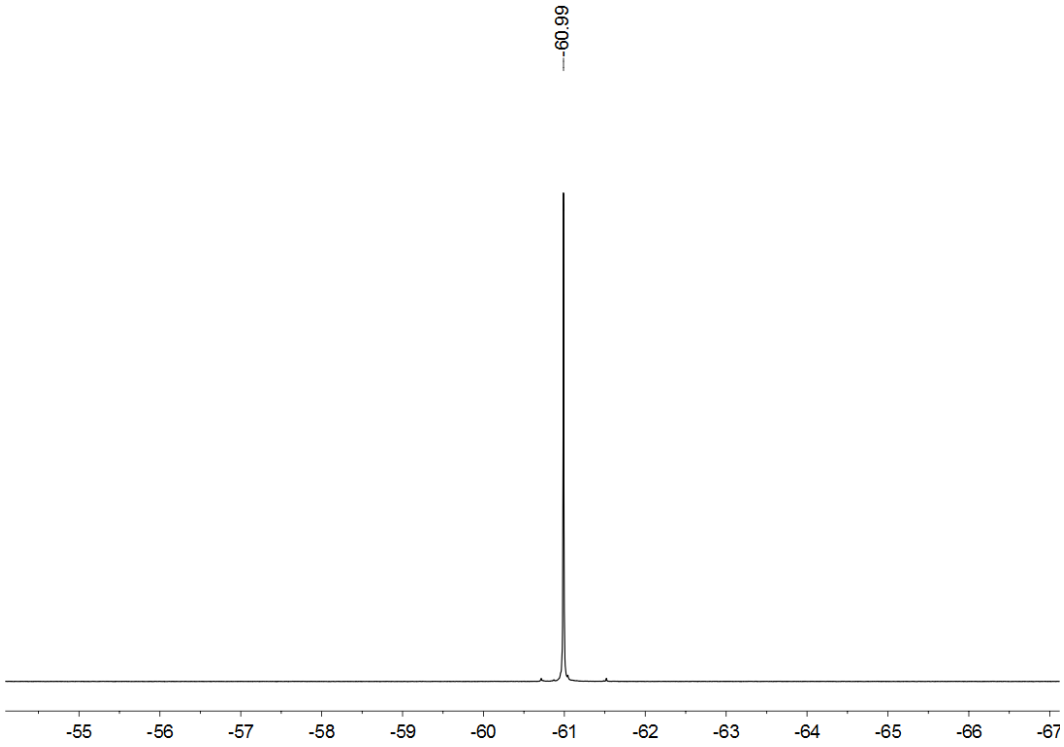

Figure 4.2.2.5 ^{19}F NMR of **KNPhAr^{F}(THF)$_{0.5}$** in pyridine-d_5.

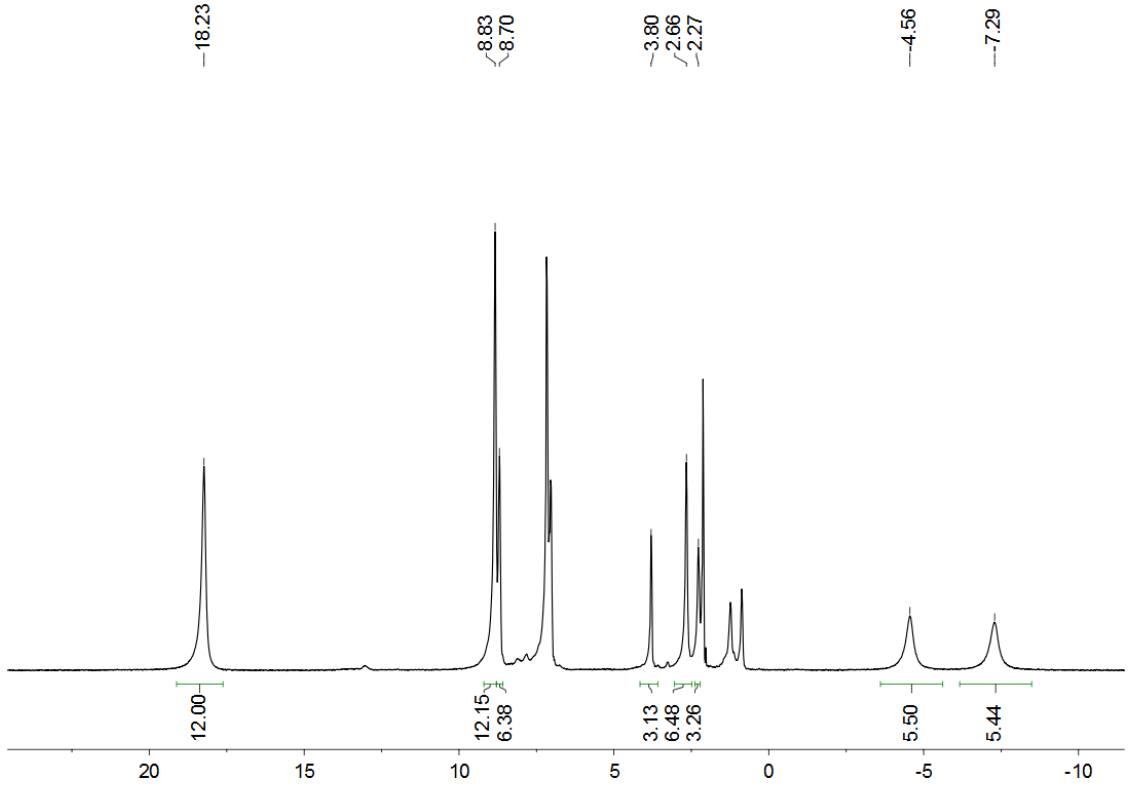

Figure 4.2.2.6 ^{1}H NMR of **4.1** in benzene-d_6.

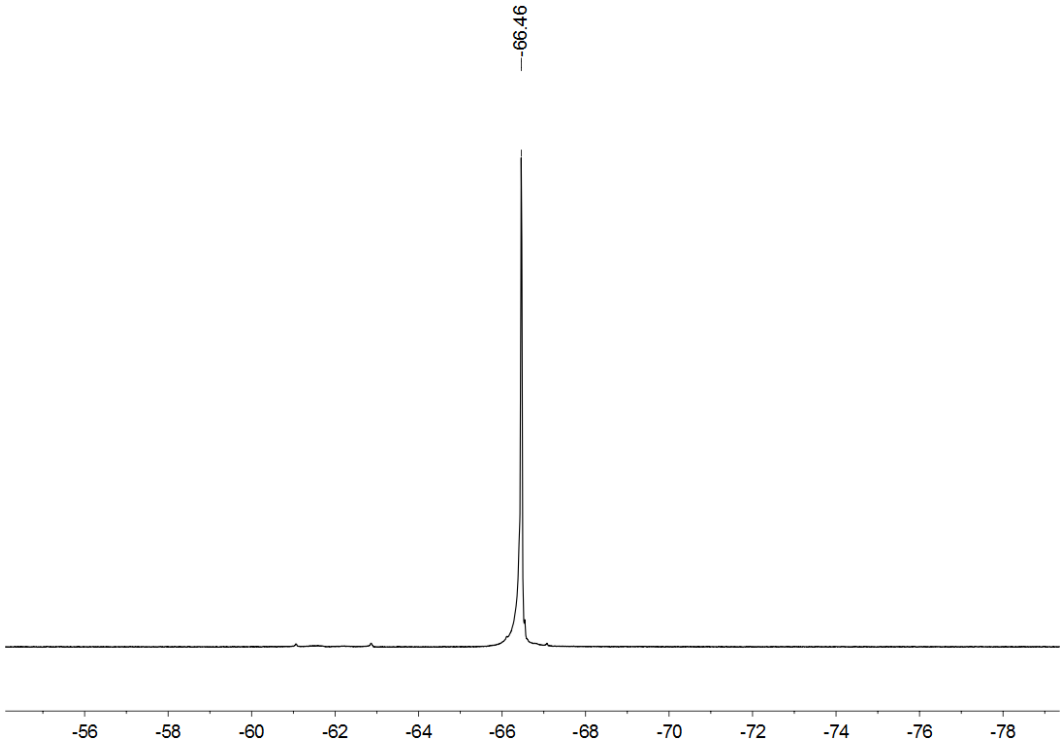

Figure 4.2.2.7 ^{19}F NMR of **4.1** in benzene-d_6.

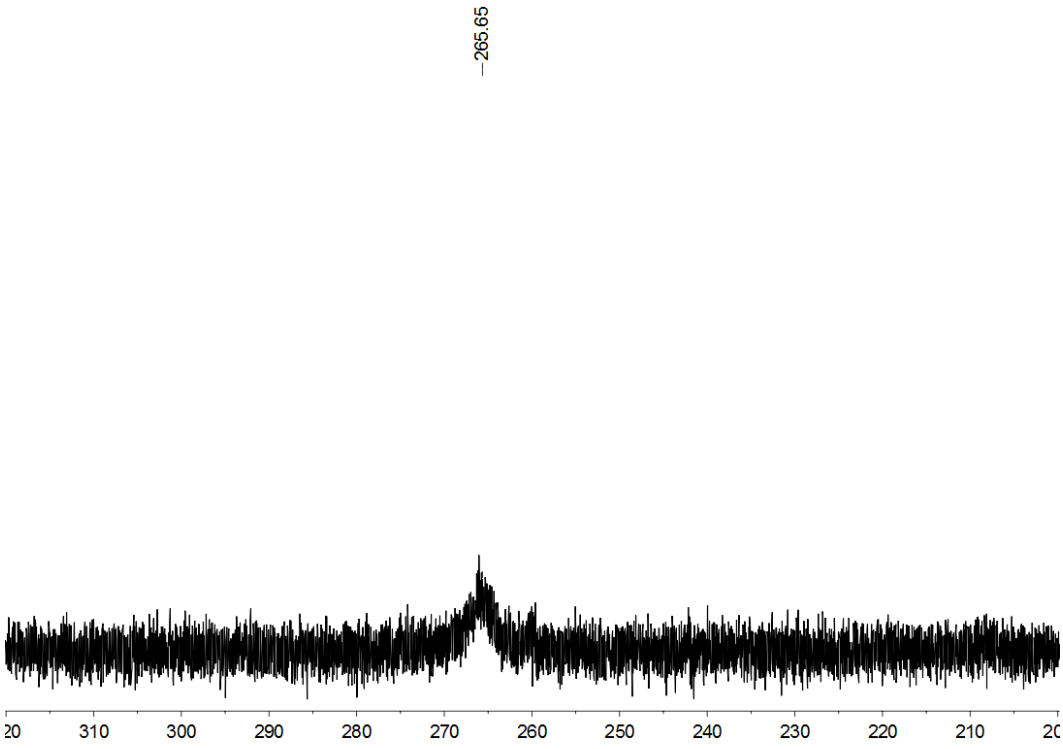

Figure 4.2.2.8 ^{31}P NMR of **4.1** in benzene-d_6.

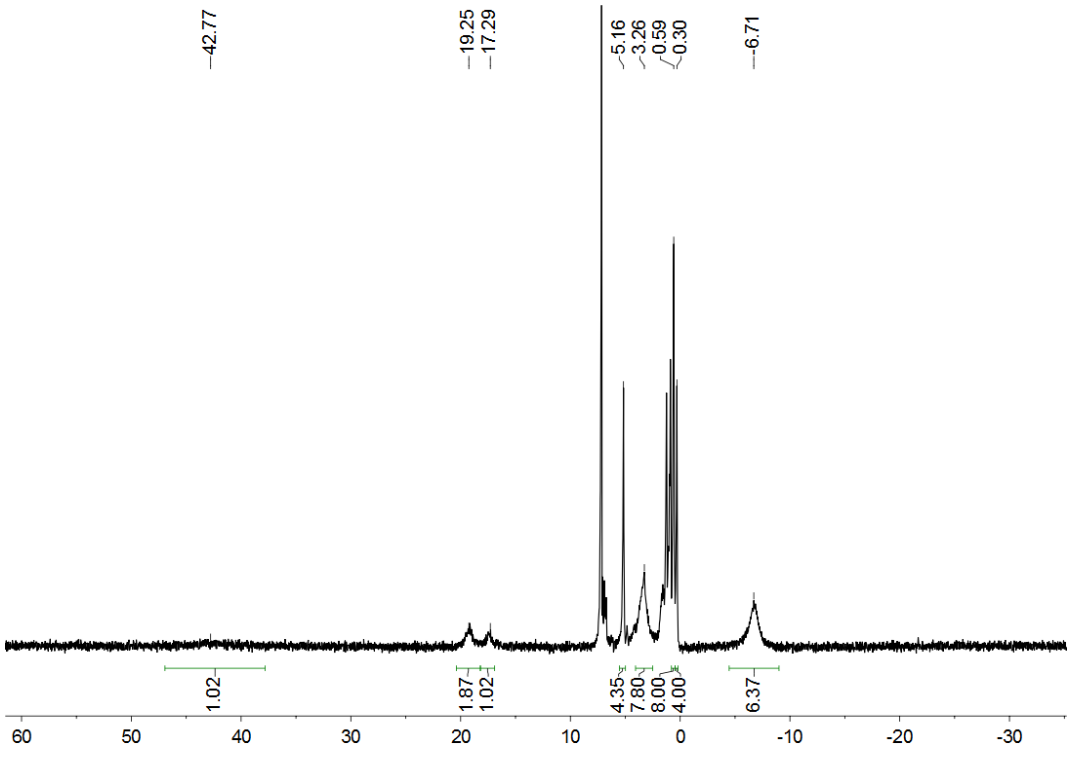

Figure 4.2.2.9 ^{1}H NMR of **4.2** in benzene-d_6.

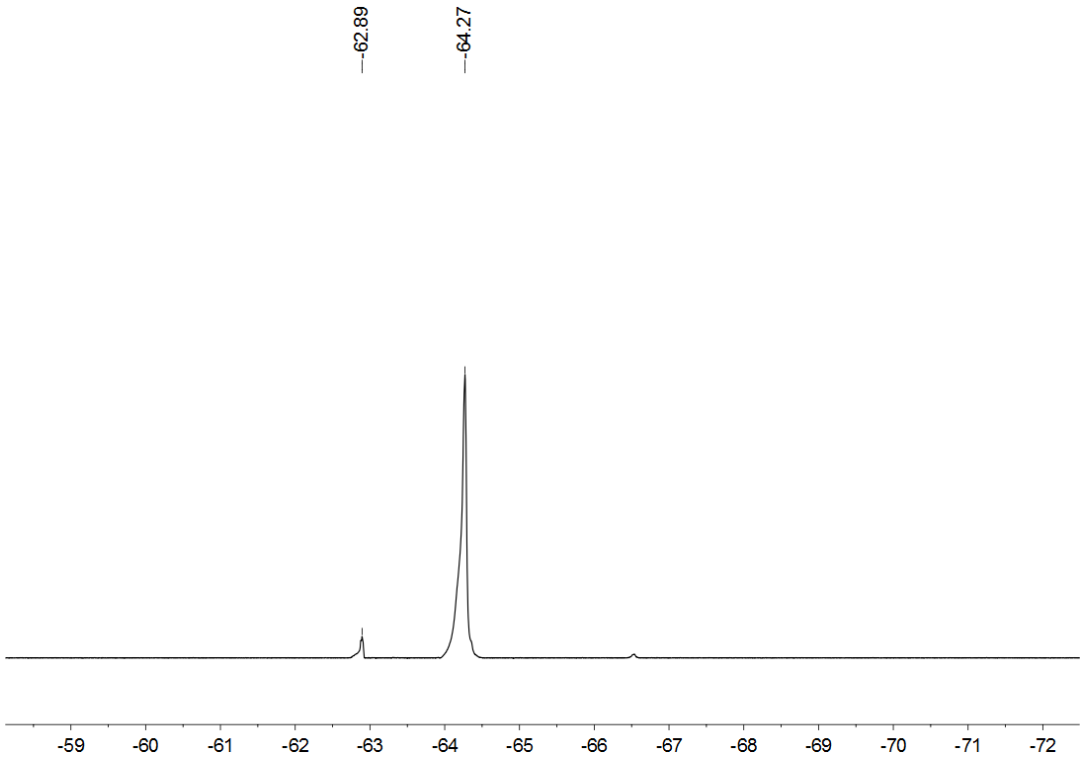

Figure 4.2.2.10 ^{19}F NMR of **4.2** in benzene-d_6. HNPhAr^F is noted as a minor impurity.

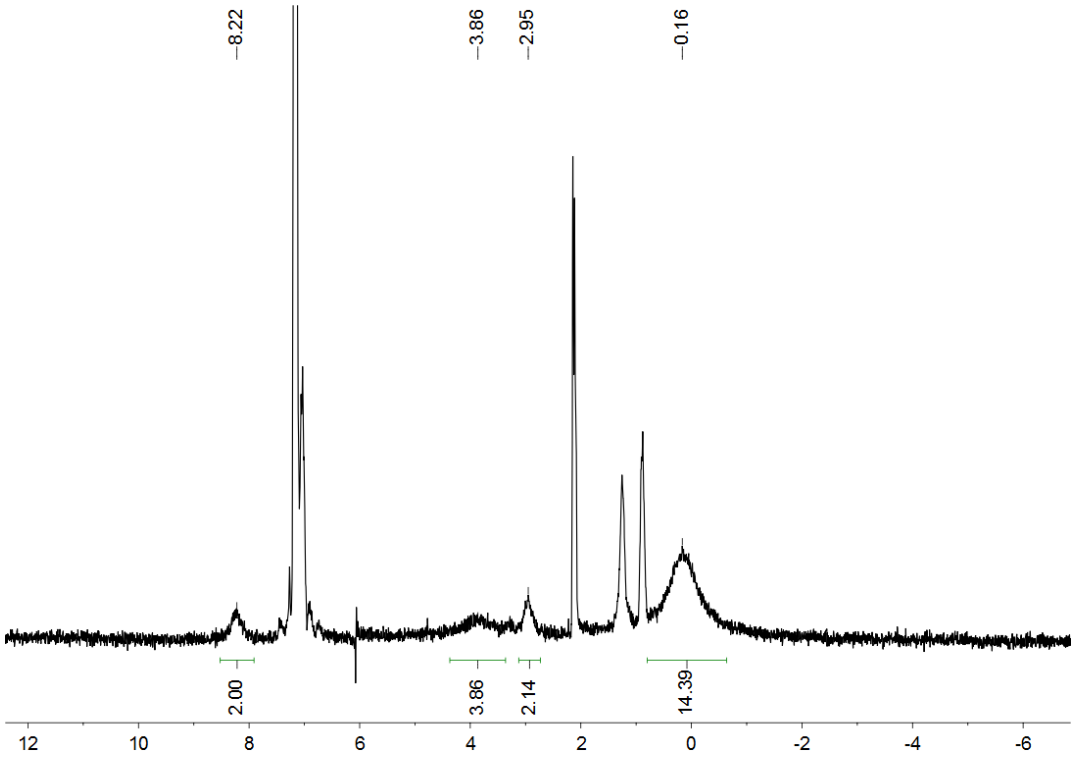

Figure 4.2.2.11 ^{1}H NMR of **4.3** in benzene-d_6.

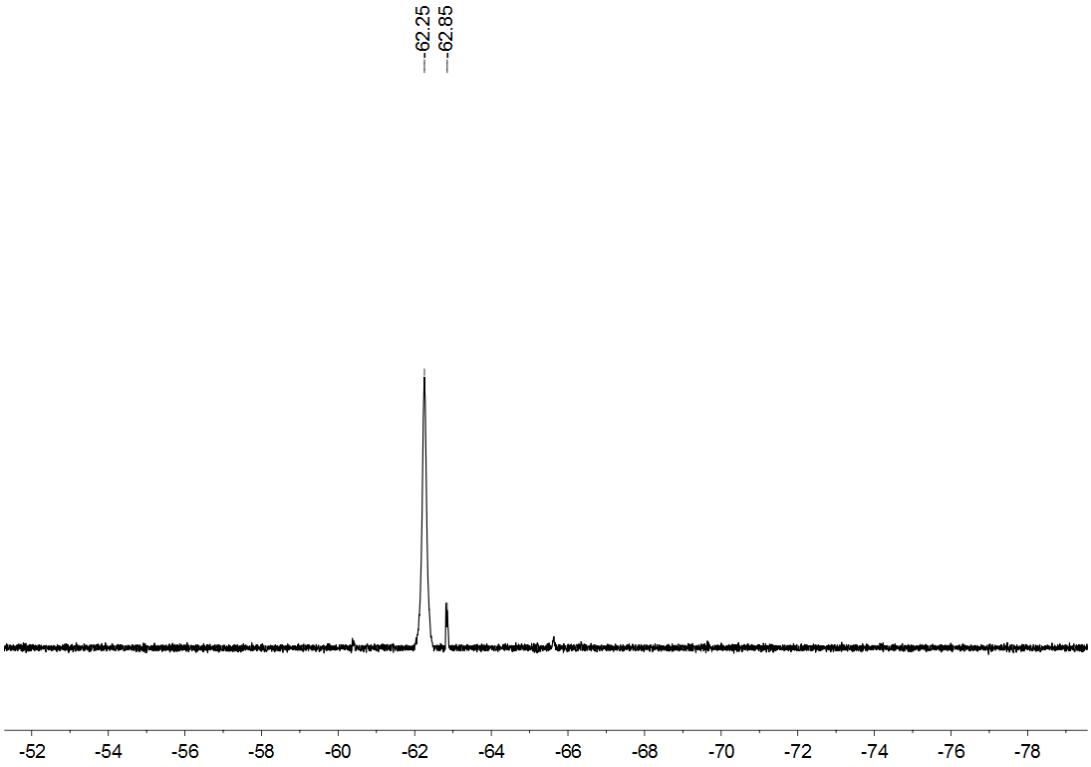

Figure 4.2.2.12 ^{19}F NMR of **4.3** in benzene-d_6. HNPhAr^F is noted as a minor impurity.

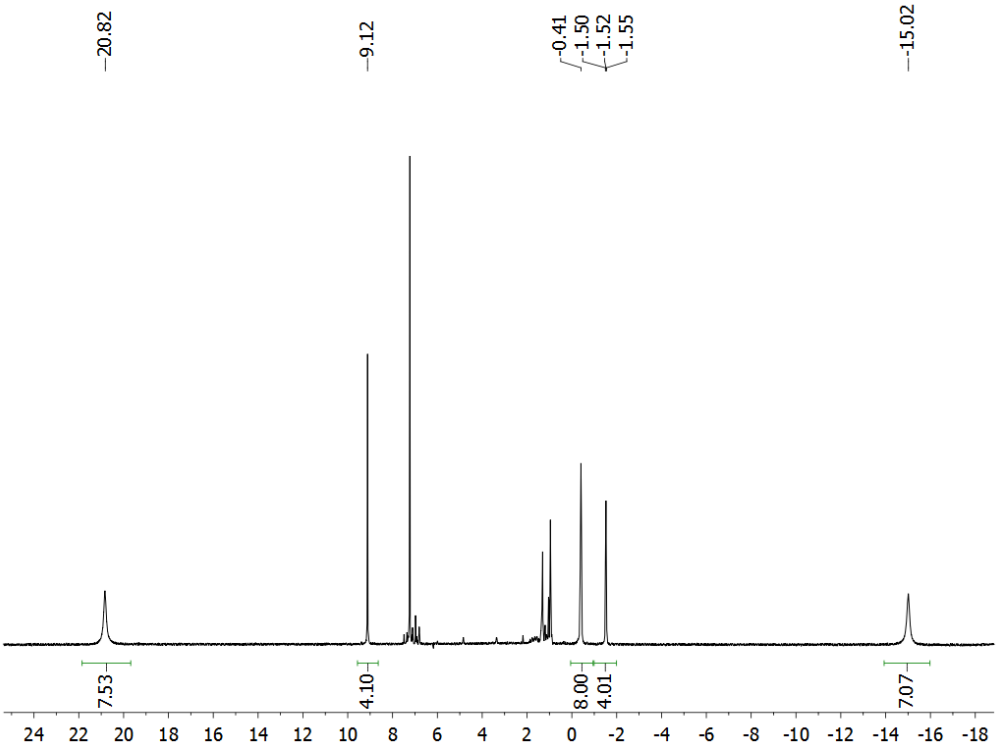

Figure 4.2.2.13 ^{1}H NMR **4.4** in benzene-d_6.

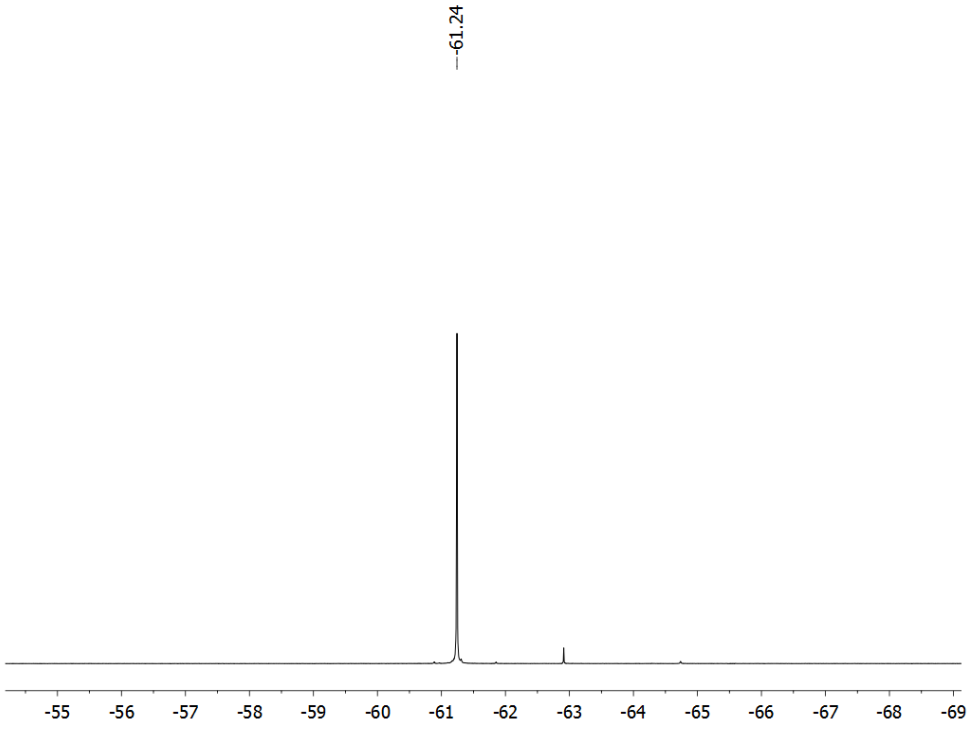

Figure 4.2.2.14 ^{19}F NMR of **4.4** in benzene-d_6. HNPhAr^F is noted as a minor impurity.

4.3 Uranyl Activation. As discussed earlier, the uranyl dication (UO_2^{2+}) is the most prevalent form of uranium in Nature, due to the thermodynamic stability of the linear *trans*-dioxo arrangement of oxygen atoms at the uranium(VI) cation.[22] Various strategies have been employed to activate the inert uranium-oxo bonds of uranyl.[23] Photo-excitation of electrons localized in U=O bonding orbitals to non-bonding U(5f) orbitals facilitates reactivity of the U=O bond.[24] Strong σ-donating ligands polarize U=O bonds as a consequence of *cis*-destabilization, a feature of the inverse *trans* influence present in high-valent uranium complexes.[22, 25-29] Polarization of the U=O bonds increases the Lewis basicity of the oxo ligands, causing them to be more prone to Lewis acid coordination.[30] Lewis acid coordination reduces the charge donation from the oxo ligand to the uranium center, which weakens the U=O bond and facilitates reduction at uranium. Reduction to uranium(V) weakens the U=O bonds, making further reactivity accessible.[31-33]

In the absence of strongly σ-donating ligands, the uranyl oxo ligands tend to be weakly Lewis basic, requiring a strong Lewis acids such as $B(C_6F_5)_3$ to achieve coordination.[30] The formation of strong B–O and Si–O bonds can also provide a substantial enthalpic driving force for U=O bond activation.[32, 34-37] Directing Lewis acid coordination to uranyl has been accomplished through the use of flexible, Pacman-type ligands, a highly successful strategy developed by Arnold and co-workers (Figure 4.3.1, left).[31, 33, 38-45] The simplest Lewis acid, H^+, was directed towards interaction with UO_2^{2+} in the stereognostic coordination chemistry developed by Raymond and co-workers (Figure 4.3.1, right).[46] However, weaker Lewis acids such as alkali metals are known to bind to uranyl oxo-groups in a variety of cases, employing much simpler ligand designs.[47-54]

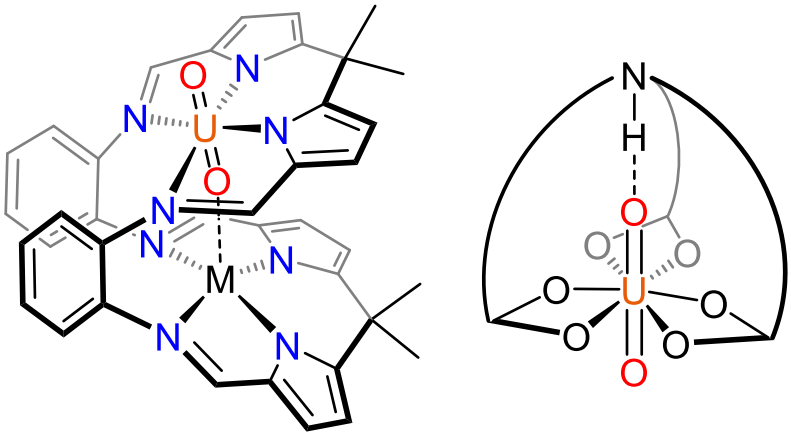

Figure 4.3.1 Lewis acid coordination to uranyl directed by macrocyclic Schiff-base (left) and tris[2-(2-carboxyphenoxy)alkyl]ammonium ligands (right).[38, 46]

Toward our goal of manipulating the coordination environments around f-block cations through collective non-covalent interactions in secondary coordination spheres,[55-59] we sought to facilitate Lewis acid binding at the weakly Lewis basic uranyl oxo ligands through the use of supramolecular design principles. In our work exploring the coordination chemistry of electron-poor diarylamide ligands,[58] we determined that these ligands provided a suitable coordination environment around uranium to create discrete, monomeric complexes.

Considering the coordination chemistry of fluorinated diarlyamides with the uranyl cation, we reasoned that the NAr^{F}Ph$^-$ ligand would create a pocket lined with aryl-fragments around each of the U=O bonds, which could serve as a scaffold to direct cation binding. In this work, we focused on directing the coordination of relatively weakly Lewis acidic K^+ ions to uranyl through self-assembly directed by cation-π and cation-fluorine interactions. The K^+ ion serves as a proof of principle of this approach, as it has only a small inherent tendency to interact with uranyl oxo ligands. For example, among complexes of the formula $[M(crown)]_2[UO_2X_4]^{2-}$ (M(crown) = Li(12-crown-4)$^+$, Na(15-crown-5)$^+$, K(18-crown-6)$^+$, X = Cl$^-$, Br$^-$), M–O=U coordination preference follows the trend $Li^+ > Na^+ > K^+$.[48] We further demonstrated that K^+ coordination provides observable activation of the U=O bonds that persists in solution.

4.4 Uranyl Complexes of the NAr^{F}Ph$^-$ Ligand. Reaction of 8 equiv KNAr^{F}Ph with $[UO_2Cl_2(THF)_2]_2$ in THF led to an immediate color change to dark red. Removal of solvent or

addition of non-coordinating solvent such as hexanes led to a dramatic color change to dark green.[60] Extraction and recrystallization of the dark green product from toluene allowed for the isolation of [K(toluene)]$_2$[UO$_2$(NAr^{F}Ph)$_4$] (**4.5-tol**) in 71% yield. X-ray structural analysis of **4.5-tol** (Figure 4) revealed close association of both potassium ions with the uranyl oxo ligands in the solid state at average K–O distances of 2.602(3). This K–O distance represents the shortest known contact between a K^+ ion and uranyl, including pentavalent uranyl complexes.[61-63] The orientation of the aryl substituents around the U=O bond create a pocket that facilitates favorable cation-π binding, directing the K^+ ion to coordinate to the uranyl oxo ligands. Furthermore, it has been previously suggested that the encapsulation of the uranyl moiety in a hydrophobic pocket strengthens the equatorial metal-ligand bonding.[64] The ^{1}H NMR spectrum of **4.5-tol** displayed a minimal number of resonances and the ^{19}F NMR spectrum showed only one resonance, supporting a symmetric ligand arrangement consistent with the X-ray structure. Attempts to desolvate **4.5-tol** through application of dynamic vacuum or addition of non-coordinating solvent such as hexanes had no effect, indicating resilience of the potassium cations towards desolvation.

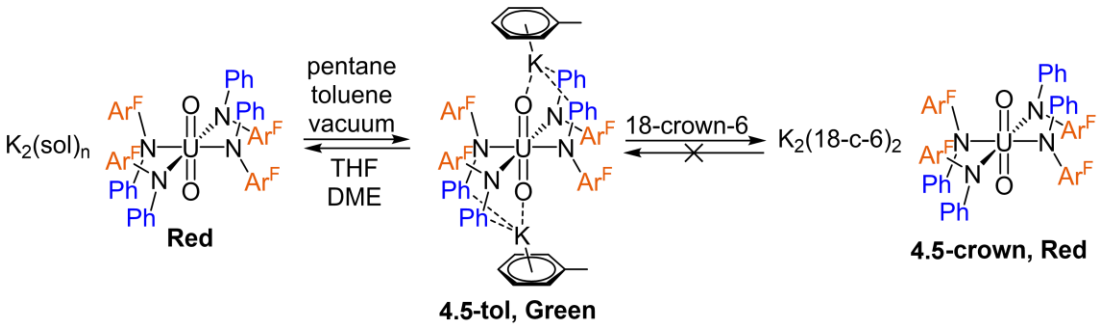

Scheme 4.4.1 Solvation dynamics of **4.5-tol** and **4.5-crown**.

Table 4.4.1 Comparison of bonding metrics in **4.5**, **4.5-crown**, **4.5-tol**.

	U–O$_{av}$	U–N$_{av}$	K–O$_{av}$
4.5-tol (exp.)	1.804(3)	2.393(3)	2.602(3)
4.5-tol (calc.)	1.807	2.449	2.589
4.5	1.802(3)	2.395(5)	2.693(4)
4.5-crown (exp.)	1.791(6)	2.437(6)	–
4.5-crown (calc.)	1.783	2.489	–

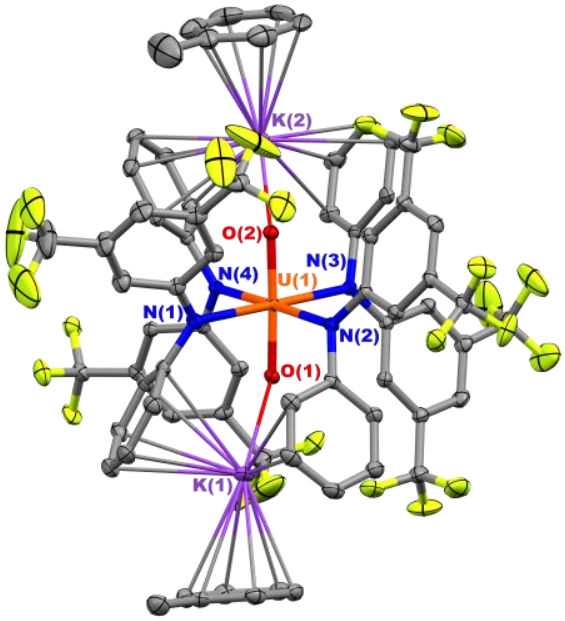

Figure 4.4.1 Thermal ellipsoid plot of **4.5-tol** at 30% probability. Hydrogen atoms omitted for clarity. Selected bond distances (Å) and angles (deg): U(1)–O(1) 1.802(2), U(1)–O(2) 1.806(2), U(1)–N(1) 2.402(3), U(1)–N(2) 2.375(3), U(1)–N(3) 2.397(3), U(1)–N(4) 2.397(3), K(1)–O(1) 2.589(2), K(2)–O(2) 2.614(2); O(1)–U(1)–O(2) 177.83(9).

Attempts to desolvate **4.5-tol** through application of dynamic vacuum or addition of non-coordinating solvent such as hexanes had no effect, indicating tight association of toluene with the potassium cations in solution. However, recrystallization from a concentrated fluorobenzene solution produced $K_2[UO_2(NAr^FPh)_4]$ (**4.5**) with no arene solvation of the potassium ions. The structure of **4.5** (Figure 4.4.2) is essentially identical to that of **4.5-tol**, where the environment around the "unsolvated" K^+ ions is saturated by coordination to $-CF_3$ groups from adjacent molecules in the unit cell. These intermolecular contacts pull the K^+ ions slightly out of their pockets, resulting in a lengthening of the K–O distance (Table 4.4.1). The presence of K^+–F interactions in **4.5** suggests that the $-CF_3$ groups in **4.5-tol** may play a role in directing K^+ coordination in solution, even though these interactions were not observed in the solid state.

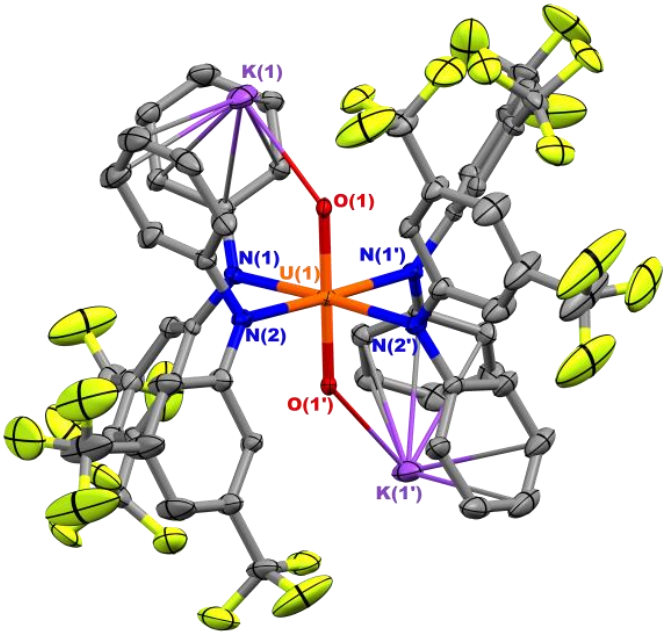

Figure 4.4.2 Thermal ellipsoid plot of **4.5** at 30% probability. Hydrogen atoms and disordered interstitial molecules of fluorobenzene are omitted for clarity. Selected bond distances (Å) and angles (deg): U(1)–O(1) 1.802(3), U(1)–N(1) 2.395(4), U(1)–N(2) 2.394(4), K(1)–O(1) 2.693(4); O(1)–U(1)–O(1') 176.5(2).

Dissolution of **4.5-tol** in a coordinating solvent such as THF reversibly restored the dark red color (Scheme 4.4.1). Addition of 2 equiv 18-crown-6 to a toluene solution of **4.5-tol** led to immediate precipitation of a red solid. Recrystallization from DME layered with hexanes produced crystals suitable for X-ray diffraction, which revealed the structure to be [K(18-crown-6)(DME)]$_2$[UO$_2$(NAr^{F}Ph)$_4$] (**4.5-crown**) (DME = 1,2-dimethyoxyethane) (Figure 4.4.3). With the exception of the removal of the K$^+$ ion from direct coordination to uranyl in **4.5-crown**, the overall structural arrangement of the different aryl functionalities is essentially the same as that of **4.5-tol**. Additionally, the ^{1}H NMR spectrum of **4.5-crown** indicated a similar symmetric ligand environment as in **4.5-tol**, and again the ^{19}F NMR displayed a single resonance.

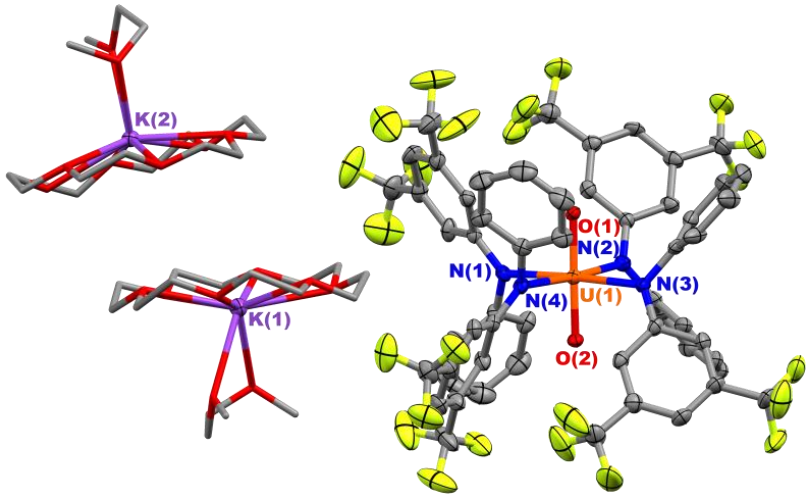

Figure 4.4.3 Thermal ellipsoid plot of **4.5-crown** at 30% probability. Hydrogen atoms are omitted for clarity. Selected bond distances (Å) and angles (deg): U(1)–O(1) 1.789(4), U(1)–O(1) 1.792(4), U(1)–N(1) 2.420(5), U(1)–N(2) 2.453(5), U(1)–N(3) 2.442(5), U(1)–N(4) 2.434(5), O(1)–U(1)–O(2) 178.94(19).

Determining the extent of activation of the U=O bonds of uranyl from the bond metrics is limited by the small variation in these bond lengths. Typical U^{VI}=O bond lengths range from 1.70 to 1.85 Å depending on the degree of activation, though in practice most uranyl complexes exhibit bond lengths of ~1.77 Å within experimental error.[65] A slight lengthening of the U=O bonds in **4.5-tol** relative to those of **4.5-crown** is consistently observed, but the different bond lengths are too close to reliably differentiate (Table 4.4.1). However, within the conserved primary coordination environment, there is a statistically significant decrease in the U–N bond lengths upon K^+ ion coordination to uranyl (Table 4.4.1). These metrics imply that K^+–O coordination weakens the U=O bonds, which strengthens the equatorial U–N bonds through the inverse *trans* influence.[22, 25] These U–N bond lengths are significantly longer than those of other structurally characterized uranyl complexes bound solely to amide ligands, including $[Na(THF)_2][UO_2(N(SiMe_3)_2)_3]$ at 2.310(5),[47] and $[Li(DME)_2Cl][Li(DME)][UO_2(NC_5H_{10})_2(\mu\text{-}NC_5H_{10})]_2$ at 2.249(7).[53] In contrast, the U–N bonds in U(IV) complexes bearing the $N(SiMe_3)_2^-$ ligand are slightly longer than those containing the NAr^FPh^- ligand.[58, 66]

DFT optimized geometries of the gas phase structures of **4.5-tol** and **4.5-crown** were obtained to support the observable differences in bond metrics (Table 4.4.1). As noted in the X-

ray crystal structures, upon K^+ coordination a slight lengthening of the U=O bonds was noted, as well as a more significant shortening of the equatorial U–N bonds. Close agreement with the experimental K–O distances was obtained in the model of **4.5-tol**, though some preference for K^+–F interactions over K^+–Ph interactions was noted over the course of the optimization, leading to minor differences in the secondary structure.

Identification of the ν_1 symmetric U=O stretching modes obtained from DFT frequency calculations established a shift from 854 cm^{-1} in **4.5-crown** to 807 cm^{-1} in **4.5-tol**, indicative of weakening of the U=O bonds. For comparison, upon coordination of $B(C_6F_5)_3$ to $UO_2(NCN)_2(THF)$ (NCN = $[(SiMe_3N)_2CPh]^-$), the ν_1 mode shifts from 803 cm^{-1} to 780 cm^{-1}.[30] We were unable to locate the ν_3 asymmetric U=O stretching mode by IR spectroscopy due to considerable overlap with ligand-based vibrations. Mayer bond order (MBO) analysis showed that K^+ coordination leads to a decrease in the average U=O MBO from 1.974 to 1.804 and an increase in the average U–N MBO from 0.462 to 0.525. Additionally, the natural charge localized on the oxygen atoms increased from –0.584 to –0.673 with K^+ coordination, signifying greater polarization of the U=O bonds. These metrics all support activation of uranyl upon K^+ coordination.

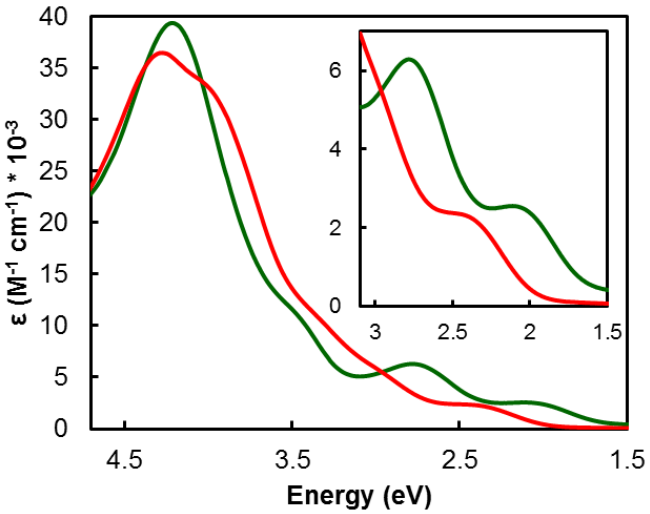

Figure 4.4.4. Electronic absorption spectrum of **4.5-tol** (green) and **4.5-crown** (red) in CH_2Cl_2.

Complexes **4.5-crown** (red) and **4.5-tol** (green) exhibited a dramatic difference in color, prompting us to collect electronic absorption spectra of these compounds To rule out

solvatochromism,[67] the absorption spectra of both compounds were collected in CH_2Cl_2, in which each compound retained its characteristic color. The intense bands of energies ≥ 3.5 eV were assigned to amide-ligand based π-π* and/or π*-π* electronic transitions (Figure 4.4.4). The lower energy absorption bands, of energies ≤ 3.5 eV were assigned to LMCT transitions between the amide ligands and uranium(VI) cations.[50] The spectra of the two compounds showed a significant shift of the LMCT bands in the visible region. Spectral deconvolution allowed for assignment of the peak maxima; a red-shift of 0.32 eV was observed upon cation coordination. The lower energy charge transfer band observed in **4.5-tol** suggests that the charge transfer occurs to a lower energy unfilled orbital centered on the uranium ion. From these data we may infer that the potassium ions are bound to the uranyl oxo ligands in solution, and that coordination of the potassium ions lowers the energy of unfilled 5f-orbitals on uranium, the putative acceptor orbitals of the charge transfer transitions. To further support this assignment, we performed excited state calculations on **4.5-tol** and **4.5-crown**.

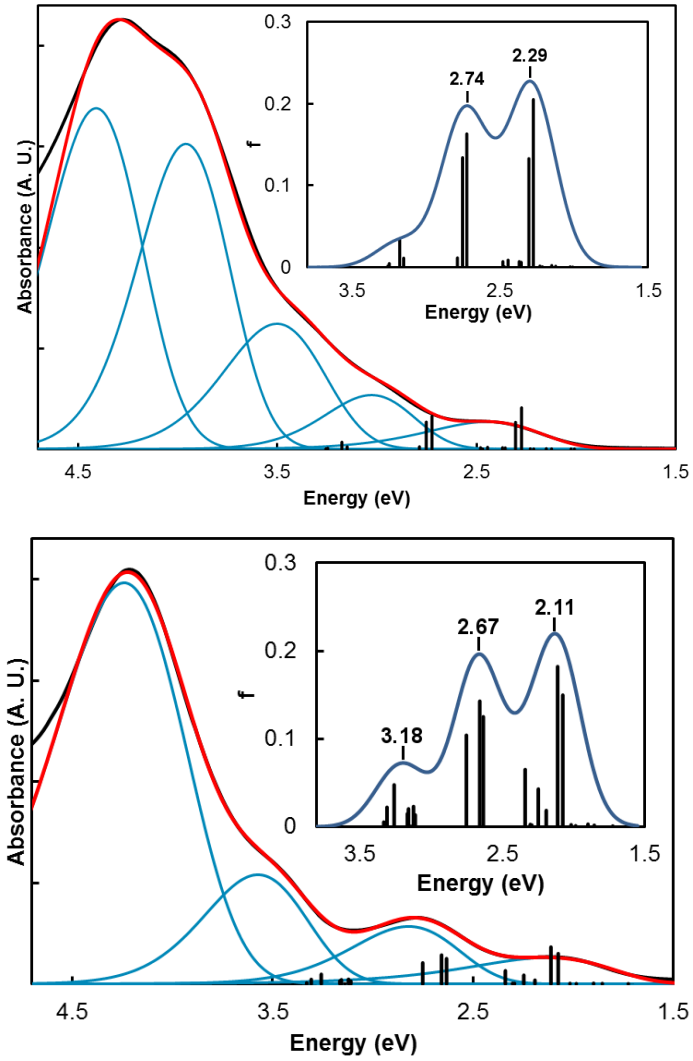

Figure 4.4.5 Spectral deconvolution of electronic absorption spectrum of **4.5-crown** (top) and **4.5-tol** (bottom). Experimental data are shown in black, component peaks are shown in blue, and the fits is shown in red. Vertical black lines indicate TD-DFT calculated excitations, with simulated spectra inset.

TD-DFT calculations were performed on **4.5-tol** and the anionic portion of **4.5-crown**. The lowest energy transitions of significant oscillator strength were centered at 2.29 eV in **4.5-tol** and 2.11 eV in **4.5-crown**, in reasonably close agreement with the lowest energy bands in the experimental spectra (Figure 4.4.5). These transitions were characterized as ligand to metal charge transfer (LMCT), primarily originating from nitrogen-centered non-bonding p-orbitals, excited into non-bonding uranium 5f orbitals. A representative transition is shown in Figure 4.4.6, from the ligand-based HOMO to the metal-based LUMO+2. While the difference in energy of the

charge transfer band in these two complexes is underestimated relative to the experimental results, the predicted red shift upon cation coordination and confirmation of these transitions as equatorial LMCT support the persistence of cation coordination in solution and the activation of the uranyl moiety by the K^+ ions. Consideration of the ground state electronic structures of **4.5-tol** and **4.5-crown** yielded further insight into the extent of the activation. Direct K^+ coordination resulted in a lowering in energy of the U=O anti-bonding orbitals and a slight increase in the energy of the U–N anti-bonding orbitals, indicating destabilization of the axial U=O bonding and stabilization of the equatorial U–N bonding (Figure 4.4.7).

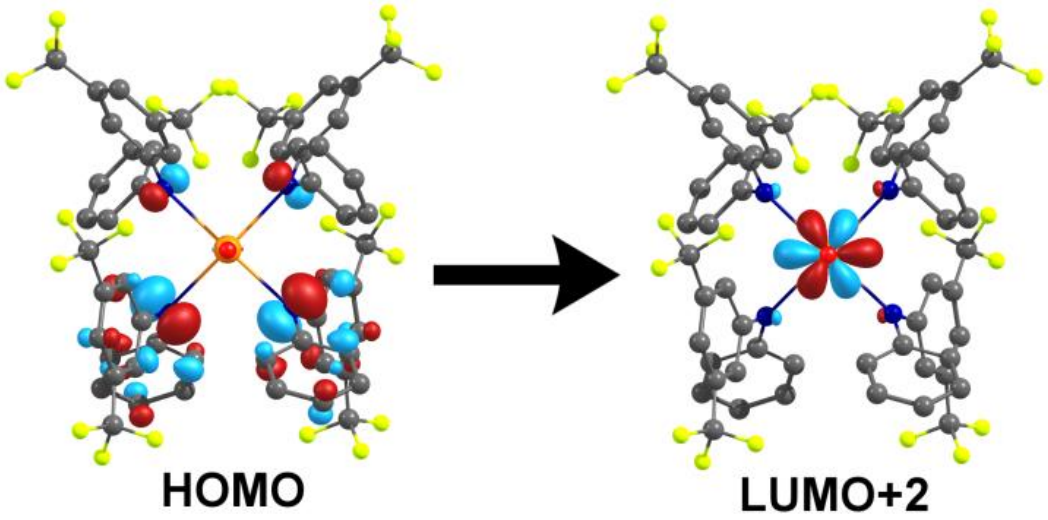

Figure 4.4.6 Representative LMCT natural transition orbitals obtained from TD-DFT calculations, giving rise to the lowest energy absorption band in **4.5-tol** and **4.5-crown**.

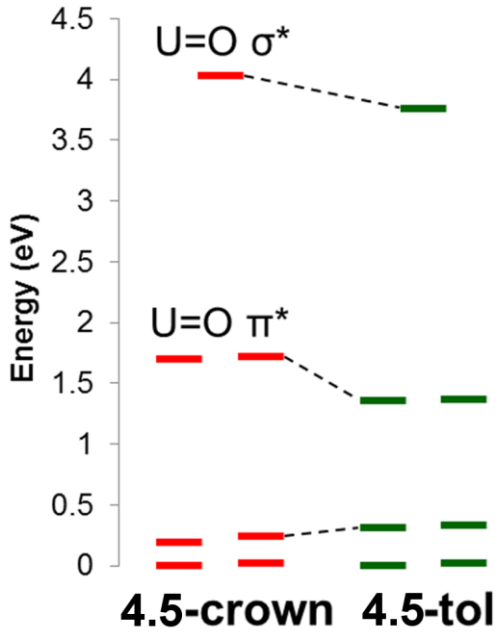

Figure 4.4.7 Calculated unoccupied molecular orbitals of primarily uranium 5f character for **4.5-crown** and **4.5-tol**. Energies are shown relative to the LUMO for each complex. Orbitals depicted: (**4.5-crown**) LUMO–LUMO+3, LUMO+11, LUMO+12, LUMO+24; (**4.5-tol**) LUMO–LUMO+5, LUMO+34.

Finally, the impact of potassium ion coordination on the electronics of the uranyl ions in **4.5-tol** and **4.5-crown** was further assessed through electrochemical measurements. Notably, cyclic voltammetry performed in CH_2Cl_2 for both complexes displayed different behavior between them (Figure 4.4.8). Multiple quasi-reversible reduction processes were noted in **4.5-tol** at –1.6 and –1.9 V whereas a single highly irreversible process at a more negative potential of –2.3 V was observed for **4.5-crown**. The larger negative potential necessary to observe the first reduction feature in **4.5-crown** implies that the coordination of K^+ ion directly to the uranyl facilitates reduction. Lewis acid coordination to iron–oxo and manganese–oxo complexes is known to have a similar effect on metal complex reduction potentials.[68-72] The electrochemical data therefore further support the coordination of K^+ ion to **4.5-tol** in solution.

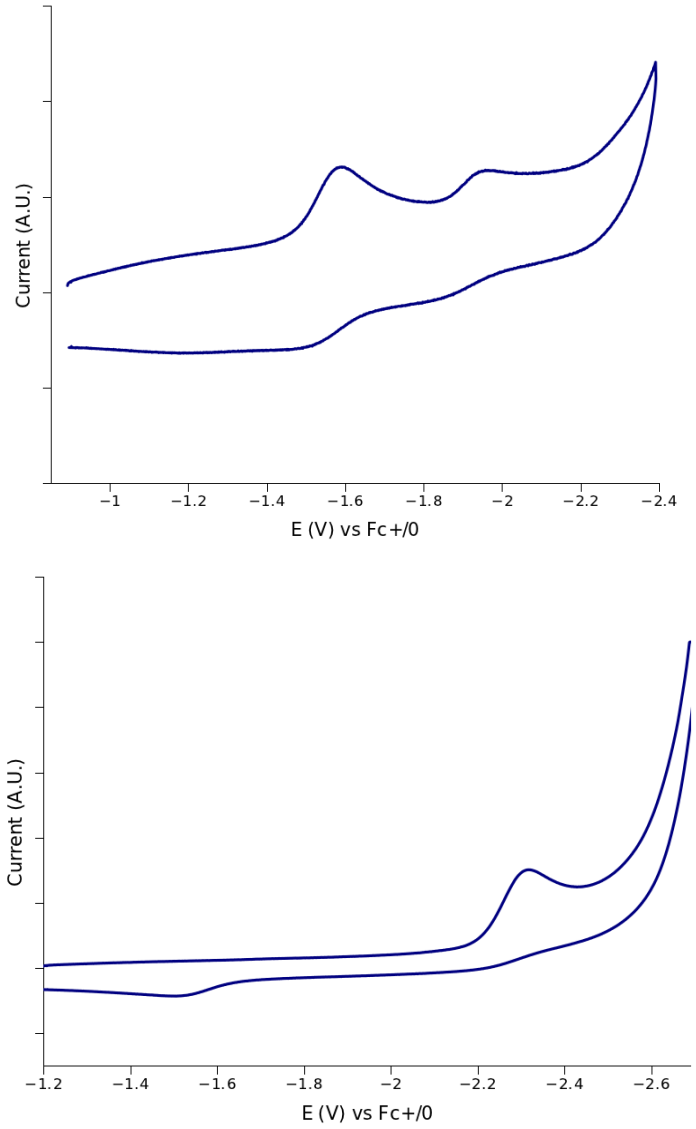

Figure 4.4.8 Cyclic voltammograms of **4.5-tol** (top) and **4.5-crown** (bottom) performed in CH_2Cl_2, referenced to an internal ferrocene/ferrocenium reference.

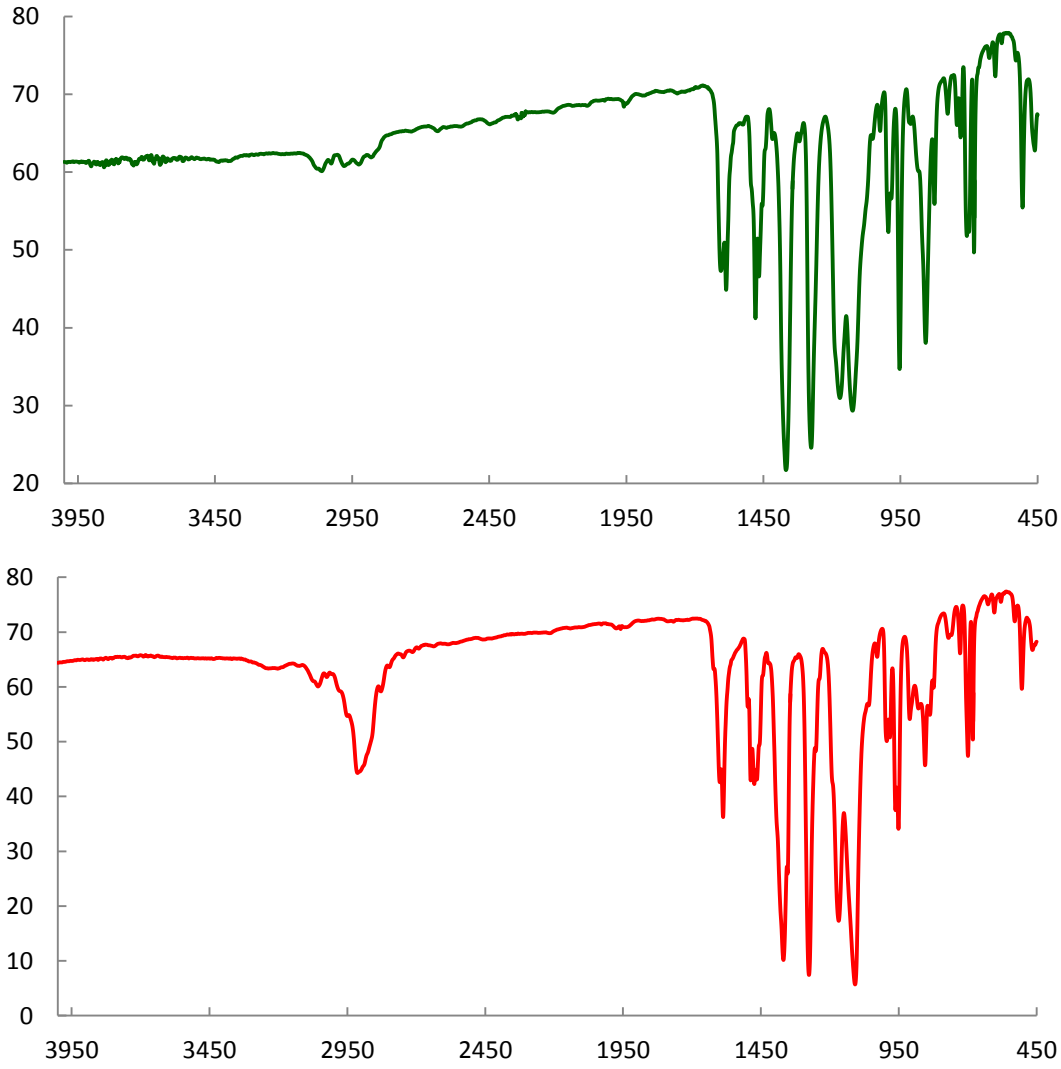

Figure 4.4.9. IR spectra of **4.5-tol** (top) and **4.5-crown** (bottom).

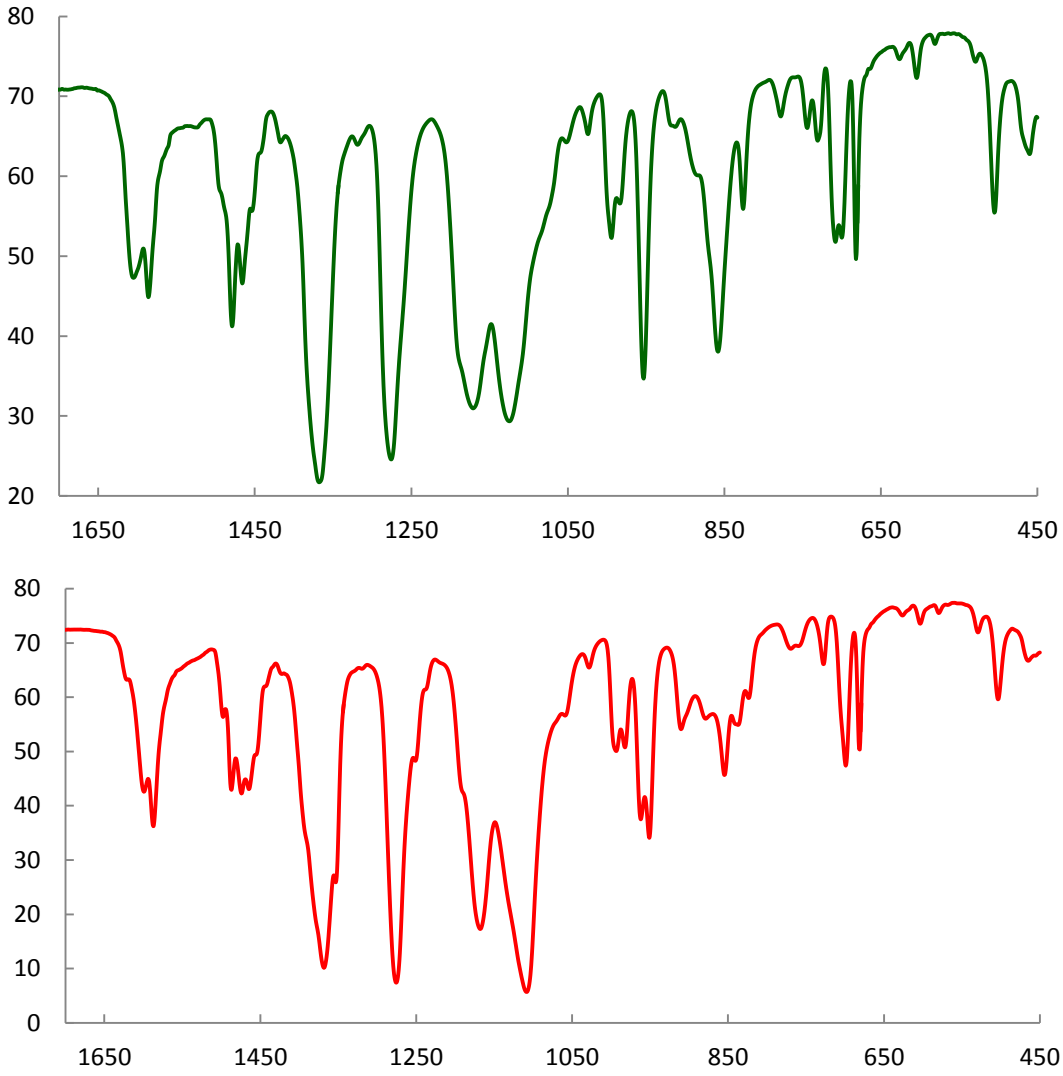

Figure 4.4.10 IR spectra of **4.5-tol** (top) and **4.5-crown** (bottom), highlighting the fingerprint region.

4.5 Experimental.

4.5.1 HNPhAr^{F}. A Teflon-sealed glass vessel was charged with $Pd_2(dba)_3$ (533 mg, 0.58 mmol, 1.5 mol %), BINAP (1.09 g, 1.75 mmol, 4.5 mol %), and 35 mL of toluene. The slurry was heated at 80 ºC for 20 min with stirring. The resulting red solution was transferred into a glass vessel containing Cs_2CO_3 (19.30 g, 59.24 mmol, 1.53 equiv) and 3,5-bis(trifluoromethyl) bromobenzene (11.36 g, 38.77 mmol, 1.00 equiv) in about 10 mL of toluene under N_2. Aniline (3.62 g, 38.88 mmol, 1.00 equiv) was added and the vessel was sealed under N_2 with a Teflon screw cap. After heating at 100 ºC for 36 h, the mixture was cooled to room temperature, filtered

through Celite packed on a coarse porosity fritted filter, and the Celite was rinsed with CH_2Cl_2. Removal of volatiles under reduced pressure yielded an oily red residue, which was purified by chromatography on silica with 1% CH_2Cl_2/hexanes, affording HNPhAr^F as a white crystalline solid. Yield: 9.80 g, 32.11 mmol, 83 %. ^{1}H NMR (benzene-d_6): δ 7.29 (s, 1H), 7.07 (t, 2H, J = 9.0 Hz), 6.92 (s, 2H), 6.85 (t, 1H, J = 9.0 Hz), 6.74 (d, 2H, J = 9.0 Hz), 4.83 (s, 1H). ^{13}C NMR (benzene-d_6): δ 145.9, 140.9, 133.4, 132.9, 130.3, 126.2, 124.2, 122.6, 120.8, 115.6. ^{19}F NMR (benzene-d_6): δ –62.9. ESI-MS (CH_2Cl_2): 304.0 ([NPhAr^F]$^-$). Elemental analysis found (calculated) for $C_{14}H_9F_6N$: C, 55.07 (55.09); H, 3.09 (2.97); N, 4.53 (4.59).

4.5.2 KNPhAr^F. To a 125 mL Erlenmeyer flask containing HNPhAr^F (1.51 g, 5.0 mmol, 1.00 equiv) dissolved in 50 mL of Et_2O, KH (0.30 g, 0.75 mmol, 1.50 equiv) was slowly added resulting in gas evolution. After stirring for 2 h, the slurry was filtered through Celite packed on a coarse porosity fritted filter and washed with 3 × 5 mL Et_2O. Removal of volatiles under vacuum yielded a yellow solid, which was collected on a fritted filter and washed with hexanes. Drying under vacuum for 5 h yielded a bright yellow powder identified by ^{1}H NMR as KNPhAr^F with negligible solvation by Et_2O. Yield: 1.50 g, 4.4 mmol, 87 %. ^{1}H NMR (pyridine-d_5): δ 7.66 (s, 2H, *o*-Ar^F), 7.54 (d, 2H, J = 8.1 Hz, *o*-Ph), 7.30 (t, 2H, J = 7.2 Hz, *m*-Ph), 6.77 (t, 1H, J = 7.2 Hz, *p*-Ph), 6.73 (s, 1H, p-Ar^F). ^{19}F NMR (pyridine-d_5) δ –62.48 (s, 6F). HRMS (MeCN) observed (calculated) for [$C_{14}H_8NF_6$]$^-$: 304.0572 (304.0561).

4.5.3 KNPhAr^F(THF)$_{0.5}$. To a vial containing HNPhAr^F (1.49 g, 4.9 mmol, 1.00 equiv) dissolved in THF, solid KH (235 mg, 5.9 mmol, 1.20 equiv) was slowly added resulting in gas evolution and a color change to bright yellow. After stirring for 2 h, the slurry was filtered through Celite packed on a coarse porosity fritted filter, which was further washed with THF. Removal of volatiles under vacuum yielded a yellow solid with tinges of brown, which was washed with n-pentane to afford KNPhAr^F(THF)$_{0.5}$ as a bright yellow powder. Yield: 1.57 g, 4.14 mmol, 85%. The product could be further purified by recrystallization from a concentrated solution in THF layered with hexanes at −21 ºC to yield KNPhAr^F (THF)$_3$ as large yellow blocks.

4.5.4 $U^{III}(NPhAr^F)_3(OPPh_3)_2$ (4.1). To a dark blue stirring slurry of UI_3 (190 mg, 0.31 mmol 1.00 equiv) in 5 mL THF, triphenylphosphine oxide (171 mg, 0.61 mmol, 2.00 equiv) was added, causing an immediate color change to dark purple and complete dissolution of residual solid. After cooling this solution to -21 ^oC, $KNPhAr^F$ $(THF)_{0.5}$ (350 mg, 0.92 mmol, 3.00 equiv) dissolved in about 6 mL THF cooled to -21 ^oC was added dropwise. The mixture was allowed to return to room temperature while stirring for one hour, then cooled to -21 °C to precipitate KI. Filtration through celite packed on a coarse porosity fritted filter followed by washing with Et_2O yielded a black filtrate. Volatiles were removed under reduced pressure, and the resulting black solid residue was dissolved in about 10 mL of toluene and filtered through celite suspended in a glass pipette. This solution was concentrated to ~3 mL and layered with ~13 mL of pentane and stored at -21 °C, leading to the growth of clusters of black crystalline needles over two days. Crystals of **4.1** were isolated on a medium porosity fritted filter, washed with ~25 mL pentane, and dried. Yield: 399 mg, 0.23 mmol, 76%. X-ray structural analysis was performed on a crystal grown in the above manner. ^1H NMR (benzene-d_6): δ 18.33 (s, 12H, PPh_3), 8.86 (s, 12H, PPh_3), 8.72 (s, 6H), 3.71 (s, 3H), 2.68 (s, 6H), 2.27 (s, 3H), -4.72 (s, 6H), -7.19 (s, 6H). ^{19}F NMR (benzene-d_6): δ -66.5 (s, 18F). ^{31}P NMR (benzene-d_6): 266.2 (s, 2P) Elemental analysis found (calculated) for $C_{78}H_{54}F_{18}N_3O_2P_2U \cdot 1.5C_7H_8$: C, 57.76 (57.60); H, 3.88 (3.60); N, 2.50 (2.28).

4.5.5 $U^{IV}(NPhAr^F)_4(py)$ (4.2). A mixture of UCl_4 (63 mg, 0.17 mmol, 1.00 equiv) and $KNPhAr^F$ $(THF)_{0.5}$ (250 mg, 0.66 mmol, 3.97 equiv) was treated with about 2 mL of pyridine, immediately generating a dark red slurry. After stirring for 30 minutes, 8 mL of hexanes was added, generating a red solution with the precipitation of a black oil. Following removal of volatiles under reduced pressure, 15 mL of hexanes was added and mixture was heated to reflux for 5 minutes on a hot plate. The boiling red solution was filtered through celite suspended in a glass pipette, and the volatiles were removed under reduced pressure from the dark red filtrate. The resulting red-black oily residue was triturated with 2 mL of hexanes, yielding **4.2** as an analytically pure orange powder. Yield: 149 mg, 0.10 mmol, 60%. Dark red crystals of **4.2** suitable for X-ray structural analysis were obtained from a dilute solution prepared from boiling hexanes stored at -

21 °C for three weeks. ^{1}H NMR (benzene-d_6): δ 44.39 (br, 1H, *p*-pyH), 19.56 (br, 2H, *o/m*-pyH), 17.67 (br, 2H, *o/m*-pyH), 5.39 (s, 4H), 4.30 (br, 8H), 0.52 (s, 8H), 0.16 (s, 4H), -7.12 (br, 8H). ^{19}F NMR (benzene-d_6): δ -64.1 (s, 24F). Elemental analysis found (calculated) for $C_{62}H_{37}F_{24}N_4U$: C, 47.41 (47.76); H 2.58 (2.43); N 4.36 (4.57).

4.5.6 $U^{IV}(NPhAr^F)_2(^tBupy)_2Cl_2$ (4.3). To a solution of UCl_4 (300 mg, 0.79 mmol, 1.00 equiv) and *p*-^{t}Bu-pyridine (220 mg, 1.63 mmol, 2.06 equiv) in about 5 mL of THF, $KNPhAr^F(THF)_{0.5}$ (600 mg, 1.58 mmol, 2.00 equiv) dissolved in minimal THF was added. After 3 h, the resulting orange solution was filtered through celite packed on a coarse porosity fritted filter and volatiles were removed under reduced pressure. The resulting residue was dissolved in minimal Et_2O, layered with pentane, and stored at -21 ºC, yielding light brown crystalline needles of **4.3** that were collected and dried on a coarse porosity fritted filter. Yield: 827 mg, 0.70 mmol, 88%. Crystals suitable for X-ray structural analysis were obtained from either a concentrated solution in hexanes stored at -21 ºC (yellow plate polymorph, **4.3a**) or a concentrated toluene solution layered with hexanes stored at -21 ºC (red block polymorph, **4.3b**). ^{1}H NMR (benzene-d_6): δ 8.21 (s, 2H), 3.87 (s, 4H), 2.95 (s, 2H), 0.16 (s, 18H); the other expected resonances were not observed, though several extremely broad features were noted. ^{19}F NMR (benzene-d_6): δ -62.2 (s, 12F). Elemental analysis found (calculated) for $C_{46}H_{42}Cl_2F_{12}N_4U$: C, 46.23 (46.52); H, 3.57 (3.56); N, 4.64 (4.72).

4.5.7 $U^{IV}(NPhAr^F)_4$ (4.4). To a vial containing $HNPhAr^F$ (0.146 g, 0.48 mmol, 4.00 equiv) dissolved in 5 mL Et_2O, slowly added KH (0.040 g, 1 mmol, 8.33 equiv), resulting in bubbling and an immediate color change to yellow. After stirring for 1 h, the slurry was filtered through celite suspended in a glass pipette, which was further washed with Et_2O. To this solution, an Et_2O solution containing $UI_4(Et_2O)_2$ (0.107 g, 0.12 mmol, 1.00 equiv) was added, causing an immediate color change to red. After stirring for 1 h, the mixture was filtered through celite suspended in a glass pipette and volatiles were removed under reduced pressure. Hexanes (5 mL) was added and the mixture was filtered through celite suspended in a glass pipette to yield a red filtrate. The hexanes solution was concentrated and stored at -21 °C to yield a dark red **4.4** as an amorphous

solid which was collected and dried under vacuum. Yield: 0.040 g, 0.028 mmol, 23%. ^{1}H NMR (benzene-d_6): δ 21.10 (br, 8H), 9.10 (br, 4H, *p*-Ar^F), -0.39 (br, 8H), -1.53 (t, 4H, *J* = 7.5 Hz, *p*-Ph), -15.09 (br, 8H). ^{19}F NMR (benzene-d_8): δ -61.20 (s, 24F) Elemental analysis found (calculated) for $C_{56}H_{32}F_{24}N_4U$: C, 46.32 (46.23); H, 2.35 (2.22); N, 3.80 (3.85).

4.5.8 [K(Toluene)]$_2$[UO$_2$(NAr^{F}Ph)$_4$] (4.5-tol). To a solution of $[UO_2Cl_2(THF)_2]_2$ (246 mg, 0.025 mmol, 1.0 equiv), KNAr^{F}Ph(THF)$_{0.5}$ (770 mg, 2.03 mmol, 8.0 equiv) was added, causing an immediate color change to dark red. After stirring 1.5 h, volatiles were removed in vacuum, leaving a green-black residue. This residue was dissolved in toluene, and the resulting green solution was filtered through Celite on a coarse porosity fritted filter. The filtrate was concentrated to a volume of 15 mL, and layered with 20 mL of pentane. Storage at –21 °C produced green-black crystals of **4.5-tol** overnight, which were collected by filtration over a medium porosity fritted filter and washed with pentane. Yield: 627 mg, 0.36 mmol, 71%. ^{1}H NMR (C_6D_6): δ 7.54 (8H), 7.32 (8H), 7.20 (4H), 7.02 (2H, tol), 6.82 (8H), 6.26 (4H), 2.12 (6H, tol-CH_3); peak multiplicity could not be assigned for this compound due to signal broadening. ^{19}F NMR (C_6D_6): δ –62.5 (24F). IR (KBr): 3060 (w), 2979 (w), 1605 (m), 1586 (m), 1479 (m), 1466 (m), 1368 (s), 1171 (s), 1125 (s), 1125 (s), 1024 (w), 994 (m), 953 (s), 858 (s), 826 (m), 778 (w), 774 (w), 731 (w), 708 (m), 700 (m), 682 (m), 604 (w), 505 (m), 460 (w). Elemental analysis found (calculated) for $C_{56}H_{32}F_{24}K_2N_4O_2U{\cdot}2C_7H_8$: C, 47.92 (48.06); H, 3.02 (2.77); N, 3.13 (3.20).

4.5.9 K$_2$[UO$_2$(NAr^{F}Ph)$_4$] (4.5). Recrystallization of **4.5-tol** from fluorobenzene at –21 °C over two weeks produced the unsolvated complex **4.5** as green-black blocks. Interstitial fluorobenzene was identified in the crystal structure, though it was easily removed under vacuum. Elemental analysis found (calculated) for $C_{56}H_{32}F_{24}K_2N_4O_2U$: C, 42.37 (42.98); H, 2.27 (2.06); N, 3.50 (3.58).

4.5.10 [K(18-c-6)]$_2$[UO$_2$(NAr^{F}Ph)$_4$] (4.5-crown). To a solution of KNAr^{F}Ph(THF)$_{0.5}$ (150 mg, 0.40 mmol, 8.0 equiv) in 4 mL THF, added $[UO_2Cl_2(THF)_2]_2$ (48 mg, 0.05 mmol, 1.0 equiv), resulting in an immediate color change to dark red. After stirring 45 minutes, volatiles were removed under reduced pressure to yield a black residue. This residue was extracted with

toluene and filtered to produce a dark green solution. To this solution, 18-crown-6 (52 mg, 0.20 mmol, 2.0 equiv) was added, causing a color change to red with immediate formation of red precipitate. The red solid was collected by filtration over a medium frit and washed with toluene and then hexanes. Recrystallization from a DME solution layered with hexanes at –21 °C produced **4.5-crown** as a red crystalline solid. Yield: 151 mg, 0.07 mmol, 73%. Alternatively, **4.5-crown** could be prepared as a THF solvate by recrystallization from a THF solution layered with hexanes at –21 °C, but the solid produced from this route was multi-crystalline. ^{1}H NMR (pyr-d_5): δ 8.26 (s, 8H), 7.89 (d, 8H), 7.29 (m, 8H), 7.10 (s, 4H), 6.80 (m, 4H), 3.68 (m, 16H), 3.43 (s, 48H, 18-c-6), 1.64 (m, 16H). ^{19}F NMR (pyr-d_5): δ –61.1 (24F). IR (KBr): 3056 (w), 2913 (m), 1599 (m), 1587 (m), 1487 (m), 1474 (m), 1465 (m), 1368 (s), 1276 (s), 1168 (s), 1108 (s), 1028 (w), 993 (m), 982 (m), 962 (m), 951 (m), 910 (w), 855 (m), 837 (w), 770 (w), 728 (w), 699 (m), 681 (m), 604 (w), 504 (m), 465 (w). Elemental analysis found (calculated) for $C_{80}H_{80}F_{24}K_2N_4O_{14}U$: C, 45.75 (45.89); H, 4.08 (3.85); N, 2.49 (2.68).

4.6 X-Ray Data.

Table 4.6.1 Summary of structure determination.

	HNAr^{F}Ph	**KNAr^{F}Ph**	**4.1**
Empirical formula	$C_{14}H_9NF_6$	$C_{26}H_{32}NO_3F_6K$	$C_{88.50}H_{66}N_3P_2O_2F_{18}U$
Formula weight	305.22	559.63	1845.41
Temperature	143(1) K	143(1) K	143(1) K
Wavelength	0.71073 Å	0.71073 Å	0.71073 Å
Crystal system	orthorhombic	triclinic	triclinic
Space group	$Pca2_1$	P-1	P-1
a	10.0174(7) Å	10.8866(7) Å	13.4814(8) Å
b	15.9406(12) Å	11.9211(7) Å	16.1925(10) Å
c	7.9776(6) Å	12.8559(8) Å	19.0979(11) Å
α	90	111.365(3)°	76.559(3)°
β	90	100.052(3)°	87.948(3)°
γ	90	109.196(3)°	84.674(3)°
Volume	1273.89(16) Å^3	1382.78(15) Å^3	4036.9(4) Å^3
Z	4	2	2
Density (calculated)	1.591 Mg/m^3	1.344 Mg/m^3	1.518 Mg/m^3
Absorption coefficient	0.155 mm^{-1}	0.260 mm^{-1}	2.142 mm^{-1}
F(000)	616	584	1836
Crystal size	0.44 x 0.10 x 0.03 mm^3	0.30 x 0.20 x 0.10 mm^3	0.42 x 0.10 x 0.02 mm^3
Theta range	2.40 to 23.55°	1.81 to 27.53°	1.86 to 27.83°
Index ranges	-11 ≤ h ≤ 11, -17 ≤	-14 ≤ h ≤ 14, -15 ≤ k ≤	-17 ≤ h ≤ 17, -19 ≤ k ≤

	k ≤ 17, -8 ≤ l ≤ 8	15, -16 ≤ l ≤ 16	21, -24 ≤ l ≤ 24
Reflections	16275	44236	96002
Independent reflections	1889 [R(int) = 0.0225]	6325 [R(int) = 0.0268]	18420 [R(int) = 0.0788]
Completeness to theta = 27.52 °	99.90%	99.20%	96.00%
Max. and min. transmission	0.7449 and 0.6650	0.7456 and 0.7007	0.7456 and 0.5265
Data / restraints / parameters	1889 / 13 / 233	6325 / 0 / 361	18420 / 0 / 999
Goodness-of-fit on F^2	1.077	1.053	1.096
Final R indices [I>2sigma(I)]	R1 = 0.0246, wR2 = 0.0642	R1 = 0.0517, wR2 = 0.1458	R1 = 0.0588, wR2 = 0.1441
R indices (all data)	R1 = 0.0263, wR2 = 0.0655	R1 = 0.0610, wR2 = 0.1545	R1 = 0.0964, wR2 = 0.1670
Largest diff. peak and hole	1.1(6)	0.661 and -0.394 e.Å^{-3}	2.449 and -3.167 e.Å^{-3}

	4.2	**4.3a**	**4.3b**
Empirical formula	$C_{61}H_{37}N_5F_{24}U$	$C_{46}H_{42}N_4F_{12}Cl_2U$	$C_{46}H_{42}N_4F_{12}Cl_2U$
Formula weight	1533.99	1187.77	1187.77
Temperature	143(1) K	100(1) K	143(1) K
Wavelength	0.71073 Å	0.71073 Å	0.71073 Å
Crystal system	monoclinic	monoclinic	monoclinic
Space group	P21/c	C2/c	C2/c
a	21.8109(14) Å	19.241(2) Å	23.2121(11) Å
b	14.6703(9) Å	19.891(2) Å	16.5531(8) Å
c	22.4352(14) Å	12.4602(13) Å	17.9213(15) Å
α	90	90	90
β	116.068(3)°	102.178(6)°	121.475(2)°
γ	90	90	90
Volume	6448.4(7) Å^3	4661.5(8) Å^3	5872.8(6) Å^3
Z	4	4	4
Density (calculated)	1.580 Mg/m^3	1.692 Mg/m^3	1.343 Mg/m^3
Absorption coefficient	2.628 mm^{-1}	3.682 mm^{-1}	2.922 mm^{-1}
F(000)	2984	2320	2320
Crystal size	0.25 x 0.20 x 0.18 mm^3	0.62 x 0.08 x 0.08 mm^3	0.79 x 0.65 x 0.48 mm^3
Theta range	1.72 to 27.59°	1.49 to 27.52°	2.06 to 27.74°
Index ranges	-28 ≤ h ≤ 28, -19 ≤ k ≤ 19, -29 ≤ l ≤ 29	-24 ≤ h ≤ 24, -25 ≤ k ≤ 25, -16 ≤ l ≤ 16	-30 ≤ h ≤ 29, -21 ≤ k ≤ 21, -23 ≤ l ≤ 23
Reflections	161531	45673	41814
Independent reflections	14876 [R(int) = 0.0536]	5266 [R(int) = 0.0431]	6772 [R(int) = 0.0361]
Completeness to theta = 27.52 °	99.60%	98.10%	97.90%
Max. and min. transmission	0.7456 and 0.6152	0.7456 and 0.4681	0.7456 and 0.5595
Data / restraints / parameters	14876 / 170 / 902	5266 / 0 / 298	6772 / 0 / 298
Goodness-of-fit on	1.15	1.1	1.13

F^2			
Final R indices [I>2sigma(I)]	R1 = 0.0394, wR2 = 0.0928	R1 = 0.0292, wR2 = 0.0707	R1 = 0.0450, wR2 = 0.1020
R indices (all data)	R1 = 0.0503, wR2 = 0.0961	R1 = 0.0347, wR2 = 0.0743	R1 = 0.0526, wR2 = 0.1063
Largest diff. peak and hole	1.940 and -0.892 e.Å^{-3}	1.703 and -1.020 e.Å^{-3}	3.486 and -1.438 e.Å^{-3}

	$U^{IV}F(NAr^FPh)_4py$	**4.5-tol**	**4.5**
Empirical formula	$C_{66}H_{42}N_6F_{25}KU$	$C_{70}H_{48}N_4O_2F_{24}K_2U$	$C_{56}H_{32}N_4O_2F_{24}K_2U$
Formula weight	1671.19	1749.35	1565.09
Temperature	143(1) K	143(1) K	143(1) K
Wavelength	0.71073 Å	0.71073 Å	0.71073 Å
Crystal system	monoclinic	monoclinic	monoclinic
Space group	P21/c	P21/n	C2/c
a	24.2328(16) Å	15.9136(9) Å	20.8532(16) Å
b	12.7508(8) Å	21.3308(13) Å	15.2370(12) Å
c	24.1585(15) Å	22.1833(12) Å	23.0364(18) Å
α	90	90	90
β	109.123(3)°	110.360(3)°	103.053(4)°
γ	90	90	90
Volume	7052.8(8) Å^3	7059.7(7) Å^3	7130.5(10) Å^3
Z	4	4	4
Density (calculated)	1.574 Mg/m^3	1.646 Mg/m^3	1.458 Mg/m^3
Absorption coefficient	2.469 mm^{-1}	2.528 mm^{-1}	2.493 mm^{-1}
F(000)	3264	3432	3032
Crystal size	0.45 x 0.25 x 0.12 mm^3	0.22 x 0.07 x 0.04 mm^3	0.32 x 0.24 x 0.16 mm^3
Theta range	1.71 to 27.51°	1.67 to 27.55°	1.67 to 27.78°
Index ranges	-28 ≤ h ≤ 31, -16 ≤ k ≤ 16, -31 ≤ l ≤ 31	-20 ≤ h ≤ 20, -27 ≤ k ≤ 27, -28 ≤ l ≤ 28	-27 ≤ h ≤ 26, -19 ≤ k ≤ 19, -29 ≤ l ≤ 29
Reflections	117168	188472	87101
Independent reflections	16218 [R(int) = 0.0328]	16272 [R(int) = 0.0526]	8273 [R(int) = 0.0878]
Completeness to theta = 27.52 °	99.90%	99.90%	98.30%
Max. and min. transmission	0.7456 and 0.5875	0.7456 and 0.6866	0.7456 and 0.6634
Data / restraints / parameters	16218 / 132 / 946	16272 / 0 / 931	8273 / 0 / 402
Goodness-of-fit on F^2	1.14	1.016	1.069
Final R indices [I>2sigma(I)]	R1 = 0.0473, wR2 = 0.1020	R1 = 0.0309, wR2 = 0.0690	R1 = 0.0517, wR2 = 0.1235
R indices (all data)	R1 = 0.0550, wR2 = 0.1046	R1 = 0.0507, wR2 = 0.0775	R1 = 0.0671, wR2 = 0.1292
Largest diff. peak and hole	2.642 and -2.516 e.Å^{-3}	1.452 and -0.737 e.Å^{-3}	2.146 and -0.775 e.Å^{-3}

	4.5-crown
Empirical formula	$C_{88}H_{100}N_4O_{18}F_{24}K_2U$

Formula weight	2273.95
Temperature	143(1) K
Wavelength	0.71073 Å
Crystal system	monoclinic
Space group	P21/c
a	14.2737(4) Å
b	22.2064(7) Å
c	32.9180(10) Å
α	90
β	95.921(2)°
γ	90
Volume	10378.3(5) Å^{3}
Z	4
Density (calculated)	1.455 Mg/m^{3}
Absorption coefficient	1.749 mm^{-1}
F(000)	4584
Crystal size	0.30 x 0.18 x 0.05 mm^{3}
Theta range	1.43 to 27.62°
Index ranges	-18 ≤ h ≤ 18, -28 ≤ k ≤ 28, -42 ≤ l ≤ 42
Reflections	157248
Independent reflections	23936 [R(int) = 0.1032]
Completeness to theta = 27.52 °	99.10%
Max. and min. transmission	0.7456 and 0.5977
Data / restraints / parameters	23936 / 0 / 1238
Goodness-of-fit on F^{2}	1.029
Final R indices [I>2sigma(I)]	R1 = 0.0676, wR2 = 0.1636
R indices (all data)	R1 = 0.1237, wR2 = 0.1822
Largest diff. peak and hole	1.848 and -1.472 e.Å^{-3}

Table 4.6.2 Bond lengths of HNAr^{F}Ph (Å).

C1-C6	1.385(3)	C1-C2	1.391(2)	C1-N1	1.410(2)
C2-C3	1.380(3)	C3-C4	1.383(3)	C4-C5	1.368(3)
C5-C6	1.382(3)	C7-C12	1.387(2)	C7-N1	1.389(2)
C7-C8	1.398(3)	C8-C9	1.386(3)	C9-C10	1.384(3)
C9-C13	1.481(3)	C10-C11	1.378(3)	C11-C12	1.385(2)
C11-C14	1.496(3)	C13-F3'	1.230(6)	C13-F2'	1.286(7)
C13-F1	1.310(3)	C13-F2	1.324(4)	C13-F3	1.402(4)
C13-F1'	1.473(8)	C14-F5'	1.265(5)	C14-F4	1.301(7)
C14-F6	1.331(4)	C14-F4'	1.343(7)	C14-F6'	1.382(5)
C14-F5	1.400(5)				

Table 4.6.3 Bond angles of HNAr^{F}Ph (°).

C6-C1-C2	119.52(16)	C6-C1-N1	119.08(15)
C3-C2-C1	119.55(17)	C2-C3-C4	120.72(17)
C4-C5-C6	120.67(18)	C5-C6-C1	120.01(17)
C12-C7-C8	118.42(15)	N1-C7-C8	118.30(15)
C10-C9-C8	120.99(17)	C10-C9-C13	120.59(17)
C11-C10-C9	118.09(16)	C10-C11-C12	121.93(15)
C12-C11-C14	118.25(16)	C11-C12-C7	120.04(16)
F3'-C13-F1	68.4(5)	F2'-C13-F1	125.2(5)

F2'-C13-F2	18.0(5)	F1-C13-F2	108.6(2)
F2'-C13-F3	91.4(5)	F1-C13-F3	104.1(2)
F3'-C13-F1'	104.3(4)	F2'-C13-F1'	101.4(4)
F2-C13-F1'	83.6(4)	F3-C13-F1'	137.7(3)
F2'-C13-C9	109.0(6)	F1-C13-C9	114.2(2)
F3-C13-C9	109.2(2)	F1'-C13-C9	104.3(4)
F5'-C14-F6	77.5(3)	F4-C14-F6	108.7(4)
F4-C14-F4'	15.5(6)	F6-C14-F4'	122.5(7)
F4-C14-F6'	87.9(4)	F6-C14-F6'	31.3(2)
F5'-C14-F5	25.8(3)	F4-C14-F5	104.7(4)
F4'-C14-F5	93.5(6)	F6'-C14-F5	132.3(3)
F4-C14-C11	116.1(6)	F6-C14-C11	115.0(3)
F6'-C14-C11	106.8(3)	F5-C14-C11	108.0(3)
C2-C1-N1	121.31(16)	F3'-C13-C9	118.9(4)
C5-C4-C3	119.51(18)	F2-C13-C9	116.3(3)
C12-C7-N1	123.25(16)	F5'-C14-F4	116.4(8)
C9-C8-C7	120.52(16)	F5'-C14-F4'	110.1(6)
C8-C9-C13	118.42(17)	F5'-C14-F6'	107.7(3)
C10-C11-C14	119.82(16)	F4'-C14-F6'	103.4(4)
F3'-C13-F2'	116.4(6)	F6-C14-F5	103.1(2)
F3'-C13-F2	119.7(5)	F5'-C14-C11	116.8(5)
F3'-C13-F3	36.1(5)	F4'-C14-C11	111.0(8)
F2-C13-F3	103.3(2)	C7-N1-C1	126.36(15)
F1-C13-F1'	36.9(3)		

Table 4.6.4 Bond lengths of KNAr^{F}Ph(THF)$_3$ (Å).

K1-O1	2.6572(17)	K1-O3	2.6687(17)	K1-O2	2.6947(18)
K1-N1#1	2.7867(15)	K1-N1	2.8797(15)	K1-C1#1	3.3433(18)
K1-C2	3.351(2)	K1-C7	3.3528(16)	K1-C2#1	3.353(2)
K1-C1	3.3868(18)	K1-C23	3.411(3)	K1-K1#1	4.1688(8)
F1-C13	1.315(3)	F2-C13	1.351(3)	F3-C13	1.303(3)
F4-F4'	0.65(3)	F4-C14	1.308(4)	F4-F5'	1.44(2)
F5-F6'	1.18(4)	F5-F5'	1.20(3)	F5-C14	1.313(3)
F6-F6'	1.10(4)	F6-C14	1.341(4)	F6-F4'	1.54(3)
F4'-C14	1.183(13)	F5'-C14	1.395(13)	F6'-C14	1.178(11)
O1-C15	1.411(3)	O1-C18	1.420(3)	O2-C22	1.420(3)
O2-C19	1.426(3)	O3-C26	1.419(3)	O3-C23	1.423(3)
N1-C7	1.362(2)	N1-C1	1.383(2)	N1-K1#1	2.7868(15)
C1-C2	1.410(2)	C1-C6	1.412(3)	C1-K1#1	3.3433(18)
C2-C3	1.382(3)	C2-K1#1	3.353(2)	C3-C4	1.384(4)
C4-C5	1.389(4)	C5-C6	1.382(3)	C7-C12	1.416(2)
C7-C8	1.421(2)	C8-C9	1.384(2)	C9-C10	1.387(3)
C9-C13	1.497(3)	C10-C11	1.388(3)	C11-C12	1.381(3)
C11-C14	1.497(3)	C15-C16	1.470(4)	C16-C17	1.428(5)
C17-C18	1.447(4)	C19-C20	1.457(4)	C20-C21	1.522(4)
C21-C22	1.500(4)	C23-C24	1.464(4)	C24-C25	1.500(4)
C25-C26	1.519(4)				

Symmetry transformations used to generate equivalent atoms:

#1 -x+1,-y+1,-z+1

Table 4.6.5 Bond angles of KNAr^{F}Ph(THF)$_3$ (°).

O1-K1-O3	95.13(6)	O1-K1-O2	89.63(6)
O1-K1-N1#1	114.08(5)	O3-K1-N1#1	149.19(5)
O1-K1-N1	112.55(5)	O3-K1-N1	92.63(5)
N1#1-K1-N1	85.28(4)	O1-K1-C1#1	90.64(5)
O2-K1-C1#1	88.53(5)	N1#1-K1-C1#1	23.93(4)
O1-K1-C2	154.67(5)	O3-K1-C2	78.24(5)
N1#1-K1-C2	78.90(5)	N1-K1-C2	44.48(4)
O1-K1-C7	90.15(5)	O3-K1-C7	87.00(6)
N1#1-K1-C7	101.84(4)	N1-K1-C7	23.72(4)
C2-K1-C7	65.30(4)	O1-K1-C2#1	76.42(5)
O2-K1-C2#1	107.80(6)	N1#1-K1-C2#1	44.81(4)
C1#1-K1-C2#1	24.31(4)	C2-K1-C2#1	103.09(4)
O1-K1-C1	130.60(5)	O3-K1-C1	76.56(5)
N1#1-K1-C1	90.55(4)	N1-K1-C1	23.77(4)
C2-K1-C1	24.15(4)	C7-K1-C1	41.53(4)
O1-K1-C23	72.35(6)	O3-K1-C23	23.21(6)
N1#1-K1-C23	164.95(7)	N1-K1-C23	105.18(6)
C2-K1-C23	100.80(6)	C7-K1-C23	91.49(7)
C1-K1-C23	94.96(6)	O1-K1-K1#1	122.52(5)
O2-K1-K1#1	124.95(5)	N1#1-K1-K1#1	43.51(3)
C1#1-K1-K1#1	52.20(3)	C2-K1-K1#1	51.57(3)
C2#1-K1-K1#1	51.52(3)	C1-K1-K1#1	51.26(3)
F4'-F4-C14	64.4(13)	F4'-F4-F5'	120.6(18)
F6'-F5-F5'	120.7(11)	F6'-F5-C14	56.1(8)
F6'-F6-C14	56.8(9)	F6'-F6-F4'	96.3(12)
F4-F4'-C14	85.8(12)	F4-F4'-F6	140.0(18)
F5-F5'-C14	60.3(9)	F5-F5'-F4	106.6(9)
F6-F6'-C14	72.1(13)	F6-F6'-F5	134.3(13)
C15-O1-C18	109.2(2)	C15-O1-K1	125.54(15)
C22-O2-C19	107.76(19)	C22-O2-K1	131.29(16)
C26-O3-C23	109.74(18)	C26-O3-K1	139.12(14)
C7-N1-C1	121.08(15)	C7-N1-K1#1	132.76(11)
C7-N1-K1	98.01(10)	C1-N1-K1	99.15(10)
N1-C1-C2	118.35(16)	N1-C1-C6	125.05(16)
N1-C1-K1#1	54.84(8)	C2-C1-K1#1	78.23(11)
N1-C1-K1	57.08(9)	C2-C1-K1	76.49(11)
K1#1-C1-K1	76.55(4)	C3-C2-C1	121.78(19)
C1-C2-K1	79.36(10)	C3-C2-K1#1	134.99(13)
K1-C2-K1#1	76.91(4)	C2-C3-C4	120.7(2)
C6-C5-C4	120.8(2)	C5-C6-C1	121.56(19)
N1-C7-C8	125.85(16)	C12-C7-C8	115.59(15)
C12-C7-K1	110.80(11)	C8-C7-K1	98.68(10)
C8-C9-C10	122.63(17)	C8-C9-C13	118.49(18)
C9-C10-C11	116.82(16)	C12-C11-C10	122.05(17)
C10-C11-C14	119.04(17)	C11-C12-C7	121.87(17)
F3-C13-F2	104.1(2)	F1-C13-F2	103.34(19)
F1-C13-C9	114.1(2)	F2-C13-C9	111.35(18)
F6'-C14-F4	130.9(7)	F4'-C14-F4	29.8(15)
F4'-C14-F5	123.6(9)	F4-C14-F5	108.2(3)
F4'-C14-F6	74.9(15)	F4-C14-F6	103.6(3)
F6'-C14-F5'	106.9(16)	F4'-C14-F5'	92.1(14)
F5-C14-F5'	52.5(13)	F6-C14-F5'	141.1(6)

F4'-C14-C11	117.7(9)	F4-C14-C11	113.5(3)
F6-C14-C11	111.6(2)	F5'-C14-C11	106.9(5)
C17-C16-C15	106.8(3)	C16-C17-C18	107.9(3)
O2-C19-C20	104.8(2)	C19-C20-C21	104.6(3)
O2-C22-C21	107.1(2)	O3-C23-C24	107.7(2)
C24-C23-K1	155.28(18)	C23-C24-C25	103.6(2)
O3-C26-C25	105.84(19)	C2-C1-C6	116.29(17)
O3-K1-O2	86.43(6)	C6-C1-K1#1	135.49(12)
O2-K1-N1#1	84.28(5)	C6-C1-K1	145.72(12)
O2-K1-N1	157.78(6)	C3-C2-K1	141.89(14)
O3-K1-C1#1	172.31(5)	C1-C2-K1#1	77.46(11)
N1-K1-C1#1	89.84(4)	C3-C4-C5	118.9(2)
O2-K1-C2	114.01(6)	N1-C7-C12	118.38(16)
C1#1-K1-C2	98.59(5)	N1-C7-K1	58.27(9)
O2-K1-C7	173.38(5)	C9-C8-C7	121.04(17)
C1#1-K1-C7	98.09(4)	C10-C9-C13	118.82(17)
O3-K1-C2#1	163.14(6)	C12-C11-C14	118.90(18)
N1-K1-C2#1	77.63(5)	F3-C13-F1	108.9(2)
C7-K1-C2#1	78.56(5)	F3-C13-C9	114.10(18)
O2-K1-C1	136.93(6)	F6'-C14-F4'	114.5(15)
C1#1-K1-C1	103.45(4)	F6'-C14-F5	56.3(19)
C2#1-K1-C1	97.69(5)	F6'-C14-F6	51.1(19)
O2-K1-C23	82.14(7)	F5-C14-F6	104.6(3)
C1#1-K1-C23	160.54(5)	F4-C14-F5'	64.4(13)
C2#1-K1-C23	147.16(6)	F6'-C14-C11	115.0(7)
O3-K1-K1#1	127.29(4)	F5-C14-C11	114.4(2)
N1-K1-K1#1	41.78(3)	O1-C15-C16	107.6(2)
C7-K1-K1#1	60.31(3)	O1-C18-C17	107.6(2)
C23-K1-K1#1	145.74(5)	C22-C21-C20	103.8(2)
C14-F4-F5'	60.7(9)	O3-C23-K1	47.65(11)
F5'-F5-C14	67.2(7)	C24-C25-C26	103.0(2)
C14-F6-F4'	47.9(5)	C23-O3-K1	109.14(14)
C14-F4'-F6	57.2(12)	C1-N1-K1#1	101.23(10)
C14-F5'-F4	54.9(6)	K1#1-N1-K1	94.72(4)
C14-F6'-F5	67.6(14)	C19-O2-K1	118.97(15)
C18-O1-K1	118.20(16)		

Symmetry transformations used to generate equivalent atoms:

#1 -x+1,-y+1,-z+1

Table 4.6.6 Bond lengths of **4.1** (Å).

U1-O2	2.387(4)	U1-O1	2.388(5)	U1-N1	2.390(5)
U1-N3	2.390(5)	U1-N2	2.426(5)	P1-O1	1.509(5)
P1-C55	1.787(7)	P1-C49	1.799(7)	P1-C43	1.814(7)
P2-O2	1.506(5)	P2-C67	1.791(6)	P2-C61	1.796(6)
P2-C73	1.799(6)	F1-C13	1.341(10)	F2-C13	1.322(11)
F3-C13	1.339(11)	F4-C14	1.335(10)	F5-C14	1.342(11)
F6-C14	1.326(9)	F7-C27	1.351(12)	F8-C27	1.300(11)
F9-C27	1.308(11)	F10-C28	1.303(10)	F11-C28	1.291(10)
F12-C28	1.296(10)	F13-C41	1.306(9)	F14-C41	1.281(9)
F15-C41	1.310(9)	F16-C42	1.236(11)	F17-C42	1.329(12)
F18-C42	1.261(10)	N1-C7	1.398(7)	N1-C1	1.402(8)
N2-C21	1.379(8)	N2-C15	1.418(8)	N3-C35	1.380(7)

N3-C29	1.408(8)	C1-C2	1.397(9)	C1-C6	1.412(8)
C2-C3	1.366(9)	C3-C4	1.375(10)	C4-C5	1.385(11)
C5-C6	1.382(10)	C7-C8	1.397(9)	C7-C12	1.398(9)
C8-C9	1.377(9)	C9-C10	1.377(11)	C9-C13	1.503(11)
C10-C11	1.366(10)	C11-C12	1.393(9)	C11-C14	1.496(11)
C15-C20	1.383(10)	C15-C16	1.406(9)	C16-C17	1.392(10)
C17-C18	1.385(12)	C18-C19	1.376(11)	C19-C20	1.386(9)
C21-C22	1.392(9)	C21-C26	1.414(10)	C22-C23	1.385(10)
C23-C24	1.380(11)	C23-C27	1.479(11)	C24-C25	1.392(10)
C25-C26	1.374(10)	C25-C28	1.491(11)	C29-C34	1.397(8)
C29-C30	1.409(9)	C30-C31	1.380(9)	C31-C32	1.391(10)
C32-C33	1.356(10)	C33-C34	1.388(9)	C35-C40	1.397(8)
C35-C36	1.401(9)	C36-C37	1.393(8)	C37-C38	1.383(9)
C37-C41	1.485(9)	C38-C39	1.373(10)	C39-C40	1.384(9)
C39-C42	1.499(10)	C43-C44	1.356(10)	C43-C48	1.358(11)
C44-C45	1.382(14)	C45-C46	1.383(16)	C46-C47	1.366(15)
C47-C48	1.471(13)	C49-C54	1.378(11)	C49-C50	1.393(11)
C50-C51	1.366(12)	C51-C52	1.367(14)	C52-C53	1.385(14)
C53-C54	1.392(11)	C55-C56	1.376(11)	C55-C60	1.385(10)
C56-C57	1.365(12)	C57-C58	1.356(13)	C58-C59	1.353(14)
C59-C60	1.373(11)	C61-C66	1.386(9)	C61-C62	1.391(9)
C62-C63	1.380(10)	C63-C64	1.369(12)	C64-C65	1.369(12)
C65-C66	1.375(10)	C67-C72	1.339(10)	C67-C68	1.375(9)
C68-C69	1.362(10)	C69-C70	1.339(12)	C70-C71	1.369(12)
C71-C72	1.402(12)	C73-C74	1.355(10)	C73-C78	1.375(10)
C74-C75	1.379(10)	C75-C76	1.340(12)	C76-C77	1.360(13)
C77-C78	1.363(12)	C79-C84	1.3949	C79-C80	1.3950
C79-C85	1.5402	C80-C81	1.3950	C81-C82	1.3950
C82-C83	1.3950	C83-C84	1.3951	C86-C87	1.3949
C86-C91	1.3950	C86-C92	1.5401	C87-C88	1.3951
C88-C89	1.3949	C89-C90	1.3950	C90-C91	1.3950

Table 4.6.7 Bond angles of **4.1** (°).

O2-U1-O1	175.99(14)	O2-U1-N1	92.45(15)
O2-U1-N3	89.15(16)	O1-U1-N3	89.70(16)
O2-U1-N2	89.14(17)	O1-U1-N2	88.23(17)
N3-U1-N2	122.26(17)	O1-P1-C55	112.6(3)
C55-P1-C49	107.5(3)	O1-P1-C43	112.1(3)
C49-P1-C43	106.6(3)	O2-P2-C67	111.5(3)
C67-P2-C61	107.7(3)	O2-P2-C73	110.6(3)
C61-P2-C73	109.6(3)	P1-O1-U1	169.7(3)
C7-N1-C1	116.6(5)	C7-N1-U1	123.4(4)
C21-N2-C15	119.0(5)	C21-N2-U1	117.9(4)
C35-N3-C29	119.8(5)	C35-N3-U1	129.8(4)
C2-C1-N1	121.3(5)	C2-C1-C6	117.4(6)
C3-C2-C1	121.2(6)	C2-C3-C4	121.5(7)
C6-C5-C4	121.2(7)	C5-C6-C1	120.1(6)
C8-C7-C12	116.9(6)	N1-C7-C12	121.3(5)
C8-C9-C10	122.1(7)	C8-C9-C13	119.1(7)
C11-C10-C9	117.4(6)	C10-C11-C12	122.1(7)
C12-C11-C14	117.7(7)	C11-C12-C7	120.5(6)
F2-C13-F1	107.5(9)	F3-C13-F1	103.9(7)

F3-C13-C9	111.6(8)	F1-C13-C9	112.4(7)
F6-C14-F5	107.2(8)	F4-C14-F5	104.4(8)
F4-C14-C11	112.2(7)	F5-C14-C11	113.3(7)
C20-C15-N2	119.6(6)	C16-C15-N2	122.6(6)
C18-C17-C16	120.7(7)	C19-C18-C17	119.3(7)
C15-C20-C19	122.0(7)	N2-C21-C22	124.5(6)
C22-C21-C26	116.7(6)	C23-C22-C21	121.4(7)
C24-C23-C27	118.7(7)	C22-C23-C27	119.6(7)
C26-C25-C24	121.8(7)	C26-C25-C28	119.6(7)
C25-C26-C21	120.9(7)	F8-C27-F9	109.8(9)
F9-C27-F7	101.3(8)	F8-C27-C23	115.2(7)
F7-C27-C23	110.8(8)	F11-C28-F12	106.5(8)
F12-C28-F10	104.1(8)	F11-C28-C25	114.7(6)
F10-C28-C25	112.8(7)	C34-C29-N3	119.7(6)
N3-C29-C30	122.9(5)	C31-C30-C29	121.2(6)
C33-C32-C31	119.2(6)	C32-C33-C34	121.6(6)
N3-C35-C40	119.3(6)	N3-C35-C36	123.7(5)
C37-C36-C35	120.9(6)	C38-C37-C36	121.3(6)
C36-C37-C41	119.5(6)	C39-C38-C37	118.0(6)
C38-C39-C42	119.8(6)	C40-C39-C42	118.4(7)
F14-C41-F13	105.7(8)	F14-C41-F15	105.9(7)
F14-C41-C37	115.3(6)	F13-C41-C37	111.5(6)
F16-C42-F18	109.4(9)	F16-C42-F17	103.4(9)
F16-C42-C39	114.9(7)	F18-C42-C39	116.0(6)
C44-C43-C48	124.2(8)	C44-C43-P1	118.4(7)
C43-C44-C45	119.4(10)	C44-C45-C46	119.9(10)
C46-C47-C48	119.6(11)	C43-C48-C47	115.8(8)
C54-C49-P1	118.7(6)	C50-C49-P1	120.4(6)
C50-C51-C52	119.6(9)	C51-C52-C53	120.7(8)
C49-C54-C53	118.2(9)	C56-C55-C60	118.5(7)
C60-C55-P1	119.7(6)	C57-C56-C55	120.2(8)
C59-C58-C57	119.4(8)	C58-C59-C60	120.8(9)
C66-C61-C62	119.7(6)	C66-C61-P2	118.9(5)
C63-C62-C61	119.4(8)	C64-C63-C62	120.6(8)
C64-C65-C66	120.9(8)	C65-C66-C61	119.5(7)
C72-C67-P2	122.8(5)	C68-C67-P2	118.7(5)
C70-C69-C68	122.0(7)	C69-C70-C71	118.3(8)
C67-C72-C71	120.7(8)	C74-C73-C78	118.4(7)
C78-C73-P2	118.0(5)	C73-C74-C75	121.0(8)
C75-C76-C77	119.8(8)	C76-C77-C78	120.6(8)
C84-C79-C80	120.0	C84-C79-C85	120.0
C81-C80-C79	120.0	C80-C81-C82	120.0
C82-C83-C84	120.0	C79-C84-C83	120.0
C87-C86-C92	120.0	C91-C86-C92	120.0
C89-C88-C87	120.0	C88-C89-C90	120.0
C86-C91-C90	120.0	C39-C40-C35	121.2(6)
O1-U1-N1	91.46(16)	F13-C41-F15	104.0(7)
N1-U1-N3	119.20(17)	F15-C41-C37	113.5(7)
N1-U1-N2	118.53(17)	F18-C42-F17	101.3(9)
O1-P1-C49	110.6(3)	F17-C42-C39	110.2(8)
C55-P1-C43	107.1(3)	C48-C43-P1	117.4(6)
O2-P2-C61	110.6(3)	C47-C46-C45	120.7(10)
C67-P2-C73	106.7(3)	C54-C49-C50	120.9(7)
P2-O2-U1	172.3(3)	C51-C50-C49	120.2(9)

C1-N1-U1	120.0(4)	C52-C53-C54	120.3(10)
C15-N2-U1	122.0(4)	C56-C55-P1	121.7(6)
C29-N3-U1	110.4(3)	C58-C57-C56	121.1(9)
N1-C1-C6	121.1(6)	C59-C60-C55	119.9(8)
C3-C4-C5	118.4(7)	C62-C61-P2	121.2(5)
C8-C7-N1	121.7(6)	C65-C64-C63	119.8(7)
C9-C8-C7	121.0(7)	C72-C67-C68	118.5(7)
C10-C9-C13	118.8(7)	C69-C68-C67	120.5(7)
C10-C11-C14	120.1(7)	C70-C71-C72	119.9(9)
F2-C13-F3	107.5(8)	C74-C73-P2	123.6(5)
F2-C13-C9	113.4(7)	C76-C75-C74	120.0(8)
F6-C14-F4	106.4(7)	C77-C78-C73	120.1(8)
F6-C14-C11	112.8(7)	C80-C79-C85	120.0
C20-C15-C16	117.6(6)	C81-C82-C83	120.0
C17-C16-C15	120.3(7)	C87-C86-C91	120.0
C18-C19-C20	120.1(8)	C86-C87-C88	120.0
N2-C21-C26	118.6(6)	C89-C90-C91	120.0
C24-C23-C22	121.6(7)	C34-C29-C30	117.1(6)
C23-C24-C25	117.4(7)	C30-C31-C32	120.3(7)
C24-C25-C28	118.5(7)	C33-C34-C29	120.6(6)
F8-C27-F7	104.3(10)	C40-C35-C36	117.0(5)
F9-C27-C23	114.0(9)	C38-C37-C41	119.2(6)
F11-C28-F10	103.8(9)	C38-C39-C40	121.7(6)
F12-C28-C25	114.0(8)		

Table 4.6.8 Bond lengths of **4.2** (Å).

U1-N4	2.279(3)	U1-N3	2.283(3)	U1-N2	2.290(3)
U1-N1	2.298(3)	U1-N5	2.637(4)	U1-C29	3.032(4)
U1-C43	3.037(4)	F1-C13	1.314(7)	F2-C13	1.319(6)
F3-C13	1.345(7)	F4-C14	1.321(6)	F5-C14	1.324(6)
F6-C14	1.338(6)	F7-C27	1.326(6)	F8-C27	1.324(6)
F9-C27	1.322(6)	F10-C28	1.327(6)	F11-C28	1.347(6)
F12-C28	1.327(6)	F16-C42	1.300(9)	F17-C42	1.298(8)
F18-C42	1.302(7)	F19-C55	1.333(11)	F20-C55	1.310(11)
F21-C55	1.286(13)	F19'-C55	1.238(13)	F20'-C55	1.361(12)
F21'-C55	1.302(16)	F22-C56	1.338(8)	F23-C56	1.308(7)
F24-C56	1.327(7)	N1-C7	1.414(5)	N1-C1	1.428(5)
N2-C21	1.401(5)	N2-C15	1.413(5)	N3-C35	1.355(14)
N3-C29	1.448(5)	N3-C35'	1.486(14)	N4-C49	1.397(5)
N4-C43	1.431(5)	N5-C61	1.332(6)	N5-C57	1.349(6)
C1-C2	1.388(6)	C1-C6	1.398(6)	C2-C3	1.403(7)
C3-C4	1.357(8)	C4-C5	1.380(8)	C5-C6	1.381(7)
C7-C12	1.392(6)	C7-C8	1.396(6)	C8-C9	1.383(6)
C9-C10	1.386(7)	C9-C13	1.494(7)	C10-C11	1.378(7)
C11-C12	1.397(6)	C11-C14	1.496(7)	C15-C16	1.397(6)
C15-C20	1.400(6)	C16-C17	1.389(7)	C17-C18	1.375(8)
C18-C19	1.381(7)	C19-C20	1.382(6)	C21-C22	1.393(6)
C21-C26	1.404(6)	C22-C23	1.387(6)	C23-C24	1.378(6)
C23-C27	1.495(7)	C24-C25	1.381(6)	C25-C26	1.385(6)
C25-C28	1.499(6)	C29-C30	1.383(6)	C29-C34	1.391(6)
C30-C31	1.388(6)	C31-C32	1.379(7)	C32-C33	1.369(7)
C33-C34	1.394(6)	C35-C40	1.3951	C35-C36	1.3951

C36-C37	1.3949	C37-C38	1.3949	C37-C41	1.539(11)
C38-C39	1.3950	C39-C40	1.3951	C39-C42	1.571(14)
C41-F13	1.3100	C41-F14	1.3101	C41-F15	1.3116
C35'-C36'	1.3949	C35'-C40'	1.3951	C36'-C37'	1.3951
C37'-C38'	1.3950	C37'-C41'	1.529(11)	C38'-C39'	1.3951
C39'-C40'	1.3949	C39'-C42	1.387(14)	C41'-F13'	1.3098
C41'-F15'	1.3100	C41'-F14'	1.3103	C43-C44	1.388(6)
C43-C48	1.394(6)	C44-C45	1.392(6)	C45-C46	1.374(7)
C46-C47	1.381(8)	C47-C48	1.380(7)	C49-C50	1.397(6)
C49-C54	1.399(6)	C50-C51	1.383(6)	C51-C52	1.376(7)
C51-C55	1.500(8)	C52-C53	1.383(7)	C53-C54	1.384(6)
C53-C56	1.496(8)	C57-C58	1.380(7)	C58-C59	1.364(8)
C59-C60	1.372(8)	C60-C61	1.379(7)		

Table 4.6.9 Bond angles of **4.2** (°).

N4-U1-N3	86.32(12)	N4-U1-N2	114.81(12)
N4-U1-N1	126.16(12)	N3-U1-N1	100.18(13)
N4-U1-N5	93.03(11)	N3-U1-N5	178.08(12)
N1-U1-N5	81.67(12)	N4-U1-C29	110.68(11)
N2-U1-C29	77.84(12)	N1-U1-C29	94.53(12)
N4-U1-C43	26.68(11)	N3-U1-C43	107.15(11)
N1-U1-C43	104.91(12)	N5-U1-C43	72.75(11)
C7-N1-C1	115.8(3)	C7-N1-U1	132.9(3)
C21-N2-C15	117.7(3)	C21-N2-U1	130.4(3)
C35-N3-C29	113.0(9)	C35-N3-C35'	11.1(14)
C35-N3-U1	139.4(9)	C29-N3-U1	106.5(2)
C49-N4-C43	116.9(3)	C49-N4-U1	135.2(3)
C61-N5-C57	117.1(4)	C61-N5-U1	118.9(3)
C2-C1-C6	118.5(4)	C2-C1-N1	120.5(4)
C1-C2-C3	120.3(5)	C4-C3-C2	120.3(5)
C4-C5-C6	120.9(5)	C5-C6-C1	120.0(5)
C12-C7-N1	120.6(4)	C8-C7-N1	121.5(4)
C8-C9-C10	121.5(4)	C8-C9-C13	119.7(5)
C11-C10-C9	118.1(4)	C10-C11-C12	121.1(4)
C12-C11-C14	118.2(4)	C7-C12-C11	120.7(4)
F1-C13-F3	105.2(5)	F2-C13-F3	104.6(5)
F2-C13-C9	113.4(5)	F3-C13-C9	111.2(5)
F4-C14-F6	105.2(5)	F5-C14-F6	105.3(4)
F5-C14-C11	112.8(5)	F6-C14-C11	112.5(4)
C16-C15-N2	119.0(4)	C20-C15-N2	123.0(4)
C18-C17-C16	120.5(5)	C17-C18-C19	119.5(5)
C19-C20-C15	120.8(4)	C22-C21-N2	122.2(4)
N2-C21-C26	120.3(4)	C23-C22-C21	121.0(4)
C24-C23-C27	121.9(4)	C22-C23-C27	116.9(4)
C24-C25-C26	121.4(4)	C24-C25-C28	118.5(4)
C25-C26-C21	120.6(4)	F9-C27-F8	106.0(5)
F8-C27-F7	106.2(4)	F9-C27-C23	111.9(4)
F7-C27-C23	112.5(4)	F10-C28-F12	106.7(5)
F12-C28-F11	105.5(5)	F10-C28-C25	112.4(5)
F11-C28-C25	111.2(4)	C30-C29-C34	119.0(4)
C34-C29-N3	120.0(4)	C30-C29-U1	107.3(3)
N3-C29-U1	46.20(18)	C29-C30-C31	120.6(4)

C33-C32-C31	120.7(4)	C32-C33-C34	119.7(5)
N3-C35-C40	112.1(13)	N3-C35-C36	127.8(13)
C37-C36-C35	120.0	C38-C37-C36	120.0
C36-C37-C41	112.7(11)	C37-C38-C39	120.0
C38-C39-C42	116.7(13)	C40-C39-C42	123.1(13)
F13-C41-F14	109.5	F13-C41-F15	109.4
F13-C41-C37	105.6(8)	F14-C41-C37	109.9(7)
C36'-C35'-C40'	120.0	C36'-C35'-N3	116.8(13)
C35'-C36'-C37'	120.0	C38'-C37'-C36'	120.0
C36'-C37'-C41'	119.2(11)	C37'-C38'-C39'	120.0
C40'-C39'-C42	115.8(14)	C38'-C39'-C42	124.2(14)
F13'-C41'-F15'	109.4	F13'-C41'-F14'	109.4
F13'-C41'-C37'	109.8(8)	F15'-C41'-C37'	111.3(8)
F17-C42-F16	103.6(5)	F17-C42-F18	105.0(6)
F17-C42-C39'	116.6(13)	F16-C42-C39'	106.9(12)
F17-C42-C39	111.1(12)	F16-C42-C39	117.9(10)
C39'-C42-C39	11.0(19)	C44-C43-C48	118.9(4)
C48-C43-N4	120.0(4)	C44-C43-U1	98.9(3)
N4-C43-U1	45.65(17)	C43-C44-C45	120.4(4)
C45-C46-C47	120.2(5)	C46-C47-C48	120.2(5)
N4-C49-C50	122.1(4)	N4-C49-C54	120.3(4)
C51-C50-C49	121.0(4)	C52-C51-C50	121.2(5)
C50-C51-C55	119.0(5)	C51-C52-C53	118.3(4)
C52-C53-C56	118.2(5)	C54-C53-C56	120.4(5)
F19'-C55-F21	130.3(12)	F19'-C55-F21'	113.5(18)
F19'-C55-F20	53.6(14)	F21-C55-F20	114.3(13)
F19'-C55-F19	49.8(16)	F21-C55-F19	102.6(9)
F20-C55-F19	101.7(10)	F19'-C55-F20'	105.4(15)
F21'-C55-F20'	97.7(14)	F20-C55-F20'	55.8(10)
F19'-C55-C51	116.0(8)	F21-C55-C51	112.5(9)
F20-C55-C51	113.5(6)	F19-C55-C51	111.1(7)
F23-C56-F24	106.6(6)	F23-C56-F22	105.9(5)
F23-C56-C53	113.1(6)	F24-C56-C53	113.6(5)
N5-C57-C58	122.8(4)	C59-C58-C57	119.0(5)
C59-C60-C61	119.1(5)	N5-C61-C60	123.0(5)
N3-U1-N2	98.99(12)	F12-C28-C25	114.2(4)
N2-U1-N1	116.68(12)	C30-C29-N3	120.9(4)
N2-U1-N5	79.64(12)	C34-C29-U1	112.7(3)
N3-U1-C29	27.25(11)	C32-C31-C30	119.6(4)
N5-U1-C29	152.49(11)	C29-C34-C33	120.2(5)
N2-U1-C43	125.34(12)	C40-C35-C36	120.0
C29-U1-C43	133.95(11)	C38-C37-C41	127.2(11)
C1-N1-U1	111.0(3)	C38-C39-C40	120.0
C15-N2-U1	111.7(2)	C35-C40-C39	120.0
C29-N3-C35'	118.7(9)	F14-C41-F15	109.4
C35'-N3-U1	134.8(8)	F15-C41-C37	113.0(8)
C43-N4-U1	107.7(2)	C40'-C35'-N3	123.1(13)
C57-N5-U1	123.4(3)	C38'-C37'-C41'	120.7(11)
C6-C1-N1	120.9(4)	C40'-C39'-C38'	120.0
C3-C4-C5	119.8(5)	C39'-C40'-C35'	120.0
C12-C7-C8	117.8(4)	F15'-C41'-F14'	109.4
C9-C8-C7	120.8(4)	F14'-C41'-C37'	107.5(9)
C10-C9-C13	118.8(4)	F16-C42-F18	107.2(7)
C10-C11-C14	120.5(4)	F18-C42-C39'	116.5(10)

F1-C13-F2	108.0(5)	F18-C42-C39	111.1(9)
F1-C13-C9	113.8(5)	C44-C43-N4	121.0(4)
F4-C14-F5	107.3(5)	C48-C43-U1	122.1(3)
F4-C14-C11	113.0(4)	C46-C45-C44	119.9(5)
C16-C15-C20	117.9(4)	C47-C48-C43	120.3(5)
C17-C16-C15	120.7(5)	C50-C49-C54	117.5(4)
C18-C19-C20	120.5(5)	C52-C51-C55	119.8(5)
C22-C21-C26	117.5(4)	C52-C53-C54	121.4(5)
C24-C23-C22	121.2(4)	C53-C54-C49	120.6(4)
C23-C24-C25	118.3(4)	F21-C55-F21'	33.9(13)
C26-C25-C28	120.1(4)	F21'-C55-F20	133.5(14)
F9-C27-F7	106.2(5)	F21'-C55-F19	71.5(13)
F8-C27-C23	113.4(4)	F21-C55-F20'	65.4(10)
F10-C28-F11	106.2(4)	F19-C55-F20'	137.7(8)
F24-C56-F22	104.7(6)	F21'-C55-C51	111.6(13)
F22-C56-C53	112.3(6)	F20'-C55-C51	110.9(6)
C58-C59-C60	119.0(5)		

Table 4.6.10 Bond lengths of **4.3a** (Å).

U1-N1	2.248(3)	U1-N1#1	2.248(3)	U1-N2#1	2.587(3)
U1-N2	2.587(3)	U1-Cl1#1	2.6475(8)	U1-Cl1	2.6475(8)
U1-C9	2.989(3)	U1-C9#1	2.989(3)	N1-C1	1.415(4)
N1-C9	1.419(4)	N2-C19	1.333(5)	N2-C15	1.339(5)
C1-C6	1.388(5)	C1-C2	1.399(5)	C2-C3	1.386(5)
C3-C4	1.384(5)	C3-C7	1.503(5)	C4-C5	1.390(5)
C5-C6	1.389(5)	C5-C8	1.498(5)	C7-F3	1.303(5)
C7-F2	1.307(6)	C7-F1	1.343(5)	C8-F6	1.265(5)
C8-F5	1.279(6)	C8-F4	1.359(7)	C9-C10	1.398(5)
C9-C14	1.403(5)	C10-C11	1.391(5)	C11-C12	1.371(6)
C12-C13	1.396(6)	C13-C14	1.371(5)	C15-C16	1.378(5)
C16-C17	1.376(5)	C17-C18	1.387(5)	C17-C20	1.518(5)
C18-C19	1.382(5)	C20-C23	1.526(5)	C20-C22	1.532(5)
C20-C21	1.539(5)				

Symmetry transformations used to generate equivalent atoms:

#1 -x+1,y,-z+1/2

Table 4.6.11 Bond angles of **4.3a** (°).

N1-U1-N1#1	83.73(14)	N1-U1-N2#1	173.60(10)
N1-U1-N2	101.81(10)	N1#1-U1-N2	173.60(10)
N1-U1-Cl1#1	89.48(7)	N1#1-U1-Cl1#1	100.02(7)
N2-U1-Cl1#1	83.34(7)	N1-U1-Cl1	100.02(7)
N2#1-U1-Cl1	83.34(7)	N2-U1-Cl1	86.42(7)
N1-U1-C9	27.00(9)	N1#1-U1-C9	110.10(10)
N2-U1-C9	75.14(9)	Cl1#1-U1-C9	90.51(6)
N1-U1-C9#1	110.10(10)	N1#1-U1-C9#1	27.00(9)
N2-U1-C9#1	147.98(9)	Cl1#1-U1-C9#1	94.16(6)
C9-U1-C9#1	136.88(12)	C1-N1-C9	116.4(3)
C9-N1-U1	107.0(2)	C19-N2-C15	116.3(3)
C15-N2-U1	118.1(2)	C6-C1-C2	118.8(3)
C2-C1-N1	120.9(3)	C3-C2-C1	120.1(3)

C4-C3-C7	120.3(3)	C2-C3-C7	118.5(3)
C6-C5-C4	120.8(3)	C6-C5-C8	119.6(3)
C1-C6-C5	120.4(3)	F3-C7-F2	109.9(4)
F2-C7-F1	103.1(4)	F3-C7-C3	113.5(3)
F1-C7-C3	112.0(3)	F6-C8-F5	110.9(5)
F5-C8-F4	99.5(5)	F6-C8-C5	115.5(4)
F4-C8-C5	111.7(4)	C10-C9-C14	118.4(3)
C14-C9-N1	121.1(3)	C10-C9-U1	92.6(2)
N1-C9-U1	45.99(15)	C11-C10-C9	120.0(3)
C11-C12-C13	119.1(4)	C14-C13-C12	120.7(4)
N2-C15-C16	123.2(3)	C17-C16-C15	121.1(3)
C16-C17-C20	121.0(3)	C18-C17-C20	123.5(3)
N2-C19-C18	123.3(3)	C17-C20-C23	111.0(3)
C23-C20-C22	108.7(3)	C17-C20-C21	107.8(3)
C22-C20-C21	108.2(3)	C6-C1-N1	120.2(3)
N1#1-U1-N2#1	101.81(10)	C4-C3-C2	121.2(3)
N2#1-U1-N2	72.85(13)	C3-C4-C5	118.5(3)
N2#1-U1-Cl1#1	86.42(7)	C4-C5-C8	119.6(3)
N1#1-U1-Cl1	89.48(7)	F3-C7-F1	105.2(4)
Cl1#1-U1-Cl1	167.27(4)	F2-C7-C3	112.4(4)
N2#1-U1-C9	147.98(9)	F6-C8-F4	104.5(5)
Cl1-U1-C9	94.16(6)	F5-C8-C5	113.2(4)
N2#1-U1-C9#1	75.14(9)	C10-C9-N1	120.2(3)
Cl1-U1-C9#1	90.51(6)	C14-C9-U1	126.9(2)
C1-N1-U1	133.4(2)	C12-C11-C10	121.1(3)
C19-N2-U1	125.0(2)	C13-C14-C9	120.7(3)
C17-C20-C22	111.1(3)	C16-C17-C18	115.4(3)
C23-C20-C21	110.0(3)	C19-C18-C17	120.7(3)

Symmetry transformations used to generate equivalent atoms:

#1 -x+1,y,-z+1/2

Table 4.6.12 Bond lengths of **4.3b** (Å).

U1-N1	2.289(4)	U1-N1#1	2.289(4)	U1-N2	2.560(3)
U1-N2#1	2.560(3)	U1-Cl1#1	2.6349(12)	U1-Cl1	2.6349(12)
N1-C1	1.393(6)	N1-C9	1.420(6)	N2-C15	1.338(5)
N2-C19	1.347(6)	C1-C6	1.390(7)	C1-C2	1.401(6)
C2-C3	1.384(7)	C3-C4	1.378(8)	C3-C7	1.499(7)
C4-C5	1.385(7)	C5-C6	1.386(7)	C5-C8	1.479(8)
C7-F1	1.275(9)	C7-F2	1.298(8)	C7-F3	1.327(9)
C8-F6	1.297(7)	C8-F5	1.303(7)	C8-F4	1.318(7)
C9-C14	1.392(6)	C9-C10	1.405(7)	C10-C11	1.371(8)
C11-C12	1.392(8)	C12-C13	1.366(8)	C13-C14	1.387(8)
C15-C16	1.371(6)	C16-C17	1.390(6)	C17-C18	1.396(6)
C17-C20	1.526(6)	C18-C19	1.381(6)	C20-C22	1.526(9)
C20-C21	1.530(8)	C20-C23	1.532(8)		

Symmetry transformations used to generate equivalent atoms:

#1 -x+1,y,-z+1/2

Table 4.6.13 Bond angles of **4.3b** (°).

N1-U1-N1#1	87.9(2)	N1-U1-N2	97.91(13)
N1-U1-N2#1	172.69(13)	N1#1-U1-N2#1	97.91(13)
N1-U1-Cl1#1	104.33(10)	N1#1-U1-Cl1#1	86.93(10)
N2#1-U1-Cl1#1	80.49(9)	N1-U1-Cl1	86.93(10)
N2-U1-Cl1	80.49(9)	N2#1-U1-Cl1	87.35(8)
C1-N1-C9	118.5(4)	C1-N1-U1	130.0(3)
C15-N2-C19	116.3(4)	C15-N2-U1	123.2(3)
C6-C1-N1	119.7(4)	C6-C1-C2	118.0(4)
C3-C2-C1	120.0(5)	C4-C3-C2	121.6(5)
C2-C3-C7	119.6(5)	C3-C4-C5	118.8(5)
C4-C5-C8	120.2(5)	C6-C5-C8	119.5(5)
F1-C7-F2	109.2(7)	F1-C7-F3	103.0(7)
F1-C7-C3	115.5(6)	F2-C7-C3	114.1(6)
F6-C8-F5	106.4(6)	F6-C8-F4	105.5(5)
F6-C8-C5	112.0(5)	F5-C8-C5	113.3(5)
C14-C9-C10	117.9(5)	C14-C9-N1	119.8(4)
C11-C10-C9	120.9(5)	C10-C11-C12	120.0(5)
C12-C13-C14	120.3(5)	C13-C14-C9	120.8(5)
C15-C16-C17	120.5(4)	C16-C17-C18	115.7(4)
C18-C17-C20	120.1(4)	C19-C18-C17	120.6(4)
C22-C20-C17	108.6(4)	C22-C20-C21	108.7(6)
C22-C20-C23	109.5(5)	C17-C20-C23	109.2(4)
N1#1-U1-N2	172.69(13)	F5-C8-F4	105.3(6)
N2-U1-N2#1	76.65(15)	F4-C8-C5	113.6(5)
N2-U1-Cl1#1	87.35(9)	C10-C9-N1	122.1(4)
N1#1-U1-Cl1	104.33(10)	C13-C12-C11	119.9(5)
Cl1#1-U1-Cl1	164.51(5)	N2-C15-C16	124.0(4)
C9-N1-U1	110.5(3)	C16-C17-C20	124.2(4)
C19-N2-U1	119.7(3)	N2-C19-C18	122.9(4)
N1-C1-C2	121.9(4)	C17-C20-C21	111.2(5)
C4-C3-C7	118.8(5)	C21-C20-C23	109.6(6)
C4-C5-C6	120.2(5)	F2-C7-F3	103.1(6)
C5-C6-C1	121.3(4)	F3-C7-C3	110.6(6)

Symmetry transformations used to generate equivalent atoms:

#1 -x+1,y,-z+1/2

Table 4.6.14 Bond lengths of U^{IV}F(NAr^{F}Ph)$_4$py (Å).

U1-F25	2.143(3)	U1-N3	2.351(4)	U1-N4	2.382(4)
U1-N2	2.385(4)	U1-N1	2.402(4)	U1-N5	2.630(4)
N1-C7	1.379(6)	N1-C1	1.438(7)	N2-C21	1.383(6)
N2-C15	1.432(6)	N3-C29	1.406(6)	N3-C35	1.408(6)
N4-C49	1.381(6)	N4-C43	1.433(6)	N5-C57	1.325(8)
N5-C61	1.338(8)	N6-C66	1.333(13)	N6-C62	1.345(14)
N6-K1	2.850(7)	C1-C6	1.344(10)	C1-C2	1.410(11)
C2-C3	1.399(12)	C3-C4	1.367(18)	C4-C5	1.32(2)
C5-C6	1.404(12)	C7-C12	1.397(7)	C7-C8	1.421(7)
C8-C9	1.375(7)	C9-C10	1.389(8)	C9-C13	1.504(8)
C10-C11	1.380(7)	C11-C12	1.391(6)	C11-C14	1.487(7)
C13-F2	1.268(8)	C13-F1	1.280(9)	C13-F3	1.385(11)
C14-F5	1.314(6)	C14-F4	1.331(7)	C14-F6	1.342(6)
C15-C20	1.386(7)	C15-C16	1.389(7)	C16-C17	1.389(8)
C17-C18	1.358(9)	C18-C19	1.382(9)	C19-C20	1.393(7)

C21-C22	1.407(7)	C21-C26	1.411(7)	C22-C23	1.389(7)
C23-C24	1.383(8)	C23-C27	1.501(7)	C24-C25	1.387(8)
C25-C26	1.377(7)	C25-C28	1.482(8)	C27-F7	1.296(8)
C27-F8'	1.302(8)	C27-F9	1.306(8)	C27-F9'	1.308(8)
C27-F8	1.361(7)	C27-F7'	1.363(7)	C28-F10	1.297(8)
C28-F11	1.306(7)	C28-F12	1.360(8)	C29-C30	1.389(7)
C29-C34	1.405(7)	C30-C31	1.395(8)	C31-C32	1.359(9)
C32-C33	1.385(10)	C33-C34	1.374(8)	C35-C36	1.410(6)
C35-C40	1.421(6)	C36-C37	1.375(7)	C37-C38	1.378(7)
C37-C41	1.502(7)	C38-C39	1.387(7)	C39-C40	1.392(6)
C39-C42	1.491(7)	C41-F15	1.303(7)	C41-F14	1.324(7)
C41-F13	1.330(7)	C42-F17	1.329(6)	C42-F16	1.338(6)
C42-F18	1.349(6)	C43-C44	1.374(7)	C43-C48	1.382(7)
C44-C45	1.384(8)	C45-C46	1.349(9)	C46-C47	1.367(8)
C47-C48	1.384(7)	C49-C54	1.404(6)	C49-C50	1.413(6)
C50-C51	1.387(7)	C51-C52	1.381(7)	C51-C55	1.496(7)
C52-C53	1.386(6)	C53-C54	1.382(6)	C53-C56	1.488(7)
C55-F20	1.266(7)	C55-F21	1.268(7)	C55-F19	1.292(8)
C56-F22	1.278(7)	C56-F23'	1.280(8)	C56-F24'	1.289(7)
C56-F23	1.307(7)	C56-F22'	1.390(8)	C56-F24	1.392(7)
C57-C58	1.396(11)	C58-C59	1.336(14)	C59-C60	1.347(12)
C60-C61	1.383(8)	F6-K1	2.837(4)	F12-K1	2.729(5)
F14-K1#1	2.934(4)	F18-K1	2.802(3)	F24-K1	2.796(9)
F24'-K1	2.760(12)	F25-K1	2.616(3)	K1-F14#1	2.934(4)
C62-C63	1.365(13)	C63-C64	1.37(2)	C64-C65	1.36(2)
C65-C66	1.349(13)				

Symmetry transformations used to generate equivalent atoms:

#1 -x+1,-y+1,-z+1

Table 4.6.15 Bond angles of U^{IV}F(NAr^{F}Ph)$_4$py (°).

F25-U1-N3	80.05(11)	F25-U1-N4	85.24(11)
F25-U1-N2	84.12(12)	N3-U1-N2	89.66(13)
F25-U1-N1	81.74(11)	N3-U1-N1	161.76(13)
N2-U1-N1	89.58(13)	F25-U1-N5	174.19(12)
N4-U1-N5	99.65(13)	N2-U1-N5	91.12(14)
C7-N1-C1	116.7(4)	C7-N1-U1	131.7(3)
C21-N2-C15	115.7(4)	C21-N2-U1	130.5(3)
C29-N3-C35	113.3(4)	C29-N3-U1	115.4(3)
C49-N4-C43	116.4(4)	C49-N4-U1	132.2(3)
C57-N5-C61	116.7(6)	C57-N5-U1	122.8(5)
C66-N6-C62	116.5(9)	C66-N6-K1	126.9(7)
C6-C1-C2	118.0(7)	C6-C1-N1	121.5(7)
C3-C2-C1	119.9(11)	C4-C3-C2	119.0(12)
C4-C5-C6	120.2(11)	C1-C6-C5	121.3(10)
N1-C7-C8	123.6(4)	C12-C7-C8	115.5(4)
C8-C9-C10	122.2(5)	C8-C9-C13	119.6(6)
C11-C10-C9	117.2(5)	C10-C11-C12	121.5(5)
C12-C11-C14	118.4(4)	C11-C12-C7	122.2(4)
F2-C13-F3	100.1(7)	F1-C13-F3	100.1(6)
F1-C13-C9	113.9(6)	F3-C13-C9	109.7(8)
F5-C14-F6	106.2(5)	F4-C14-F6	103.3(5)
F4-C14-C11	113.5(4)	F6-C14-C11	112.8(4)

C20-C15-N2	121.0(4)	C16-C15-N2	120.8(4)
C18-C17-C16	120.5(6)	C17-C18-C19	119.8(5)
C15-C20-C19	120.4(5)	N2-C21-C22	123.6(4)
C22-C21-C26	116.7(4)	C23-C22-C21	120.8(5)
C24-C23-C27	118.9(5)	C22-C23-C27	118.9(5)
C26-C25-C24	122.4(5)	C26-C25-C28	118.6(5)
C25-C26-C21	120.9(5)	F7-C27-F8'	47.4(8)
F8'-C27-F9	129.4(11)	F7-C27-F9'	134.1(11)
F9-C27-F9'	31.9(11)	F7-C27-F8	97.6(8)
F9-C27-F8	100.4(8)	F9'-C27-F8	69.9(10)
F8'-C27-F7'	97.3(8)	F9-C27-F7'	76.7(8)
F8-C27-F7'	136.7(7)	F7-C27-C23	112.7(6)
F9-C27-C23	112.5(8)	F9'-C27-C23	113.1(9)
F7'-C27-C23	112.2(5)	F10-C28-F11	107.6(5)
F11-C28-F12	104.0(6)	F10-C28-C25	114.9(6)
F12-C28-C25	111.0(5)	C30-C29-C34	117.2(4)
C34-C29-N3	121.2(4)	C29-C30-C31	121.2(5)
C31-C32-C33	119.0(6)	C34-C33-C32	121.1(6)
N3-C35-C36	124.7(4)	N3-C35-C40	119.9(4)
C37-C36-C35	122.2(4)	C36-C37-C38	122.1(5)
C38-C37-C41	119.1(5)	C37-C38-C39	117.4(4)
C38-C39-C42	120.6(4)	C40-C39-C42	117.6(4)
F15-C41-F14	107.4(5)	F15-C41-F13	105.1(6)
F15-C41-C37	113.1(5)	F14-C41-C37	113.6(5)
F17-C42-F16	106.2(4)	F17-C42-F18	106.4(4)
F17-C42-C39	113.9(4)	F16-C42-C39	112.6(4)
C44-C43-C48	117.0(5)	C44-C43-N4	120.7(4)
C43-C44-C45	121.1(5)	C46-C45-C44	121.3(6)
C46-C47-C48	120.4(5)	C43-C48-C47	121.3(5)
N4-C49-C50	123.9(4)	C54-C49-C50	115.9(4)
C52-C51-C50	122.1(4)	C52-C51-C55	118.5(5)
C51-C52-C53	117.3(4)	C54-C53-C52	121.7(4)
C52-C53-C56	119.4(4)	C53-C54-C49	121.9(4)
F20-C55-F19	104.8(6)	F21-C55-F19	102.7(6)
F21-C55-C51	113.4(5)	F19-C55-C51	114.2(5)
F22-C56-F24'	52.3(7)	F23'-C56-F24'	113.6(10)
F23'-C56-F23	28.9(9)	F24'-C56-F23	127.7(8)
F23'-C56-F22'	104.0(9)	F24'-C56-F22'	98.7(8)
F22-C56-F24	101.6(7)	F23'-C56-F24	73.5(9)
F23-C56-F24	100.9(6)	F22'-C56-F24	141.6(7)
F23'-C56-C53	116.3(9)	F24'-C56-C53	115.6(6)
F22'-C56-C53	105.8(6)	F24-C56-C53	109.4(5)
C59-C58-C57	120.8(8)	C58-C59-C60	118.2(7)
N5-C61-C60	123.0(7)	C14-F6-K1	140.8(3)
C41-F14-K1#1	145.9(4)	C42-F18-K1	127.6(3)
C56-F24'-K1	134.5(9)	U1-F25-K1	175.59(13)
F25-K1-F24'	88.6(3)	F12-K1-F24'	174.5(2)
F12-K1-F24	154.7(2)	F24'-K1-F24	24.5(3)
F12-K1-F18	72.21(15)	F24'-K1-F18	104.5(3)
F25-K1-F6	86.43(10)	F12-K1-F6	99.18(16)
F24-K1-F6	65.6(2)	F18-K1-F6	171.36(12)
F12-K1-N6	69.0(2)	F24'-K1-N6	108.7(4)
F18-K1-N6	109.62(18)	F6-K1-N6	66.65(18)
F12-K1-F14#1	115.06(17)	F24'-K1-F14#1	59.4(2)

F18-K1-F14#1	65.93(13)	F6-K1-F14#1	119.78(14)
N6-C62-C63	123.7(13)	C62-C63-C64	118.0(15)
C66-C65-C64	120.1(14)	N6-C66-C65	122.9(13)
N3-U1-N4	91.18(13)	C38-C39-C40	121.7(4)
N4-U1-N2	169.02(13)	C39-C40-C35	121.3(4)
N4-U1-N1	86.19(13)	F14-C41-F13	103.9(5)
N3-U1-N5	96.63(14)	F13-C41-C37	113.0(5)
N1-U1-N5	101.60(14)	F16-C42-F18	105.3(4)
C1-N1-U1	111.6(3)	F18-C42-C39	111.9(4)
C15-N2-U1	112.9(3)	C48-C43-N4	122.3(4)
C35-N3-U1	131.3(3)	C45-C46-C47	118.8(5)
C43-N4-U1	110.6(3)	N4-C49-C54	120.3(4)
C61-N5-U1	120.1(4)	C51-C50-C49	121.2(4)
C62-N6-K1	110.6(7)	C50-C51-C55	119.5(5)
C2-C1-N1	120.5(6)	C54-C53-C56	119.0(4)
C5-C4-C3	121.4(10)	F20-C55-F21	106.4(6)
N1-C7-C12	120.9(4)	F20-C55-C51	114.2(5)
C9-C8-C7	121.4(5)	F22-C56-F23'	123.5(10)
C10-C9-C13	118.3(5)	F22-C56-F23	108.9(7)
C10-C11-C14	120.1(4)	F22-C56-F22'	46.6(6)
F2-C13-F1	115.3(8)	F23-C56-F22'	76.8(8)
F2-C13-C9	115.4(6)	F24'-C56-F24	52.0(7)
F5-C14-F4	106.0(4)	F22-C56-C53	118.1(5)
F5-C14-C11	114.2(5)	F23-C56-C53	115.6(6)
C20-C15-C16	118.3(5)	N5-C57-C58	121.7(8)
C17-C16-C15	120.8(5)	C59-C60-C61	119.5(8)
C18-C19-C20	120.3(6)	C28-F12-K1	136.8(4)
N2-C21-C26	119.7(4)	C56-F24-K1	125.4(6)
C24-C23-C22	122.1(5)	F25-K1-F12	95.99(13)
C23-C24-C25	117.0(5)	F25-K1-F24	102.68(16)
C24-C25-C28	118.9(5)	F25-K1-F18	93.79(10)
F7-C27-F9	122.0(10)	F24-K1-F18	122.6(2)
F8'-C27-F9'	111.4(11)	F24'-K1-F6	84.1(3)
F8'-C27-F8	50.9(8)	F25-K1-N6	145.45(17)
F7-C27-F7'	53.5(8)	F24-K1-N6	86.1(3)
F9'-C27-F7'	105.4(10)	F25-K1-F14#1	132.87(13)
F8'-C27-C23	116.0(7)	F24-K1-F14#1	62.74(17)
F8-C27-C23	108.7(6)	N6-K1-F14#1	80.98(19)
F10-C28-F12	103.1(6)	C65-C64-C63	118.6(11)
F11-C28-C25	115.1(5)	C33-C34-C29	120.7(5)
C30-C29-N3	121.4(4)	C36-C35-C40	115.3(4)
C32-C31-C30	120.7(6)	C36-C37-C41	118.7(5)

Symmetry transformations used to generate equivalent atoms:

#1 -x+1,-y+1,-z+1

Table 4.6.16 Bond lengths of **4.5-tol** (Å).

U1-O1	1.802(2)	U1-O2	1.806(2)	U1-N2	2.375(3)
U1-N4	2.397(3)	U1-N3	2.397(3)	U1-N1	2.402(3)
U1-K2	4.1541(8)	U1-K1	4.2415(8)	N1-C7	1.387(4)
N1-C1	1.420(4)	N2-C21	1.394(4)	N2-C15	1.431(4)
N3-C35	1.384(4)	N3-C29	1.435(4)	N4-C49	1.388(4)
N4-C43	1.422(4)	O1-K1	2.589(2)	O2-K2	2.614(2)

C1-C2	1.389(5)	C1-C6	1.404(5)	C1-K1	3.388(3)
C2-C3	1.390(5)	C2-K1	3.333(4)	C3-C4	1.376(6)
C3-K1	3.293(4)	C4-C5	1.373(6)	C4-K1	3.309(4)
C5-C6	1.394(5)	C5-K1	3.381(4)	C6-K1	3.414(4)
C7-C12	1.397(5)	C7-C8	1.409(5)	C8-C9	1.390(5)
C9-C10	1.379(6)	C9-C13	1.476(6)	C10-C11	1.374(6)
C11-C12	1.385(6)	C11-C14	1.478(7)	C13-F3	1.270(6)
C13-F2	1.279(6)	C13-F1	1.299(6)	C14-F4	1.243(7)
C14-F6	1.277(10)	C14-F5	1.324(12)	C15-C16	1.379(5)
C15-C20	1.389(5)	C16-C17	1.392(5)	C16-K1	3.374(4)
C17-C18	1.377(6)	C17-K1	3.249(4)	C18-C19	1.378(6)
C18-K1	3.436(4)	C19-C20	1.380(5)	C21-C22	1.399(5)
C21-C26	1.407(5)	C22-C23	1.381(5)	C23-C24	1.388(5)
C23-C27	1.495(6)	C24-C25	1.380(5)	C25-C26	1.392(5)
C25-C28	1.498(5)	C27-F9	1.311(5)	C27-F8	1.324(5)
C27-F7	1.353(6)	C28-F12	1.325(4)	C28-F10	1.330(4)
C28-F11	1.336(4)	C29-C30	1.385(5)	C29-C34	1.397(5)
C29-K2	3.405(3)	C30-C31	1.386(5)	C30-K2	3.286(4)
C31-C32	1.377(6)	C31-K2	3.188(4)	C32-C33	1.384(6)
C32-K2	3.203(4)	C33-C34	1.390(5)	C33-K2	3.298(4)
C34-K2	3.404(4)	C35-C40	1.408(5)	C35-C36	1.413(5)
C36-C37	1.391(5)	C37-C38	1.371(5)	C37-C41	1.490(5)
C38-C39	1.383(5)	C39-C40	1.377(5)	C39-C42	1.500(5)
C41-F14	1.282(6)	C41-F15	1.303(5)	C41-F13	1.323(5)
C42-F16	1.327(5)	C42-F17	1.329(5)	C42-F18	1.332(5)
C43-C44	1.393(5)	C43-C48	1.396(5)	C43-K2	3.222(3)
C44-C45	1.396(5)	C44-K2	3.188(3)	C45-C46	1.377(6)
C45-K2	3.252(4)	C46-C47	1.380(6)	C46-K2	3.336(4)
C47-C48	1.384(5)	C47-K2	3.379(4)	C48-K2	3.307(4)
C49-C50	1.408(4)	C49-C54	1.409(4)	C50-C51	1.383(4)
C51-C52	1.380(5)	C51-C55	1.496(5)	C52-C53	1.390(5)
C53-C54	1.384(5)	C53-C56	1.492(5)	C55-F21	1.331(4)
C55-F20	1.332(4)	C55-F19	1.348(4)	C56-F24	1.252(5)
C56-F22	1.307(5)	C56-F23	1.339(6)	K1-C61	3.152(4)
K1-C62	3.212(4)	K1-C60	3.212(4)	K1-C59	3.329(4)
K1-C57	3.361(4)	C57-C62	1.388(5)	C57-C58	1.389(5)
C57-C63	1.506(6)	C58-C59	1.385(6)	C59-C60	1.379(6)
C60-C61	1.379(6)	C61-C62	1.380(6)	K2-C67	3.147(5)
K2-C66	3.150(5)	K2-C65	3.227(5)	K2-C68	3.242(5)
C64-C65	1.327(7)	C64-C69	1.368(7)	C64-C70	1.503(8)
C65-C66	1.270(8)	C66-C67	1.298(9)	C67-C68	1.442(10)
C68-C69	1.451(10)				

Table 4.6.17 Bond angles of **4.5-tol** (°).

O1-U1-O2	177.83(9)	O1-U1-N2	87.72(9)
O1-U1-N4	89.81(9)	O2-U1-N4	89.03(9)
O1-U1-N3	93.11(9)	O2-U1-N3	88.66(9)
N4-U1-N3	86.92(9)	O1-U1-N1	86.89(9)
N2-U1-N1	90.03(10)	N4-U1-N1	91.84(9)
O1-U1-K2	155.54(7)	O2-U1-K2	24.22(7)
N4-U1-K2	67.88(6)	N3-U1-K2	76.42(6)
O1-U1-K1	18.07(7)	O2-U1-K1	160.67(7)

N4-U1-K1	97.24(6)	N3-U1-K1	109.85(7)
K2-U1-K1	163.964(17)	C7-N1-C1	115.8(3)
C1-N1-U1	119.1(2)	C21-N2-C15	113.7(3)
C15-N2-U1	113.94(18)	C35-N3-C29	113.9(3)
C29-N3-U1	114.89(19)	C49-N4-C43	114.9(3)
C43-N4-U1	120.0(2)	U1-O1-K1	149.47(11)
C2-C1-C6	117.4(3)	C2-C1-N1	120.9(3)
C2-C1-K1	75.9(2)	C6-C1-K1	79.1(2)
C1-C2-C3	121.8(4)	C1-C2-K1	80.3(2)
C4-C3-C2	119.9(4)	C4-C3-K1	78.6(2)
C5-C4-C3	119.7(4)	C5-C4-K1	81.1(2)
C4-C5-C6	120.7(4)	C4-C5-K1	75.2(2)
C5-C6-C1	120.4(4)	C5-C6-K1	76.8(2)
N1-C7-C12	122.5(3)	N1-C7-C8	120.3(3)
C9-C8-C7	120.7(3)	C10-C9-C8	121.5(4)
C8-C9-C13	118.6(4)	C11-C10-C9	117.8(4)
C10-C11-C14	118.6(4)	C12-C11-C14	119.2(5)
F3-C13-F2	106.1(5)	F3-C13-F1	105.1(5)
F3-C13-C9	114.8(5)	F2-C13-C9	113.7(4)
F4-C14-F6	110.6(9)	F4-C14-F5	102.3(8)
F4-C14-C11	118.8(6)	F6-C14-C11	113.4(7)
C16-C15-C20	118.3(3)	C16-C15-N2	119.9(3)
C15-C16-C17	121.2(4)	C15-C16-K1	91.6(2)
C18-C17-C16	119.7(4)	C18-C17-K1	85.9(2)
C17-C18-C19	119.7(4)	C17-C18-K1	70.6(2)
C18-C19-C20	120.3(4)	C19-C20-C15	120.8(4)
N2-C21-C26	123.3(3)	C22-C21-C26	116.3(3)
C22-C23-C24	121.3(3)	C22-C23-C27	119.4(3)
C25-C24-C23	117.7(3)	C24-C25-C26	121.5(3)
C26-C25-C28	118.1(3)	C25-C26-C21	121.2(3)
F9-C27-F7	105.0(4)	F8-C27-F7	103.6(4)
F8-C27-C23	113.4(3)	F7-C27-C23	111.3(4)
F12-C28-F11	105.4(3)	F10-C28-F11	105.4(3)
F10-C28-C25	113.1(3)	F11-C28-C25	112.6(3)
C30-C29-N3	120.8(3)	C34-C29-N3	120.9(3)
C34-C29-K2	78.13(19)	N3-C29-K2	118.58(19)
C29-C30-K2	82.9(2)	C31-C30-K2	73.7(2)
C32-C31-K2	78.2(2)	C30-C31-K2	81.7(2)
C31-C32-K2	76.9(2)	C33-C32-K2	81.6(2)
C32-C33-K2	73.9(2)	C34-C33-K2	82.4(2)
C33-C34-K2	73.8(2)	C29-C34-K2	78.19(19)
N3-C35-C36	123.2(3)	C40-C35-C36	116.3(3)
C38-C37-C36	122.3(3)	C38-C37-C41	120.3(3)
C37-C38-C39	117.5(3)	C40-C39-C38	121.8(3)
C38-C39-C42	118.6(3)	C39-C40-C35	121.5(3)
F14-C41-F13	104.4(5)	F15-C41-F13	103.6(4)
F15-C41-C37	114.3(4)	F13-C41-C37	112.9(4)
F16-C42-F18	106.2(3)	F17-C42-F18	105.4(4)
F17-C42-C39	112.4(3)	F18-C42-C39	113.4(3)
C44-C43-N4	121.4(3)	C48-C43-N4	120.8(3)
C48-C43-K2	81.1(2)	N4-C43-K2	109.80(19)
C43-C44-K2	78.8(2)	C45-C44-K2	80.0(2)
C46-C45-K2	81.4(2)	C44-C45-K2	74.9(2)
C45-C46-K2	74.5(2)	C47-C46-K2	79.9(2)

C46-C47-K2	76.4(2)	C48-C47-K2	75.1(2)
C47-C48-K2	81.0(2)	C43-C48-K2	74.27(19)
N4-C49-C54	120.7(3)	C50-C49-C54	116.5(3)
C52-C51-C50	122.0(3)	C52-C51-C55	120.4(3)
C51-C52-C53	117.6(3)	C54-C53-C52	121.5(3)
C52-C53-C56	119.6(3)	C53-C54-C49	121.2(3)
F21-C55-F19	106.0(3)	F20-C55-F19	105.7(3)
F20-C55-C51	113.1(3)	F19-C55-C51	111.6(3)
F24-C56-F23	104.3(5)	F22-C56-F23	100.4(4)
F22-C56-C53	114.2(4)	F23-C56-C53	110.7(4)
O1-K1-C62	158.97(9)	C61-K1-C62	25.02(10)
C61-K1-C60	25.01(10)	C62-K1-C60	43.72(10)
C61-K1-C17	86.11(11)	C62-K1-C17	76.01(10)
O1-K1-C3	84.45(9)	C61-K1-C3	131.66(10)
C60-K1-C3	117.61(10)	C17-K1-C3	117.67(11)
C61-K1-C4	115.26(11)	C62-K1-C4	94.94(11)
C17-K1-C4	103.34(11)	C3-K1-C4	24.06(10)
C61-K1-C59	42.95(10)	C62-K1-C59	49.60(10)
C17-K1-C59	125.41(10)	C3-K1-C59	93.56(10)
O1-K1-C2	62.30(8)	C61-K1-C2	155.82(9)
C60-K1-C2	139.28(10)	C17-K1-C2	106.01(10)
C4-K1-C2	42.25(10)	C59-K1-C2	116.26(10)
C61-K1-C57	43.40(10)	C62-K1-C57	24.25(9)
C17-K1-C57	89.94(10)	C3-K1-C57	92.26(10)
C59-K1-C57	42.33(10)	C2-K1-C57	114.41(9)
C61-K1-C16	107.82(10)	C62-K1-C16	100.17(10)
C17-K1-C16	24.18(9)	C3-K1-C16	107.43(10)
C59-K1-C16	149.28(10)	C2-K1-C16	89.05(9)
O1-K1-C5	102.63(9)	C61-K1-C5	116.35(11)
C60-K1-C5	122.75(10)	C17-K1-C5	79.84(11)
C4-K1-C5	23.65(11)	C59-K1-C5	103.31(11)
C57-K1-C5	74.62(10)	C16-K1-C5	79.97(10)
C62-C57-C63	121.0(4)	C58-C57-C63	121.5(4)
C58-C57-K1	79.4(2)	C63-C57-K1	118.8(3)
C59-C58-K1	75.5(2)	C57-C58-K1	76.8(2)
C60-C59-K1	73.1(2)	C58-C59-K1	80.7(2)
C59-C60-K1	82.6(2)	C61-C60-K1	75.0(2)
C60-C61-K1	79.9(2)	C62-C61-K1	79.9(2)
C61-C62-K1	75.1(2)	C57-C62-K1	83.9(2)
O2-K2-C66	156.85(15)	C67-K2-C66	23.79(17)
C67-K2-C31	91.73(13)	C66-K2-C31	102.06(16)
C67-K2-C44	135.00(18)	C66-K2-C44	111.25(17)
O2-K2-C32	107.23(9)	C67-K2-C32	74.56(14)
C31-K2-C32	24.89(11)	C44-K2-C32	134.59(11)
C67-K2-C43	143.2(2)	C66-K2-C43	121.95(16)
C44-K2-C43	25.10(9)	C32-K2-C43	109.57(10)
C67-K2-C65	41.36(17)	C66-K2-C65	22.94(15)
C44-K2-C65	96.08(13)	C32-K2-C65	114.26(15)
O2-K2-C68	125.18(19)	C67-K2-C68	26.03(19)
C31-K2-C68	104.01(19)	C44-K2-C68	142.21(14)
C43-K2-C68	163.92(12)	C65-K2-C68	49.66(14)
C67-K2-C45	110.00(18)	C66-K2-C45	86.29(18)
C44-K2-C45	25.01(10)	C32-K2-C45	141.58(12)
C65-K2-C45	71.82(13)	C68-K2-C45	120.49(12)

C67-K2-C30	115.96(13)	C66-K2-C30	126.15(15)
C44-K2-C30	93.42(10)	C32-K2-C30	43.41(10)
C65-K2-C30	147.50(14)	C68-K2-C30	123.87(16)
O2-K2-C33	89.29(9)	C67-K2-C33	82.15(16)
C31-K2-C33	43.02(11)	C44-K2-C33	139.96(9)
C43-K2-C33	117.27(9)	C65-K2-C33	123.14(14)
C45-K2-C33	160.07(11)	C30-K2-C33	49.53(10)
C65-C64-C70	120.6(6)	C69-C64-C70	120.4(7)
C69-C64-K2	77.9(3)	C70-C64-K2	119.6(4)
C66-C65-K2	75.1(3)	C64-C65-K2	82.8(3)
C65-C66-K2	81.9(3)	C67-C66-K2	78.0(3)
C66-C67-K2	78.2(3)	C68-C67-K2	80.6(3)
C67-C68-K2	73.3(3)	C69-C68-K2	80.5(3)
C64-C69-K2	78.4(3)	C68-C69-K2	74.0(3)
O2-U1-N2	93.50(9)	O1-K1-C17	91.39(9)
N2-U1-N4	176.82(9)	C60-K1-C17	110.86(11)
N2-U1-N3	91.21(9)	C62-K1-C3	116.24(10)
O2-U1-N1	91.32(10)	O1-K1-C4	104.43(9)
N3-U1-N1	178.76(10)	C60-K1-C4	110.77(11)
N2-U1-K2	114.17(6)	O1-K1-C59	137.96(10)
N1-U1-K2	103.11(7)	C60-K1-C59	24.25(10)
N2-U1-K1	80.97(6)	C4-K1-C59	87.54(11)
N1-U1-K1	70.30(7)	C62-K1-C2	137.05(10)
C7-N1-U1	125.0(2)	C3-K1-C2	24.21(9)
C21-N2-U1	132.4(2)	O1-K1-C57	176.69(9)
C35-N3-U1	131.0(2)	C60-K1-C57	50.38(10)
C49-N4-U1	124.5(2)	C4-K1-C57	72.31(10)
U1-O2-K2	139.33(11)	O1-K1-C16	68.02(8)
C6-C1-N1	121.6(3)	C60-K1-C16	131.16(10)
N1-C1-K1	110.68(19)	C4-K1-C16	102.45(10)
C3-C2-K1	76.3(2)	C57-K1-C16	112.93(10)
C2-C3-K1	79.5(2)	C62-K1-C5	91.80(10)
C3-C4-K1	77.3(2)	C3-K1-C5	41.71(11)
C6-C5-K1	79.5(2)	C2-K1-C5	48.34(10)
C1-C6-K1	77.0(2)	C62-C57-C58	117.5(4)
C12-C7-C8	117.1(3)	C62-C57-K1	71.8(2)
C10-C9-C13	119.9(4)	C59-C58-C57	121.1(4)
C10-C11-C12	122.2(4)	C60-C59-C58	120.4(4)
C11-C12-C7	120.7(4)	C59-C60-C61	119.2(4)
F2-C13-F1	100.8(6)	C60-C61-C62	120.2(4)
F1-C13-C9	115.0(4)	C61-C62-C57	121.6(4)
F6-C14-F5	95.6(7)	O2-K2-C67	151.18(19)
F5-C14-C11	113.2(8)	O2-K2-C31	100.64(9)
C20-C15-N2	121.8(3)	O2-K2-C44	64.38(8)
C17-C16-K1	72.9(2)	C31-K2-C44	109.85(11)
C16-C17-K1	82.9(2)	C66-K2-C32	91.78(17)
C19-C18-K1	89.9(2)	O2-K2-C43	64.55(8)
N2-C21-C22	120.4(3)	C31-K2-C43	84.99(10)
C23-C22-C21	121.9(3)	O2-K2-C65	134.90(14)
C24-C23-C27	119.2(3)	C31-K2-C65	124.44(15)
C24-C25-C28	120.4(3)	C43-K2-C65	114.26(12)
F9-C27-F8	108.9(4)	C66-K2-C68	43.67(18)
F9-C27-C23	113.8(4)	C32-K2-C68	80.93(17)
F12-C28-F10	107.3(3)	O2-K2-C45	86.72(10)

F12-C28-C25	112.5(3)	C31-K2-C45	118.84(12)
C30-C29-C34	118.3(3)	C43-K2-C45	43.99(9)
C30-C29-K2	73.3(2)	O2-K2-C30	76.90(8)
C29-C30-C31	120.9(4)	C31-K2-C30	24.66(9)
C32-C31-C30	120.7(4)	C43-K2-C30	68.76(9)
C31-C32-C33	119.1(4)	C45-K2-C30	110.60(10)
C32-C33-C34	120.5(4)	C66-K2-C33	104.33(17)
C33-C34-C29	120.5(4)	C32-K2-C33	24.52(11)
N3-C35-C40	120.5(3)	C68-K2-C33	77.39(13)
C37-C36-C35	120.5(3)	C65-C64-C69	119.0(6)
C36-C37-C41	117.4(3)	C65-C64-K2	73.9(3)
C40-C39-C42	119.5(3)	C66-C65-C64	124.4(6)
F14-C41-F15	106.3(4)	C65-C66-C67	122.5(7)
F14-C41-C37	114.3(4)	C66-C67-C68	120.4(6)
F16-C42-F17	106.5(3)	C67-C68-C69	114.7(5)
F16-C42-C39	112.3(4)	C64-C69-C68	119.0(6)
C44-C43-C48	117.7(3)	C54-C53-C56	118.9(3)
C44-C43-K2	76.09(19)	F21-C55-F20	107.1(3)
C43-C44-C45	120.8(4)	F21-C55-C51	112.8(3)
C46-C45-C44	120.0(4)	F24-C56-F22	110.8(5)
C45-C46-C47	120.4(4)	F24-C56-C53	115.0(4)
C46-C47-C48	119.5(4)	O1-K1-C61	139.73(9)
C47-C48-C43	121.7(4)	O1-K1-C60	131.64(9)
N4-C49-C50	122.6(3)	C50-C51-C55	117.5(3)
C51-C50-C49	121.0(3)		

Table 4.6.18 Bond lengths of **4.5** (Å).

U1-O1#1	1.802(3)	U1-O1	1.802(3)	U1-N2#1	2.394(4)
U1-N2	2.394(4)	U1-N1#1	2.395(4)	U1-N1	2.395(4)
U1-K1	4.2424(14)	U1-K1#1	4.2425(14)	K1-O1	2.693(4)
K1-F4#2	2.924(5)	K1-F6#2	3.068(5)	K1-C6	3.167(6)
K1-C1	3.201(5)	K1-C17	3.218(8)	K1-F8#3	3.255(7)
K1-C5	3.263(7)	K1-C2	3.325(6)	K1-C18	3.363(8)
K1-C16	3.401(7)	K1-C4	3.406(7)	F1-C13	1.313(9)
F2-C13	1.238(9)	F3-C13	1.301(9)	F4-C14	1.335(7)
F4-K1#4	2.923(5)	F5-C14	1.325(8)	F6-C14	1.344(9)
F6-K1#4	3.068(5)	F7-C27	1.40(3)	F8-C27	1.29(2)
F8-K1#5	3.255(7)	F9-C27	1.307(12)	F10-C28	1.335(9)
F11-C28	1.297(10)	F12-C28	1.339(8)	N1-C7	1.404(6)
N1-C1	1.423(6)	N2-C21	1.387(7)	N2-C15	1.430(6)
C1-C6	1.392(8)	C1-C2	1.411(8)	C2-C3	1.374(9)
C3-C4	1.371(10)	C4-C5	1.391(10)	C5-C6	1.391(8)
C7-C8	1.387(8)	C7-C12	1.394(7)	C8-C9	1.381(8)
C9-C10	1.379(9)	C9-C13	1.498(9)	C10-C11	1.370(9)
C11-C12	1.386(7)	C11-C14	1.488(9)	C15-C20	1.372(8)
C15-C16	1.397(9)	C16-C17	1.386(9)	C17-C18	1.335(12)
C18-C19	1.361(13)	C19-C20	1.425(10)	C21-C22	1.399(9)
C21-C26	1.410(7)	C22-C23	1.371(10)	C23-C24	1.397(11)
C23-C27	1.507(12)	C24-C25	1.375(9)	C25-C26	1.366(8)
C25-C28	1.498(9)				

Symmetry transformations used to generate equivalent atoms:

#1 -x,y,-z+1/2 #2 x,-y+1,z-1/2 #3 -x+1/2,y+1/2,-z+1/2

#4 x,-y+1,z+1/2 #5 -x+1/2,y-1/2,-z+1/2

Table 4.6.19 Bond angles of **4.5** (°).

O1#1-U1-O1	176.5(2)	O1#1-U1-N2#1	88.36(14)
O1#1-U1-N2	94.09(14)	O1-U1-N2	88.36(14)
O1#1-U1-N1#1	88.29(14)	O1-U1-N1#1	89.33(14)
N2-U1-N1#1	177.16(14)	O1#1-U1-N1	89.33(14)
N2#1-U1-N1	177.16(14)	N2-U1-N1	88.79(15)
O1#1-U1-K1	154.44(10)	O1-U1-K1	23.78(10)
N2-U1-K1	81.74(10)	N1#1-U1-K1	96.76(10)
O1#1-U1-K1#1	23.78(10)	O1-U1-K1#1	154.44(10)
N2-U1-K1#1	116.70(10)	N1#1-U1-K1#1	65.47(10)
K1-U1-K1#1	155.10(4)	O1-K1-F4#2	125.50(14)
F4#2-K1-F6#2	41.35(12)	O1-K1-C6	64.81(12)
F6#2-K1-C6	126.65(14)	O1-K1-C1	64.77(12)
F6#2-K1-C1	151.64(14)	C6-K1-C1	25.25(14)
F4#2-K1-C17	84.10(17)	F6#2-K1-C17	122.16(18)
C1-K1-C17	85.43(19)	O1-K1-F8#3	156.4(2)
F6#2-K1-F8#3	97.84(19)	C6-K1-F8#3	107.40(17)
C17-K1-F8#3	69.3(3)	O1-K1-C5	87.16(13)
F6#2-K1-C5	112.56(15)	C6-K1-C5	24.93(14)
C17-K1-C5	123.5(2)	F8#3-K1-C5	91.4(2)
F4#2-K1-C2	141.05(15)	F6#2-K1-C2	159.01(15)
C1-K1-C2	24.88(14)	C17-K1-C2	73.6(2)
C5-K1-C2	49.91(16)	O1-K1-C18	96.38(17)
F6#2-K1-C18	99.03(19)	C6-K1-C18	133.00(19)
C17-K1-C18	23.3(2)	F8#3-K1-C18	72.3(3)
C2-K1-C18	96.6(2)	O1-K1-C16	69.44(13)
F6#2-K1-C16	134.23(15)	C6-K1-C16	92.93(15)
C17-K1-C16	23.96(15)	F8#3-K1-C16	89.5(3)
C2-K1-C16	65.93(17)	C18-K1-C16	40.80(18)
F4#2-K1-C4	125.24(17)	F6#2-K1-C4	117.45(16)
C1-K1-C4	49.89(15)	C17-K1-C4	108.9(2)
C5-K1-C4	23.96(17)	C2-K1-C4	41.64(16)
C16-K1-C4	107.16(18)	C14-F4-K1#4	108.7(4)
C27-F8-K1#5	122.1(11)	U1-O1-K1	140.57(16)
C7-N1-U1	123.3(3)	C1-N1-U1	120.6(3)
C21-N2-U1	130.6(3)	C15-N2-U1	114.0(3)
C6-C1-N1	121.2(5)	C2-C1-N1	120.5(5)
C2-C1-K1	82.5(3)	N1-C1-K1	109.4(3)
C3-C2-K1	82.4(4)	C1-C2-K1	72.6(3)
C4-C3-K1	77.7(4)	C2-C3-K1	74.2(4)
C3-C4-K1	79.2(4)	C5-C4-K1	72.2(4)
C6-C5-K1	73.7(3)	C4-C5-K1	83.8(4)
C5-C6-K1	81.4(4)	C1-C6-K1	78.8(3)
C8-C7-N1	122.2(5)	C12-C7-N1	119.9(5)
C10-C9-C8	122.0(6)	C10-C9-C13	119.5(6)
C11-C10-C9	117.5(5)	C10-C11-C12	121.8(6)
C12-C11-C14	118.0(5)	C11-C12-C7	120.4(5)
F2-C13-F1	104.2(7)	F3-C13-F1	102.4(7)
F3-C13-C9	113.2(6)	F1-C13-C9	112.3(7)

F5-C14-F6	105.7(6)	F4-C14-F6	104.6(6)
F4-C14-C11	113.5(6)	F6-C14-C11	113.1(6)
C20-C15-N2	122.0(6)	C16-C15-N2	119.8(5)
C17-C16-K1	70.6(4)	C15-C16-K1	92.9(4)
C18-C17-K1	84.5(5)	C16-C17-K1	85.4(4)
C17-C18-K1	72.2(4)	C19-C18-K1	93.7(5)
C15-C20-C19	119.2(7)	N2-C21-C22	123.8(5)
C22-C21-C26	115.3(5)	C23-C22-C21	121.7(7)
C22-C23-C27	119.1(8)	C24-C23-C27	118.4(7)
C26-C25-C24	123.0(6)	C26-C25-C28	119.7(5)
C25-C26-C21	121.8(5)	F8-C27-F9	108.9(16)
F9-C27-F7	108.0(16)	F8-C27-C23	114.8(14)
F7-C27-C23	109.0(16)	F11-C28-F10	106.0(7)
F10-C28-F12	103.4(6)	F11-C28-C25	113.3(7)
F12-C28-C25	113.7(5)	O1-K1-C4	107.46(15)
O1-U1-N2#1	94.10(14)	C6-K1-C4	42.67(16)
N2#1-U1-N2	89.7(2)	F8#3-K1-C4	67.7(2)
N2#1-U1-N1#1	88.79(15)	C18-K1-C4	128.2(3)
O1-U1-N1	88.29(14)	C14-F6-K1#4	101.3(4)
N1#1-U1-N1	92.8(2)	C7-N1-C1	115.8(4)
N2#1-U1-K1	116.70(10)	C21-N2-C15	115.1(4)
N1-U1-K1	65.47(10)	C6-C1-C2	118.3(5)
N2#1-U1-K1#1	81.74(10)	C6-C1-K1	76.0(3)
N1-U1-K1#1	96.76(10)	C3-C2-C1	119.9(6)
O1-K1-F6#2	104.49(13)	C4-C3-C2	121.4(6)
F4#2-K1-C6	162.71(15)	C3-C4-C5	119.9(6)
F4#2-K1-C1	165.55(15)	C6-C5-C4	119.4(6)
O1-K1-C17	91.99(15)	C5-C6-C1	121.1(5)
C6-K1-C17	110.67(19)	C8-C7-C12	117.8(5)
F4#2-K1-F8#3	68.56(17)	C9-C8-C7	120.4(6)
C1-K1-F8#3	98.37(16)	C8-C9-C13	118.4(6)
F4#2-K1-C5	138.54(15)	C10-C11-C14	120.2(5)
C1-K1-C5	44.02(15)	F2-C13-F3	110.4(9)
O1-K1-C2	87.49(12)	F2-C13-C9	113.4(6)
C6-K1-C2	43.44(15)	F5-C14-F4	106.2(6)
F8#3-K1-C2	73.75(16)	F5-C14-C11	113.0(5)
F4#2-K1-C18	63.02(17)	C20-C15-C16	118.2(6)
C1-K1-C18	108.01(19)	C17-C16-C15	121.3(7)
C5-K1-C18	146.3(2)	C18-C17-C16	120.2(8)
F4#2-K1-C16	103.68(15)	C17-C18-C19	120.7(7)
C1-K1-C16	69.00(15)	C18-C19-C20	120.4(7)
C5-K1-C16	112.35(17)	N2-C21-C26	120.9(5)
O1-K1-C4	107.46(15)	C22-C23-C24	122.5(7)
C6-K1-C4	42.67(16)	C25-C24-C23	115.6(6)
F8#3-K1-C4	67.7(2)	C24-C25-C28	117.3(6)
C18-K1-C4	128.2(3)	F8-C27-F7	102.9(10)
C14-F6-K1#4	101.3(4)	F9-C27-C23	112.5(9)
C7-N1-C1	115.8(4)	F11-C28-F12	106.8(7)
C21-N2-C15	115.1(4)	F10-C28-C25	112.8(7)
C6-C1-C2	118.3(5)	C22-C23-C24	122.5(7)
C6-C1-K1	76.0(3)	C25-C24-C23	115.6(6)
C3-C2-C1	119.9(6)	C24-C25-C28	117.3(6)
C4-C3-C2	121.4(6)	F8-C27-F7	102.9(10)
C3-C4-C5	119.9(6)	F9-C27-C23	112.5(9)

C6-C5-C4	119.4(6)	F11-C28-F12	106.8(7)
C5-C6-C1	121.1(5)	F10-C28-C25	112.8(7)
C8-C7-C12	117.8(5)	C18-C17-C16	120.2(8)
C9-C8-C7	120.4(6)	C17-C18-C19	120.7(7)
C8-C9-C13	118.4(6)	C18-C19-C20	120.4(7)
C10-C11-C14	120.2(5)	N2-C21-C26	120.9(5)
F2-C13-F3	110.4(9)	F5-C14-C11	113.0(5)
F2-C13-C9	113.4(6)	C20-C15-C16	118.2(6)
F5-C14-F4	106.2(6)	C17-C16-C15	121.3(7)

Symmetry transformations used to generate equivalent atoms:

#1 -x,y,-z+1/2 #2 x,-y+1,z-1/2 #3 -x+1/2,y+1/2,-z+1/2

#4 x,-y+1,z+1/2 #5 -x+1/2,y-1/2,-z+1/2

Table 4.6.20 Bond lengths of **4.5-crown** (Å).

U1-O1	1.789(4)	U1-O2	1.792(4)	U1-N1	2.420(5)
U1-N4	2.434(5)	U1-N3	2.442(5)	U1-N2	2.453(5)
K2-O18	2.731(7)	K2-O16	2.761(6)	K2-O12	2.788(6)
K2-O17	2.792(7)	K2-O15	2.851(6)	K2-O14	2.860(7)
K2-O13	2.889(7)	K2-O11	2.895(6)	K2-C86	3.344(12)
K1-O10	2.733(6)	K1-O6	2.790(6)	K1-O4	2.812(6)
K1-O7	2.843(6)	K1-O5	2.844(6)	K1-O3	2.852(7)
K1-O9	2.869(6)	K1-O8	2.883(6)	K1-C70	3.459(9)
K1-C64	3.539(8)	F1-C13	1.311(12)	F2-C13	1.303(11)
F3-C13	1.287(11)	F4-C14	1.268(12)	F5-C14	1.296(12)
F6-C14	1.318(12)	F7-C27	1.343(10)	F8-C27	1.356(10)
F9-C27	1.305(10)	F10-C28	1.319(10)	F11-C28	1.311(11)
F12-C28	1.299(11)	F13-C41	1.275(10)	F14-C41	1.377(11)
F15-C41	1.261(10)	F16-C42	1.271(11)	F17-C42	1.291(11)
F18-C42	1.312(11)	F19-C55	1.356(10)	F20-C55	1.291(11)
F21-C55	1.330(10)	F22-C56	1.333(13)	F23-C56	1.311(15)
F24-C56	1.272(11)	O3-C57	1.402(13)	O3-C68	1.446(13)
O4-C58	1.355(14)	O4-C59	1.395(13)	O5-C60	1.409(12)
O5-C61	1.420(13)	O6-C62	1.402(11)	O6-C63	1.413(9)
O7-C64	1.403(10)	O7-C65	1.411(10)	O8-C67	1.379(11)
O8-C66	1.384(11)	O9-C69	1.415(11)	O9-C70	1.450(10)
O10-C71	1.419(10)	O10-C72	1.449(11)	O11-C84	1.410(11)
O11-C73	1.421(12)	O12-C74	1.419(12)	O12-C75	1.457(12)
O13-C77	1.387(13)	O13-C76	1.448(14)	O14-C79	1.345(14)
O14-C78	1.426(15)	O15-C80	1.421(14)	O15-C81	1.426(13)
O16-C82	1.436(12)	O16-C83	1.460(12)	O17-C86	1.352(13)
O17-C85	1.520(15)	O18-C88	1.403(12)	O18-C87	1.486(13)
N1-C7	1.367(8)	N1-C1	1.434(9)	N2-C21	1.371(8)
N2-C15	1.415(9)	N3-C35	1.364(8)	N3-C29	1.424(9)
N4-C49	1.370(8)	N4-C43	1.416(8)	C1-C6	1.356(10)
C1-C2	1.375(11)	C2-C3	1.377(13)	C3-C4	1.323(15)
C4-C5	1.387(15)	C5-C6	1.425(11)	C7-C8	1.410(9)
C7-C12	1.416(9)	C8-C9	1.381(10)	C9-C10	1.373(11)
C9-C13	1.504(12)	C10-C11	1.405(11)	C11-C12	1.394(11)
C11-C14	1.511(12)	C15-C20	1.405(10)	C15-C16	1.419(11)
C16-C17	1.387(11)	C17-C18	1.382(13)	C18-C19	1.395(13)
C19-C20	1.375(10)	C21-C26	1.384(9)	C21-C22	1.401(9)

C22-C23	1.396(10)	C23-C24	1.384(10)	C23-C27	1.484(11)
C24-C25	1.368(10)	C25-C26	1.415(10)	C25-C28	1.490(11)
C29-C34	1.385(11)	C29-C30	1.387(11)	C30-C31	1.385(11)
C31-C32	1.402(14)	C32-C33	1.358(15)	C33-C34	1.408(12)
C35-C36	1.409(9)	C35-C40	1.415(10)	C36-C37	1.377(10)
C37-C38	1.380(11)	C37-C41	1.489(11)	C38-C39	1.406(10)
C39-C40	1.365(10)	C39-C42	1.492(11)	C43-C44	1.380(10)
C43-C48	1.420(10)	C44-C45	1.404(12)	C45-C46	1.338(13)
C46-C47	1.392(13)	C47-C48	1.368(11)	C49-C54	1.397(9)
C49-C50	1.419(9)	C50-C51	1.373(10)	C51-C52	1.356(11)
C51-C55	1.494(11)	C52-C53	1.394(12)	C53-C54	1.407(10)
C53-C56	1.487(12)	C57-C58	1.545(18)	C59-C60	1.540(17)
C61-C62	1.476(14)	C63-C64	1.496(13)	C65-C66	1.541(14)
C67-C68	1.501(15)	C70-C71	1.503(12)	C73-C74	1.451(15)
C75-C76	1.403(16)	C77-C78	1.483(19)	C79-C80	1.503(19)
C81-C82	1.462(16)	C83-C84	1.464(14)	C86-C87	1.533(19)

Table 4.6.21 Bond angles of**4.5-crown** (°).

O1-U1-O2	178.94(19)	O1-U1-N1	91.84(18)
O1-U1-N4	89.24(19)	O2-U1-N4	91.76(18)
O1-U1-N3	90.97(18)	O2-U1-N3	88.66(18)
N4-U1-N3	90.07(19)	O1-U1-N2	88.01(19)
N1-U1-N2	88.60(19)	N4-U1-N2	175.55(18)
O18-K2-O16	112.8(2)	O18-K2-O12	104.2(3)
O18-K2-O17	59.7(2)	O16-K2-O17	73.1(2)
O18-K2-O15	101.0(3)	O16-K2-O15	59.6(2)
O17-K2-O15	116.0(2)	O18-K2-O14	79.4(2)
O12-K2-O14	116.1(2)	O17-K2-O14	137.7(2)
O18-K2-O13	88.1(2)	O16-K2-O13	158.21(19)
O17-K2-O13	125.7(3)	O15-K2-O13	112.1(2)
O18-K2-O11	130.0(2)	O16-K2-O11	58.6(2)
O17-K2-O11	71.6(2)	O15-K2-O11	110.4(2)
O13-K2-O11	113.2(2)	O18-K2-C86	45.6(3)
O12-K2-C86	75.9(4)	O17-K2-C86	23.3(3)
O14-K2-C86	123.8(3)	O13-K2-C86	103.1(3)
O10-K1-O6	96.11(19)	O10-K1-O4	119.4(2)
O10-K1-O7	80.17(18)	O6-K1-O7	59.92(17)
O10-K1-O5	129.82(19)	O6-K1-O5	59.46(19)
O7-K1-O5	113.74(18)	O10-K1-O3	103.9(2)
O4-K1-O3	58.6(2)	O7-K1-O3	113.8(2)
O10-K1-O9	59.70(17)	O6-K1-O9	77.61(18)
O7-K1-O9	117.27(18)	O5-K1-O9	71.87(18)
O10-K1-O8	76.76(18)	O6-K1-O8	118.82(18)
O7-K1-O8	58.99(18)	O5-K1-O8	152.72(19)
O9-K1-O8	135.41(18)	O10-K1-C70	43.07(19)
O4-K1-C70	104.4(2)	O7-K1-C70	94.02(19)
O3-K1-C70	133.6(2)	O9-K1-C70	24.28(18)
O10-K1-C64	74.2(2)	O6-K1-C64	41.9(2)
O7-K1-C64	22.13(19)	O5-K1-C64	100.7(2)
O9-K1-C64	96.8(2)	O8-K1-C64	79.0(2)
C57-O3-C68	114.2(10)	C57-O3-K1	108.4(7)
C58-O4-C59	108.7(10)	C58-O4-K1	121.7(7)

C60-O5-C61	108.8(9)	C60-O5-K1	111.7(6)
C62-O6-C63	113.2(7)	C62-O6-K1	117.8(6)
C64-O7-C65	112.7(7)	C64-O7-K1	108.1(5)
C67-O8-C66	110.9(8)	C67-O8-K1	117.1(6)
C69-O9-C70	116.1(7)	C69-O9-K1	124.1(7)
C71-O10-C72	111.8(7)	C71-O10-K1	121.4(5)
C84-O11-C73	111.2(8)	C84-O11-K2	108.7(6)
C74-O12-C75	114.2(8)	C74-O12-K2	117.5(6)
C77-O13-C76	113.6(10)	C77-O13-K2	110.4(7)
C79-O14-C78	110.9(11)	C79-O14-K2	117.3(8)
C80-O15-C81	113.2(10)	C80-O15-K2	112.8(6)
C82-O16-C83	113.7(8)	C82-O16-K2	119.3(7)
C86-O17-C85	116.1(11)	C86-O17-K2	101.9(8)
C88-O18-C87	114.3(8)	C88-O18-K2	127.0(7)
C7-N1-C1	114.8(5)	C7-N1-U1	128.2(4)
C21-N2-C15	115.8(5)	C21-N2-U1	124.4(4)
C35-N3-C29	115.9(5)	C35-N3-U1	122.9(4)
C49-N4-C43	115.6(5)	C49-N4-U1	129.6(4)
C6-C1-C2	120.0(7)	C6-C1-N1	120.9(7)
C1-C2-C3	118.4(9)	C4-C3-C2	124.1(10)
C4-C5-C6	119.3(9)	C1-C6-C5	119.8(8)
N1-C7-C12	121.8(6)	C8-C7-C12	116.3(6)
C10-C9-C8	124.6(8)	C10-C9-C13	116.2(7)
C9-C10-C11	115.2(7)	C12-C11-C10	122.4(7)
C10-C11-C14	120.0(8)	C11-C12-C7	121.0(7)
F3-C13-F1	108.0(11)	F2-C13-F1	101.3(9)
F2-C13-C9	113.3(9)	F1-C13-C9	111.9(9)
F4-C14-F6	109.1(9)	F5-C14-F6	103.1(10)
F5-C14-C11	113.8(8)	F6-C14-C11	111.6(10)
C20-C15-C16	115.9(7)	N2-C15-C16	120.6(7)
C18-C17-C16	120.6(9)	C17-C18-C19	120.3(8)
C19-C20-C15	123.7(8)	N2-C21-C26	120.6(6)
C26-C21-C22	117.2(6)	C23-C22-C21	120.8(7)
C24-C23-C27	121.2(7)	C22-C23-C27	117.4(7)
C24-C25-C26	120.6(7)	C24-C25-C28	120.5(7)
C21-C26-C25	121.5(6)	F9-C27-F7	105.7(7)
F7-C27-F8	102.4(8)	F9-C27-C23	115.1(8)
F8-C27-C23	112.9(7)	F12-C28-F11	103.7(9)
F11-C28-F10	104.5(8)	F12-C28-C25	113.7(8)
F10-C28-C25	113.3(8)	C34-C29-C30	118.1(7)
C30-C29-N3	121.2(7)	C31-C30-C29	122.8(9)
C33-C32-C31	120.6(8)	C32-C33-C34	120.7(9)
N3-C35-C36	122.4(7)	N3-C35-C40	122.1(6)
C37-C36-C35	122.3(7)	C36-C37-C38	121.8(7)
C38-C37-C41	118.9(7)	C37-C38-C39	116.6(7)
C40-C39-C42	118.5(7)	C38-C39-C42	119.2(7)
F15-C41-F13	110.9(9)	F15-C41-F14	102.3(8)
F15-C41-C37	114.1(8)	F13-C41-C37	115.5(7)
F16-C42-F17	109.7(9)	F16-C42-F18	102.7(9)
F16-C42-C39	115.1(9)	F17-C42-C39	113.9(8)
C44-C43-N4	121.3(7)	C44-C43-C48	118.1(7)
C43-C44-C45	119.9(8)	C46-C45-C44	121.4(9)
C48-C47-C46	120.3(9)	C47-C48-C43	120.5(8)
N4-C49-C50	122.9(6)	C54-C49-C50	115.0(6)

C52-C51-C50	122.4(7)	C52-C51-C55	118.1(7)
C51-C52-C53	118.1(7)	C52-C53-C54	120.2(7)
C54-C53-C56	118.0(8)	C49-C54-C53	122.3(7)
F20-C55-F19	104.0(8)	F21-C55-F19	104.3(8)
F21-C55-C51	112.0(8)	F19-C55-C51	112.5(7)
F24-C56-F22	110.5(10)	F23-C56-F22	101.7(9)
F23-C56-C53	111.3(10)	F22-C56-C53	110.9(10)
O4-C58-C57	105.9(9)	O4-C59-C60	109.8(9)
O5-C61-C62	108.4(9)	O6-C62-C61	110.2(8)
O7-C64-C63	108.2(7)	O7-C64-K1	49.8(4)
O7-C65-C66	106.5(7)	O8-C66-C65	108.1(8)
O3-C68-C67	107.6(9)	O9-C70-C71	111.2(7)
C71-C70-K1	86.1(5)	O10-C71-C70	108.5(7)
O12-C74-C73	111.3(9)	C76-C75-O12	109.7(9)
O13-C77-C78	106.9(11)	O14-C78-C77	107.2(10)
O15-C80-C79	109.3(10)	O15-C81-C82	109.2(8)
O16-C83-C84	108.9(8)	O11-C84-C83	110.6(8)
O17-C86-K2	54.8(6)	C87-C86-K2	89.5(7)
O2-U1-N1	88.57(18)	C30-C31-C32	117.9(10)
N1-U1-N4	87.99(19)	C29-C34-C33	119.9(10)
N1-U1-N3	176.57(18)	C36-C35-C40	115.4(6)
O2-U1-N2	91.02(18)	C36-C37-C41	119.2(7)
N3-U1-N2	93.47(19)	C40-C39-C38	122.3(7)
O16-K2-O12	118.0(2)	C39-C40-C35	121.6(7)
O12-K2-O17	86.1(2)	F13-C41-F14	102.9(8)
O12-K2-O15	152.74(19)	F14-C41-C37	109.7(8)
O16-K2-O14	118.3(2)	F17-C42-F18	101.0(9)
O15-K2-O14	58.7(2)	F18-C42-C39	113.0(8)
O12-K2-O13	59.0(2)	N4-C43-C48	120.6(6)
O14-K2-O13	57.4(2)	C45-C46-C47	119.9(8)
O12-K2-O11	59.37(19)	N4-C49-C54	122.0(6)
O14-K2-O11	150.49(19)	C51-C50-C49	122.1(7)
O16-K2-C86	96.4(3)	C50-C51-C55	119.4(7)
O15-K2-C86	130.4(4)	C52-C53-C56	121.8(8)
O11-K2-C86	84.7(3)	F20-C55-F21	108.2(8)
O6-K1-O4	119.0(2)	F20-C55-C51	115.1(8)
O4-K1-O7	159.59(19)	F24-C56-F23	104.7(11)
O4-K1-O5	59.7(2)	F24-C56-C53	116.5(8)
O6-K1-O3	157.8(2)	O3-C57-C58	109.5(11)
O5-K1-O3	111.9(2)	O5-C60-C59	105.4(10)
O4-K1-O9	80.3(2)	O6-C63-C64	109.1(7)
O3-K1-O9	120.9(2)	C63-C64-K1	82.6(4)
O4-K1-O8	116.8(2)	O8-C67-C68	109.7(8)
O3-K1-O8	58.3(2)	O9-C70-K1	54.4(4)
O6-K1-C70	68.33(19)	O11-C73-C74	109.4(8)
O5-K1-C70	86.9(2)	C75-C76-O13	109.8(10)
O8-K1-C70	118.7(2)	O14-C79-C80	109.4(11)
O4-K1-C64	160.2(2)	O16-C82-C81	110.3(9)
O3-K1-C64	135.7(2)	O17-C86-C87	109.2(13)
C70-K1-C64	75.1(2)	O18-C87-C86	106.5(8)
C68-O3-K1	115.4(6)	F4-C14-F5	104.2(11)
C59-O4-K1	116.4(6)	F4-C14-C11	114.2(9)
C61-O5-K1	111.5(5)	C20-C15-N2	123.5(7)
C63-O6-K1	117.3(5)	C17-C16-C15	121.0(9)

C65-O7-K1	111.6(5)	C20-C19-C18	118.5(8)
C66-O8-K1	116.0(6)	N2-C21-C22	122.2(6)
C70-O9-K1	101.3(5)	C24-C23-C22	121.4(7)
C72-O10-K1	120.7(6)	C25-C24-C23	118.5(6)
C73-O11-K2	111.4(6)	C26-C25-C28	118.8(7)
C75-O12-K2	118.7(6)	F9-C27-F8	107.1(8)
C76-O13-K2	106.5(6)	F7-C27-C23	112.6(7)
C78-O14-K2	118.1(7)	F12-C28-F10	106.9(8)
C81-O15-K2	107.8(6)	F11-C28-C25	113.8(7)
C83-O16-K2	121.5(6)	C34-C29-N3	120.8(7)
C85-O17-K2	124.8(8)	C3-C4-C5	118.0(9)
C87-O18-K2	117.7(6)	N1-C7-C8	121.9(6)
C1-N1-U1	116.0(4)	C9-C8-C7	120.4(7)
C15-N2-U1	119.1(4)	C8-C9-C13	119.2(7)
C29-N3-U1	120.9(4)	C12-C11-C14	117.6(8)
C43-N4-U1	114.7(4)	F3-C13-F2	105.7(10)
C2-C1-N1	119.1(7)	F3-C13-C9	115.6(8)

4.7 Coordinates of Optimized Geometries.

Table 4.7.1 Optimized geometry of anion of **4.5-crown**

U	-0.00002097	0.38614611	-0.00007017	F	-6.22552818	5.40882152	-0.47646329
F	-4.46809042	6.17863017	0.55293035	F	-4.36444395	5.69560337	-1.55973919
F	-7.01844446	0.68408933	-0.58172230	F	-5.68465363	-0.60972829	0.55307872
F	-5.33625391	-0.27971941	-1.56323172	F	-5.47682540	-4.50435283	2.81668640
F	-3.57173248	-5.46119409	3.21632490	F	-4.85926083	-6.21365001	1.63015197
F	-5.14833566	-3.76508280	-2.64666569	F	-3.06909622	-4.19352420	-3.10281308
F	-3.76407774	-2.13552183	-3.05616153	O	1.20554059	0.40712232	1.31277642
N	-1.38373937	2.11911599	1.13361149	N	-1.23814201	-1.37550515	1.24369764
C	-0.86780304	3.00856700	2.09892297	C	-1.62863174	3.40662158	3.22350249
H	-2.64405419	3.03432560	3.33034499	C	-1.09819159	4.25686516	4.19149118
H	-1.71209649	4.53751592	5.04619313	C	0.20899032	4.73978375	4.07980847
H	0.62074973	5.40362384	4.83671057	C	0.97540073	4.35366204	2.97727777
H	1.99102534	4.72370064	2.85294178	C	0.44637831	3.50836709	2.00374216
H	1.04656396	3.23283419	1.14641117	C	-2.69207726	2.35537418	0.71974380
C	-3.18889942	3.66365400	0.49244383	H	-2.54995594	4.51240922	0.71032457
C	-4.46040534	3.87546765	-0.03516881	C	-5.30887190	2.80675552	-0.33871338
H	-6.29848834	2.97624414	-0.74201170	C	-4.84469719	1.51407185	-0.08906106
C	-3.57283280	1.28621087	0.43385311	H	-3.24290359	0.27487506	0.63711533
C	-4.87782655	5.27569549	-0.37086107	C	-5.71345786	0.33091510	-0.41710406
C	-0.84985058	-1.45712086	2.61538124	C	-1.32363748	-0.51802795	3.54524642
H	-2.00291791	0.25520219	3.20225592	C	-0.90207409	-0.55312667	4.87574340
H	-1.26873528	0.19898020	5.57102922	C	-0.00542179	-1.53166847	5.30764876
H	0.33276561	-1.55025473	6.34151198	C	0.46831464	-2.47682128	4.39329134
H	1.19040309	-3.22840655	4.70064599	C	0.04623144	-2.44415063	3.06478774
H	0.42876981	-3.17028174	2.35395329	C	-2.17285770	-2.29943468	0.82729677
C	-2.79248128	-3.24034919	1.69787517	H	-2.52202143	-3.25225952	2.74582656
C	-3.73516659	-4.15569913	1.23285066	C	-4.12655230	-4.19233009	-0.10537724
H	-4.85802438	-4.90675250	-0.46010166	C	-3.53924694	-3.26281450	-0.97083794
C	-2.59471787	-2.34331070	-0.53199009	H	-2.17744883	-1.63152708	-1.23241971
C	-4.39904153	-5.07559020	2.21465513	C	-3.88093243	-3.32113223	-2.43191870
F	6.22440421	5.40975139	0.47684750	F	4.46689443	6.17927666	-0.55263643
F	4.36314768	5.69604734	1.55997639	F	7.01827444	0.68514788	0.58170727

F	5.68479995	-0.60884623	-0.55326429	F	5.33619972	-0.27904618	1.56304285
F	5.47752921	-4.50409909	-2.81610289	F	3.57247710	-5.46103893	-3.21571565
F	4.85991184	-6.21320608	-1.62933091	F	5.14943605	-3.76298069	2.64674912
F	3.07051078	-4.19255403	3.10319626	F	3.76430974	-2.13415772	3.05622841
O	-1.20559272	0.40682930	-1.31290704	N	1.38342435	2.11918677	-1.13395099
N	1.23825986	-1.37540502	-1.24369955	C	0.86738364	3.00843306	-2.09940347
C	1.62811555	3.40631208	-3.22410696	H	2.64357069	3.03409610	-3.33092710
C	1.09753808	4.25629129	-4.19225521	H	1.71136907	4.53681540	-5.04705221
C	-0.20968664	4.73909713	-4.08061386	H	-0.62154903	5.40272874	-4.83764235
C	-0.97601316	4.35312908	-2.97797013	H	-1.99167250	4.72308331	-2.85367054
C	-0.44685143	3.50809702	-2.00428352	H	-1.04694793	3.23265412	-1.14686513
C	2.69167847	2.35569303	-0.71998434	C	3.18823492	3.66405347	-0.49251547
H	2.54913549	4.51270041	-0.71035529	C	4.45963832	3.87607087	0.03525557
C	5.30829515	2.80750442	0.33878719	H	6.29784348	2.97715361	0.74218314
C	4.84439913	1.51475423	0.08896117	C	3.57262927	1.28668511	-0.43409031
H	3.24296699	0.27529372	-0.63751198	C	4.87673952	5.27635419	0.37111384
C	5.71336467	0.33173980	0.41697980	C	0.85007439	-1.45717554	-2.61542309
C	1.32395662	-0.51820459	-3.54535016	H	2.00322581	0.25505832	-3.20240222
C	0.90249151	-0.55345303	-4.87587767	H	1.26922851	0.19855579	-5.57122988
C	0.00583564	-1.53201363	-5.30773248	H	-0.33226100	-1.55071006	-6.34162337
C	-0.46800463	-2.47703951	-4.39329819	H	-1.19008570	-3.22864961	-4.70060944
C	-0.04601803	-2.44421652	-3.06476604	H	-0.42861603	-3.17025511	-2.35387654
C	2.17320168	-2.29909454	-0.82720773	C	2.79290596	-3.24010851	-1.69761742
H	2.52239541	-3.25230102	-2.74554858	C	3.73575590	-4.15521454	-1.23244207
C	4.12724596	-4.19147578	0.10576403	H	4.85884266	-4.90572211	0.46059589
C	3.53987755	-3.26184158	0.97105475	C	2.59517849	-2.34258633	0.53205585
H	2.17784541	-1.63072172	1.23236434	C	4.39970530	-5.07525299	-2.21405968
C	3.88176009	-3.31977238	2.43210754	C	-0.46800463	-2.47703951	-4.39329819
H	-1.19008570	-3.22864961	-4.70060944	C	-0.04601803	-2.44421652	-3.06476604
H	-0.42861603	-3.17025511	-2.35387654	C	2.17320168	-2.29909454	-0.82720773
C	2.79290596	-3.24010851	-1.69761742	H	2.52239541	-3.25230102	-2.74554858
C	3.73575590	-4.15521454	-1.23244207	C	4.12724596	-4.19147578	0.10576403
H	4.85884266	-4.90572211	0.46059589	C	3.53987755	-3.26184158	0.97105475
C	2.59517849	-2.34258633	0.53205585	H	2.17784541	-1.63072172	1.23236434
C	4.39970530	-5.07525299	-2.21405968	C	3.88176009	-3.31977238	2.43210754

Table 4.7.2. Optimized coordinates of **4.5-tol**.

U	0.00662906	0.16751801	-0.03412401	N	-0.68434896	1.79452615	-1.69394014
N	-0.36919901	-1.64191412	-1.64461014	N	0.47306806	-1.46774712	1.74163912
N	0.60721314	1.94973814	1.55255811	O	1.72169619	0.18870998	-0.60020106
O	-1.69765407	0.17104505	0.56728203	C	0.18650412	2.67540720	-2.37691419
C	1.31344622	3.22690822	-1.73790615	H	1.47697323	3.01159420	-0.69025906
C	2.19070530	4.07228527	-2.41800820	H	3.02439337	4.51174428	-1.87526816
C	1.97392129	4.39150529	-3.76119630	H	2.64512036	5.06713933	-4.28486834
C	0.86118520	3.84975228	-4.41239135	H	0.67127919	4.08903030	-5.45622543
C	-0.01874589	3.00682123	-3.73601230	H	-0.88095596	2.59886622	-4.25623234
C	-2.05398607	1.99361519	-1.92937316	C	-2.92702915	0.90274413	-2.10915317
H	-2.51428714	-0.09628496	-2.17236418	C	-4.30704825	1.09453817	-2.20196518
C	-4.86458327	2.37010028	-2.14925417	H	-5.93389236	2.51521432	-2.23513318
C	-4.00596319	3.46147835	-1.98373916	C	-2.62889808	3.28649230	-1.89204115
H	-1.98381802	4.14758036	-1.75632614	C	-5.20879235	-0.10698790	-2.26103218
C	-4.60641720	4.81925447	-1.75501214	C	0.58652606	-1.78329515	-2.68384821
C	0.85237210	-0.71874507	-3.56714729	H	0.26320908	0.18662801	-3.48249328
C	1.85779618	-0.81690310	-4.53356036	H	2.02951521	0.02060896	-5.20587141

C	2.62130621	-1.98456721	-4.65123337	H	3.39214227	-2.06706923	-5.41312543
C	2.35457617	-3.05874728	-3.79219630	H	2.93530319	-3.97428637	-3.86384131
C	1.34980609	-2.96219526	-2.82836423	H	1.15764006	-3.79983532	-2.16540218
C	-1.44897511	-2.52345916	-1.66678814	C	-2.26464818	-2.68024816	-0.52397205
H	-1.99726014	-2.16217312	0.38469902	C	-3.42522428	-3.44797419	-0.55400505
C	-3.80716333	-4.14828424	-1.69842014	H	-4.71215440	-4.74111126	-1.72098214
C	-2.98936326	-4.03750524	-2.82490723	C	-1.84460916	-3.24406621	-2.82201123
H	-1.26688811	-3.15494421	-3.73384729	C	-4.25003535	-3.52862918	0.69742204
C	-3.32951530	-4.82351830	-4.06373032	C	-0.40759001	-1.44809610	2.86243821
C	-0.39219399	-0.39486202	3.79670828	H	0.32477608	0.40687302	3.66741227
C	-1.28465605	-0.37416400	4.87484736	H	-1.24021503	0.44528606	5.58837343
C	-2.21851015	-1.40378506	5.04223238	H	-2.90352520	-1.39350305	5.88595943
C	-2.24207217	-2.45930714	4.12163730	H	-2.96034224	-3.26743519	4.22862231
C	-1.34115210	-2.48590716	3.05487722	H	-1.36200312	-3.31091523	2.35109117
C	1.57136912	-2.30927421	1.87918013	C	2.06378615	-2.72743625	3.14391323
H	1.55181212	-2.41627922	4.04590430	C	3.20345822	-3.51509234	3.25649524
C	3.90994027	-3.94162738	2.13025415	H	4.79371232	-4.55824745	2.22648916
C	3.42651124	-3.55871634	0.87949405	C	2.28010017	-2.77257426	0.74540904
H	1.89675214	-2.52982623	-0.23835803	C	3.74222526	-3.84038437	4.62463934
C	4.12821328	-4.03402639	-0.35889904	C	-0.32712192	2.78007122	2.19835416
C	-1.52926900	3.15346727	1.55746711	H	-1.67461202	2.88106526	0.52035303
C	-2.50816806	3.89913435	2.21817716	H	-3.39667112	4.20134439	1.66731212
C	-2.31995603	4.30614038	3.54350626	H	-3.07057308	4.90451144	4.05233930
C	-1.12390695	3.96907632	4.18569331	H	-0.94812293	4.29125935	5.20952339
C	-0.14523389	3.22332925	3.53069226	H	0.77486717	2.97282821	4.05153130
C	1.96378325	2.23079713	1.75834312	C	2.48206631	3.54543022	1.66805511
H	1.79747328	4.37736229	1.54410311	C	3.85449143	3.77598721	1.66915211
C	4.76962747	2.72403911	1.79082012	H	5.83594858	2.91259610	1.78948613
C	4.26667341	1.43146702	1.92003813	C	2.89284130	1.18585403	1.93025513
H	2.52665425	0.17322496	2.04009114	C	4.38335849	5.15212030	1.37663909
C	5.19566645	0.25307791	1.96297814	F	-4.70404233	-1.10173499	-3.01249124
F	-5.40618040	-0.62482294	-1.00964209	F	-6.43688644	0.19224215	-2.73990922
F	-5.73117630	5.01318050	-2.47561220	F	-3.75788711	5.82495254	-2.03720317
F	-4.96640022	4.96968848	-0.44161705	F	-3.67590132	-4.30946025	1.64922711
F	-4.41062933	-2.29913208	1.28369509	F	-5.48661047	-4.01561419	0.48473703
F	-4.65779541	-5.05023129	-4.17188233	F	-2.93370626	-4.19348626	-5.19216641
F	-2.72600328	-6.03686940	-4.06380332	F	2.76731818	-3.89652536	5.55867240
F	4.63053534	-2.90659432	5.04054337	F	4.38849028	-5.02817247	4.64267034
F	5.25863635	-4.71225747	-0.10381702	F	3.35043320	-4.82090044	-1.13458710
F	4.49796634	-2.97689832	-1.17052310	F	3.50643445	6.12681641	1.68118412
F	5.53276256	5.40958629	2.03700614	F	4.67108552	5.28328431	0.04667399
F	4.90943841	-0.60936915	2.95093122	F	5.11331543	-0.47218814	0.79282005
F	6.49235057	0.61081291	2.08306115	K	3.86977934	-0.44475011	-1.89108216
C	5.86769551	1.10495596	-4.21070833	C	5.43272451	2.14244005	-3.36842227
H	4.75294947	2.89724512	-3.75580730	C	5.85440353	2.21748305	-2.03618117
H	5.50896054	3.03340912	-1.40660312	C	6.71679560	1.24421096	-1.51738513
H	7.03711463	1.28907595	-0.48150805	C	7.14562560	0.19658687	-2.34003119
H	7.81307962	-0.56547620	-1.94593016	C	6.72281054	0.12903587	-3.67230629
H	7.07441760	-0.68243920	-4.30590534	C	5.45620448	1.06558997	-5.66482742
H	6.13019055	1.67968500	-6.27624548	H	4.44359342	1.45773902	-5.80717044
H	5.48976749	0.04755689	-6.06680348	K	-3.36044820	0.47465711	2.53464618
C	-6.64756842	1.34629024	2.10773015	C	-6.33575041	2.06203029	3.27775524
H	-6.33264138	3.14941137	3.25264823	C	-6.04744739	1.39681423	4.47272133
H	-5.82396737	1.97025827	5.36872941	C	-6.05940140	-0.00259087	4.51982634

H	-5.85453043	-0.51969692	5.45317139	C	-6.34714645	-0.72743392	3.36112625
H	-6.34473345	-1.81338900	3.37768925	C	-6.63309246	-0.05760887	2.16599615
H	-6.84063948	-0.63036890	1.26678309	C	-7.02250246	2.06502730	0.83254005
H	-6.40699539	2.95503836	0.66269504	H	-8.06865254	2.39608735	0.87119106
H	-6.91540847	1.40602825	-0.03264701				

4.8 References.

(1) Bart, S.; Meyer, K., Highlights in Uranium Coordination Chemistry Organometallic and Coordination Chemistry of the Actinides. In Albrecht-Schmitt, T., Ed. Springer Berlin / Heidelberg: 2008; Vol. 127, pp 119.
(2) Lam, O. P.; Anthon, C.; Meyer, K., *Dalton Trans.* **2009**, 9677.
(3) Roussel, P.; Hitchcock, P. B.; Tinker, N. D.; Scott, P., *Inorg. Chem.* **1997,** *36*, 5716.
(4) Roussel, P.; Boaretto, R.; Kingsley, A. J.; Alcock, N. W.; Scott, P., *J. Chem. Soc., Dalton Trans.* **2002**, 1423.
(5) Patel, D.; Lewis, W.; Blake, A. J.; Liddle, S. T., *Dalton Transactions* **2010,** *39*, 6638.
(6) Gardner, B. M.; Lewis, W.; Blake, A. J.; Liddle, S. T., *Inorg. Chem.* **2011,** *50*, 9631.
(7) Reynolds, J. G.; Zalkin, A.; Templeton, D. H.; Edelstein, N. M.; Templeton, L. K., *Inorganic Chemistry* **1976,** *15*, 2498.
(8) Reynolds, J. G.; Zalkin, A.; Templeton, D. H.; Edelstein, N. M., *Inorganic Chemistry* **1977,** *16*, 1858.
(9) Van der Sluys, W. G.; Burns, C. J.; Sattelberger, A. P., *Organometallics* **1989,** *8*.
(10) Stewart, J. L.; Andersen, R. A., *Polyhedron* **1998,** *17*.
(11) Mansell, S. M.; Perandones, B. F.; Arnold, P. L., *J. Organomet. Chem.* **2010,** *695*, 2814.
(12) Kraft, S. J.; Fanwick, P. E.; Bart, S. C., *J. Am. Chem. Soc.* **2012,** *134*, 6160.
(13) Odom, A. L.; Arnold, P. L.; Cummins, C. C., *J. Am. Chem. Soc.* **1998,** *120*.
(14) Jiang, L.; Buckwald, S. L., Palladium-catalyzed aromatic carbon-nitrogen bond formation. In *Metal-Catalyzed Cross-Coupling Reactions*, 2nd ed.; Wiley: 2004; pp 699.
(15) Brennan, J. G.; Andersen, R. A.; Zalkin, A., *Inorg. Chem.* **1986,** *25*.
(16) Stewart, J. L. *Tris[bis(trimethylsilyl)amido]uranium: compounds with tri-, tetra-, and pentavalent uranium*; Lawrence Berkeley Lab.: 1988; p 200 pp.
(17) Avens, L. R.; Barnhart, D. M.; Burns, C. J.; McKee, S. D.; Smith, W. H., *Inorg. Chem.* **1994,** *33*, 4245.
(18) Arliguie, T. r. s.; lug, M.; Le Floch, P.; M z ailles, N.; Thu ry , P.; Ephritikhine, M., *Organometallics* **2008,** *27*, 4158.
(19) Lam, O. P.; Franke, S. M.; Heinemann, F. W.; Meyer, K., *J. Am. Chem. Soc.* **2012,** *134*, 16877.
(20) Brown, J. L.; Wu, G.; Hayton, T. W., *Organometallics* **2012,** *32*, 1193.
(21) Franke, S. M.; Heinemann, F. W.; Meyer, K., *Chem. Sci.* **2013**.
(22) Denning, R. G., *J. Phys. Chem. A* **2007,** *111*, 4125.
(23) Fortier, S.; Hayton, T. W., *Coord. Chem. Rev.* **2010,** *254*, 197.
(24) Kannan, S.; Moody, M. A.; Barnes, C. L.; Duval, P. B., *Inorg. Chem.* **2006,** *45*, 9206.
(25) O'Grady, E.; Kaltsoyannis, N., *J. Chem. Soc., Dalton Trans.* **2002**, 1233.
(26) Kosog, B.; La Pierre, H. S.; Heinemann, F. W.; Liddle, S. T.; Meyer, K., *J. Am. Chem. Soc.* **2012,** *134*, 5284.

(27) La Pierre, H. S.; Meyer, K., *Inorg. Chem.* **2013,** *52*, 529.
(28) Lewis, A. J.; Carroll, P. J.; Schelter, E. J., *J. Am. Chem. Soc.* **2013,** *135*, 511.
(29) Lewis, A. J.; Carroll, P. J.; Schelter, E. J., *J. Am. Chem. Soc.* **2013,** *135*, 13185.
(30) Sarsfield, M. J.; Helliwell, M., *J. Am. Chem. Soc.* **2004,** *126*, 1036.
(31) Arnold, P. L.; Patel, D.; Wilson, C.; Love, J. B., *Nature* **2008,** *451*, 315.
(32) Schnaars, D. D.; Wu, G.; Hayton, T. W., *J. Am. Chem. Soc.* **2009,** *131*, 17532.
(33) Arnold, P. L.; Jones, G. M.; Odoh, S. O.; Schreckenbach, G.; Magnani, N.; Love, J. B., *Nat. Chem.* **2012,** *4*, 221.
(34) Brown, J. L.; Wu, G.; Hayton, T. W., *J. Am. Chem. Soc.* **2010,** *132*, 7248.
(35) Schnaars, D. D.; Wu, G.; Hayton, T. W., *Inorg. Chem.* **2011,** *50*, 4695.
(36) Schnaars, D. D.; Wu, G.; Hayton, T. W., *Inorg. Chem.* **2011,** *50*, 9642.
(37) Brown, J. L.; Mokhtarzadeh, C. C.; Lever, J. M.; Wu, G.; Hayton, T. W., *Inorg. Chem.* **2011,** *50*, 5105.
(38) Arnold, P. L.; Patel, D.; Blake, A. J.; Wilson, C.; Love, J. B., *J. Am. Chem. Soc.* **2006,** *128*, 9610.
(39) Arnold, P. L.; Pécharman, A.-F.; Hollis, E.; Yahia, A.; Maron, L.; Parsons, S.; Love, J. B., *Nat. Chem.* **2010,** *2*, 1056.
(40) Arnold, P. L.; Pécharman, A.-F.; Love, J. B., *Angew. Chem. Int. Ed.* **2011,** *50*, 9456.
(41) Arnold, P. L.; Hollis, E.; White, F. J.; Magnani, N.; Caciuffo, R.; Love, J. B., *Angew. Chem. Int. Ed.* **2011,** *50*, 887.
(42) Jones, G. M.; Arnold, P. L.; Love, J. B., *Angew. Chem. Int. Ed.* **2012,** *51*, 12584.
(43) Arnold, P. L.; Jones, G. M.; Pan, Q.-J.; Schreckenbach, G.; Love, J. B., *Dalton Trans.* **2012,** *41*, 6595.
(44) Arnold, P. L.; Hollis, E.; Nichol, G. S.; Love, J. B.; Griveau, J.-C.; Caciuffo, R.; Magnani, N.; Maron, L.; Castro, L.; Yahia, A.; Odoh, S. O.; Schreckenbach, G., *J. Am. Chem. Soc.* **2013,** *135*, 3841.
(45) Jones, G. M.; Arnold, P. L.; Love, J. B., *Chem. - Eur. J.* **2013,** *19*, 10287.
(46) Franczyk, T. S.; Czerwinski, K. R.; Raymond, K. N., *J. Am. Chem. Soc.* **1992,** *114*, 8138.
(47) Burns, C. J.; Clark, D. L.; Donohoe, R. J.; Duval, P. B.; Scott, B. L.; Tait, C. D., *Inorg. Chem.* **2000,** *39*, 5464.
(48) Danis, J. A.; Lin, M. R.; Scott, B. L.; Eichhorn, B. W.; Runde, W. H., *Inorg. Chem.* **2001,** *40*, 3389.
(49) Thuery, P.; Masci, B., *Dalton Trans.* **2003**, 2411.
(50) Sarsfield, M. J.; Helliwell, M.; Raftery, J., *Inorg. Chem.* **2004,** *43*, 3170.
(51) Masci, B.; Thuery, P., *CrystEngComm* **2007,** *9*, 582.
(52) Thuéry, P.; Masci, B.; Takimoto, M.; Yamato, T., *Inorg. Chem. Commun.* **2007,** *10*, 795.
(53) Seaman, L. A.; Schnaars, D. D.; Wu, G.; Hayton, T. W., *Dalton Trans.* **2010,** *39*, 6635.
(54) Seaman, L. A.; Hrobarik, P.; Schettini, M. F.; Fortier, S.; Kaupp, M.; Hayton, T. W., *Angew. Chem. Int. Ed.* **2013,** *52*, 3259.
(55) Lewis, A. J.; Williams, U. J.; Kikkawa, J. M.; Carroll, P. J.; Schelter, E. J., *Inorg. Chem.* **2012,** *51*, 37.
(56) Robinson, J. R.; Carroll, P. J.; Walsh, P. J.; Schelter, E. J., *Angew. Chem., Int. Ed. Engl.* **2012,** *51*, 10159.
(57) Levin, J. R.; Gu, J.; Carroll, P. J.; Schelter, E. J., *Dalton Trans.* **2012,** *41*, 7870.

(58) Yin, H.; Lewis, A. J.; Williams, U. J.; Carroll, P. J.; Schelter, E. J., *Chem. Sci.* **2013,** *4*, 798.
(59) Yin, H.; Lewis, A. J.; Carroll, P.; Schelter, E. J., *Inorg. Chem.* **2013,** *52*, 8234.
(60) Direct crystallization of this product from hexanes was attempted several times, which produced complexes of variable K-THF solvation in which the potassium ions were bound directly to the uranyl oxo ligands. The variable solvation of this product prevented adequate structural refinement or full characterization.
(61) Berthet, J.-C.; Siffredi, G.; Thuery, P.; Ephritikhine, M., *Chem. Commun.* **2006,** *0*, 3184.
(62) Natrajan, L.; Burdet, F.; Pécaut, J.; Mazzanti, M., *J. Am. Chem. Soc.* **2006,** *128*, 7152.
(63) Berthet, J.-C.; Siffredi, G.; Thuery, P.; Ephritikhine, M., *Dalton Trans.* **2009,** *0*, 3478.
(64) Beer, S.; Berryman, O. B.; Ajami, D.; Rebek Jr, J., *Chem. Sci.* **2010,** *1*, 43.
(65) Allen, F., *Acta Crystallogr., Sect. B: Struct. Sci* **2002,** *58*, 380.
(66) Lewis, A. J.; Williams, U. J.; Carroll, P. J.; Schelter, E. J., *Inorg. Chem.* **2013,** *52*, 7326.
(67) Marini, A.; Mu oz-Losa, A.; Biancardi, A.; Mennucci, B., *J. Phys. Chem. B* **2010,** *114*, 17128.
(68) Miller, C. G.; Gordon-Wylie, S. W.; Horwitz, C. P.; Strazisar, S. A.; Peraino, D. K.; Clark, G. R.; Weintraub, S. T.; Collins, T. J., *J. Am. Chem. Soc.* **1998,** *120*, 11540.
(69) Lam, W. W. Y.; Yiu, S.-M.; Lee, J. M. N.; Yau, S. K. Y.; Kwong, H.-K.; Lau, T.-C.; Liu, D.; Lin, Z., *J. Am. Chem. Soc.* **2006,** *128*, 2851.
(70) Fukuzumi, S.; Morimoto, Y.; Kotani, H.; Naumov, P.; Lee, Y.-M.; Nam, W., *Nat. Chem.* **2010,** *2*, 756.
(71) Park, Y. J.; Ziller, J. W.; Borovik, A. S., *J. Am. Chem. Soc.* **2011,** *133*, 9258.
(72) Tsui, E. Y.; Tran, R.; Yano, J.; Agapie, T., *Nat. Chem.* **2013,** *5*, 293.

Chapter 5

Incorporating Non-Covalent Interactions in a Directed Binding Pocket at Low Valent Uranium

5.1 Introduction. The incorporation of non-covalent interactions into the secondary coordination sphere of metal complexes is a proven strategy for stabilizing reactive fragments and effecting new chemistry.[1, 2] As the metal-ligand bonding in many f-block complexes is largely ionic and non-directional,[3] we postulated that non-covalent interactions between ligands could promote directed coordination chemistry at f-block ions by providing *collective secondary structures*.[4] Such collective secondary structures could contribute to several research themes including: the stabilization of U^{III} and U^{V} complexes that are prone to disproportionation,[5, 6] the isolation of complexes of reactive small molecule fragments at f-block ions,[7] and the mitigation of kinetic factors, such as large inner sphere electron transfer reorganization energy, which are understood to impede the oxidation of Ce^{III} compounds.[8]

As a first step to probe these ideas we set out to prepare complexes showing attractive non-covalent interactions between ligands in the coordination sphere of a uranium ion that could be detected in the solid state using X-ray crystallography and in solution using NMR spectroscopy. We reasoned that a well-defined molecular pocket at a metal ion picketed by electron deficient arene groups could bind aryl-based ligands cooperatively through dative and arene-arene interactions. The *C*$_3$-symmetric Ar$_3$TPA^{3-} and other tris(pyrrolyl) ligands have been used recently in transition metal chemistry for small molecule activation,[9-12] and magnetism studies.[13, 14] In this work we focused on the synthesis of uranium complexes of the Ar$^F_3$TPA^{3-}

Portions of this chapter have been adapted from a previous publication. Sections 5.3 and 5.7 are adapted with permission from "Uranium Pyrrolylamine Complexes Featuring a Trigonal Binding Pocket and Interligand Noncovalent Interactions" Lewis, A. J.; Williams, U. J.; Kikkawa, J. M.; Carroll, P. J.; Schelter, E. J. *Inorg. Chem.* **2012**, *51*, 37-39.

ligand (Ar^F = 3,5-bis(trifluoromethyl)phenyl, TPA = tris(pyrrolyl-α-methylamine)). In contrast to related transition metal complexes of the $Ar^F{}_3TPA^{3-}$ ligand, the uranium complexes form trigonal frameworks with three open coordination sites. Importantly, the three coordination sites reside in a trigonal binding pocket lined with electron deficient arene groups at a reactive metal center. The uranium complexes show evidence for arene-arene interactions[15] between the $Ar^F{}_3TPA^{3-}$ ligand and pyridyl ligands bound in the trigonal pocket in the solid state and in solution.

5.2 The Ar_3TPA^{3-} Ligand: Its Synthesis and Utility. The Ar_3TPA^{3-} ligand belongs to a class of chelates involving four nitrogen donors, inspired from the tris(aminoethyl)amine (TREN) framework. Derivatives of the TREN ligand have provided substantial advances in transition metal chemistry, directing reactivity to a single coordination site at a 3-fold symmetric sterically protected pocket with a proclivity for axial π-bonding.[16] TREN complexes of uranium have now been explored in great detail,[17-32] including the recent landmark synthesis of a terminal uranium-nitride,[33-35] discussed earlier. In contrast to transition metal complexes, the arrangement of the amide tethers of the TREN ligand is of the requisite symmetry for π-donation into the empty $5f_{x(x2-3y2)}$ orbital of high valent uranium. However, incorporation of the nitrogen atoms into pyrrolyl groups eliminates the ability for the ligand to act as a π-donor, due to favorable conjugation of the lone pair into the aromatic ring. The pyrrolyl group additionally has the ability to access variable hapticity akin to the cyclopentadienyl ligand, shifting from κ^1- to η^5-coordination to better suit the electronic demand of the metal center. [36-38] Variable hapticity has also been observed in uranium complexes bearing substituted pyrrolyl ligands.[39, 40]

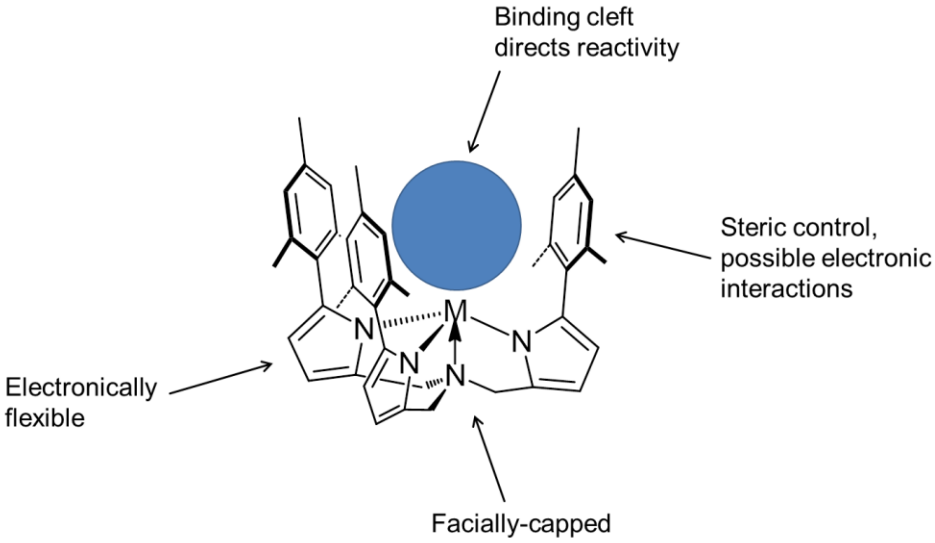

Figure 5.2.1 Design aspects of the Mes_3TPA^{3-} ligand.

The synthesis of the unfunctionalized H_3TPA ligand was originally reported by Odom and coworkers, through the one-pot triple Mannich condensation reaction between NH_4Cl, formaldehyde, and pyrrole.[41] Convenient access to functionalized derivatives was made possible from methodology developed by Sadighi and coworkers, involving palladium catalyzed cross-coupling of deprotonated pyrrole and an aryl halide.[42] The resulting 2-arylpyrroles allowed for the synthesis of the corresponding H_3Ar_3TPA ligands following the procedure for the preparation of H_3TPA.[9, 10] The $Ar^F{}_3TPA^{3-}$ ligand was investigated in complexes of Zr, Hf, and Mo, but in no case was the anticipated 5-coordianate complex formed.[43] The Mes_3TPA^{3-} and Ph_3TPA^{3-} ligands were shown to be capable of stabilizing reactive Fe(IV)-oxo complexes active in C-H bond activation reactions,[44, 45] and enabled the synthesis of the first example of a N_2O complex of vanadium.[46]

5.3 Uranium Complexes of the $Ar^F{}_3TPA^{3-}$ Ligand.

5.3.1 Synthesis and Characterization of U($Ar^F{}_3TPA$) Complexes. Green-black $U^{III}(Ar^FTPA)(py)_3$ (**5.1**) was produced from slow addition of a dilute THF solution of $K_3Ar^F{}_3TPA(THF)_{1.5}$ to a stirred solution of UI_3 in a mixture of 20 mL THF and 0.5 mL pyridine at –25 °C (Scheme 5.3.1.1). The product was obtained in 55 % yield following crystallization. The moderate yield of the complex is due to its high solubility in organic solvents. Attempts to synthesize a THF analog of **5.1** failed, generating only mixtures of intractable products in the

absence of pyridine. The X-ray structure of **5.1** (Figure 5.3.1.1) displays a seven-coordinate, C_3-symmetric geometry at the U^{III} ion where the $Ar^F{}_3TPA^{3-}$ ligand binds in a tetradentate fashion and three pyridine molecules complete the coordination sphere of the ion. The U^{III} ion in **5.1** is displaced ~0.86 Å above the plane of the pyrrolyl–nitrogen atoms, in contrast to the ~0.4–0.7 Å displacements observed in related transition metal TPA complexes.[9-11, 13, 14, 41]

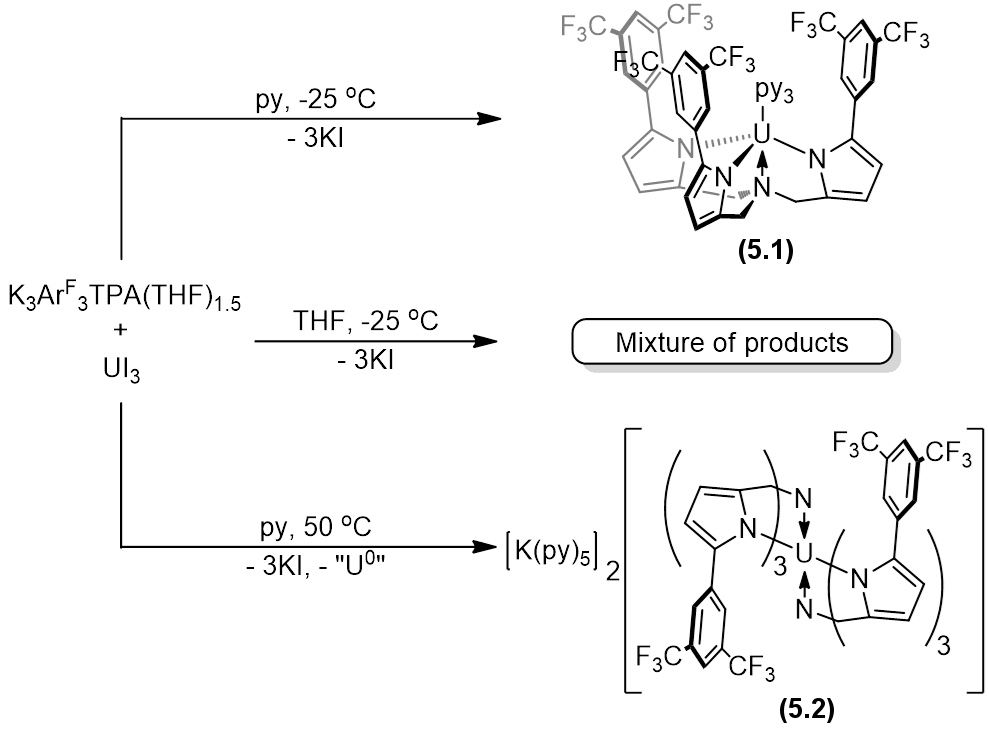

Scheme 5.3.1.1 Synthesis of complexes **5.1** and **5.2**.

The U–$N_{(pyrrolyl)}$ bond lengths in **5.1** are long at an average distance of 2.602(6) Å. Reported U^{III}–$N_{(pyrrolyl)}$ bonds in calix[4]pyrrole complexes are ~2.52 Å.[47, 48] The long U–$N_{(pyrrolyl)}$ distances are presumably the result of a poor fit of the U^{III} ion with three bound pyridines into the pocket of the Ar^FTPA^{3-} ligand. Notably, each pyridine within the uranium coordination sphere is found in an offset face-to-face orientation with respect to an adjacent Ar^F-substituent on the $Ar^F{}_3TPA^{3-}$ ligand at an observed pyridine-Ar^F inter-aryl-centroid distance of ~3.5 Å. These metrics support the presence of face-to-face inter-arene interactions between the pyridine ligands and Ar^F substituents. Face-to-face arene-arene interactions are typically ~3.5 Å,[49] though can be expected to be longer with more bulky substituents. Assignment of the ^{1}H NMR spectrum of **5.1**

confirms the C_3–symmetry of the complex in solution at room temperature, as eight resonances are observed as expected. A single, sharp resonance is observed in the ^{19}F NMR spectrum at –65.8 ppm, consistent with a symmetric ligand environment. Magnetic susceptibility measurements carried out on **5.1** displayed a RT magnetic moment of 2.91 μ_B, typical for the 5f^3 electronic configuration of a U^{III} ion.[50] Variable temperature- and low temperature/variable field- magnetism studies also supported assignment of **5.1** as a U^{III} complex (see Section 5.3.4).

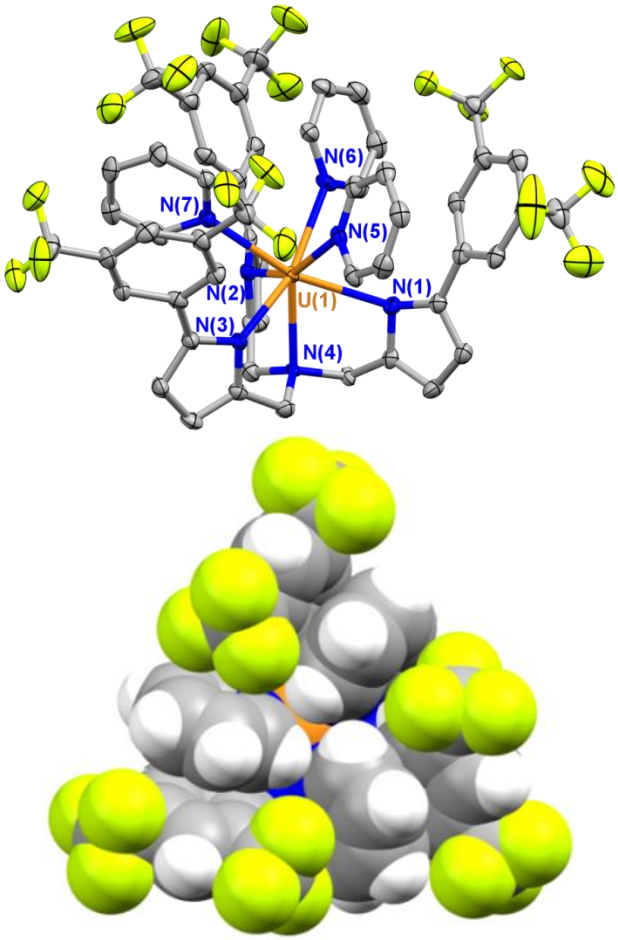

Figure 5.3.1.1 Thermal ellipsoid plot of U^{III}(Ar^{F}TPA)(py)$_3$ (**5.1**) at the 50% probability (top) and space-filling model viewed into the trigonal pocket along the U(1)–N(4) axis and illustrating the Ar^F–py face-to-face interactions (bottom). Hydrogen atoms and interstitial solvents omitted for clarity. U–N(1) 2.605(6), U–N(2) 2.595(5), U–N(3) 2.605(6), U–N(4) 2.561(5), U–N(5) 2.641(6), U–N(6) 2.653(6), U–N(7) 2.632(6) (Å). N(4)–U-N(1) 71.1(2), N(4)–U–N(2) 70.8(2), N(4)–U–N(3) 69.9(2), N(4)–U–N(5) 130.0(2), N(4)–U–N(6) 128.7(2), N(4)–U–N(7) 128.5(2) (°).

To further characterize complex **5.1**, electronic structure calculations were carried out using the crystal structure coordinates of **5.1** at the B3LYP hybrid DFT level of theory. The three

highest occupied molecular orbitals of the optimized structure are singly occupied and primarily non-bonding 5f-character centered on uranium. The highest occupied SOMO is largely $5f_{x(x^2-3y^2)}$ in character and the singly occupied SOMO–1 and SOMO–2 comprise degenerate $5f_{xyz}$ and $5f_{z(x^2-y^2)}$ orbitals. The electronic structure of the optimized geometry demonstrates that the valence 5f orbitals are largely uninvolved in bonding in this complex (Figure 5.3.1.2).

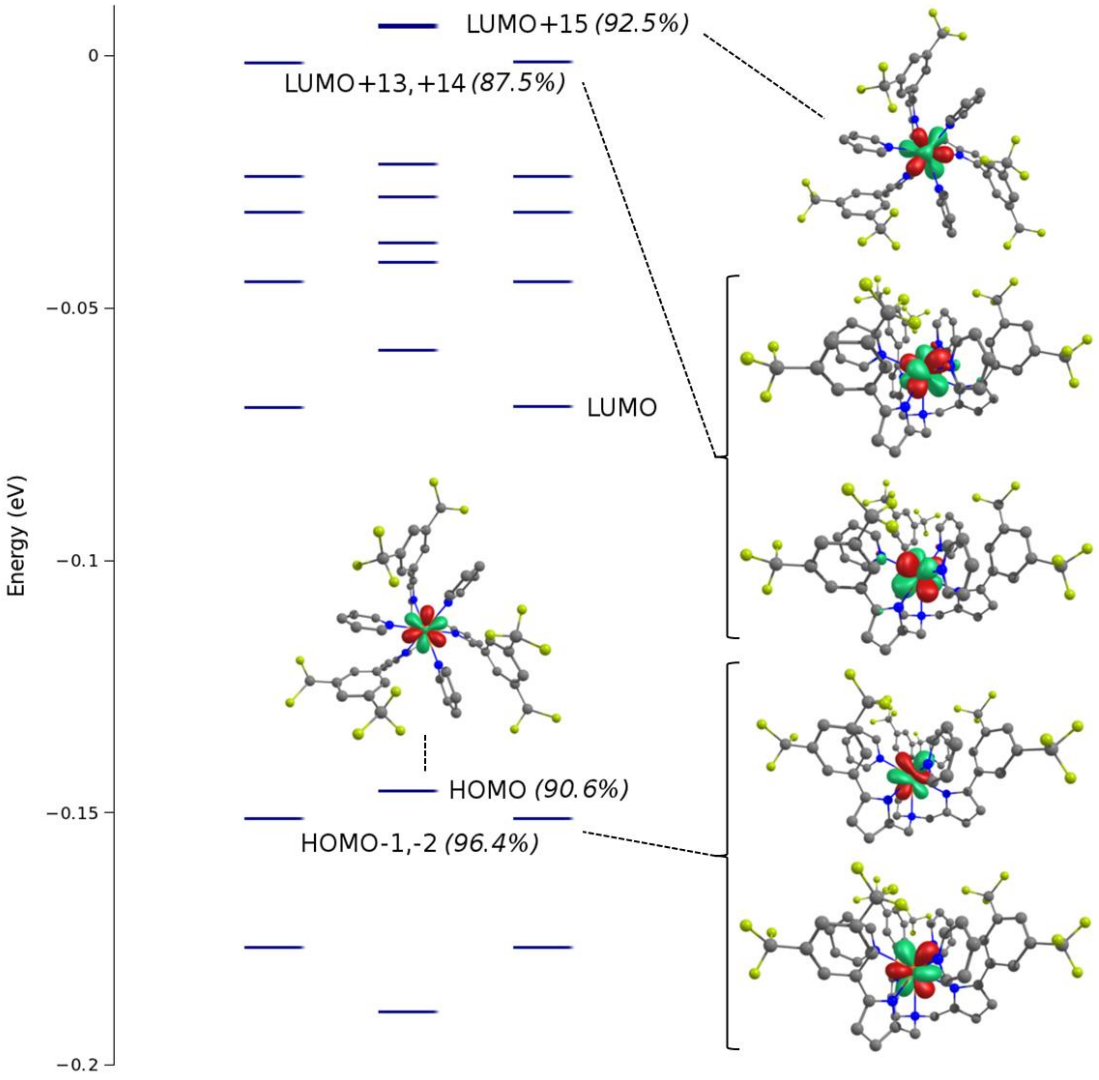

Figure 5.3.1.2 Calculated MO diagram for **5.1**, with orbitals of primarily f-character illustrated. Numbers in parentheses indicate percent uranium f-character in the given MO. The seventh f-orbital is distributed among several MOs immediately above the LUMO+15.

Following the same reaction conditions for the synthesis of **5.1** but performing the addition at room temperature resulted in the formation of the bright yellow complex

$[K(py)_5]_2[U^{IV}(Ar^F{}_3TPA)_2]$ (**5.2**) (Scheme 5.3.1.1). Heating at 50 ºC rapidly produced **5.2** as the major product. The generation of this U^{IV} product from a U^{III} starting material implicates a disproportionation pathway ($4U^{III} \rightarrow 3U^{IV} + U^0$).[51] Crystallization from diethyl ether provided **5.2** in 52 % yield. The crystal structure of **5.2** (Figure 5.3.1.3) shows tetradentate coordination of the U^{IV} ion by each of the two $Ar^F{}_3TPA^{3-}$ ligands in an eight-coordinate, pseudo-cubic geometry. This structure also contains inter-arene interactions between all of the Ar^F- and pyrrolyl- groups. The arms of the two $Ar^F{}_3TPA^{3-}$ ligands interdigitate such that each Ar^F-ring is aligned with an adjacent pyrrolyl ring in a staggered orientation with an average Ar^F–centroid to pyrrolyl–centroid distance of ~3.7 Å. The U^{IV} ion in **5.2** is displaced ~1.0 Å above each plane of three pyrrolyl nitrogen atoms.

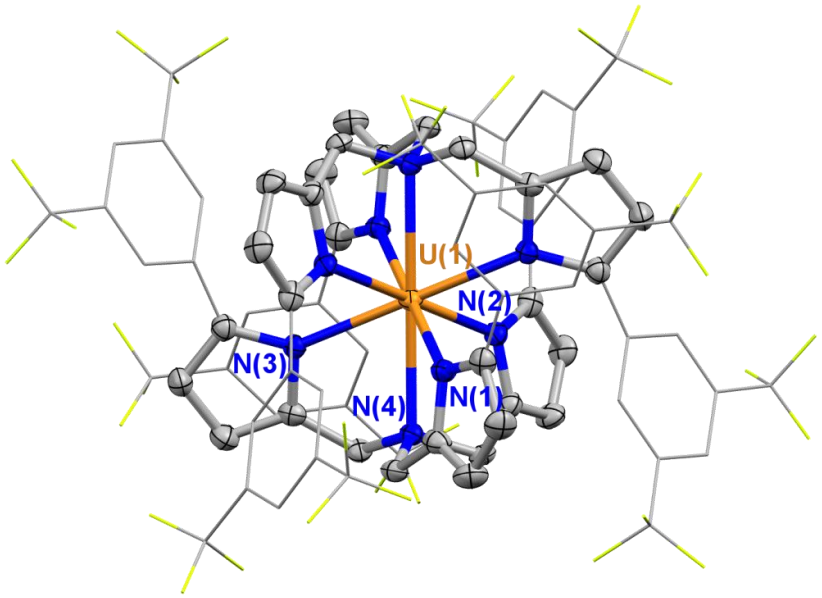

Figure 5.3.1.3 Thermal ellipsoid plot of $[K(py)_5]_2[U^{IV}(Ar^F{}_3TPA)_2]$ (**5.2**) at 50% probability. Hydrogen atoms and potassium ions are omitted, and Ar^F-rings shown in wireframe for clarity. U–N(1) 2.508(4), U–N(2) 2.493(4), U–N(3) 2.490(4), U–N(4) 2.649(4) (Å). N(4)–U–N(1) 65.9(1), N(4)–U–N(2) 66.5(1), N(4)–U–N(3) 66.4(1) (°).

The ^{1}H NMR of **5.2** in pyridine-d_5 at room temperature displays six resonances in a 2:1:1:1:1:1 ratio. Five resonances are expected based on equivalency of the six Ar^F-pyrrolyl-methylene- arms of the two ligands. The appearance of a sixth resonance is rationalized on the basis that the *ortho*-hydrogens on the Ar^F-substituents are inequivalent on the NMR timescale.

The ^{19}F NMR spectrum supports this assignment. It displays two broad peaks in a 1:1 integration due to hindered rotation of the Ar^F rings nestled into the cleft of the adjacent ligand. It is evident that the self-complimentary arrangement of arene groups in the structure of **5.2** contributes to the formation of the 1:2 complex. Noting the tendency of the U^{IV} complex **5.2** to form from UI_3, we sought to prepare it directly from UCl_4.

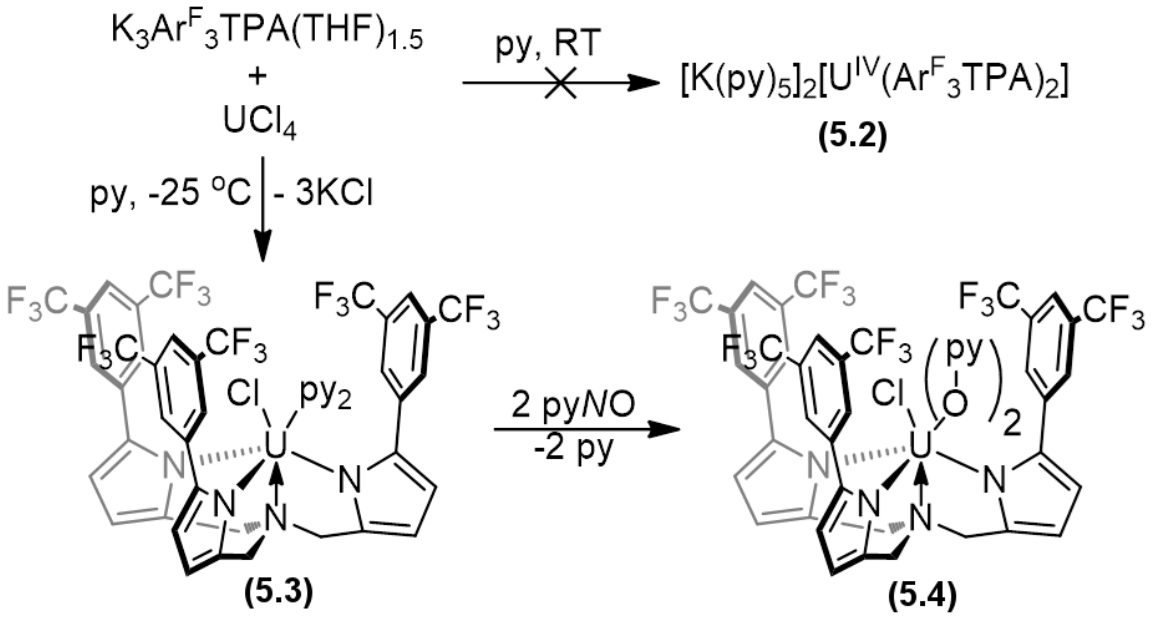

Scheme 5.3.1.2 Syntheses of complexes **5.3** and **5.4** and failed synthesis of **5.2** from UCl_4.

Addition of $K_3Ar^F{}_3TPA(THF)_{1.5}$ to a solution of UCl_4 in THF/pyridine at –25 °C produced red $U^{IV}(Ar^F{}_3TPA)(py)_2Cl$ (**5.3**) (Scheme 5.3.1.2). Surprisingly, performing this reaction at room temperature led to no observable formation of **5.2** even when two equiv of $K_3Ar^F{}_3TPA(THF)_{1.5}$ were added (Scheme 5.3.1.2). In our hands complex **5.2** was only accessible through disproportionation reaction of the U^{III} starting material. As in the study of **5.1,** attempts to prepare the analogous THF-adduct of **5.3** in the absence of pyridine were unsuccessful due to the formation of multiple products.

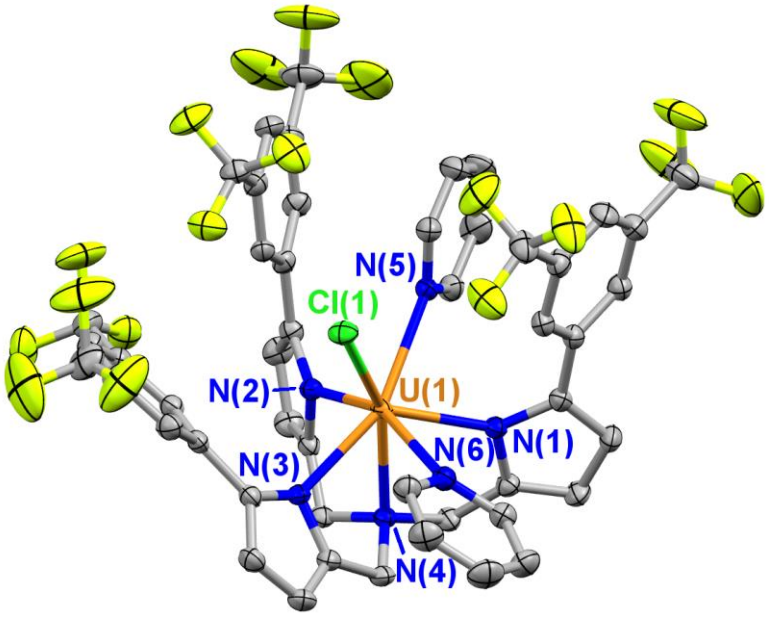

Figure 5.3.1.4 Thermal ellipsoid plot of $U^{IV}(Ar^F{}_3TPA)(py)_2Cl$ (**5.3**) at the 50% probability level. Hydrogen atoms and interstitial pyridine omitted for clarity. U–N(1) 2.3663(17), U–N(2) 2.3752(17), U–N(3) 2.3836(18), U–N(5) 2.5537(16), U–N(6) 2.6583(18), U–Cl(1) 2.6188(5) (Å). N(4)–U–N(1) 69.98(6), N(4)–U–N(2) 65.01(6), N(4)–U–N(3) 71.59(6), N(4)–U–N(5) 122.60(6), N(4)–U–N(6) 89.23(6), N(4)–U–Cl(1) 155.43(4) (°).

The structure of **5.3** reveals a seven-coordinate geometry (Figure 5.3.1.4). The average U–N(pyrrolyl) bond length in **5.3** is 2.375(9) Å, ~0.23 Å shorter than the related distances in **5.1** and slightly shorter than previously reported U^{IV}–pyrrolyl bond lengths in calix[4]pyrrole complexes.[47] In complex **5.3** one pyridine ligand is sandwiched between two Ar^F-rings at an average Ar^F-centroid to pyridine-centroid distance of ~3.6 Å in a staggered arrangement. The second pyridine ligand is displaced into a pseudo-equatorial position, and shows no short inter-arene distances with the Ar^F groups. The U^{IV} ion lies ~0.87 Å above the plane of the three pyrrolyl-nitrogen atoms, nearly identical to **5.1**. Magnetic susceptibility measurements carried out on **5.3** displayed a room temperature magnetic moment of 3.32 μ_B and variable temperature and field responses typical for a $5f^2$ ion.[50]

The number of ^{1}H and ^{19}F NMR resonances of **5.3** are highly dependent on temperature as well as solvent (Figure 5.3.1.6). In pyridine-d_5 five $Ar^F{}_3TPA$ ligand resonances are observed for **5.3** in the ^{1}H NMR spectrum between –23 °C and +62 °C, indicating the complex is effectively C_3 symmetric in pyridine-d_5 solution at room temperature. These peaks appear sharp at higher

temperature and broaden at lower temperature, until they can no longer be observed below –23 °C. The absence of resonances observed for bound pyridine and the effective C_3 symmetry is consistent with fast exchange of the pyridine ligands with pyridine-d_5. Similar behavior is observed in the ^{19}F NMR, where a single sharp peak broadens at lower temperature. Spectra collected for **5.3** in toluene-d_8 exhibit more complicated features. At room temperature, the ^{1}H NMR spectrum displays a number of broad, overlapping peaks, consistent with an unsymmetric ligand environment. Below room temperature, multiple decoalescence processes are evident in the ^{19}F NMR spectrum. The appearance of multiple decoalescence processes in the VT NMR experiment suggests that the molecule adopts multiple low energy conformations that readily equilibrate. These conformations likely correspond to interactions between the Ar^F rings and the pyridine ligands, leading to inequivalent chemical environments of the Ar^F rings and the resulting appearance of multiple peaks in the ^{19}F NMR spectrum. To further investigate the role of inter-arene interactions in **5.3**, we prepared a second Lewis base adduct of **5.3**.

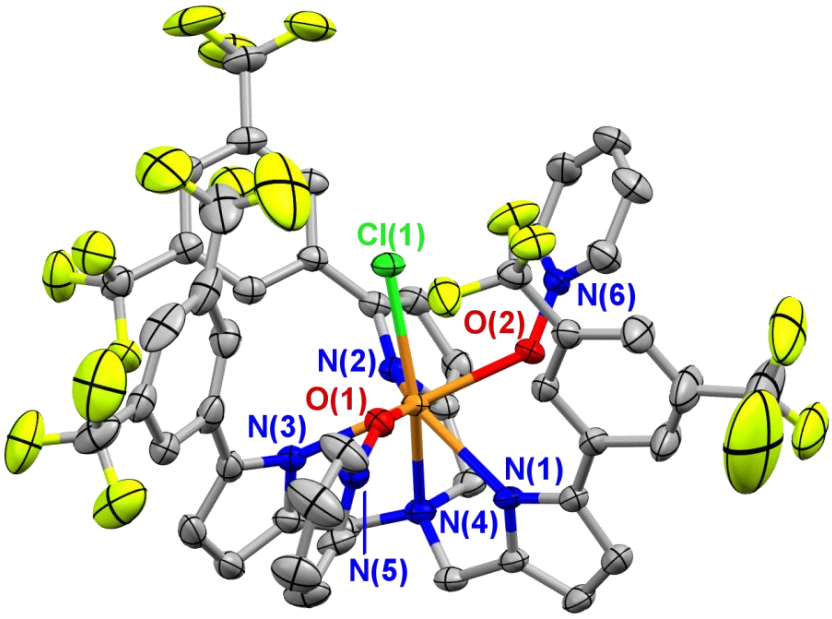

Figure 5.3.1.5 Thermal ellipsoid plot of **5.4** shown at 50% probability. Hydrogen atoms (from thermal ellipsoid plot) and interstitial solvent, as well as minor disorder has been omitted for clarity. U(1)–N(1) 2.417(4), U(1)–N(2) 2.479(3), U(1)–N(3) 2.433(4), U(1)–N(4) 2.535(3), U(1)–O(1) 2.299(3), U(1)–O(2) 2.270(3), U(1)–Cl(1) 2.6115(10) (Å). N(4)–U(1)–N(1) 65.17(11), N(4)–U(1)–N(2) 69.18(12), N(4)–U(1)–N(3) 71.60(12), N(4)–U(1)–O(1) 100.74(11), N(4)–U(1)–O(2) 121.28(11), N(4)–U(1)–Cl(1) 150.71(9) (°).

Addition of two equiv of pyridine *N*-oxide (py–O) to **5.3** leads to immediate formation of green-yellow $U^{IV}(Ar^F{}_3TPA)(py–O)_2Cl$ (**5.4**). Complex **5.4** was obtained by crystallization at –25 °C from a concentrated solution in toluene layered with hexane in 90 % yield and the structure was determined. A similar local geometry at the U^{IV} ion is observed in **5.4** as in **5.3** (Figure 5.3.1.5), though there is an elongation (~0.07 Å) of the $U–N_{(pyrrolyl)}$ bonds in **5.4** consistent with the increased electron donating nature of the py–O ligand relative to pyridine. The major difference in the solid state structures of **5.3** and **5.4** is that the py–O ligands in **5.4** are unable to orient into the same inter-arene interactions with the Ar^F-rings due to the extension of the aryl group of the py–O ligand out of the trigonal pocket. The U^{IV}–O–py bonds are evidently stronger than the U^{IV}–*N*py bonds in **5.3**, as observed by the complete substitution of pyridine for py–O in the synthesis of **5.4**. Importantly, the absence of inter-arene interactions in **5.4** results in a significant change in the ^{1}H NMR of **5.4** relative to **5.3**. Apart from broadening of the single ^{19}F signal ~280 K, complex **5.4** is largely C_3 symmetric in toluene-d_8 by ^{1}H- and ^{19}F NMR between room temperature and –50 ºC. No decoalescence of the ^{19}F peak for **5.4** into multiple peaks was observed, signifying equivalent chemical environments of the Ar^F rings on the NMR timescale. The C_3 solution symmetry of **5.4** implies that there is minimal interaction between the Ar^F-substituents and the py–O ligands, allowing the complex to rearrange faster than the time scale of the experiment.

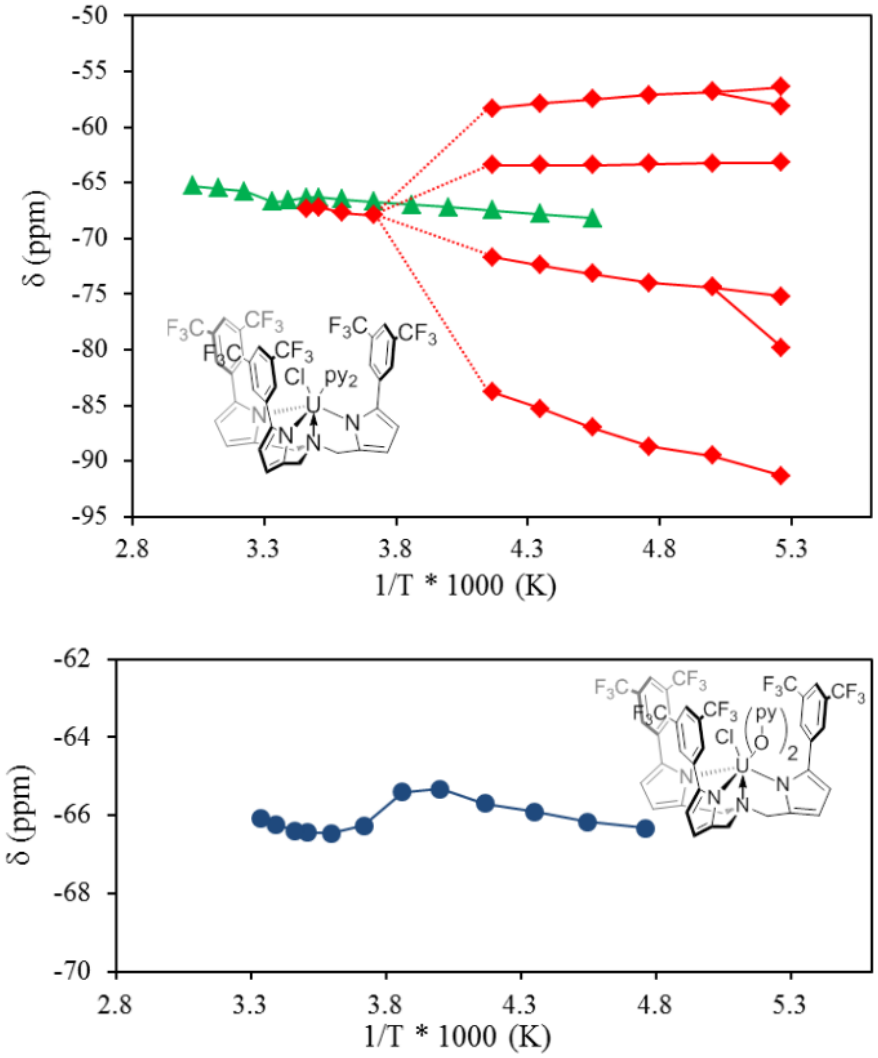

Figure 5.3.1.6 VT-^{19}F NMR data for complex **5.3** (top) and complex **5.4** (bottom). Lines are provided as a guide for the eye. Dotted lines indicate the region around coalescence, where the peak center is ambiguous due to extreme peak broadening.

5.3.2 VT-^{19}F NMR Spectra.

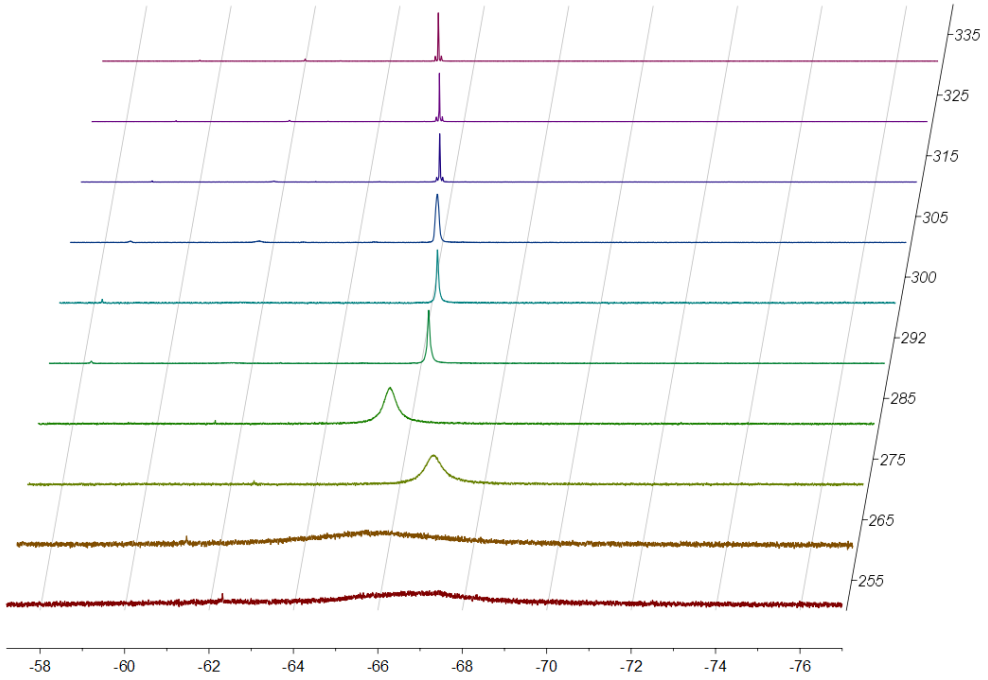

Figure 5.3.2.1 VT-^{19}F-NMR spectra of U^{IV}(Ar$^{F}_{3}$TPA)(py)$_2$Cl (**5.3**) in pyridine-d_5.

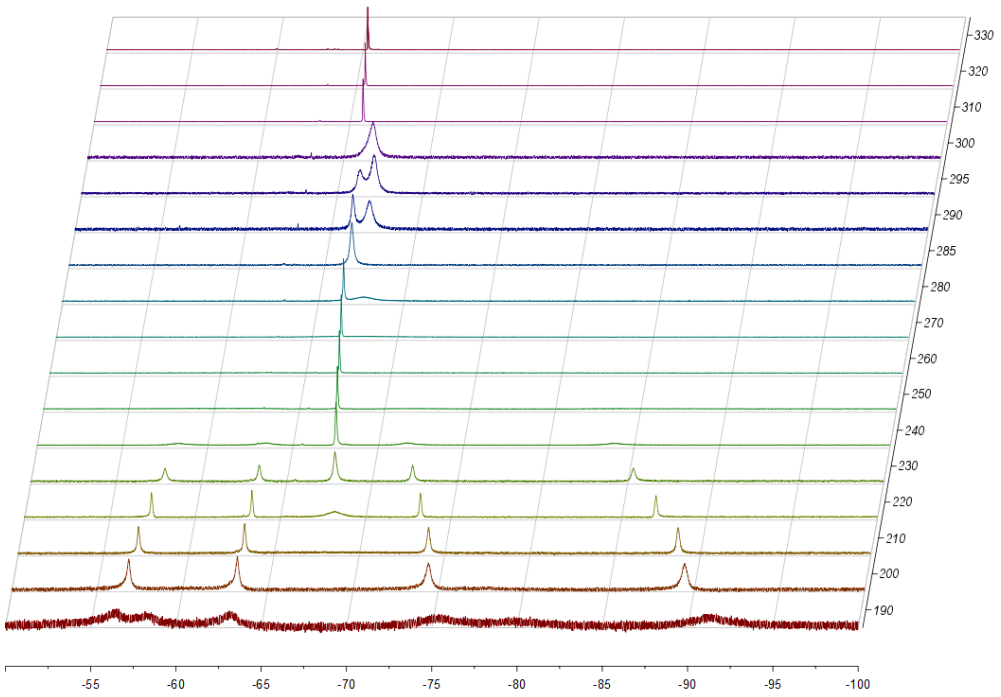

Figure 5.3.2.2 VT-^{19}F-NMR spectra of U^{IV}(Ar$^{F}_{3}$TPA)(py)$_2$Cl (**5.3**) in toluene-d_8.

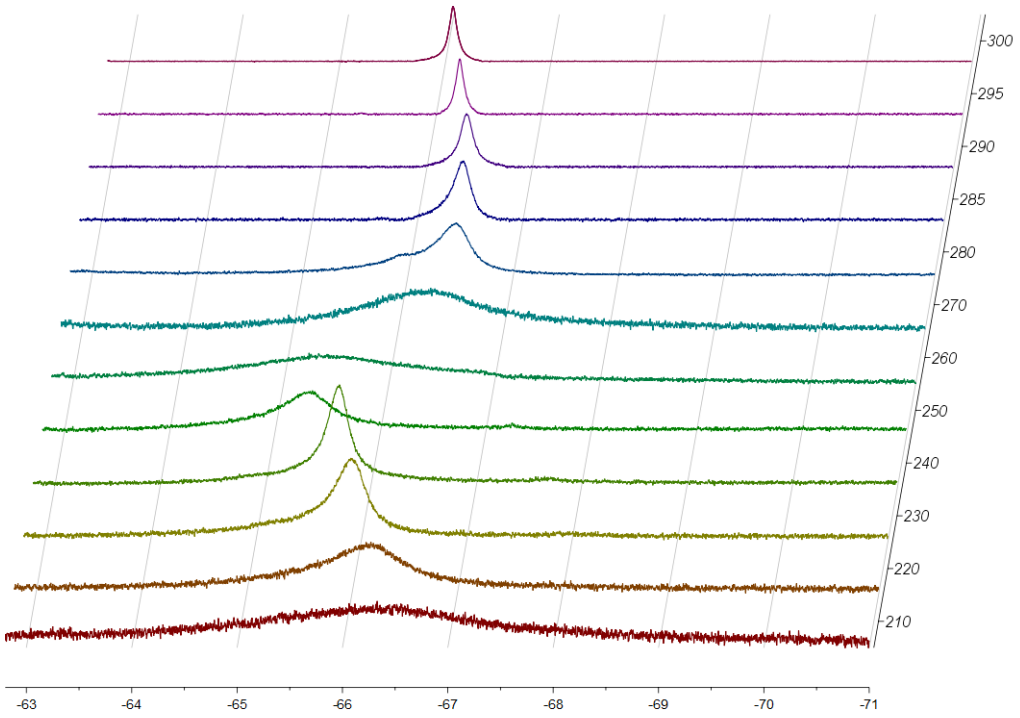

Figure 5.3.2.3 VT-^{19}F-NMR spectra of U^{IV}(Ar$^{F}_3$TPA)(py*N*O)$_2$Cl (**5.4**) in toluene-d_8.

5.3.3 ^{1}H and ^{19}F NMR Spectra.

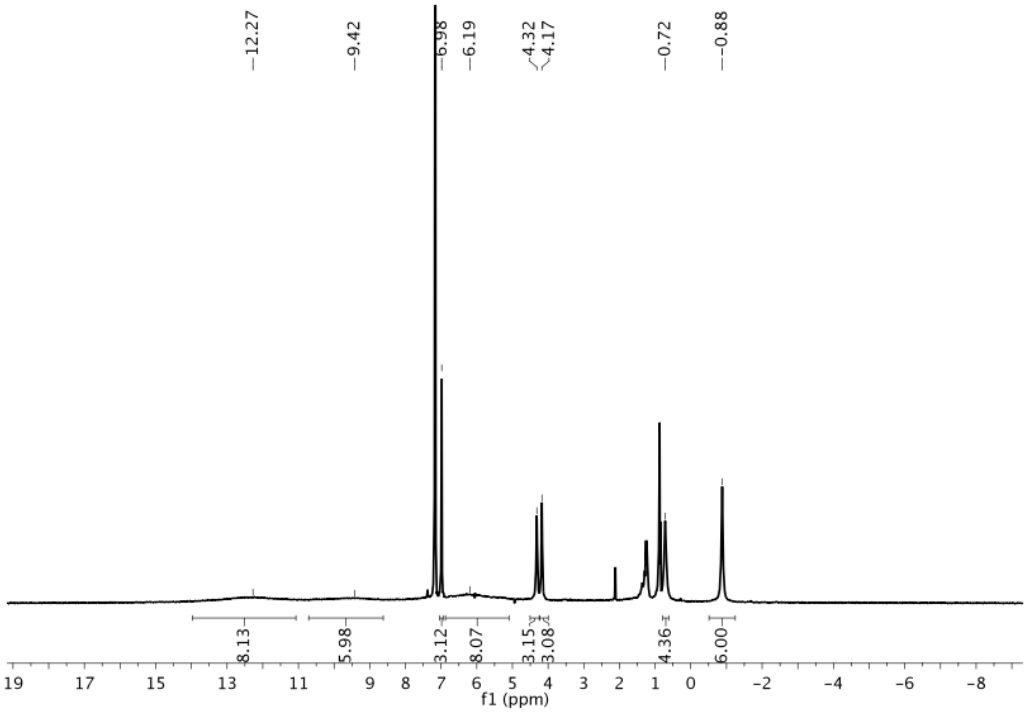

Figure 5.3.3.1 ^{1}H NMR of U^{III}(Ar$^{F}_3$TPA)(py)$_3$ (**5.1**) collected in benzene-d_6 at 25 °C.

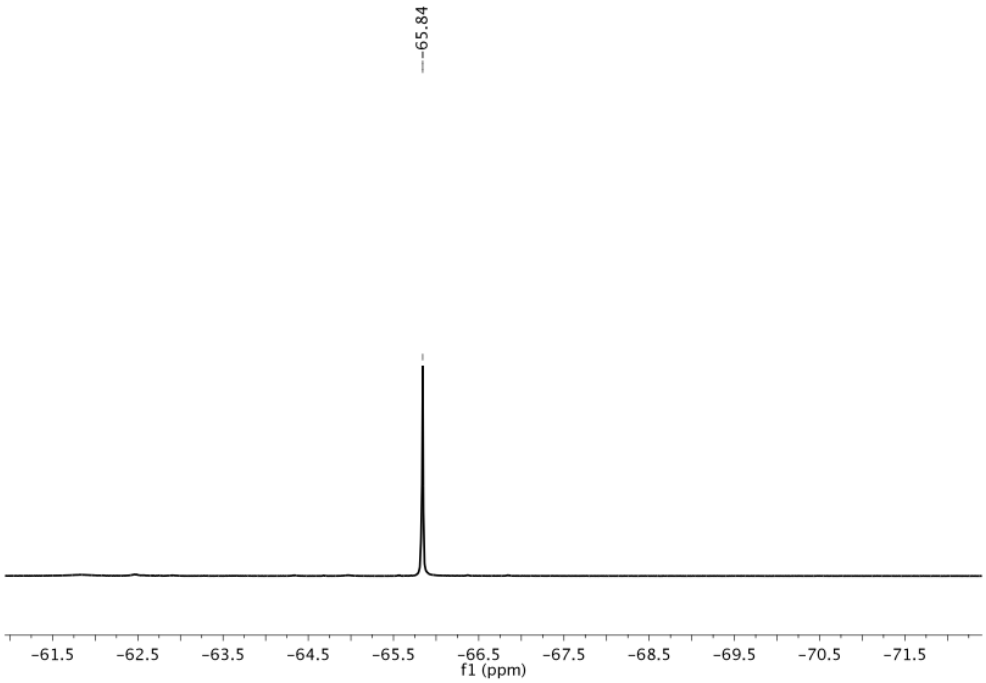

Figure 5.3.3.2 ^{19}F NMR of U^{III}(Ar$^{F}_{3}$TPA)(py)$_3$ (**5.1**) collected in benzene-d_6 at 25 °C.

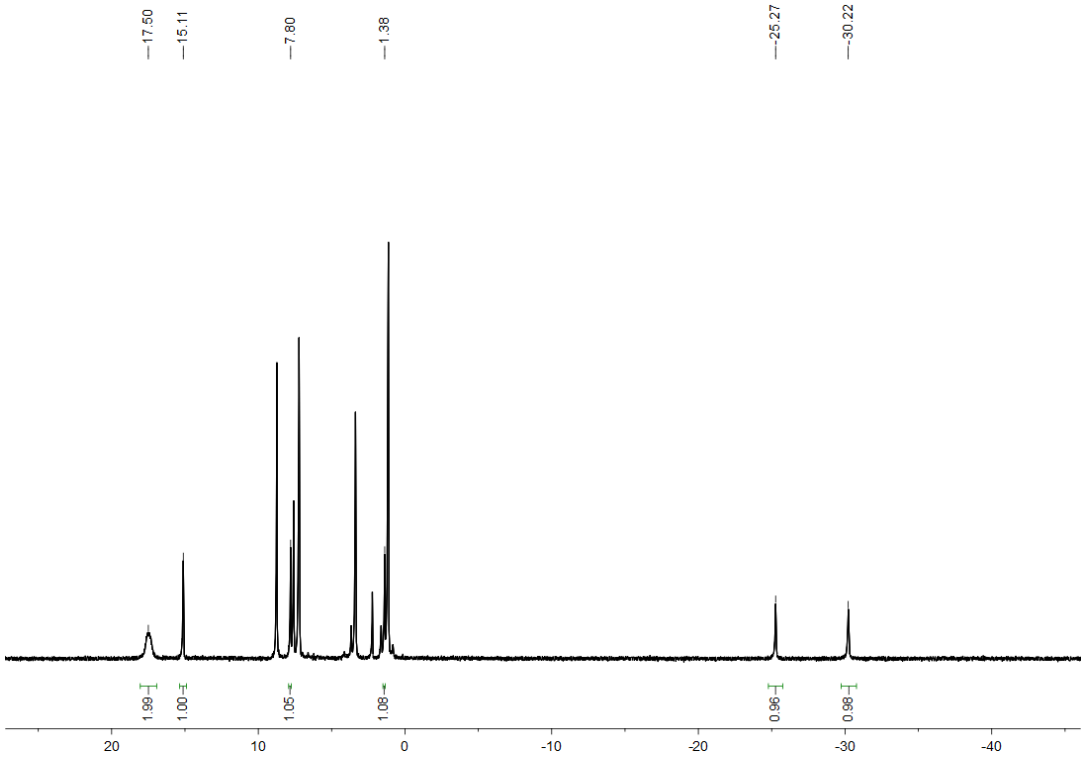

Figure 5.3.3.3 ^{1}H NMR of [K(py)$_5$]$_2$[U^{IV}(Ar$^{F}_{3}$TPA)$_2$] (**5.2**) collected in pyridine-d_5 at 25 °C.

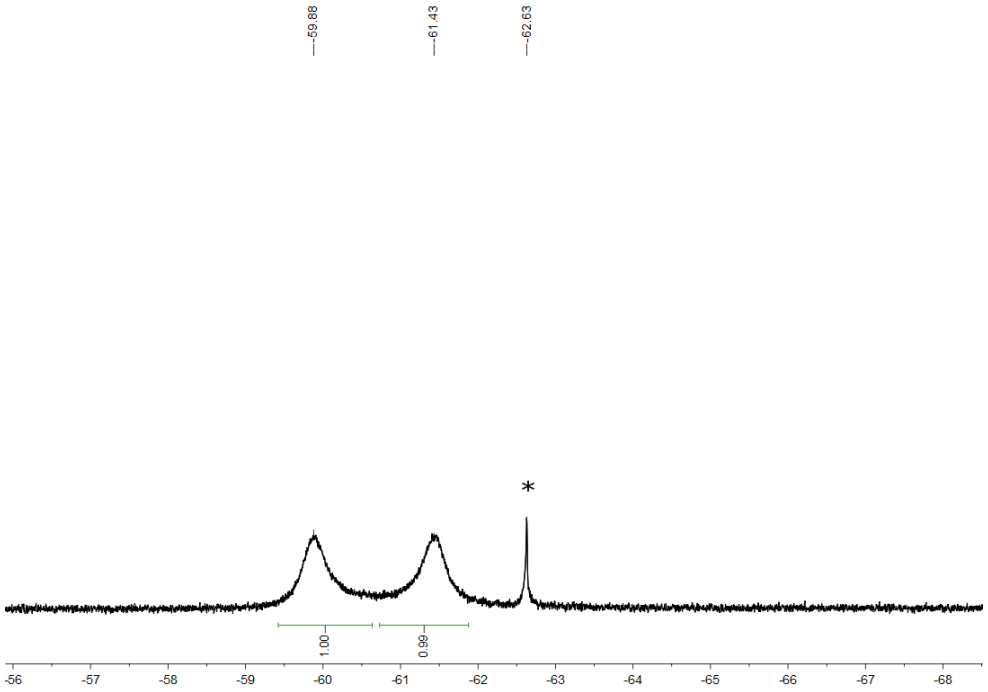

Figure 5.3.3.4 ^{19}F NMR of $[K(py)_5]_2[U^{IV}(Ar^{F}{}_3TPA)_2]$ (**5.2**) collected in pyridine-d_5 at 25 °C. *$H_3Ar^{F}{}_3TPA$

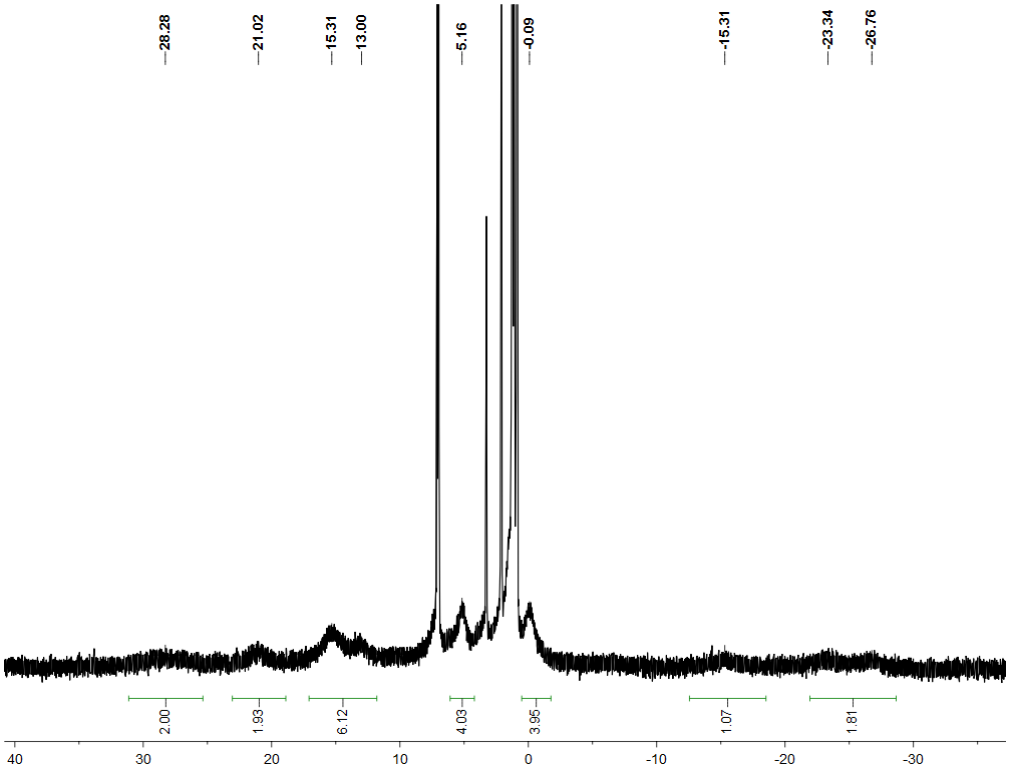

Figure 5.3.3.5 ^{1}H NMR of $U^{IV}(Ar^{F}{}_3TPA)(py)_2Cl$ (**5.3**) collected in toluene-d_8 at 25 °C.

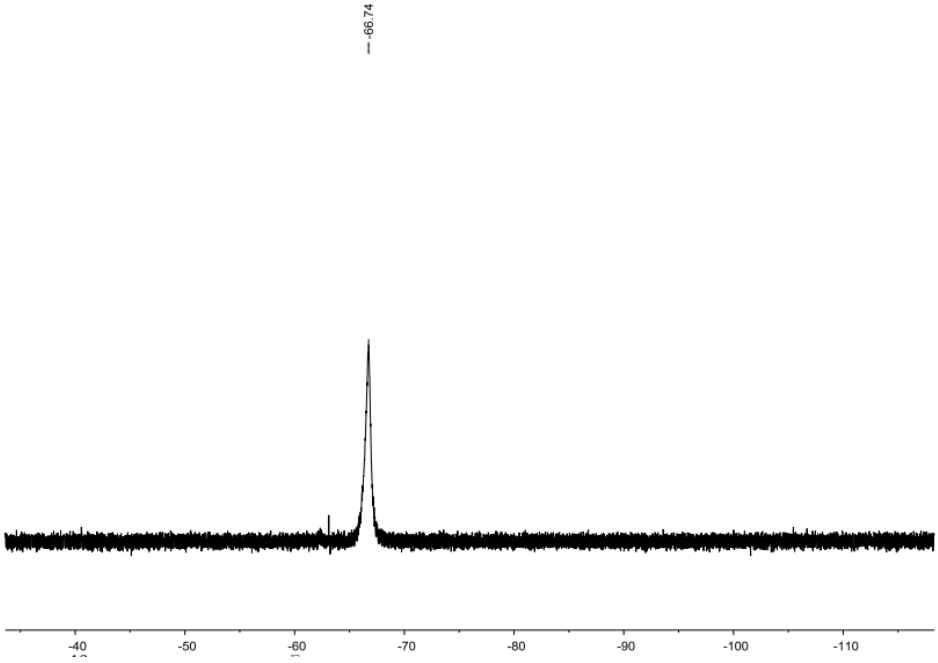

Figure 5.3.3.6 ^{19}F NMR of U^{IV}(Ar$^{F}_3$TPA)(py)$_2$Cl (**5.3**) collected in toluene-d_8 at 25 °C.

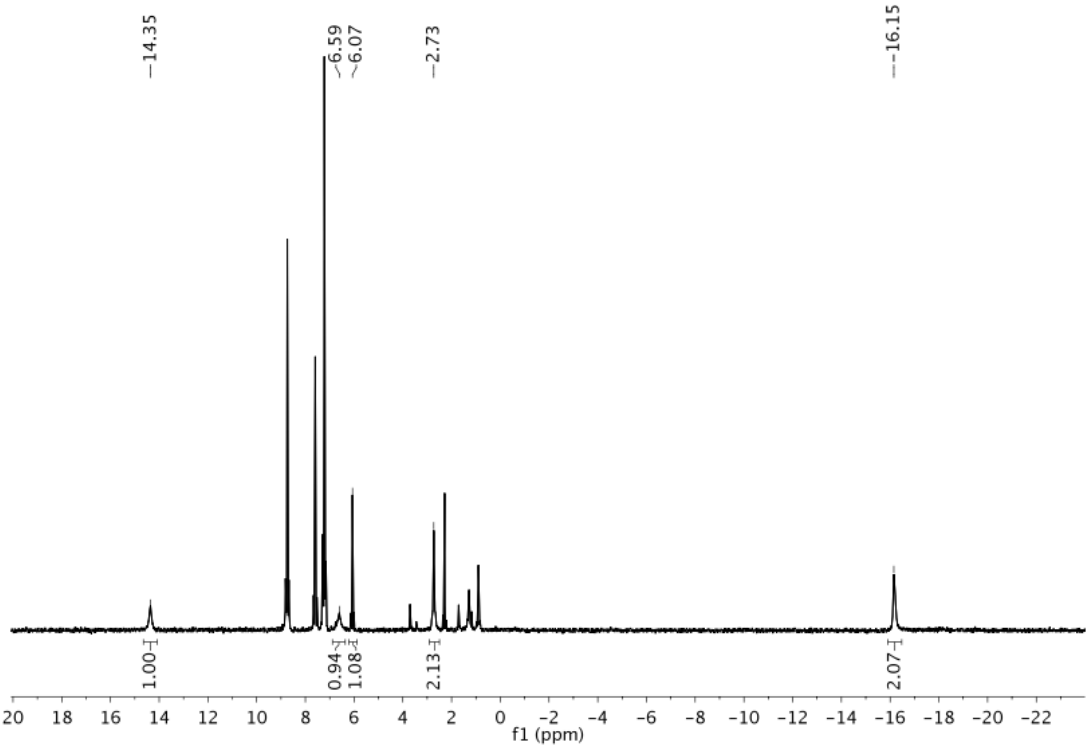

Figure 5.3.3.7 ^{1}H NMR of U^{IV}(Ar$^{F}_3$TPA)(py)$_2$Cl (**5.3**) collected in pyridine-d_6 at 62 °C.

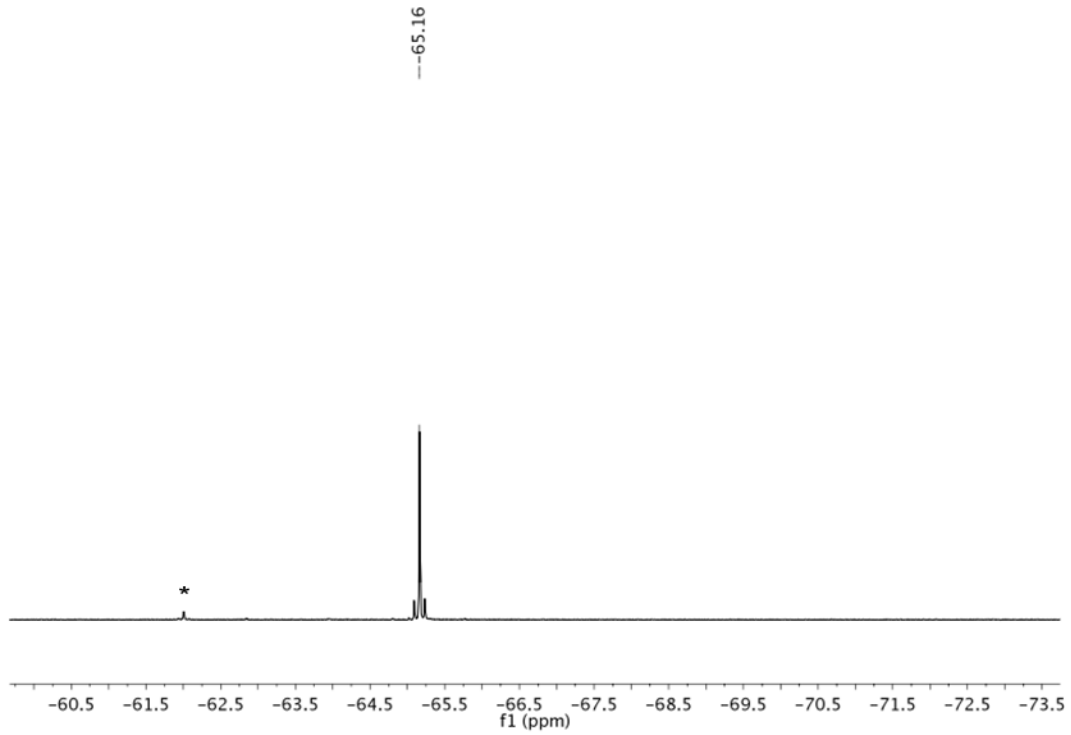

Figure 5.3.3.8 ^{19}F NMR of U^{IV}(Ar$^{F}_3$TPA)(py)$_2$Cl (**5.3**) collected in pyridine-d_6 at 62 °C. *H$_3$Ar$^{F}_3$TPA

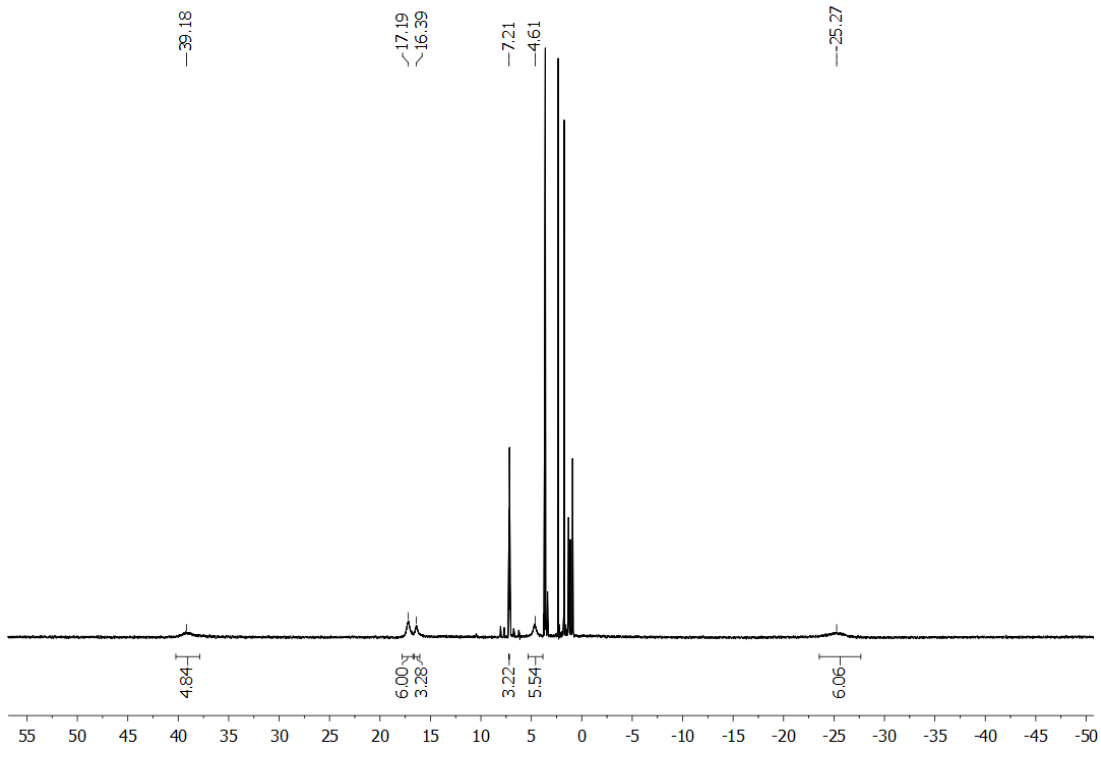

Figure 5.3.3.9 ^{1}H NMR of U^{IV}(Ar$^{F}_3$TPA)(pyNO)$_2$Cl (**5.4**) collected in toluene-d_8 at 25 °C.

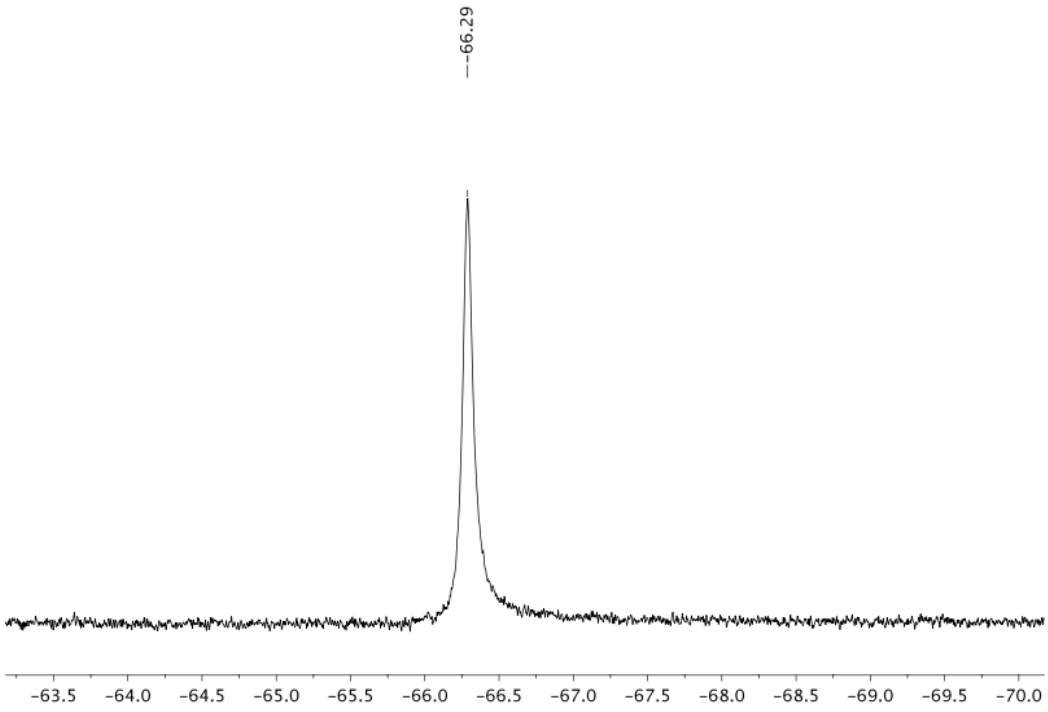

Figure 5.3.3.10 ^{19}F NMR of U^{IV}(Ar$^F_3$TPA)(pyNO)$_2$Cl (**5.4**) collected in toluene-d_8 at 25 °C.

5.3.4 Magnetic Data

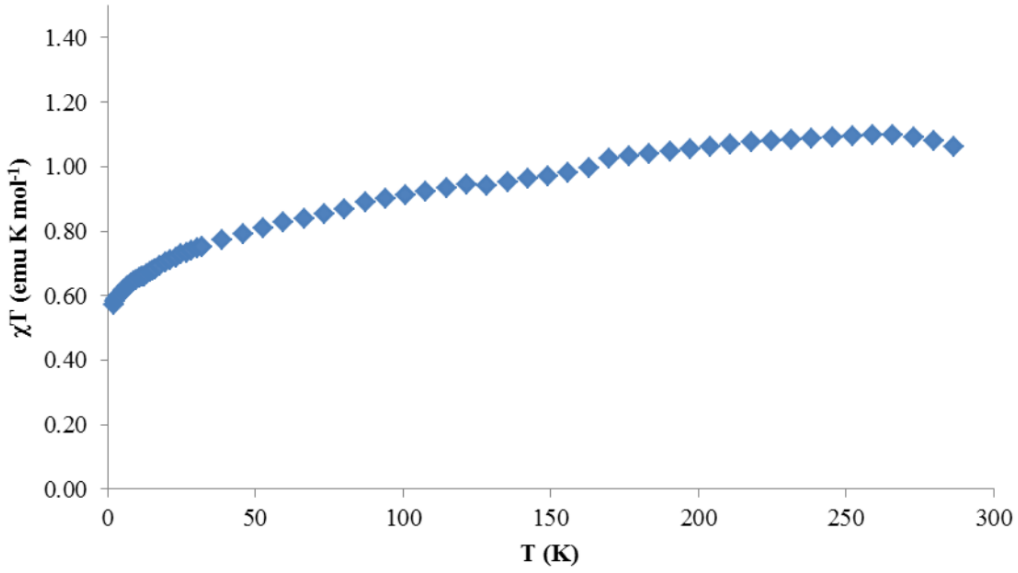

Figure 5.3.4.1 Temperature dependent magnetic data for U^{III}(Ar$^F_3$TPA)(py)$_3$ (**5.1**) collected at H = 0.1 T.

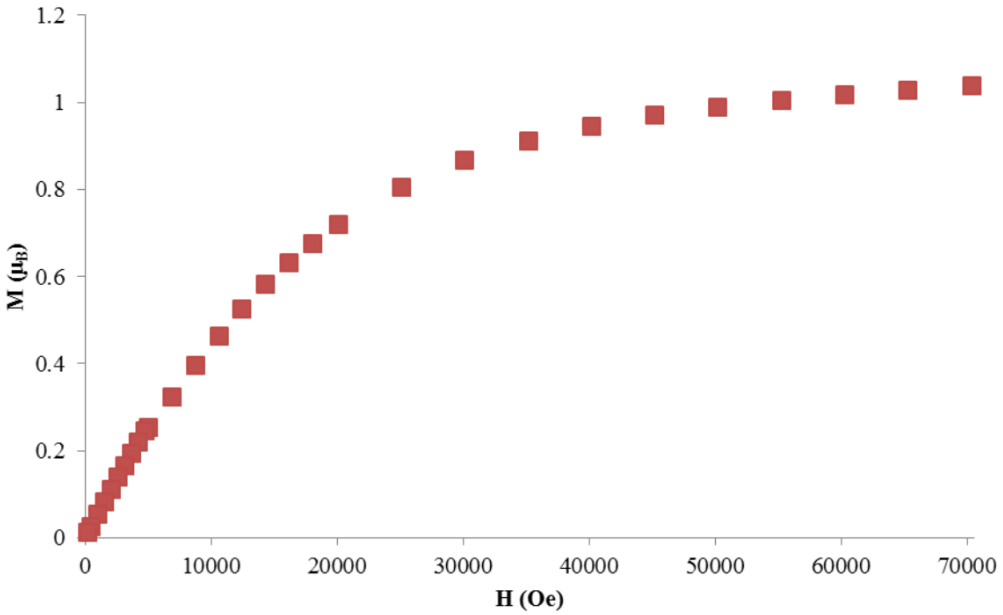

Figure 5.3.4.2 Field dependent magnetic data for $U^{III}(Ar^F_3TPA)(py)_3$ (**5.1**) collected at T = 2 K.

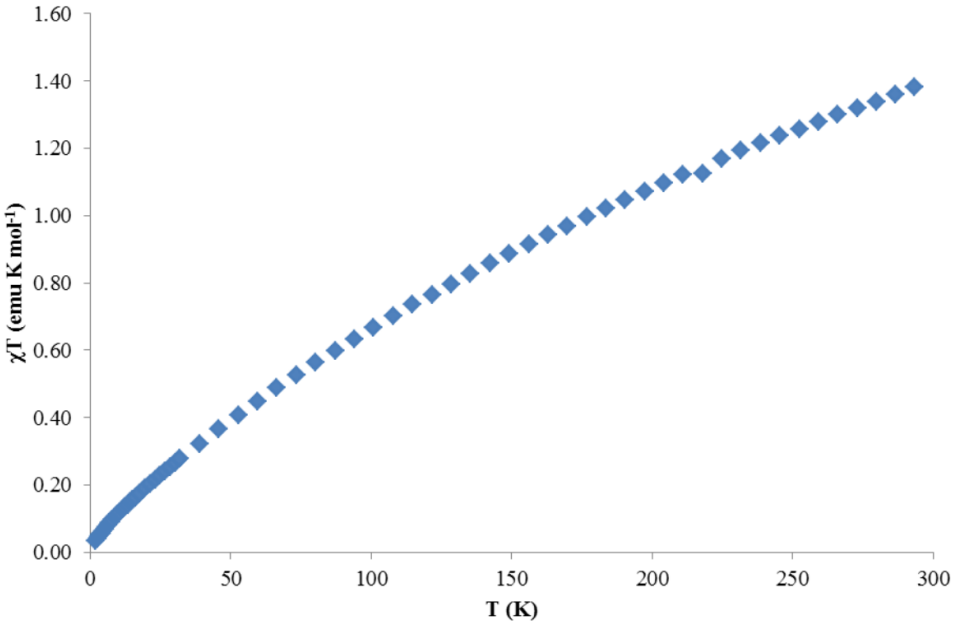

Figure 5.3.4.3 Temperature dependent magnetic data for $U^{IV}(Ar^F_3TPA)(py)_2Cl$ (**5.3**) collected at H = 0.1 T.

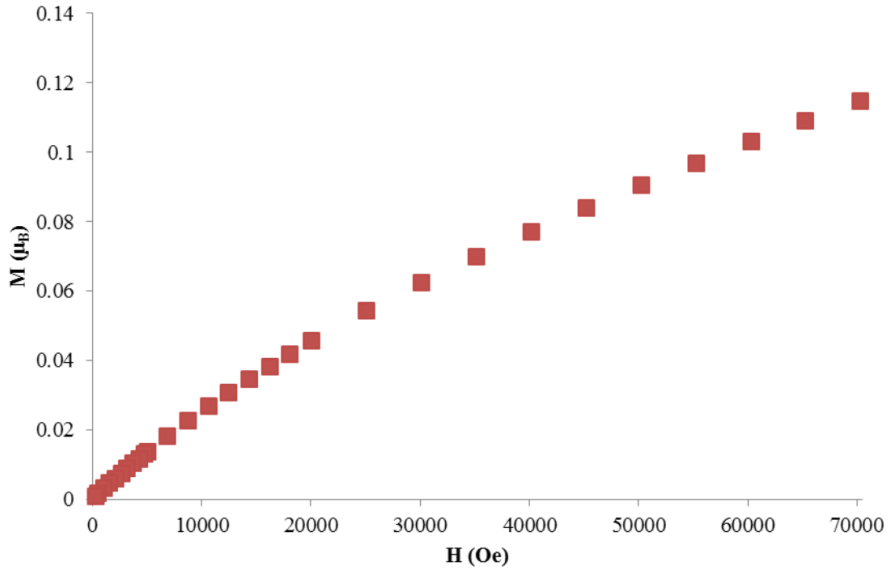

Figure 5.3.4.4 Field dependent magnetic data for U^{IV}(Ar$^{F}_3$TPA)(py)$_2$Cl (**5.3**) collected at T = 2 K.

5.4 Uranium Complexes of the Mes$_3$TPA^{3-} Ligand.

5.4.1 Synthesis and Characterization. The Mes$_3$TPA^{3-} ligand provides better steric protection and is expected to be more electron donating than the Ar$^{F}_3$TPA^{3-} ligand. The synthesis of uranium complexes of the Mes$_3$TPA^{3-} ligand was rapid and facile (Scheme 5.4.1.1). Addition of 1 equiv K$_3$Mes$_3$TPA to a DME solution of UI$_3$ led to a the formation of a dark purple solution with visible precipitation of KI. Recrystallization of a saturated DME solution layered with hexanes at –25 °C produced black crystals of U^{III}(Mes$_3$TPA)(DME) (**5.5**) in 74% yield. Alternately, performing this synthesis in THF rather than DME produced U^{III}(Mes$_3$TPA)(THF) (**5.6**) in 84% yield. Single crystals of **5.5** and **5.6** suitable for X-ray diffraction were obtained by cooling hot hexanes solutions to –25 °C (Figures 5.4.1.1, 5.4.1.2). In contrast to **5.1**, these complexes exhibit coordination to only a single solvent molecule, due to the larger steric demand of the mesityl groups.

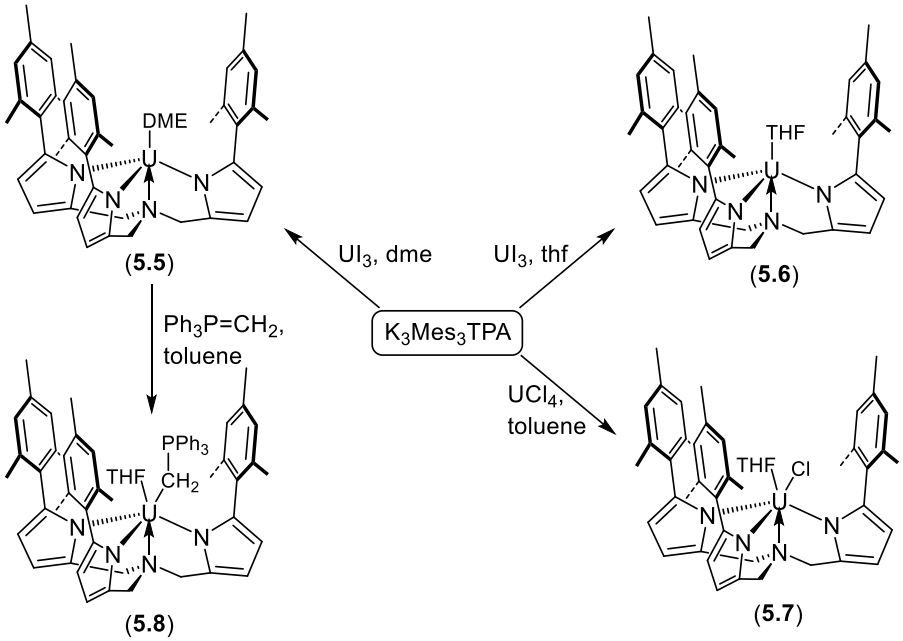

Scheme 5.4.1.1 Synthesis of low valent uranium complexes bound to the Mes_3TPA^{3-} ligand.

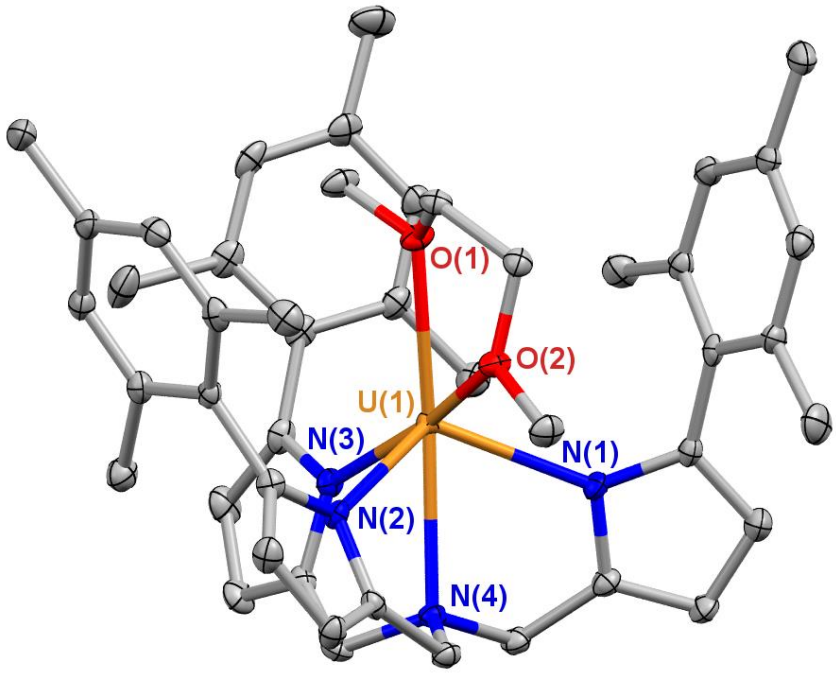

Figure 5.4.1.1 Thermal ellipsoid plot of $U^{III}(Mes_3TPA)(DME)$ (**5.5**) at 30% probability. Hydrogen atoms are omitted for clarity. Selected bond metrics are listed in Table 5.4.1.1.

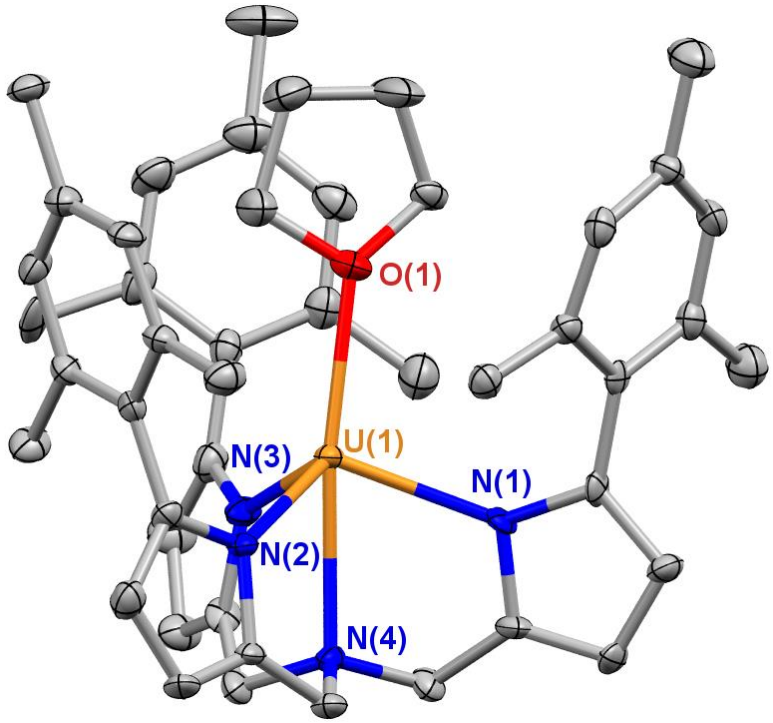

Figure 5.4.1.2 Thermal ellipsoid plot of U^{III};(Mes$_3$TPA)(THF) (**5.6**) at 30% probability. Hydrogen atoms are omitted for clarity. Selected bond metrics are listed in Table 5.4.1.1.

The ^{1}H NMR spectrum of **5.5** exhibited six resonances for the Mes$_3$TPA^{3-} ligand, indicating that the complex is C_3 symmetric on the NMR time scale. This observation indicates that the DME ligand either rapidly exchanges or that there is a low barrier to reorganization of the complex. Similarly, the ^{1}H NMR spectrum of **5.6** displayed the minimal number of resonances indicative of C_3 solution symmetry.

Table 5.4.1.1 Selected bond metrics for **5.5**–**5.7.**

	U–N$_{pyr}$	U–N$_{Am}$	U–L^1	U–L^2	N$_{Am}$–U–N$_{Pyrr}$	N$_{Am}$–U–X
5.5	2.424(7)	2.622(5)	2.572(5)	2.582(5)	65.9(2)	166.26(19)
5.6	2.386(17)	2.627(13)	2.497(12) U(1)–O(1)	–	67.9(5)	169.9(5)
5.7	2.326(5)	2.572(5)	2.456(4) U(1)–O(1)	2.5987(14) U(1)–Cl(1)	66.9(2)	160.36(11)
5.8	2.457(2)	2.6370(19)	2.540(2) U(1)–O(1)	2.757(2) U(1)–C(1)	65.84(7)	153.72(6)

Synthesis of a uranium(IV) complex of the Mes$_3$TPA ligand was carried out through addition of 1 equiv K$_3$Mes$_3$TPA to a THF solution of UCl$_4$, resulting in an immediate color change to red. Recrystallization of this product from a saturated toluene solution layered with hexanes at

–25 °C produced red blocks of U^{IV}(Mes$_3$TPA)(THF)Cl (**5.6**) in 61% yield. The ^{1}H NMR spectrum of **5.6** exhibited chemical equivalence of the three arms of the ligand despite the overall desymmetrization of the complex imparted by the THF and chloride ligands.

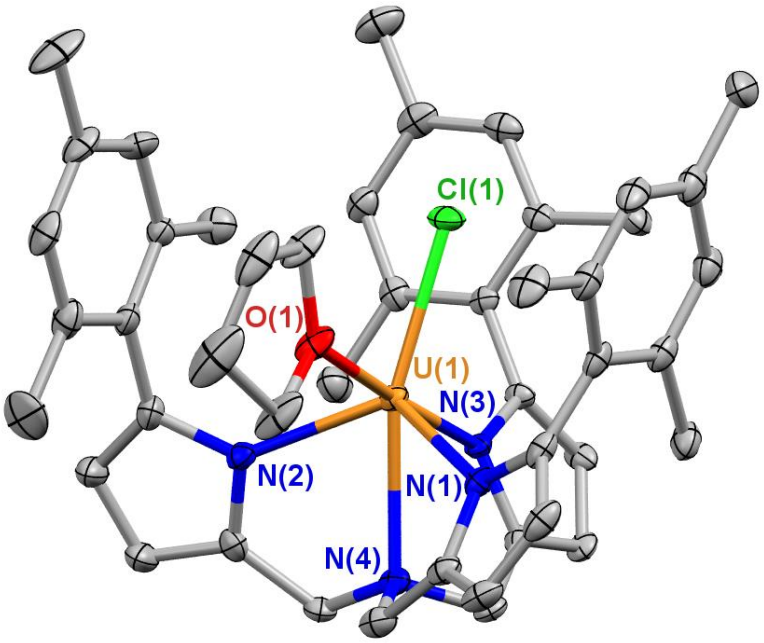

Figure 5.4.1.3 Thermal ellipsoid plot of U^{IV}(Mes$_3$TPA)(THF)Cl (**5.7**) at 30% probability. Hydrogen atoms are omitted for clarity. Selected bond metrics are listed in Table 5.4.1.1.

Numerous oxidation reactions to produce uranium(V) or uranium(VI) complexes of the Mes$_3$TPA^{3-} were attempted. Addition of 1 equiv pyridine-*N*-oxide to **5.5** led to an immediate color change to dark red. This product resisted all attempts at obtaining structural evidence for the expected product formulation, U^{V}(Mes$_3$TPA)O(py), so the formation of a dimeric or unexpected decomposition product cannot be ruled out in this case. Treatment of **5.7** with $CuCl_2$ in THF led to a very slow color change to dark red, requiring 48 hours to achieve full conversion. The ^{1}H spectrum of the formed produce showed apparent desymmetrization of the Mes$_3$TPA ligand (Figure 5.4.1.4), expected due to installation of the chloride ligand. Furthermore, treatment of **2.1-Cl** with 1 equiv H$_3$Mes$_3$TPA led to formation of the same product identified by ^{1}H NMR, supporting an assignment of U^{V}(Mes$_3$TPA)Cl$_2$. Confirmation of the structure of this product was not obtained due to poor stability.

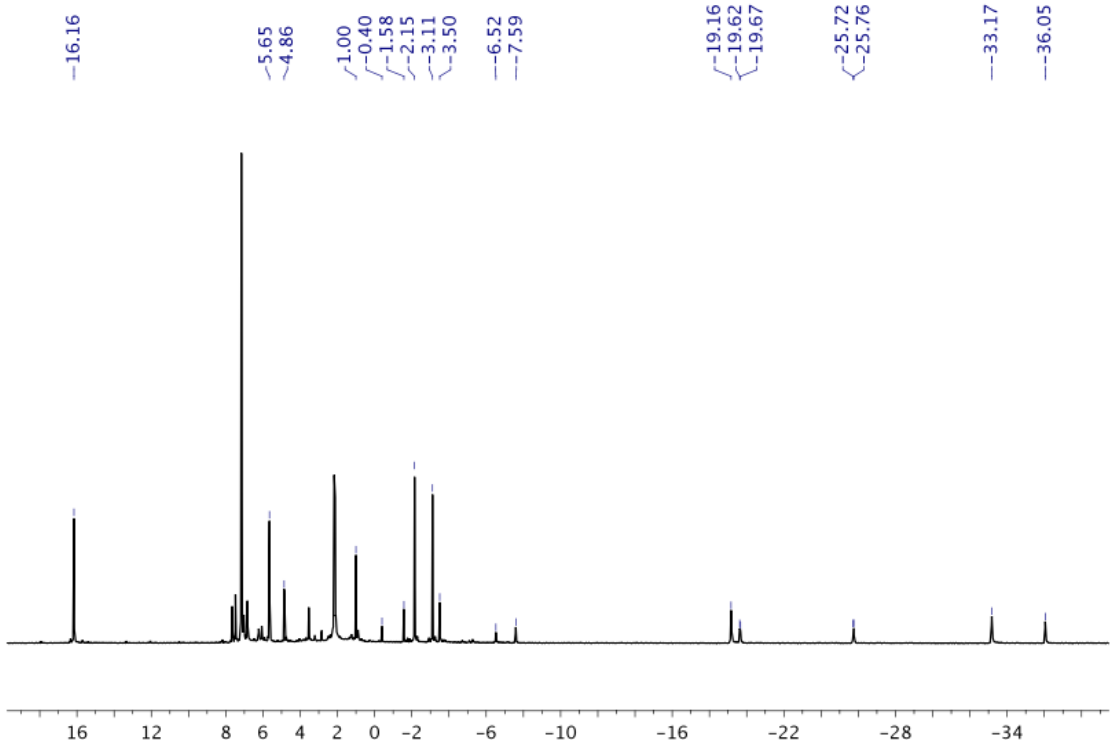

Figure 5.4.1.4 ^{1}H NMR of putative product $U^{V}(Mes_3TPA)Cl_2$.

Attempts to oxidize the uranium(III) center in **5.5** with phosphorus ylide also met with limited success. Addition of 1 equiv Ph_3PCH_2 to **5.5** in THF led to a color change to dark green, and formation of a single product by identified by ^{1}H NMR spectroscopy. Recrystallization of this product from a toluene solution layered with hexanes at –25 °C produced black crystals of $U^{III}(Mes_3TPA)(CH_2PPh_3)(THF)$ (**5.8**). The X-ray structure revealed the surprising coordination of both the ylide ligand as well as a THF ligand, in contrast to the single THF ligand bound to **5.6** (Figure 5.4.1.5). The thermal stability of **5.8** was poor, with gradual loss of PPh_3 observed over time at room temperature as judged by the appearance of a resonance at –5.2 ppm in the ^{31}P NMR spectrum. Addition of a second equivalent of Ph_3PCH_2 led to a color change to brown, with some PPh_3 formation noted. The ^{1}H NMR spectrum of the resulting brown product was invariably extremely convoluted regardless of the reaction conditions investigated, including variation of solvent, reaction temperature, and time. No identifiable product was obtained from any of these reactions.

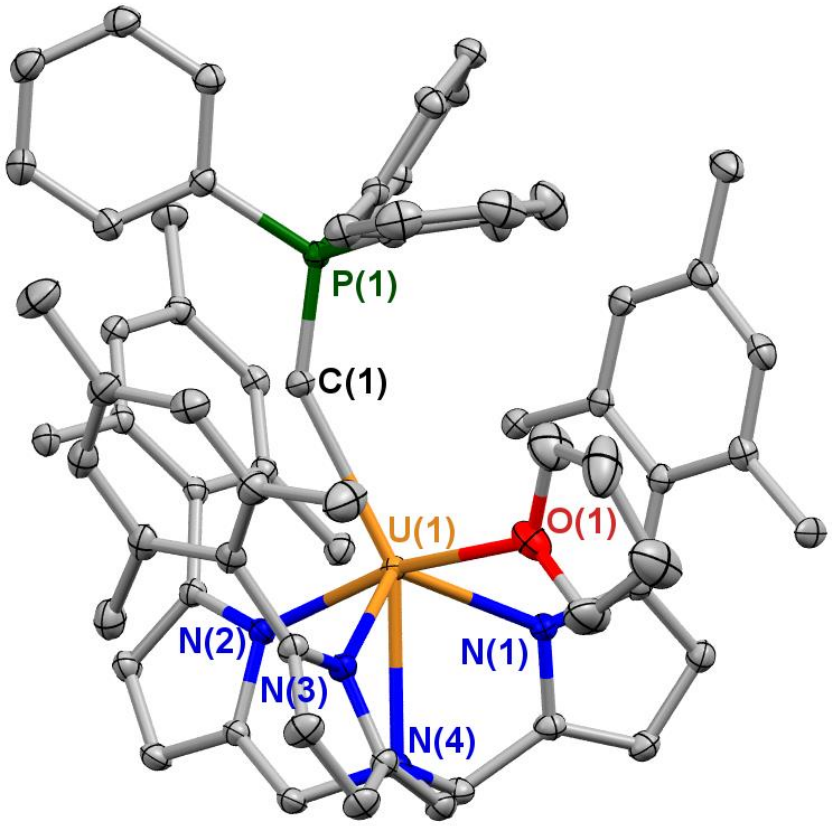

Figure 5.4.1.5 Thermal ellipsoid plot of $U^{III}(Mes_3TPA)(CH_2PPh_3)(THF)$ (**5.8**) at 30% probability. Hydrogen atoms are omitted for clarity. Selected bond metrics are listed in Table 5.4.1.1.

While the chemistry of uranium(IV) with deprotonated ylide ligands was well established in the work of Gilje and Cramer,[52-69] prior to the synthesis of **5.8**, no uranium(III) ylide adduct had been reported. More recently, the reactivity of $U^{III}[N(SiMe_3)_2]_3$ with Ph_3PCH_2 was explored by Hayton and coworkers,[70] where unstable $U^{III}(CH_2PPh_3)[N(SiMe_3)_2]_3$ was shown to undergo loss of 0.5 equiv PPh_3 to form $U^{IV}(CHPPh_3)[N(SiMe_3)_2]_3$ and $U^{IV}(CH_3)[N(SiMe_3)_2]_3$ through a proposed intermolecular hydrogen atom transfer route. A similar reactivity pathway is likely operative in the decomposition of **5.8**.

5.4.2 ^{1}H NMR Spectra.

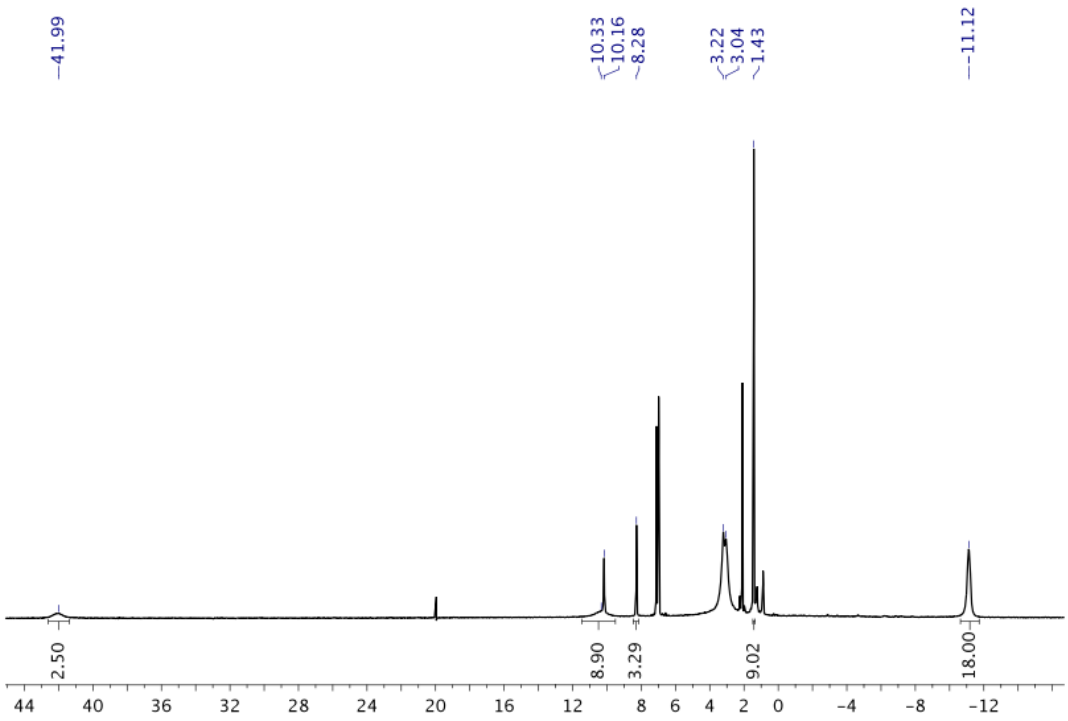

Figure 5.4.2.1 ^{1}H NMR spectrum of **5.5** in toluene-d_8.

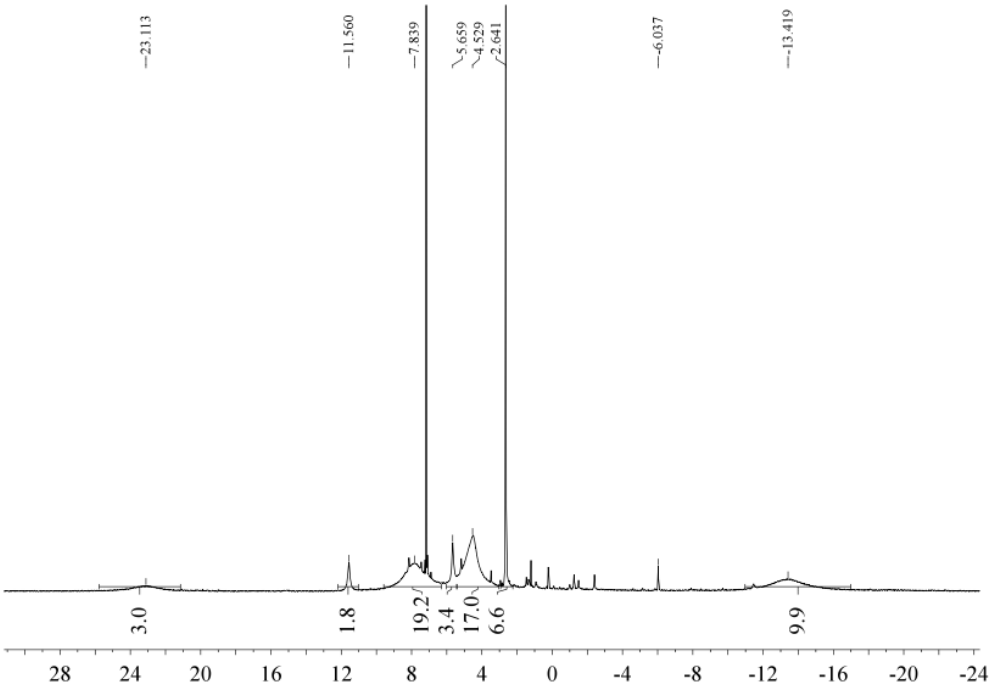

Figure 5.4.2.2 ^{1}H NMR spectrum of **5.6** in benzene-d_6.

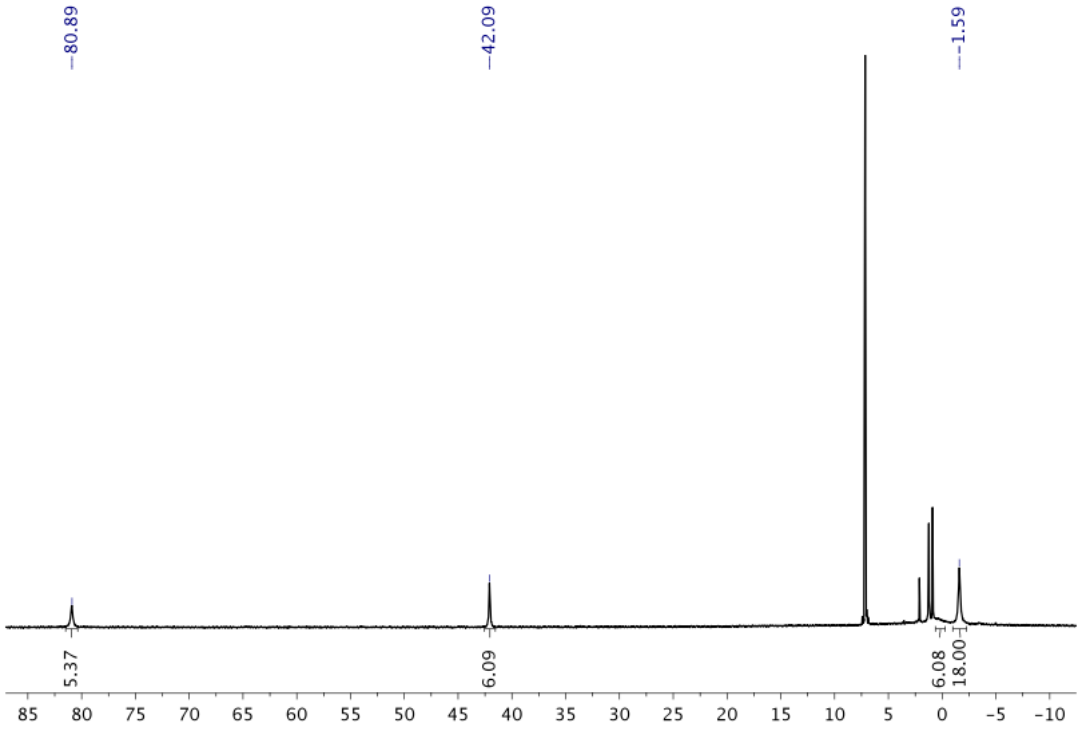

Figure 5.4.2.3 ^{1}H NMR spectrum of **5.7** in benzene-d_6.

5.5 Rare Earth Complexes of the Mes$_3$TPA^{3-} Ligand. Having successfully controlled the coordination environment at a reactive uranium center, the Mes$_3$TPA^{3-} ligand was also applied to the coordination chemistry of the lanthanides. Addition of 1 equiv K$_3$Mes$_3$TPA to a DME solution of CeCl$_3$ led to the slow formation of Ce^{III}(Mes$_3$TPA)(DME) (**5.9**) as a colorless product. Recrystallization from a DME solution layered with hexanes at –35 °C allowed for structural characterization, revealing a geometry isostructural to **5.5**. Due to the close match of the ionic radii at 1.025 and 1.01 Å for 6-coordinate uranium(III) and cerium(III) respectively,[71] the unit cell parameters of **5.5** and **5.9** were almost identical.

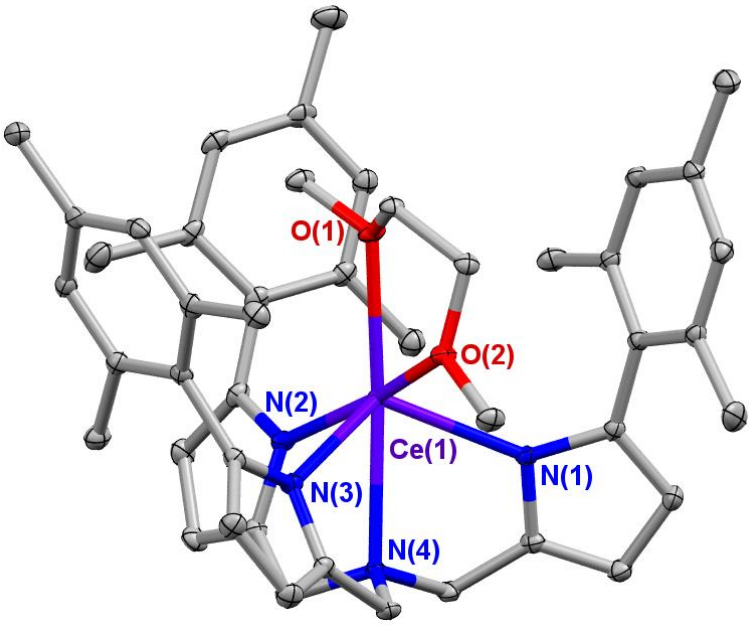

Figure 5.5.1 Thermal ellipsoid plot of **5.9** at 30% probability. Hydrogen atoms are omitted for clarity. Bond distances (Å) and angles (°): Ce(1)–N(1) 2.399(3), Ce(1)–N(2) 2.430(3), Ce(1)–N(3) 2.452(3), Ce(1)–N(4) 2.606(3), Ce(1)–O(1) 2.559(3), Ce(1)–O(2) 2.571(3), N(4)–Ce(1)–N_{pyr} 66.29(13), N(4)–Ce(1)–O(1) 117.14(10), N(4)–Ce(1)–O(2) 172.21(10).

Oxidation of **5.9** was attempted with a variety of oxidants, such as I_2, $CuCl_2$, and *p*-benzoquinone, all of which primarily produced free H_3Mes_3TPA. The sensitivity of pyrrolyl ligands towards oxidizing conditions is now well known;[72] it is likely that the cerium(III) ion does not sufficiently stabilize an intermediate ligand-centered radical, which undergoes hydrogen atom abstraction as a mechanism of decomposition. With this limitation in mind, we instead pursued reducing conditions. Treatment of **5.9** with 1 equiv 2,2'-bipyridine (bpy) led to an immediate color change to light orange attributed to formation of $Ce^{III}(Mes_3TPA)(bpy)$ (**5.10**). The orange solution was then transferred to a vial mirrored with excess K^0 metal, leading to a slow color change to dark magenta. Recrystallization of the magenta product from a DME solution layered with hexanes at –21 °C revealed the structure to be $[K(DME)_4][Ce^{III}(Mes_3TPA)(bpy)]$ (**5.11**).

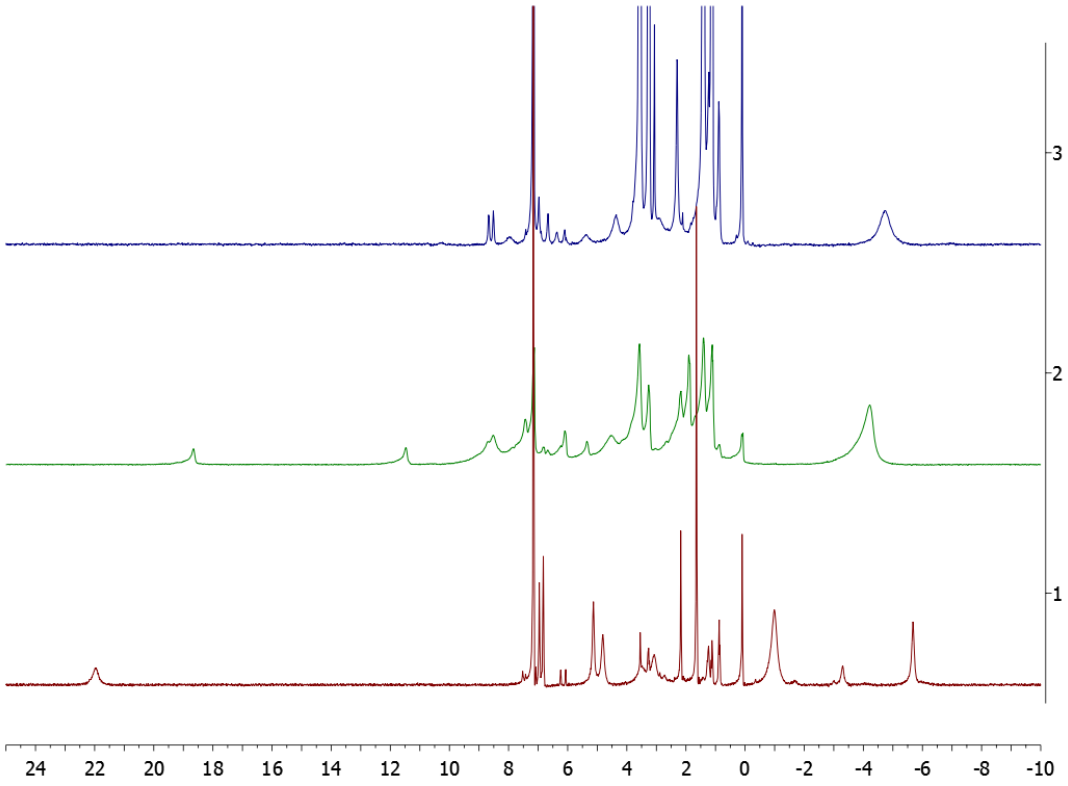

Figure 5.5.2 ^{1}H NMR spectrum of **5.9** (bottom), **5.10** (middle), and **5.11** (top), illustrating bpy adduct formation and reduction.

The X-ray structure of **5.11** was consistent with a one-electron reduced bpy$^{\cdot-}$ ligand bound to a cerium(III) ion. Neutral cerium(III) complexes of bpy$^{\cdot-}$ have been reported,[73, 74] though no anionic examples are known. The internal bond metrics of the bpy$^{\cdot-}$ ligand in **5.11** are consistent with those in $(C_5Me_5)_2Ce(bpy)$, supporting the assignment.[74] The single electron stored in the bipyridyl ligand is capable of facilitating multi-electron transfer reactions, potentially providing new routes to otherwise inaccessible cerium(IV) complexes. A similar strategy has been implemented in work from Walter and coworkers, where thorium bound to a doubly reduced bpy^{2-} ligand acts as a "Th(II)" synthon, facilitating the synthesis of thorium-imido, -oxo, and -sulfido moieties.[75, 76] This reactivity has been demonstrated a number of times in uranium chemistry, recently in the conversion of a U(III)-bpy$^{\cdot-}$ complex to a U(IV)-oxo multiple bond.[77]

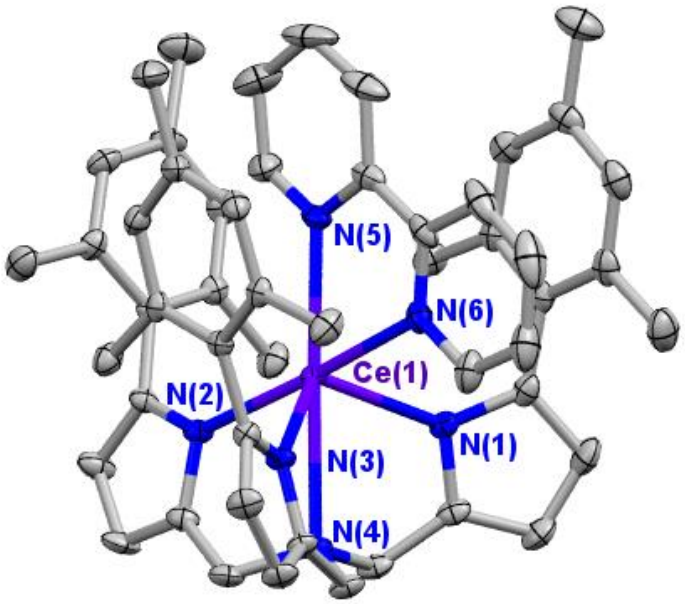

Figure 5.5.3 Thermal ellipsoid plot of **5.11** at 30% probability. Hydrogen atoms and $[K(DME)_4]^+$ counter-ion are omitted for clarity. Bond distances (Å) and angles (°):Ce(1)–N(1) 2.4499(17), Ce(1)–N(2) 2.4541(18), Ce(1)–N(3) 2.5566(17), Ce(1)–N(4) 2.6960(17), Ce(1)–N(5) 2.4798(18), Ce(1)–N(6) 2.5545(19), N(4)–Ce(1)–N_{pyr} 66.38(7), N(4)–Ce(1)–N(5) 178.04(6), N(4)–Ce(1)–N(6) 114.66(6).

The synthesis of **5.9** was adapted to other rare earth metals as well. Treatment of $TbCl_3$ or YCl_3 with 1 equiv K_3Mes_3TPA in DME gave Tb(Mes_3TPA)(DME) (**5.12**) and Y(Mes_3TPA)(DME) (**5.13**) respectively. Crystallization of both **5.12** and **5.13** from DME solutions layered with hexanes at –35 °C allowed for X-ray structural analysis (Figures 5.5.4 and 5.5.5). The ionic radii of the complexes **5.5**, **5.9**, **5.12**, and **5.13** span from 0.9 Å in **5.13** to 1.025 Å in **5.5**, causing minor differences in crystal packing, but isostructural coordination environments. The strongly paramagnetic Tb(III) ion caused the ^{1}H NMR spectrum of **5.12** to exhibit dramatically shifted resonances, in the range of +246 to –123 ppm. The ^{1}H NMR spectrum of diamagnetic **5.13** was comparably easily interpretable.

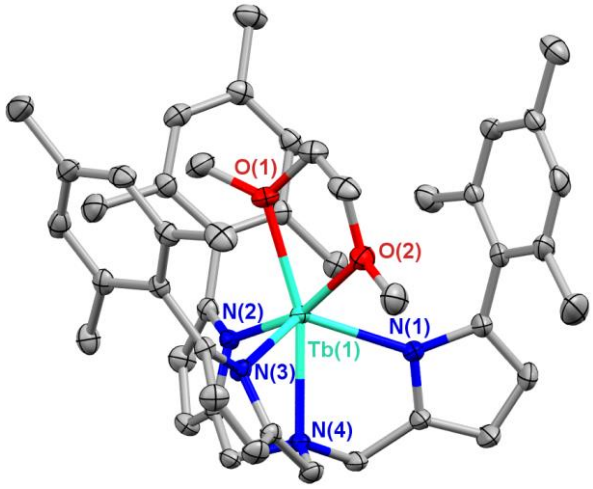

Figure 5.5.4 Thermal ellipsoid plot of **5.12** at 30% probability. Hydrogen atoms are omitted for clarity. Bond distances (Å) and angles (°): Tb(1)–N(1) 2.338(3), Tb(1)–N(2) 2.351(3), Tb(1)–N(3) 2.366(3), Tb(1)–N(4) 2.461(3), Tb(1)–O(1) 2.380(3), Tb(1)–O(2) 2.422(3), N(4)–Tb(1)–N_{pyr} 70.88(13), N(4)–Tb(1)–O(1) 123.09(10), N(4)–Tb(1)–O(2) 163.19(10).

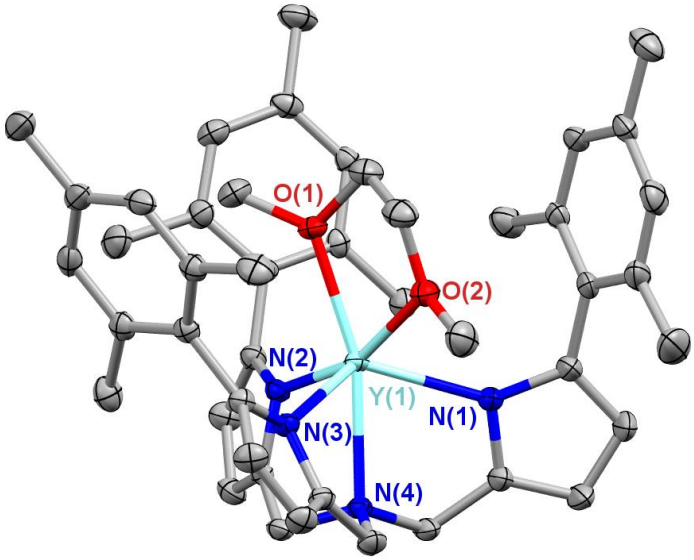

Figure 5.5.5 Thermal ellipsoid plot of **5.13** at 30% probability. Hydrogen atoms are omitted for clarity. Bond distances (Å) and angles (°): Y(1)–N(1) 2.324(3), Y(1)–N(2) 2.334(3), Y(1)–N(3) 2.358(3), Y(1)–N(4) 2.421(3), Y(1)–O(1) 2.334(2), Y(1)–O(2) 2.391(2), N(4)–Y(1)–N_{pyr} 71.78(11), N(4)–Y(1)–O(1) 123.54(9), N(4)–Y(1)–O(2) 163.17(9).

In the course of investigating the oxidation chemistry of **5.9**, the reaction with TEMPO (2,2,6,6-tetramethylpiperidine-*N*-oxyl) was attempted. TEMPO was shown to be an effective ligand in homoleptic complexes with samarium in work from Evans and coworkers.[78] Upon addition of TEMPO to **5.9**, a color change to an intense dark red was observed. The ^{1}H NMR spectrum of an aliquot showed an apparent diamagnetic product. Crystallization of a DME

solution layered with hexanes at –35 °C produced red crystals identified by X-ray structural analysis to be [K(DME)$_4$][Ce^{III}(Mes$_3$TPA)(TEMPO)] (**5.14**, Figure 5.5.6), a decidedly paramagnetic species. Reanalysis of the ^{1}H NMR spectrum showed extremely broad paramagnetically shifted resonances presumably attributable to **5.14**. The TEMPO ligand of **5.14** was assigned as the product one-electron reduction on the basis of bond lengths and charge balance considerations. The unidentified "diamagnetic" product observed in the ^{1}H NMR spectrum was assumed to be the corresponding oxidation product. The presence of K^+ in the crystallized product was attributed to adventitious residual KCl in the sample of **5.9**. Indeed, addition of TEMPO to a sample of **5.9** prepared from a protonolysis route that avoided the generation of KCl led to no reaction.

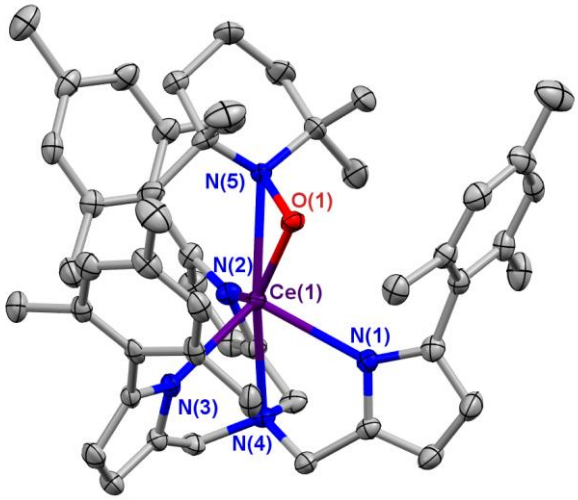

Figure 5.5.6 Thermal ellipsoid plot of **5.14** at 30% probability. Hydrogen atoms are omitted for clarity. Bond distances (Å) and angles: Ce(1)–N(1) 2.517(3), Ce(1)–N(2) 2.533(3), Ce(1)–N(3) 2.559(3), Ce(1)–N(4) 2.638(3), Ce(1)–N(5) 2.581(3), Ce(1)–O(1) 2.231(3), O(1)–N(5) 1.435(4), N(4)–Ce(1)–N$_{pyr}$ 66.43(13), N(4)–Ce(1)–O(1) 154.22(11), N(4)–Ce(1)–N(5) 163.57(10).

In an effort to determine whether the unidentified side product produced in the reaction to form **5.14** may contain Ce(IV), we also considered the same reactivity at redox inactive **5.12**. Addition of TEMPO to **5.12** similarly generated an intense red color, and crystallization of a DME solution layered with hexanes at –35 °C allowed for structural characterization of the product as [K(DME)$_4$][Tb^{III}(Mes$_3$TPA)(TEMPO)] (**5.15**, Figure 5.5.7). The resonances corresponding to the diamagnetic oxidation product in the reaction that produced **5.14** were also noted in the synthesis of **5.15**. Based on this evidence we conclude that in the presence of KCl, TEMPO induces ligand

based oxidation to generate an unidentified organic decomposition product, and the side-product K(TEMPO) undergoes „-ate" complex formation with **5.9**. Alternative procedures to generate **5.14** or **5.15**, such as treatment of **5.9** with K(TEMPO) or addition of TEMPO to **5.11**, were not pursued.

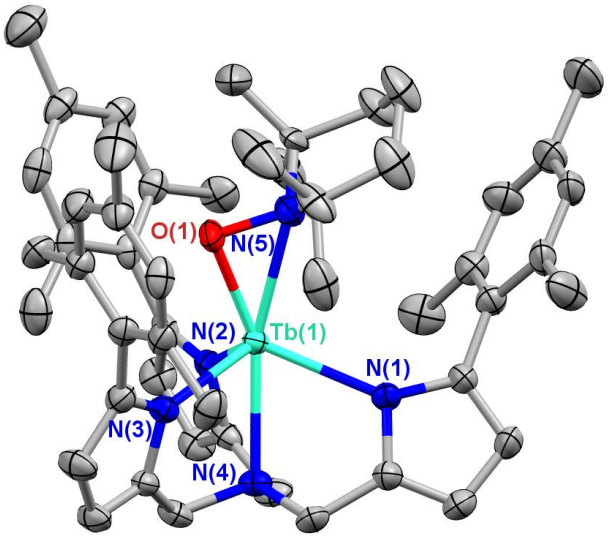

Figure 5.5.7 Thermal ellipsoid plot of **5.15** at 30% probability. Hydrogen atoms are omitted for clarity. Bond distances (Å) and angles (°): Tb(1)–N(1) 2.409(6), Tb(1)–N(2) 2.435(6), Tb(1)–N(3) 2.455(6), Tb(1)–N(4) 2.503(6), Tb(1)–N(5) 2.490(7), Tb(1)–O(1) 2.140(5), O(1)–N(5) 1.416(8), N(4)–Tb(1)–N_{pyr} 68.8(2), N(4)–Tb(1)–O(1) 156.2(2), N(4)–Tb(1)–N(5) 164.2(2).

5.6 Synthesis of $H_3{}^t$BuXyl$_3$TPA and U^{III}(^{t}BuXyl$_3$TPA). The stable uranium(III)-Ph_3PCH_2 adduct in **5.8** led us to pursue methods to facilitate the two-electron process that would lead to formation of the uranium(V) methylidene product. That **5.5** did not undergo redox reactivity with a single equivalent of ylide led us to the conclusion that either the metal center was not sufficiently electron rich, or that the intermediate was not sufficiently destabilized. In an effort to address both of these issues, the ligand $H_3{}^t$BuXyl$_3$TPA was prepared (^{t}BuXyl = 4-*tert*-butyl-2,6-dimethylphenyl). The synthesis of 2-^{t}BuXylpyrrole was carried out following conditions analogous to the known 2-arylpyrrole derivatives, with the exception that it was isolated as a viscous yellow oil following distillation, contrary to the other derivatives that were isolated by sublimation as colorless crystalline solids. Assembly of the tripodal ligand scaffold through the Mannich reaction with NH_4Cl and formaldehyde proceeded in high yield.

Addition of 1 equiv K$_3$^{t}BuXyl$_3$TPA to a DME solution of UI$_3$ cleanly generated a hexanes-soluble dark purple product. Crystallization of this product from hexanes revealed the structure to be U^{III}(Mes$_3$TPA)(DME) (**5.16**, Figure 5.6.1), roughly isostructural to **5.5**. The three *tert*-butyl functionalities sterically block the coordination site above the trigonal pocket formed by the arene groups, as expected. However, reaction of **5.16** with Ph$_3$PCH$_2$ led to immediate decomposition to intractable, insoluble products under various conditions.

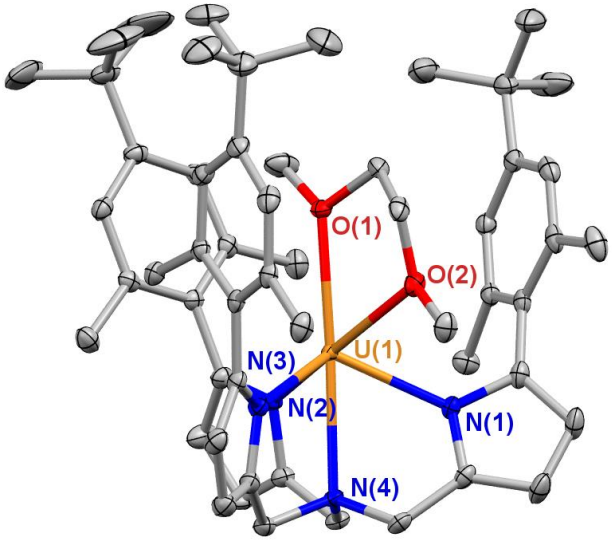

Figure 5.6.1 Thermal ellipsoid plot of **5.16** at 30% probability. Hydrogen atoms are omitted for clarity. Bond distances (Å) and angles (°):U(1)–N(1) 2.397(2), U(1)–N(2) 2.433(2), U(1)–N(3) 2.445(2), U(1)–N(4) 2.612(2), U(1)–O(1) 2.5813(18), U(1)–O(2) 2.5904(17), N(4)–U(1)–N$_{pyr}$ 67.10(9), N(4)–U(1)–O(1) 118.18(6), N(4)–U(1)–O(2) 176.73(6).

The reactivity of **5.16** as a reductant was screened with various reagents. Treatment of **5.16** with 5 equiv CuI led to rapid color change to red-orange consistent with formation of a uranium(IV) product. Comparison of the ^{1}H NMR spectrum with that of **5.6** showed good agreement, suggesting that the intended product U^{IV}(^{t}BuXyl$_3$TPA)(THF)I was formed. Reaction of UCl$_4$ with 1 equiv K$_3$^{t}BuXyl$_3$TPA produced the analogous complex U^{IV}(^{t}BuXyl$_3$TPA)(THF)Cl (**5.17**) in 68% yield, which also exhibited similar resonances in the ^{1}H NMR spectrum, supporting the assignment of U^{IV}(^{t}BuXyl$_3$TPA)(THF)I. Treatment of **5.16** with 1 equiv I$_2$ produced a dark red product that exhibited a highly desymmetrized ^{1}H NMR spectrum similar to the putative product U^V(Mes$_3$TPA)Cl$_2$ proposed in Section 5.4.1, with no evidence for the aforementioned

U^{IV}(^{t}BuXyl$_3$TPA)(THF)I product. Similarly, addition of pyridine-*N*-oxide to a THF solution of **5.16** led to a color change to dark red-brown, with a dramatic shift in the ^{1}H NMR spectrum. The minimal number of resonances suggested a symmetric product, tentatively assigned as U^V(^{t}BuXyl$_3$TPA)(py)O.

5.7 Experimental. Starting materials: Pyrrolylsodium,[42] Ar^{F}pyrrole,[42] Mes-pyrrole,[42] H$_3$Mes$_3$TPA,[44] 2-bromo-5-(tert-butyl)-1,3-dimethylbenzene (^{t}BuXyl-Br),[79] prepared according to literature procedures.

5.7.1 H$_3$Ar$^F_3$TPA. The reported synthesis[4] was adapted as follows: A 500 mL Schlenk flask was charged with 2-Ar^{F}pyrrole (22.53 g, 80.7 mmol, 3 equiv), formaldehyde (2.42 g, 80.7 mmol, 37% w/w solution in H_2O, 3 equiv), and ammonium chloride (1.44 g, 26.9 mmol, 1 equiv) in 38 mL EtOH/H_2O (70% by volume). The mixture was purged with nitrogen three times followed by heating at 60 °C under nitrogen for 24 h with vigorous stirring, which induced precipitation of a white solid. The precipitate was collected by filtration over a fine porosity fritted filter and washed with 40 mL of cold ethanol (0 °C) until the pink filtrate ran colorless. The solid was transferred to a 1 L separatory funnel, to which 320 mL of 20% NaOH and 500 mL of dichloromethane were added. After vigorous shaking, the organic layer was collected and the aqueous layer was extracted with 2 × 125 mL dichloromethane. The combined organics were dried over $MgSO_4$, filtered, and concentrated under reduced pressure to yield an off-white solid (Yield 22.60 g, 25.4 mmol, 94%). The ^{1}H and ^{19}F NMR data were consistent with reported values for the compound.[4]

5.7.2 K$_3$Ar$^F_3$TPA(THF)$_{1.5}$. A solution of H$_3$Ar$^F_3$TPA (5.00 g, 5.61 mmol) dissolved in 35 mL THF was prepared in a 125 mL Erlenmeyer flask. Potassium hydride (1.35 g, 33.67 mmol, 6 equiv) was added in small quantities resulting in vigorous bubbling and a color change to brown. The reaction was stirred at room temperature overnight. Residual KH was removed by filtration over a Celite-packed coarse porosity fritted filter and the volatiles were removed under reduced pressure to yield K$_3$Ar$^F_3$TPA(THF)$_{1.5}$ as a tan solid. On storage at room temperature the solid is unstable, as evident by a slow color change to dark purple. The solid can be stored indefinitely without decomposition at –25 °C. Yield: 4.9 g, 4.4 mmol, 98%. ^{1}H NMR (tetrahydrofuran-d_8): δ

7.98 (6H, Ar^F *o*-CH), 7.22 (3H, Ar^F *p*-CH), 6.59 (3H, pyr-H), 6.10 (3H, pyr-H), 3.62 (6H, THF), 3.53 (6H, CH_2), 1.78 (6H, THF). ^{19}F NMR (benzene-d_6): δ –63.49 (18F).

5.7.3 U^{III}(Ar$^F_3$TPA)(py)$_3$ (5.1). A solution of $K_3Ar^F_3TPA(THF)_{1.5}$ (1.80 g, 1.6 mmol, 1 equiv) in 25 mL of THF was prepared in a 125 mL vacuum flask and chilled to –25 °C. The dark brown solution was then added dropwise over 20 minutes to a stirred solution of UI_3 (1.00 g, 1.6 mmol, 1 equiv) dissolved in a mixture of 20 mL of THF and 0.5 mL pyridine at –25°C. Upon addition, the mixture turned green-black with precipitation of a white solid. This solution was allowed to warm to room temperature while stirring over 45 minutes, then cooled to –25 °C to precipitate KI. Filtration through Celite on a coarse porosity fritted filter followed by concentration of the black filtrate under reduced pressure produced a black, oily residue. Extraction of this solid with toluene followed by filtration through Celite and removal of the volatiles under reduced pressure produced a green-black solid. The black-green solid was dissolved in minimal toluene, layered with hexane, and stored at –25 °C overnight yielding black, crystalline needles. Crystals of **5.1** disintegrated under vacuum due to loss of pyridine, consistent with the observed elemental analysis. Yield: 1.21 g, 0.89 mmol, 55%. ^{1}H NMR (benzene-d_6): δ 12.27 (8H), 9.42 (6H), 6.98 (3H), 6.19 (8H), 4.32 (3H), 4.17 (3H), 0.72 (4H), –0.88 (6H). ^{19}F NMR (benzene-d_6): δ –65.84 (18F). Analysis calculated for $C_{39}H_{21}F_{18}N_4U{\cdot}2.5C_5H_5N$: C, 46.74; H 2.55; N, 6.88. Found: C, 46.48; H, 2.92; N, 6.43.

5.7.4 [K(py)$_5$]$_2$[U^{IV}(Ar$^F_3$TPA)$_2$] (5.2). $K_3Ar^F_3TPA(THF)_{1.5}$ (0.30 g, 0.27 mmol, 1.5 equiv) dissolved in a mixture of 3 mL of THF and 1 mL of pyridine was added to a stirred solution of UI_3 (0.11 g, 0.18 mmol, 1 equiv) in THF at room temperature, producing a cloudy green solution. Heating this solution to 50 °C resulted in the rapid color change to brown. After stirring for one hour, the reaction mixture was filtered over Celite packed on a coarse porosity frit, and the brown filtrate was concentrated under reduced pressure to a brown residue. This residue was extracted with minimal Et_2O, filtered, and stored at –25 °C. Bright yellow crystals of **5.2** were isolated in two crops. Crystals satisfactory for X-ray diffraction were grown from a mixture of toluene, pyridine, and hexane cooled to –25 °C. Crystals of **5.2** disintegrated under vacuum due to loss of pyridine,

consistent with the observed elemental analysis. Yield: 0.27 g, 0.12 mmol, 52% (based on UI_3). ^{1}H NMR (pyridine-d_5): δ 17.50 (12H), 15.11 (6H), 7.80 (6H), 1.38 (6H), –25.27 (6H), –30.22 (6H). ^{19}F NMR (pyridine-d_5): δ –59.88 (18F), –61.43 (18F). Analysis calculated for $C_{78}H_{42}F_{36}K_2N_8U\cdot3C_5H_5N$: C, 47.97; H, 2.47; N 6.62. Found: C, 48.02; H, 2.82; N, 6.64.

5.7.5 $U^{IV}(Ar^F_3TPA)(py)_2Cl$ (5.3). $K_3Ar^F_3TPA(THF)_{1.5}$ (0.50 g, 0.45 mmol, 1 equiv) dissolved in a mixture of 6 mL of THF and 0.5 mL pyridine was chilled to –25 °C. The mixture was slowly added to a stirred solution of UCl_4 (0.17 g, 0.45 mmol, 1 equiv) in 10 mL of THF that had been chilled to –25 °C, resulting in the immediate formation of a cloudy, dark red suspension. The dark red suspension was stirred for 40 minutes, filtered through Celite on a coarse porosity fritted filter and concentrated under reduced pressure to a red-brown solid. The solid was extracted with toluene, filtered, layered with pentane, and stored at –25 °C. Crystals of **5.3** were obtained from the toluene/pentane mixture in two crops as red blocks. Yield: 0.38 g, 0.29 mmol, 68%. ^{1}H NMR (pyridine-d_5, 62 ºC): δ 14.34 (3H), 6.59 (3H), 6.05 (3H), 2.72 (6H), –16.16 (6H). ^{19}F NMR (pyridine-d_5, 62 ºC): δ 65.16 (18F). ^{19}F NMR (benzene-d_6, 25 ºC) –66.49 (18F). Elemental analysis was performed on a sample prepared analogously using pyridine-d_5. Analysis calculated for $C_{49}H_{21}D_{10}ClF_{18}N_6U$: C, 44.27; H, 3.11; N, 6.32. Found: C, 44.06; H, 2.80; N, 5.94.

5.7.6 $U^{IV}(Ar^F_3TPA)(pyNO)_2Cl$ (5.4). To a stirred solution of **5.3** (0.025 g, 0.02 mmol) in 5 mL of THF, a solution of pyridine *N*-oxide (0.004 g, 0.04 mmol, 2 equiv) dissolved in THF was added, resulting in an immediate color change to yellow-green. After ~5 minutes the volatiles were removed under reduced pressure leaving a yellow-green residue. The residue was dissolved in a 1:1 mixture of toluene and hexane, filtered through celite, and stored at –25 °C. Crystals of **5.4** were isolated as green-yellow plates. Yield: 0.023 g, 90%. ^{1}H NMR (toluene-d_8): δ 37.15 (6H), 15.29 (6H), 14.64 (3H), 8.41 (4H), 4.62 (6H), –24.93 (6H). ^{19}F NMR (toluene-d_8): δ –66.29 (18F). Analysis calculated for $C_{49}H_{31}ClF_{18}N_6O_2U\cdot1.5C_5H_5N$: C, 46.17; H, 2.64; N, 7.15. Found: C, 46.45; H, 2.62; N, 6.99.

5.7.7 $U^{III}(Mes_3TPA)(DME)$ (5.5). To a solution of UI_3 (1.83 g, 2.96 mmol) in 40 mL DME, a solution of K_3Mes_3TPA (2.14 mg, 2.96 mmol, 1.0 equiv) was added, producing a dark purple

solution. After stirring 15 h, visible colorless precipitate was filtered on Celite on a coarse fritted filter and the solution was concentrated to minimal volume to a saturated solution. An equal volume of hexanes was added, and the mixture was stored at –25 °C for one week. The green-black supernatant was decanted and discarded. The recrystallized purple multi-crystalline solid was isolated, and volatiles were removed under reduced pressure to yield **5.5**. Yield: 2.05 g, 2.20 mmol, 74%. ^{1}H NMR (toluene-d_8): δ 42.0 (3H), 10.3 (3H), 10.2 (6H), 8.3 (3H), 1.4 (9H), 11.1 (18H).

5.7.8 U^{III}(Mes$_3$TPA)(THF) (5.6). To a solution of UI_3 (0.856 g, 1.38 mmol) in 30 mL THF, a solution of K_3Mes_3TPA (1.00 g, 1.38 mmol, 1.0 equiv) was added, producing a dark blue solution. After stirring 12 h, the solution was filtered through Celite on a coarse fritted filter. Following removal of volatiles under reduced pressure, dissolved residual black solid in hexanes, and filtered through Celite on a coarse fritted filter. Volatiles were removed under reduced pressure to yield dark blue **5.6** as a powder. Yield: 1.07 g, 1.17 mmol, 84%. ^{1}H NMR (benzene-d_6): δ 23.1 (3H), 11.6 (3H), 7.8 (18H), 5.7 (3H), 4.5 (16H), 2.6 (6H), –13.4 (9H).

5.7.9 U^{IV}(Mes$_3$TPA)(THF)Cl (5.7). To a solution of K_3Mes_3TPA (1.37 g, 1.89 mmol, 1.0 equiv) in 25 mL THF in a 125 mL side-arm flask, UCl_4 (720 mg, 1.89 mmol) was added, resulting in an immediate color change to dark red. After stirring 24 h, volatiles were removed under reduced pressure. The resulting red solid residue was dissolved in toluene, leaving a colorless precipitate that was filtered through Celite on a coarse fritted filter. The filtrate was concentrated to 20 mL, then layered with 50 mL hexanes and stored at –25 °C to produce a red solid, which was collected after 24 h on a medium fritted filter and washed with hexanes to yield **5.7** as a red powder. Yield: 1.10 g, 1.16 mmol, 61%. ^{1}H NMR (benzene-d_6): δ 81.0, 42.1, –1.6; only 3 peaks were observable at room temperature.

5.7.10 U^{III}(Mes$_3$TPA)(CH$_2$PPh$_3$)(THF) (5.8). To a mixture of **5.5** (800 mg, 0.86 mmol) and Ph_3PCH_2 (284 mg, 1.03 mmol, 1.2 equiv) in a 125 mL side arm flask, 30 mL toluene was added. After stirring 6 hours, the resulting dark green solution was filtered through Celite on a coarse fritted filter, separating an insoluble light brown solid. Removal of volatiles under reduced

pressure provided crude **5.8** as a green-black solid, with good purity as a judged by ^{1}H NMR. Yield: 770mg, 0.65 mmol, 75%. Single crystals of **5.8** were obtained from a toluene solution layered with hexanes stored at –25 °C. ^{1}H NMR (benzene-d_6): δ 37.3 (3H), 32.8 (3H), 20.2 (9H), 13.3 (6H), 9.4 (9H), 9.0 (6H), 4.1 (6H), 3.1 (18H); the methylene resonance of the ylide ligand was not identified.

5.7.11 Ce^{III}(Mes$_3$TPA)(DME) (5.9).

5.7.11a *From CeCl$_3$.* To a vial containing K_3Mes_3TPA (1.5 g, 2.1 mmol, 1.0 equiv) and $CeCl_3$ (511 mg, 2.07 mmol), 40 mL DME was added. The mixture was stirred 20 hours, and then filtered through Celite on a coarse fritted filter to yield a light orange filtrate. Removal of volatiles under reduced pressure gave **5.12** as a light tan foam of good purity. Crystalline **5.12** was obtained by layering a DME solution with hexanes at –35 °C). Yield: 1.43 g, 1.7 mmol, 81%.

5.7.11a *From Ce[N(SiMe$_3$)$_2$]$_3$.* To a 50 mL glass bomb, $Ce[N(SiMe_3)_2]_3$ (674 mg, 1.08 mmol) and H_3Mes_3TPA (660 mg, 1.08 mmol, 1.0 equiv) were dissolved in 15 mL DME. The mixture was heated and stirred at 60 °C for 5 h, then cooled and returned to the glovebox. The mixture was filtered through Celite on a coarse fritted filter, and volatiles were removed under reduced pressure. The resulting tan residue was dissolved in minimal DME then layered with hexanes and stored at –25 °C, affording **5.9** as a tan solid. Yield: 660 mg, 0.79 mmol, 73%.^{1}H NMR (benzene-d_6): δ 21.9 (4H), 7.0 (3H), 6.8 (3H), 5.1 (6H), 4.8 (6H), 1.7 (9H), –1.0 (18H), –5.7 (6H). Elemental analysis found (calculated) for $C_{46}H_{55}CeN_4O_2$: C, 66.20 (66.08); H, 6.71 (6.63); N, 7.09 (6.70).

5.7.12 [K(DME)$_4$][Ce^{III}(Mes$_3$TPA)(bipy)] (5.11). To a solution of **5.9** (250 mg, 0.3 mmol) in 3 mL THF, 2,2'-bipyridine (47 mg, 0.3 mmol, 1.0 equiv) was added, resulting in a color change to pale orange. After 15 min, the solution was transferred to a vial mirrored with K^0 (58 mg, 1.5 mmol, 5.0 equiv). The solution turned dark maroon, and was allowed to stir for 20 min, at which point volatiles were removed under reduced pressure. The resulting dark residue was dissolved in DME, filtered through Celite suspended in a pipet, and then concentrated to 2 mL and layered with 12 mL hexanes. Storage at –25 °C yielded dark maroon crystals of **5.11**, which were rinsed

with hexanes. Yield: 310 mg, 0.24 mmol, 80%. ^{1}H NMR (benzene-d_6): δ 21.9 (4H), 7.0 (3H), 6.8 (3H), 5.1 (6H), 4.8 (6H), –1.0 (18H), –5.7 (6H).

5.7.13 Tb^{III}(Mes$_3$TPA)(DME) (5.12). To a vial containing K$_3$Mes$_3$TPA (500 mg, 0.69 mmol, 1.0 equiv) and TbCl$_3$ (183 mg, 0.69 mmol), 20 mL DME was added. The mixture was stirred 24 hours, and then filtered through Celite on a coarse fritted filter to yield a grapefruit colored filtrate. Removal of volatiles under reduced pressure gave a light pink residue, which was dissolved in minimal DME, filtered, and layered with hexanes to yield almost colorless plates of **5.12**. Yield: 330 mg, 0.39 mmol, 56%. ^{1}H NMR (benzene-d_6): δ 246.1, 6.3, –0.8, –5.0, –10.7, –40.0, –58.2, -123.3. Integration was not feasible due to extreme spectral broadening in this compound from significant paramagnetism.

5.7.14 Y^{III}(Mes$_3$TPA)(DME) (5.13). To a vial containing K$_3$Mes$_3$TPA (250 mg, 0.35 mmol, 1.0 equiv) and YCl$_3$ (68 mg, 0.35 mmol), 10 mL DME was added. The pale orange-pink cloudy mixture was stirred 16 h, then concentrated and filtered through Celite on a coarse fritted filter. Removal of volatiles under reduced pressure yielded **5.13**. Yield: 150 mg, 0.21 mmol, 61%. Single crystals of **5.13** were obtained by layering a DME solution with pentane and storing at –35 °C. %. ^{1}H NMR (benzene-d_6): δ 6.64 (6H), 6.42 (3H), 6.28 (3H), 4.18 (6H), 2.47 (6H), 2.19 (18H), 2.1 (6H).

5.7.15 [K(DME)$_4$][Ce^{III}(Mes$_3$TPA)(TEMPO)] (5.14). To a THF solution of **5.9** (515 mg, 0.62 mmol), TEMPO (96 mg, 0.62 mmol, 1.0 equiv) was added, resulting in an immediate color change to dark red. The mixture was stirred 17 h, then volatiles were removed under reduced pressure. The resulting red-brown solid was recrystallized from a concentrated DME solution layered with pentane at –35 °C to produce orange plates of **5.14** suitable for X-ray diffraction.

5.7.16 [K(DME)$_4$][Tb^{III}(Mes$_3$TPA)(TEMPO)] (5.15). To a toluene solution of **5.12** (200 mg, 0.23 mmol), TEMPO (37 mg, 0.24 mmol, 1.0 equiv) was added, resulting in a slow color change to orange. The mixture was strired overnight, then volatiles were removed under reduced pressure. The resulting residue was triturated with hexanes then washed with hexanes on a medium fritted filter to yield 78 mg of dark pink-purple solid. Recrystallization of the resulting dark

pink solid from a concentrated DME solution layered with hexanes stored at –35 °C produced crystals of **5.15** suitable for X-ray diffraction.

5.7.17 2-^{t}BuXyl-pyrrole. Pyrrolylsodium (14.76 g, 166 mmol, 4 equiv) and $ZnCl_2$ (22.60 g, 166 mmol, 4.0 equiv) were loaded into a 100 mL Teflon-screw cap glass bomb, and THF was slowly added over the course of 15 minutes, generating a quite exothermic reaction. Pd_2dba_3 (760 mg, 0.83, 2 mol%), and PCy_2(biphenyl) (581 mg, 1.66 mmol, 4 mol%) were added, then ^{t}BuXyl-Br was (10.0 g, 41.5 mmol, 1 equiv) was added. The reaction vessel was sealed and heated at 100 °C with stirring for 3 days. The mixture was cooled to room temperature and then extracted with Et_2O/H_2O. After drying with $MgSO_4$, volatiles were removed by rotovap to produce a dark brown oil. The residual oil was dissolved in EtOAc, and eluted through silica to produce a yellow eluent, from which volatiles were removed under reduced pressure to produce a dark yellow oil. Distillation under slight vacuum at 165 °C with a short path condenser yielded 2-^{t}BuXyl-pyrrole as a highly viscous bright yellow oil. Yield: 4.64 g, 20.4 mmol, 49%. ^{1}H NMR ($CDCl_3$): δ 7.93 (1H, bs, NH), 7.22 (2H, s, ArH), 6.90 (1H, m, pyrH), 6.39 (1H, m, pyrH), 6.16 (1H, m, pyrH), 2.26 (6H, s, CH_3), 1.44 (9H, s, ^{t}Bu). ^{13}C NMR ($CDCl_3$): 151.0, 138.4, 131.0, 129.8, 124.5, 117.0, 108.6, 108.4, 34.6, 31.6, 21.1. ESI-MS (pos.): 228.2 (H^+-2-^{t}BuXyl-pyrrole, calc"d 228.2).

5.7.18 H$_3$^{t}BuXyl$_3$TPA. To a 250 mL round bottom flask, 2-^{t}BuXyl-pyrrole (4.14 g, 18.2 mmol, 3.0 equiv) and sublimed NH_4Cl (325 mg, 6.07 mmol) was dissolved in 30 mL 70% $EtOH/H_2O$. A solution of 37% formaldehyde (1.42 mL, 18.2 mmol, 3.0 equiv) was added, leading to precipitation of a colorless solid. The mixture was stirred at 50 °C for two days, then cooled to room temperature. The resulting slurry was extracted with DCM/20% NaOH, and the red solution was rotovap"d to a tan oil. Under reduced pressure a pale brown foam was formed, which was repeatedly mechanically agitated and treated to reduced pressure until a tan powder was formed. Yield: 4.17 g, 5.7 mmol, 93%. ^{1}H NMR (benzene-d_6): δ 7.51 (3H, NH), 7.14 (6H, ArH), 6.23 (3H, pyrH), 6.07 (3H, pyrH), 3.55 (6H, CH_2), 2.20 (18H, CH_3), 1.29 (27H, ^{t}Bu). ^{13}C NMR ($CDCl_3$): δ150.9. 138.2, 131.1, 129.5, 127.5, 124.5, 108.4, 108.3, 49.4, 34.6, 31.6, 21.2. ESI-MS (pos.): 735.6 (H_4^{t}BuXyl$_3$TPA$^+$, calc"d 735.5).

5.7.19 K$_3$^{t}BuXyl$_3$TPA(THF)$_{1.5}$. To a THF solution of H$_3$^{t}BuXyl$_3$TPA (2.25 g, 3.1 mmol), KH (736 mg, 18.4 mmol, 6.0 equiv) was added slowly, leading to vigorous gas evolution. The slurry was stirred overnight, then filtered through Celite on a coarse fritted filter. Removal of volatiles under reduced pressure yielded K$_3$^{t}BuXyl$_3$TPA(THF)$_{1.5}$ as a tan solid. Yield: 2.91 g, 3.04, 99%.^{1}H NMR (toluene-d_8): δ 7.1 (6H, ArH), 6.4 (3H, pyrH), 6.1 (3H, pyrH), 3.4 (6H, CH_2), 2.2 (9H, CH_3), 1.4 (27H, ^{t}Bu); significant spectral broadening was observed due to mild insolubility.

5.7.20 U^{III}(^{t}BuXyl$_3$TPA) (5.16). To a 125 mL side arm flask containing a –25 °C DME solution of K$_3$^{t}BuXyl$_3$TPA(THF)$_{1.5}$ (1.0 g, 1.04 mmol, 1.0 equiv), UI$_3$ (646 mg, 1.04 mmol) was slowly added. The mixture was stirred 1 h, allowing it to return to room temperature, then was stored at –25 °C for 15 h. Volatiles were removed under reduced pressure to yield an oily dark purple residue, which was dissolved in 150 mL hexanes, and filtered through Celite on a coarse fritted filter. Removal of volatiles under reduced pressure yielded **5.16** as a purple-black solid. Yield: 730 mg, 0.69 mmol, 66%.^{1}H NMR (benzene-d_6): δ 42.9 (3H), 10.0 (3H), 8.9 (3H), 8.4 (6H), 3.3 (4H), 0.6 (27H), –9.9 (18H).

5.7.21 U^{IV}(^{t}BuXyl$_3$TPA)Cl (5.17). A THF solution of K$_3$^{t}BuXyl$_3$TPA(THF)$_{1.5}$ (600 mg, 0.63 mmol, 1.0 equiv) was added to a stirring THF solution of UCl$_4$ (238 mg, 0.63 mmol), resulting in an immediate color change to dark red. The mixture was stirred 15 h, then filtered through Celite on a coarse fritted filter. Volatiles were removed under reduced pressure, and the resulting dark red residue was dissolved in toluene and filtered through Celite on a coarse fritted filter. Volatiles were removed under reduced pressure and the resulting oily dark red residue was dissolved in hexanes and filtered through Celite, yielding a red filtrate that was concentrated and stored at –25 °C. Pure **5.17** was isolated as a red powder. Yield: 462 mg, 0.43 mmol, 68%. ^{1}H NMR (benzene-d_6): δ 76.9, 40.8, 3.7, 1.3, –2.1; as in **5.7**, some resonances could be observed at room temperature.

5.8 X-Ray Data.

Table 5.8.1 Summary of structure determination.

	5.1	**5.2**	**5.3**
Empirical formula	$C_{67}H_{53}N_9F_{18}U$	$C_{128}H_{92}N_{18}F_{36}K_2U$	$C_{123}H_{87}N_{17}F_{36}Cl_2U_2$
Formula weight	1564.21	2882.43	3034.06
Temperature	143(1) K	143(1) K	143(1) K
Wavelength	0.71073 Å	0.71073 Å	0.71073 Å
Crystal system	triclinic	monoclinic	triclinic
Space group	P-1	$P2_1/c$	P-1
a	14.9137(6) Å	14.8967(6) Å	12.5198(8) Å
b	15.0306(5) Å	29.6220(13) Å	13.4380(10) Å
c	16.7526(7) Å	15.2447(6) Å	20.5761(14) Å
α	65.774(2)°	90	72.021(3)°
β	67.054(2)°	113.741(2)°	75.321(3)°
γ	86.440(2)°	90	63.759(3)°
Volume	3132.1(2) Å^3	6157.8(4) Å^3	2925.5(3) Å^3
Z	2	2	1
Density (calculated)	1.659 Mg/m^3	1.555 Mg/m^3	1.722 Mg/m^3
Absorption coefficient	2.695 mm^{-1}	1.498 mm^{-1}	2.926 mm^{-1}
F(000)	1544	2880	1486
Crystal size	0.15 x 0.05 x 0.02 mm^3	0.28 x 0.12 x 0.10 mm^3	0.18 x 0.12 x 0.10 mm^3
Theta range	1.45 to 27.54°	1.61 to 27.61°	1.73 to 27.55°
Index ranges	-17 ≤ h ≤ 19, -17 ≤ k ≤ 19, 0 ≤ l ≤ 21	-19 ≤ h ≤ 17, -38 ≤ k ≤ 38, -19 ≤ l ≤ 19	-16 ≤ h ≤ 16, -16 ≤ k ≤ 17, -26 ≤ l ≤ 26
Reflections	120114	84402	61667
Independent reflections	14286 [R(int) = 0.0865]	14113 [R(int) = 0.0619]	13362 [R(int) = 0.0321]
Completeness to theta = 27.52 °	98.70%	98.60%	98.80%
Max. and min. transmission	0.7456 and 0.6310	0.7456 and 0.6017	0.7456 and 0.6633
Data / restraints / parameters	14286 / 111 / 834	14113 / 120 / 889	13362 / 0 / 865
Goodness-of-fit on F^2	1.166	1.467	1.035
Final R indices [I>2sigma(I)]	R1 = 0.0539, wR2 = 0.1343	R1 = 0.0705, wR2 = 0.1312	R1 = 0.0207, wR2 = 0.0476
R indices (all data)	R1 = 0.0758, wR2 = 0.1486	R1 = 0.0999, wR2 = 0.1392	R1 = 0.0250, wR2 = 0.0491
Largest diff. peak and hole	2.066 and -1.677 e.Å^{-3}	1.290 and -0.850 e.Å^{-3}	0.759 and -0.427 e.Å^{-3}

	5.4	**5.5**	**5.6**
Empirical formula	$C_{56}H_{39}N_6O_2ClF_{18}U$	$C_{52}H_{70}N_4O_5U$	$C_{46}H_{53}N_4OU$
Formula weight	1443.41	1069.15	915.95
Temperature	143(1) K	143(1) K	143(1) K
Wavelength	0.71073 Å	0.71073 Å	0.71073 Å
Crystal system	monoclinic	monoclinic	orthorhombic
Space group	$P2_1/n$	$P2_1/c$	Pbca

a	14.9900(15) Å	10.9178(18) Å	17.911(3) Å
b	22.203(2) Å	26.088(4) Å	15.326(3) Å
c	17.6681(17) Å	16.827(3) Å	29.782(6) Å
α	90	90	90
β	111.455(4)°	92.003(8)°	90
γ	90	90	90
Volume	5472.9(9) Å^3	4789.8(14) Å^3	8175(3) Å^3
Z	4	4	8
Density (calculated)	1.752 Mg/m^3	1.483 Mg/m^3	1.488 Mg/m^3
Absorption coefficient	3.125 mm^{-1}	3.439 mm^{-1}	4.009 mm^{-1}
F(000)	2816	2168	3656
Crystal size	0.50 x 0.25 x 0.03 mm3	0.42 x 0.35 x 0.06 mm3	0.58 x 0.25 x 0.08 mm3
Theta range	1.72 to 27.56°	1.87 to 27.52°	1.78 to 27.52°
Index ranges	-19 ≤ h ≤ 19, -28 ≤ k ≤ 28, -22 ≤ l ≤ 22	-14 ≤ h ≤ 14, -33 ≤ k ≤ 33, -21 ≤ l ≤ 21	-19 ≤ h ≤ 23, -19 ≤ k ≤ 19, -38 ≤ l ≤ 28
Reflections	135927	95321	89084
Independent reflections	12593 [R(int) = 0.0453]	10955 [R(int) = 0.0525]	9369 [R(int) = 0.0656]
Completeness to theta = 27.52 °	99.60%	99.30%	99.50%
Max. and min. transmission	0.7456 and 0.5635	0.7456 and 0.4880	1.0000 and 0.5640
Data / restraints / parameters	12593 / 152 / 812	10955 / 6 / 574	9369 / 31 / 488
Goodness-of-fit on F^2	1.137	1.33	1.241
Final R indices [I>2sigma(I)]	R1 = 0.0350, wR2 = 0.0762	R1 = 0.0595, wR2 = 0.1222	R1 = 0.1043, wR2 = 0.2401
R indices (all data)	R1 = 0.0541, wR2 = 0.0879	R1 = 0.0709, wR2 = 0.1273	R1 = 0.1336, wR2 = 0.2564
Largest diff. peak and hole	2.617 and -1.174 e.Å^{-3}	2.837 and -5.290 e.Å^{-3}	7.351 and -14.533 e.Å^{-3}

	5.7	**5.8**	**5.9**
Empirical formula	$C_{46}H_{53}N_4OClU$	$C_{79}H_{86}N_4POU$	$C_{56}H_{79}N_4O_4Ce$
Formula weight	951.4	1376.52	1012.35
Temperature	143(1) K	143(1) K	100(1) K
Wavelength	0.71073 Å	0.71073 Å	0.71073 Å
Crystal system	orthorhombic	triclinic	monoclinic
Space group	Fdd2	P-1	$P2_1/c$
a	43.240(8) Å	12.894(3) Å	10.8933(6) Å
b	47.735(10) Å	17.567(4) Å	26.0349(15) Å
c	9.0997(19) Å	18.817(4) Å	16.7286(9) Å
α	90	72.572(11)°	90
β	90	71.319(10)°	92.227(3)°
γ	90	69.782(10)°	90
Volume	18782(7) Å^3	3702.4(14) Å^3	4740.7(5) Å^3
Z	16	2	4
Density (calculated)	1.346 Mg/m^3	1.235 Mg/m^3	1.418 Mg/m^3
Absorption coefficient	3.548 mm^{-1}	2.257 mm^{-1}	1.013 mm^{-1}
F(000)	7584	1406	2132
Crystal size	0.32 x 0.32 x 0.28 mm3	0.40 x 0.15 x 0.04 mm3	0.42 x 0.38 x 0.06 mm3
Theta range	1.71 to 27.49°	1.53 to 27.58°	1.87 to 27.65°

Index ranges	-55 ≤ h ≤ 55, -61 ≤ k ≤ 61, -11 ≤ l ≤ 11	-16 ≤ h ≤ 16, -22 ≤ k ≤ 22, -24 ≤ l ≤ 24	-14 ≤ h ≤ 14, -33 ≤ k ≤ 33, -21 ≤ l ≤ 21
Reflections	112787	101930	101224
Independent reflections	10704 [R(int) = 0.0317]	16891 [R(int) = 0.0294]	10939 [R(int) = 0.0296]
Completeness to theta = 27.52 °	99.70%	98.50%	99.00%
Max. and min. transmission	1.0000 and 0.8140	1.0000 and 0.7733	0.7456 and 0.6437
Data / restraints / parameters	10704 / 1 / 488	16891 / 4 / 796	10939 / 0 / 574
Goodness-of-fit on F^2	1.101	1.092	1.26
Final R indices [I>2sigma(I)]	R1 = 0.0351, wR2 = 0.0974	R1 = 0.0243, wR2 = 0.0616	R1 = 0.0473, wR2 = 0.1109
R indices (all data)	R1 = 0.0361, wR2 = 0.0985	R1 = 0.0284, wR2 = 0.0640	R1 = 0.0559, wR2 = 0.1168
Largest diff. peak and hole	1.168 and -1.246 e.Å^{-3}	1.591 and -1.049 e.Å^{-3}	1.211 and -2.276 e.Å^{-3}

	5.11	**5.12**	**5.13**
Empirical formula	$C_{68}H_{93}N_6O_8KCe$	$C_{46}H_{55}N_4O_2Tb$	$C_{46}H_{55}N_4O_2Y$
Formula weight	1301.7	854.86	784.85
Temperature	143(1) K	143(1) K	143(1) K
Wavelength	0.71073 Å	0.71073 Å	0.71073 Å
Crystal system	monoclinic	Monoclinic	Monoclinic
Space group	$P2_1/n$	$P2_1/n$	$P2_1/n$
a	21.0899(12) Å	12.7398(16) Å	12.7501(19) Å
b	16.8233(9) Å	22.283(3) Å	22.218(3) Å
c	21.1324(10) Å	15.0994(18) Å	15.108(2) Å
α	90	90	90
β	115.146(2)°	108.563(7)°	108.948(8)°
γ	90	90	90
Volume	6787.2(6) Å^3	4063.4(9) Å^3	4047.9(10) Å^3
Z	4	4	4
Density (calculated)	1.274 Mg/m^3	1.397 Mg/m^3	1.288 Mg/m^3
Absorption coefficient	0.788 mm^{-1}	1.782 mm^{-1}	1.483 mm^{-1}
F(000)	2736	1760	1656
Crystal size	0.45 x 0.12 x 0.05 mm3	0.12 x 0.12 x 0.03 mm3	0.20 x 0.18 x 0.03 mm3
Theta range	1.61 to 27.53°	1.69 to 27.56°	1.69 to 27.66°
Index ranges	-27 ≤ h ≤ 26, -21 ≤ k ≤ 21, -26 ≤ l ≤ 27	-16 ≤ h ≤ 16, -28 ≤ k ≤ 28, -19 ≤ l ≤ 19	-16 ≤ h ≤ 16, -28 ≤ k ≤ 28, -19 ≤ l ≤ 19
Reflections	99303	71304	70033
Independent reflections	15603 [R(int) = 0.0270]	9341 [R(int) = 0.0580]	9345 [R(int) = 0.0965]
Completeness to theta = 27.52 °	99.70%	99.40%	98.80%
Max. and min. transmission	0.7456 and 0.6669	1.0000 and 0.9008	1.0000 and 0.7678
Data / restraints / parameters	15603 / 0 / 775	9341 / 0 / 490	9345 / 0 / 490
Goodness-of-fit on F^2	1.049	1.188	1.033
Final R indices [I>2sigma(I)]	R1 = 0.0295, wR2 = 0.0655	R1 = 0.0432, wR2 = 0.0727	R1 = 0.0540, wR2 = 0.1031

R indices (all data)	R1 = 0.0446, wR2 = 0.0747	R1 = 0.0672, wR2 = 0.0776	R1 = 0.1071, wR2 = 0.1193
Largest diff. peak and hole	1.488 and -0.651 e.Å^{-3}	0.824 and -0.628 e.Å^{-3}	0.435 and -0.442 e.Å^{-3}

	5.14	**5.15**	**5.16**
Empirical formula	$C_{67}H_{103}N_5O_9KCe$	$C_{67}H_{103}N_5O_9KTb$	$C_{58}H_{80}N_4O_2U$
Formula weight	1301.76	1320.56	1103.29
Temperature	143(1) K	143(1) K	143(1) K
Wavelength	0.71073 Å	0.71073 Å	0.71073 Å
Crystal system	monoclinic	monoclinic	monoclinic
Space group	$P2_1/n$	$P2_1/n$	$P2_1/n$
a	12.8571(18) Å	12.9213(16) Å	13.0180(13) Å
b	14.250(2) Å	14.2146(16) Å	24.202(3) Å
c	37.846(5) Å	37.224(4) Å	17.4701(18) Å
α	90	90	90
β	94.479(8)°	93.929(7)°	91.450(5)°
γ	90	90	90
Volume	6912.7(16) Å^3	6820.9(14) Å^3	5502.4(10) Å^3
Z	4	4	4
Density (calculated)	1.251 Mg/m^3	1.286 Mg/m^3	1.332 Mg/m^3
Absorption coefficient	0.774 mm^{-1}	1.154 mm^{-1}	2.992 mm^{-1}
F(000)	2756	2784	2256
Crystal size	0.15 x 0.12 x 0.03 mm3	0.11 x 0.09 x 0.03 mm3	0.35 x 0.12 x 0.04 mm3
Theta range	1.53 to 27.62°	1.53 to 27.71°	1.68 to 27.56°
Index ranges	-16 ≤ h ≤ 16, -17 ≤ k ≤ 18, -48 ≤ l ≤ 49	-16 ≤ h ≤ 16, -16 ≤ k ≤ 18, -48 ≤ l ≤ 48	-16 ≤ h ≤ 16, -31 ≤ k ≤ 31, -22 ≤ l ≤ 22
Reflections	134453	157000	115644
Independent reflections	15882 [R(int) = 0.1326]	15880 [R(int) = 0.1761]	12597 [R(int) = 0.0403]
Completeness to theta = 27.52 °	98.70%	99.30%	99.10%
Max. and min. transmission	1.0000 and 0.9167	1.0000 and 0.8588	0.7456 and 0.5742
Data / restraints / parameters	15882 / 0 / 770	15880 / 0 / 770	12597 / 0 / 605
Goodness-of-fit on F^2	1.051	1.026	1.057
Final R indices [I>2sigma(I)]	R1 = 0.0599, wR2 = 0.1061	R1 = 0.0795, wR2 = 0.1565	R1 = 0.0248, wR2 = 0.0522
R indices (all data)	R1 = 0.1134, wR2 = 0.1209	R1 = 0.1775, wR2 = 0.1938	R1 = 0.0383, wR2 = 0.0572
Largest diff. peak and hole	0.816 and -1.292 e.Å^{-3}	1.219 and -0.842 e.Å^{-3}	1.225 and -0.707 e.Å^{-3}

Table 5.8.2 Bond lengths of **5.1** (Å)

U1-N1	2.561(5)	U1-N2	2.595(5)	U1-N3	2.605(6)
U1-N4	2.606(6)	U1-N5	2.632(6)	U1-N6	2.641(6)
U1-N7	2.652(6)	N1-C1	1.459(9)	N1-C27	1.469(8)
N1-C14	1.495(8)	N2-C2	1.386(9)	N2-C5	1.400(9)
N3-C15	1.382(9)	N3-C18	1.393(9)	N4-C28	1.388(9)

N4-C31	1.398(9)	N5-C44	1.333(9)	N5-C40	1.369(9)
N6-C49	1.321(10)	N6-C45	1.346(10)	N7-C54	1.321(10)
N7-C50	1.342(10)	C1-C2	1.484(10)	C2-C3	1.384(11)
C3-C4	1.398(11)	C4-C5	1.395(10)	C5-C6	1.460(10)
C6-C11	1.395(11)	C6-C7	1.409(10)	C7-C8	1.382(11)
C8-C9	1.372(12)	C8-C12	1.470(12)	C9-C10	1.377(11)
C10-C11	1.399(10)	C10-C13	1.477(13)	C12-F2	1.320(10)
C12-F1	1.350(12)	C12-F3	1.354(11)	C13-F4	1.324(11)
C13-F5	1.336(10)	C13-F6	1.343(11)	C14-C15	1.470(10)
C15-C16	1.399(10)	C16-C17	1.396(11)	C17-C18	1.394(10)
C18-C19	1.471(10)	C19-C24	1.385(11)	C19-C20	1.395(10)
C20-C21	1.392(11)	C21-C22	1.384(12)	C21-C25	1.498(12)
C22-C23	1.403(11)	C23-C24	1.377(10)	C23-C26	1.483(12)
C25-F7	1.277(11)	C25-F9	1.309(11)	C25-F8	1.349(12)
C26-F10	1.317(10)	C26-F12	1.345(9)	C26-F11	1.360(10)
C27-C28	1.499(10)	C28-C29	1.376(10)	C29-C30	1.412(11)
C30-C31	1.407(10)	C31-C32	1.454(10)	C32-C37	1.373(10)
C32-C33	1.425(10)	C33-C34	1.350(11)	C34-C35	1.397(11)
C34-C38	1.488(11)	C35-C36	1.381(11)	C36-C37	1.411(11)
C36-C39	1.496(11)	C38-F15	1.315(10)	C38-F13	1.328(11)
C38-F14	1.342(10)	C39-F17	1.319(10)	C39-F16	1.323(11)
C39-F18	1.344(11)	C40-C41	1.352(11)	C41-C42	1.393(12)
C42-C43	1.339(11)	C43-C44	1.392(10)	C45-C46	1.369(11)
C46-C47	1.374(12)	C47-C48	1.368(12)	C48-C49	1.403(11)
C50-C51	1.354(11)	C51-C52	1.383(12)	C52-C53	1.382(13)
C53-C54	1.383(11)	N8-C59	1.34	N8-C55	1.3413
C55-C56	1.3949	C56-C57	1.3949	C57-C58	1.3951
C58-C59	1.395	N9-C64	1.34	N9-C60	1.3413
C60-C61	1.3949	C61-C62	1.3949	C62-C63	1.3951
C63-C64	1.395	C65-C66	1.489(18)	C65-C65#1	1.53(3)
C66-C67	1.52(2)				

Symmetry transformations used to generate equivalent atoms:
#1 -x,-y,-z+2

Table 5.8.3 Bond angles of **5.1** (°)

N1-U1-N2	70.78(17)	N1-U1-N3	71.10(17)
N1-U1-N4	69.94(17)	N2-U1-N4	109.89(18)
N1-U1-N5	128.47(17)	N2-U1-N5	86.62(18)
N4-U1-N5	75.93(18)	N1-U1-N6	130.01(18)
N3-U1-N6	76.03(18)	N4-U1-N6	87.73(18)
N1-U1-N7	128.64(18)	N2-U1-N7	75.62(17)
N4-U1-N7	160.39(18)	N5-U1-N7	85.84(18)
C1-N1-C27	112.6(5)	C1-N1-C14	111.1(5)
C1-N1-U1	106.8(4)	C27-N1-U1	108.4(4)
C2-N2-C5	103.8(6)	C2-N2-U1	108.2(4)
C15-N3-C18	105.3(6)	C15-N3-U1	106.3(4)
C28-N4-C31	104.1(6)	C28-N4-U1	108.3(4)
C44-N5-C40	115.8(6)	C44-N5-U1	127.9(5)
C49-N6-C45	117.1(7)	C49-N6-U1	130.0(5)
C54-N7-C50	117.2(6)	C54-N7-U1	115.6(5)
N1-C1-C2	112.5(6)	C3-C2-N2	112.0(6)
N2-C2-C1	120.1(6)	C2-C3-C4	106.5(7)
C4-C5-N2	110.9(6)	C4-C5-C6	123.3(6)
C11-C6-C7	117.1(7)	C11-C6-C5	122.8(6)
C8-C7-C6	121.2(8)	C9-C8-C7	120.8(7)

C7-C8-C12	121.2(8)	C8-C9-C10	119.5(7)
C9-C10-C13	120.6(7)	C11-C10-C13	118.9(7)
F2-C12-F1	106.6(9)	F2-C12-F3	105.5(8)
F2-C12-C8	113.6(7)	F1-C12-C8	114.1(7)
F4-C13-F5	105.4(8)	F4-C13-F6	104.4(8)
F4-C13-C10	113.2(8)	F5-C13-C10	113.5(8)
C15-C14-N1	110.0(5)	N3-C15-C16	110.8(6)
C16-C15-C14	127.5(7)	C17-C16-C15	106.5(6)
N3-C18-C17	110.2(6)	N3-C18-C19	125.3(6)
C24-C19-C20	118.0(7)	C24-C19-C18	122.5(6)
C21-C20-C19	120.1(8)	C22-C21-C20	121.9(7)
C20-C21-C25	120.2(8)	C21-C22-C23	117.4(8)
C24-C23-C26	119.7(7)	C22-C23-C26	119.6(7)
F7-C25-F9	108.1(9)	F7-C25-F8	105.6(10)
F7-C25-C21	113.9(8)	F9-C25-C21	112.7(8)
F10-C26-F12	106.6(7)	F10-C26-F11	105.6(7)
F10-C26-C23	113.7(7)	F12-C26-C23	113.2(7)
N1-C27-C28	109.4(5)	C29-C28-N4	112.7(6)
N4-C28-C27	119.6(6)	C28-C29-C30	106.1(6)
N4-C31-C30	110.5(6)	N4-C31-C32	124.8(6)
C37-C32-C33	117.6(7)	C37-C32-C31	123.0(7)
C34-C33-C32	121.7(7)	C33-C34-C35	120.7(7)
C35-C34-C38	116.8(7)	C36-C35-C34	118.7(7)
C35-C36-C39	120.3(7)	C37-C36-C39	119.0(7)
F15-C38-F13	105.7(7)	F15-C38-F14	107.4(8)
F15-C38-C34	113.3(7)	F13-C38-C34	113.0(8)
F17-C39-F16	107.0(8)	F17-C39-F18	106.2(7)
F17-C39-C36	113.6(7)	F16-C39-C36	113.0(7)
C41-C40-N5	123.0(7)	C40-C41-C42	119.9(7)
C42-C43-C44	120.1(8)	N5-C44-C43	123.2(7)
C45-C46-C47	119.7(8)	C48-C47-C46	119.1(7)
N6-C49-C48	123.9(8)	N7-C50-C51	123.5(8)
C53-C52-C51	118.5(8)	C52-C53-C54	118.1(8)
C59-N8-C55	119.6	N8-C55-C56	121.4
C56-C57-C58	118.3	C59-C58-C57	118.9
C64-N9-C60	119.6	N9-C60-C61	121.4
C61-C62-C63	118.3	C64-C63-C62	118.9
C66-C65-C65#1	112.4(13)	C65-C66-C67	113.8(14)
N2-U1-N3	108.92(18)	C24-C23-C22	120.7(8)
N3-U1-N4	109.82(18)	C23-C24-C19	121.8(7)
N3-U1-N5	159.25(18)	F9-C25-F8	103.2(8)
N2-U1-N6	157.66(18)	F8-C25-C21	112.5(7)
N5-U1-N6	84.47(18)	F12-C26-F11	106.0(7)
N3-U1-N7	84.92(18)	F11-C26-C23	111.2(7)
N6-U1-N7	83.32(18)	C29-C28-C27	127.7(7)
C27-N1-C14	111.2(5)	C31-C30-C29	106.6(6)
C14-N1-U1	106.4(4)	C30-C31-C32	124.0(7)
C5-N2-U1	135.9(4)	C33-C32-C31	119.1(6)
C18-N3-U1	135.5(5)	C33-C34-C38	122.5(7)
C31-N4-U1	135.9(4)	C35-C36-C37	120.6(7)
C40-N5-U1	116.0(5)	C32-C37-C36	120.6(7)
C45-N6-U1	112.5(5)	F13-C38-F14	105.3(7)
C50-N7-U1	126.7(5)	F14-C38-C34	111.6(7)
C3-C2-C1	127.8(7)	F16-C39-F18	105.9(7)

C5-C4-C3	106.7(6)	F18-C39-C36	110.6(8)
N2-C5-C6	125.0(6)	C43-C42-C41	117.8(7)
C7-C6-C5	119.7(7)	N6-C45-C46	122.6(7)
C9-C8-C12	118.0(7)	C47-C48-C49	117.6(8)
C9-C10-C11	120.5(8)	C50-C51-C52	119.0(8)
C6-C11-C10	121.0(7)	N7-C54-C53	123.6(7)
F1-C12-F3	103.1(7)	C55-C56-C57	119.6
F3-C12-C8	113.1(9)	N8-C59-C58	122.2
F5-C13-F6	107.0(8)	C60-C61-C62	119.6
F6-C13-C10	112.6(7)	N9-C64-C63	122.2
N3-C15-C14	121.7(6)	C17-C18-C19	123.8(6)
C18-C17-C16	107.3(6)	C20-C19-C18	119.2(7)
C22-C21-C25	117.8(8)		

Symmetry transformations used to generate equivalent atoms:
#1 -x,-y,-z+2

Table 5.8.4 Bond lengths of **5.2** (Å)

U1-N4	2.490(4)	U1-N4#1	2.490(4)	U1-N3#1	2.493(4)
U1-N3	2.493(4)	U1-N2#1	2.508(4)	U1-N2	2.508(4)
U1-N1	2.649(4)	U1-N1#1	2.649(4)	N1-C14	1.468(6)
N1-C1	1.473(6)	N1-C27	1.477(6)	N2-C2	1.384(6)
N2-C5	1.390(7)	N3-C15	1.371(7)	N3-C18	1.394(7)
N4-C31	1.383(6)	N4-C28	1.400(6)	C1-C2	1.483(7)
C2-C3	1.368(8)	C3-C4	1.407(8)	C4-C5	1.383(8)
C5-C6	1.483(7)	C6-C11	1.389(8)	C6-C7	1.396(8)
C7-C8	1.380(8)	C8-C9	1.382(10)	C8-C12	1.492(10)
C9-C10	1.378(9)	C10-C11	1.395(8)	C10-C13	1.479(9)
C12-F1	1.273(10)	C12-F3	1.277(10)	C12-F2	1.310(11)
C13-F6	1.323(9)	C13-F5	1.335(8)	C13-F4	1.335(9)
C14-C15	1.492(8)	C15-C16	1.356(8)	C16-C17	1.398(8)
C17-C18	1.375(7)	C18-C19	1.485(8)	C19-C20	1.388(8)
C19-C24	1.396(8)	C20-C21	1.395(8)	C21-C22	1.379(8)
C21-C25	1.488(8)	C22-C23	1.374(9)	C23-C24	1.389(8)
C23-C26	1.503(9)	C25-F7	1.321(8)	C25-F9	1.340(7)
C25-F8	1.342(8)	C26-F11	1.263(10)	C26-F10	1.273(9)
C26-F12	1.308(10)	C27-C28	1.475(7)	C28-C29	1.368(7)
C29-C30	1.390(8)	C30-C31	1.376(7)	C31-C32	1.478(7)
C32-C37	1.399(8)	C32-C33	1.401(8)	C33-C34	1.385(7)
C34-C35	1.387(8)	C34-C38	1.492(8)	C35-C36	1.389(9)
C36-C37	1.376(8)	C36-C39	1.486(8)	C38-F15'	1.299(9)
C38-F14	1.301(7)	C38-F13	1.315(7)	C38-F14'	1.318(9)
C38-F13'	1.320(9)	C38-F15	1.329(7)	C39-F17	1.280(8)
C39-F16'	1.289(8)	C39-F17'	1.333(8)	C39-F18	1.337(8)
C39-F18'	1.343(8)	C39-F16	1.349(8)	F8-K1	2.778(4)
K1-N8	2.770(8)	K1-N6	2.796(7)	K1-N5	2.802(8)
K1-N9	2.820(11)	K1-N7	2.851(8)	K1-C55	3.496(12)
N5-C40	1.306(12)	N5-C44	1.317(11)	N6-C49	1.318(11)
N6-C45	1.336(10)	N7-C54	1.313(11)	N7-C50	1.322(11)
N8-C59	1.302(13)	N8-C55	1.308(14)	N9-C60	1.34(2)
N9-C64	1.353(17)	C40-C41	1.358(17)	C41-C42	1.313(18)
C42-C43	1.376(17)	C43-C44	1.377(13)	C45-C46	1.342(11)
C46-C47	1.371(12)	C47-C48	1.356(12)	C48-C49	1.360(11)
C50-C51	1.334(13)	C51-C52	1.364(15)	C52-C53	1.399(15)

C53-C54	1.364(13)	C55-C56	1.312(17)	C56-C57	1.317(19)
C57-C58	1.383(18)	C58-C59	1.352(15)	C60-C61	1.327(19)
C61-C62	1.348(18)	C62-C63	1.332(17)	C63-C64	1.366(16)

Symmetry transformations used to generate equivalent atoms:

#1 -x+1,-y+1,-z+1

Table 5.8.5 Bond angles of **5.2** (°)

N4-U1-N4#1	180.0	N4-U1-N3#1	75.27(14)
N4-U1-N3	104.73(14)	N4#1-U1-N3	75.27(14)
N4-U1-N2#1	75.02(13)	N4#1-U1-N2#1	104.98(13)
N3-U1-N2#1	75.16(13)	N4-U1-N2	104.98(13)
N3#1-U1-N2	75.16(13)	N3-U1-N2	104.84(13)
N4-U1-N1	66.45(13)	N4#1-U1-N1	113.55(13)
N3-U1-N1	66.37(13)	N2#1-U1-N1	114.14(13)
N4-U1-N1#1	113.55(13)	N4#1-U1-N1#1	66.45(13)
N3-U1-N1#1	113.63(13)	N2#1-U1-N1#1	65.86(13)
N1-U1-N1#1	180.000(1)	C14-N1-C1	110.6(4)
C1-N1-C27	109.4(4)	C14-N1-U1	108.3(3)
C27-N1-U1	109.2(3)	C2-N2-C5	104.1(4)
C5-N2-U1	136.7(3)	C15-N3-C18	103.4(4)
C18-N3-U1	136.4(3)	C31-N4-C28	104.5(4)
C28-N4-U1	118.0(3)	N1-C1-C2	109.8(4)
C3-C2-C1	128.6(5)	N2-C2-C1	119.2(4)
C5-C4-C3	106.8(5)	C4-C5-N2	110.8(5)
N2-C5-C6	128.6(5)	C11-C6-C7	117.5(5)
C7-C6-C5	117.1(5)	C8-C7-C6	121.1(6)
C7-C8-C12	119.2(7)	C9-C8-C12	119.8(6)
C9-C10-C11	120.4(6)	C9-C10-C13	119.6(6)
C6-C11-C10	121.2(5)	F1-C12-F3	106.2(8)
F3-C12-F2	104.2(9)	F1-C12-C8	114.9(7)
F2-C12-C8	111.9(7)	F6-C13-F5	105.7(6)
F5-C13-F4	104.9(6)	F6-C13-C10	114.2(6)
F4-C13-C10	113.4(6)	N1-C14-C15	110.0(4)
C16-C15-C14	128.6(5)	N3-C15-C14	118.3(5)
C18-C17-C16	106.9(5)	C17-C18-N3	110.7(5)
N3-C18-C19	127.8(5)	C20-C19-C24	118.3(5)
C24-C19-C18	117.8(5)	C19-C20-C21	120.3(5)
C22-C21-C25	119.4(6)	C20-C21-C25	119.5(5)
C22-C23-C24	121.1(6)	C22-C23-C26	118.9(6)
C23-C24-C19	120.5(6)	F7-C25-F9	106.5(5)
F9-C25-F8	105.0(6)	F7-C25-C21	113.5(6)
F8-C25-C21	112.6(5)	F11-C26-F10	106.9(9)
F10-C26-F12	103.4(8)	F11-C26-C23	113.6(7)
F12-C26-C23	111.9(7)	C28-C27-N1	110.8(4)
C29-C28-C27	129.5(5)	N4-C28-C27	119.6(4)
C31-C30-C29	107.9(5)	C30-C31-N4	110.2(5)
N4-C31-C32	127.2(4)	C37-C32-C33	117.1(5)
C33-C32-C31	124.3(5)	C34-C33-C32	120.9(5)
C33-C34-C38	120.1(5)	C35-C34-C38	118.5(5)
C37-C36-C35	120.9(5)	C37-C36-C39	119.7(5)
C36-C37-C32	121.7(5)	F15'-C38-F14	128.0(11)
F14-C38-F13	107.2(7)	F15'-C38-F14'	106.0(12)
F13-C38-F14'	133.6(10)	F15'-C38-F13'	105.9(12)

F13-C38-F13'	46.9(11)	F14'-C38-F13'	104.0(11)
F14-C38-F15	106.3(8)	F13-C38-F15	103.7(7)
F13'-C38-F15	134.4(10)	F15'-C38-C34	115.6(9)
F13-C38-C34	113.1(6)	F14'-C38-C34	111.8(9)
F15-C38-C34	111.2(6)	F17-C39-F16'	117.6(13)
F16'-C39-F17'	110.1(9)	F17-C39-F18	106.5(10)
F17'-C39-F18	132.8(9)	F17-C39-F18'	31.4(8)
F17'-C39-F18'	99.9(8)	F18-C39-F18'	83.2(11)
F16'-C39-F16	71.8(9)	F17'-C39-F16	46.1(7)
F18'-C39-F16	134.4(9)	F17-C39-C36	119.0(9)
F17'-C39-C36	112.4(6)	F18-C39-C36	110.2(8)
F16-C39-C36	111.1(6)	C25-F8-K1	137.2(4)
N8-K1-N6	168.4(3)	F8-K1-N6	98.35(18)
F8-K1-N5	75.45(18)	N6-K1-N5	102.1(2)
F8-K1-N9	161.2(3)	N6-K1-N9	91.1(3)
N8-K1-N7	88.2(3)	F8-K1-N7	86.51(19)
N5-K1-N7	160.5(2)	N9-K1-N7	110.2(4)
F8-K1-C55	104.3(3)	N6-K1-C55	154.7(3)
N9-K1-C55	64.0(3)	N7-K1-C55	104.7(3)
C40-N5-K1	116.7(7)	C44-N5-K1	124.2(6)
C49-N6-K1	115.9(6)	C45-N6-K1	126.8(6)
C54-N7-K1	126.5(6)	C50-N7-K1	116.0(7)
C59-N8-K1	121.7(8)	C55-N8-K1	113.0(8)
C60-N9-K1	117.3(11)	C64-N9-K1	122.8(11)
C42-C41-C40	118.2(12)	C41-C42-C43	120.0(12)
N5-C44-C43	123.3(9)	N6-C45-C46	123.7(8)
C48-C47-C46	118.4(8)	C47-C48-C49	119.2(9)
N7-C50-C51	124.2(10)	C50-C51-C52	118.7(10)
C54-C53-C52	117.1(11)	N7-C54-C53	123.8(9)
N8-C55-K1	46.8(6)	C56-C55-K1	152.4(12)
C56-C57-C58	121.8(13)	C59-C58-C57	115.7(13)
C61-C60-N9	126.8(18)	C60-C61-C62	116.3(18)
C62-C63-C64	117.8(14)	N9-C64-C63	123.2(14)
N4#1-U1-N3#1	104.73(14)	F16'-C39-F18	28.1(9)
N3#1-U1-N3	180.000(1)	F16'-C39-F18'	104.5(9)
N3#1-U1-N2#1	104.84(13)	F17-C39-F16	108.5(9)
N4#1-U1-N2	75.02(13)	F18-C39-F16	99.8(8)
N2#1-U1-N2	180.0	F16'-C39-C36	117.8(9)
N3#1-U1-N1	113.63(13)	F18'-C39-C36	110.3(8)
N2-U1-N1	65.86(13)	N8-K1-F8	92.1(3)
N3#1-U1-N1#1	66.37(13)	N8-K1-N5	85.2(3)
N2-U1-N1#1	114.14(13)	N8-K1-N9	80.3(3)
C14-N1-C27	109.6(4)	N5-K1-N9	86.8(4)
C1-N1-U1	109.6(3)	N6-K1-N7	87.6(2)
C2-N2-U1	118.2(3)	N8-K1-C55	20.1(3)
C15-N3-U1	118.4(3)	N5-K1-C55	73.4(3)
C31-N4-U1	136.9(3)	C40-N5-C44	115.8(9)
C3-C2-N2	112.1(5)	C49-N6-C45	116.6(7)
C2-C3-C4	106.1(5)	C54-N7-C50	117.4(9)
C4-C5-C6	120.6(5)	C59-N8-C55	119.2(11)
C11-C6-C5	124.6(5)	C60-N9-C64	113.8(13)
C7-C8-C9	121.0(6)	N5-C40-C41	125.3(11)
C10-C9-C8	118.8(6)	C42-C43-C44	117.3(11)
C11-C10-C13	119.9(6)	C45-C46-C47	118.9(8)

F1-C12-F2	104.1(9)	N6-C49-C48	123.3(8)
F3-C12-C8	114.4(8)	C51-C52-C53	118.8(10)
F6-C13-F4	105.0(7)	N8-C55-C56	123.2(15)
F5-C13-C10	112.8(6)	C55-C56-C57	117.8(14)
C16-C15-N3	113.1(6)	N8-C59-C58	122.0(11)
C15-C16-C17	105.9(5)	C63-C62-C61	122.0(14)
C17-C18-C19	121.4(5)	C34-C35-C36	118.1(5)
C20-C19-C18	123.3(5)	C35-C36-C39	119.3(5)
C22-C21-C20	121.1(5)	F15'-C38-F13	63.7(11)
C23-C22-C21	118.7(6)	F14-C38-F14'	41.0(11)
C24-C23-C26	120.1(6)	F14-C38-F13'	65.2(11)
F7-C25-F8	106.0(6)	F15'-C38-F15	41.7(11)
F9-C25-C21	112.6(6)	F14'-C38-F15	69.8(12)
F11-C26-F12	106.3(8)	F14-C38-C34	114.6(7)
F10-C26-C23	113.9(7)	F13'-C38-C34	112.6(9)
C29-C28-N4	110.9(5)	F17-C39-F17'	68.7(9)
C28-C29-C30	106.5(5)	C37-C32-C31	117.8(5)
C30-C31-C32	122.5(5)	C33-C34-C35	121.3(5)

Symmetry transformations used to generate equivalent atoms:

#1 -x+1,-y+1,-z+1

Table 5.8.6 Bond lengths of **5.3** (Å)

U1-N2	2.3663(17)	U1-N4	2.3752(17)	U1-N3	2.3836(18)
U1-N1	2.5537(16)	U1-N6	2.5996(17)	U1-Cl1	2.6188(5)
U1-N5	2.6583(18)	N1-C27	1.485(3)	N1-C1	1.487(3)
N1-C14	1.495(3)	N2-C5	1.391(3)	N2-C2	1.396(3)
N3-C15	1.397(2)	N3-C18	1.399(3)	N4-C31	1.390(3)
N4-C28	1.391(2)	N5-C40	1.346(3)	N5-C44	1.351(3)
N6-C49	1.340(3)	N6-C45	1.353(3)	C1-C2	1.489(3)
C2-C3	1.369(3)	C3-C4	1.406(3)	C4-C5	1.375(3)
C5-C6	1.474(3)	C6-C11	1.393(3)	C6-C7	1.404(3)
C7-C8	1.388(3)	C8-C9	1.381(3)	C8-C12	1.496(3)
C9-C10	1.389(3)	C10-C11	1.389(3)	C10-C13	1.496(3)
C12-F2	1.302(4)	C12-F3	1.311(3)	C12-F1	1.315(4)
C13-F6	1.328(3)	C13-F5	1.334(3)	C13-F4	1.337(3)
C14-C15	1.486(3)	C15-C16	1.362(3)	C16-C17	1.408(3)
C17-C18	1.378(3)	C18-C19	1.462(3)	C19-C20	1.394(3)
C19-C24	1.397(3)	C20-C21	1.386(3)	C21-C22	1.381(3)
C21-C25	1.498(3)	C22-C23	1.379(3)	C23-C24	1.388(3)
C23-C26	1.504(3)	C25-F8	1.331(3)	C25-F7	1.339(3)
C25-F9	1.342(3)	C26-F10'	1.182(10)	C26-F11	1.255(4)
C26-F12'	1.300(9)	C26-F10	1.331(5)	C26-F12	1.344(5)
C26-F11'	1.372(7)	C27-C28	1.503(3)	C28-C29	1.364(3)
C29-C30	1.410(3)	C30-C31	1.383(3)	C31-C32	1.467(3)
C32-C37	1.398(3)	C32-C33	1.401(3)	C33-C34	1.388(3)
C34-C35	1.383(3)	C34-C38	1.501(3)	C35-C36	1.386(4)
C36-C37	1.388(3)	C36-C39	1.499(4)	C38-F15	1.331(3)

C38-F13	1.336(3)	C38-F14	1.343(3)	C39-F17'	1.218(10)
C39-F18'	1.267(9)	C39-F16	1.297(5)	C39-F18	1.316(5)
C39-F16'	1.316(8)	C39-F17	1.322(5)	C40-C41	1.380(3)
C41-C42	1.374(4)	C42-C43	1.377(4)	C43-C44	1.382(3)
C45-C46	1.378(3)	C46-C47	1.374(4)	C47-C48	1.382(4)
C48-C49	1.384(3)	F10-F10'	0.89(2)	F10-F11'	1.547(15)
F11-F11'	1.067(10)	F11-F12'	1.185(13)	F12-F12'	1.206(17)
F12-F10'	1.32(2)	F16-F16'	1.139(13)	F16-F18'	1.22(2)
F17-F17'	1.09(3)	F17-F16'	1.327(17)	F18-F18'	1.17(2)
F18-F17'	1.21(3)	N7-C54	1.315(5)	N7-C50	1.351(5)
C50-C51	1.344(5)	C51-C52	1.344(5)	C52-C53	1.378(5)
C53-C54	1.360(5)	N8-C55	1.327(4)	N8-C59	1.334(4)
C55-C56	1.369(4)	C56-C57	1.362(5)	C57-C58	1.370(4)
C58-C59	1.371(4)	C60-N62	1.361(5)	C60-C61#1	1.379(5)
C61-N62	1.350(5)	C61-C60#1	1.379(5)		

Symmetry transformations used to generate equivalent atoms:

#1 -x,-y+2,-z

Table 5.8.7 Bond angles of **5.3** (°)

N2-U1-N4	126.63(6)	N2-U1-N3	106.42(6)
N2-U1-N1	69.98(6)	N4-U1-N1	65.01(6)
N2-U1-N6	73.68(6)	N4-U1-N6	157.30(6)
N1-U1-N6	122.60(6)	N2-U1-Cl1	127.71(4)
N3-U1-Cl1	112.40(4)	N1-U1-Cl1	155.43(4)
N2-U1-N5	75.22(6)	N4-U1-N5	76.97(6)
N1-U1-N5	89.23(6)	N6-U1-N5	122.14(6)
C27-N1-C1	112.13(16)	C27-N1-C14	110.92(16)
C27-N1-U1	105.11(12)	C1-N1-U1	111.20(12)
C5-N2-C2	105.04(17)	C5-N2-U1	135.82(13)
C15-N3-C18	105.18(17)	C15-N3-U1	114.56(13)
C31-N4-C28	105.44(17)	C31-N4-U1	130.31(13)
C40-N5-C44	117.14(19)	C40-N5-U1	116.54(14)
C49-N6-C45	117.86(19)	C49-N6-U1	115.64(14)
N1-C1-C2	111.43(17)	C3-C2-N2	110.84(19)
N2-C2-C1	119.07(18)	C2-C3-C4	106.47(19)
C4-C5-N2	109.98(18)	C4-C5-C6	125.2(2)
C11-C6-C7	118.0(2)	C11-C6-C5	124.1(2)
C8-C7-C6	120.8(2)	C9-C8-C7	120.8(2)
C7-C8-C12	118.9(2)	C8-C9-C10	118.7(2)
C9-C10-C13	117.8(2)	C11-C10-C13	121.0(2)
F2-C12-F3	106.3(3)	F2-C12-F1	105.5(3)
F2-C12-C8	113.1(2)	F3-C12-C8	113.6(2)
F6-C13-F5	106.5(2)	F6-C13-F4	105.8(2)
F6-C13-C10	113.8(2)	F5-C13-C10	112.5(2)
C15-C14-N1	110.29(16)	C16-C15-N3	110.70(18)
N3-C15-C14	119.69(18)	C15-C16-C17	107.07(19)
C17-C18-N3	109.58(18)	C17-C18-C19	127.0(2)
C20-C19-C24	117.79(19)	C20-C19-C18	122.80(19)
C21-C20-C19	121.0(2)	C22-C21-C20	120.9(2)
C20-C21-C25	121.3(2)	C23-C22-C21	118.5(2)

C22-C23-C26	119.2(2)	C24-C23-C26	119.7(2)
F8-C25-F7	106.6(2)	F8-C25-F9	106.5(2)
F8-C25-C21	113.67(18)	F7-C25-C21	112.27(19)
F10'-C26-F11	129.0(7)	F10'-C26-F12'	109.6(10)
F10'-C26-F10	40.8(11)	F11-C26-F10	109.6(4)
F10'-C26-F12	62.7(11)	F11-C26-F12	105.9(4)
F10-C26-F12	101.9(4)	F10'-C26-F11'	106.9(10)
F12'-C26-F11'	101.6(8)	F10-C26-F11'	69.8(7)
F10'-C26-C23	115.5(6)	F11-C26-C23	114.7(3)
F10-C26-C23	112.5(3)	F12-C26-C23	111.3(3)
N1-C27-C28	108.75(16)	C29-C28-N4	110.58(19)
N4-C28-C27	118.38(18)	C28-C29-C30	107.18(19)
C30-C31-N4	109.93(18)	C30-C31-C32	127.4(2)
C37-C32-C33	118.1(2)	C37-C32-C31	120.9(2)
C34-C33-C32	120.7(2)	C35-C34-C33	120.9(2)
C33-C34-C38	121.0(2)	C34-C35-C36	118.7(2)
C35-C36-C39	118.6(2)	C37-C36-C39	120.3(2)
F15-C38-F13	106.9(2)	F15-C38-F14	106.1(2)
F15-C38-C34	113.2(2)	F13-C38-C34	111.9(2)
F17'-C39-F18'	107.7(13)	F17'-C39-F16	134.1(6)
F17'-C39-F18	56.6(16)	F18'-C39-F18	53.9(11)
F17'-C39-F16'	107.5(13)	F18'-C39-F16'	105.7(9)
F18-C39-F16'	134.0(5)	F17'-C39-F17	50.5(16)
F16-C39-F17	107.1(4)	F18-C39-F17	102.9(4)
F17'-C39-C36	112.0(6)	F18'-C39-C36	112.2(5)
F18-C39-C36	114.6(3)	F16'-C39-C36	111.4(5)
N5-C40-C41	123.1(2)	C42-C41-C40	119.1(2)
C42-C43-C44	119.2(2)	N5-C44-C43	122.6(2)
C47-C46-C45	119.2(2)	C46-C47-C48	119.1(2)
N6-C49-C48	122.6(2)	F10'-F10-C26	60.5(8)
C26-F10-F11'	56.3(4)	F11'-F11-F12'	133.7(10)
F12'-F11-C26	64.3(6)	F12'-F12-F10'	106.7(8)
F10'-F12-C26	52.6(6)	F10-F10'-C26	78.7(12)
C26-F10'-F12	64.7(8)	F11-F11'-C26	60.4(4)
C26-F11'-F10	53.9(5)	F11-F12'-F12	120.4(9)
F12-F12'-C26	64.8(7)	F16'-F16-F18'	121.9(10)
F18'-F16-C39	60.4(7)	F17'-F17-C39	59.8(9)
C39-F17-F16'	59.6(5)	F18'-F18-F17'	115.2(11)
F17'-F18-C39	57.6(9)	F16-F16'-C39	63.3(5)
C39-F16'-F17	60.0(6)	F17-F17'-F18	128.3(12)
F18-F17'-C39	65.8(10)	F18-F18'-F16	120.7(10)
F16-F18'-C39	62.9(7)	C54-N7-C50	116.6(3)
C52-C51-C50	119.1(4)	C51-C52-C53	118.6(4)
N7-C54-C53	122.9(4)	C55-N8-C59	116.6(3)
C57-C56-C55	119.2(3)	C56-C57-C58	118.8(3)
N8-C59-C58	123.7(3)	N62-C60-C61#1	121.6(3)
C61-N62-C60	117.1(3)	F11-C26-F12'	55.3(7)
N4-U1-N3	85.37(6)	F12'-C26-F10	133.3(5)
N3-U1-N1	71.59(6)	F12'-C26-F12	54.3(8)
N3-U1-N6	78.17(6)	F11-C26-F11'	47.7(5)
N4-U1-Cl1	90.76(4)	F12-C26-F11'	139.5(4)
N6-U1-Cl1	81.35(4)	F12'-C26-C23	113.7(4)
N3-U1-N5	158.20(6)	F11'-C26-C23	108.3(4)
Cl1-U1-N5	80.86(4)	C29-C28-C27	131.03(19)

C1-N1-C14	109.83(16)	C31-C30-C29	106.8(2)
C14-N1-U1	107.47(11)	N4-C31-C32	121.71(18)
C2-N2-U1	118.61(13)	C33-C32-C31	120.9(2)
C18-N3-U1	135.51(13)	C35-C34-C38	118.1(2)
C28-N4-U1	110.75(13)	C35-C36-C37	121.2(2)
C44-N5-U1	124.91(15)	C36-C37-C32	120.5(2)
C45-N6-U1	126.49(15)	F13-C38-F14	106.8(2)
C3-C2-C1	129.00(19)	F14-C38-C34	111.7(2)
C5-C4-C3	107.6(2)	F18'-C39-F16	56.7(10)
N2-C5-C6	124.79(18)	F16-C39-F18	105.3(4)
C7-C6-C5	117.93(19)	F16-C39-F16'	51.7(7)
C9-C8-C12	120.2(2)	F18'-C39-F17	135.4(6)
C9-C10-C11	121.1(2)	F16'-C39-F17	60.4(8)
C10-C11-C6	120.6(2)	F16-C39-C36	113.8(3)
F3-C12-F1	105.0(3)	F17-C39-C36	112.2(3)
F1-C12-C8	112.6(2)	C41-C42-C43	118.9(2)
F5-C13-F4	105.8(2)	N6-C45-C46	122.4(2)
F4-C13-C10	111.9(2)	C47-C48-C49	118.9(2)
C16-C15-C14	129.47(19)	F10'-F10-F11'	112.4(10)
C18-C17-C16	107.5(2)	F11'-F11-C26	71.9(6)
N3-C18-C19	123.39(18)	F12'-F12-C26	61.0(5)
C24-C19-C18	119.4(2)	F10-F10'-F12	139.7(14)
C22-C21-C25	117.76(19)	F11-F11'-F10	106.5(7)
C22-C23-C24	121.2(2)	F11-F12'-C26	60.4(5)
C23-C24-C19	120.6(2)	F16'-F16-C39	65.1(6)
F7-C25-F9	105.48(19)	F17'-F17-F16'	115.4(11)
F9-C25-C21	111.7(2)	F18'-F18-C39	60.9(7)
C54-C53-C52	119.1(4)	F16-F16'-F17	117.2(9)
N8-C55-C56	123.4(3)	F17-F17'-C39	69.7(12)
C57-C58-C59	118.3(3)	F18-F18'-C39	65.1(8)
N62-C61-C60#1	121.4(3)	C51-C50-N7	123.5(4)

Symmetry transformations used to generate equivalent atoms:

#1 -x,-y+2,-z

Table 5.8.8 Bond lengths of **5.4** (Å)

U1-O2	2.270(3)	U1-O1	2.299(3)	U1-N2	2.417(4)
U1-N3	2.433(4)	U1-N4	2.479(3)	U1-N1	2.535(3)
U1-Cl1	2.6115(10)	F1-C12	1.330(5)	F2-C12	1.336(5)
F3-C12	1.332(5)	F4-C13	1.322(5)	F5-C13	1.320(5)
F6-C13	1.333(6)	F7-C25	1.347(8)	F8-C25	1.347(8)
F7'-C25'	1.320(9)	F8'-C25'	1.315(9)	F9-C25'	1.289(9)
F9-C25	1.384(7)	F10-C26	1.313(7)	F11-C26	1.332(7)
F12-C26	1.334(6)	F13-C38	1.323(5)	F14-C38	1.339(5)
F15-C38	1.327(5)	F16-C39	1.304(7)	F17-C39	1.371(8)
F18-C39	1.340(7)	O1-N5	1.342(4)	O2-N6	1.338(5)
N1-C27	1.482(5)	N1-C1	1.483(6)	N1-C14	1.490(6)
N2-C2	1.384(5)	N2-C5	1.387(5)	N3-C15	1.396(5)
N3-C18	1.397(6)	N4-C28	1.380(5)	N4-C31	1.393(6)
N5-C44	1.331(6)	N5-C40	1.344(6)	N6-C49	1.342(6)
N6-C45	1.345(6)	C1-C2	1.500(6)	C2-C3	1.373(6)
C3-C4	1.412(6)	C4-C5	1.384(6)	C5-C6	1.462(6)
C6-C7	1.398(6)	C6-C11	1.401(6)	C7-C8	1.388(6)
C8-C9	1.390(6)	C8-C12	1.496(6)	C9-C10	1.380(7)

C10-C11	1.389(7)	C10-C13	1.501(6)	C14-C15	1.487(7)
C15-C16	1.377(6)	C16-C17	1.390(8)	C17-C18	1.382(7)
C18-C19	1.467(7)	C19-C24	1.392(7)	C19-C20'	1.409(8)
C19-C20	1.411(7)	C20-C21	1.392(8)	C21-C22	1.400(8)
C21-C25	1.527(12)	C22-C23	1.436(8)	C20'-C21'	1.385(9)
C21'-C22'	1.399(9)	C21'-C25'	1.480(16)	C22'-C23	1.375(9)
C23-C24	1.386(7)	C23-C26	1.505(9)	C27-C28	1.483(6)
C28-C29	1.381(6)	C29-C30	1.393(7)	C30-C31	1.389(6)
C31-C32	1.458(6)	C32-C33	1.394(6)	C32-C37	1.400(7)
C33-C34	1.381(6)	C34-C35	1.366(7)	C34-C38	1.501(6)
C35-C36	1.387(8)	C36-C37	1.383(8)	C36-C39	1.521(7)
C40-C41	1.370(7)	C41-C42	1.374(8)	C42-C43	1.370(8)
C43-C44	1.376(7)	C45-C46	1.364(8)	C46-C47	1.374(8)
C47-C48	1.370(8)	C48-C49	1.375(7)	C50-C51	1.348(10)
C50-C55	1.382(10)	C50-C56	1.490(10)	C51-C52	1.388(12)
C52-C53	1.365(14)	C53-C54	1.368(14)	C54-C55	1.358(12)

Table 5.8.9 Bond angles of **5.4** (°)

O2-U1-O1	116.80(11)	O2-U1-N2	153.94(11)
O2-U1-N3	75.65(11)	O1-U1-N3	167.51(12)
O2-U1-N4	80.02(11)	O1-U1-N4	73.27(11)
N3-U1-N4	111.67(11)	O2-U1-N1	121.28(11)
N2-U1-N1	65.17(11)	N3-U1-N1	71.60(12)
O2-U1-Cl1	83.37(8)	O1-U1-Cl1	78.45(8)
N3-U1-Cl1	103.25(9)	N4-U1-Cl1	135.79(8)
C25'-F9-C25	66.9(6)	N5-O1-U1	136.1(2)
C27-N1-C1	111.6(3)	C27-N1-C14	109.3(3)
C27-N1-U1	110.8(3)	C1-N1-U1	103.4(2)
C2-N2-C5	106.0(3)	C2-N2-U1	110.0(3)
C15-N3-C18	105.0(4)	C15-N3-U1	112.9(3)
C28-N4-C31	104.9(3)	C28-N4-U1	115.4(3)
C44-N5-O1	118.7(4)	C44-N5-C40	121.7(4)
O2-N6-C49	120.3(4)	O2-N6-C45	117.6(4)
N1-C1-C2	108.8(3)	C3-C2-N2	110.5(4)
N2-C2-C1	118.7(4)	C2-C3-C4	106.7(4)
C4-C5-N2	109.7(4)	C4-C5-C6	127.3(4)
C7-C6-C11	117.6(4)	C7-C6-C5	120.8(4)
C8-C7-C6	121.2(4)	C7-C8-C9	120.6(4)
C9-C8-C12	118.2(4)	C10-C9-C8	118.6(4)
C9-C10-C13	119.2(4)	C11-C10-C13	119.5(4)
F1-C12-F3	106.3(4)	F1-C12-F2	106.2(4)
F1-C12-C8	113.1(4)	F3-C12-C8	113.1(4)
F5-C13-F4	105.6(4)	F5-C13-F6	107.6(4)
F5-C13-C10	113.6(4)	F4-C13-C10	111.7(4)
C15-C14-N1	110.5(4)	C16-C15-N3	110.6(4)
N3-C15-C14	120.2(4)	C15-C16-C17	106.8(4)
C17-C18-N3	109.5(4)	C17-C18-C19	126.1(4)
C24-C19-C20'	107.0(6)	C24-C19-C20	124.2(5)
C24-C19-C18	123.3(4)	C20'-C19-C18	128.5(6)
C21-C20-C19	115.8(7)	C20-C21-C22	118.9(8)
C22-C21-C25	120.9(7)	C21-C22-C23	125.9(8)
C20'-C21'-C22'	121.8(9)	C20'-C21'-C25'	127.3(9)

C23-C22'-C21'	107.4(8)	C22'-C23-C24	130.7(7)
C24-C23-C22	113.1(6)	C22'-C23-C26	106.6(7)
C22-C23-C26	125.4(6)	C23-C24-C19	121.4(5)
F7-C25-F9	114.9(8)	F8-C25-F9	106.2(7)
F8-C25-C21	111.7(7)	F9-C25-C21	109.5(7)
F9-C25'-F7'	92.7(9)	F8'-C25'-F7'	109.3(11)
F8'-C25'-C21'	117.4(10)	F7'-C25'-C21'	108.7(10)
F10-C26-F12	107.3(6)	F11-C26-F12	108.1(6)
F11-C26-C23	110.9(7)	F12-C26-C23	110.6(6)
N4-C28-C29	111.6(4)	N4-C28-C27	119.5(4)
C28-C29-C30	106.1(4)	C31-C30-C29	107.7(4)
C30-C31-C32	125.7(4)	N4-C31-C32	124.6(4)
C33-C32-C31	124.4(4)	C37-C32-C31	119.5(4)
C35-C34-C33	121.4(5)	C35-C34-C38	118.7(4)
C34-C35-C36	117.9(5)	C37-C36-C35	121.2(5)
C35-C36-C39	118.2(6)	C36-C37-C32	121.4(5)
F13-C38-F14	106.0(4)	F15-C38-F14	105.0(3)
F15-C38-C34	113.0(4)	F14-C38-C34	111.4(4)
F16-C39-F17	105.0(8)	F18-C39-F17	109.7(8)
F18-C39-C36	110.6(6)	F17-C39-C36	112.6(7)
C40-C41-C42	120.4(5)	C43-C42-C41	118.7(5)
N5-C44-C43	120.0(5)	N6-C45-C46	119.1(5)
C48-C47-C46	118.7(5)	C47-C48-C49	120.1(5)
C51-C50-C55	118.9(8)	C51-C50-C56	120.9(8)
C50-C51-C52	121.5(8)	C53-C52-C51	118.7(9)
C55-C54-C53	120.7(10)	C54-C55-C50	120.1(9)
O1-U1-N2	83.84(12)	C21'-C20'-C19	130.0(10)
N2-U1-N3	83.95(12)	C22'-C21'-C25'	110.0(9)
N2-U1-N4	123.25(12)	C22'-C23-C22	26.4(6)
O1-U1-N1	100.74(11)	C24-C23-C26	121.1(5)
N4-U1-N1	69.18(12)	F7-C25-F8	104.2(8)
N2-U1-Cl1	85.76(8)	F7-C25-C21	110.2(7)
N1-U1-Cl1	150.71(9)	F9-C25'-F8'	112.4(10)
N6-O2-U1	143.5(3)	F9-C25'-C21'	113.4(10)
C1-N1-C14	112.8(4)	F10-C26-F11	106.0(6)
C14-N1-U1	108.8(2)	F10-C26-C23	113.8(5)
C5-N2-U1	135.9(3)	N1-C27-C28	111.1(3)
C18-N3-U1	136.2(3)	C29-C28-C27	128.9(4)
C31-N4-U1	136.7(3)	C30-C31-N4	109.7(4)
O1-N5-C40	119.6(4)	C33-C32-C37	116.1(4)
C49-N6-C45	122.0(4)	C34-C33-C32	121.9(4)
C3-C2-C1	130.6(4)	C33-C34-C38	119.9(4)
C5-C4-C3	107.0(4)	C37-C36-C39	120.2(6)
N2-C5-C6	122.0(4)	F13-C38-F15	107.2(4)
C11-C6-C5	121.2(4)	F13-C38-C34	113.6(4)
C7-C8-C12	121.1(4)	F16-C39-F18	106.5(7)
C9-C10-C11	121.2(4)	F16-C39-C36	112.1(7)
C10-C11-C6	120.7(4)	N5-C40-C41	119.3(5)
F3-C12-F2	105.9(4)	C42-C43-C44	119.9(5)
F2-C12-C8	111.7(4)	C45-C46-C47	120.7(6)
F4-C13-F6	105.2(4)	N6-C49-C48	119.3(5)
F6-C13-C10	112.5(4)	C55-C50-C56	120.2(8)
C16-C15-C14	129.1(4)	C52-C53-C54	120.0(9)
C18-C17-C16	108.0(4)	C20-C19-C18	111.8(5)

N3-C18-C19	124.3(4)	C20-C21-C25	120.2(7)
C20'-C19-C20	26.5(5)		

Table 5.8.10 Bond lengths of **5.5** (Å)

U1-N3	2.391(6)	U1-N2	2.437(6)	U1-N4	2.444(5)
U1-O2	2.572(5)	U1-O1	2.582(5)	U1-N1	2.622(5)
O1-C43	1.427(8)	O1-C45	1.436(8)	O2-C46	1.431(9)
O2-C44	1.451(8)	N1-C29	1.480(9)	N1-C1	1.484(9)
N1-C15	1.488(9)	N2-C2	1.379(9)	N2-C5	1.382(9)
N3-C16	1.377(9)	N3-C19	1.393(9)	N4-C30	1.371(8)
N4-C33	1.387(8)	C1-C2	1.498(10)	C2-C3	1.370(10)
C3-C4	1.414(11)	C4-C5	1.380(10)	C5-C6	1.489(10)
C6-C11	1.411(10)	C6-C7	1.412(10)	C7-C8	1.400(10)
C7-C12	1.501(11)	C8-C9	1.373(11)	C9-C10	1.391(11)
C9-C13	1.511(11)	C10-C11	1.390(11)	C11-C14	1.497(11)
C15-C16	1.503(10)	C16-C17	1.377(10)	C17-C18	1.406(11)
C18-C19	1.379(10)	C19-C20	1.487(10)	C20-C21	1.415(10)
C20-C25	1.415(10)	C21-C22	1.382(10)	C21-C26	1.512(10)
C22-C23	1.382(11)	C23-C24	1.390(11)	C23-C27	1.514(10)
C24-C25	1.394(11)	C25-C28	1.508(11)	C29-C30	1.496(9)
C30-C31	1.378(10)	C31-C32	1.400(11)	C32-C33	1.384(10)
C33-C34	1.470(10)	C34-C39	1.409(10)	C34-C35	1.413(11)
C35-C36	1.387(11)	C35-C40	1.506(11)	C36-C37	1.408(11)
C37-C38	1.375(12)	C37-C41	1.504(12)	C38-C39	1.398(11)
C39-C42	1.508(12)	C43-C44	1.490(10)	O3-C47	1.388(18)
O3-C49	1.47(2)	O4-C48	1.362(18)	O4-C50	1.47(2)
C47-C48	1.51(2)	O5-C51	1.363(13)	O5-C52	1.398(13)
C51-C51#1	1.48(2)				

Symmetry transformations used to generate equivalent atoms:

#1 -x+2,-y,-z

Table 5.8.11 Bond angles of **5.5** (°)

N3-U1-N2	113.50(19)	N3-U1-N4	93.35(19)
N3-U1-O2	108.60(18)	N2-U1-O2	115.69(18)
N3-U1-O1	74.81(18)	N2-U1-O1	85.45(18)
O2-U1-O1	61.47(15)	N3-U1-N1	63.95(19)
N4-U1-N1	66.32(18)	O2-U1-N1	172.25(17)
C43-O1-C45	113.8(5)	C43-O1-U1	120.6(4)
C46-O2-C44	112.4(5)	C46-O2-U1	116.2(4)
C29-N1-C1	111.1(5)	C29-N1-C15	110.8(5)
C29-N1-U1	109.4(4)	C1-N1-U1	107.7(4)
C2-N2-C5	106.1(6)	C2-N2-U1	118.3(5)
C16-N3-C19	106.5(6)	C16-N3-U1	117.9(4)
C30-N4-C33	106.7(6)	C30-N4-U1	119.4(4)
N1-C1-C2	110.4(6)	C3-C2-N2	110.7(6)
N2-C2-C1	119.4(6)	C2-C3-C4	106.4(7)
C4-C5-N2	109.7(6)	C4-C5-C6	126.0(7)
C11-C6-C7	118.5(7)	C11-C6-C5	121.6(6)
C8-C7-C6	119.5(7)	C8-C7-C12	117.6(7)
C9-C8-C7	122.3(7)	C8-C9-C10	117.9(7)
C10-C9-C13	121.2(7)	C11-C10-C9	122.2(7)

C10-C11-C14	118.4(7)	C6-C11-C14	121.8(7)
N3-C16-C17	110.2(6)	N3-C16-C15	117.5(6)
C16-C17-C18	106.6(6)	C19-C18-C17	107.7(7)
C18-C19-C20	130.2(7)	N3-C19-C20	120.5(6)
C21-C20-C19	120.8(6)	C25-C20-C19	120.4(6)
C22-C21-C26	119.2(7)	C20-C21-C26	120.9(7)
C22-C23-C24	116.8(7)	C22-C23-C27	120.6(8)
C23-C24-C25	123.2(7)	C24-C25-C20	118.6(7)
C20-C25-C28	121.7(7)	N1-C29-C30	110.8(5)
N4-C30-C29	119.5(6)	C31-C30-C29	130.2(6)
C33-C32-C31	107.3(7)	C32-C33-N4	109.0(7)
N4-C33-C34	120.0(6)	C39-C34-C35	119.4(7)
C35-C34-C33	119.2(7)	C36-C35-C34	119.3(7)
C34-C35-C40	120.8(7)	C35-C36-C37	121.8(8)
C38-C37-C41	122.5(8)	C36-C37-C41	119.7(8)
C38-C39-C34	119.0(7)	C38-C39-C42	119.9(7)
O1-C43-C44	107.5(6)	O2-C44-C43	108.4(6)
C48-O4-C50	109.8(15)	O3-C47-C48	108.9(14)
C51-O5-C52	116.4(10)	O5-C51-C51#1	111.7(13)
N2-U1-N4	106.0(2)	N1-C15-C16	108.3(5)
N4-U1-O2	117.73(17)	C17-C16-C15	132.3(7)
N4-U1-O1	166.26(19)	C18-C19-N3	108.9(6)
N2-U1-N1	67.58(19)	C21-C20-C25	118.7(6)
O1-U1-N1	112.88(16)	C22-C21-C20	119.7(7)
C45-O1-U1	120.9(4)	C23-C22-C21	122.9(7)
C44-O2-U1	121.2(4)	C24-C23-C27	122.6(7)
C1-N1-C15	112.2(5)	C24-C25-C28	119.7(7)
C15-N1-U1	105.4(4)	N4-C30-C31	110.1(6)
C5-N2-U1	135.3(5)	C30-C31-C32	106.9(7)
C19-N3-U1	131.5(5)	C32-C33-C34	130.8(7)
C33-N4-U1	133.4(5)	C39-C34-C33	121.4(7)
C3-C2-C1	129.9(7)	C36-C35-C40	119.7(7)
C5-C4-C3	107.1(7)	C38-C37-C36	117.8(7)
N2-C5-C6	124.3(6)	C37-C38-C39	122.5(7)
C7-C6-C5	119.8(6)	C34-C39-C42	121.1(7)
C6-C7-C12	122.9(7)	C47-O3-C49	110.5(14)
C8-C9-C13	120.8(8)	O4-C48-C47	107.9(14)
C10-C11-C6	119.7(7)		

Symmetry transformations used to generate equivalent atoms:

#1 -x+2,-y,-z

Table 5.8.12 Bond lengths of **5.6** (Å)

U1-N3	2.368(13)	U1-N4	2.386(14)	U1-N2	2.405(14)
U1-O1	2.497(12)	U1-N1	2.627(13)	O1-C46	1.459(10)
O1-C43	1.46(2)	O1-C46'	1.462(10)	N1-C15	1.48(2)
N1-C29	1.49(2)	N1-C1	1.49(2)	N2-C5	1.37(2)
N2-C2	1.410(18)	N3-C16	1.38(2)	N3-C19	1.40(2)
N4-C33	1.406(18)	N4-C30	1.406(19)	C1-C2	1.48(2)
C2-C3	1.36(3)	C3-C4	1.42(3)	C4-C5	1.38(2)
C5-C6	1.49(2)	C6-C7	1.42(2)	C6-C11	1.42(2)
C7-C8	1.42(2)	C7-C12	1.52(3)	C8-C9	1.39(3)
C9-C10	1.35(3)	C9-C13	1.53(2)	C10-C11	1.39(2)
C11-C14	1.53(2)	C15-C16	1.47(3)	C16-C17	1.38(2)

C17-C18	1.43(3)	C18-C19	1.38(3)	C19-C20	1.49(3)
C20-C21	1.40(3)	C20-C25	1.41(2)	C21-C22	1.40(3)
C21-C26	1.52(3)	C22-C23	1.41(3)	C23-C24	1.38(3)
C23-C27	1.51(3)	C24-C25	1.42(3)	C25-C28	1.46(3)
C29-C30	1.47(2)	C30-C31	1.39(2)	C31-C32	1.41(2)
C32-C33	1.37(2)	C33-C34	1.49(2)	C34-C35	1.40(2)
C34-C39	1.43(2)	C35-C36	1.43(2)	C35-C40	1.50(2)
C36-C37	1.38(2)	C37-C38	1.38(3)	C37-C41	1.53(3)
C38-C39	1.39(3)	C39-C42	1.50(3)	C43-C44	1.48(3)
C44-C45	1.48(4)	C45-C46	1.518(10)	C45-C46'	1.521(10)

Table 5.8.13 Bond angles of **5.6** (°)

N3-U1-N4	106.9(5)	N3-U1-N2	104.8(5)
N3-U1-O1	109.0(5)	N4-U1-O1	103.8(4)
N3-U1-N1	67.9(4)	N4-U1-N1	69.1(4)
O1-U1-N1	169.9(5)	C46-O1-C43	109.0(15)
C43-O1-C46'	100(2)	C46-O1-U1	114.4(11)
C46'-O1-U1	121.5(17)	C15-N1-C29	112.9(14)
C29-N1-C1	110.6(13)	C15-N1-U1	107.2(9)
C1-N1-U1	108.6(9)	C5-N2-C2	105.7(14)
C2-N2-U1	120.4(11)	C16-N3-C19	105.7(14)
C19-N3-U1	134.6(12)	C33-N4-C30	104.7(13)
C30-N4-U1	117.2(10)	C2-C1-N1	108.9(13)
C3-C2-C1	133.6(14)	N2-C2-C1	117.3(14)
C5-C4-C3	105.1(17)	N2-C5-C4	111.3(15)
C4-C5-C6	129.4(17)	C7-C6-C11	118.8(15)
C11-C6-C5	120.4(15)	C6-C7-C8	119.2(16)
C8-C7-C12	120.2(16)	C9-C8-C7	120.2(16)
C10-C9-C13	120.4(18)	C8-C9-C13	119.3(17)
C10-C11-C6	119.2(15)	C10-C11-C14	121.9(16)
C16-C15-N1	109.7(14)	C17-C16-N3	110.9(16)
N3-C16-C15	119.2(13)	C16-C17-C18	106.3(17)
C18-C19-N3	110.1(18)	C18-C19-C20	128.6(19)
C21-C20-C25	119.6(18)	C21-C20-C19	121.6(17)
C20-C21-C22	119.8(19)	C20-C21-C26	120.8(19)
C21-C22-C23	122(2)	C24-C23-C22	117.0(19)
C22-C23-C27	122(2)	C23-C24-C25	123(2)
C20-C25-C28	123.5(19)	C24-C25-C28	118.0(18)
C31-C30-N4	110.0(15)	C31-C30-C29	131.7(16)
C30-C31-C32	107.0(15)	C33-C32-C31	107.2(16)
C32-C33-C34	127.0(14)	N4-C33-C34	121.9(13)
C35-C34-C33	121.6(15)	C39-C34-C33	119.9(15)
C34-C35-C40	122.9(15)	C36-C35-C40	118.9(16)
C38-C37-C36	116.4(16)	C38-C37-C41	123.8(17)
C37-C38-C39	123.5(17)	C38-C39-C34	119.6(17)
C34-C39-C42	121.5(17)	O1-C43-C44	104.5(17)
C44-C45-C46	104.9(18)	C44-C45-C46'	90(3)
O1-C46-C45	106.6(16)	O1-C46'-C45	106.4(16)
N4-U1-N2	108.3(5)	N3-C19-C20	121.1(16)
N2-U1-O1	123.3(4)	C25-C20-C19	118.8(17)
N2-U1-N1	66.6(5)	C22-C21-C26	119.4(19)
C46-O1-C46'	38(3)	C24-C23-C27	121(2)

C43-O1-U1	134.8(11)	C20-C25-C24	118.4(19)
C15-N1-C1	111.2(14)	C30-C29-N1	109.5(14)
C29-N1-U1	106.1(10)	N4-C30-C29	118.3(15)
C5-N2-U1	132.8(10)	C32-C33-N4	111.1(15)
C16-N3-U1	119.6(10)	C35-C34-C39	118.4(16)
C33-N4-U1	134.3(11)	C34-C35-C36	117.9(16)
C3-C2-N2	109.1(14)	C37-C36-C35	123.4(18)
C2-C3-C4	108.8(15)	C36-C37-C41	119.8(18)
N2-C5-C6	119.0(14)	C38-C39-C42	118.9(18)
C7-C6-C5	120.7(15)	C43-C44-C45	110(2)
C6-C7-C12	120.5(15)	C46-C45-C46'	37(3)
C10-C9-C8	120.3(17)	C17-C16-C15	129.4(16)
C9-C10-C11	122.3(17)	C19-C18-C17	107.0(18)
C6-C11-C14	118.9(15)		

Table 5.8.14 Bond lengths of **5.7** (Å)

U1-N4	2.305(4)	U1-N3	2.329(4)	U1-N2	2.345(5)
U1-O1	2.456(4)	U1-N1	2.572(5)	U1-Cl1	2.5987(14)
O1-C43	1.458(9)	O1-C46	1.462(9)	N1-C15	1.469(7)
N1-C1	1.478(7)	N1-C29	1.506(8)	N2-C2	1.385(8)
N2-C5	1.398(7)	N3-C16	1.409(6)	N3-C19	1.425(6)
N4-C30	1.373(8)	N4-C33	1.387(7)	C1-C2	1.504(8)
C2-C3	1.377(8)	C3-C4	1.409(9)	C4-C5	1.335(9)
C5-C6	1.484(8)	C6-C11	1.388(8)	C6-C7	1.418(9)
C7-C8	1.387(10)	C7-C12	1.533(11)	C8-C9	1.393(11)
C9-C10	1.394(10)	C9-C13	1.527(10)	C10-C11	1.407(8)
C11-C14	1.506(8)	C15-C16	1.492(8)	C16-C17	1.382(7)
C17-C18	1.420(8)	C18-C19	1.356(7)	C19-C20	1.482(7)
C20-C21	1.395(7)	C20-C25	1.410(8)	C21-C22	1.417(8)
C21-C26	1.519(8)	C22-C23	1.344(10)	C23-C24	1.405(10)
C23-C27	1.505(9)	C24-C25	1.381(9)	C25-C28	1.530(9)
C29-C30	1.510(9)	C30-C31	1.353(8)	C31-C32	1.390(10)
C32-C33	1.401(9)	C33-C34	1.477(9)	C34-C39	1.398(8)
C34-C35	1.426(8)	C35-C36	1.386(10)	C35-C40	1.530(8)
C36-C37	1.393(10)	C37-C38	1.403(11)	C37-C41	1.539(10)
C38-C39	1.380(10)	C39-C42	1.512(9)	C43-C44	1.545(10)
C44-C45	1.462(17)	C45-C46	1.521(10)		

Table 5.8.15 Bond angles of **5.7** (°)

N4-U1-N3	99.35(14)	N4-U1-N2	117.99(17)
N4-U1-O1	78.49(14)	N3-U1-O1	176.34(16)
N4-U1-N1	65.91(15)	N3-U1-N1	66.46(16)
O1-U1-N1	114.87(17)	N4-U1-Cl1	111.71(12)
N2-U1-Cl1	124.93(11)	O1-U1-Cl1	82.51(13)
C43-O1-C46	110.7(5)	C43-O1-U1	119.5(4)
C15-N1-C1	109.5(5)	C15-N1-C29	110.8(4)
C15-N1-U1	108.1(3)	C1-N1-U1	110.3(3)
C2-N2-C5	106.0(5)	C2-N2-U1	119.5(3)
C16-N3-C19	105.5(4)	C16-N3-U1	118.5(3)
C30-N4-C33	107.9(5)	C30-N4-U1	117.7(3)

N1-C1-C2	110.8(5)	C3-C2-N2	110.2(5)
N2-C2-C1	120.1(5)	C2-C3-C4	105.1(6)
C4-C5-N2	108.8(5)	C4-C5-C6	128.7(5)
C11-C6-C7	119.2(6)	C11-C6-C5	122.2(5)
C8-C7-C6	119.6(7)	C8-C7-C12	121.2(7)
C7-C8-C9	121.6(6)	C8-C9-C10	118.7(6)
C10-C9-C13	120.8(8)	C9-C10-C11	120.7(6)
C6-C11-C14	121.9(5)	C10-C11-C14	117.8(5)
C17-C16-N3	109.9(5)	C17-C16-C15	131.4(5)
C16-C17-C18	106.5(4)	C19-C18-C17	109.0(5)
C18-C19-C20	128.3(5)	N3-C19-C20	121.7(4)
C21-C20-C19	121.3(5)	C25-C20-C19	119.4(5)
C20-C21-C26	121.8(5)	C22-C21-C26	119.2(5)
C22-C23-C24	118.4(6)	C22-C23-C27	121.2(7)
C25-C24-C23	121.8(5)	C24-C25-C20	119.3(5)
C20-C25-C28	119.7(5)	N1-C29-C30	108.3(5)
C31-C30-C29	132.5(6)	N4-C30-C29	117.3(5)
C31-C32-C33	108.5(5)	N4-C33-C32	106.4(6)
C32-C33-C34	133.4(6)	C39-C34-C35	118.6(6)
C35-C34-C33	119.4(5)	C36-C35-C34	119.8(6)
C34-C35-C40	121.8(6)	C35-C36-C37	121.4(6)
C36-C37-C41	120.7(7)	C38-C37-C41	121.2(6)
C38-C39-C34	120.2(6)	C38-C39-C42	118.5(6)
O1-C43-C44	104.0(7)	C45-C44-C43	105.4(8)
O1-C46-C45	105.8(7)	C6-C7-C12	119.1(7)
N3-U1-N2	98.24(15)	C8-C9-C13	120.5(7)
N2-U1-O1	85.39(16)	C6-C11-C10	120.2(5)
N2-U1-N1	68.22(15)	N1-C15-C16	108.2(4)
N3-U1-Cl1	95.64(11)	N3-C16-C15	118.7(4)
N1-U1-Cl1	160.36(11)	C18-C19-N3	109.1(5)
C46-O1-U1	129.6(4)	C21-C20-C25	119.3(5)
C1-N1-C29	113.8(5)	C20-C21-C22	119.0(5)
C29-N1-U1	104.1(3)	C23-C22-C21	122.3(6)
C5-N2-U1	133.3(4)	C24-C23-C27	120.4(7)
C19-N3-U1	134.3(3)	C24-C25-C28	121.0(6)
C33-N4-U1	130.6(4)	C31-C30-N4	110.0(6)
C3-C2-C1	129.6(6)	C30-C31-C32	107.1(6)
C5-C4-C3	109.9(6)	N4-C33-C34	120.0(5)
N2-C5-C6	122.3(5)	C39-C34-C33	122.1(5)
C7-C6-C5	118.6(6)	C36-C35-C40	118.4(6)
C34-C39-C42	121.3(6)	C36-C37-C38	118.1(6)
C44-C45-C46	106.2(7)	C39-C38-C37	121.7(6)

Table 5.8.16 Bond lengths of **5.8** (Å)

N4-U1-N3	99.35(14)	N4-U1-N2	117.99(17)
N4-U1-O1	78.49(14)	N3-U1-O1	176.34(16)
N4-U1-N1	65.91(15)	N3-U1-N1	66.46(16)
O1-U1-N1	114.87(17)	N4-U1-Cl1	111.71(12)
N2-U1-Cl1	124.93(11)	O1-U1-Cl1	82.51(13)
C43-O1-C46	110.7(5)	C43-O1-U1	119.5(4)
C15-N1-C1	109.5(5)	C15-N1-C29	110.8(4)
C15-N1-U1	108.1(3)	C1-N1-U1	110.3(3)

C2-N2-C5	106.0(5)	C2-N2-U1	119.5(3)
C16-N3-C19	105.5(4)	C16-N3-U1	118.5(3)
C30-N4-C33	107.9(5)	C30-N4-U1	117.7(3)
N1-C1-C2	110.8(5)	C3-C2-N2	110.2(5)
N2-C2-C1	120.1(5)	C2-C3-C4	105.1(6)
C4-C5-N2	108.8(5)	C4-C5-C6	128.7(5)
C11-C6-C7	119.2(6)	C11-C6-C5	122.2(5)
C8-C7-C6	119.6(7)	C8-C7-C12	121.2(7)
C7-C8-C9	121.6(6)	C8-C9-C10	118.7(6)
C10-C9-C13	120.8(8)	C9-C10-C11	120.7(6)
C6-C11-C14	121.9(5)	C10-C11-C14	117.8(5)
C17-C16-N3	109.9(5)	C17-C16-C15	131.4(5)
C16-C17-C18	106.5(4)	C19-C18-C17	109.0(5)
C18-C19-C20	128.3(5)	N3-C19-C20	121.7(4)
C21-C20-C19	121.3(5)	C25-C20-C19	119.4(5)
C20-C21-C26	121.8(5)	C22-C21-C26	119.2(5)
C22-C23-C24	118.4(6)	C22-C23-C27	121.2(7)
C25-C24-C23	121.8(5)	C24-C25-C20	119.3(5)
C20-C25-C28	119.7(5)	N1-C29-C30	108.3(5)
C31-C30-C29	132.5(6)	N4-C30-C29	117.3(5)
C31-C32-C33	108.5(5)	N4-C33-C32	106.4(6)
C32-C33-C34	133.4(6)	C39-C34-C35	118.6(6)
C35-C34-C33	119.4(5)	C36-C35-C34	119.8(6)
C34-C35-C40	121.8(6)	C35-C36-C37	121.4(6)
C36-C37-C41	120.7(7)	C38-C37-C41	121.2(6)
C38-C39-C34	120.2(6)	C38-C39-C42	118.5(6)
O1-C43-C44	104.0(7)	C45-C44-C43	105.4(8)
O1-C46-C45	105.8(7)	C21-C20-C25	119.3(5)
N3-U1-N2	98.24(15)	C20-C21-C22	119.0(5)
N2-U1-O1	85.39(16)	C23-C22-C21	122.3(6)
N2-U1-N1	68.22(15)	C24-C23-C27	120.4(7)
N3-U1-Cl1	95.64(11)	C24-C25-C28	121.0(6)
N1-U1-Cl1	160.36(11)	C31-C30-N4	110.0(6)
C46-O1-U1	129.6(4)	C30-C31-C32	107.1(6)
C1-N1-C29	113.8(5)	N4-C33-C34	120.0(5)
C29-N1-U1	104.1(3)	C39-C34-C33	122.1(5)
C5-N2-U1	133.3(4)	C36-C35-C40	118.4(6)
C19-N3-U1	134.3(3)	C36-C37-C38	118.1(6)
C33-N4-U1	130.6(4)	C39-C38-C37	121.7(6)
C3-C2-C1	129.6(6)	C34-C39-C42	121.3(6)
C5-C4-C3	109.9(6)	C44-C45-C46	106.2(7)
N2-C5-C6	122.3(5)	C6-C11-C10	120.2(5)
C7-C6-C5	118.6(6)	N1-C15-C16	108.2(4)
C6-C7-C12	119.1(7)	N3-C16-C15	118.7(4)
C8-C9-C13	120.5(7)	C18-C19-N3	109.1(5)

Table 5.8.17 Bond angles of **5.8** (°)

N2-U1-N4	116.31(7)	N2-U1-N3	96.81(6)
N2-U1-O1	74.87(7)	N4-U1-O1	78.59(7)
N2-U1-N1	64.63(6)	N4-U1-N1	66.76(6)
O1-U1-N1	102.88(7)	N2-U1-C47	108.04(7)
N3-U1-C47	90.99(7)	O1-U1-C47	98.94(7)

C46-O1-C43	106.0(3)	C46-O1-U1	123.2(2)
C1-N1-C29	112.58(18)	C1-N1-C15	110.53(18)
C1-N1-U1	104.75(13)	C29-N1-U1	110.10(13)
C2-N2-C5	105.79(19)	C2-N2-U1	117.43(15)
C19-N3-C16	104.79(18)	C19-N3-U1	138.58(15)
C30-N4-C33	105.76(18)	C30-N4-U1	120.47(15)
N1-C1-C2	108.65(19)	C3-C2-N2	110.7(2)
N2-C2-C1	118.2(2)	C2-C3-C4	106.6(2)
C4-C5-N2	109.6(2)	C4-C5-C6	128.1(2)
C7-C6-C11	118.6(2)	C7-C6-C5	121.2(2)
C8-C7-C6	119.6(3)	C8-C7-C12	118.9(3)
C9-C8-C7	122.3(3)	C10-C9-C8	117.3(3)
C8-C9-C13	120.9(3)	C9-C10-C11	122.7(3)
C10-C11-C14	119.5(2)	C6-C11-C14	120.9(2)
C17-C16-N3	111.2(2)	C17-C16-C15	127.6(2)
C16-C17-C18	106.5(2)	C19-C18-C17	106.9(2)
C18-C19-C20	122.9(2)	N3-C19-C20	125.97(19)
C25-C20-C19	120.51(19)	C21-C20-C19	119.5(2)
C22-C21-C26	120.1(2)	C20-C21-C26	120.4(2)
C24-C23-C22	118.0(2)	C24-C23-C27	121.6(2)
C23-C24-C25	121.6(2)	C24-C25-C20	119.8(2)
C20-C25-C28	120.3(2)	N1-C29-C30	111.03(19)
C31-C30-C29	130.7(2)	N4-C30-C29	118.6(2)
C33-C32-C31	107.3(2)	C32-C33-N4	109.6(2)
N4-C33-C34	121.7(2)	C35-C34-C39	119.2(2)
C39-C34-C33	120.6(2)	C36-C35-C34	119.7(2)
C34-C35-C40	121.3(2)	C37-C36-C35	122.0(2)
C38-C37-C41	120.9(2)	C36-C37-C41	121.5(3)
C38-C39-C34	118.8(2)	C38-C39-C42	118.5(2)
C44-C43-O1	109.0(3)	C43-C44-C45	102.1(5)
C45-C44-C45'	26.8(5)	C44-C45-C46	104.0(6)
O1-C46-C45'	110.3(4)	O1-C46-C45	107.5(5)
C47-P1-C54	110.95(12)	C47-P1-C60	113.24(11)
C47-P1-C48	116.27(11)	C54-P1-C48	104.28(11)
P1-C47-U1	145.56(12)	C49-C48-C53	119.0(2)
C53-C48-P1	120.34(18)	C48-C49-C50	120.3(2)
C50-C51-C52	119.6(2)	C53-C52-C51	120.4(2)
C59-C54-C55	118.6(2)	C59-C54-P1	122.7(2)
C54-C55-C56	120.1(3)	C57-C56-C55	120.4(3)
C57-C58-C59	120.7(3)	C58-C59-C54	120.3(3)
C61-C60-P1	119.05(17)	C65-C60-P1	121.70(18)
C63-C62-C61	120.5(2)	C62-C63-C64	119.8(2)
C64-C65-C60	120.3(2)	C71-C66-C67	117.7(4)
C67-C66-C72	121.0(4)	C68-C67-C66	120.8(4)
C70-C69-C68	119.9(4)	C69-C70-C71	120.1(4)
C78-C73-C74	118.9(4)	C78-C73-C79	119.2(4)
C75-C74-C73	121.0(4)	C74-C75-C76	120.1(5)
C78-C77-C76	122.7(5)	C77-C78-C73	120.0(4)
N4-U1-N3	98.75(6)	C22-C21-C20	119.3(2)
N3-U1-O1	168.61(7)	C21-C22-C23	122.0(2)
N3-U1-N1	66.13(6)	C22-C23-C27	120.4(2)
N4-U1-C47	132.81(7)	C24-C25-C28	119.8(2)
N1-U1-C47	153.72(6)	C31-C30-N4	110.7(2)
C43-O1-U1	129.16(19)	C30-C31-C32	106.7(2)

C29-N1-C15	110.40(18)	C32-C33-C34	128.7(2)
C15-N1-U1	108.26(13)	C35-C34-C33	120.2(2)
C5-N2-U1	135.67(15)	C36-C35-C40	118.9(2)
C16-N3-U1	116.13(14)	C38-C37-C36	117.5(2)
C33-N4-U1	133.04(15)	C37-C38-C39	122.8(2)
C3-C2-C1	131.1(2)	C34-C39-C42	122.7(2)
C5-C4-C3	107.3(2)	C43-C44-C45'	107.3(4)
N2-C5-C6	122.1(2)	C44-C45'-C46	104.3(5)
C11-C6-C5	120.0(2)	C45'-C46-C45	26.4(5)
C6-C7-C12	121.4(3)	C54-P1-C60	108.76(11)
C10-C9-C13	121.8(3)	C60-P1-C48	102.60(10)
C10-C11-C6	119.5(3)	C49-C48-P1	120.57(18)
N1-C15-C16	110.13(18)	C51-C50-C49	120.4(3)
N3-C16-C15	121.11(19)	C52-C53-C48	120.3(2)
C18-C19-N3	110.7(2)	C55-C54-P1	118.6(2)
C25-C20-C21	119.2(2)	C58-C57-C56	119.8(3)
C71-C66-C72	121.3(4)	C61-C60-C65	119.1(2)
C69-C68-C67	120.0(4)	C62-C61-C60	120.1(2)
C66-C71-C70	121.5(4)	C63-C64-C65	120.2(2)
C74-C73-C79	121.9(4)	C75-C76-C77	117.4(5)

Table 5.8.18 Bond lengths of **5.9** (Å)

Ce1-N3	2.399(3)	Ce1-N2	2.430(3)	Ce1-N4	2.452(3)
Ce1-O2	2.559(3)	Ce1-O1	2.571(3)	Ce1-N1	2.606(3)
O1-C43	1.431(5)	O1-C45	1.436(5)	O2-C46	1.441(5)
O2-C44	1.444(5)	N1-C1	1.476(5)	N1-C29	1.487(5)
N1-C15	1.488(5)	N2-C2	1.378(5)	N2-C5	1.387(5)
N3-C16	1.375(5)	N3-C19	1.387(5)	N4-C33	1.380(5)
N4-C30	1.381(5)	C1-C2	1.503(6)	C2-C3	1.370(6)
C3-C4	1.417(6)	C4-C5	1.381(6)	C5-C6	1.489(6)
C6-C7	1.409(6)	C6-C11	1.410(6)	C7-C8	1.398(6)
C7-C12	1.512(6)	C8-C9	1.381(6)	C9-C10	1.382(7)
C9-C13	1.512(6)	C10-C11	1.397(6)	C11-C14	1.511(6)
C15-C16	1.508(6)	C16-C17	1.373(6)	C17-C18	1.421(6)
C18-C19	1.385(6)	C19-C20	1.488(6)	C20-C25	1.405(6)
C20-C21	1.411(6)	C21-C22	1.393(6)	C21-C26	1.511(6)
C22-C23	1.381(6)	C23-C24	1.387(6)	C23-C27	1.520(6)
C24-C25	1.398(6)	C25-C28	1.510(6)	C29-C30	1.492(5)
C30-C31	1.378(6)	C31-C32	1.417(6)	C32-C33	1.383(6)
C33-C34	1.477(6)	C34-C39	1.404(6)	C34-C35	1.408(6)
C35-C36	1.403(6)	C35-C40	1.497(6)	C36-C37	1.403(6)
C37-C38	1.379(7)	C37-C41	1.506(7)	C38-C39	1.411(6)
C39-C42	1.496(7)	C43-C44	1.501(6)	O3-C47	1.404(8)
O3-C49	1.427(9)	O4-C48	1.394(8)	O4-C50	1.431(9)
C47-C48	1.492(10)	O5-C51	1.401(7)	O5-C52	1.403(7)
C51-C51#1	1.499(11)				

Symmetry transformations used to generate equivalent atoms:

#1 -x+2,-y,-z

Table 5.8.19 Bond angles of **5.9** (°)

N3-Ce1-N2	114.87(11)	N3-Ce1-N4	92.65(12)

N3-Ce1-O2	108.18(11)	N2-Ce1-O2	115.60(11)
N3-Ce1-O1	75.92(11)	N2-Ce1-O1	84.95(11)
O2-Ce1-O1	61.65(9)	N3-Ce1-N1	64.23(11)
N4-Ce1-N1	66.44(11)	O2-Ce1-N1	172.21(10)
C43-O1-C45	113.5(3)	C43-O1-Ce1	121.0(2)
C46-O2-C44	112.0(3)	C46-O2-Ce1	115.7(2)
C1-N1-C29	111.2(3)	C1-N1-C15	112.0(3)
C1-N1-Ce1	107.8(2)	C29-N1-Ce1	110.0(2)
C2-N2-C5	105.3(3)	C2-N2-Ce1	117.6(3)
C16-N3-C19	107.0(3)	C16-N3-Ce1	116.9(3)
C33-N4-C30	106.1(3)	C33-N4-Ce1	134.4(3)
N1-C1-C2	110.2(3)	C3-C2-N2	111.3(4)
N2-C2-C1	119.6(4)	C2-C3-C4	106.4(4)
C4-C5-N2	110.3(4)	C4-C5-C6	126.2(4)
C7-C6-C11	118.1(4)	C7-C6-C5	120.3(4)
C8-C7-C6	120.0(4)	C8-C7-C12	117.6(4)
C9-C8-C7	122.1(4)	C8-C9-C10	117.7(4)
C10-C9-C13	121.4(4)	C9-C10-C11	122.3(4)
C10-C11-C14	118.1(4)	C6-C11-C14	122.1(4)
C17-C16-N3	110.7(4)	C17-C16-C15	131.8(4)
C16-C17-C18	106.1(4)	C19-C18-C17	107.6(4)
C18-C19-C20	130.2(4)	N3-C19-C20	120.9(4)
C25-C20-C19	121.1(4)	C21-C20-C19	120.0(4)
C22-C21-C26	118.4(4)	C20-C21-C26	121.6(4)
C22-C23-C24	117.9(4)	C22-C23-C27	120.1(4)
C23-C24-C25	122.3(4)	C24-C25-C20	119.2(4)
C20-C25-C28	121.5(4)	N1-C29-C30	110.6(3)
C31-C30-C29	129.8(4)	N4-C30-C29	119.5(3)
C33-C32-C31	106.6(4)	N4-C33-C32	110.2(4)
C32-C33-C34	130.3(4)	C39-C34-C35	120.2(4)
C35-C34-C33	118.8(4)	C36-C35-C34	119.1(4)
C34-C35-C40	121.6(4)	C35-C36-C37	121.5(4)
C38-C37-C41	122.8(4)	C36-C37-C41	119.0(5)
C34-C39-C38	118.5(4)	C34-C39-C42	121.8(4)
O1-C43-C44	106.8(3)	O2-C44-C43	108.6(3)
C48-O4-C50	111.8(6)	O3-C47-C48	109.2(6)
C51-O5-C52	113.2(5)	O5-C51-C51#1	108.4(6)
N2-Ce1-N4	106.44(12)	C18-C19-N3	108.7(4)
N4-Ce1-O2	117.11(10)	C25-C20-C21	118.9(4)
N4-Ce1-O1	166.64(11)	C22-C21-C20	119.8(4)
N2-Ce1-N1	68.21(11)	C23-C22-C21	121.9(4)
O1-Ce1-N1	113.14(10)	C24-C23-C27	121.9(4)
C45-O1-Ce1	121.1(2)	C24-C25-C28	119.4(4)
C44-O2-Ce1	121.4(2)	C31-C30-N4	110.4(4)
C29-N1-C15	110.7(3)	C30-C31-C32	106.6(4)
C15-N1-Ce1	104.9(2)	N4-C33-C34	119.3(4)
C5-N2-Ce1	136.4(3)	C39-C34-C33	121.0(4)
C19-N3-Ce1	131.4(3)	C36-C35-C40	119.2(4)
C30-N4-Ce1	119.1(2)	C38-C37-C36	118.2(4)
C3-C2-C1	129.1(4)	C37-C38-C39	122.4(4)
C5-C4-C3	106.7(4)	C38-C39-C42	119.7(4)
N2-C5-C6	123.5(4)	C47-O3-C49	112.3(6)
C11-C6-C5	121.5(4)	O4-C48-C47	109.1(6)
C6-C7-C12	122.3(4)	N1-C15-C16	108.3(3)

C8-C9-C13	120.8(4)	N3-C16-C15	117.5(3)
C10-C11-C6	119.8(4)		

Symmetry transformations used to generate equivalent atoms:

#1 -x+2,-y,-z

Table 5.8.20 Bond lengths of **5.11** (Å)

Ce1-N4	2.4499(17)	Ce1-N2	2.4541(18)	Ce1-N6	2.4798(18)
Ce1-N5	2.5545(19)	Ce1-N3	2.5566(17)	Ce1-N1	2.6960(17)
N1-C15	1.467(3)	N1-C1	1.478(3)	N1-C29	1.480(3)
N2-C2	1.378(3)	N2-C5	1.388(3)	N3-C19	1.377(3)
N3-C16	1.381(3)	N4-C30	1.367(3)	N4-C33	1.376(3)
N5-C43	1.345(3)	N5-C47	1.368(3)	N6-C52	1.356(3)
N6-C48	1.391(3)	C1-C2	1.491(4)	C2-C3	1.378(3)
C3-C4	1.398(4)	C4-C5	1.377(3)	C5-C6	1.477(3)
C6-C11	1.406(3)	C6-C7	1.419(3)	C7-C8	1.383(4)
C7-C12	1.508(4)	C8-C9	1.380(4)	C9-C10	1.386(4)
C9-C13	1.508(4)	C10-C11	1.388(3)	C11-C14	1.508(3)
C15-C16	1.495(3)	C16-C17	1.368(3)	C17-C18	1.409(3)
C18-C19	1.371(3)	C19-C20	1.487(3)	C20-C25	1.402(3)
C20-C21	1.407(3)	C21-C22	1.384(3)	C21-C26	1.508(3)
C22-C23	1.385(3)	C23-C24	1.385(4)	C23-C27	1.510(3)
C24-C25	1.390(3)	C25-C28	1.508(3)	C29-C30	1.498(3)
C30-C31	1.371(3)	C31-C32	1.414(3)	C32-C33	1.377(3)
C33-C34	1.484(3)	C34-C39	1.400(3)	C34-C35	1.409(3)
C35-C36	1.385(3)	C35-C40	1.513(3)	C36-C37	1.379(4)
C37-C38	1.379(3)	C37-C41	1.511(3)	C38-C39	1.393(3)
C39-C42	1.508(3)	C43-C44	1.370(4)	C44-C45	1.390(5)
C45-C46	1.354(5)	C46-C47	1.420(4)	C47-C48	1.426(4)
C48-C49	1.412(4)	C49-C50	1.391(5)	C50-C51	1.444(5)
C51-C52	1.371(4)	K1-O3	2.7607(18)	K1-O6	2.789(2)
K1-O8	2.793(2)	K1-O2	2.793(2)	K1-O5	2.801(2)
K1-O7	2.899(2)	K1-O4	2.907(2)	K1-O1	3.100(3)
K1-C62	3.529(3)	O1-C53	1.400(4)	O1-C55	1.417(4)
O2-C54	1.364(4)	O2-C56	1.404(4)	O3-C57	1.399(4)
O3-C59	1.420(3)	O4-C58	1.405(4)	O4-C60	1.426(4)
O5-C61	1.411(4)	O5-C63	1.419(4)	O6-C62	1.413(4)
O6-C64	1.414(4)	O7-C65	1.421(5)	O7-C67	1.426(4)
O8-C66	1.397(4)	O8-C68	1.436(4)	C53-C54	1.475(5)
C57-C58	1.489(5)	C61-C62	1.488(5)	C65-C66	1.478(5)

Table 5.8.21 Bond angles of **5.11** (°)

N4-Ce1-N2	113.49(6)	N4-Ce1-N6	114.96(6)
N4-Ce1-N5	75.85(6)	N2-Ce1-N5	84.87(6)
N4-Ce1-N3	100.99(6)	N2-Ce1-N3	99.94(6)
N5-Ce1-N3	175.05(6)	N4-Ce1-N1	64.10(6)
N6-Ce1-N1	178.04(6)	N5-Ce1-N1	114.66(6)
C15-N1-C1	113.19(18)	C15-N1-C29	110.36(17)
C15-N1-Ce1	107.13(12)	C1-N1-Ce1	106.34(13)
C2-N2-C5	106.20(19)	C2-N2-Ce1	116.83(15)
C19-N3-C16	105.07(17)	C19-N3-Ce1	139.15(14)
C30-N4-C33	106.57(17)	C30-N4-Ce1	122.19(13)

C43-N5-C47	118.5(2)	C43-N5-Ce1	120.27(17)
C52-N6-C48	118.1(2)	C52-N6-Ce1	118.90(16)
N1-C1-C2	111.12(18)	N2-C2-C3	110.1(2)
C3-C2-C1	131.0(2)	C2-C3-C4	106.7(2)
C4-C5-N2	109.3(2)	C4-C5-C6	129.1(2)
C11-C6-C7	118.0(2)	C11-C6-C5	121.1(2)
C8-C7-C6	119.6(2)	C8-C7-C12	118.3(2)
C9-C8-C7	122.6(2)	C8-C9-C10	117.4(2)
C10-C9-C13	121.4(3)	C9-C10-C11	122.3(2)
C10-C11-C14	117.7(2)	C6-C11-C14	122.4(2)
C17-C16-N3	111.0(2)	C17-C16-C15	127.6(2)
C16-C17-C18	106.4(2)	C19-C18-C17	106.7(2)
C18-C19-C20	127.2(2)	N3-C19-C20	121.43(18)
C25-C20-C19	122.8(2)	C21-C20-C19	118.19(19)
C22-C21-C26	119.8(2)	C20-C21-C26	120.3(2)
C22-C23-C24	117.7(2)	C22-C23-C27	121.0(2)
C23-C24-C25	122.5(2)	C24-C25-C20	119.0(2)
C20-C25-C28	121.5(2)	N1-C29-C30	109.30(17)
N4-C30-C29	117.87(18)	C31-C30-C29	131.51(19)
C33-C32-C31	106.9(2)	N4-C33-C32	109.66(19)
C32-C33-C34	131.5(2)	C39-C34-C35	118.8(2)
C35-C34-C33	120.28(19)	C36-C35-C34	119.5(2)
C34-C35-C40	122.0(2)	C37-C36-C35	122.2(2)
C38-C37-C41	121.4(2)	C36-C37-C41	120.6(2)
C38-C39-C34	119.4(2)	C38-C39-C42	118.8(2)
N5-C43-C44	124.1(3)	C43-C44-C45	117.8(3)
C45-C46-C47	120.7(3)	N5-C47-C46	119.1(3)
C46-C47-C48	124.8(3)	N6-C48-C49	119.5(3)
C49-C48-C47	124.2(3)	C50-C49-C48	121.6(3)
C52-C51-C50	117.2(3)	N6-C52-C51	125.5(3)
O3-K1-O8	81.47(6)	O6-K1-O8	88.32(6)
O6-K1-O2	107.86(7)	O8-K1-O2	127.61(7)
O6-K1-O5	60.33(7)	O8-K1-O5	143.52(7)
O3-K1-O7	108.83(7)	O6-K1-O7	72.05(7)
O2-K1-O7	172.75(8)	O5-K1-O7	91.16(7)
O6-K1-O4	131.40(7)	O8-K1-O4	106.68(7)
O5-K1-O4	84.53(7)	O7-K1-O4	76.66(7)
O6-K1-O1	80.64(7)	O8-K1-O1	80.25(7)
O5-K1-O1	109.68(7)	O7-K1-O1	131.02(7)
O3-K1-C62	163.50(8)	O6-K1-C62	22.14(8)
O2-K1-C62	90.56(8)	O5-K1-C62	42.15(8)
O4-K1-C62	124.23(8)	O1-K1-C62	80.92(8)
C53-O1-K1	115.51(19)	C55-O1-K1	129.4(3)
C54-O2-K1	118.4(2)	C56-O2-K1	108.0(2)
C57-O3-K1	119.38(17)	C59-O3-K1	122.24(18)
C58-O4-K1	106.08(18)	C60-O4-K1	117.3(2)
C61-O5-K1	117.3(2)	C63-O5-K1	125.9(2)
C62-O6-K1	109.84(19)	C64-O6-K1	109.55(19)
C65-O7-K1	112.31(19)	C67-O7-K1	117.5(2)
C66-O8-K1	115.2(2)	C68-O8-K1	108.66(17)
O2-C54-C53	111.9(3)	O3-C57-C58	110.1(2)
O5-C61-C62	110.0(3)	O6-C62-C61	109.9(3)
C61-C62-K1	83.43(18)	O7-C65-C66	109.6(3)
N2-Ce1-N6	110.82(6)	N4-C33-C34	118.83(18)

N6-Ce1-N5	63.38(7)	C39-C34-C33	120.84(19)
N6-Ce1-N3	115.41(6)	C36-C35-C40	118.5(2)
N2-Ce1-N1	68.49(6)	C38-C37-C36	118.0(2)
N3-Ce1-N1	66.55(5)	C37-C38-C39	122.1(2)
C1-N1-C29	111.45(17)	C34-C39-C42	121.7(2)
C29-N1-Ce1	108.06(12)	C46-C45-C44	119.7(3)
C5-N2-Ce1	130.65(14)	N5-C47-C48	116.2(2)
C16-N3-Ce1	115.77(13)	N6-C48-C47	116.3(2)
C33-N4-Ce1	131.09(13)	C49-C50-C51	118.1(3)
C47-N5-Ce1	121.15(16)	O3-K1-O6	167.08(7)
C48-N6-Ce1	122.95(16)	O3-K1-O2	72.95(7)
N2-C2-C1	118.8(2)	O3-K1-O5	131.84(7)
C5-C4-C3	107.6(2)	O2-K1-O5	82.72(7)
N2-C5-C6	121.53(19)	O8-K1-O7	59.53(7)
C7-C6-C5	120.9(2)	O3-K1-O4	59.91(6)
C6-C7-C12	122.1(2)	O2-K1-O4	98.80(7)
C8-C9-C13	121.2(3)	O3-K1-O1	89.79(6)
C10-C11-C6	119.9(2)	O2-K1-O1	55.34(6)
N1-C15-C16	112.36(18)	O4-K1-O1	146.44(7)
N3-C16-C15	121.28(19)	O8-K1-C62	110.05(8)
C18-C19-N3	110.8(2)	O7-K1-C62	87.46(8)
C25-C20-C21	119.0(2)	C53-O1-C55	110.7(3)
C22-C21-C20	119.9(2)	C54-O2-C56	113.4(3)
C21-C22-C23	121.8(2)	C57-O3-C59	111.9(2)
C24-C23-C27	121.3(2)	C58-O4-C60	110.8(3)
C24-C25-C28	119.5(2)	C61-O5-C63	112.6(3)
N4-C30-C31	110.56(19)	C62-O6-C64	111.8(3)
C30-C31-C32	106.3(2)	C65-O7-C67	113.1(3)
O6-C62-K1	48.02(14)	C66-O8-C68	110.8(3)
O8-C66-C65	109.0(3)	O1-C53-C54	109.8(3)
O4-C58-C57	110.2(3)		

Table 5.8.22 Bond lengths of **5.12** (Å)

Tb1-N3	2.338(3)	Tb1-N2	2.351(3)	Tb1-N4	2.366(3)
Tb1-O2	2.380(3)	Tb1-O1	2.422(3)	Tb1-N1	2.461(3)
O1-C43	1.429(5)	O1-C45	1.436(5)	O2-C46	1.418(5)
O2-C44	1.430(5)	N1-C15	1.471(5)	N1-C1	1.480(5)
N1-C29	1.486(5)	N2-C2	1.381(5)	N2-C5	1.399(5)
N3-C19	1.387(5)	N3-C16	1.389(5)	N4-C33	1.390(5)
N4-C30	1.394(4)	C1-C2	1.501(6)	C2-C3	1.364(6)
C3-C4	1.405(6)	C4-C5	1.371(6)	C5-C6	1.484(6)
C6-C7	1.402(6)	C6-C11	1.404(5)	C7-C8	1.387(6)
C7-C12	1.506(6)	C8-C9	1.380(6)	C9-C10	1.382(6)
C9-C13	1.509(6)	C10-C11	1.395(6)	C11-C14	1.508(6)
C15-C16	1.500(6)	C16-C17	1.362(5)	C17-C18	1.412(6)
C18-C19	1.380(5)	C19-C20	1.479(5)	C20-C25	1.409(5)
C20-C21	1.412(5)	C21-C22	1.397(6)	C21-C26	1.518(6)
C22-C23	1.392(7)	C23-C24	1.369(7)	C23-C27	1.509(6)
C24-C25	1.388(6)	C25-C28	1.500(6)	C29-C30	1.493(5)
C30-C31	1.362(6)	C31-C32	1.417(6)	C32-C33	1.368(6)
C33-C34	1.488(5)	C34-C35	1.400(5)	C34-C39	1.403(6)
C35-C36	1.393(6)	C35-C40	1.499(6)	C36-C37	1.380(6)

C37-C38	1.385(6)	C37-C41	1.509(6)	C38-C39	1.391(6)
C39-C42	1.509(6)	C43-C44	1.486(7)		

Table 5.8.23 Bond angles of **5.12** (°)

N3-Tb1-N2	119.72(11)	N3-Tb1-N4	102.79(10)
N3-Tb1-O2	100.12(11)	N2-Tb1-O2	125.45(10)
N3-Tb1-O1	83.53(11)	N2-Tb1-O1	82.02(11)
O2-Tb1-O1	66.18(10)	N3-Tb1-N1	69.17(11)
N4-Tb1-N1	72.23(10)	O2-Tb1-N1	163.19(10)
C43-O1-C45	114.7(4)	C43-O1-Tb1	120.5(3)
C46-O2-C44	113.6(3)	C46-O2-Tb1	128.5(3)
C15-N1-C1	111.9(3)	C15-N1-C29	113.6(3)
C15-N1-Tb1	105.9(2)	C1-N1-Tb1	109.0(2)
C2-N2-C5	105.3(3)	C2-N2-Tb1	116.3(2)
C19-N3-C16	105.9(3)	C19-N3-Tb1	135.9(2)
C33-N4-C30	104.6(3)	C33-N4-Tb1	140.4(2)
N1-C1-C2	110.7(3)	C3-C2-N2	111.0(4)
N2-C2-C1	119.2(3)	C2-C3-C4	106.7(4)
C4-C5-N2	109.5(4)	C4-C5-C6	126.7(4)
C7-C6-C11	118.4(4)	C7-C6-C5	120.7(4)
C8-C7-C6	119.4(4)	C8-C7-C12	118.2(5)
C9-C8-C7	123.2(4)	C8-C9-C10	116.8(4)
C10-C9-C13	121.8(4)	C9-C10-C11	122.3(4)
C10-C11-C14	118.9(4)	C6-C11-C14	121.3(4)
C17-C16-N3	110.6(4)	C17-C16-C15	130.2(4)
C16-C17-C18	106.8(4)	C19-C18-C17	107.3(4)
C18-C19-C20	128.2(4)	N3-C19-C20	122.1(3)
C25-C20-C19	121.5(4)	C21-C20-C19	119.9(4)
C22-C21-C26	118.6(4)	C20-C21-C26	121.9(4)
C24-C23-C22	117.8(4)	C24-C23-C27	122.2(5)
C23-C24-C25	122.8(4)	C24-C25-C20	119.6(4)
C20-C25-C28	122.5(4)	N1-C29-C30	109.6(3)
C31-C30-C29	129.5(3)	N4-C30-C29	119.2(3)
C33-C32-C31	107.3(4)	C32-C33-N4	110.5(3)
N4-C33-C34	122.2(3)	C35-C34-C39	119.4(4)
C39-C34-C33	120.8(4)	C36-C35-C34	119.5(4)
C34-C35-C40	120.3(4)	C37-C36-C35	121.9(4)
C36-C37-C41	121.3(4)	C38-C37-C41	120.9(4)
C38-C39-C34	118.8(4)	C38-C39-C42	119.9(4)
O1-C43-C44	108.6(4)	O2-C44-C43	109.7(4)
N2-Tb1-N4	106.14(11)	N1-C15-C16	111.1(3)
N4-Tb1-O2	98.73(10)	N3-C16-C15	119.1(3)
N4-Tb1-O1	164.63(10)	C18-C19-N3	109.4(4)
N2-Tb1-N1	71.25(10)	C25-C20-C21	118.5(4)
O1-Tb1-N1	123.09(10)	C22-C21-C20	119.5(4)
C45-O1-Tb1	119.7(3)	C23-C22-C21	121.8(4)
C44-O2-Tb1	117.8(3)	C22-C23-C27	119.9(5)
C1-N1-C29	110.4(3)	C24-C25-C28	117.9(4)
C29-N1-Tb1	105.6(2)	C31-C30-N4	111.4(3)
C5-N2-Tb1	138.2(3)	C30-C31-C32	106.2(4)
C16-N3-Tb1	111.6(2)	C32-C33-C34	127.1(4)
C30-N4-Tb1	113.2(2)	C35-C34-C33	119.6(3)

C3-C2-C1	129.8(4)	C36-C35-C40	120.1(4)
C5-C4-C3	107.6(4)	C36-C37-C38	117.7(4)
N2-C5-C6	123.6(4)	C37-C38-C39	122.6(4)
C11-C6-C5	120.8(4)	C34-C39-C42	121.3(4)
C6-C7-C12	122.3(4)	C10-C11-C6	119.8(4)
C8-C9-C13	121.4(4)		

Table 5.8.24 Bond lengths of **5.13** (Å)

Y1-N3	2.324(3)	Y1-O2	2.334(2)	Y1-N2	2.334(3)
Y1-N4	2.358(3)	Y1-O1	2.391(2)	Y1-N1	2.421(3)
O1-C43	1.422(4)	O1-C45	1.441(4)	O2-C46	1.432(4)
O2-C44	1.439(4)	N1-C1	1.473(4)	N1-C29	1.483(4)
N1-C15	1.487(4)	N2-C2	1.384(4)	N2-C5	1.390(4)
N3-C19	1.382(4)	N3-C16	1.385(4)	N4-C33	1.392(4)
N4-C30	1.394(4)	C1-C2	1.492(5)	C2-C3	1.360(5)
C3-C4	1.408(5)	C4-C5	1.363(5)	C5-C6	1.490(5)
C6-C7	1.404(5)	C6-C11	1.405(5)	C7-C8	1.387(5)
C7-C12	1.507(5)	C8-C9	1.378(5)	C9-C10	1.382(5)
C9-C13	1.506(5)	C10-C11	1.393(5)	C11-C14	1.509(5)
C15-C16	1.492(5)	C16-C17	1.371(5)	C17-C18	1.403(5)
C18-C19	1.380(4)	C19-C20	1.475(4)	C20-C25	1.410(5)
C20-C21	1.412(5)	C21-C22	1.391(5)	C21-C26	1.514(5)
C22-C23	1.380(6)	C23-C24	1.380(5)	C23-C27	1.508(5)
C24-C25	1.386(5)	C25-C28	1.510(5)	C29-C30	1.497(4)
C30-C31	1.366(5)	C31-C32	1.410(5)	C32-C33	1.366(5)
C33-C34	1.481(4)	C34-C39	1.402(5)	C34-C35	1.404(4)
C35-C36	1.388(5)	C35-C40	1.495(5)	C36-C37	1.382(5)
C37-C38	1.383(5)	C37-C41	1.502(5)	C38-C39	1.383(5)
C39-C42	1.511(5)	C43-C44	1.502(5)		

Table 5.8.25 Bond angles of **5.13** (°)

N3-Y1-O2	100.43(9)	N3-Y1-N2	120.69(9)
N3-Y1-N4	103.96(9)	O2-Y1-N4	96.69(9)
N3-Y1-O1	83.56(9)	O2-Y1-O1	67.03(8)
N4-Y1-O1	163.28(8)	N3-Y1-N1	70.04(9)
N2-Y1-N1	72.13(9)	N4-Y1-N1	73.17(9)
C43-O1-C45	113.6(3)	C43-O1-Y1	120.4(2)
C46-O2-C44	112.8(3)	C46-O2-Y1	128.9(2)
C1-N1-C29	110.5(3)	C1-N1-C15	112.2(3)
C1-N1-Y1	109.22(18)	C29-N1-Y1	105.64(17)
C2-N2-C5	104.9(3)	C2-N2-Y1	115.0(2)
C19-N3-C16	105.9(3)	C19-N3-Y1	136.9(2)
C33-N4-C30	104.5(3)	C33-N4-Y1	141.7(2)
N1-C1-C2	110.4(3)	C3-C2-N2	110.9(3)
N2-C2-C1	119.5(3)	C2-C3-C4	106.7(3)
C4-C5-N2	110.4(3)	C4-C5-C6	126.4(3)
C7-C6-C11	119.0(3)	C7-C6-C5	120.1(3)
C8-C7-C6	119.2(3)	C8-C7-C12	118.0(4)
C9-C8-C7	122.9(4)	C8-C9-C10	117.1(3)
C10-C9-C13	121.7(4)	C9-C10-C11	122.6(3)

C10-C11-C14	119.5(3)	C6-C11-C14	121.4(3)
C17-C16-N3	110.5(3)	C17-C16-C15	130.3(3)
C16-C17-C18	106.5(3)	C19-C18-C17	107.6(3)
C18-C19-C20	127.9(3)	N3-C19-C20	122.3(3)
C25-C20-C19	121.1(3)	C21-C20-C19	120.4(3)
C22-C21-C26	119.0(3)	C20-C21-C26	121.4(3)
C24-C23-C22	118.0(3)	C24-C23-C27	121.6(4)
C23-C24-C25	122.4(4)	C24-C25-C20	119.6(3)
C20-C25-C28	122.6(3)	N1-C29-C30	109.5(2)
C31-C30-C29	129.8(3)	N4-C30-C29	119.4(3)
C33-C32-C31	106.9(3)	C32-C33-N4	110.9(3)
N4-C33-C34	122.3(3)	C39-C34-C35	118.9(3)
C35-C34-C33	119.4(3)	C36-C35-C34	119.7(3)
C34-C35-C40	120.2(3)	C37-C36-C35	121.8(3)
C36-C37-C41	121.1(3)	C38-C37-C41	121.1(4)
C38-C39-C34	119.1(3)	C38-C39-C42	119.9(3)
O1-C43-C44	107.5(3)	O2-C44-C43	108.8(3)
O2-Y1-N2	124.35(9)	C25-C20-C21	118.4(3)
N2-Y1-N4	106.66(9)	C22-C21-C20	119.5(3)
N2-Y1-O1	81.21(9)	C23-C22-C21	122.1(4)
O2-Y1-N1	163.17(9)	C22-C23-C27	120.4(4)
O1-Y1-N1	123.54(9)	C24-C25-C28	117.8(3)
C45-O1-Y1	119.9(2)	C31-C30-N4	110.8(3)
C44-O2-Y1	118.0(2)	C30-C31-C32	106.9(3)
C29-N1-C15	113.1(2)	C32-C33-C34	126.7(3)
C15-N1-Y1	105.78(19)	C39-C34-C33	121.5(3)
C5-N2-Y1	139.7(2)	C36-C35-C40	119.9(3)
C16-N3-Y1	111.6(2)	C36-C37-C38	117.7(3)
C30-N4-Y1	112.0(2)	C39-C38-C37	122.6(3)
C3-C2-C1	129.4(3)	C34-C39-C42	120.9(3)
C5-C4-C3	107.1(3)	N1-C15-C16	111.1(3)
N2-C5-C6	123.1(3)	N3-C16-C15	119.2(3)
C11-C6-C5	120.9(3)	C18-C19-N3	109.4(3)
C6-C7-C12	122.8(4)	C10-C11-C6	119.1(3)
C8-C9-C13	121.2(4)		

Table 5.8.26 Bond lengths of **5.14** (Å)

Ce1-O1	2.231(3)	Ce1-N2	2.517(3)	Ce1-N4	2.533(3)
Ce1-N3	2.559(3)	Ce1-N5	2.581(3)	Ce1-N1	2.638(3)
O1-N5	1.435(4)	N1-C15	1.467(5)	N1-C29	1.471(5)
N1-C1	1.484(5)	N2-C5	1.376(5)	N2-C2	1.385(5)
N3-C19	1.381(5)	N3-C16	1.385(5)	N4-C30	1.389(5)
N4-C33	1.391(6)	N5-C47	1.491(5)	N5-C43	1.498(6)
C1-C2	1.493(6)	C2-C3	1.363(6)	C3-C4	1.404(7)
C4-C5	1.389(6)	C5-C6	1.488(6)	C6-C11	1.387(6)
C6-C7	1.412(6)	C7-C8	1.377(7)	C7-C12	1.507(7)
C8-C9	1.386(7)	C9-C10	1.384(7)	C9-C13	1.515(7)
C10-C11	1.399(6)	C11-C14	1.516(6)	C15-C16	1.495(6)
C16-C17	1.363(6)	C17-C18	1.398(7)	C18-C19	1.373(6)
C19-C20	1.482(6)	C20-C25	1.407(6)	C20-C21	1.410(6)
C21-C22	1.388(6)	C21-C26	1.505(7)	C22-C23	1.389(7)
C23-C24	1.380(7)	C23-C27	1.518(7)	C24-C25	1.378(6)

C25-C28	1.501(7)	C29-C30	1.484(6)	C30-C31	1.368(6)
C31-C32	1.395(7)	C32-C33	1.367(7)	C33-C34	1.495(6)
C34-C35	1.404(6)	C34-C39	1.405(6)	C35-C36	1.380(7)
C35-C40	1.513(7)	C36-C37	1.387(7)	C37-C38	1.386(7)
C37-C41	1.500(7)	C38-C39	1.386(7)	C39-C42	1.500(6)
C43-C44	1.521(7)	C43-C49	1.529(8)	C43-C48	1.534(7)
C44-C45	1.506(7)	C45-C46	1.511(7)	C46-C47	1.519(6)
C47-C50	1.526(7)	C47-C51	1.529(6)	K2-O3	2.722(4)
K2-O7	2.760(4)	K2-O9	2.824(4)	K2-O5	2.837(4)
K2-O4	2.844(4)	K2-O8	2.860(4)	K2-O6	2.929(5)
K2-O2	2.945(4)	O2-C54	1.399(7)	O2-C52	1.417(7)
O3-C55	1.408(7)	O3-C53	1.413(7)	O4-C58	1.412(7)
O4-C56	1.434(7)	O5-C57	1.411(6)	O5-C59	1.418(6)
O6-C60	1.412(8)	O6-C62	1.427(7)	O7-C61	1.400(7)
O7-C63	1.429(7)	O8-C64	1.399(6)	O8-C66	1.416(6)
O9-C65	1.373(7)	O9-C67	1.395(8)	C52-C53	1.444(9)
C56-C57	1.508(8)	C60-C61	1.482(10)	C64-C65	1.474(9)

Table 5.8.27 Bond angles of **5.14** (°)

O1-Ce1-N2	118.54(11)	O1-Ce1-N4	87.20(11)
O1-Ce1-N3	131.49(11)	N2-Ce1-N3	101.34(11)
O1-Ce1-N5	33.72(10)	N2-Ce1-N5	127.28(11)
N3-Ce1-N5	100.21(11)	O1-Ce1-N1	154.22(11)
N4-Ce1-N1	67.33(11)	N3-Ce1-N1	65.69(11)
N5-O1-Ce1	86.63(19)	C15-N1-C29	112.3(3)
C29-N1-C1	110.7(3)	C15-N1-Ce1	105.3(2)
C1-N1-Ce1	107.5(2)	C5-N2-C2	105.3(3)
C2-N2-Ce1	116.8(3)	C19-N3-C16	105.1(3)
C16-N3-Ce1	114.4(3)	C30-N4-C33	104.6(4)
C33-N4-Ce1	140.4(3)	O1-N5-C47	108.8(3)
C47-N5-C43	117.1(3)	O1-N5-Ce1	59.66(16)
C43-N5-Ce1	120.9(3)	N1-C1-C2	110.8(3)
C3-C2-C1	129.3(4)	N2-C2-C1	119.7(4)
C5-C4-C3	106.6(4)	N2-C5-C4	110.2(4)
C4-C5-C6	127.9(4)	C11-C6-C7	119.3(4)
C7-C6-C5	119.3(4)	C8-C7-C6	119.0(5)
C6-C7-C12	120.4(4)	C7-C8-C9	122.7(5)
C10-C9-C13	120.9(5)	C8-C9-C13	121.4(5)
C6-C11-C10	119.8(4)	C6-C11-C14	121.1(4)
N1-C15-C16	109.8(4)	C17-C16-N3	111.1(4)
N3-C16-C15	119.5(4)	C16-C17-C18	106.4(4)
C18-C19-N3	110.0(4)	C18-C19-C20	126.4(4)
C25-C20-C21	119.0(4)	C25-C20-C19	120.9(4)
C22-C21-C20	119.4(4)	C22-C21-C26	119.0(5)
C21-C22-C23	121.9(5)	C24-C23-C22	117.7(5)
C22-C23-C27	120.4(5)	C25-C24-C23	122.8(5)
C24-C25-C28	120.4(5)	C20-C25-C28	120.3(4)
C31-C30-N4	110.8(4)	C31-C30-C29	127.9(4)
C30-C31-C32	106.9(4)	C33-C32-C31	107.3(5)
C32-C33-C34	124.3(4)	N4-C33-C34	125.3(4)
C35-C34-C33	119.0(4)	C39-C34-C33	122.5(4)
C36-C35-C40	119.9(5)	C34-C35-C40	119.9(5)

C38-C37-C36	116.1(5)	C38-C37-C41	121.8(5)
C39-C38-C37	123.5(5)	C38-C39-C34	119.2(5)
C34-C39-C42	120.7(4)	N5-C43-C44	108.0(4)
C44-C43-C49	111.6(5)	N5-C43-C48	105.2(4)
C49-C43-C48	109.2(5)	C45-C44-C43	113.9(5)
C45-C46-C47	113.5(4)	N5-C47-C46	109.4(4)
C46-C47-C50	108.3(4)	N5-C47-C51	114.2(4)
C50-C47-C51	107.6(4)	O3-K2-O7	149.22(14)
O7-K2-O9	134.29(13)	O3-K2-O5	76.98(12)
O9-K2-O5	143.81(13)	O3-K2-O4	88.03(12)
O9-K2-O4	97.46(13)	O5-K2-O4	60.14(11)
O7-K2-O8	92.80(12)	O9-K2-O8	59.08(12)
O4-K2-O8	154.07(12)	O3-K2-O6	150.61(14)
O9-K2-O6	80.75(14)	O5-K2-O6	118.61(13)
O8-K2-O6	84.59(13)	O3-K2-O2	58.57(13)
O9-K2-O2	107.14(13)	O5-K2-O2	74.48(11)
O8-K2-O2	72.85(12)	O6-K2-O2	146.23(13)
C54-O2-K2	113.0(4)	C52-O2-K2	103.7(4)
C55-O3-K2	119.5(4)	C53-O3-K2	122.2(4)
C58-O4-K2	114.9(4)	C56-O4-K2	109.2(3)
C57-O5-K2	117.4(3)	C59-O5-K2	123.6(3)
C60-O6-K2	106.3(4)	C62-O6-K2	115.3(4)
C61-O7-K2	119.2(4)	C63-O7-K2	117.1(4)
C64-O8-K2	117.5(3)	C66-O8-K2	123.1(4)
C65-O9-K2	110.4(4)	C67-O9-K2	117.4(5)
O3-C53-C52	111.5(5)	O4-C56-C57	109.6(4)
O6-C60-C61	109.8(6)	O7-C61-C60	110.9(6)
O9-C65-C64	113.2(6)	C35-C34-C39	118.2(4)
N2-Ce1-N4	102.59(11)	C36-C35-C34	120.2(5)
N4-Ce1-N3	111.08(11)	C35-C36-C37	122.8(5)
N4-Ce1-N5	113.31(11)	C36-C37-C41	122.1(6)
N2-Ce1-N1	66.27(11)	C38-C39-C42	120.1(4)
N5-Ce1-N1	163.57(10)	N5-C43-C49	113.9(5)
C15-N1-C1	113.0(3)	C44-C43-C48	108.6(5)
C29-N1-Ce1	107.8(2)	C44-C45-C46	107.6(4)
C5-N2-Ce1	137.9(3)	N5-C47-C50	105.1(3)
C19-N3-Ce1	140.2(3)	C46-C47-C51	111.9(4)
C30-N4-Ce1	115.0(3)	O3-K2-O9	74.02(13)
O1-N5-C43	108.7(3)	O7-K2-O5	79.83(12)
C47-N5-Ce1	121.4(3)	O7-K2-O4	97.73(12)
C3-C2-N2	111.0(4)	O3-K2-O8	94.95(12)
C2-C3-C4	106.9(4)	O5-K2-O8	145.53(12)
N2-C5-C6	121.7(4)	O7-K2-O6	59.83(13)
C11-C6-C5	121.3(4)	O4-K2-O6	80.44(12)
C8-C7-C12	120.5(4)	O7-K2-O2	95.83(13)
C10-C9-C8	117.7(5)	O4-K2-O2	129.00(12)
C9-C10-C11	121.5(5)	C54-O2-C52	115.2(5)
C10-C11-C14	119.1(4)	C55-O3-C53	112.7(5)
C17-C16-C15	129.3(4)	C58-O4-C56	111.9(5)
C19-C18-C17	107.5(4)	C57-O5-C59	112.3(4)
N3-C19-C20	123.4(4)	C60-O6-C62	114.7(6)
C21-C20-C19	120.0(4)	C61-O7-C63	112.1(6)
C20-C21-C26	121.6(4)	C64-O8-C66	113.5(5)
C24-C23-C27	121.9(5)	C65-O9-C67	110.7(6)

C24-C25-C20	119.2(5)	O2-C52-C53	111.7(6)
N1-C29-C30	111.7(4)	O5-C57-C56	109.0(5)
N4-C30-C29	121.1(4)	O8-C64-C65	112.3(5)
C32-C33-N4	110.4(4)		

Table 5.8.28 Bond lengths of **5.15** (Å)

Tb1-O1	2.140(5)	Tb1-N2	2.409(6)	Tb1-N4	2.435(6)
Tb1-N3	2.455(6)	Tb1-N5	2.490(7)	Tb1-N1	2.503(6)
O1-N5	1.416(8)	N1-C15	1.470(10)	N1-C1	1.478(10)
N1-C29	1.506(10)	N2-C5	1.380(10)	N2-C2	1.391(10)
N3-C19	1.374(10)	N3-C16	1.375(10)	N4-C30	1.379(9)
N4-C33	1.389(10)	N5-C47	1.488(11)	N5-C43	1.507(12)
C1-C2	1.500(12)	C2-C3	1.360(12)	C3-C4	1.374(12)
C4-C5	1.373(11)	C5-C6	1.481(11)	C6-C7	1.382(11)
C6-C11	1.412(12)	C7-C8	1.385(13)	C7-C12	1.487(13)
C8-C9	1.362(14)	C9-C10	1.379(13)	C9-C13	1.531(13)
C10-C11	1.390(12)	C11-C14	1.513(12)	C15-C16	1.517(12)
C16-C17	1.342(12)	C17-C18	1.384(12)	C18-C19	1.364(11)
C19-C20	1.485(12)	C20-C25	1.420(13)	C20-C21	1.432(13)
C21-C22	1.362(13)	C21-C26	1.493(14)	C22-C23	1.420(15)
C23-C24	1.365(15)	C23-C27	1.520(14)	C24-C25	1.372(13)
C25-C28	1.528(14)	C29-C30	1.474(11)	C30-C31	1.363(11)
C31-C32	1.353(12)	C32-C33	1.390(12)	C33-C34	1.493(12)
C34-C35	1.393(12)	C34-C39	1.407(11)	C35-C36	1.391(12)
C35-C40	1.505(12)	C36-C37	1.364(13)	C37-C38	1.380(13)
C37-C41	1.509(13)	C38-C39	1.395(12)	C39-C42	1.508(12)
C43-C48	1.508(15)	C43-C44	1.519(14)	C43-C49	1.565(15)
C44-C45	1.492(16)	C45-C46	1.509(14)	C46-C47	1.561(13)
C47-C51	1.485(13)	C47-C50	1.532(14)	K2-O3	2.716(8)
K2-O7	2.737(9)	K2-O9	2.821(9)	K2-O4	2.839(8)
K2-O5	2.843(7)	K2-O8	2.872(9)	K2-O6	2.924(10)
K2-O2	2.932(10)	O2-C54	1.408(15)	O2-C52	1.454(16)
O3-C55	1.371(14)	O3-C53	1.406(17)	O4-C58	1.388(13)
O4-C56	1.423(14)	O5-C57	1.409(13)	O5-C59	1.409(13)
O6-C60	1.429(17)	O6-C62	1.436(15)	O7-C63	1.385(15)
O7-C61	1.421(16)	O8-C64	1.409(14)	O8-C66	1.429(14)
O9-C65	1.350(16)	O9-C67	1.397(17)	C52-C53	1.41(2)
C56-C57	1.593(18)	C60-C61	1.53(2)	C64-C65	1.46(2)

Table 5.8.29 Bond angles of **5.15** (°)

O1-Tb1-N2	111.8(2)	O1-Tb1-N4	87.4(2)
O1-Tb1-N3	131.5(2)	N2-Tb1-N3	103.9(2)
O1-Tb1-N5	34.6(2)	N2-Tb1-N5	123.2(2)
N3-Tb1-N5	98.0(2)	O1-Tb1-N1	156.2(2)
N4-Tb1-N1	69.9(2)	N3-Tb1-N1	67.7(2)
N5-O1-Tb1	86.4(4)	C15-N1-C1	113.3(7)
C1-N1-C29	109.5(7)	C15-N1-Tb1	106.6(5)
C29-N1-Tb1	107.8(5)	C5-N2-C2	104.1(7)
C2-N2-Tb1	115.5(5)	C19-N3-C16	103.4(7)
C16-N3-Tb1	113.5(5)	C30-N4-C33	104.6(7)

C33-N4-Tb1	140.7(5)	O1-N5-C47	106.9(6)
C47-N5-C43	116.0(7)	O1-N5-Tb1	59.0(3)
C43-N5-Tb1	118.8(6)	N1-C1-C2	109.5(7)
C3-C2-C1	128.8(8)	N2-C2-C1	119.6(7)
C5-C4-C3	108.5(8)	C4-C5-N2	109.8(8)
N2-C5-C6	122.0(7)	C7-C6-C11	119.0(8)
C11-C6-C5	120.1(7)	C6-C7-C8	119.5(9)
C8-C7-C12	120.1(9)	C9-C8-C7	122.7(9)
C8-C9-C13	123.1(10)	C10-C9-C13	119.0(11)
C10-C11-C6	119.0(8)	C10-C11-C14	121.0(9)
N1-C15-C16	107.1(7)	C17-C16-N3	112.1(8)
N3-C16-C15	119.7(7)	C16-C17-C18	106.9(8)
C18-C19-N3	111.4(7)	C18-C19-C20	124.1(8)
C25-C20-C21	117.6(9)	C25-C20-C19	120.1(9)
C22-C21-C20	119.8(9)	C22-C21-C26	121.0(10)
C21-C22-C23	121.9(10)	C24-C23-C22	117.8(10)
C22-C23-C27	117.9(11)	C23-C24-C25	122.6(11)
C24-C25-C28	120.0(10)	C20-C25-C28	119.5(9)
C31-C30-N4	111.3(8)	C31-C30-C29	127.9(7)
C32-C31-C30	106.9(8)	C31-C32-C33	108.5(8)
N4-C33-C34	127.3(8)	C32-C33-C34	123.8(8)
C35-C34-C33	119.1(8)	C39-C34-C33	121.6(8)
C36-C35-C40	120.4(9)	C34-C35-C40	120.7(9)
C36-C37-C38	117.5(9)	C36-C37-C41	122.1(10)
C37-C38-C39	121.8(9)	C38-C39-C34	119.5(9)
C34-C39-C42	120.8(8)	N5-C43-C48	105.3(8)
C48-C43-C44	111.8(10)	N5-C43-C49	112.2(10)
C44-C43-C49	109.3(9)	C45-C44-C43	117.1(10)
C45-C46-C47	111.2(9)	C51-C47-N5	117.4(10)
N5-C47-C50	103.4(7)	C51-C47-C46	113.9(8)
C50-C47-C46	104.8(9)	O3-K2-O7	149.3(3)
O7-K2-O9	134.2(3)	O3-K2-O4	86.8(3)
O9-K2-O4	98.7(3)	O3-K2-O5	76.6(2)
O9-K2-O5	145.0(3)	O4-K2-O5	60.5(2)
O7-K2-O8	93.0(3)	O9-K2-O8	58.7(3)
O5-K2-O8	144.1(3)	O3-K2-O6	148.8(3)
O9-K2-O6	79.4(3)	O4-K2-O6	80.7(3)
O8-K2-O6	84.8(3)	O3-K2-O2	59.6(3)
O9-K2-O2	106.2(3)	O4-K2-O2	129.2(3)
O8-K2-O2	71.5(3)	O6-K2-O2	146.6(3)
C54-O2-K2	115.0(8)	C52-O2-K2	102.7(8)
C55-O3-K2	119.8(8)	C53-O3-K2	122.0(8)
C58-O4-K2	114.9(8)	C56-O4-K2	109.8(7)
C57-O5-K2	118.2(7)	C59-O5-K2	123.2(7)
C60-O6-K2	104.3(8)	C62-O6-K2	114.4(9)
C63-O7-K2	120.3(9)	C61-O7-K2	118.0(9)
C64-O8-K2	118.1(9)	C66-O8-K2	121.9(8)
C65-O9-K2	112.1(10)	C67-O9-K2	114.9(10)
O3-C53-C52	112.2(13)	O4-C56-C57	108.2(10)
O6-C60-C61	108.7(13)	O7-C61-C60	108.7(12)
O9-C65-C64	115.9(15)	C30-C29-N1	111.0(6)
N2-Tb1-N4	104.1(2)	N4-C30-C29	120.6(7)
N4-Tb1-N3	114.9(2)	N4-C33-C32	108.7(8)
N4-Tb1-N5	112.8(2)	C35-C34-C39	118.8(8)

N2-Tb1-N1	68.9(2)	C36-C35-C34	118.9(8)
N5-Tb1-N1	164.2(2)	C37-C36-C35	123.4(9)
C15-N1-C29	110.9(6)	C38-C37-C41	120.5(10)
C1-N1-Tb1	108.6(5)	C38-C39-C42	119.7(8)
C5-N2-Tb1	140.4(5)	N5-C43-C44	108.0(8)
C19-N3-Tb1	142.9(5)	C48-C43-C49	110.3(10)
C30-N4-Tb1	114.8(5)	C44-C45-C46	106.3(9)
O1-N5-C43	110.0(7)	C51-C47-C50	107.4(10)
C47-N5-Tb1	124.9(6)	N5-C47-C46	108.6(8)
C3-C2-N2	111.6(8)	O3-K2-O9	74.4(3)
C2-C3-C4	106.0(8)	O7-K2-O4	97.5(3)
C4-C5-C6	128.0(8)	O7-K2-O5	79.2(3)
C7-C6-C5	120.9(8)	O3-K2-O8	95.6(3)
C6-C7-C12	120.4(9)	O4-K2-O8	155.2(3)
C8-C9-C10	117.9(9)	O7-K2-O6	61.4(3)
C9-C10-C11	121.9(10)	O5-K2-O6	119.9(3)
C6-C11-C14	120.0(8)	O7-K2-O2	95.8(3)
C17-C16-C15	128.0(8)	O5-K2-O2	74.5(3)
C19-C18-C17	106.3(8)	C54-O2-C52	117.4(13)
N3-C19-C20	124.4(7)	C55-O3-C53	112.9(12)
C21-C20-C19	122.1(8)	C58-O4-C56	112.9(11)
C20-C21-C26	119.2(9)	C57-O5-C59	112.3(10)
C24-C23-C27	124.3(11)	C60-O6-C62	117.6(12)
C24-C25-C20	120.3(10)	C63-O7-C61	107.8(13)
C53-C52-O2	114.5(15)	C64-O8-C66	113.8(11)
O5-C57-C56	107.3(10)	C65-O9-C67	113.4(14)
O8-C64-C65	112.1(12)		

Table 5.8.30 Bond lengths of **5.16** (Å)

U1-N2	2.397(2)	U1-N3	2.433(2)	U1-N4	2.445(2)
U1-O1	2.5813(18)	U1-O2	2.5904(17)	U1-N1	2.612(2)
O1-C52	1.430(3)	O1-C54	1.439(3)	O2-C55	1.422(3)
O2-C53	1.435(3)	N1-C1	1.478(3)	N1-C35	1.487(3)
N1-C18	1.484(3)	N2-C2	1.377(3)	N2-C5	1.386(3)
N3-C19	1.385(3)	N3-C22	1.393(3)	N4-C39	1.388(3)
N4-C36	1.390(3)	C1-C2	1.488(4)	C2-C3	1.373(4)
C3-C4	1.409(5)	C4-C5	1.374(4)	C5-C6	1.476(4)
C6-C7	1.401(4)	C6-C11	1.412(4)	C7-C8	1.394(5)
C7-C12	1.509(4)	C8-C9	1.383(4)	C9-C10	1.399(4)
C9-C13	1.536(4)	C10-C11	1.390(4)	C11-C17	1.510(4)
C13-C15	1.515(5)	C13-C14	1.527(5)	C13-C16	1.530(5)
C18-C19	1.493(4)	C19-C20	1.372(4)	C20-C21	1.402(4)
C21-C22	1.377(4)	C22-C23	1.480(4)	C23-C24	1.401(4)
C23-C28	1.416(4)	C24-C25	1.395(4)	C24-C29	1.504(4)
C25-C26	1.383(4)	C26-C27	1.395(4)	C26-C30	1.528(4)
C27-C28	1.382(4)	C28-C34	1.510(4)	C30-C33	1.526(5)
C30-C31	1.531(5)	C30-C32	1.532(5)	C35-C36	1.491(4)
C36-C37	1.360(4)	C37-C38	1.412(4)	C38-C39	1.370(4)
C39-C40	1.486(4)	C40-C41	1.397(4)	C40-C45	1.408(4)
C41-C42	1.391(4)	C41-C46	1.511(4)	C42-C43	1.389(4)
C43-C44	1.393(4)	C43-C47	1.538(4)	C44-C45	1.389(4)
C45-C51	1.504(4)	C47-C50	1.499(6)	C47-C49	1.505(6)

C47-C48	1.512(6)	C52-C53	1.493(4)	C56-C57	1.514(10)
C57-C58	1.510(7)	C58-C58#1	1.540(13)		

Symmetry transformations used to generate equivalent atoms:

#1 -x+1,-y+1,-z+2

Table 5.8.31 Bond angles of **5.16** (°)

N2-U1-N3	112.66(7)	N2-U1-N4	99.48(7)
N2-U1-O1	73.72(7)	N3-U1-O1	90.70(7)
N2-U1-O2	118.04(7)	N3-U1-O2	108.85(7)
O1-U1-O2	61.77(6)	N2-U1-N1	64.47(7)
N4-U1-N1	68.89(7)	O1-U1-N1	118.18(6)
C52-O1-C54	113.1(2)	C52-O1-U1	120.17(14)
C55-O2-C53	112.5(2)	C55-O2-U1	123.40(17)
C1-N1-C35	111.33(19)	C1-N1-C18	110.8(2)
C1-N1-U1	108.40(15)	C35-N1-U1	106.38(14)
C2-N2-C5	107.1(2)	C2-N2-U1	119.90(17)
C19-N3-C22	105.5(2)	C19-N3-U1	118.23(16)
C39-N4-C36	105.5(2)	C39-N4-U1	137.96(17)
N1-C1-C2	109.3(2)	C3-C2-N2	109.7(3)
N2-C2-C1	117.9(2)	C2-C3-C4	106.8(3)
C4-C5-N2	108.7(3)	C4-C5-C6	132.0(3)
C7-C6-C11	118.1(3)	C7-C6-C5	122.6(3)
C8-C7-C6	119.9(3)	C8-C7-C12	118.9(3)
C9-C8-C7	122.9(3)	C8-C9-C10	116.5(3)
C10-C9-C13	120.2(3)	C11-C10-C9	122.4(3)
C10-C11-C17	119.3(2)	C6-C11-C17	120.6(3)
C15-C13-C16	107.0(3)	C14-C13-C16	109.1(3)
C14-C13-C9	109.2(3)	C16-C13-C9	110.0(3)
C20-C19-N3	110.7(2)	C20-C19-C18	130.8(3)
C19-C20-C21	106.6(3)	C22-C21-C20	107.7(2)
C21-C22-C23	129.1(2)	N3-C22-C23	121.4(2)
C24-C23-C22	120.9(2)	C28-C23-C22	120.9(2)
C25-C24-C29	118.0(2)	C23-C24-C29	122.0(3)
C25-C26-C27	116.1(3)	C25-C26-C30	123.7(3)
C28-C27-C26	123.3(3)	C27-C28-C23	119.4(3)
C23-C28-C34	121.7(3)	C33-C30-C26	108.9(3)
C26-C30-C31	112.2(3)	C33-C30-C32	110.1(3)
C31-C30-C32	108.2(3)	N1-C35-C36	110.5(2)
C37-C36-C35	128.9(3)	N4-C36-C35	120.2(2)
C39-C38-C37	107.6(3)	C38-C39-N4	109.7(2)
N4-C39-C40	122.4(2)	C41-C40-C45	119.0(2)
C45-C40-C39	119.7(2)	C42-C41-C40	119.7(3)
C40-C41-C46	120.9(3)	C43-C42-C41	122.5(3)
C42-C43-C47	122.8(3)	C44-C43-C47	120.4(3)
C44-C45-C40	119.4(2)	C44-C45-C51	120.4(3)
C50-C47-C49	109.9(4)	C50-C47-C48	107.1(5)
C50-C47-C43	110.4(3)	C49-C47-C43	109.1(3)
O1-C52-C53	107.7(2)	O2-C53-C52	108.2(2)
C57-C58-C58#1	113.8(7)	C24-C23-C28	118.2(3)
N3-U1-N4	104.75(7)	C25-C24-C23	119.8(3)
N4-U1-O1	164.55(7)	C26-C25-C24	123.0(3)
N4-U1-O2	112.02(6)	C27-C26-C30	120.2(3)
N3-U1-N1	67.93(7)	C27-C28-C34	118.9(3)

O2-U1-N1	176.73(6)	C33-C30-C31	108.3(4)
C54-O1-U1	117.42(17)	C26-C30-C32	109.1(3)
C53-O2-U1	119.68(15)	C37-C36-N4	110.8(2)
C35-N1-C18	111.3(2)	C36-C37-C38	106.5(3)
C18-N1-U1	108.45(14)	C38-C39-C40	127.9(2)
C5-N2-U1	130.42(18)	C41-C40-C39	121.2(2)
C22-N3-U1	134.26(18)	C42-C41-C46	119.4(3)
C36-N4-U1	115.90(16)	C42-C43-C44	116.9(3)
C3-C2-C1	132.4(3)	C45-C44-C43	122.5(3)
C5-C4-C3	107.7(3)	C40-C45-C51	120.1(2)
N2-C5-C6	119.1(2)	C49-C47-C48	108.3(5)
C11-C6-C5	119.2(2)	C48-C47-C43	112.0(3)
C6-C7-C12	121.2(3)	C56-C57-C58	114.1(7)
C8-C9-C13	123.3(3)	N1-C18-C19	109.5(2)
C10-C11-C6	119.9(3)	N3-C19-C18	118.4(2)
C15-C13-C14	108.6(3)	C21-C22-N3	109.5(2)
C15-C13-C9	112.8(3)		

Symmetry transformations used to generate equivalent atoms:

#1 -x+1,-y+1,-z+2

5.9 Coordinates of Optimized Geometries.

Table 5.9.1 Optimized geometry of **5.1**.

U 0.00000000 0.00000000 1.18050000	F -0.82910000 7.75860000 0.40210000
F 0.00000000 8.14690000 -1.52510000	F -1.77410000 6.99010000 -1.34400000
F 3.57160000 3.54500000 -2.73260000	F 2.22070000 4.59790000 -4.00010000
F 1.75270000 2.62640000 -3.34130000	F -5.16660000 -5.03150000 -1.34400000
F -6.30460000 -4.59730000 0.40210000	F -7.05540000 -4.07340000 -1.52510000
F -4.85580000 1.32060000 -2.73260000	F -3.15090000 0.20460000 -3.34130000
F -5.09230000 -0.37580000 -4.00010000	F 6.94070000 -1.95860000 -1.34400000
F 7.05540000 -4.07340000 -1.52510000	F 7.13360000 -3.16130000 0.40210000
F 1.28430000 -4.86550000 -2.73260000	F 2.87160000 -4.22210000 -4.00010000
F 1.39820000 -2.83100000 -3.34130000	N 0.00000000 0.00000000 4.02080000
N 0.96010000 2.10500000 2.27150000	N -2.30300000 -0.22110000 2.27150000
N 1.34300000 -1.88390000 2.27150000	N 2.35810000 0.27000000 0.03610000
N -0.94530000 -2.17720000 0.03610000	N -1.41290000 1.90720000 0.03610000
C 1.16670000 0.77970000 4.39760000	C 1.24260000 2.05350000 3.61050000
C 1.59080000 3.27890000 4.10280000	C 1.52850000 4.16630000 3.01250000
C 1.14740000 3.42890000 1.92060000	C 1.01470000 4.06120000 0.58480000
C 0.28990000 5.25660000 0.48700000	C 0.23180000 5.97100000 -0.69130000
C 0.88150000 5.51380000 -1.82980000	C 1.59160000 4.33580000 -1.75130000
C 1.66740000 3.62380000 -0.55850000	C -0.59100000 7.22450000 -0.78250000
C 2.28990000 3.78590000 -2.96040000	C -1.25860000 0.62060000 4.39760000
C -2.39960000 0.04940000 3.61050000	C -3.63500000 -0.26180000 4.10280000
C -4.37230000 -0.75950000 3.01250000	C -3.54330000 -0.72070000 1.92060000
C -4.02450000 -1.15180000 0.58480000	C -4.69730000 -2.37720000 0.48700000
C -5.28690000 -2.78480000 -0.69130000	C -5.21590000 -1.99350000 -1.82980000
C -4.55070000 -0.78950000 -1.75130000	C -3.97200000 -0.36790000 -0.55850000
C -5.96110000 -4.12410000 -0.78250000	C -4.42370000 0.09020000 -2.96040000
C 0.09190000 -1.40020000 4.39760000	C 1.15710000 -2.10290000 3.61050000
C 2.04430000 -3.01710000 4.10280000	C 2.84390000 -3.40680000 3.01250000

C 2.39580000 -2.70820000 1.92060000	C 3.00970000 -2.90940000 0.58480000
C 4.40740000 -2.87940000 0.48700000	C 5.05510000 -3.18620000 -0.69130000
C 4.33430000 -3.52030000 -1.82980000	C 2.95910000 -3.54630000 -1.75130000
C 2.30460000 -3.25600000 -0.55850000	C 6.55210000 -3.10040000 -0.78250000
C 2.13370000 -3.87610000 -2.96040000	C 3.38510000 0.64120000 0.79760000
C 4.65230000 0.85820000 0.29170000	C 4.86760000 0.67720000 -1.06260000
C 3.80610000 0.27740000 -1.85760000	C 2.57820000 0.08170000 -1.26220000
C -1.13730000 -3.25210000 0.79760000	C -1.58290000 -4.45810000 0.29170000
C -1.84730000 -4.55410000 -1.06260000	C -1.66290000 -3.43490000 -1.85760000
C -1.21830000 -2.27360000 -1.26220000	C -1.35990000 2.19190000 -1.26220000
C -2.14330000 3.15750000 -1.85760000	C -3.02030000 3.87690000 -1.06260000
C -3.06940000 3.59990000 0.29170000	C -2.24780000 2.61100000 0.79760000
H 2.04020000 0.16280000 4.22010000	H 1.16410000 1.01730000 5.46230000
H 1.85470000 3.50550000 5.11730000	H 1.76320000 5.21280000 3.01130000
H -0.22430000 5.61840000 1.35510000	H 0.83630000 6.06950000 -2.74530000
H 2.26950000 2.74100000 -0.51610000	H -1.16110000 1.68540000 4.22010000
H -1.46300000 0.49950000 5.46230000	H -3.96320000 -0.14650000 5.11730000
H -5.39600000 -1.07950000 3.01130000	H -4.75350000 -3.00340000 1.35510000
H -5.67450000 -2.31050000 -2.74530000	H -3.50850000 0.59490000 -0.51610000
H -0.87910000 -1.84820000 4.22010000	H 0.29890000 -1.51680000 5.46230000
H 2.10850000 -3.35890000 5.11730000	H 3.63290000 -4.13340000 3.01130000
H 4.97780000 -2.61490000 1.35510000	H 4.83820000 -3.75900000 -2.74530000
H 1.23900000 -3.33590000 -0.51610000	H 3.18030000 0.78700000 1.83710000
H 5.44210000 1.16460000 0.95010000	H 5.83960000 0.83770000 -1.48960000
H 3.92000000 0.12290000 -2.91280000	H 1.74050000 -0.23650000 -1.85210000
H -0.90860000 -3.14780000 1.83710000	H -1.71250000 -5.29530000 0.95010000
H -2.19430000 -5.47610000 -1.48960000	H -1.85350000 -3.45630000 -2.91280000
H -1.07510000 -1.38900000 -1.85210000	H -0.66540000 1.62550000 -1.85210000
H -2.06650000 3.33340000 -2.91280000	H -3.64520000 4.63840000 -1.48960000
H -3.72960000 4.13070000 0.95010000	H -2.27180000 2.36070000 1.83710000

5.10 References.

(1) Lam, O. P.; Anthon, C.; Meyer, K., *Dalton Trans.* **2009**, 9677.
(2) Shook, R. L.; Borovik, A. S., *Inorg. Chem.* **2010,** *49*, 3646.
(3) Cotton, S., *Lanthanide and Actinide Chemistry*. 2nd ed.; Wiley: 2006.
(4) Balland, V.; Hureau, C.; Savéant, J.-M., *Proc. Natl. Ad. Sci. USA* **2010,** *107*, 17113.
(5) Ekstrom, A., *Inorg. Chem.* **1974,** *13*, 2237.
(6) Monreal, M. J.; Diaconescu, P. L., *Organometallics* **2008,** *27*, 1702.
(7) Castro-Rodriguez, I.; Nakai, H.; Zakharov, L. N.; Rheingold, A. L.; Meyer, K., *Science* **2004,** *305*, 1757.
(8) Casely, I. J.; Liddle, S. T.; Blake, A. J.; Wilson, C.; Arnold, P. L., *Chem. Commun.* **2007**, 5037.
(9) Wampler, K. M.; Schrock, R. R., *Inorg. Chem.* **2007,** *46*, 8463.
(10) Harman, W. H.; Chang, C. J., *J. Am. Chem. Soc.* **2007,** *129*, 15128.
(11) Piro, N. A.; Lichterman, M. F.; Harman, W. H.; Chang, C. J., *J. Am. Chem. Soc.* **2011,** *133*, 2108.
(12) Sazama, G. T.; Betley, T. A., *Organometallics* **2011,** *30*, 4315.

(13) Harman, W. H.; Harris, T. D.; Freedman, D. E.; Fong, H.; Chang, A.; Rinehart, J. D.; Ozarowski, A.; Sougrati, M. T.; Grandjean, F.; Long, G. J.; Long, J. R.; Chang, C. J., *J. Am. Chem. Soc.* **2010,** *132*, 18115.
(14) Freedman, D. E.; Harman, W. H.; Harris, T. D.; Long, G. J.; Chang, C. J.; Long, J. R., *J. Am. Chem. Soc.* **2010,** *132*, 1224.
(15) Though commonly refered to as "π stacking", the interactions in these molecules likely incorporate coupling of the dipole moments of these aryl fragments.
(16) Schrock, R. R., *Acc. Chem. Res.* **1997,** *30*, 9.
(17) Scott, P.; Hitchcock, P. B., *J. Chem. Soc., Dalton Trans.* **1995**, 603.
(18) Roussel, P.; Hitchcock, P. B.; Tinker, N.; Scott, P., *Chem. Commun.* **1996**.
(19) Roussel, P.; Hitchcock, P. B.; Tinker, N. D.; Scott, P., *Inorg. Chem.* **1997,** *36*, 5716.
(20) Roussel, P.; Scott, P., *J. Am. Chem. Soc.* **1998,** *120*, 1070.
(21) Roussel, P.; Alcock, N. W.; Boaretto, R.; Kingsley, A. J.; Munslow, I. J.; Sanders, C. J.; Scott, P., *Inorg. Chem.* **1999,** *38*, 3651.
(22) Boaretto, R.; Roussel, P.; J. Kingsley, A.; J. Munslow, I.; J. Sanders, C.; W. Alcock, N.; Scott, P., *Chem. Commun.* **1999**, 1701.
(23) Duval, P. B.; Burns, C. J.; Buschmann, W. E.; Clark, D. L.; Morris, D. E.; Scott, B. L., *Inorg. Chem.* **2001,** *40*, 5491.
(24) Roussel, P.; Boaretto, R.; Kingsley, A. J.; Alcock, N. W.; Scott, P., *J. Chem. Soc., Dalton Trans.* **2002**, 1423.
(25) Gardner, B. M.; McMaster, J.; Lewis, W.; Blake, A. J.; Liddle, S. T., *J. Am. Chem. Soc.* **2009,** *131*, 10388.
(26) Liddle, S. T.; McMaster, J.; Mills, D. P.; Blake, A. J.; Jones, C.; Woodul, W. D., *Angew. Chem. Int. Ed.* **2009,** *48*, 1077.
(27) Gardner, B. M.; Patel, D.; Lewis, W.; Blake, A. J.; Liddle, S. T., *Angew. Chem. Int. Ed.* **2011,** *50*, 10440.
(28) Gardner, B. M.; McMaster, J.; Moro, F.; Lewis, W.; Blake, A. J.; Liddle, S. T., *Chem. - Eur. J.* **2011,** *17*, 6909.
(29) Gardner, B. M.; Patel, D.; Cornish, A. D.; McMaster, J.; Lewis, W.; Blake, A. J.; Liddle, S. T., *Chem. - Eur. J.* **2011,** *17*, 11266.
(30) Gardner, B. M.; Lewis, W.; Blake, A. J.; Liddle, S. T., *Inorg. Chem.* **2011,** *50*, 9631.
(31) Patel, D.; King, D. M.; Gardner, B. M.; McMaster, J.; Lewis, W.; Blake, A. J.; Liddle, S. T., *Chem. Commun.* **2011,** *47*, 295.
(32) King, D. M.; Tuna, F.; McMaster, J.; Lewis, W.; Blake, A. J.; McInnes, E. J.; Liddle, S. T., *Angew . Chem. Int. Ed.* **2013,** *52*, 4921.
(33) King, D. M.; Tuna, F.; McInnes, E. J. L.; McMaster, J.; Lewis, W.; Blake, A. J.; Liddle, S. T., *Science* **2012,** *337*, 717.
(34) King, D. M.; Tuna, F.; McInnes, E. J.; McMaster, J.; Lewis, W.; Blake, A. J.; Liddle, S. T., *Nat. Chem.* **2013,** *5*, 482.
(35) King, D. M.; Liddle, S. T., *Coord. Chem. Rev.* **2014**.
(36) Swartz, D. L.; Odom, A. L., *Organometallics* **2006,** *25*, 6125.
(37) Ferreira da Silva, J. L.; Galvão, A. C.; Ferreira, A. P.; Galvão, A. M.; Dias, A. R.; Gomes, P. T.; Salema, M. S., *J. Organomet. Chem.* **2010,** *695*, 1533.
(38) Swartz Ii, D. L.; Staples, R. J.; Odom, A. L., *Dalton Trans.* **2011,** *40*, 7762.
(39) Swartz, D. L.; Spencer, L. P.; Scott, B. L.; Odom, A. L.; Boncella, J. M., *Dalton Trans.* **2010,** *39*, 6841.

(40) Arnold, P. L.; Farnaby, J. H.; White, R. C.; Kaltsoyannis, N.; Gardiner, M. G.; Love, J. B., *Chem. Sci.* **2014,** *5*, 756.
(41) Shi, Y.; Cao, C.; Odom, A. L., *Inorg. Chem.* **2004,** *43*, 275.
(42) Rieth, R. D.; Mankad, N. P.; Calimano, E.; Sadighi, J. P., *Org. Lett.* **2004,** *6*, 3981.
(43) Wampler, K. M.; Schrock, R. R., *Inorg. Chem.* **2007,** *46*, 8463.
(44) Harman, W. H.; Chang, C. J., *J. Am. Chem. Soc.* **2007,** *129*, 15128.
(45) Bigi, J. P.; Harman, W. H.; Lassalle-Kaiser, B.; Robles, D. M.; Stich, T. A.; Yano, J.; Britt, R. D.; Chang, C. J., *J. Am. Chem. Soc.* **2012,** *134*, 1536.
(46) Piro, N. A.; Lichterman, M. F.; Harman, W. H.; Chang, C. J., *J. Am. Chem. Soc.* **2011,** *133*, 2108.
(47) Korobkov, I.; Gambarotta, S.; Yap, G. P. A., *Organometallics* **2001,** *20*, 2552.
(48) Korobkov, I.; Gambarotta, S.; Yap, G. P. A., *Angew. Chem. Int. Ed.* **2002,** *41*, 3433.
(49) Steed, J. W. T., D.R.; Wallace, K.J., *Core Concepts in Supramolecular Chemistry and Nanochemistry*. Wiley: 2007.
(50) Castro-Rodriguez, I.; Olsen, K.; Gantzel, P.; Meyer, K., *J. Am. Chem. Soc.* **2003,** *125*, 4565.
(51) Odom, A. L.; Arnold, P. L.; Cummins, C. C., *J. Am. Chem. Soc.* **1998,** *120*, 5836.
(52) Cramer, R. E.; Maynard, R. B.; Gilje, J. W., *J. Am. Chem. Soc.* **1978,** *100*, 5562.
(53) Cramer, R. E.; Maynard, R. B.; Gilje, J. W., *Inorg. Chem.* **1980,** *19*, 2564.
(54) Cramer, R. E.; Maynard, R. B.; Paw, J. C.; Gilje, J. W., *J. Am. Chem. Soc.* **1981,** *103*.
(55) Cramer, R. E.; Maynard, R. B.; Gilje, J. W., *Inorg. Chem.* **1981,** *20*, 2466.
(56) Cramer, R. E.; Maynard, R. B.; Paw, J. C.; Gilje, J. W., *Organometallics* **1982,** *1*, 869.
(57) Cramer, R. E.; Maynard, R. B.; Paw, J. C.; Gilje, J. W., *Organometallics* **1983,** *2*, 1336.
(58) Cramer, R. E.; Higa, K. T.; Pruskin, S. L.; Gilje, J. W., *J. Am. Chem. Soc.* **1983,** *105*, 6749.
(59) Cramer, R. E.; Panchanatheswaran, K.; Gilje, J. W., *Angew. Chem. Int. Ed.* **1984,** *23*, 912.
(60) Cramer, R. E.; Panchanatheswaran, K.; Gilje, J. W., *J. Am. Chem. Soc.* **1984,** *106*, 1853.
(61) Cramer, R. E.; Mori, A. L.; Maynard, R. B.; Gilje, J. W.; Tatsumi, K.; Nakamura, A., *J. Am. Chem. Soc.* **1984,** *106*, 5920.
(62) Cramer, R. E.; Higa, K. T.; Gilje, J. W., *J. Am. Chem. Soc.* **1984,** *106*, 7245.
(63) Cramer, R. E.; Higa, K. T.; Gilje, J. W., *Organometallics* **1985,** *4*, 1140.
(64) Cramer, R. E.; Jeong, J. H.; Gilje, J. W., *Organometallics* **1986,** *5*, 2555.
(65) Cramer, R. E.; Engelhardt, U.; Higa, K. T.; Gilje, J. W., *Organometallics* **1987,** *6*, 41.
(66) Cramer, R. E.; Jeong, J. H.; Gilje, J. W., *Organometallics* **1987,** *6*, 2010.
(67) Cramer, R. E.; Roth, S.; Edelmann, F.; Bruck, M. A.; Cohn, K. C.; Gilje, J. W., *Organometallics* **1989,** *8*, 1192.
(68) Stevens, R. C.; Bau, R.; Cramer, R. E.; Afzal, D.; Gilje, J. W.; Koetzle, T. F., *Organometallics* **1990,** *9*, 694.
(69) Cramer, R. E.; Jeong, J. H.; Richmann, P. N.; Gilje, J. W., *Organometallics* **1990,** *9*, 1141.

(70) Fortier, S.; Walensky, J. R.; Wu, G.; Hayton, T. W., *J. Am. Chem. Soc.* **2011,** *133*, 6894.
(71) Shannon, R., *Acta Crystallogr. Sect. A* **1976,** *32*, 751.
(72) Sazama, G. T.; Betley, T. A., *Inorg. Chem.* **2010,** *49*, 2512.
(73) Mehdoui, T.; Berthet, J.-C.; Thuéry, P.; Salmon, L.; Rivière, E.; Ephritikhine, M., *Chem. - Eur. J.* **2005,** *11*, 6994.
(74) Kazhdan, D. Coupling of the 4f Electrons in Lanthanide Molecules. Ph.D. Dissertation, 2008.
(75) Ren, W.; Zi, G.; Fang, D.-C.; Walter, M. D., *J. Am. Chem. Soc.* **2011,** *133*, 13183.
(76) Ren, W.; Zi, G.; Walter, M. D., *Organometallics* **2012,** *31*.
(77) Kraft, S. J.; Walensky, J.; Fanwick, P. E.; Hall, M. B.; Bart, S. C., *Inorg. Chem.* **2010,** *49*, 7620.
(78) Evans, W. J.; Perotti, J. M.; Doedens, R. J.; Ziller, J. W., *Chem. Commun.* **2001**, 2326.
(79) Field, J. E.; Hill, T. J.; Venkataraman, D., *J. Org. Chem.* **2003,** *68*, 6071.

Chapter 6

Concluding Remarks

6.1 Strategies for Directing Structure and Reactivity at Uranium: The Lessons Learned. In this dissertation, new synthetic routes have been presented, producing complexes that exemplify the potential for controlling structural geometry, stabilizing reactive uranium-ligand bonds, and enabling new reactivity at uranium. The principle design elements—steric pressure, multidentate coordination, inverse trans influence stabilization, and non-covalent interactions—were of varying success.

Through the use of the uranium tris(bis(trimethylsilyl)amide) framework, a series of trigonal bipyramidal complexes was prepared, allowing for variation in the axial bonding with a conserved equatorial bonding framework. A wide variety of one-electron oxidants were tested, leading to new routes to the synthesis of uranium(V) and uranium(VI) complexes directly from uranium(III) starting materials. A combination of steric protection and inverse trans influence stabilization provided axial uranium-ligand bonding stability that allowed for the synthesis of reactive U^{VI}–C bonds, including methyl and acetylide derivatives. An unprecedented oxygen atom transfer reaction involving the one-electron deoxygenation of nitrite under non-aqueous, ambient conditions was discovered. An inverse trans influence ligand series was determined for the first time: $CN^- < I^- \approx Br^- < Cl^- \approx PhS^- < PhCC^- \approx F^- < MeO^- < NMe_2^- < Me^- < H^-$.[1] The inverse trans influence was found to contribute to the stabilization of axial uranium(V) complexes as well, allowing for the synthesis of a complex bearing an unusually short U^V–CN bond through coordination trans to an oxo ligand.[2]

Organization of secondary structure through the directed application of non-covalent interactions was demonstrated in a tethered, functionalized tris(pyrrolyl)amine framework. The collective arrangement of ligands in a binding cleft was observed in the solid state and in solution.

In an untethered ligand framework, use of the electron-poor NAr^FPh^- ligand exhibited some evidence for π-stacking interactions, apparently affecting the outcome of reactivity. However, collective organization of the secondary structure through alignment of electron-rich and electron-poor aryl groups was not observed. The NAr^FPh^- ligand was successfully applied in directing K^+ ion coordination to the weakly Lewis basic oxo groups of uranyl, directly impacting the electronic structure and bonding at the uranium center both in solution and in the solid state. Efforts to leverage non-covalent interactions to stabilize reactive uranium-ligand bonds, a long term goal of this project, are still ongoing.

6.2 Future Opportunities. By this point, the enterprising young reader will have realized that there are many new avenues for exploration in synthetic uranium chemistry. In the pursuit of new reactivity and the synthesis of metal-ligand bonds of long-standing interest, there are a number of factors should be taken into account.

The role of ionicity in uranium-ligand bonding cannot be ignored. There is an increasing drive toward preparing uranium-ligand bonds that possess more significant covalency, which has unquestionably yielded significant insight into the role of the 5f-orbtials in bonding.[3-14] However, the highly stable U=O bond is more ionic than the highly unstable U≡N bond.[15] Ligands that stabilize the negative charge on the donor atom of a ligand may prove more effective at stabilizing the uranium center. This point may prove to be important in the synthesis of a uranium-alkylidene, where attenuation of the negative charge at the dianionic carbon center could lead to stronger bonding and greater kinetic stability. At the extreme end of this spectrum lie pincer ligands such as bis(iminophosphorane)methandiide, which have been used extensively in the synthesis of uranium complexes.[11, 16-19] The U–C bonding of these complexes includes a C→U π-bonding MO with most electron density polarized onto the carbon atom.[17] A ligand with a stabilized dianionic carbon center more reminiscent of a traditional alkylidene may offer more covalent bonding.

Higher oxidation states of uranium engender greater covalency.[20] The smaller ionic radius and corresponding shorter bond length in high valent complexes allows for greater π-

bonding. However, uranium(VI) is potentially a strong oxidant in the absence of uranyl or electronic saturation with hard donor ligands. For example, U(VI/V) redox couples of UF_6 and $U^{V}F_2[N(SiMe_3)_2]_3$ are 1.91 eV and 0.90 eV vs $Fc^{+/0}$ respectively.[21] The bis(trimethylsilyl)amide ligand stabilizes the uranium center effectively, but not to the point where the $[U^{VI}F_2[N(SiMe_3)_2]_3]^+$ complex is chemically accessible.

The tris(bis(trimethylsilyl)amide) framework is not ideal for enabling inverse trans influence stabilization. While this ligand provides excellent steric protection and tends to prefer 3-fold coordination, it also competes for covalent interactions with the axial ligands. A more ideal supporting ligand should take inspiration from poorly activated uranyl complexes, in which the equatorial ligands saturate the equatorial coordination sites and protect the axial ligands. Of course, poorer donor ligands will generally stabilize the 6+ oxidation state less effectively, so the ideal conditions for preparing reactive uranium-ligand bonds may lie in the 5+ oxidation state.

Thorium-carbon bonds are stronger than uranium-carbon bonds.[22] This is an underappreciated fact that can help to explain variations in reactivity between the two elements.[23] Also, as discussed in Section 1.2, thorium(IV) complexes are considerably more stable towards reduction than uranium in any oxidation state, so thorium should prove to be more resilient toward M–R homolytic bond cleavage. These are important facts to consider, as synthetically interesting ligands such as the alkylidene may be challenging to prepare at uranium centers due to the propensity for reduction may be more accessible at thorium. Recent work in reductive preparation of thorium-ligand multiple bonds suggests that routes to these complexes may be feasible.[24, 25]

6.3 Miscellaneous Reactions. During the course of the syntheses described in Chapters 2–5, a number of other reactions were attempted that produced unexpected results. A short compendium of interesting products is provided in the following section, in the chance that they may be of interest.

A common issue faced in the synthesis of low valent uranium complexes lies in the erratic difficulties involved in preparing suitable starting materials.[26-30] The facile preparation of UI_3 in the absence of coordinating solvents allowed for the more versatile synthesis of new

uranium(III) complexes,[26] though in our hands, depending on the batch of uranium(0) turnings used, this reaction proceeded in either ~100% or ~0% yield, generating $UI_4(OEt_2)_2$ in the latter case. We therefore attempted to make use of the related preparation of $UI_4(OEt_2)_2$ as a starting point to access $UI_3(THF)_4$. Treatment of $UI_4(OEt_2)_2$ with Zn^0 powder led to a gradual color change from red to dark blue, indicative of reduction to uranium(III). Extraction of the resulting product and recrystallization from THF at –21 °C revealed that this reaction produced $[U^{III}I_2(THF)_5][ZnI_3(THF)]$ as a dark blue crystalline product (Figure 6.3.1), in poor yield and exhibiting very poor stability, particularly in the presence of non-coordinating solvents. This complex was isostructural to the reported complex $[NdI_2(THF)_5][ZnI_3(THF)]$, prepared from the reaction of Nd^0, I_2, and Zn^0 in THF.[31]

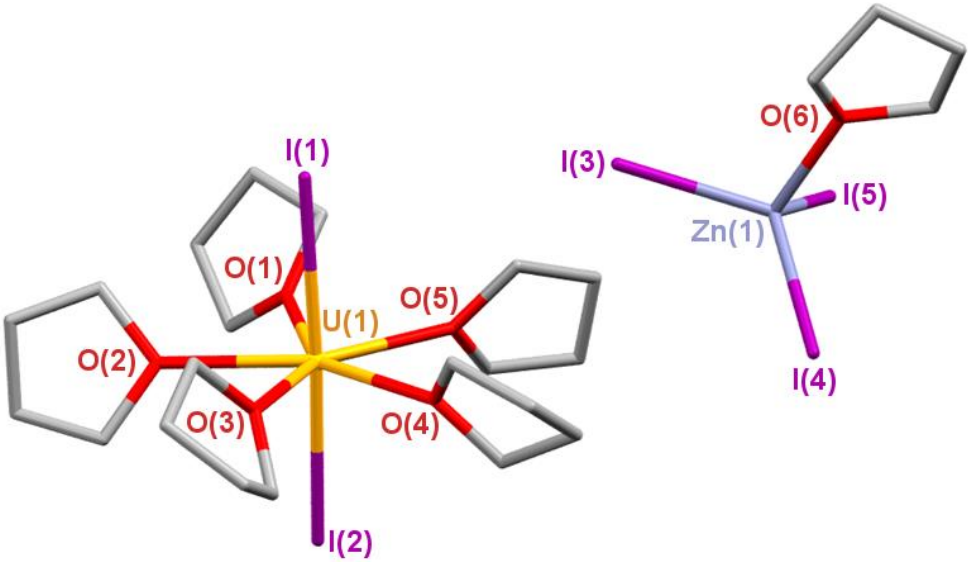

Figure 6.3.1 Structure of $[U^{III}I_2(THF)_5][ZnI_3(THF)]$.

During the course of investigating fluorinated ligands as a means to control secondary geometry, the synthesis of "$U^{III}(OPh^F)_3(py)_n$" (Ph^F = C_6F_5) was attempted. Addition of 3 equiv $HOPh^F$ to a Et_2O solution of $U^{III}(py)[N(SiMe_3)_2]_3$[32] in the presence of a small volume of pyridine led to an immediate color change to light aquamarine. Recrystallization from pyridine layered with hexanes at –21 °C produced teal crystals that were revealed by X-ray structural analysis to be $U^{IV}(OPh^F)_4(py)_4$ (Figure 6.3.2), presumably the product of disproportionation. The arrangement of

the four aryloxide ligands in this product closely resemble that of $U^{VI}(O^tBu)_2(OPh^F)_4$, reported by Hayton and coworkers.[33]

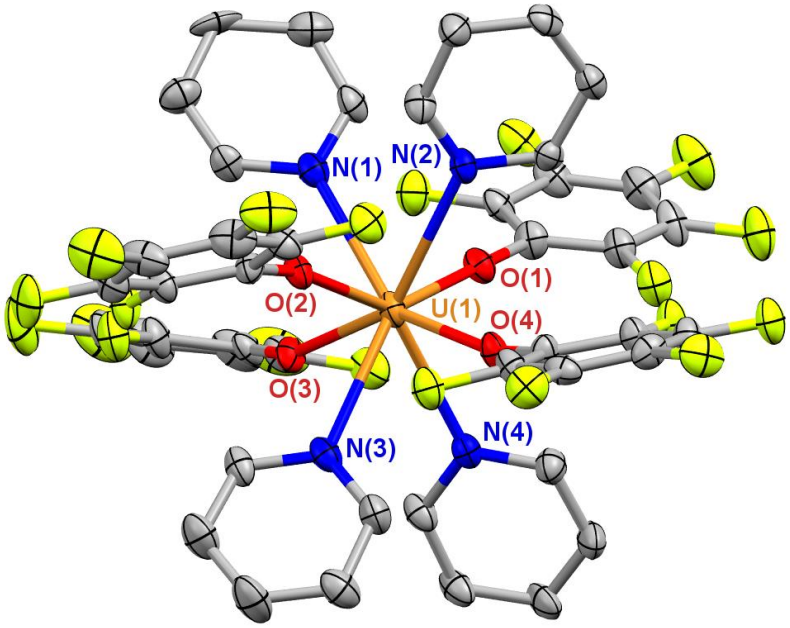

Figure 6.3.2 Thermal ellipsoid plot of $U^{IV}(OPh^F)_4(py)_4$, at 30% probability. Hydrogen atoms are omitted for clarity. Bond lengths (Å) and angles (°): U(1)–O(1) 2.187(8), U(1)–O(2) 2.241(8), U(1)–O(3) 2.215(8), U(1)–O(4) 2.211(8), U(1)–N(1) 2.634(10), U(1)–N(2) 2.682(10), U(1)–N(3) 2.667(10), U(1)–N(4) 2.667 (10).

The preparation of other simple uranium(III) complexes was investigated. Attempting to perform the synthesis of $U^{III}[N(SiMe_3)_2]_3$ through the addition of 3 equiv $NaN(SiMe_3)_2$ to a DME solution of $UI_3(THF)_4$, rather than the reported conditions involving THF as a solvent,[34] produced a dark purple product that was insoluble in hexanes. Dissolution of this product with toluene resulted in precipitation of a colorless solid, presumed to be NaI, with the product $U^{III}[N(SiMe_3)_2]_3$ confirmed by ^1H NMR. Therefore, it was concluded that the initial reaction produced $Na(DME)_4[U^{III}I[N(SiMe_3)_2]_3]$. NaI contamination is a noted difficulty in the preparation of $U^{III}[N(SiMe_3)_2]_3$;[35] in our hands, it was most effectively removed through trituration with hexanes followed by removal of solvent to fully desolvate the NaI, followed by extraction with hexanes.

The putative uranium(III)-iodide ‗-ate' complex inspired us to prepare another simple uranium(III)-iodide complex as another potential starting material. Slow addition of 2 equiv $KN(SiMe_3)_2$ to a THF solution of $UI_3(THF)_4$ produced $[U^{III}[N(SiMe_3)_2]_2(THF)(\mu\text{-}I)]_2$, structurally

identified by X-ray crystallography (Figure 6.3.3). THF solvation was apparently preferred over coordination of a second iodide ligand, so ‗-ate' complex formation was not observed in this instance, though it should be noted that several minor side products appeared in the ^{1}H NMR spectrum of an aliquot. The optimal conditions to prepare this complex were not determined, and its potential as a starting material was not investigated.

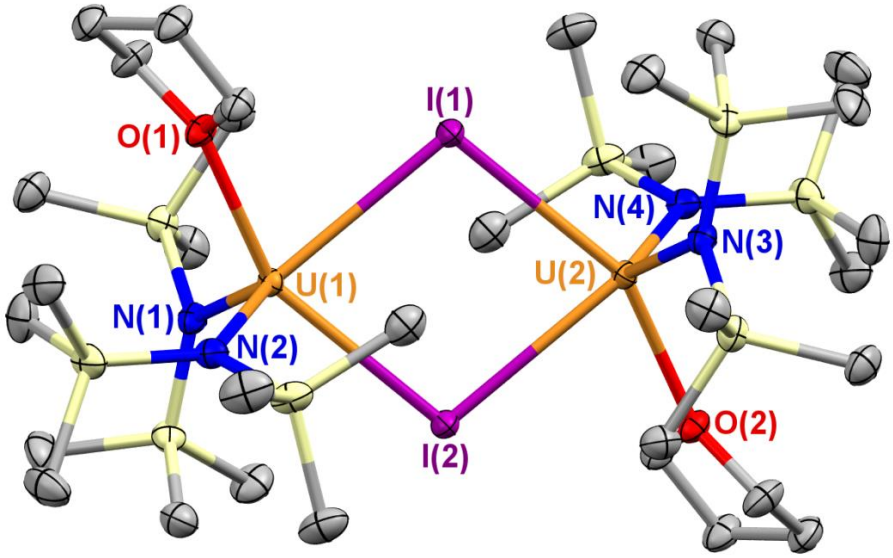

Figure 6.3.3 Thermal ellipsoid plot of $[U^{III}[N(SiMe_3)_2]_2(THF)(\mu\text{-}I)]_2$, at 30% probability. Hydrogen atoms are omitted for clarity. Bond lengths (Å) and angles (°): U(1)–I(1) 3.2107(6), U(1)–I(2) 3.2422(5), U(1)–N(1) 2.296(3), U(1)–N(2) 2.313(3), U(1)–O(1) 2.547(3), I(1)–U(1)–I(2) 78.765(10), N(1)–U(1)–N(2) 116.75(12), O(1)–U(1)–I(1) 76.99(7), O(1)–U(1)–I(2) 153.02(6).

The difficulty in completely removing NaI from $U^{III}[N(SiMe_3)_2]_3$ led to some unexpected reactivity. Addition of 0.5 equiv N_2CPh_2 to $U^{III}[N(SiMe_3)_2]_3$ dissolved in hexanes in the presence of a small volume of pyridine led to a color change to dark orange. Extraction of the resulting product in Et_2O and layering with hexanes at –21 °C selectively crystallized the uranium(IV) product $[Na(py)_2][U^{IV}[N(SiMe_3)_2]_3(\eta^2\text{-}N_2CPh_2)]$ (Figure 6.3.4). Consideration of charge balance indicates that the diazo-moiety undergoes 2-electron reduction, with one electron presumably originating from the uranium center and the second from adventitious NaI. Close association of the Na^+ cation with one of the phenyl rings was retained in solution, based on the asymmetry observed in the ^{1}H NMR spectrum (Figure 6.3.5). One and two electron reductions of Ph_2CN_2 by uranium complexes to form $Ph_2CN_2^-$ and $Ph_2CN_2^{2-}$ have been previously observed.[8, 36]

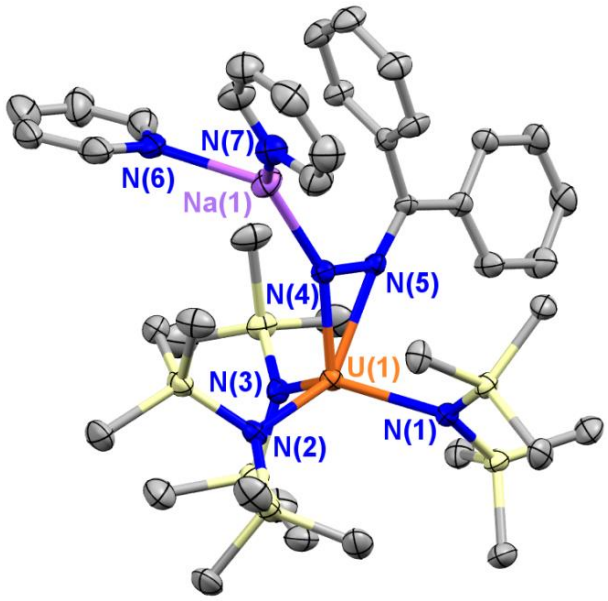

Figure 6.3.4 Thermal ellipsoid plot of $[Na(py)_2][U^{IV}[N(SiMe_3)_2]_3(\eta^2\text{-}N_2CPh_2)]$ at 30% probability. Hydrogen atoms are omitted for clarity. Bond lengths (Å) and angles (°): U(1)–N(1) 2.325(4), U(1)–N(2) 2.346(4), U(1)–N(3) 2.330(4), U(1)–N(4) 2.162(4), U(1)–N(5) 2.373(4), Na(1)–N(4) 2.342(4), N(4)–N(5) 1.349(5), N(4)–U(1)–N(5) 34.20(13).

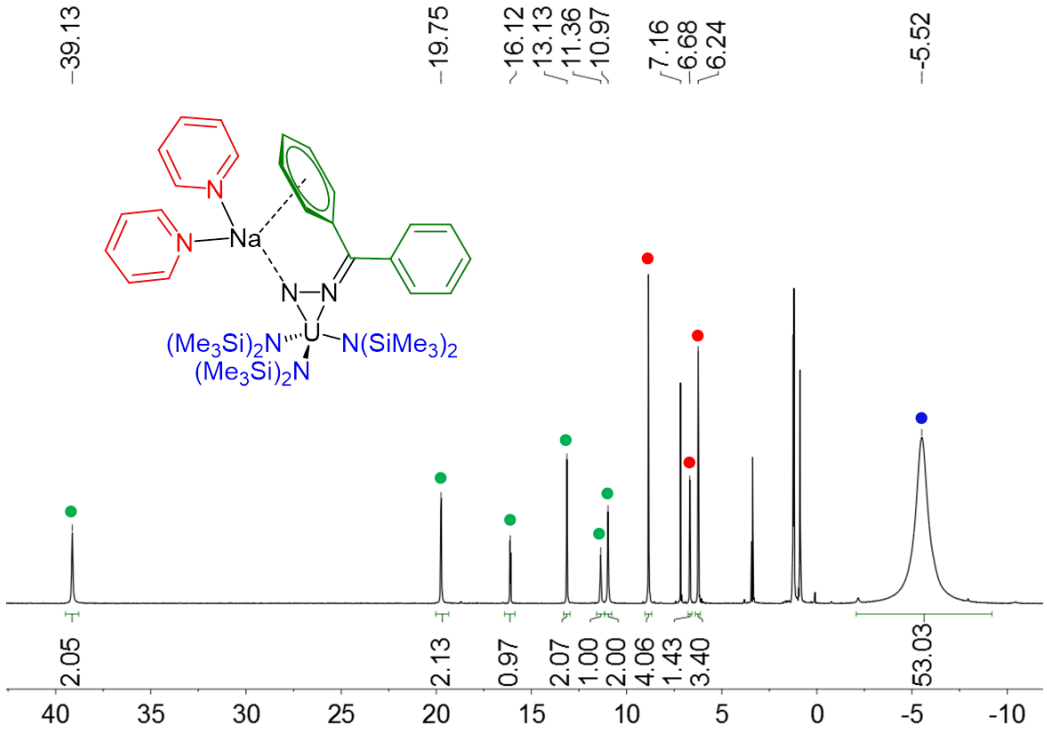

Figure 6.3.5 ^{1}H NMR spectrum of $[Na(py)_2][U^{IV}[N(SiMe_3)_2]_3(\eta^2\text{-}N_2CPh_2)]$ in benzene-d_6. Unlabeled resonances correspond to C_6D_5H, as well as Et_2O and hexanes from crystallization.

Over the course of exploring the one-electron oxidation chemistry of $U^{III}[N(SiMe_3)_2]_3$, new reactivity of the uranium(IV)-metallacyclic complexes was observed. Addition of 1 equiv I_2 to a THF solution of $U^{IV}(CH_2SiMe_3NSiMe_3)[N(SiMe_3)_2]_2$ produced an orange product with an unusual ^1H NMR spectrum (Figure 6.3.6). The expected product, $U^{V}I(CH_2SiMe_3NSiMe_3)[N(SiMe_3)_2]_2$, was not ruled out, but was deemed unlikely due to the dissimilarity of the ^1H NMR spectrum to the known uranium(V) tris-amide complexes. A more likely possibility is that the I_2 adds across the U–C bond, to produce $U^{IV}I(ICH_2SiMe_2NSiMe_3)[N(SiMe_3)_2]_2$. This exact reaction was mentioned by Ephritikhine and coworkers, who observed decomposition into unknown products, though were able to observe addition of I_2 over the U–C bond in another complex.[37]

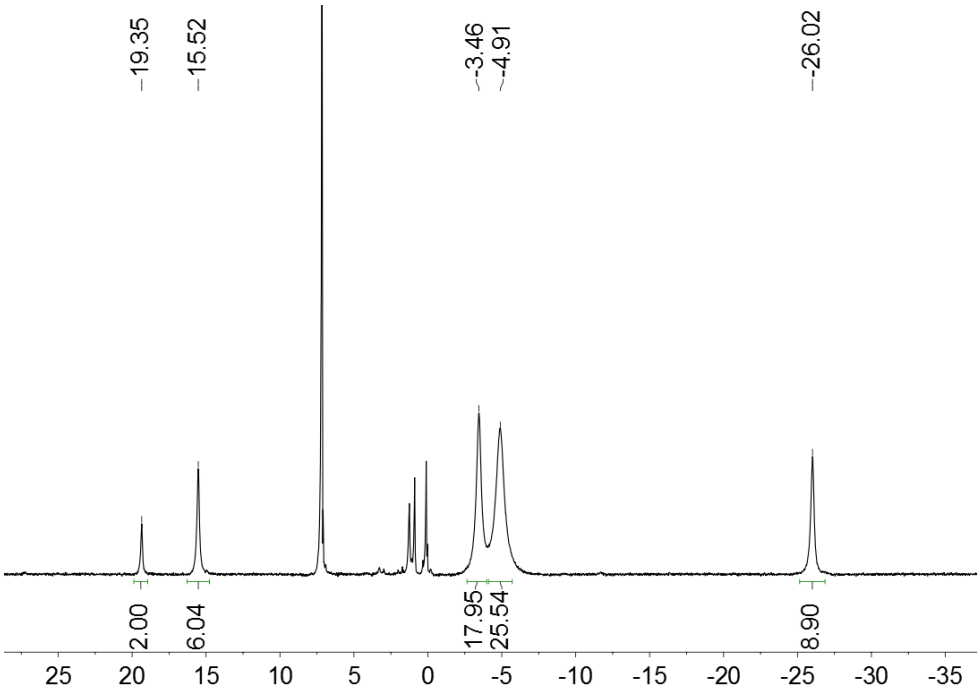

Figure 6.3.6 ^1H NMR spectrum of the product of the reaction of $U^{IV}(CH_2SiMe_3NSiMe_3)[N(SiMe_3)_2]_2$ with 1 equiv I_2 in THF.

We also prepared new metallacyclic derivatives in our attempts to synthesize U(IV)-alkyl complexes. Addition of 1 equiv $Li(THF)_3CHPH_2$ to a THF solution of $U^{IV}Cl[N(SiMe_3)_2]_3$ in THF produced the bis-metallacycle $Li(THF)_n[U(CH_2SiMe_3NSiMe_3)_2[N(SiMe_3)_2]_2]$, with variable THF solvation. Recrystallization from a concentrated THF solution layered with hexanes stored at –21 °C produced a mixture of colorless and green crystals, both of which were structurally

characterized. Both polymorphs of $[Li(THF)_n][U(CH_2SiMe_3NSiMe_3)_2[N(SiMe_3)_2]]$ exhibited close contact of the Li^+ ion, where the structure of the colorless (n = 2 THF) crystal showed close contact with both of the tethered alkyl ligands, and the green (n = 1 THF) crystal showed close contact with one CH_2 and one amide nitrogen (Figure 6.3.7). Uranium(IV) bis-metallacycles of the other alkali metals are now well known.[38]

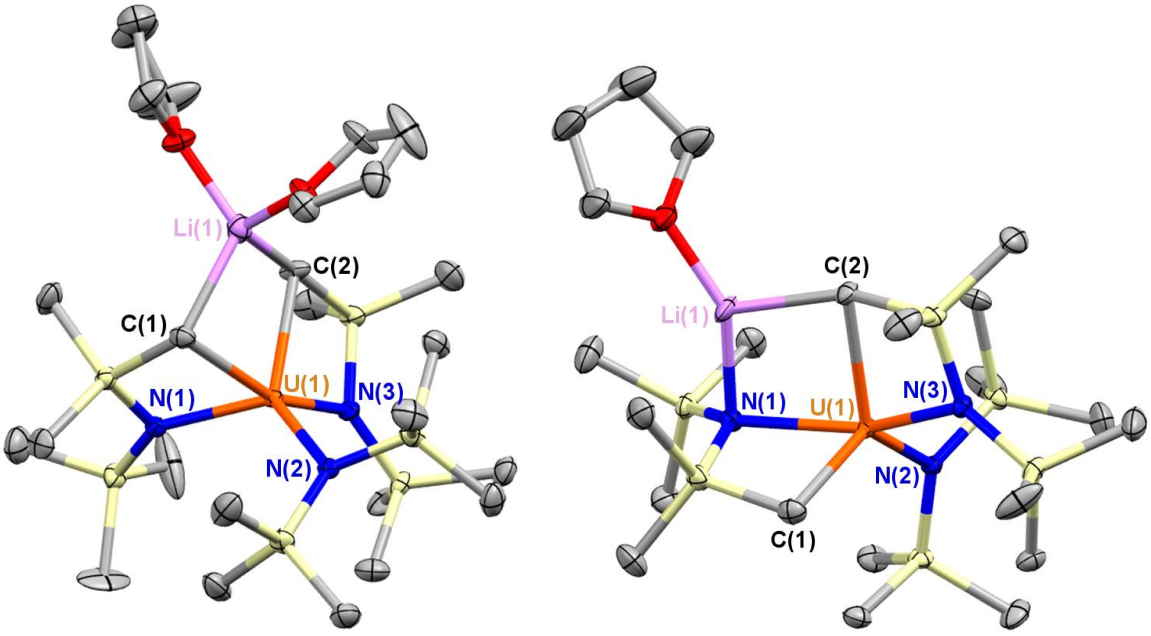

Figure 6.3.7 Thermal ellipsoid plots of colorless (left) and green (right) polymorphs of $[Li(THF)_n][U^{IV}(CH_2SiMe_3NSiMe_3)_2[N(SiMe_3)_2]]$ at 30% probability. Bond lengths (Å) and angles (°): U(1)–N(1) 2.3327(16), U(1)–N(2) 2.2633(17), U(1)–N(3) 2.2711(17), U(1)–C(1) 2.485(2), U(1)–C(2) 2.524(2).

In the course of testing the reactivity of $U^{IV}(py)(NAr^FPh)_4$ (**4.2**) with various oxidants, the reaction with TEMPO was considered. Addition of TEMPO led to a color change to brown, producing a mixture of products. A product was isolated from this reaction through recrystallization from hexanes at –21 °C: $U^{IV}(TEMPO)_2(NAr^FPh)_2$. No examples of TEMPO coordinated to uranium have been previously reported, though TEMPO has been used as an oxygen atom donor towards uranium(III) and uranium(IV).[35, 39]

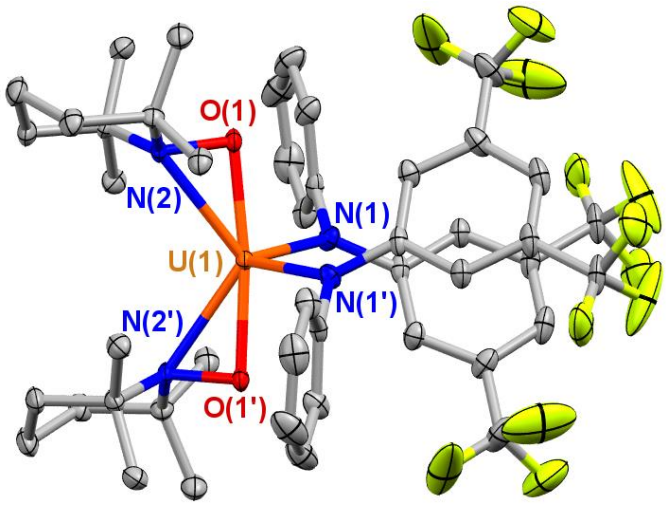

Figure 6.3.8 Thermal ellipsoid plot of $U^{IV}(NAr^{F}Ph)_2(TEMPO)_2$, at 30% probability. Hydrogen atoms are omitted for clarity. Bond lengths (Å) and angles (°): U(1)–O(1) 2.155(4), U(1)–N(1) 2.334(5), U(1)–N(2) 2.561(5), N(2)–O(1) 1.432(6), O(1)–U(1)–O(1') 172.6(2), N(1)–U(1)–N(1') 97.8(2), N(2)–U(1)–N(2') 109.3(2), N(2)–O(1)–U(1) 88.7(3).

6.4 Experimental (Miscellaneous).

6.4.1 $[U^{III}I_2(THF)_5][ZnI_3(THF)]$. To an Et_2O solution of $UI_4(OEt_2)_2$ (200 mg, 0.22 mmol), Zn^0 powder (74 mg, 1.12 mmol, 5.1 equiv) was added. The mixture was stirred for 4 h, over which time it gradually became dark blue. The mixture was filtered through Celite packed on a coarse fritted filter, which was rinsed with Et_2O to produce a purple filtrate after separating a grey solid precipitate. The residual solid was extracted with THF to produce a blue filtrate, which was concentrated and stored at –21 °C to produce dark blue crystals of $[U^{III}I_2(THF)_5][ZnI_3(THF)]$. Yield: 15 mg, 0.01 mmol, 5%. Attempts to collect the ^{1}H NMR spectrum in benzene-d_6 led to immediate color change to pale yellow.

6.4.2 $U^{IV}(OC_6F_5)_4(py)_4$. To an Et_2O solution of $U^{III}(py)[N(SiMe_3)_2]_3$ (171 mg, 0.21 mmol), an Et_2O solution of HOC_6F_5 (118mg, 0.64 mmol, 3.0 equiv) with a small volume of pyridine was added, resulting in a color change to aquamarine. After stirring 45 min, the mixture was filtered through Celite suspended in a glass pipet, and the filtrate was layered with hexanes and stored at –21 °C to yield $U^{IV}(OC_6F_5)_4(py)_4$ as a teal crystalline solid. Yield: 132 mg, 0.10 mmol, 64% (based on 4 U^{III} → 3 U^{IV} + U^0). ^{1}H NMR (Tol-d_8): δ 2.54 (4H), –0.06 (8H), –5.55 (8H). ^{19}F NMR (Tol-d_8): δ –148.0 (d, 8F), –161.3 (t, 8F), –168.1 (t, 4F).

Recrystallization from THF/hexanes at –21 °C produced the complex $U^{IV}(OC_6F_5)_4(py)_3(THF)$ as judged by ^1H NMR spectroscopy and elemental analysis. ^1H NMR (benzene-d_6): δ –0.29 (3H), –2.58 (4H), –4.26 (6H), –4.67 (4H), –14.26 (6H). ^{19}F NMR (benzene-d_6): δ –149.1 (8F), –161.2 (8F), –168.0 (4F). Elemental analysis found (calculated) for $C_{43}H_{23}F_{20}N_3O_5U$: C, 40.19 (40.36); H, 1.86 (1.81); N, 3.51 (3.28).

6.4.3 $[U^{III}[N(SiMe_3)_2]_2(THF)(\mu\text{-}I)]_2$. To a solution of $UI_3(THF)_4$ (500 mg, 0.55 mmol) in 5 mL THF, $KN(SiMe_3)_2$ (220 mg, 1.10 mmol, 2.0 equiv) dissolved in 7 mL THF was added dropwise, resulting in a color change to dark purple. After stirring 1.5 h, visible KI was allowed to settle, then the mixture was filtered through Celite and volatiles were removed under reduced pressure. The resulting black residue was extracted with hexanes, filtered through Celite, and stored at –21 °C to produce black crystals of $[U^{III}[N(SiMe_3)_2]_2(THF)(\mu\text{-}I)]_2$. A yield was not determined for this product, as the reaction was not optimized to avoid significant side-product formation. ^1H NMR (benzene-d_6): δ –8.98 (72H). The coordinated THF resonances were not definitively assigned.

6.4.4 $[Na(py)_2][U^{IV}[N(SiMe_3)_2]_3(\eta^2\text{-}N_2CPh_2)]$. To a solution of $U[N(SiMe_3)_2]_3$ (200 mg, 0.28 mmol) in hexanes with 0.5 mL pyridine cooled to –21 °C, added N_2CPh_2 (27 mg, 0.14 mmol, 0.5 equiv), leading to a rapid color change to dark orange. After stirring 10 min, volatiles were removed under reduced pressure. Recyrstallization of an Et_2O solution layered with hexanes produced orange crystals of $[Na(py)_2][U^{IV}[N(SiMe_3)_2]_3(\eta^2\text{-}N_2CPh_2)]$. Yield: 23 mg, percent yield unknown due to presumable dependency on NaI contamination. ^1H NMR (benzene-d_6): δ 39.13 (2H), 19.75 (2H), 16.12 (1H), 13.13 (2H), 11.36 (1H), 10.97 (2H), 8.85 (4H), 6.68 (2H), 6.24 (4H), –5.52 (54H).

6.4.5 $[Li(THF)_n][U(CH_2SiMe_2\mathit{N}SiMe_3)_2[N(SiMe_3)_2]]$ (n = 1, 2). To a –21 °C THF solution of $U^{IV}Cl[N(SiMe_3)_2]_3$ (300 mg, 0.40 mmol), a –21 °C THF solution of $Li(THF)_3CHPh_2$ (320 mg, 0.82 mmol, 2.06 equiv) was added, resulting in a color change to dark red-brown. After stirring 3 h, volatiles were removed under reduced pressure, and the resulting brown residue was dissolved in hexanes to precipitate a colorless soled. The mixture was filtered through Celite

suspended in a glass pipette, concentrated, and stored at –21 °C overnight to produce a mixture of colorless and light green crystals, which were identified as $[Li(THF)_2][U(CH_2SiMe_2NSiMe_3)_2[N(SiMe_3)_2]]$ and $[Li(THF)][U(CH_2SiMe_2NSiMe_3)_2[N(SiMe_3)_2]]$ respectively. The isolated solid was dried under reduced pressure to remove excess THF solvation. Yield: 180 mg, 0.23 mmol, 57%. ^{1}H NMR (benzene-d_6): δ 44.56 (18H), 29.26 (6H), –6.92 (6H), –42.62 (18H). The CH_2 resonances were not identified, but are expected to appear ~ –290 ppm based on related the U(IV)-bis-metallacycles.[38]

6.4.6 $U^{IV}(NAr^FPh)_2(TEMPO)_2$. To an Et_2O solution of **4.2** (20 mg, 0.01 mmol), an Et_2O solution of TEMPO (2 mg, 0.01 mmol, 1.0 equiv) was added, resulting in a color change to brown. After stirring 30 min, volatiles were removed under reduced pressure, and the resulting brown residue was recrystallized from hexanes at –21 °C to produce scant crystals of $U^{IV}(NAr^FPh)_2(TEMPO)_2$.

6.5 X-Ray Data.

Table 6.5.1 Summary of structure determination.

	$U^{IV}(OC_6F_5)_4(py)_4$	$[U^{III}[N(SiMe_3)_2]_2(THF)(\mu\text{-}I)]_2$	$[Na(py)_2][U^{IV}[N(SiMe_3)_2]_3(\eta^2\text{-}N_2CPh_2)]$
Empirical formula	$C_{54}H_{30}N_6O_4F_{20}U$	$C_{32}H_{88}N_4Si_8O_2I_2U_2$	$C_{41}H_{74}N_7Si_6NaU$
Formula weight	1444.87	1515.64	1094.63
Temperature	143(1) K	143(1) K	143(1) K
Wavelength	0.71073 Å	0.71073 Å	0.71073 Å
Crystal system	monoclinic	orthorhombic	monoclinic
Space group	$P2_1/c$	Pbca	$P2_1/n$
a	20.814(4) Å	18.448(4) Å	20.199(3) Å
b	16.858(3) Å	16.360(3) Å	13.4796(18) Å
c	16.196(3) Å	18.991(4) Å	24.166(3) Å
α	90	90	90
β	109.981(10)°	90	94.444(7)°
γ	90	90	90
Volume	5340.8(17) Å^3	5731(2) Å^3	6559.9(16) Å^3
Z	4	4	4
Density (calculated)	1.797 Mg/m^3	1.756 Mg/m^3	1.108 Mg/m^3
Absorption coefficient	3.162 mm^{-1}	6.917 mm^{-1}	2.618 mm^{-1}
F(000)	2800	2904	2224
Crystal size	0.38 x 0.20 x 0.06 mm3	0.25 x 0.12 x 0.12 mm3	0.35 x 0.25 x 0.10 mm3
Theta range	1.59 to 27.67°	1.98 to 27.61°	1.82 to 27.57°
Index ranges	-27 ≤ h ≤ 26, -22 ≤ k ≤ 21, -19 ≤ l ≤ 21	-24 ≤ h ≤ 23, -21 ≤ k ≤ 21, -24 ≤ l ≤ 24	-26 ≤ h ≤ 26, -17 ≤ k ≤ 17, -31 ≤ l ≤ 30

Reflections	68339	106764	163596
Independent reflections	12404 [R(int) = 0.3827]	6609 [R(int) = 0.0339]	15100 [R(int) = 0.0350]
Completeness to theta = 27.52 °	99.40%	99.30%	99.50%
Max. and min. transmission	0.7456 and 0.3833	0.7456 and 0.6572	0.7456 and 0.5858
Data / restraints / parameters	12404 / 744 / 767	6609 / 0 / 238	15100 / 0 / 523
Goodness-of-fit on F^2	0.934	1.095	1.095
Final R indices [I>2sigma(I)]	R1 = 0.0818, wR2 = 0.1320	R1 = 0.0235, wR2 = 0.0550	R1 = 0.0481, wR2 = 0.1129
R indices (all data)	R1 = 0.2767, wR2 = 0.1970	R1 = 0.0344, wR2 = 0.0621	R1 = 0.0627, wR2 = 0.1211
Largest diff. peak and hole	2.206 and -1.098 e.Å^{-3}	2.616 and -0.621 e.Å^{-3}	2.092 and -1.972 e.Å^{-3}

	$Li(THF)U[N(SiMe_3)_2](\kappa_2\text{-}CH_2SiMe_2NSiMe_3)_2$	$U^{IV}(NAr^FPh)_2(TEMPO)_2$
Empirical formula	$C_{26}H_{68}Si_6N_3O_2LiU$	$C_{46}H_{52}N_4O_2F_{12}U$
Formula weight	868.34	1158.95
Temperature	143(2) K	143(1) K
Wavelength	0.71073 Å	0.71073 Å
Crystal system	orthorhombic	orthorhombic
Space group	$P2_12_12_1$	$C222_1$
a	12.4940(5) Å	13.0246(8) Å
b	15.4123(6) Å	20.3327(14) Å
c	21.6821(8) Å	19.8206(13) Å
α	90	90
β	90	90
γ	90	90
Volume	4175.1(3) Å^3	5249.0(6) Å^3
Z	4	4
Density (calculated)	1.381 Mg/m^3	1.467 Mg/m^3
Absorption coefficient	4.084 mm^{-1}	3.172 mm^{-1}
F(000)	1760	2288
Crystal size	0.25 x 0.12 x 0.08 mm3	0.48 x 0.32 x 0.20 mm3
Theta range	1.62 to 27.54°	1.86 to 27.54°
Index ranges	-16 ≤ h ≤ 16, -20 ≤ k ≤ 20, -28 ≤ l ≤ 28	-16 ≤ h ≤ 16, -26 ≤ k ≤ 26, -25 ≤ l ≤ 25
Reflections	202840	79523
Independent reflections	9617 [R(int) = 0.0328]	6032 [R(int) = 0.0368]
Completeness to theta = 27.52 °	99.90%	99.70%
Max. and min. transmission	0.7456 and 0.6416	0.7456 and 0.5309
Data / restraints / parameters	9617 / 0 / 369	6032 / 0 / 298
Goodness-of-fit on	1.04	1.231

F^2		
Final R indices [I>2sigma(I)]	R1 = 0.0139, wR2 = 0.0322	R1 = 0.0352, wR2 = 0.1048
R indices (all data)	R1 = 0.0155, wR2 = 0.0328	R1 = 0.0392, wR2 = 0.1090
Largest diff. peak and hole	0.795 and -0.393 e.Å^{-3}	2.419 and -1.190 e.Å^{-3}

Table 6.5.2 Bond lengths of $U^{IV}(OC_6F_5)_4(py)_4$ (Å).

U1-O1	2.187(8)	U1-O4	2.211(8)	U1-O3	2.215(8)
U1-O2	2.241(8)	U1-N1	2.634(10)	U1-N4	2.667(10)
U1-N3	2.667(10)	U1-N2	2.682(10)	N1-C5	1.328(14)
N1-C1	1.344(15)	N2-C10	1.346(15)	N2-C6	1.344(15)
N3-C11	1.322(15)	N3-C15	1.333(15)	N4-C16	1.326(15)
N4-C20	1.370(15)	O1-C21	1.346(14)	O2-C27	1.306(14)
O3-C33	1.317(13)	O4-C39	1.342(14)	C1-C2	1.334(17)
C2-C3	1.390(19)	C3-C4	1.46(2)	C4-C5	1.397(18)
C6-C7	1.408(18)	C7-C8	1.372(19)	C8-C9	1.40(2)
C9-C10	1.366(18)	C11-C12	1.359(17)	C12-C13	1.404(18)
C13-C14	1.335(17)	C14-C15	1.387(17)	C16-C17	1.383(17)
C17-C18	1.345(18)	C18-C19	1.379(18)	C19-C20	1.380(17)
C21-C22	1.368(17)	C21-C26	1.389(17)	C22-F1	1.340(14)
C22-C23	1.358(17)	C23-F2	1.348(15)	C23-C24	1.349(19)
C24-F3	1.339(15)	C24-C25	1.377(19)	C25-F4	1.331(15)
C25-C26	1.381(17)	C26-F5	1.344(14)	C27-C28	1.387(17)
C27-C32	1.421(17)	C28-C29	1.354(19)	C28-F6	1.375(16)
C29-F7	1.313(17)	C29-C30	1.36(2)	C30-C31	1.36(2)
C30-F8	1.364(17)	C31-F9	1.333(18)	C31-C32	1.391(19)
C32-F10	1.357(15)	C33-C34	1.364(17)	C33-C38	1.417(17)
C34-F11	1.351(14)	C34-C35	1.370(16)	C35-C36	1.331(19)
C35-F12	1.339(15)	C36-F13	1.321(15)	C36-C37	1.40(2)
C37-F14	1.344(15)	C37-C38	1.371(18)	C38-F15	1.331(15)
C39-C40	1.375(17)	C39-C44	1.412(17)	C40-F16	1.345(14)
C40-C41	1.365(18)	C41-F17	1.353(14)	C41-C42	1.364(17)
C42-C43	1.354(16)	C42-F18	1.382(14)	C43-F19	1.306(14)
C43-C44	1.389(17)	C44-F20	1.363(13)	N5-C45	1.290(18)
N5-C49	1.338(17)	C45-C46	1.37(2)	C46-C47	1.37(2)
C47-C48	1.36(2)	C48-C49	1.371(19)	N6-C54	1.34(3)
N6-C50	1.39(3)	C50-C51	1.30(3)	C51-C52	1.34(2)
C52-C53	1.37(3)	C53-C54	1.36(3)		

Table 6.5.3 Bond angles of $U^{IV}(OC_6F_5)_4(py)_4$ (°).

O1-U1-O4	96.6(3)	O1-U1-O3	146.6(3)
O1-U1-O2	93.6(3)	O4-U1-O2	145.0(3)
O1-U1-N1	77.6(3)	O4-U1-N1	141.9(3)
O2-U1-N1	73.1(3)	O1-U1-N4	73.3(3)
O3-U1-N4	140.2(3)	O2-U1-N4	78.7(3)
O1-U1-N3	76.0(3)	O4-U1-N3	73.1(3)
O2-U1-N3	141.9(3)	N1-U1-N3	68.9(3)
O1-U1-N2	141.2(3)	O4-U1-N2	77.2(3)
O2-U1-N2	74.0(3)	N1-U1-N2	129.8(3)

N3-U1-N2	134.9(3)	C5-N1-C1	115.9(11)
C1-N1-U1	119.4(8)	C10-N2-C6	117.8(12)
C6-N2-U1	122.6(9)	C11-N3-C15	116.8(11)
C15-N3-U1	118.7(8)	C16-N4-C20	115.7(11)
C20-N4-U1	122.2(9)	C21-O1-U1	178.1(8)
C33-O3-U1	165.0(9)	C39-O4-U1	160.0(8)
C1-C2-C3	123.2(15)	C2-C3-C4	112.7(13)
N1-C5-C4	124.0(14)	N2-C6-C7	123.0(13)
C7-C8-C9	119.4(15)	C10-C9-C8	119.0(15)
N3-C11-C12	125.1(13)	C11-C12-C13	116.4(13)
C13-C14-C15	118.8(13)	N3-C15-C14	122.7(13)
C18-C17-C16	118.9(14)	C17-C18-C19	119.9(14)
N4-C20-C19	123.3(13)	O1-C21-C22	120.7(12)
C22-C21-C26	117.2(13)	F1-C22-C23	118.8(13)
C23-C22-C21	121.2(14)	F2-C23-C24	119.7(13)
C24-C23-C22	121.7(15)	F3-C24-C23	121.4(15)
C23-C24-C25	119.5(14)	F4-C25-C24	120.6(13)
C24-C25-C26	118.8(14)	F5-C26-C25	117.5(13)
C25-C26-C21	121.7(14)	O2-C27-C28	126.1(13)
C28-C27-C32	112.8(13)	C29-C28-F6	119.4(14)
F6-C28-C27	114.8(13)	F7-C29-C28	120.4(17)
C28-C29-C30	118.4(17)	C29-C30-C31	121.6(17)
C31-C30-F8	118.7(19)	F9-C31-C30	122.3(17)
C30-C31-C32	118.3(17)	F10-C32-C31	117.8(13)
C31-C32-C27	123.0(15)	O3-C33-C34	124.0(12)
C34-C33-C38	115.4(12)	F11-C34-C33	117.6(11)
C33-C34-C35	124.0(13)	C36-C35-F12	120.4(13)
F12-C35-C34	119.2(13)	F13-C36-C35	121.7(16)
C35-C36-C37	119.2(14)	F14-C37-C38	118.8(15)
C38-C37-C36	120.3(14)	F15-C38-C37	119.2(13)
C37-C38-C33	120.9(14)	O4-C39-C40	122.1(12)
C40-C39-C44	114.5(13)	F16-C40-C41	117.6(12)
C41-C40-C39	122.5(13)	F17-C41-C40	119.7(13)
C40-C41-C42	120.1(13)	C43-C42-C41	122.0(13)
C41-C42-F18	120.4(12)	F19-C43-C42	123.6(13)
C42-C43-C44	116.5(13)	F20-C44-C43	118.1(11)
C43-C44-C39	124.2(13)	C45-N5-C49	117.3(15)
C47-C46-C45	118.0(18)	C48-C47-C46	119.5(17)
N5-C49-C48	123.0(16)	C54-N6-C50	121(2)
C50-C51-C52	122(2)	C51-C52-C53	116(3)
N6-C54-C53	116(3)	F3-C24-C25	119.1(14)
O4-U1-O3	95.2(3)	F4-C25-C26	120.6(14)
O3-U1-O2	94.4(3)	F5-C26-C21	120.7(12)
O3-U1-N1	73.8(3)	O2-C27-C32	121.1(12)
O4-U1-N4	72.5(3)	C29-C28-C27	125.7(16)
N1-U1-N4	137.6(3)	F7-C29-C30	121.1(17)
O3-U1-N3	77.7(3)	C29-C30-F8	119.1(18)
N4-U1-N3	130.1(3)	F9-C31-C32	119.2(16)
O3-U1-N2	72.0(3)	F10-C32-C27	119.1(12)
N4-U1-N2	68.3(3)	O3-C33-C38	120.6(12)
C5-N1-U1	124.8(9)	F11-C34-C35	118.5(12)
C10-N2-U1	119.5(9)	C36-C35-C34	120.2(15)
C11-N3-U1	124.5(8)	F13-C36-C37	119.1(14)
C16-N4-U1	122.1(8)	F14-C37-C36	120.8(14)

C27-O2-U1	152.4(8)	F15-C38-C33	119.9(12)
C2-C1-N1	124.8(13)	O4-C39-C44	123.4(12)
C5-C4-C3	119.3(14)	F16-C40-C39	119.6(12)
C8-C7-C6	117.8(15)	F17-C41-C42	120.2(13)
N2-C10-C9	123.1(15)	C43-C42-F18	117.3(13)
C14-C13-C12	120.1(13)	F19-C43-C44	119.9(12)
N4-C16-C17	124.1(13)	F20-C44-C39	117.7(11)
C18-C19-C20	118.0(14)	N5-C45-C46	124.1(18)
O1-C21-C26	122.1(13)	C47-C48-C49	117.9(16)
F1-C22-C21	119.9(12)	C51-C50-N6	121(2)
F2-C23-C22	118.7(13)	C54-C53-C52	125(3)

Table 6.5.4 Bond lengths of $[U^{III}[N(SiMe_3)_2]_2(THF)(\mu\text{-}I)]_2$ (Å).

U1-N1	2.296(3)	U1-N2	2.313(3)	U1-O1	2.547(3)
U1-I1#1	3.2107(6)	U1-I1	3.2422(5)	I1-U1#1	3.2107(6)
Si1-N1	1.724(3)	Si1-C3	1.865(5)	Si1-C2	1.867(5)
Si1-C1	1.873(5)	Si2-N1	1.728(3)	Si2-C6	1.857(5)
Si2-C4	1.869(5)	Si2-C5	1.879(5)	Si3-N2	1.724(4)
Si3-C9	1.863(5)	Si3-C8	1.867(6)	Si3-C7	1.876(5)
Si4-N2	1.722(4)	Si4-C11	1.868(6)	Si4-C12	1.868(5)
Si4-C10	1.876(5)	O1-C13	1.437(5)	O1-C16	1.457(5)
C13-C14	1.490(7)	C14-C15	1.492(7)	C15-C16	1.515(6)

Symmetry transformations used to generate equivalent atoms:

#1 -x+1,-y+1,-z+1

Table 6.5.5 Bond angles of $[U^{III}[N(SiMe_3)_2]_2(THF)(\mu\text{-}I)]_2$ (°).

N1-U1-N2	116.75(12)	N1-U1-O1	110.94(10)
N1-U1-I1#1	91.07(8)	N2-U1-I1#1	101.82(8)
N1-U1-I1	118.80(8)	N2-U1-I1	124.43(9)
I1#1-U1-I1	78.765(10)	U1#1-I1-U1	101.235(10)
N1-Si1-C2	111.69(19)	C3-Si1-C2	106.7(2)
C3-Si1-C1	107.3(3)	C2-Si1-C1	105.7(3)
N1-Si2-C4	111.5(2)	C6-Si2-C4	108.2(2)
C6-Si2-C5	105.5(2)	C4-Si2-C5	107.2(2)
N2-Si3-C8	110.5(2)	C9-Si3-C8	108.1(3)
C9-Si3-C7	106.8(2)	C8-Si3-C7	105.3(3)
N2-Si4-C12	113.1(2)	C11-Si4-C12	107.3(3)
C11-Si4-C10	104.8(3)	C12-Si4-C10	106.7(2)
C13-O1-U1	135.4(3)	C16-O1-U1	116.6(2)
Si1-N1-U1	121.14(17)	Si2-N1-U1	117.28(17)
Si4-N2-U1	120.24(18)	Si3-N2-U1	118.79(18)
C13-C14-C15	103.4(4)	C14-C15-C16	104.9(4)
N2-U1-O1	82.54(10)	N2-Si4-C11	110.3(2)
O1-U1-I1#1	153.02(6)	N2-Si4-C10	114.0(2)
O1-U1-I1	76.99(7)	C13-O1-C16	108.0(3)
N1-Si1-C3	112.8(2)	Si1-N1-Si2	121.6(2)
N1-Si1-C1	112.2(2)	Si4-N2-Si3	121.0(2)
N1-Si2-C6	110.51(19)	O1-C13-C14	105.0(4)
N1-Si2-C5	113.6(2)	O1-C16-C15	106.2(3)

N2-Si3-C9	111.8(2)	N2-Si3-C7	113.8(2)

Symmetry transformations used to generate equivalent atoms:

#1 -x+1,-y+1,-z+1

Table 6.5.6 Bond lengths of $[Na(py)_2][U^{IV}[N(SiMe_3)_2]_3(\eta^2\text{-}N_2CPh_2)]$ (Å).

U1-N4	2.162(4)	U1-N1	2.325(4)	U1-N3	2.330(4)
U1-N2	2.346(4)	U1-N5	2.373(4)	U1-Si2	3.4011(14)
U1-Si3	3.4283(15)	U1-Si5	3.4383(13)	Si1-N1	1.736(4)
Si1-C1	1.859(6)	Si1-C2	1.866(7)	Si1-C3	1.875(7)
Si2-N1	1.724(4)	Si2-C6	1.865(6)	Si2-C5	1.870(7)
Si2-C4	1.882(6)	Si3-N2	1.733(4)	Si3-C7	1.860(6)
Si3-C8	1.876(6)	Si3-C9	1.885(6)	Si4-N2	1.726(4)
Si4-C12	1.873(7)	Si4-C10	1.879(7)	Si4-C11	1.887(6)
Si5-N3	1.725(4)	Si5-C15	1.868(5)	Si5-C13	1.877(5)
Si5-C14	1.884(5)	Si6-N3	1.733(4)	Si6-C17	1.867(6)
Si6-C16	1.876(6)	Si6-C18	1.878(5)	Na1-N4	2.342(4)
Na1-N6	2.415(6)	Na1-N7	2.423(6)	N4-N5	1.349(5)
N5-C19	1.314(6)	N6-C36	1.314(8)	N6-C32	1.336(9)
N7-C37	1.313(8)	N7-C41	1.336(9)	C19-C26	1.466(6)
C19-C20	1.500(6)	C20-C21	1.385(7)	C20-C25	1.386(7)
C21-C22	1.378(8)	C22-C23	1.361(8)	C23-C24	1.396(8)
C24-C25	1.387(8)	C26-C31	1.384(7)	C26-C27	1.397(7)
C27-C28	1.386(7)	C28-C29	1.357(8)	C29-C30	1.395(8)
C30-C31	1.381(7)	C32-C33	1.364(10)	C33-C34	1.344(11)
C34-C35	1.355(11)	C35-C36	1.385(10)	C37-C38	1.444(13)
C38-C39	1.353(13)	C39-C40	1.298(13)	C40-C41	1.374(10)

Table 6.5.7 Bond angles of $[Na(py)_2][U^{IV}[N(SiMe_3)_2]_3(\eta^2\text{-}N_2CPh_2)]$ (°).

N4-U1-N1	109.06(14)	N4-U1-N3	107.74(14)
N4-U1-N2	100.14(14)	N1-U1-N2	104.87(14)
N4-U1-N5	34.20(13)	N1-U1-N5	98.61(13)
N2-U1-N5	134.05(13)	N4-U1-Si2	134.26(10)
N3-U1-Si2	110.36(9)	N2-U1-Si2	87.13(10)
N4-U1-Si3	78.67(10)	N1-U1-Si3	95.79(10)
N2-U1-Si3	27.61(10)	N5-U1-Si3	112.27(9)
N4-U1-Si5	86.87(10)	N1-U1-Si5	145.67(10)
N2-U1-Si5	101.75(11)	N5-U1-Si5	77.36(9)
Si3-U1-Si5	117.49(4)	N1-Si1-C1	114.5(2)
C1-Si1-C2	106.7(3)	N1-Si1-C3	112.4(3)
C2-Si1-C3	108.0(4)	N1-Si2-C6	110.2(2)
C6-Si2-C5	104.9(3)	N1-Si2-C4	114.2(3)
C5-Si2-C4	108.5(3)	N1-Si2-U1	38.86(13)
C5-Si2-U1	114.2(2)	C4-Si2-U1	136.4(2)
N2-Si3-C8	110.0(3)	C7-Si3-C8	107.7(3)
C7-Si3-C9	104.5(3)	C8-Si3-C9	107.9(3)
C7-Si3-U1	76.98(19)	C8-Si3-U1	105.0(2)
N2-Si4-C12	112.3(2)	N2-Si4-C10	112.7(3)
N2-Si4-C11	113.4(3)	C12-Si4-C11	105.1(3)
N3-Si5-C15	113.3(2)	N3-Si5-C13	110.8(2)

N3-Si5-C14	112.6(2)	C15-Si5-C14	107.4(3)
N3-Si5-U1	37.85(13)	C15-Si5-U1	136.73(19)
C14-Si5-U1	113.89(17)	N3-Si6-C17	112.0(3)
C17-Si6-C16	105.5(3)	N3-Si6-C18	111.1(2)
C16-Si6-C18	104.8(3)	N4-Na1-N6	130.87(19)
N6-Na1-N7	104.3(2)	Si2-N1-Si1	119.5(2)
Si1-N1-U1	127.1(2)	Si4-N2-Si3	118.0(2)
Si3-N2-U1	113.5(2)	Si5-N3-Si6	118.9(2)
Si6-N3-U1	125.9(2)	N5-N4-U1	81.5(2)
U1-N4-Na1	151.55(19)	C19-N5-N4	125.5(4)
N4-N5-U1	64.3(2)	C36-N6-C32	116.2(6)
C32-N6-Na1	122.7(5)	C37-N7-C41	116.7(7)
C41-N7-Na1	119.1(4)	N5-C19-C26	119.9(4)
C26-C19-C20	120.1(4)	C21-C20-C25	118.1(5)
C25-C20-C19	121.8(4)	C22-C21-C20	120.7(5)
C22-C23-C24	119.4(5)	C25-C24-C23	119.2(5)
C31-C26-C27	116.9(5)	C31-C26-C19	122.0(4)
C28-C27-C26	121.2(5)	C29-C28-C27	121.2(5)
C31-C30-C29	120.2(6)	C30-C31-C26	121.8(5)
C34-C33-C32	120.0(7)	C33-C34-C35	118.7(7)
N6-C36-C35	124.0(7)	N7-C37-C38	121.5(9)
C40-C39-C38	122.1(9)	C39-C40-C41	118.3(10)
N1-U1-N3	119.79(13)	C19-N5-U1	170.2(3)
N3-U1-N2	113.44(14)	C36-N6-Na1	120.6(5)
N3-U1-N5	86.66(13)	C37-N7-Na1	124.0(6)
N1-U1-Si2	27.72(10)	N5-C19-C20	119.9(4)
N5-U1-Si2	125.61(9)	C21-C20-C19	120.1(4)
N3-U1-Si3	137.26(10)	C23-C22-C21	121.2(5)
Si2-U1-Si3	89.81(4)	C20-C25-C24	121.4(5)
N3-U1-Si5	27.02(9)	C27-C26-C19	121.1(4)
Si2-U1-Si5	136.12(4)	C28-C29-C30	118.7(5)
N1-Si1-C2	111.1(3)	N6-C32-C33	122.9(7)
C1-Si1-C3	103.7(3)	C34-C35-C36	118.2(7)
N1-Si2-C5	114.0(3)	C39-C38-C37	117.0(8)
C6-Si2-C4	104.2(3)	N7-C41-C40	124.5(8)
C6-Si2-U1	73.15(18)	C13-Si5-C14	105.3(3)
N2-Si3-C7	111.2(2)	C13-Si5-U1	74.46(16)
N2-Si3-C9	115.2(3)	N3-Si6-C16	114.5(2)
N2-Si3-U1	38.85(14)	C17-Si6-C18	108.4(3)
C9-Si3-U1	144.7(2)	N4-Na1-N7	118.98(18)
C12-Si4-C10	106.9(3)	Si2-N1-U1	113.43(19)
C10-Si4-C11	105.9(3)	Si4-N2-U1	128.1(2)
C15-Si5-C13	107.0(3)	Si5-N3-U1	115.12(19)
N5-N4-Na1	126.5(3)		

Table 6.5.8 Bond lengths of Li(THF)U[N(SiMe$_3$)$_2$](κ$_2$-CH$_2$SiMe$_2$NSiMe$_3$)$_2$ (Å).

U1-N2	2.2633(17)	U1-N3	2.2711(17)	U1-N1	2.3327(16)
U1-C18	2.485(2)	U1-C12	2.524(2)	U1-Si6	3.0403(6)
U1-Si4	3.0790(6)	U1-Si2	3.4565(6)	Si6-N3	1.7355(19)
Si6-C17	1.870(3)	Si6-C18	1.872(2)	Si6-C16	1.875(2)
N3-Si5	1.7215(19)	Si2-N1	1.7103(19)	Si2-C4	1.872(3)
Si2-C5	1.874(3)	Si2-C6	1.877(3)	Si3-N2	1.7123(18)

Si3-C7	1.867(3)	Si3-C8	1.871(3)	Si3-C9	1.883(3)
Si4-N2	1.7407(19)	Si4-C12	1.851(2)	Si4-C11	1.872(3)
Si4-C10	1.877(3)	Si5-C14	1.850(3)	Si5-C15	1.858(3)
Si5-C13	1.862(4)	N1-Si1	1.7223(18)	C22-C21	1.435(5)
C22-O1	1.437(3)	O1-C19	1.429(3)	O1-Li1	1.933(4)
C23-O2	1.423(4)	C23-C24	1.475(5)	Si1-C1	1.866(3)
Si1-C2	1.869(3)	Si1-C3	1.869(3)	C19-C20	1.486(4)
C20-C21	1.474(5)	O2-C26	1.412(4)	O2-Li1	1.947(4)
C25-C26	1.411(5)	C25-C24	1.483(5)		

Table 6.5.9 Bond angles of Li(THF)U[N(SiMe$_3$)$_2$](κ$_2$-CH$_2$SiMe$_2$NSiMe$_3$)$_2$ (°).

N2-U1-N3	106.79(7)	N2-U1-N1	106.27(6)
N2-U1-C18	157.43(7)	N3-U1-C18	72.38(7)
N2-U1-C12	70.76(7)	N3-U1-C12	102.75(7)
C18-U1-C12	87.26(8)	N2-U1-Si6	137.27(5)
N1-U1-Si6	110.62(4)	C18-U1-Si6	37.94(5)
N2-U1-Si4	33.87(5)	N3-U1-Si4	107.08(4)
C18-U1-Si4	123.85(6)	C12-U1-Si4	36.93(5)
N2-U1-Si2	94.67(5)	N3-U1-Si2	146.12(4)
C18-U1-Si2	97.38(6)	C12-U1-Si2	109.03(6)
Si4-U1-Si2	105.314(17)	N3-Si6-C17	114.20(11)
C17-Si6-C18	106.27(12)	N3-Si6-C16	110.97(11)
C18-Si6-C16	114.54(12)	N3-Si6-U1	47.73(6)
C18-Si6-U1	54.74(6)	C16-Si6-U1	127.80(10)
Si5-N3-U1	137.62(10)	Si6-N3-U1	97.83(8)
N1-Si2-C5	114.19(11)	C4-Si2-C5	107.02(15)
C4-Si2-C6	107.85(13)	C5-Si2-C6	105.99(13)
C4-Si2-U1	127.43(11)	C5-Si2-U1	124.08(10)
N2-Si3-C7	109.39(11)	N2-Si3-C8	112.27(11)
N2-Si3-C9	112.01(11)	C7-Si3-C9	108.56(14)
N2-Si4-C12	101.40(9)	N2-Si4-C11	112.17(11)
N2-Si4-C10	113.17(12)	C12-Si4-C10	111.20(14)
N2-Si4-U1	46.43(6)	C12-Si4-U1	55.03(7)
C10-Si4-U1	128.65(11)	N3-Si5-C14	111.12(13)
C14-Si5-C15	106.02(18)	N3-Si5-C13	113.05(13)
C15-Si5-C13	104.11(19)	Si2-N1-Si1	120.97(10)
Si1-N1-U1	121.86(9)	C21-C22-O1	107.2(3)
C19-O1-Li1	129.6(2)	C22-O1-Li1	121.4(2)
N1-Si1-C1	114.02(11)	N1-Si1-C2	109.75(11)
N1-Si1-C3	112.52(12)	C1-Si1-C3	106.61(14)
Si3-N2-Si4	128.70(11)	Si3-N2-U1	131.16(10)
O1-C19-C20	106.8(2)	C21-C20-C19	105.0(3)
C26-O2-C23	108.0(2)	C26-O2-Li1	128.6(2)
Si6-C18-U1	87.31(8)	C26-C25-C24	106.8(3)
C22-C21-C20	108.9(3)	C25-C26-O2	109.5(3)
N3-U1-N1	120.23(6)	C11-Si4-C10	106.64(15)
N1-U1-C18	92.72(7)	C11-Si4-U1	124.55(11)
N1-U1-C12	134.84(8)	N3-Si5-C15	113.72(12)
N3-U1-Si6	34.44(5)	C14-Si5-C13	108.3(2)
C12-U1-Si6	96.59(6)	Si2-N1-U1	116.66(9)
N1-U1-Si4	127.51(5)	C19-O1-C22	108.8(2)
Si6-U1-Si4	121.382(16)	O2-C23-C24	107.0(3)

N1-U1-Si2	26.24(5)	C1-Si1-C2	106.01(14)
Si6-U1-Si2	127.691(17)	C2-Si1-C3	107.53(16)
N3-Si6-C18	102.47(9)	Si4-N2-U1	99.70(8)
C17-Si6-C16	108.37(13)	Si4-C12-U1	88.05(9)
C17-Si6-U1	123.80(9)	C23-O2-Li1	122.8(2)
Si5-N3-Si6	124.54(10)	C23-C24-C25	103.6(3)
N1-Si2-C4	112.98(12)	O1-Li1-O2	100.6(2)
N1-Si2-C6	108.42(10)	C7-Si3-C8	106.93(13)
N1-Si2-U1	37.09(6)	C8-Si3-C9	107.49(13)
C6-Si2-U1	71.37(8)	C12-Si4-C11	112.37(13)

Table 6.5.10 Bond lengths of $U^{IV}(NAr^{F}Ph)_2(TEMPO)_2$ (Å).

U1-O1#1	2.155(4)	U1-O1	2.155(4)	U1-N2	2.334(5)
U1-N2#1	2.334(5)	U1-N1#1	2.561(5)	U1-N1	2.561(5)
F1-C22	1.296(11)	F2-C22	1.341(10)	F3-C22	1.272(10)
F4-C23	1.312(10)	F5-C23	1.307(12)	F6-C23	1.228(11)
O1-N1	1.432(6)	N1-C1	1.505(7)	N1-C5	1.520(8)
N2-C16	1.396(7)	N2-C10	1.443(7)	C1-C6	1.520(9)
C1-C7	1.523(9)	C1-C2	1.534(9)	C2-C3	1.530(10)
C3-C4	1.520(10)	C4-C5	1.536(9)	C5-C8	1.520(9)
C5-C9	1.531(8)	C10-C11	1.378(9)	C10-C15	1.395(8)
C11-C12	1.404(9)	C12-C13	1.384(13)	C13-C14	1.352(13)
C14-C15	1.409(11)	C16-C21	1.392(10)	C16-C17	1.408(9)
C17-C18	1.375(10)	C18-C19	1.369(12)	C18-C22	1.497(10)
C19-C20	1.395(12)	C20-C21	1.374(9)	C20-C23	1.497(10)

Symmetry transformations used to generate equivalent atoms:

#1 x,-y+1,-z

Table 6.5.11 Bond angles of $U^{IV}(NAr^{F}Ph)_2(TEMPO)_2$ (°).

O1#1-U1-O1	172.6(2)	O1#1-U1-N2	98.52(16)
O1#1-U1-N2#1	86.38(16)	O1-U1-N2#1	98.52(16)
O1#1-U1-N1#1	33.99(14)	O1-U1-N1#1	138.95(15)
N2#1-U1-N1#1	115.92(16)	O1#1-U1-N1	138.95(15)
N2-U1-N1	115.92(16)	N2#1-U1-N1	108.90(16)
N1-O1-U1	88.7(3)	O1-N1-C1	108.6(4)
C1-N1-C5	118.7(5)	O1-N1-U1	57.3(2)
C5-N1-U1	116.0(4)	C16-N2-C10	114.6(5)
C10-N2-U1	122.3(4)	N1-C1-C6	107.6(5)
C6-C1-C7	107.7(5)	N1-C1-C2	108.3(5)
C7-C1-C2	111.7(5)	C3-C2-C1	113.1(6)
C3-C4-C5	114.1(5)	C8-C5-N1	107.0(5)
N1-C5-C9	113.7(5)	C8-C5-C4	109.2(5)
C9-C5-C4	111.9(5)	C11-C10-C15	118.5(6)
C15-C10-N2	119.5(6)	C10-C11-C12	121.0(6)
C14-C13-C12	120.1(7)	C13-C14-C15	120.7(7)
C21-C16-N2	120.5(6)	C21-C16-C17	117.6(5)
C18-C17-C16	120.4(6)	C19-C18-C17	121.0(8)
C17-C18-C22	121.4(7)	C18-C19-C20	119.4(8)
C21-C20-C23	121.2(7)	C19-C20-C23	119.0(7)
F3-C22-F1	111.7(10)	F3-C22-F2	102.5(8)

F3-C22-C18	113.9(7)	F1-C22-C18	113.6(6)
F6-C23-F5	104.7(11)	F6-C23-F4	111.4(10)
F6-C23-C20	115.2(7)	F5-C23-C20	111.7(8)
O1-U1-N2	86.38(16)	C11-C10-N2	122.0(5)
N2-U1-N2#1	97.8(2)	C13-C12-C11	119.6(7)
N2-U1-N1#1	108.90(16)	C10-C15-C14	119.9(7)
O1-U1-N1	33.99(14)	N2-C16-C17	121.9(6)
N1#1-U1-N1	109.3(2)	C19-C18-C22	117.6(8)
O1-N1-C5	108.3(4)	C21-C20-C19	119.8(6)
C1-N1-U1	125.0(4)	C20-C21-C16	121.5(6)
C16-N2-U1	122.8(4)	F1-C22-F2	102.5(7)
N1-C1-C7	113.1(5)	F2-C22-C18	111.5(8)
C6-C1-C2	108.3(5)	F5-C23-F4	100.7(8)
C4-C3-C2	108.4(5)	F4-C23-C20	111.9(7)
C8-C5-C9	107.8(6)	N1-C5-C4	107.0(5)

Symmetry transformations used to generate equivalent atoms:

#1 x,-y+1,-z

6.6 References.

(1) Lewis, A. J.; Carroll, P. J.; Schelter, E. J., *J. Am. Chem. Soc.* **2013,** *135*, 13185.
(2) Lewis, A. J.; Nakamaru-Ogiso, E.; Carroll, P. J.; Schelter, E. J. **2014**, *submitted to Inorg. Chem.*
(3) Edelstein, N.; Brown, D.; Whittaker, B., *Inorg. Chem.* **1974,** *13*, 563.
(4) Choppin, G. R., *J. Alloys Compd.* **2002,** *344*.
(5) Jensen, M. P.; Bond, A. H., *IJ. Am. Chem. Soc.* **2002,** *124*, 9870.
(6) Graves, C. R.; Vaughn, A. E.; Schelter, E. J.; Scott, B. L.; Thompson, J. D.; Morris, D. E.; Kiplinger, J. L., *Inorg. Chem.* **2008,** *47*, 11879.
(7) Cantat, T.; Graves, C. R.; Jantunen, K. C.; Burns, C. J.; Scott, B. L.; Schelter, E. J.; Morris, D. E.; Hay, P. J.; Kiplinger, J. L., *J. Am. Chem. Soc.* **2008,** *130*, 17537.
(8) Cantat, T.; Graves, C. R.; Scott, B. L.; Kiplinger, J. L., *Angew. Chem. Int. Ed.* **2009,** *48*, 3681.
(9) Arnold, P. L.; Turner, Z. R.; Kaltsoyannis, N.; Pelekanaki, P.; Bellabarba, R. M.; Tooze, R. P., *Chem. - Eur. J.* **2010,** *16*, 9623.
(10) Minasian, S. G.; Keith, J. M.; Batista, E. R.; Boland, K. S.; Clark, D. L.; Conradson, S. D.; Kozimor, S. A.; Martin, R. L.; Schwarz, D. E.; Shuh, D. K.; Wagner, G. L.; Wilkerson, M. P.; Wolfsberg, L. E.; Yang, P., *J. Am. Chem. Soc.* **2012**.
(11) Cooper, O. J.; Mills, D. P.; McMaster, J.; Tuna, F.; McInnes, E. J.; Lewis, W.; Blake, A. J.; Liddle, S. T., *Chem. - Eur. J.* **2013,** *19*, 7071.
(12) Kaltsoyannis, N., *Inorg. Chem.* **2013,** *52*, 3407.
(13) Lukens, W. W.; Edelstein, N. M.; Magnani, N.; Hayton, T. W.; Fortier, S.; Seaman, L. A., *J. Am. Chem. Soc.* **2013,** *135*, 10742.
(14) Roy, L. E.; Bridges, N. J.; Martin, L. R., *Dalton Trans.* **2013,** *42*, 2636.
(15) King, D. M.; Tuna, F.; McInnes, E. J.; McMaster, J.; Lewis, W.; Blake, A. J.; Liddle, S. T., *Nat. Chem.* **2013,** *5*, 482.
(16) Cooper, O. J.; Mills, D. P.; McMaster, J.; Moro, F.; Davies, E. S.; Lewis, W.; Blake, A. J.; Liddle, S. T., *Angew. Chem. Int. Ed.* **2011,** *50*, 2383.
(17) Mills, D. P.; Cooper, O. J.; Tuna, F.; McInnes, E. J. L.; Davies, E. S.; McMaster, J.; Moro, F.; Lewis, W.; Blake, A. J.; Liddle, S. T., *J. Am. Chem. Soc.* **2012,** *134*, 10047.

(18) antat, T.; rliguie, T. r. s.; No l, .; Thu ry, P.; phriti hine, .; Floch, P. .; zailles, N., *J. Am. Chem. Soc.* **2009,** *131*, 963.
(19) Tourneux, J.-C.; Berthet, J.-C.; Cantat, T.; Thu ry , P.; z ailles, N.; e Floch, P.; Ephritikhine, M., *Organometallics* **2011,** *30*.
(20) Bogart, J. A.; Lewis, A. J.; Medling, S. A.; Piro, N. A.; Carroll, P. J.; Booth, C. H.; Schelter, E. J., *Inorg. Chem.* **2013,** *52*, 11600.
(21) Anderson, G. M.; Iqbal, J.; Sharp, D. W. A.; Winfield, J. M.; Cameron, J. H.; McLeod, A. G., *J. Fluor. Chem.* **1984,** *24*, 303.
(22) Simoes, J. A. M.; Beauchamp, J. L., *Chem. Rev.* **1990,** *90*, 629.
(23) Gardner, B. M.; Cleaves, P. A.; Kefalidis, C. E.; Fang, J.; Maron, L.; Lewis, W.; Blake, A. J.; Liddle, S., *Chem. Sci.* **2014**.
(24) Ren, W.; Zi, G.; Fang, D.-C.; Walter, M. D., *J. Am. Chem. Soc.* **2011,** *133*, 13183.
(25) Ren, W.; Zi, G.; Walter, M. D., *Organometallics* **2012,** *31*.
(26) Carmichael, C. D.; Jones, N. A.; Arnold, P. L., *Inorg. Chem.* **2008,** *47*, 8577.
(27) Schnaars, D. D.; Wu, G.; Hayton, T. W., *Dalton Trans.* **2008,** *0*, 6121.
(28) Schnaars, D. D.; Wu, G.; Hayton, T. W., *Dalton Trans.* **2009**, 3681.
(29) Monreal, M. J.; Thomson, R. K.; Cantat, T.; Travia, N. E.; Scott, B. L.; Kiplinger, J. L., *Organometallics* **2011,** *30*, 2031.
(30) La Pierre, H. S.; Heinemann, F. W.; Meyer, K., *Chem. Commun.* **2014**.
(31) Huebner, L.; Kornienko, A.; Emge, T. J.; Brennan, J. G., *Inorg. Chem.* **2004,** *43*, 5659.
(32) Stewart, J. L. *Tris[bis(trimethylsilyl)amido]uranium: compounds with tri-, tetra-, and pentavalent uranium*; Lawrence Berkeley Lab.: 1988; p 200 pp.
(33) Fortier, S.; Wu, G.; Hayton, T. W., *Inorg. Chem.* **2009,** *48*, 3000.
(34) Avens, L. R.; Bott, S. G.; Clark, D. L.; Sattelberger, A. P.; Watkin, J. G.; Zwick, B. D., *Inorg. Chem.* **1994,** *33*, 2248.
(35) Fortier, S.; Brown, J. L.; Kaltsoyannis, N.; Wu, G.; Hayton, T. W., *Inorg. Chem.* **2012,** *51*, 1625.
(36) Lam, O. P.; Feng, P. L.; Heinemann, F. W.; O'Connor, J. M.; Meyer, K., *J. Am. Chem. Soc.* **2008,** *130*, 2806.
(37) Bénaud, O.; Berthet, J.-C.; Thuéry, P.; Ephritikhine, M., *Chem. Commun.* **2011,** *47*, 9057.
(38) n aud, O.; erthet, . - .; Thu ry, P.; phriti hine, ., *Inorg. Chem.* **2010,** *49*, 8117.
(39) Fortier, S.; Kaltsoyannis, N.; Wu, G.; Hayton, T. W., *J. Am. Chem. Soc.* **2011,** *133*, 14224.